

STEREOSPECIFIC REACTIONS OF
 α -AMINO- β -DIAZONIUM INTERMEDIATES: MECHANISTIC STUDIES, NEW
REACTION DISCOVERY AND THEIR APPLICATION TO A TWO-DIRECTIONAL
TOTAL SYNTHESIS OF (+)-ZWITTERMICIN A

By

Hubert Muchalski

Dissertation

Submitted to the Faculty of the
Graduate School of Vanderbilt University
in partial fulfillment of the requirements
for the degree of

DOCTOR OF PHILOSOPHY

in

Chemistry

August, 2012

Nashville, Tennessee

Approved:

Jeffrey N. Johnston (Chair)

Timothy P. Hanusa

Ned A. Porter

Gary A. Sulikowski

*To my wife Kasia and son Olaf.
To my mom, dad, and brother.*

Acknowledgments

Though only my name appears on the cover of this dissertation, a great many people have contributed to its production. I owe my gratitude to all those people who have made this dissertation possible and because of whom my graduate experience has been one that I will cherish forever.

First and foremost, I would like to express my gratitude to my advisor, Dr. Jeffrey N. Johnston, for his support, patience, and encouragement throughout my graduate studies. It is not often that one finds an advisor and colleague that always finds the time for listening to the little problems and roadblocks that unavoidably crop up in the course of performing research. The extensive knowledge, vision, and creative thinking of Dr. Johnston have been the source of inspiration for me throughout this work.

Secondly, I must acknowledge my close co-workers. I thank Dr. Timothy L. Troyer for his teamwork, support, and intellectual contribution to the aziridine and glycolate Mannich projects and Dr. Ki Bum Hong for his contribution in the zwittermicin project. My work drew heavily on the results of their early efforts. I owe big thanks to Amanda B. Doody for her friendship and contribution to the large scale diazo preparation.

I would like to acknowledge my committee members Dr. Timothy P. Hanusa, Dr. Gary A. Sulikowski, Dr. Piotr Kaszynski, and Dr. Ned A. Porter for their commitment to my education. I'm especially thankful to Dr. Ned A. Porter, for agreeing to be on my Ph.D. committee on last minute notice. I acknowledge Dr. Eva Harth for her support during the summer of 2005 and for recruiting me into Vanderbilt's Graduate School. I thank my advisor at Wrocław University of Technology, Dr. Mirosław Giurg, for igniting my passion for chemistry.

The great amount of experimental data that I collected during my graduate work wouldn't be possible without the help of Dr. Don Stec and Dr. Markus Voehler. I especially appreciate the support of Dr. Stec during night hours and weekends. I acknowledge Dr. Maren Pink and Dr. Jonathan Karty (Indiana University) for their service and support.

A big part of being a graduate student is teaching. I had the privilege to work and interact with wonderful people when I was a TA. My thanks go to Dr. Adam List, Dr. Pat Tellinghuisen, and Clara Johnson for their help in my teaching assignments.

It was an honor to work with a group of extraordinary people in the Johnston Lab. My deep thanks go to Dr. Matthew Donahue, Dr. Julie Pigza for training me during my early days in the group, Dr. Jeremy Wilt, Dr. Anand Singh, Dr. Bo Shen, Dr. Aroop Chandra, Dr. Tyler Davis, Dr. Matthew Leighty, Mark Dobish, Dawn Makley, Priya Mathew, Jessica Shackelford, Dain Beezer, Brandon Vara, Daniel Sprague, Kenneth Schwieter, and Michael

Danneman for their intellectual support, friendship, and hard work. I also thank the current group members for prompt proofreading of this dissertation.

I would like to thank my friends in the Chemistry Department, Dr. Bryan Ringstrand, Dr. Aleksandra Barańczak, and, especially, Dr. Stephen Chau for visiting me almost everyday and for his always positive attitude.

I acknowledge Vanderbilt University, the National Science Foundation, and Warren Fund for financial support.

Perfect typesetting in this dissertation would not be possible without the support of the developers and enthusiasts of L^AT_EX system. I owe big thanks to Joseph Wright for developing and maintaining `achemso`, `chemstyle`, and `siunitx` packages. Big thanks go to developers of MiKTeX, JabRef, and Autohotkey software as well as contributors to L^AT_EX Community Forum.

Many individuals added to my enjoyment of doing research by producing extraordinary podcasts and shows that I listened to while working in the lab. I'm grateful to George Hrab, Dan Benjamin, Merlin Mann, John Siracusa, SGU Team, Colin Marshall, Desiree Schell, Russ Roberts, Chris Mooney, Robynn "Swoopy" McCarthy, Derek Colanduno, Brian Dunning, and people behind NPR Radiolab.

I'm also extremely grateful to my parents for their endless love and support. My parents have continually sacrificed their own interests so that Konrad and I could have the best education possible. Even more importantly, my mother and father have provided two role models of hard work, persistence, and integrity.

Finally, I extend my deepest gratitude to my wife, Kasia, for her love and patience. She has been with me from the beginning of my Ph.D., and through all the ups and downs she has continued her support and encouragement. My son Olaf, a.k.a my first natural product, has brought me incredible joy and continually cheers me up with his exuberant greetings upon my return from work in the evenings.

Table of Contents

DEDICATION	i
ACKNOWLEDGMENTS	ii
LIST OF FIGURES	xiv
LIST OF SCHEMES	xix
LIST OF TABLES	xx
LIST OF ABBREVIATIONS	xxi
Chapter	
1 Mechanism of the Brønsted acid-catalyzed aza-Darzens reaction. Influence of diazoalkane structure on the stereoselectivity of carbon–carbon bond formation.	1
1.1 Introduction to diazoalkanes	1
1.1.1 Diazoalkanes in organic synthesis	1
1.1.2 Synthetic approaches to diazoalkanes	4
1.2 Stereoselective reactions involving α -aminodiazonium intermediates	8
1.2.1 Metal catalyzed reactions	8
1.2.2 Brønsted acid catalyzed reactions	12
1.3 Origins of selectivity in the aza-Darzens aziridine synthesis	17
1.4 Results and discussion	21
1.4.1 Stereochemistry of triazoline imide fragmentation	22
1.4.2 Stereochemistry of the carbon–carbon bond formation in α -diazo imide addition to azomethines	25
1.4.3 Diazoalkane scope of the aza-Darzens reaction	30
1.4.4 Summary and conclusions	31
2 Stereoselective reactions of α-diazo imides	33
2.1 Stereoselective approaches to α -oxy- β -amino acid motif	33
2.1.1 Olefin functionalization	33
2.1.2 Vicinal aminoalcohols via C–C bond forming reactions	37
2.2 Diastereoselective Brønsted acid-catalyzed glycolate Mannich reaction	40
2.2.1 Large scale synthesis of α -diazo imide	40
2.2.2 Optimization of reaction conditions and substrate scope	43
2.2.3 Functionalization of the oxazolidine dione ring	48

2.3	Development of enantioselective glycolate Mannich reaction	54
2.3.1	Evaluation of chiral Brønsted acids in reactions of α -diazo imide with azomethines	54
2.3.2	Evaluation of Lewis acids in the <i>syn</i> -glycolate Mannich reaction . . .	55
2.3.3	Glycolate Mannich reaction catalyzed by chiral Cu(II)–BOX complexes	61
2.3.4	New reactivity of α -diazo imide in presence of copper(I) catalysts . .	72
2.3.5	Exploration of α -diazo imide–copper(I) system	77
2.3.6	Summary and conclusions	89
3	Progress towards the total synthesis of (+)-zwittermicin A	90
3.1	Background	90
3.1.1	Isolation, structural assignment and biological activity	90
3.1.2	Revision of the absolute stereochemistry	91
3.1.3	Biosynthesis	93
3.2	Two-directional synthesis	96
3.2.1	Introduction	96
3.2.2	Two-directional synthesis of natural products	96
3.2.3	Approach to (+)-zwittermicin A via a two-directional azide–alkene cycloaddition	100
3.3	Previous work	101
3.3.1	Diastereoselective azide–alkene reaction: a model study	101
3.3.2	Synthesis of bis(imide) 312	103
3.3.3	Summary of previous work	105
3.4	Results and discussion	106
3.4.1	Optimization of the synthesis of bis(imide) 312	106
3.4.2	Studies of facial discrimination in the acid-promoted azide–olefin cycloaddition	110
3.4.3	Functionalization of the bis(oxazolidine dione)	113
3.4.4	Desymmetrization and synthesis of the aldehyde for Passerini coupling	120
3.4.5	Synthesis of the isonitrile fragment	124
3.4.6	First generation synthesis of the Passerini adduct and its functionalization	127
3.4.7	Studies towards the desymmetriation and decarbonylation	131
3.4.8	Second generation synthesis of the Passerini adduct	134
3.4.9	The end game strategy	139

Appendix

A Experimental Section	141
Compounds relevant to Chapter 1	141
Compounds relevant to Chapter 2	147
Compounds relevant to Chapter 3	164
B X-Ray Crystallography of the compound 345	200
C Spectral data and characterization.	225
References	434

List of Figures

1.1	Approaches to aziridines by addition to double bonds.	9
1.2	Proposed mechanism of metallocarbene addition to azomethine	10
1.3	Lewis acid-catalyzed aziridination with diazo compounds.	11
1.4	Boron catalysts for asymmetric aziridination	12
1.5	Mechanistic outline connecting aza-Darzens and triazoline decomposition reactions in the presence of a Brønsted acid.	18
1.6	Intersecting paths of triazoline imide fragmentation and α -diazo imide addition to imines.	22
1.7	Outline of triazoline imide decomposition.	23
1.8	Diazo imide–imine reaction hypothesis.	25
1.9	$^1\text{H NMR}$ (CDCl_3) of a) aziridine <i>cis</i> - 74 , b) oxazolidine dione <i>syn</i> - 80 , c) oxazolidine dione <i>syn</i> - 75 , d) oxazolidine dione <i>anti</i> - 75 , and e) crude reaction mixture (Scheme 1.34). The resonance at 4.28 ppm (dq) corresponding to the oxazolidine dione <i>syn</i> - 75 is absent in the spectrum of the crude reaction mixture. Resonances marked with an asterisk (*) are assigned to the aziridine <i>methyl</i> ester.	29
1.10	Origin of stereoselectivity in Brønsted acid-promoted diazo–azomethine reactions.	31
2.1	Natural products containing <i>vic</i> -aminoalcohol fragment.	34
2.2	Decomposition pathways of α -diazo imide.	43
2.3	Bis(amidine) (BAM) catalysts for enantioselective aza-Henry reaction.	54
2.4	Equilibrium reaction between $\text{BF}_3 \cdot \text{OEt}_2$ and TMSOTf.	56
2.5	Origin of stereoselectivity in Brønsted acid-promoted diazo–azomethine reactions.	74
2.6	Mechanistic pathways of the α -aminodiazonium formed from <i>N</i> -Boc imine and α -diazo imide.	79
2.7	Brønsted acid promoted formation of <i>N</i> -Ts oxazolidine dione 230 . (a) $^1\text{H NMR}$ (CDCl_3) spectrum of the crude reaction mixture without addition of triflic acid (b) $^1\text{H NMR}$ (CDCl_3) spectrum of the crude reaction mixture after addition of triflic acid.	83
2.8	Postulated mechanism for the formation of 236 and 237	87

3.1	(+)-Zwittermicin A	90
3.2	Proposed biosynthesis of zwittermicin A (adapted from ref. 145)	95
3.3	General strategies for the synthesis of acyclic compounds.	96
3.4	Mechanism of the competitive acyl transfer during Horner–Wadsworth–Emmons reaction	109
3.5	Depictions of the likely major conformations of the siloxane (A) and disiloxane (B) rings.	112
3.6	Perspective view of the disiloxane view in bis(ester) 352	117
3.7	The X-ray structure of the bis(ester) 352	118
3.8	Dess–Martin oxidation of 406 followed by ¹ H NMR. (A) Alcohol 406 ; (B) Reaction mixture after 5 min; (C) reaction mixture after 15 min; (D) reaction mixture after addition of PhCO ₂ H; (E) reaction mixture after addition of isonitrile 383	138
C.1	¹ H NMR (CDCl ₃) of 75	226
C.2	¹³ C NMR (CDCl ₃) of 75	227
C.3	¹ H NMR (CDCl ₃) of 76	228
C.4	¹³ C NMR (CDCl ₃) of 76	229
C.5	¹ H NMR (CDCl ₃) of 78	230
C.6	¹³ C NMR (CDCl ₃) of 78	231
C.7	¹ H NMR (CDCl ₃) of 81	232
C.8	¹³ C NMR (CDCl ₃) of 81	233
C.9	¹ H NMR (CDCl ₃) of 82	234
C.10	¹³ C NMR (CDCl ₃) of 82	235
C.11	¹ H NMR (CDCl ₃) of 83	236
C.12	¹³ C NMR (CDCl ₃) of 83	237
C.13	¹ H NMR (CDCl ₃) of 85	238
C.14	¹³ C NMR (CDCl ₃) of 85	239
C.15	¹ H NMR (CDCl ₃) of 86	240
C.16	¹³ C NMR (CDCl ₃) of 86	241
C.17	¹ H NMR (CDCl ₃) of 87	242
C.18	¹³ C NMR (CDCl ₃) of 87	243
C.19	¹ H NMR (CDCl ₃) of 88	244
C.20	¹³ C NMR (CDCl ₃) of 88	245
C.21	¹ H NMR (CDCl ₃) of 131	246
C.22	¹³ C NMR (CDCl ₃) of 131	247

C.23	^1H NMR (CDCl_3) of 132	248
C.24	^{13}C NMR (CDCl_3) of 132	249
C.25	^1H NMR (CDCl_3) of 133	250
C.26	^{13}C NMR (CDCl_3) of 133	251
C.27	^1H NMR (CDCl_3) of 134	252
C.28	^{13}C NMR (CDCl_3) of 134	253
C.29	^1H NMR (CDCl_3) of 138	254
C.30	^{13}C NMR (CDCl_3) of 138	255
C.31	^1H NMR (CDCl_3) of 139	256
C.32	^{13}C NMR (CDCl_3) of 139	257
C.33	^1H NMR (CDCl_3) of 140	258
C.34	^{13}C NMR (CDCl_3) of 140	259
C.35	^1H NMR (CDCl_3) of 141	260
C.36	^{13}C NMR (CDCl_3) of 141	261
C.37	^1H NMR (CDCl_3) of 162	262
C.38	^{13}C NMR (CDCl_3) of 162	263
C.39	^1H NMR (CDCl_3) of 415	264
C.40	^{13}C NMR (CDCl_3) of 415	265
C.41	^1H NMR (CDCl_3) of 416	266
C.42	^{13}C NMR (CDCl_3) of 416	267
C.43	^1H NMR (CDCl_3) of 417	268
C.44	^{13}C NMR (CDCl_3) of 417	269
C.45	^1H NMR (CDCl_3) of 418	270
C.46	^{13}C NMR (CDCl_3) of 418	271
C.47	^1H NMR (CDCl_3) of 150	272
C.48	^{13}C NMR (CDCl_3) of 150	273
C.49	^1H NMR (CDCl_3) of 151	274
C.50	^{13}C NMR (CDCl_3) of 151	275
C.51	^1H NMR (CDCl_3) of 156	276
C.52	^{13}C NMR (CDCl_3) of 156	277
C.53	^1H NMR (CDCl_3) of 157	278
C.54	^{13}C NMR (CDCl_3) of 157	279
C.55	^1H NMR (CDCl_3) of 203	280
C.56	^{13}C NMR (CDCl_3) of 203	281
C.57	^1H NMR (CDCl_3) of 204	282
C.58	^{13}C NMR (CDCl_3) of 204	283

C.59	^1H NMR (CDCl_3) of 215	284
C.60	^{13}C NMR (CDCl_3) of 215	285
C.61	^1H NMR (CDCl_3) of 216	286
C.62	^{13}C NMR (CDCl_3) of 216	287
C.63	^1H NMR (CDCl_3) of 217	288
C.64	^{13}C NMR (CDCl_3) of 217	289
C.65	^1H NMR (CDCl_3) of 218	290
C.66	^{13}C NMR (CDCl_3) of 218	291
C.67	^1H NMR (CDCl_3) of 219	292
C.68	^{13}C NMR (CDCl_3) of 219	293
C.69	^1H NMR ($\text{DMSO}-d_6$) of 223	294
C.70	^{13}C NMR ($\text{DMSO}-d_6$) of 223	295
C.71	^1H NMR (CDCl_3) of 236	296
C.72	^{13}C NMR (CDCl_3) of 236	297
C.73	^1H NMR (CDCl_3) of 420	298
C.74	^{13}C NMR (CDCl_3) of 420	299
C.75	^1H NMR (CDCl_3) of 230a	300
C.76	^{13}C NMR (CDCl_3) of 230a	301
C.77	^1H NMR (CDCl_3) of 230b	302
C.78	^{13}C NMR (CDCl_3) of 230b	303
C.79	^1H NMR (CDCl_3) of 232	304
C.80	^{13}C NMR (CDCl_3) of 232	305
C.81	^1H NMR (CDCl_3) of 421	306
C.82	^{13}C NMR (CDCl_3) of 421	307
C.83	^1H NMR (CDCl_3) of 236	308
C.84	^{13}C NMR (CDCl_3) of 236	309
C.85	^1H NMR (CDCl_3) of 237	310
C.86	^{13}C NMR (CDCl_3) of 237	311
C.87	^1H NMR (CDCl_3) of 238	312
C.88	^{13}C NMR (CDCl_3) of 238	313
C.89	^1H NMR (CDCl_3) of 240	314
C.90	^{13}C NMR (CDCl_3) of 240	315
C.91	^1H NMR (CDCl_3) of 242	316
C.92	^{13}C NMR (CDCl_3) of 242	317
C.93	^1H NMR (CDCl_3) of 319	318
C.94	^{13}C NMR (CDCl_3) of 319	319

C.95	^1H NMR (CDCl_3) of 322	320
C.96	^{13}C NMR (CDCl_3) of 322	321
C.97	^1H NMR (CDCl_3) of 312	322
C.98	^{13}C NMR (CDCl_3) of 312	323
C.99	^1H NMR (CDCl_3) of 422	324
C.100	^{13}C NMR (CDCl_3) of 422	325
C.101	^1H NMR (CDCl_3) of 423	326
C.102	^{13}C NMR (CDCl_3) of 423	327
C.103	^1H NMR (CDCl_3) of 328	328
C.104	^{13}C NMR (CDCl_3) of 328	329
C.105	^1H NMR (CDCl_3) of 331	330
C.106	^{13}C NMR (CDCl_3) of 331	331
C.107	^1H NMR (CDCl_3) of 335	332
C.108	^{13}C NMR (CDCl_3) of 335	333
C.109	^1H NMR (CDCl_3) of 336	334
C.110	^{13}C NMR (CDCl_3) of 336	335
C.111	^1H NMR (CDCl_3) of 337	336
C.112	^{13}C NMR (CDCl_3) of 337	337
C.113	^1H NMR (CDCl_3) of 338	338
C.114	^{13}C NMR (CDCl_3) of 338	339
C.115	^1H NMR (CDCl_3) of 339	340
C.116	^{13}C NMR (CDCl_3) of 339	341
C.117	^1H NMR (CDCl_3) of 340	342
C.118	^{13}C NMR (CDCl_3) of 340	343
C.119	^1H NMR (CDCl_3) of 341	344
C.120	^{13}C NMR (CDCl_3) of 341	345
C.121	^1H NMR (CDCl_3) of 342	346
C.122	^{13}C NMR (CDCl_3) of 342	347
C.123	^1H NMR (CDCl_3) of 343	348
C.124	^{13}C NMR (CDCl_3) of 343	349
C.125	^1H NMR (CDCl_3) of 316	350
C.126	^{13}C NMR (CDCl_3) of 316	351
C.127	^1H NMR (CDCl_3) of 344	352
C.128	^{13}C NMR (CDCl_3) of 344	353
C.129	^1H NMR (CDCl_3) of 345	354
C.130	^{13}C NMR (CDCl_3) of 345	355

C.131 ^1H NMR (CDCl_3) of 424	356
C.132 ^{13}C NMR (CDCl_3) of 424	357
C.133 ^1H NMR (CDCl_3) of 347	358
C.134 ^{13}C NMR (CDCl_3) of 347	359
C.135 ^1H NMR (CDCl_3) of 350	360
C.136 ^{13}C NMR (CDCl_3) of 350	361
C.137 ^1H NMR (CDCl_3) of 351	362
C.138 ^{13}C NMR (CDCl_3) of 351	363
C.139 ^1H NMR (CDCl_3) of 346	364
C.140 ^{13}C NMR (CDCl_3) of 346	365
C.141 ^1H NMR (CDCl_3) of 352	366
C.142 ^{13}C NMR (CDCl_3) of 352	367
C.143 ^1H NMR (CDCl_3) of 355	368
C.144 ^{13}C NMR (CDCl_3) of 355	369
C.145 ^1H NMR (CDCl_3) of 353	370
C.146 ^{13}C NMR (CDCl_3) of 353	371
C.147 ^1H NMR (CDCl_3) of 359	372
C.148 ^{13}C NMR (CDCl_3) of 359	373
C.149 ^1H NMR (CDCl_3) of 360	374
C.150 ^{13}C NMR (MeOD) of 360	375
C.151 ^1H NMR (CDCl_3) of 361	376
C.152 ^{13}C NMR (CDCl_3) of 361	377
C.153 ^1H NMR (CDCl_3) of 361	378
C.154 ^{13}C NMR (CDCl_3) of 361	379
C.155 ^1H NMR (CDCl_3) of 356	380
C.156 ^{13}C NMR (CDCl_3) of 356	381
C.157 ^1H NMR (CDCl_3) of 427	382
C.158 ^{13}C NMR (CDCl_3) of 427	383
C.159 ^1H NMR (CDCl_3) of 357	384
C.160 ^{13}C NMR (CDCl_3) of 357	385
C.161 ^1H NMR (CDCl_3) of 376	386
C.162 ^{13}C NMR (CDCl_3) of 376	387
C.163 ^1H NMR (CDCl_3) of 374	388
C.164 ^{13}C NMR (CDCl_3) of 374	389
C.165 ^1H NMR (CDCl_3) of 380	390
C.166 ^{13}C NMR (CDCl_3) of 380	391

C.167 ^1H NMR (CDCl_3) of 381	392
C.168 ^{13}C NMR (CDCl_3) of 381	393
C.169 ^1H NMR (CDCl_3) of 385	394
C.170 ^{13}C NMR (CDCl_3) of 385	395
C.171 ^1H NMR (CDCl_3) of 386a	396
C.172 ^{13}C NMR (CDCl_3) of 386a	397
C.173 ^1H NMR (CDCl_3) of 386b	398
C.174 ^{13}C NMR (CDCl_3) of 386b	399
C.175 ^1H NMR (CDCl_3) of 391	400
C.176 ^{13}C NMR (CDCl_3) of 391	401
C.177 ^1H NMR (CDCl_3) of 392	402
C.178 ^{13}C NMR (CDCl_3) of 392	403
C.179 ^1H NMR (CDCl_3) of 431	404
C.180 ^{13}C NMR (CDCl_3) of 431	405
C.181 ^1H NMR (CDCl_3) of 394	406
C.182 ^{13}C NMR (CDCl_3) of 394	407
C.183 ^1H NMR (CDCl_3) of 394	408
C.184 ^{13}C NMR (CDCl_3) of 394	409
C.185 ^1H NMR (CDCl_3) of 394	410
C.186 ^{13}C NMR (CDCl_3) of 394	411
C.187 ^1H NMR (CDCl_3) of 398	412
C.188 ^{13}C NMR (CDCl_3) of 398	413
C.189 ^1H NMR (CDCl_3) of 399	414
C.190 ^{13}C NMR (CDCl_3) of 399	415
C.191 ^1H NMR (CDCl_3) of 432	416
C.192 ^{13}C NMR (CDCl_3) of 432	417
C.193 ^1H NMR (CDCl_3) of 433	418
C.194 ^{13}C NMR (CDCl_3) of 433	419
C.195 ^1H NMR (CDCl_3) of 402	420
C.196 ^{13}C NMR (CDCl_3) of 402	421
C.197 ^1H NMR (CDCl_3) of 404	422
C.198 ^{13}C NMR (CDCl_3) of 404	423
C.199 ^1H NMR (CDCl_3) of 405	424
C.200 ^{13}C NMR (CDCl_3) of 405	425
C.201 ^1H NMR (CDCl_3) of 406	426
C.202 ^{13}C NMR (CDCl_3) of 406	427

C.203 ^1H NMR (CDCl_3) of 408	428
C.204 ^{13}C NMR (CDCl_3) of 408	429
C.205 ^1H NMR (CDCl_3) of 409	430
C.206 ^{13}C NMR (CDCl_3) of 409	431
C.207 ^1H NMR (CDCl_3) of 410	432
C.208 ^{13}C NMR (CDCl_3) of 410	433

List of Schemes

1.1	Esterification of carboxylic acids with diazomethane.	1
1.2	Maruoka's enantioselective cycloaddition of diazoesters and enals.	2
1.3	Enantioselective Roskamp reaction of diazoesters.	2
1.4	Examples of utility of diazo compounds in metallocarbene mediated reactions.	3
1.5	Rearrangement–benzannulation reaction of α -diazo enones.	3
1.6	Regitz diazo-transfer reaction.	4
1.7	Diazo-transfer reaction using imidazolium-based reagents.	5
1.8	Detrifluoroacetylative diazo transfer reaction.	5
1.9	Preparation of diazoalkanes by rearrangement of 1,2,3-triazoles.	6
1.10	Preparation of diazo analogs of steroids via Forster reaction.	6
1.11	Formation of diazoesters from tosyl hydrazones.	6
1.12	Preparation of diazoalkanes by dehydrogenation of hydrazones.	7
1.13	Synthesis of diazoalkanes via the Bamford–Stevens reaction.	7
1.14	Arndt's synthesis of diazomethane from <i>N</i> -methyl- <i>N</i> -nitrosourea.	8
1.15	Cross-coupling of diazoesters.	8
1.16	Aziridination of <i>N</i> -Ph benzaldimines with ethyl diazoacetate.	9
1.17	Wulff's asymmetric aziridination.	11
1.18	Triflic acid-catalyzed aza-Darzens reaction.	12
1.19	Terada's phosphoric acid-catalyzed synthesis of α -diazoamines.	13
1.20	Maruoka's synthesis of α -diazoamine esters and phosphonates.	14
1.21	Phosphoric acid-catalyzed <i>cis</i> -aziridination of glyoxal-derived aldimines.	14
1.22	<i>trans</i> -Selective asymmetric aziridination.	15
1.23	Improved asymmetric <i>trans</i> -aziridination of benzaldimines.	16
1.24	Substrate controlled synthesis of trisubstituted aziridines.	16
1.25	Brønsted acid-catalyzed asymmetric synthesis of trisubstituted aziridines.	17
1.26	Stereochemical outcome of Brønsted acid-promoted fragmentation of chiral <i>trans</i> -triazolines to <i>cis</i> -aziridines.	19
1.27	Fate of α -diazonium intermediate.	20
1.28	Brønsted acid-promoted formal aminohydroxylation of α,β -unsaturated imides.	21
1.29	Brønsted acid-promoted conversion of α -diazoamine 76	24
1.30	Control experiment testing <i>syn-anti</i> interconversion.	25
1.31	Unexpected diastereoselectivity in diazo imide–imine reaction.	26

1.32	Diazo imide–imine control reactions.	27
1.33	Acid-promoted diastereospecific aziridine opening.	27
1.34	Cross-over experiment testing aziridine intermediacy diazo imide–imine reaction.	28
2.1	Synthesis of Taxol side chain via Sharpless asymmetric aminohydroxylation.	34
2.2	Donohoe’s intramolecular asymmetric aminohydroxylation.	35
2.3	Aminoacetoxylation approach to <i>vic</i> -aminoalcohol derivatives.	35
2.4	Yoon’s radical aminohydroxylation using oxaziridines.	36
2.5	Brønsted acid-promoted formal aminohydroxylation of α,β -unsaturated imides.	36
2.6	Metal free, acid promoted intramolecular oxyamination.	37
2.7	Kobayashi’s asymmetric glycolate Mannich reaction with silyl ketene acetal nucleophiles.	38
2.8	Proline catalyzed direct Mannich reaction of α -hydroxy ketones.	38
2.9	Enantioselective Lewis acid catalyzed glycolate Mannich reactions.	39
2.10	Hoveyda’s silver-catalyzed vinylogous Mannich reaction of siloxyfurans.	40
2.11	Small scale preparation of α -diazo imide 69	40
2.12	Alkyl transfer side reaction of α -diazo imide addition to imines.	41
2.13	Large scale preparation of α -diazo imide 119	42
2.14	Preparative procedure for the synthesis of the 139	46
2.15	Hydrogenation of the benzhydryl group.	48
2.16	Preliminary result of oxazolidine dione hydrolysis	48
2.17	Opening of oxazolidine dione ring using alcohol solution of ammonia.	50
2.18	Opening of the oxazolidine dione using more reactive nucleophiles.	50
2.19	Opening of oxazolidine dione with ethyl thiolate.	51
2.20	Opening of oxazolidine dione with lithium acetylide.	51
2.21	Opening of the oxazolidine dione 80 and structural assignment of the methanolysis product.	53
2.22	Glycolate Mannich reaction promoted by chiral Brønsted acid.	55
2.23	Chiral Brønsted acid screen	56
2.24	Evaluation of chiral borate complexes in <i>syn</i> -glycolate reaction.	59
2.25	Evaluation of chiral borate complexes in the <i>syn</i> -glycolate reaction with glyoxal imines.	60
2.26	Evaluation of indium(III)–BINOL complexes in the <i>syn</i> -glycolate reaction.	60
2.27	Preliminary results of Cu(II)–bis(oxazoline) catalyzed glycolate Mannich reaction of benzhydryl imines.	62

2.28	Preliminary results of Cu(II)–bis(oxazoline) catalyzed glycolate Mannich reaction of <i>N</i> -Boc benzaldimines.	62
2.29	Preparation of bis(oxazoline) complexes with different counterions.	64
2.30	Synthesis of bis(oxazoline) 166	68
2.31	Synthesis of bis(oxazoline) 172	68
2.32	Synthesis of bis(oxazoline) 173	69
2.33	Synthesis of the 1-naphthyl substituted aminoalcohol.	69
2.34	Synthesis of 1-naphthyl substituted bis(oxazolines).	70
2.35	Survey of various bis(oxazoline) ligands in the copper(II) catalyzed glycolate Mannich reaction.	71
2.36	Lewis acid activation of imines using copper(I) complexes.	73
2.37	Copper(I) aziridination of imines using α -diazo imide.	74
2.38	Lewis acid activation of imines using copper(I) complexes.	76
2.39	Copper(I) promoted α -diazo imide dimerization.	76
2.40	Copper(I) promoted α -diazo imide dimerization.	77
2.41	Reactivity of <i>N</i> -Boc imines and α -diazo imide in presence of copper(I) catalysts.	77
2.42	Result of slow addition of α -diazo imide to <i>N</i> -Boc imines in the presence of copper(I) catalyst.	78
2.43	Evaluation of chiral copper(I) complexes	81
2.44	Control reaction of ethyl diazoacetate with <i>N</i> -Boc imines in the presence of copper(I) catalyst.	82
2.45	Glycolate Mannich reaction with bulky sulfonyl alkyl imines.	84
2.46	Postulated mechanism of formation of <i>N</i> -Ts glycolate Mannich products.	84
2.47	The outcome of the reaction of α -diazo imide with <i>N</i> -TMS imine.	85
2.48	Reaction of α -diazo imide with <i>N</i> -TMS imine in the presence of a proton source.	88
2.49	Attempted cyclopropanation with the α -diazo imide.	88
2.50	Control experiment for the formation of an azomethine ylide.	89
3.1	Synthesis of the initially proposed stereoisomer of zwittermicin A.	91
3.2	Synthesis of zwittermicin A enantiomer	92
3.3	Formal Total Synthesis of (+)-Zwittermicin A	93
3.4	Two-directional synthesis of the intermediate in a total synthesis of hemibrevetoxin B.	97
3.5	Two-directional synthesis of merrilactone A.	97
3.6	Assembly of an intermediate for a formal synthesis of anatoxin-a.	98
3.7	Enzymatic desymmetrization–resolution of <i>meso</i> -epoxides.	98

3.8	Enzymatic desymmetrization en route to (+)-crocacin C.	99
3.9	Synthesis of the <i>pseudo-C</i> ₂ -symmetric bisacetal en route to dermostatin A. . .	100
3.10	Retrosynthetic analysis	101
3.11	Substrate-controlled diastereoselectivity in [3+2] cycloaddition	102
3.12	Diastereoselectivity in acid-promoted reaction	102
3.13	Preparation of the di(<i>tert</i> -butyl)silyl bis(imide).	103
3.14	Attempted Two-Directional Triflic Acid-Catalyzed [3+2] Reaction	104
3.15	Thermal Two-Directional [3+2] Reaction	104
3.16	Horner–Wadsworth–Emmons reaction with <i>tert</i> -butyl imidophosphonate. . .	105
3.17	Synthesis of the imidophosphonate.	106
3.18	Improved synthesis of the bis(imide) 312	107
3.19	Unsuccessful synthesis of acyclic silyl ether aldehydes.	108
3.20	Preliminary synthesis of the TIPDS bis(imide).	108
3.21	Removal of the <i>N</i> -Boc group during Brønsted acid-promoted reaction with benzyl azide.	110
3.22	Synthesis of the isopropyl bis(imide).	110
3.23	Confirmation of the relative stereochemistry of TIPDS bis(oxazolidine dione). .	113
3.24	Synthesis of the <i>N</i> -Ph substituted bis(triazoline).	115
3.25	Lewis acid-promoted opening of the bis(oxazolidine dione) 347	116
3.26	Base promoted cyclization to bis(oxazolidinone).	119
3.27	Mechanism of the base-promoted isomerization of 347	120
3.28	A strategy for desymmetrization and removal of C16 carbon.	121
3.29	Preparation of bis(carboxylic acid) 361	121
3.30	Desymmetrization of alcohol 357	122
3.31	Synthesis of albizziine-derived isonitrile	124
3.32	Synthesis of albizziine amide-derived isonitrile	125
3.33	Synthesis of albizziine methyl ester-derived isonitrile	125
3.34	Synthesis of albizziine methyl ester-derived isonitrile	126
3.35	Synthesis of DAP methyl ester-derived isonitrile	127
3.36	Synthesis of the first generation Passerini adduct.	127
3.37	Functionalization of the Passerini adduct: transformation of a methyl ester to primary amide.	128
3.38	Removal of the Boc and trityl groups.	129
3.39	Global hydrolysis of the Passerini adduct.	130
3.40	Undesired opening–cyclization of <i>N</i> -Boc bis(oxazolidinone).	130
3.41	Successful hydrolysis of <i>N</i> -Ts derivative 395	131

3.42 Radical decarbonylation of the bis(selenoester) 397	132
3.43 Fischer esterification of the bis(carboxylic acid).	133
3.44 Preparation and decarbonylation of the selenoester 402	135
3.45 Elaboration of the monoester 403	135
3.46 One-pot oxidation and Passerini coupling.	137
3.47 End-game strategy for the synthesis of zwittermicin A.	140

List of Tables

1.1	Fragmentation of triazoline 73	24
1.2	Scope of the <i>syn</i> -glycolate Mannich reaction. ^a	30
2.1	<i>syn</i> -Glycolate Mannich reaction: Brønsted acid survey. ^a	44
2.2	Screen of <i>N</i> -protecting group on the imine substrate. ^a	45
2.3	Synthesis of α -keto imines	46
2.4	Scope of the <i>syn</i> -glycolate Mannich reaction. ^a	47
2.5	Opening of oxazolidine dione using alcohol nucleophiles.	49
2.6	Lewis acid-assisted opening of oxazolidine dione ring.	52
2.7	Evaluation of Lewis acid catalysts in the <i>syn</i> -glycolate Mannich reaction. ^a .	57
2.8	Evaluation of Lewis acid catalysts in the <i>syn</i> -glycolate Mannich reaction. ^a .	58
2.9	Correlation between enantioselection and the counter-ion for copper. ^a	64
2.10	Temperature profile of the reaction catalyzed by copper(II)–bis(oxazoline) 166 complex. ^a	65
2.11	Copper–bis(oxazoline) catalyzed glycolate Mannich reaction: solvent screen. ^a	66
2.12	Correlation between enantioselection reaction termination protocol. ^a	67
2.13	Substrate scope of the enantioselective glycolate Mannich. ^a	72
2.14	Optimization of the copper(I) catalyzed reaction of α -diazo imide with <i>N</i> - DPM imines. ^a	75
2.15	Correlation between reaction termination protocol and product outcome. ^a . .	80
2.16	Correlation between enantioselection and counterion	81
2.17	Solvent and quench-dependent product distribution in α -diazo imide addition to silyl imines. ^a	86
3.1	Substrate-Controlled Double (3+2) Cycloaddition	111
3.2	Functionalization of the bis(oxazolidine dione) 345	114
3.3	Optimization of fragmentation of the bis(triazoline) to bis(oxazolidine dione). .	116
3.4	Optimization of the reduction of bis(ester).	122
3.5	Survey of oxidation conditions for the synthesis of aldehyde 364	123
3.6	Synthesis of the symmetric phenylselenoester.	132
3.7	Selective monoesterification promoted by DOWEX ion-exchange resin. ^a . . .	134
3.8	Survey of oxidation conditions for the synthesis of the aldehyde 408	136

List of Abbreviations

<i>i</i> Pr	isopropyl
<i>n</i> Pr	<i>n</i> -propyl
18-crown-6	1,4,7,10,13,16-hexaoxacyclooctadecane
<i>n</i> Bu	<i>n</i> -butyl
<i>s</i> Bu	<i>sec</i> -butyl
<i>t</i> Bu	<i>tert</i> -butyl
Ac ₂ O	acetic anhydride
BF ₃ · OEt ₂	boron trifluoride diethyletherate
Et ₂ O	diethyl ether
Ph ₂ CO ₂ H	benzoic acid
PPh ₃	triphenylphosphine
Tf ₂ O	trifluoromethanesulfonyl anhydride
Ac	acetyl
AcO	acetate
AIBN	azobis(isobutyronitrile)
Aq	aqueous
Ar	aryl
BINAP	2,2'-bis(diphenylphosphino)-1,1'-binaphthyl
Bn	benzyl
Boc	<i>tert</i> -butyloxycarbonyl
Bz	benzoyl
cat.	catalytic
Cbz	carbobenzyloxy
CSA	camphorsulphonic acid
d	doublet
DBU	1,8-Diazabicyclo[5.4.0]undec-7-ene
DCC	dicyclohexyl carbodiimide
DCE	1,2-dichloroethane
DCM	dichloromethane
dd	doublet of doublets
ddd	doublet of doublets of doublets
DIBAL	diisobutylaluminum hydride
DIPEA	diisopropylethylamine

DIPS	diisopropylsilyl
DMAP	4-dimethylaminopyridine
DMDO	2,2-dimethyldioxirane
DMF	dimethylformamide
DMI	dimethylimidazole
DMP	Dess–Martin periodinane
DMS	dimethylsulphide
DMSO	dimethyl sulfoxide
DPM	benzhydryl, diphenylmethyl
dq	doublet of quartets
dr	diastereomeric ratio
dt	doublet of triplets
DTBS	di(<i>tert</i> -butyl)silyl
EDA	ethyl diazoacetate
EDC	1-ethyl-3-(3-dimethylaminopropyl)carbodiimide
EDCI	1-ethyl-3-(3-dimethylaminopropyl)carbodiimide hydrochloride
EDTA	ethylenediaminetetraacetic acid
ee	enantiomeric excess
equiv	equivalents
Et	ethyl
HMDS	hexamethyldisilazide
HOBT	hydroxybenzotriazole
Im	imidazole
IPA	isopropyl alcohol
KHMDS	potassium bis(trimethylsilyl)amide
LA	Lewis acid
LAH	lithium aluminum hydride
LC/MS	liquid chromatography/ mass spectrometry
LDA	lithium diisopropylamide
LHMDS	lithium hexamethyldisilazide
mCPBA	<i>meta</i> -chloroperoxybenzoic acid
Me	methyl
MOM	methoxymethyl
MS	molecular sieves
Ms	methanesulphonyl
NMO	<i>N</i> -methyldmorpholine- <i>N</i> -oxide

p-ABSA	<i>p</i> -acetamididosulfonyl azide
PCC	pyridinium chlorochromate
PG	protecting group
Ph	phenyl
PMB	<i>p</i> -methoxybenzyl
PPTS	pyridinium <i>p</i> -toluenesulfonate
Pr	propyl
PTSA	<i>p</i> -toluenesulphonic acid
py	pyridine
rt	room temperature
t	triplet
TBAF	tetra- <i>n</i> -butylammonium fluoride
TBDMS	<i>tert</i> -butyldimethylsilyl
TBDPS	<i>tert</i> -butyldiphenylsilyl
TBHP	<i>tert</i> -butylhydroperoxide
TBS	<i>tert</i> -butyldimethylsilyl
TEA	triethylamine
TFA	trifluoroacetic acid
TFAA	trifluoroacetic anhydride
TFEA	2,2,2-trifluoroethyl trifluoroacetate
TfO	trifluoromethanesulfonate, triflate
TfOH	trifluoromethanesulfonic acid, triflic acid
THF	tetrahydrofuran
TIPDS	tetraisopropoxydisiloxane
TIPS	triisopropylsilyl
TMS	trimethylsilyl
TPAP	tetra- <i>n</i> -propylammonium perruthenate
Tr	trityl, triphenylmethyl
Ts	<i>p</i> -toluenesulphonyl, tosyl
TsOH	4-toluenesulphonic acid

I have not failed, I've just found ten thousand ways that won't work.
—*Thomas Edison*

CHAPTER 1

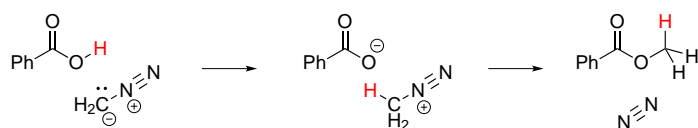
Mechanism of the Brønsted acid-catalyzed aza-Darzens reaction. Influence of diazoalkane structure on the stereoselectivity of carbon–carbon bond formation.

1.1 Introduction to diazoalkanes

1.1.1 Diazoalkanes in organic synthesis

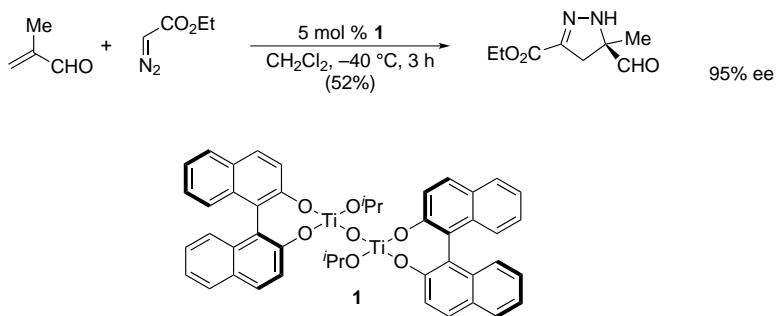
Nearly 130 years since their discovery, diazo compounds continue to attract the attention of organic chemists and new reactions utilizing diazoalkanes are still reported frequently. What started with diazotization of ethyl glycinate to form ethyl diazoacetate,¹ developed into a branch of organic chemistry with an array of useful reagents and indispensable chemical transformations. Probably one of the most widely recognized reactions of the simplest diazoalkane reagent, diazomethane, is a reaction with carboxylic acids to form esters (Scheme 1.1). Because of its simplicity and high efficiency, this reaction was quickly adopted in the field of natural product discovery and lipid chemistry where treatment of extracts with diazomethane became a standard protocol for conversion of carboxylic acids to more soluble esters.

Scheme 1.1. Esterification of carboxylic acids with diazomethane.



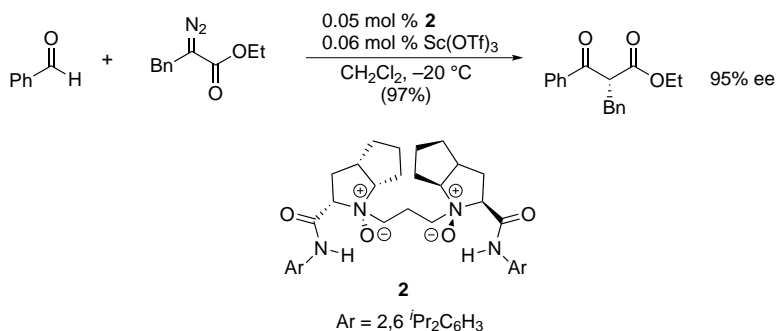
A very interesting aspect of the chemistry of diazoalkanes is the fact that their reactivity can be considered in two separate contexts. On one hand the diazo group natively possesses substantial reactivity both on carbon and nitrogen atoms. When left intact, diazoalkanes participate in 1,3-dipolar cycloaddition reactions with π -bonds of alkenes and alkynes. Maruoka and co-workers demonstrated that titanium(IV) catalyst **1** promotes a reaction between α -substituted acroleins and ethyl diazoacetate to give chiral 2-pyrazolines containing a quaternary stereogenic center in good yield and high enantioselection (Scheme 1.2).²

Scheme 1.2. Maruoka's enantioselective cycloaddition of diazoesters and enals.



When a sufficiently activated electrophile such as aldehyde or imine (see also section 1.2) is used, one can take advantage of the nucleophilicity of the diazo carbon to perform selective addition reactions. In 2010 Feng and co-workers reported the highly enantioselective addition of α -alkyl- α -diazoesters to aromatic aldehydes (the Roskamp reaction) in the presence of scandium(III)- N,N' -dioxide ligand **2**. With just 0.05 mol % of the catalyst α -alkyl- β -ketoesters form in very high yield and enantioselectivity (Scheme 1.3).³

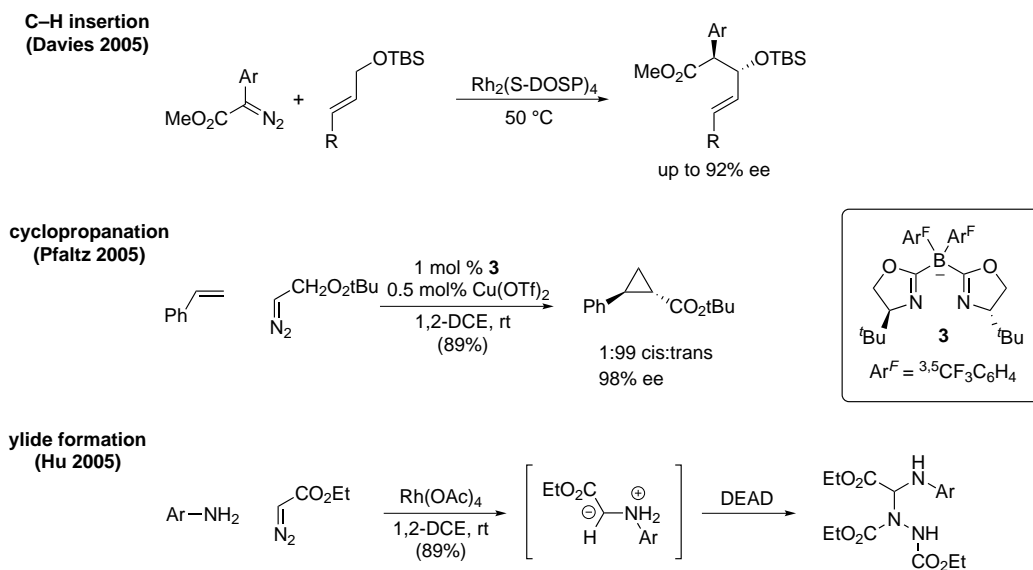
Scheme 1.3. Enantioselective Roskamp reaction of diazoesters.



In addition to non-redox reactions, transition metal catalysts and diazoalkanes react readily to give Fischer-type carbenes which are employed in a variety of stereoselective reactions. Functionalization of X-H bonds ($X = \text{C}, \text{O}, \text{S}, \text{N}$) is now a mature field of organic synthesis in which many efficient and selective transformations have been developed.^{4,5} Application of donor-acceptor rhodium carbenes in stereoselective C-H functionalization reactions has been extensively studied by Davies and co-workers.⁶ For example allylic silyl ethers will undergo asymmetric C-H insertion reaction to give products in up to 92% ee (Scheme 1.4).⁷ Electrophilic carbenes can also be attacked by nucleophilic amines to form azomethine ylides. Hu and co-workers reported a three component reaction between ethyl diazoacetate, anilines and azodicarboxylates catalyzed by $\text{Rh}_2(\text{OAc})_4$ to give aminal products in good yield with

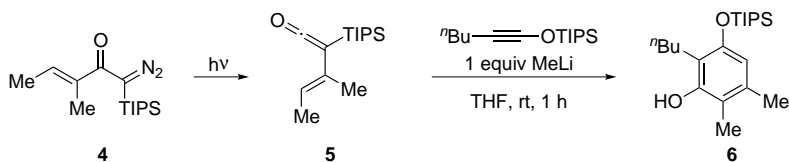
no N–H insertion products.⁸ Diazoalkanes are often utilized as methylene transfer agents to alkenes. Highly enantioselective cyclopropanation reactions were developed over the last few decades (Scheme 1.4).^{9,10}

Scheme 1.4. Examples of utility of diazo compounds in metalcarbene mediated reactions.



More elaborate diazo compounds will undergo rearrangement reactions to form more reactive intermediates such as ketenes. The Danheiser group demonstrated a new benzannulation strategy based on the photochemical decomposition–rearrangement of diazo **4** to 3-(oxido)dienylketene **5**. Compound **5** reacts with electron-rich alkynes in a 6 π electrocyclic reaction to give highly substituted benzene rings **6** (Scheme 1.5).¹¹

Scheme 1.5. Rearrangement–benzannulation reaction of α -diazo enones.



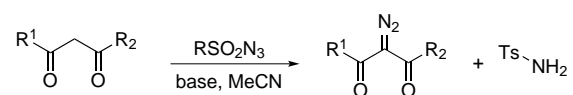
1.1.2 Synthetic approaches to diazoalkanes

Due to more than a century of research exploring the reactivity of diazoalkanes, numerous methods have been developed for their preparation. More general methods for the synthesis of whole classes of diazo compounds exist next to more specific approaches towards individual examples of diazoalkanes.^{12–15} The available synthetic routes can be divided into four groups:

- transfer of the dinitrogen functionality
- manipulations of functional groups containing one nitrogen atom
- manipulations of functional groups containing two nitrogen atoms
- substitution of an existing diazo compound

One of the best methods for preparing diazo compounds consists of the direct introduction of both nitrogen atoms in a single reaction step. The entire azo group is transferred by a donor, generally an azide, to an acceptor (C–H acidic compound), a process that is often referred to as the Regitz diazo transfer (Scheme 1.6).¹⁶ Diazo transfer to 1,3-dicarbonyl compounds usually works efficiently due to high proton activation by the carbonyl groups in the presence of weak base, to give 2-diazo-1,3-dicarbonyl compounds in yields usually over 80%.^{17–19} The diazo transfer reaction produces a stoichiometric amount of a sulfonamide which must be separated from the desired diazo compound, a challenging procedure in certain cases.

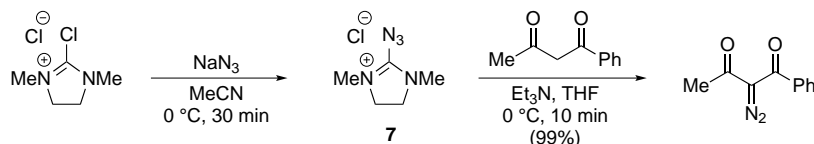
Scheme 1.6. Regitz diazo-transfer reaction.



4-Toluenesulfonyl azide is the standard reagent used, but because of safety problems resulting from its potentially explosive nature, and because of the difficulty of product separation, several alternative reagents have been developed. *N*-Dodecylbenzenesulfonyl azide²⁰ has been reported to be very effective for the preparation of crystalline diazo compounds, while *p*-acetamidobenzenesulfonyl azide²¹ offers the advantages of low cost, safety, and ease of removal of the sulfonamide by-product through a simple trituration–filtration. The latter significantly broadened the scope of the diazo transfer reaction. A different approach to the problem of azide safety and removal of by-product was addressed by Kitamura and co-workers.²² They developed a reagent based on imidazolium salts that undergo an efficient

diazo-transfer reaction with diketones under mild conditions. The ionic character of the 2-azido-1,3-dimethylimidazolium salt **7** allows for easy and efficient removal of by-products by a simple water wash. Additionally, differential scanning calorimetry (DSC) experiment showed exothermic decomposition at around 200 °C which suggests that **7** could be used at higher temperatures with a sufficiently large safety margin.

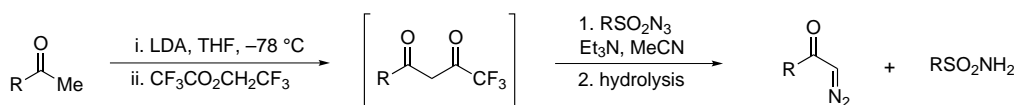
Scheme 1.7. Diazo-transfer reaction using imidazolium-based reagents.



If the carbon acid is activated by only one electron-withdrawing group (e.g. methyl ketones) diazo transfer can be problematic. This challenge can be addressed by introduction of a second electron-withdrawing group, which can be easily removed after the diazo transfer process. Early examples utilized formylation under Claisen conditions followed by treatment with sulfonyl azide. It was used sporadically and only for simple ketones because of lack of regioselectivity in thermodynamically controlled Claisen formylation.

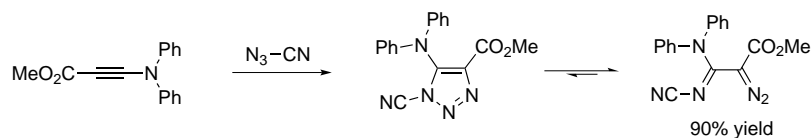
Currently, diazo transfer to less reactive substrates is carried out with the assistance of a trifluoroacetyl group. First reported by Doyle²³ and popularized by Danheiser,²⁴ it is a powerful alternative to the use of a formyl group. This method has proved particularly valuable in the preparation of diazo derivatives of enones. First, the substrate is converted to an α -trifluoroacetyl derivative by reaction of the enolate with 2,2,2-trifluoroethyl trifluoroacetate. The intermediate is not isolated but subjected to a diazo transfer reaction with an azide of choice and the trifluoroacetyl group is hydrolyzed during work-up to give the diazo compound in good yield (Scheme 1.8).

Scheme 1.8. Detrifuoroacetylativ diazo transfer reaction.



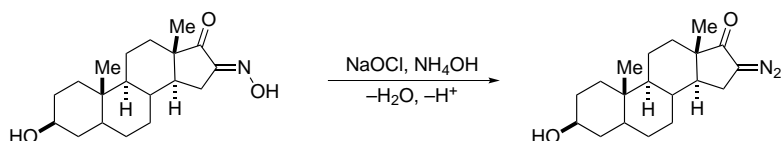
A conceptually different diazo transfer from azides can be realized via rearrangement reactions of 1,2,3-triazoles. This method is based on functionalization of ynamines or ynyl ethers. Cycloaddition with azide bearing an electron-withdrawing group affords a 1,2,3-triazole which is in equilibrium with the α -imino diazoalkane which can be isolated (Scheme 1.9).²⁵

Scheme 1.9. Preparation of diazoalkanes by rearrangement of 1,2,3-triazoles.



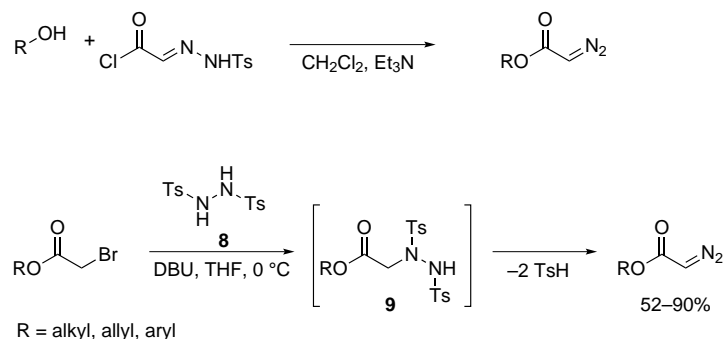
A second group of reactions producing diazo compounds are modifications of nitrogen-containing functional groups such as oximes, hydrazones and ureas. Conversion of oximes to diazoalkanes can be achieved through the Forster reaction in which oximes react with chloramines with concomitant dehydration. This method was often practiced in the synthesis of diazo analogs of steroids (Scheme 1.10).²⁶

Scheme 1.10. Preparation of diazo analogs of steroids via Forster reaction.



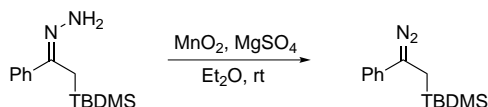
Hydrazones, mostly tosylhydrazones, are often utilized masked diazo groups. Under strongly basic conditions, the sulfinate fragment is eliminated to give the diazo functionality. Using this approach, diazoesters can be prepared in a reaction of tosylhydrazone of glyoxylic acid chloride with alcohols under basic conditions. Alcohol acylation is followed by elimination to give the diazoester.^{27,28} More recently, Fukuyama and co-workers introduced disulfonylhydrazine **8** as a precursor to the diazo group. Diazoacetates are prepared from α -bromo esters after elimination of two molecules of sulfinate from the intermediate **9** (Scheme 1.11).²⁹

Scheme 1.11. Formation of diazoesters from tosyl hydrazones.



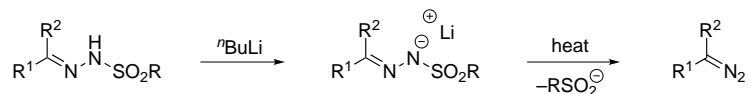
Electron rich diazoalkanes can be prepared by dehydrogenation of hydrazones, one of the oldest methods for the synthesis of diazo compounds. Mercury(II) oxide has been used for a long time as an oxidant for this transformation but since the mid-20th century numerous alternatives, such as silver oxide or manganese(IV) oxide, have been developed (Scheme 1.12).³⁰

Scheme 1.12. Preparation of diazoalkanes by dehydrogenation of hydrazones.



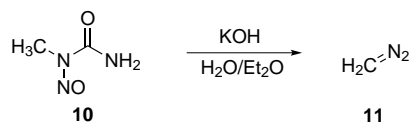
The Bamford–Stevens reaction is an alternative to dehydrogenation of hydrazones. Although this reaction is used mostly for the synthesis of alkenes, intermediate diazo compounds can be isolated. In a typical procedure an *N*-sulfonylhydrazone of the carbonyl compound is converted to the lithium salt followed by elimination (Scheme 1.13). Generation of diazo compounds under mild conditions is also possible. Elimination of the suspension of a tosylhydrazone salt in the presence of a phase-transfer catalyst was utilized by Aggarwal for the in situ generation of the desired diazoalkanes.^{31–35}

Scheme 1.13. Synthesis of diazoalkanes via the Bamford–Stevens reaction.



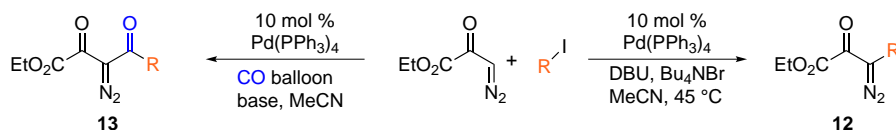
Diazomethane (**11**) is a gas at room temperature and is usually generated from precursors such as *N*-methyl-*N*-nitrosourea (**10**). Treatment with base in a biphasic system (aq KOH–diethyl ether) at room temperature affords an ethereal solution of diazomethane (Scheme 1.14).³⁶ The potentially explosive nature of diazomethane didn't prevent it from use in large industrial processes, such as the synthesis of the key intermediate to prepare the HIV protease inhibitor nelfinavir.³⁷ In a continuous process, diazomethane is generated from *N*-methyl-*N*-nitroso-*p*-toluenesulfonamide with a production rate of 50–60 tons per year but less than 80 g of diazomethane is present in the production unit.

Scheme 1.14. Arndt's synthesis of diazomethane from *N*-methyl-*N*-nitrosourea.



More elaborate diazo compounds are prepared by substitution at the diazo carbon. Probably the most common reaction of this type is acylation of diazomethane with acid chlorides. Recently, Wang and co-workers demonstrated a transition metal-catalyzed C–C coupling using diazo compounds. Palladium catalyzed cross-coupling of ethyl diazo acetate with various aryl or vinyl iodides gives coupled product **12** in good yield. When carbon monoxide is added, 2-diazo-3-oxocarboxylates **13** are the major products in good yield (Scheme 1.15).⁸

Scheme 1.15. Cross-coupling of diazoesters.



1.2 Stereoselective reactions involving α -aminodiazonium intermediates

1.2.1 Metal catalyzed reactions

α -Aminodiazonium intermediates are commonly suggested in aziridination reactions. Cyclization of the amine onto neighboring diazonium carbon with concomitant removal of N_2 , yields the heterocycle. Aziridines, the smallest heterocycles with one nitrogen atom have been a subject of intensive research^{38,39} since 1888, when Gabrel synthesized the aziridine (**14**, $\text{R}^1, \text{R}^2, \text{R}^3 = \text{H}$).⁴⁰ From the synthetic standpoint, aziridine can be prepared in one of four ways (Figure 1.1):

- functionalization of the C–C π bond with a nitrene
- functionalization of the C–N π bond with a carbene
- addition–cyclization sequence
- substitution

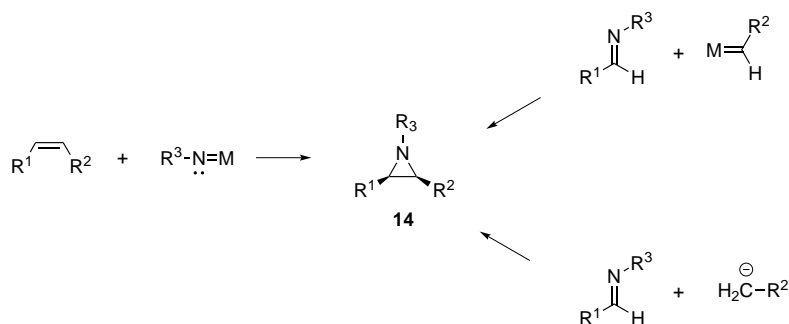
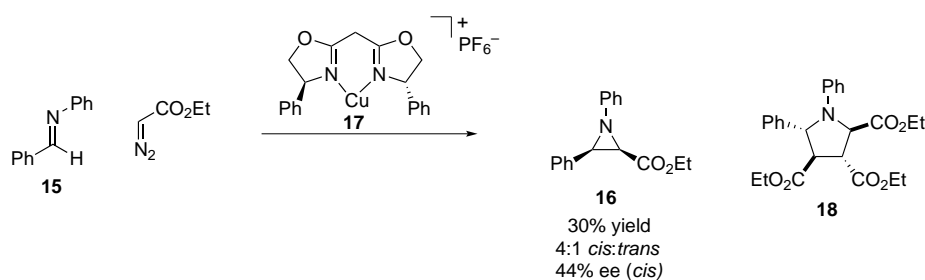


Figure 1.1. Approaches to aziridines by addition to double bonds.

Delivery of the nitrogen as a nitrene equivalent to a carbon–carbon double bond is a well developed branch of stereoselective synthesis that has been reviewed recently.^{41,42} Approach to aziridines that use carbene equivalents in addition to azomethines, are more relevant to this chapter and will be discussed in detail.

Early studies in a carbene delivery to imines met with limited success^{43–45} until 1995 when Rasmussen and Jørgensen reported aziridination of *N*-Ph imines, such as **15** with ethyl diazoacetate in the presence of 10 mol % of Cu(OTf)₂ (95 % yield, 6:1 *cis:trans*).⁴⁶ When copper(II)–bis(oxazoline) complexes were used, a fair enantioselection for **16** was observed but the yield suffered significantly. Simultaneously, Jacobsen and co-workers reported that in the presence of CuPF₆–bis(oxazoline) complex **17** such aziridination can also be achieved with modest enantioselectivity, up to 44 % ee, but still in poor yield (Scheme 1.16).⁴⁷

Scheme 1.16. Aziridination of *N*-Ph benzaldimines with ethyl diazoacetate.



Small amounts of pyrrolidine **18** were observed which suggested the presence of azomethine ylide **20**. Metal carbenoid **19** reacts with benzaldimine **15** to give **20**. Cycloaddition to diethyl fumarate **21**, the diazo homocoupling product, yields pyrrolidine **18**. Low enantioselection was attributed to a low degree of association between the chiral catalyst and the ylide. Dissociation of the ylide from the catalyst allows for the formation of racemic aziridine **22** and pyrrolidine **18** (Figure 1.2).

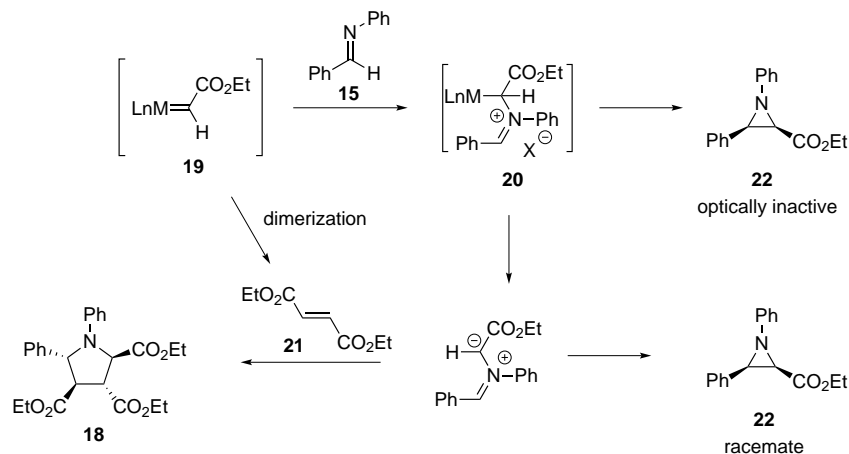


Figure 1.2. Proposed mechanism of metallocarbene addition to azomethine

Later reports of metal catalyzed additions of ethyl diazoacetate to imines started to suggest an alternative available pathway that takes advantage of diazo nucleophilicity. First Bartnik and Mloston,^{44,45} then Brookhart and Templeton,⁴⁸ and later Jørgensen⁴⁹ showed that various Lewis acids are able to promote the reaction to deliver predominantly *cis*-aziridine **23** in good to excellent yield (Figure 1.3). In contrast to Cu and Rh catalyzed reactions characteristic by-products—fumarate, maleate and pyrrolidine—were not observed. This time enamines of type **25** and **26** were present as side products and became the evidence to support addition–cyclization mechanism. According to this mechanism, the Lewis acid binds to the imine nitrogen and activates it towards diazo nucleophile. The putative intermediate **24** that forms upon addition can close in S_Ni fashion to form aziridine or undergo rearrangement to arrive at vinylogous amides **25** and **26** (Figure 1.3, path **a** and **b**). Control experiments that attempt to trap a possible azomethine ylide intermediate didn't show any evidence of pyrrolidine **18**.

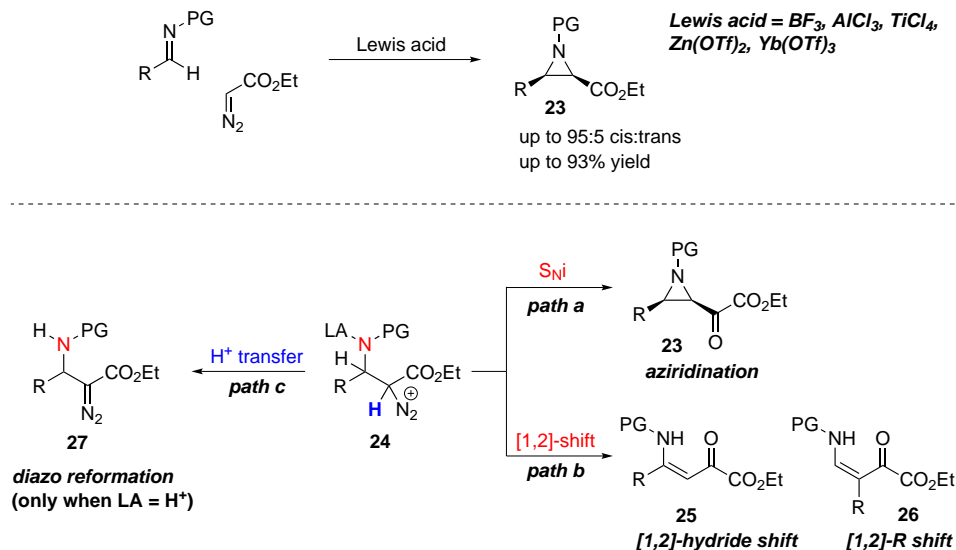
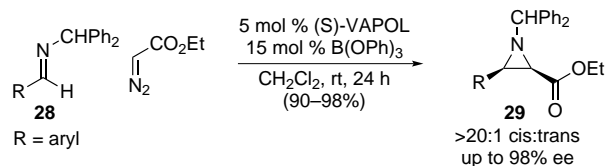


Figure 1.3. Lewis acid-catalyzed aziridination with diazo compounds.

Despite extensive studies of the active catalyst,^{50,51} chiral complexes of Lewis acids with various ligands didn't deliver products in highly enantioenriched form,⁵² until the breakthrough contribution by Antilla and Wulff^{53,54} who developed a chiral boron-VAPOL complexes that were able to activate benzhydryl imines **28** towards the nucleophilic addition to provide *cis*-aziridines **29** almost exclusively with enantioselectivities in 90–98 % ee range (Scheme 1.17). Small amounts of secondary products of type **25** and **26** were also observed. Over the years this methodology became a standard protocol for asymmetric aziridine synthesis and its utility has been demonstrated in the synthesis of biologically active molecules.^{55–57}

Scheme 1.17. Wulff's asymmetric aziridination.



Over course of several years, the active catalyst preparation protocol has been empirically optimized but the nature of the actual catalyst species was not well understood. In the initially proposed model, catalyst activity was attributed to a single boron atom in a chiral environment. However, investigation of the active catalyst by boron nuclear magnetic resonance suggested that the active catalyst is the pyroborate **30**.⁵⁶ Further NMR and

X-ray studies revealed that the catalytic system acts as a chiral Brønsted acid where a protonated imine is surrounded by a singular boroxinate counterion **31** (Figure 1.4).⁵⁸ This result provided an additional explanation for the empirically established optimal ratio of VAPOL ligand to B(OPh)₃ (1:3).

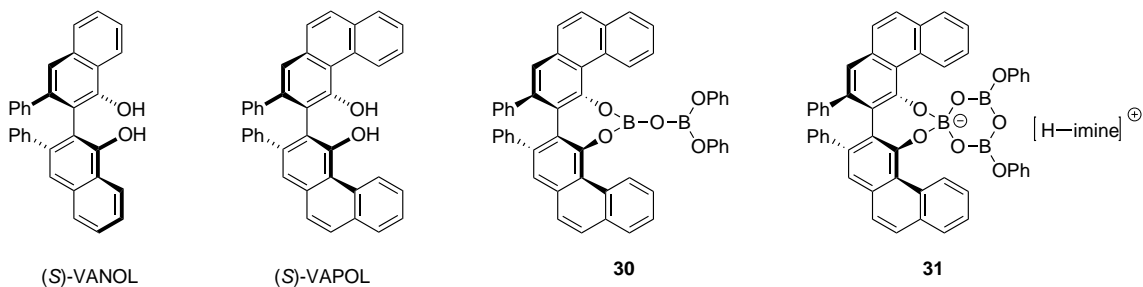
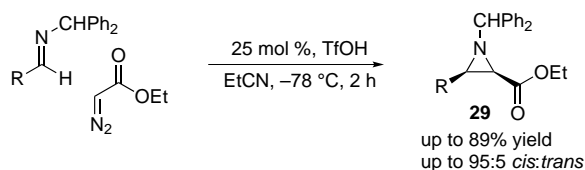


Figure 1.4. Boron catalysts for asymmetric aziridination

1.2.2 Brønsted acid catalyzed reactions

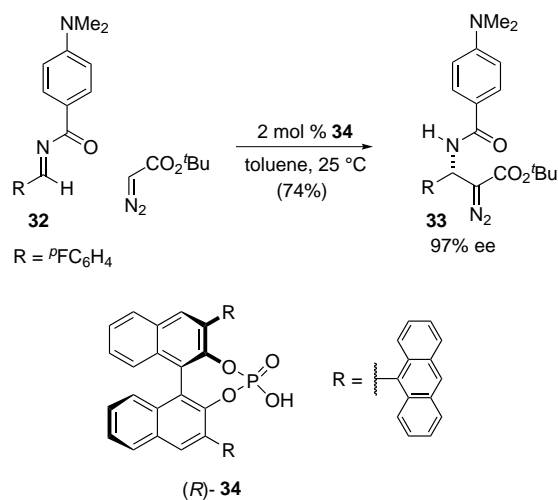
Historically, diazoalkanes were considered incompatible with Brønsted acid catalysis because protonation of the diazo carbon would be the dominant reaction pathway, a non-existent process in reactions catalyzed by aprotic Lewis acids or metal catalysts. This paradigm changed when Williams and Johnston reported that in the presence of a competitive Lewis base (azomethine nitrogen), diazo decomposition by protonation is slow even in the presence of very strong Brønsted acid (triflic acid). The presumed iminium triflate ion pair is exceptionally reactive towards ethyl diazoacetate; the reaction proceeds smoothly at $-78\text{ }^{\circ}\text{C}$ to give *cis*-aziridines **29** in high diastereoselection with good catalyst turnover (Scheme 1.18).⁵⁹ Since that work was published, Brønsted acid activation of azomethines towards diazoalkanes has developed into a dynamic area of research with a range of useful carbon-carbon bond forming reactions.

Scheme 1.18. Triflic acid-catalyzed aza-Darzens reaction.



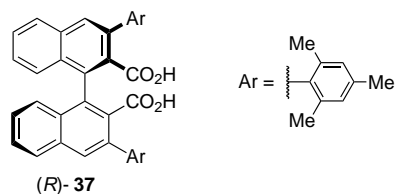
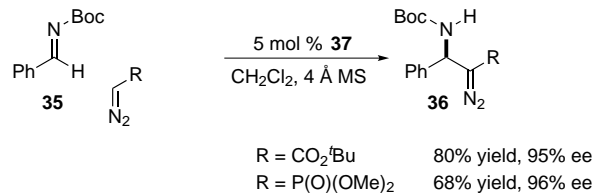
In 2005 the Terada group developed the first enantioselective addition of *tert*-butyl diazoacetate to *N*-acyl imines **32** using axially chiral phosphoric acid **34**. α -Diazo esters **33** form in good yields and excellent enantioselectivities that don't seem to be influenced by either electronics of the nitrogen protecting group or by electronics of the parent aldimine (Scheme 1.19).⁶⁰ Products presumably form via an addition/deprotonation pathway. The diazonium intermediate doesn't close to an aziridine ring but instead loses a proton to give an α -diazo amine, a formal C–H insertion product (see also Figure 1.3).

Scheme 1.19. Terada's phosphoric acid-catalyzed synthesis of α -diazoamines.



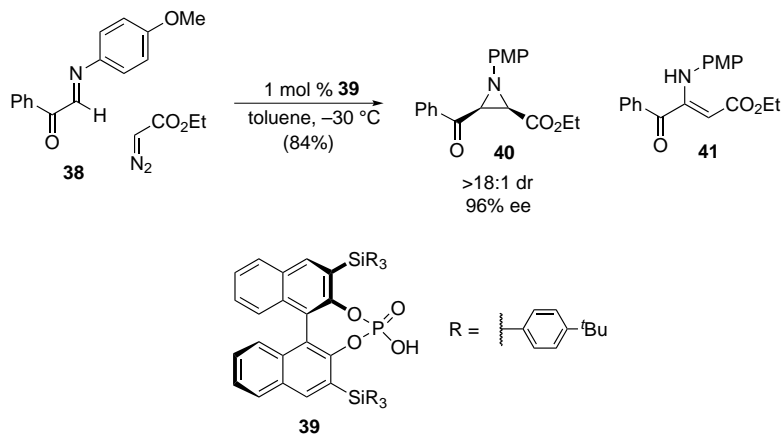
Similar reactivity was recognized by Maruoka in 2007. An axially chiral dicarboxylic acid **37** activates *N*-Boc imines towards *tert*-butyl diazoacetate or dimethyl (diazomethyl)phosphonate (Scheme 1.20) to yield the the corresponding α -diazo- β -amino esters or α -diazo- β -amino phosphonates **36** in good yield and excellent enantioselectivity.⁶¹ An intriguing aspect of this report is the fact that when compared to Terada's system (Scheme 1.19), catalysts **34** and **37** are homochiral but deliver opposite enantiomers, suggesting that stereoselection might be rooted in the nitrogen substituent. Somewhat lower reactivity of diazophosphonates has been later improved by Peng and co-workers.⁶²

Scheme 1.20. Maruoka's synthesis of α -diazamine esters and phosphonates.



There seems to be a delicate balance between the aminodiazonium structure and its end product. Akiyama and co-workers reported a chiral phosphoric acid-catalyzed aziridination reaction where a more electrophilic azomethine with an electron-rich nitrogen is used. In contrast to Terada's system, catalyst **39** favors formation of *cis*-aziridine **40** with a small amount of vinylogous amide **41** (Scheme 1.21).⁶³

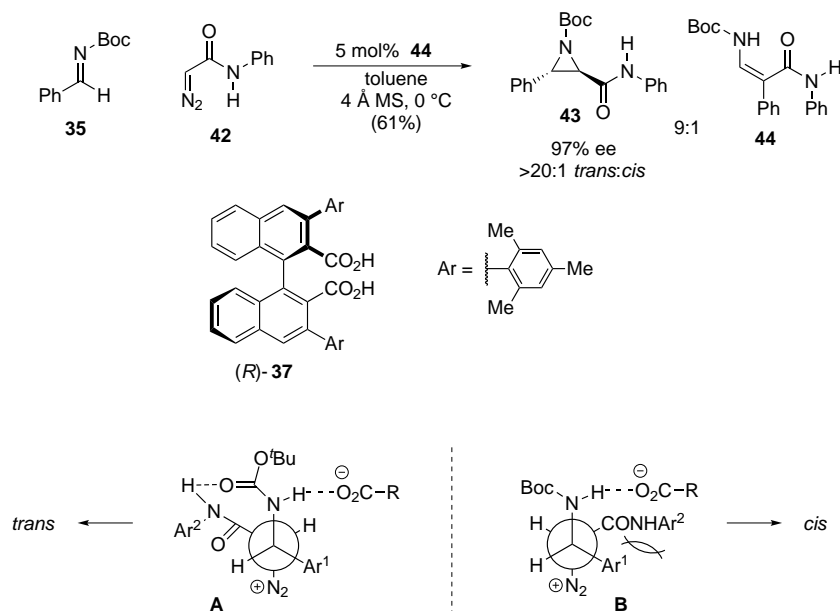
Scheme 1.21. Phosphoric acid-catalyzed *cis*-aziridination of glyoxal-derived aldimines.



For years since the first successful reaction, publications of stereoselective aza-Darzens aziridinations reported *cis*-product as the major diastereomer. This changed in 2008 when the Maruoka group reported a Brønsted acid-catalyzed enantioselective *trans*-aziridination of *N*-Boc benzaldimines with α -diazo amide **42** to give *trans*-aziridine amides **43** in moderate yield and high enantioselection (Scheme 1.22). The main byproduct was vinylogous amide **44**, the result of a 1,2-aryl shift.⁶⁴ Compared to their previous work (Scheme 1.20),

diastereoselectivity reversal to *trans*-aziridine seems to be solely correlated to the use of a diazo amide compound capable of hydrogen bond donation.

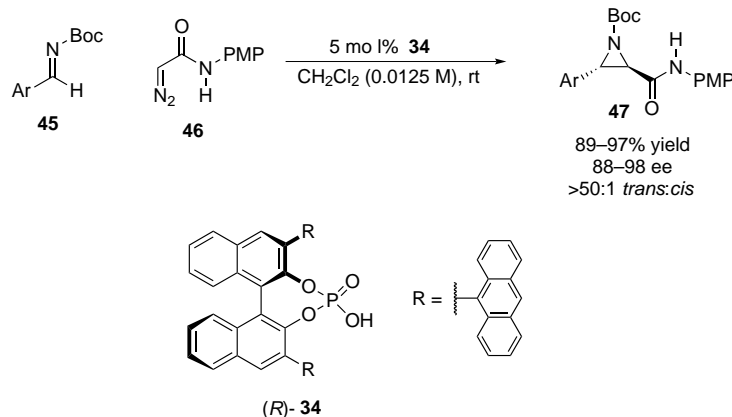
Scheme 1.22. *trans*-Selective asymmetric aziridination.



A model was advanced to explain this observation. A hydrogen bond donation from the amide N–H hydrogen bonds to the Boc group positions the diazo compound for *anti* carbon–carbon bond formation (Scheme 1.22, **A**). Cyclization of the amine nitrogen onto the diazonium carbon affords *trans* product. Since α -diazo amide **42** is larger than ethyl diazoacetate, *syn*-aminodiazonium required for *cis*-aziridine (Scheme 1.22, **B**) is disfavored. Furthermore, when less acidic *N*-Bn diazoamide was used, the yield suffered considerably.

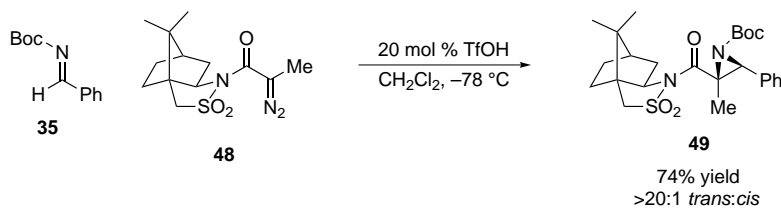
Shortly after, other groups reported asymmetric *trans*-aziridinations. The Zhong group optimized the reaction by using axially chiral phosphoric acid **34**, imine **45**, and *N*-PMP diazoamide **46**. With just 5 mol% of the catalyst at low concentration in CH₂Cl₂, the reaction proceeds in 89–97% yield and 88–98% ee for various aldimine substrates (Scheme 1.23).⁶⁵ In 2010, the Wulff group reported that α -diazoamides are compatible with their reaction system, providing both alkyl and aryl *N*-benzhydryl *trans*-aziridine products in very high yield and ee (Scheme 1.23).⁶⁶

Scheme 1.23. Improved asymmetric *trans*-aziridination of benzaldimines.



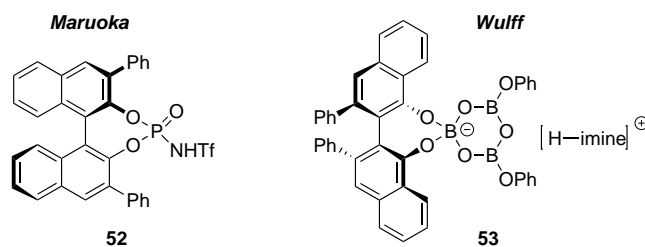
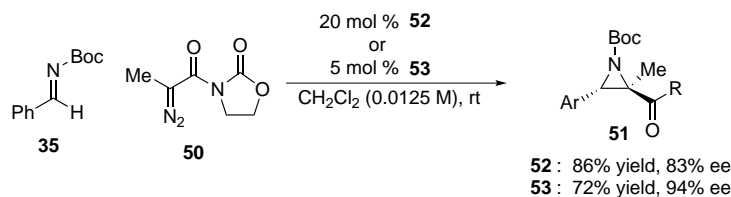
To complete the spectrum of asymmetric aziridination of imines, efforts were directed at methods for the synthesis of trisubstituted aziridines. Early examples utilized substrate control to achieve acceptable levels of diastereoselection. The Maruoka group presented in 2010 a Brønsted acid-catalyzed reaction of α -substituted α -diazocarbonyl compound **48**, containing camphorsultam chiral auxiliary, and *N*-Boc imines. In the presence of a substoichiometric amount of triflic acid, the desired trisubstituted aziridine **49** forms in acceptable yield favoring the *trans* diastereomer exclusively (Scheme 1.24).⁶⁷

Scheme 1.24. Substrate controlled synthesis of trisubstituted aziridines.



This area of research was significantly improved in 2011 when the asymmetric Brønsted acid-catalyzed aza-Darzens reaction was published simultaneously by groups of Maruoka⁶⁸ and Wulff.⁶⁹ Both groups utilized their signature catalysts, **52** and **53** respectively, and a diazo compound **50** derived from *N*-acyl oxazolidinone. Other α -substituted diazo donors were not reactive enough in this reaction. Empirical investigation of substrate scope established that only *N*-Boc imines are suitable substrates, a limitation of this methodology. Uniformly excellent asymmetric induction was observed for nearly all tested aldimines except *ortho*-substituted aldimines which were unreactive (Scheme 1.25).

Scheme 1.25. Brønsted acid-catalyzed asymmetric synthesis of trisubstituted aziridines.



1.3 Origins of selectivity in the aza-Darzens aziridine synthesis

Since the first examples of *cis*-aziridine synthesis from diazo compounds and imines, the underlying mechanism responsible for high *cis*-selectivity was not known. The most frequently proposed mechanism suggested a *syn* carbon–carbon bond creation to arrive at α -aminodiazonium **C** which undergoes $\text{S}_{\text{N}}\text{i}$ cyclization to form a *cis*-aziridine. Intermediacy of **C** (Figure 1.5), however, is not directly supported with published experimental evidence.

In 2011, Johnston and co-workers established experimentally that *cis*-aziridine forms exclusively from independently generated *syn*-aminodiazonium **C**.^{70,71} The main hypothesis behind the study was that the Brønsted acid-promoted fragmentation of a triazolone ring would provide an intermediate that would mechanistically intersect with the aza-Darzens reaction. This simple model utilizes a Brønsted acid as a catalyst which has an advantage over Lewis acids and metal catalysts because redox pathways involving carbenoids and azomethine ylides are excluded from the discussion.

Figure 1.5 shows mechanistic pathways studied, and the relative stereochemistry of the products was used to investigate the reaction outcome. Using a chiral substituent on the N3 of the triazolone, relative stereochemistry determination was possible by proton NMR. *trans*-Triazolone **A**, when subjected to a Brønsted acid will fragment the N–N bond to reveal the intermediate **B**, the same intermediate required for *cis*-aziridination. An alternative route is also possible, where protonation of the ester oxygen causes C–N bond fragmentation to give **E**. Ring closure of **E** occurs with retention of the relative stereochemistry and produces *trans*-aziridine **F**.

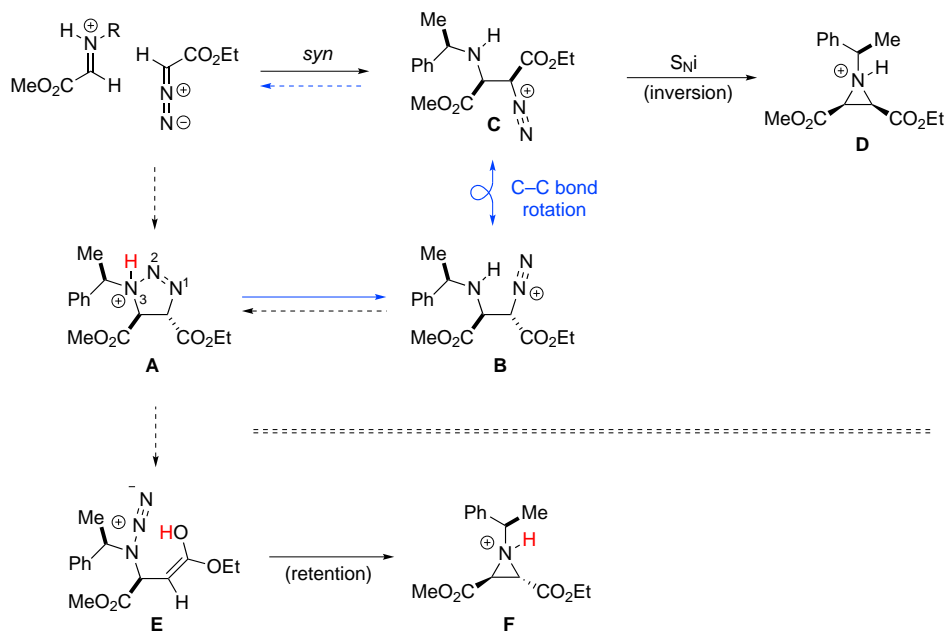
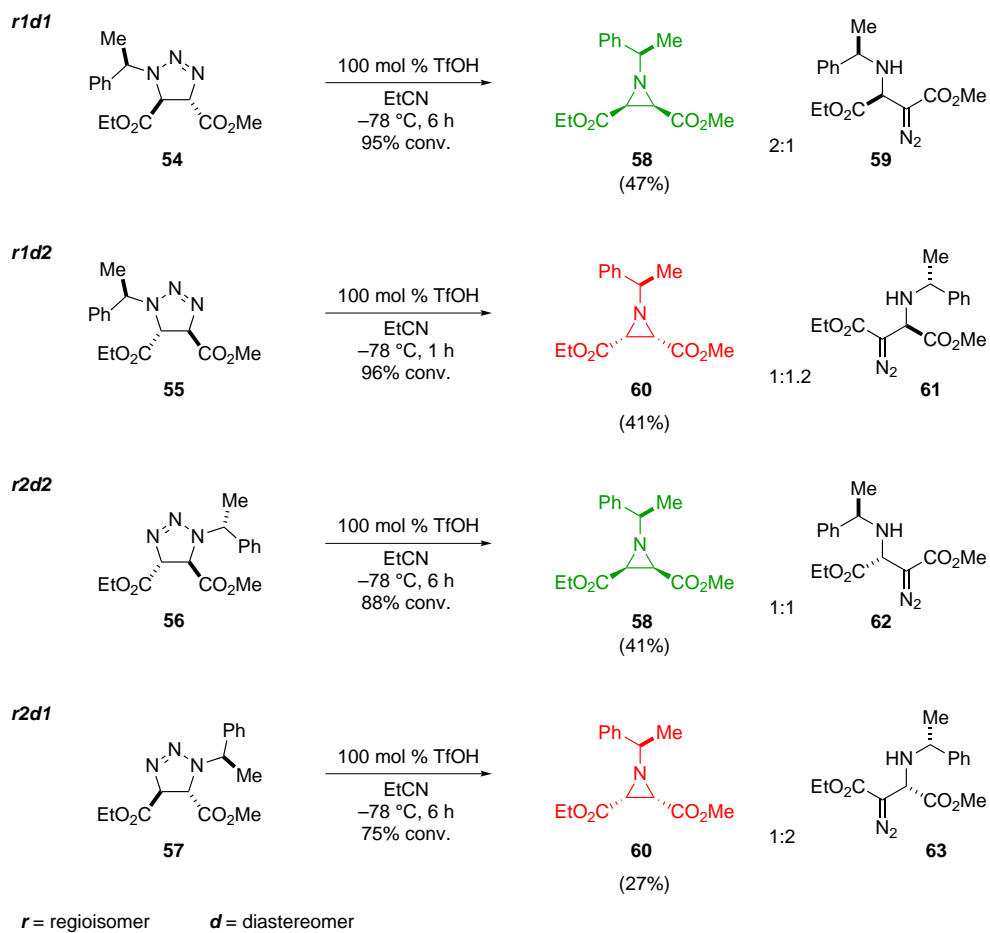


Figure 1.5. Mechanistic outline connecting aza-Darzens and triazoline decomposition reactions in the presence of a Brønsted acid.

Although the aza-Darzens reaction proceeds efficiently with a substoichiometric amount of triflic acid, a study of the fragmentation of four stereoisomers of *trans*-triazolines **54–57** was performed using a full equivalent of TfOH to ensure kinetic control. All four triazolines provided only two products (in varying ratio)—*cis*-aziridine and α -diazo- β -amino-ester (Scheme 1.26, r=regioisomer, d=diastereomer). The diazo by-product is a result of proton transfer and doesn't give aziridine when resubjected to reaction conditions. In each case, only *cis*-aziridine was observed which was confirmed by ¹H NMR and X-ray crystallography. These results are consistent with the hypothesis illustrated in Figure 1.5, that *trans*-triazoline conversion is a stereospecific process with inversion of configuration at diazonium carbon. If intermediate **E** was a product of fragmentation, *trans*-aziridine would be observed instead. Formation of **E** is unlikely because it requires an energetically unfavorable C–N bond fragmentation.

The stereochemical fate of triazoline fragmentation is detailed in Scheme 1.27. Upon protonation, the triazolone ring fragments to an α -aminodiazonium species but the resulting *gauche* conformation is not productive. Rotation around the C–C bond to the antiperiplanar arrangement is followed by cyclization to aziridine product **58**. Further support, albeit more circumstantial, was a finding that substoichiometric triflic acid (as low as 7 mol %) was sufficient to drive aza-Darzens reactions to completion.⁵⁹ This contrasted with the observation that excess triflic acid was necessary to fully convert triazolines **54–57** and suggests that

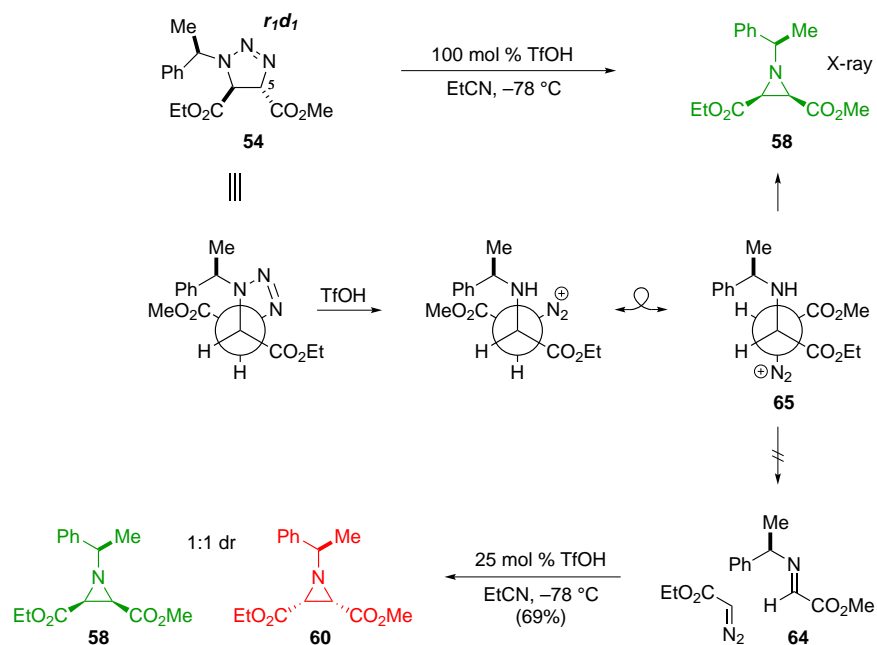
Scheme 1.26. Stereochemical outcome of Brønsted acid-promoted fragmentation of chiral *trans*-triazolines to *cis*-aziridines.



initial [2 + 1] cycloaddition between the imine and diazo to form triazoline is unlikely.

The creation of the C–C bond between diazo and imine is theoretically reversible. This is important whenever enantioselective reactions are discussed, as the retro process is a potential path for racemization. When ethyl diazoacetate and imine **64** (retro products of **65**) were subjected to triflic acid, aziridines **58** and **60** formed nonselectively. This established that under the standard reaction conditions, the *retro*-Mannich reaction of aminodiazonium **65** is not operative (Scheme 1.27).

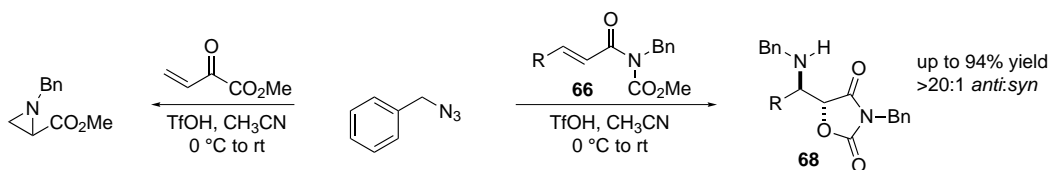
Scheme 1.27. Fate of α -diazonium intermediate.



1.4 Results and discussion

Johnston and co-workers demonstrated in 2005 that strong Brønsted acid promotes a reaction of alkyl azides with electron deficient alkenes.⁷² In reaction with acrylates, benzyl azide furnished aziridines but when the dipolarophile contains a pendant nucleophile (such as **66**), *anti*-oxazolidine dione is the product. In the follow-up publication, *trans*-triazoline **67** was proposed to be a resting state and perhaps an intermediate (Scheme 1.28).

Scheme 1.28. Brønsted acid-promoted formal aminohydroxylation of α,β -unsaturated imides.



The mechanism of formation of *anti*-**68** might intersect the aza-Darzens reaction at the *vic*-aminodiazonium intermediate. We sought to determine the stereochemical outcome of the reaction between α -diazo imide **69** and imine. The end goal is the development of a new carbon-carbon bond forming reaction as a complementary approach to *anti*-oxazolidine dione scaffolds (Figure 1.6).

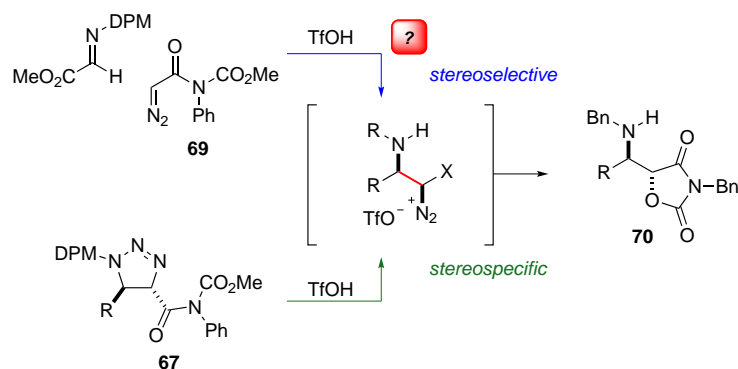


Figure 1.6. Intersecting paths of triazolone imide fragmentation and α -diazo imide addition to imines.

1.4.1 Stereochemistry of triazolone imide fragmentation

Triazolone imide **72** was prepared by a thermal cycloaddition reaction of α,β -unsaturated imide **71** with diphenylmethyl azide. We hypothesized that analogous to triazolone esters **54**–**57**, acid treatment of **72** will form *syn*-aminodiazonium intermediate **73** which will undergo *cis*-aziridine formation. If protonated aziridine **74** is sufficiently activated, the carbamate will undergo cyclization to open the *cis*-aziridine to give *syn*-oxazolidine dione **75**. Alternatively, direct carbamate 5-*exo* displacement of dinitrogen in **73** (without prior aziridine formation) would lead to *anti*-oxazolidine dione **75** (Figure 1.7).

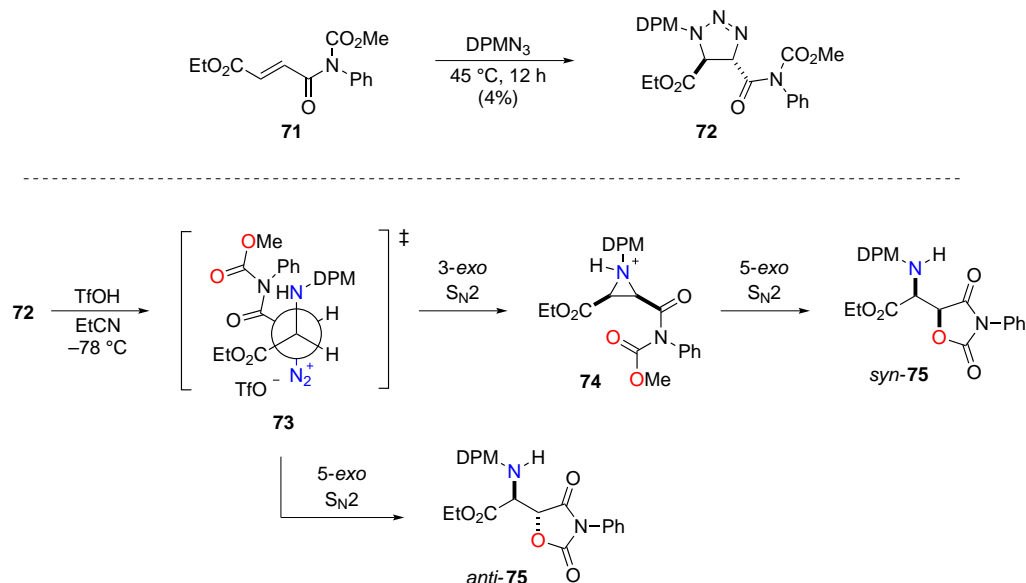
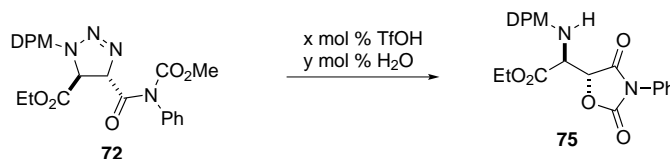


Figure 1.7. Outline of triazolone imide decomposition.

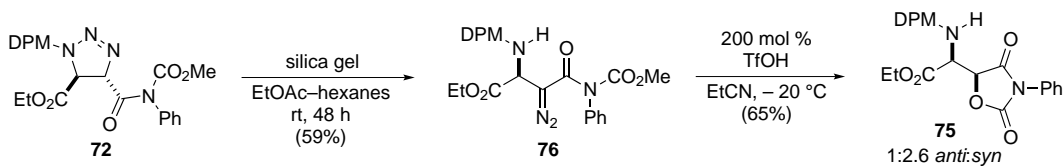
Treatment of **72** with 100 mol % of TfOH at -78°C in propionitrile returned unreacted starting material (Table 1.1, entry 1). In dichloromethane, under the same reaction conditions, very slow conversion (ca. 40%) was observed, and the *anti*-oxazolidine dione forms predominantly (Table 1.1, entry 2). In order to achieve moderate yield, reaction in propionitrile has to be carried at a higher temperature; after 5 h at 0°C , *anti*-oxazolidine dione **75** was isolated in 37% yield and 4:1 dr (Table 1.1, entry 3). The same reaction in dichloromethane was more efficient and significantly more selective (Table 1.1, entry 4). Addition of water accelerates the reaction rate⁷³ but has no effect on the selectivity of the reaction (Table 1.1, entry 5). Water-accelerated conditions allowed us to perform the reaction at -20°C to achieve optimal yield (78%) and exclusive *anti* selectivity (Table 1.1, entry 6). These results demonstrate that the 5-exo cyclization to form a 5-membered ring is significantly faster than formation of the *syn*-product by *cis*-aziridine formation and its diastereospecific opening. Rate acceleration by a secondary catalyst (water) is consistent with our previous studies.^{73,74}

Table 1.1. Fragmentation of triazoline **73**.


entry	TfOH mol %	H ₂ O mol %	solvent	T (°C)	time (h)	yield (%)	dr ^a
1	100	0	EtCN	-78	5	0 ^b	—
2	100	100	CH ₂ Cl ₂	-78	5	— ^c	10:1
3	100	0	EtCN	0	5	37	4:1
4	100	0	CH ₂ Cl ₂	0	5	55	15:1
5	100	100	EtCN	0	5	61	4:1
6	200	100	EtCN	-20	6	78	20:1

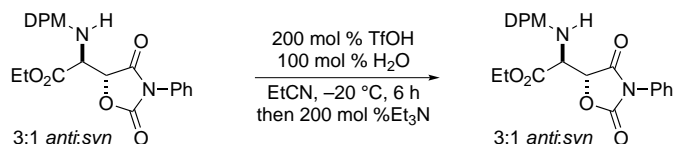
^aDiastereoselectivity was estimated using ¹H NMR of the crude reaction mixture. ^bStarting material was fully recovered. ^cProduct not isolated (40% conversion measured by ¹H NMR).

During chromatographic purification of **72** we noticed that this compound readily isomerizes to α -diazo amine **76**. Exposure of this *vic*-amino diazo compound to triflic acid at -78°C returned unreacted starting material. But the reaction carried out at -20°C provided the oxazolidinone as a 1:2.6 *anti:syn* mixture of diastereomers and no *cis*-**74** was observed (Scheme 1.29). This established that 1) the intermediate diazonium triflate is a competent precursor to oxazolidinone product, and 2) if the diazonium triflate formation is not diastereoselective (no facial selectivity for C=N₂ bond protonation), a mixture of oxazolidinone diastereomers will result, 3) carbamate cyclization is substantially faster than aziridine formation if discrete diazonium triflate **73** (analogous to **65**, Scheme 1.27) is formed in the conversion of **72** to **75**. This contrasts the highly selective transformation of *trans*-triazoline to *anti*-oxazolidinone (Table 1.1), which presumably differs by diastereospecific fragmentation to the intermediate diazonium triflate, followed by diastereospecific cyclization to the *anti*-**75**.

Scheme 1.29. Brønsted acid-promoted conversion of α -diazoamine **76**.

To test *syn-anti* interconversion under the reaction conditions, a 3:1 *anti-syn* oxazolidine dione mixture was resubjected to the reaction conditions, returning the same ratio of diastereomers following reaction workup (Scheme 1.30), which established that the diastereomeric oxazolidine diones do not interconvert under the reaction conditions. This observation supports the contention that diastereomeric ratios observed represent kinetic selectivities.

Scheme 1.30. Control experiment testing *syn-anti* interconversion.



1.4.2 Stereochemistry of the carbon–carbon bond formation in α -diazo imide addition to azomethines

This stereochemical course provided a behavioral test for the intermediacy of *vic*-aminodiazonium **73** in the examination of the triflic acid-catalyzed aza-Darzens reaction. α -Diazo imide **69** was prepared (see Section sec:diazo-prep for synthesis) for that purpose. We expected that compound **69** will react similarly to ethyl diazoacetate in reaction with benzhydryl imine **77** in presence of triflic acid. The *syn* carbon–carbon bond formation will provide the intermediate **73** and cross mechanistic path of triazolone imide **72** fragmentation (Table 1.1). As described above, we expected 5-*exo* carbamate cyclization to be faster than aziridine formation and *anti*-**75** was expected to be the major product (Figure 1.8).

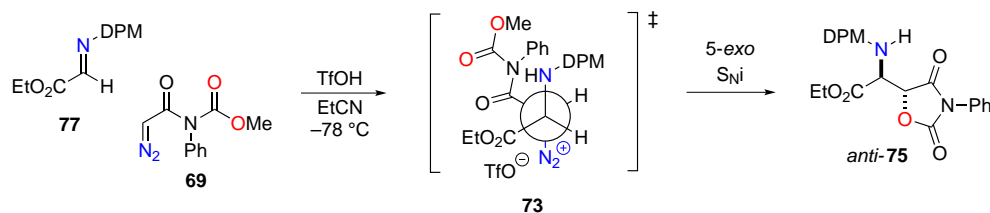
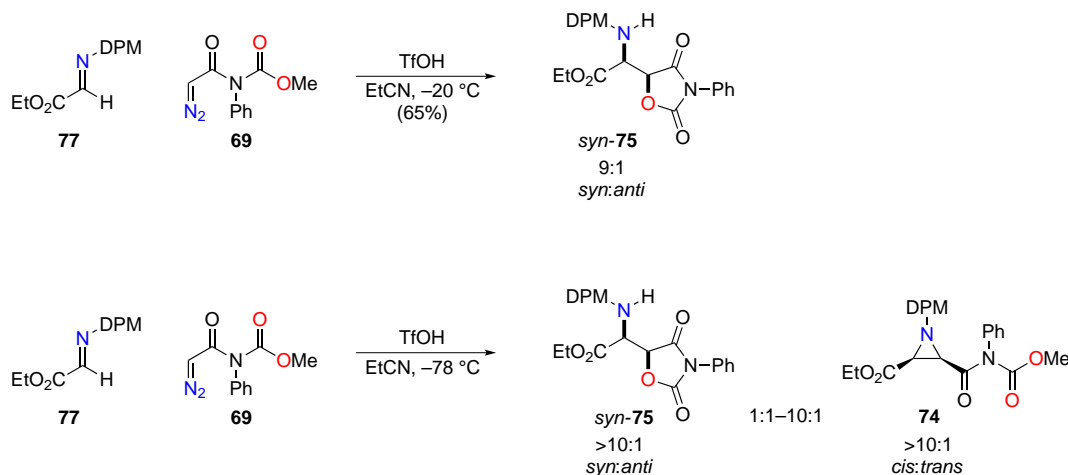


Figure 1.8. Diazo imide–imine reaction hypothesis.

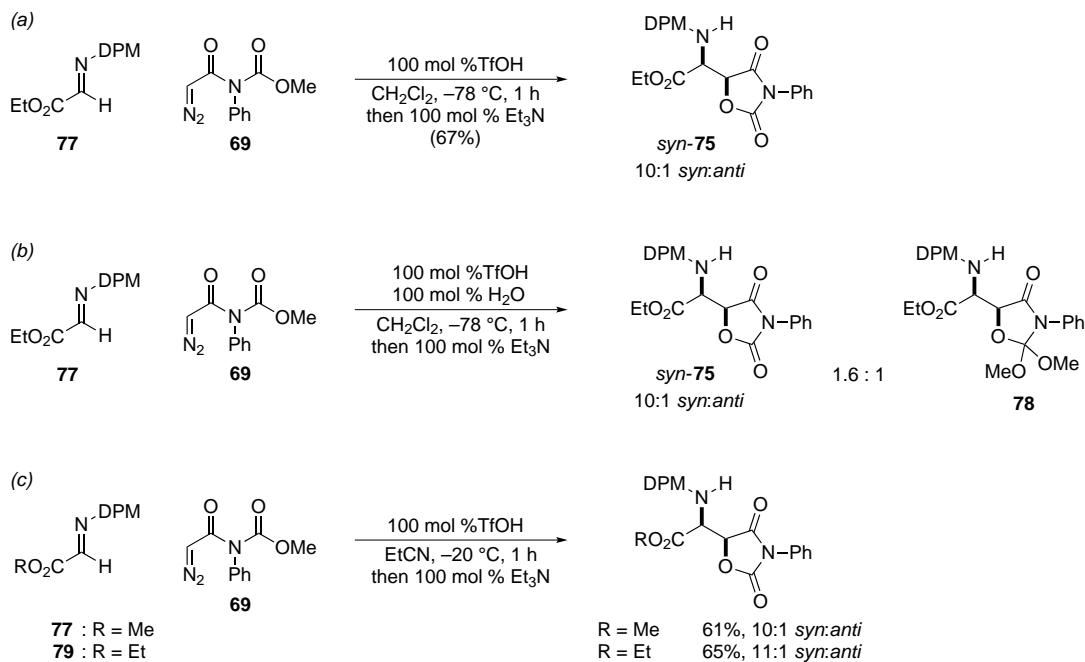
To our surprise, when imine **77** and diazo **69** are treated with 200 mol % of triflic acid in propionitrile at $-20\text{ }^{\circ}\text{C}$, the reaction afforded oxazolidine dione **75** in 65 % yield in 9:1 ratio favoring the *syn* diastereomer. At low temperature ($-78\text{ }^{\circ}\text{C}$, including reaction quench), the result was similar but on a few occasions this combination led to a mixture of *syn*-oxazolidine dione **75** and *cis*-aziridine **74**. No evidence for *trans*-aziridine was ever observed (Scheme 1.31). The selective formation of *cis*-aziridine **74** suggests that diazoimide **69** behaves similarly to ethyl diazoacetate in the mechanism of the aza-Darzens reaction but if the *cis*-aziridine and *syn*-oxazolidine dione were to share the intermediacy of discrete diazonium triflate *syn*-**73**, however, *anti*-oxazolidine dione **75** would have resulted.

Scheme 1.31. Unexpected diastereoselectivity in diazo imide–imine reaction.



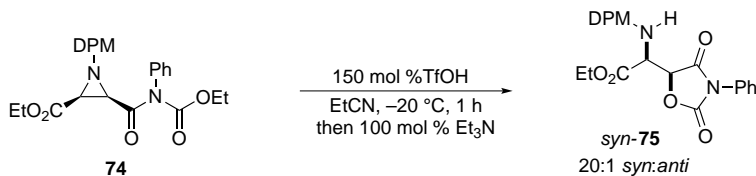
To probe the origins of aziridine and oxazolidine dione in the triflic acid-catalyzed α -diazo imide–imine reaction a series of control reactions was completed. A reaction carried out in dichloromethane at $-78\text{ }^{\circ}\text{C}$ favored *syn*-oxazolidine dione **75** and *cis*-aziridine **74** was never observed (a, Scheme 1.32). Addition of 100 mol % of water resulted in formation of compound **78** next to *syn*-**75** in 1:1.6 ratio (b, Scheme 1.32). The triflic acid catalyzed addition of α -imino methyl and ethyl esters (**77** and **79** respectively) with α -diazoimide in propionitrile at $-20\text{ }^{\circ}\text{C}$ yields the respective products cleanly and with 10:1 and 11:1 *syn*-selectivity as evidenced by ¹H NMR analysis of their crude reaction mixtures (c, Scheme 1.32).

Scheme 1.32. Diazo imide–imine control reactions.



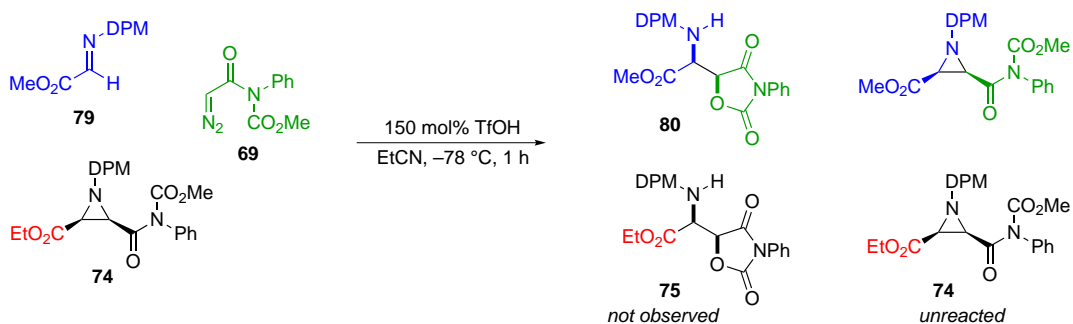
The purified aziridine from the reaction in Scheme 1.31 was resubjected to the low temperature reaction conditions, but would not convert to the oxazolidine dione. However, at higher temperatures ($-20\text{ }^{\circ}\text{C}$ or above), the *cis*-aziridine converted to the *syn*-oxazolidine dione without formation of the *anti* diastereomer (Scheme 1.33). Although this outcome is consistent with a diastereospecific, intramolecular aziridine ring opening it was not clear if *cis*-aziridine **74** is the intermediate of *syn*-**75** or if they form in two distinctive and independent pathways.

Scheme 1.33. Acid-promoted diastereospecific aziridine opening.



While these reactions established the apparent stability of the *cis*-aziridine at low temperature, an experiment was designed to show unequivocally that the *cis*-aziridine and *syn*-oxazolidine dione are produced independently of one another (Scheme 1.34). The *ethyl* ester variant of the *cis*-aziridine **74** was added (50 mol %) to a reaction of α -imino *methyl* ester **79** and α -diazo imide **69**. Triflic acid was added, and following low temperature quench, the crude reaction mixture was analyzed by ^1H NMR (Figure 1.9). Production of the expected *syn*-oxazolidine dione **80** (spectrum c in stacked plot) was observed in the crude reaction mixture (spectrum e). Unchanged *cis*-aziridine *ethyl* ester **74** (spectrum a) added at the reaction start is also observed (quartet at 4.18 ppm), and the diagnostic dq at 4.3 ppm of the *syn*-oxazolidine dione *ethyl* ester **75** (spectrum b) is absent.

Scheme 1.34. Cross-over experiment testing aziridine intermediacy diazo imide–imine reaction.



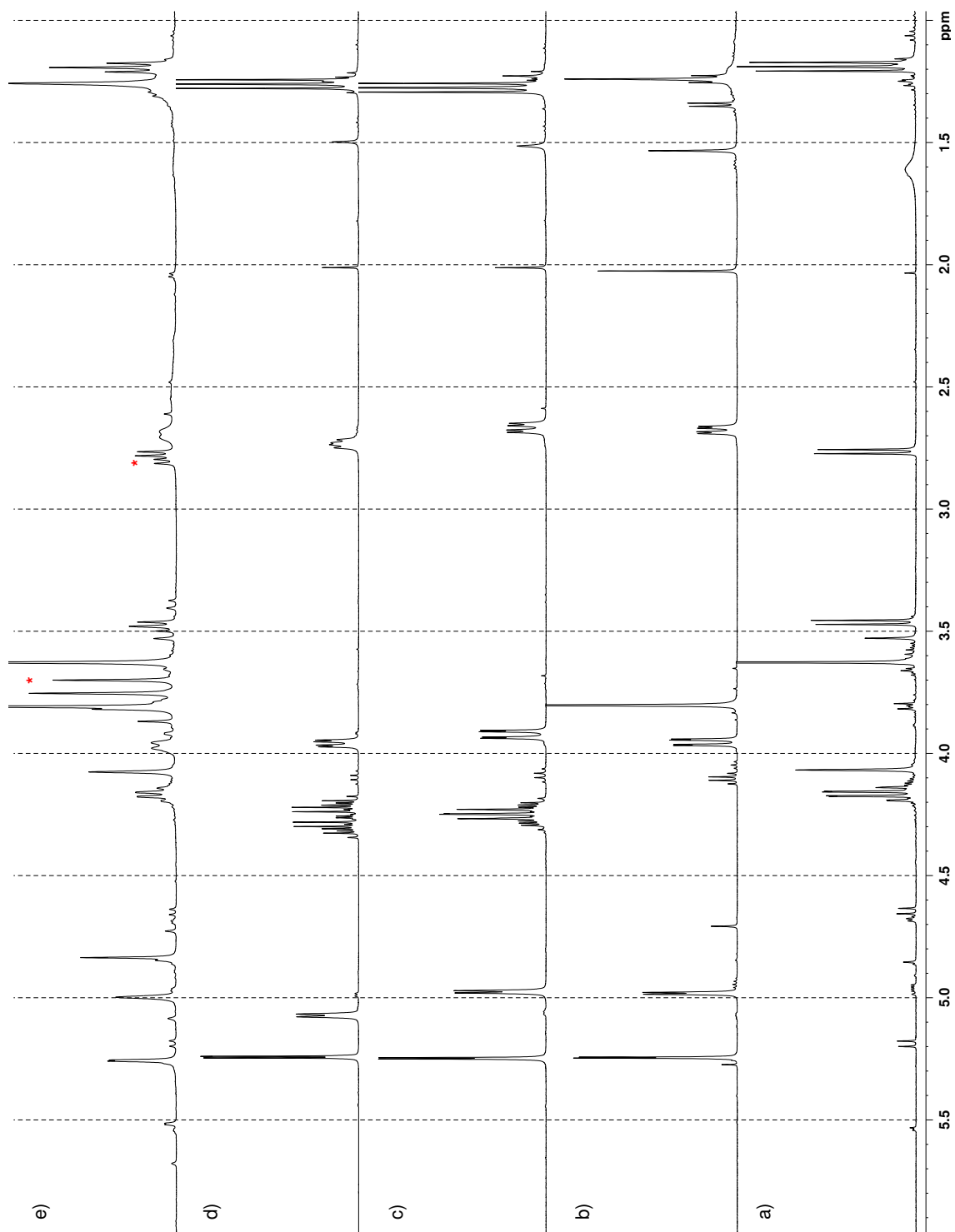


Figure 1.9. ¹H NMR (CDCl₃) of a) aziridine *cis*-74, b) oxazolidine dione *syn*-80, c) oxazolidine dione *syn*-75, d) oxazolidine dione *anti*-75, and e) crude reaction mixture (Scheme 1.34). The resonance at 4.28 ppm (dq) corresponding to the oxazolidine dione *syn*-75 is absent in the spectrum of the crude reaction mixture. Resonances marked with an asterisk (*) are assigned to the aziridine *methyl* ester.

1.4.3 Diazoalkane scope of the aza-Darzens reaction

It was clear to us that stereoselectivity of carbon-carbon bond formation is correlated with the structure of a diazo compound as ethyl diazoacetate prefers *syn* C-C bond formation and α -diazo imide forms *anti*-aminodiazonium. This prompted us to evaluate other diazo compounds in the reaction with benzhydryl imine **79** (Table 1.2).

Table 1.2. Scope of the *syn*-glycolate Mannich reaction.^a

entry	R	product	<i>cis:trans</i> ^b	yield ^c (%)
1		81	>20:1	88
2		82	>20:1	83
3		83	>20:1	81
4		84	>20:1	81 ^d
5		85	>20:1	48
6		86	>20:1	67
7		87	>20:1	67
8		88	>20:1	92 ^e

^aAll reactions were 0.3 M in imine. ^bDetermined by ¹H NMR analysis. ^cIsolated yield. ^dProduct suffers from elimination during chromatography. Yield estimated using ¹H NMR. ^eReaction was carried out at -20 °C for 18 h.

Diazoketones bearing cyclopropyl, cyclohexyl or heteroaromatic substituents delivered the corresponding *cis*-aziridines in high yield (Table 1.2 entries 1–3). Diazoalkanes containing a primary chloride gave selectively the chloroethyl substituted aziridine, which was evident from the proton NMR spectrum but it suffered from elimination during chromatography (entry 4). An ester substituted diazoalkane delivered aziridine in lower yield but without loss in diastereoselection (entry 5). A diazo with a remote 2-bromophenyl substituent, utilized in our approach to ambiguine G,⁷⁵ afforded the corresponding aziridine in 67 % yield (entry

7). Diethyl (diazomethyl)phosphonate delivered the *cis*-aziridine exclusively in very high yield but required a full equivalent of triflic acid and higher reaction temperature (Table 6, entry 8). We speculate that this is due to the Lewis basicity of the phosphonate group that competes with imine for the proton catalyst.⁷⁶ In all examples presented in Table 1.2, *cis*-aziridine was the only observed isomer. This suggests that the structure of the α -diazo imide responsible for the unique reactivity when compared to other diazo donors.

1.4.4 Summary and conclusions

This divergent behavior of diazoacetate and α -diazo imide in the Brønsted acid promoted reaction with azomethines is a result of different stereoselectivity of C–C bond formation. In the case of ethyl diazoacetate, as described in section 1.3, the reaction proceeds with *syn*-selectivity (intermediate **89**, Figure 1.10). Hence, the aza-Darzens synthesis of aziridines is exclusively *cis*-selective.

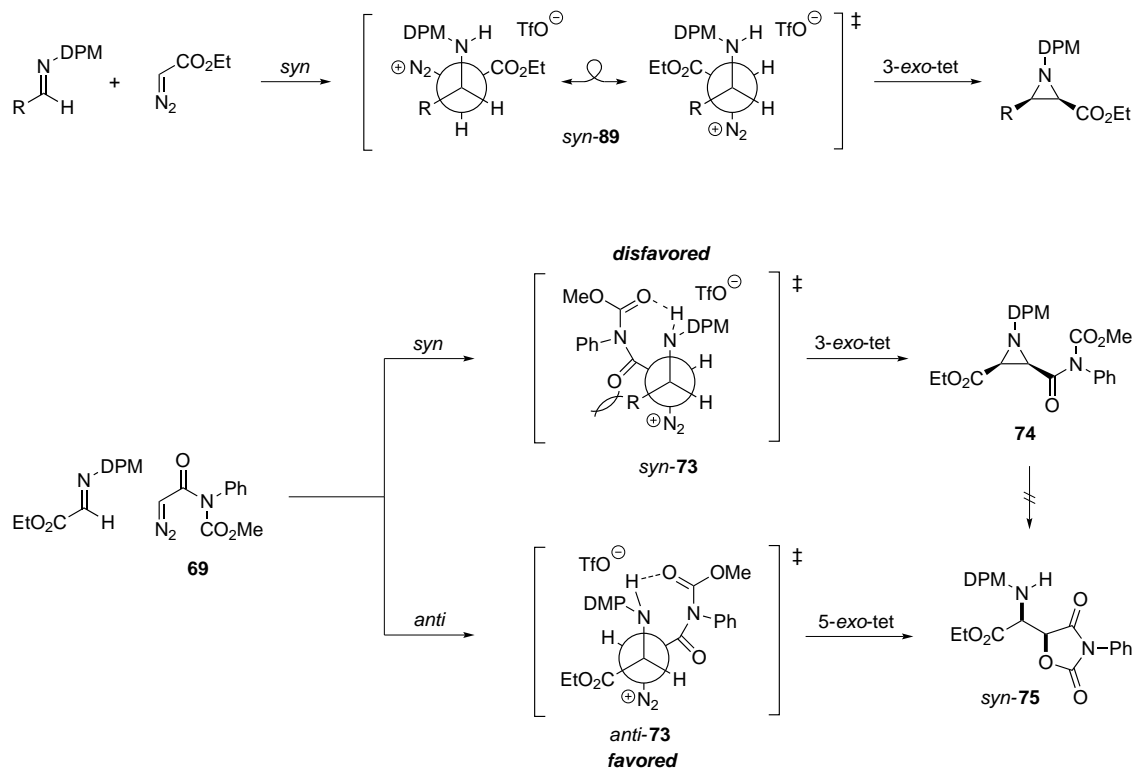


Figure 1.10. Origin of stereoselectivity in Brønsted acid-promoted diazo-azomethine reactions.

In case of α -diazo imide **69**, our results and observations suggest the following:

1. The *syn*-Aminodiazonium generated by fragmentation of *trans*-triazoline **72** leads directly to the *anti*-oxazolidine dione product.
2. Proton transfer isomerization of the *syn*-aminodiazonium **73** to α -diazo amine **76** prior to cyclization is unlikely because acid-promoted conversion of **76** to oxazolidine dione is very slow at $-78\text{ }^{\circ}\text{C}$ and nonselective at $-20\text{ }^{\circ}\text{C}$.
3. Cyclization of *syn*-**73** to *anti*-oxazolidine dione (5-*exo*-tet) is significantly faster than cyclization to *trans*-aziridine (3-*exo*-tet).
4. Carbon-carbon bond formation between α -diazo imide and azomethine electrophile favors *anti*-aminodiazonium intermediate, a precursor to *syn*-**75**. Preference for *anti* bond formation might be caused by steric interactions between the carbamate and substituents on the imine carbon. In addition to steric factors, extended hydrogen bonding of the pendant carbamate group could also be involved.
5. Under certain conditions (low temperature, propionitrile solvent) C-C bond formation occurs with *syn*-selectivity and the 3-*exo*-tet cyclization product, *cis*-aziridine **74** is produced. Additionally, aziridine **74** does not convert further to *syn*-oxazolidine dione which suggests that it forms independently of, and *is not* an intermediate to, *syn*-oxazolidine dione.
6. Diastereomer interconversion (*syn-anti*) under the reaction conditions does not contribute to the observed selectivity.

CHAPTER 2

Stereoselective reactions of α -diazo imides

2.1 Stereoselective approaches to α -oxy- β -amino acid motif

2.1.1 Olefin functionalization

Biological activity of natural products and pharmaceuticals is often a result of their unique structure. Some structural motifs, however, are prevalent in a diverse range of important natural and synthetic small molecules. 1,2-Aminoalcohol is one of these motifs and can be found in natural amino acids such as serine and threonine. Regioisomeric α -hydroxy- β -amino acid backbone has been found in clinically valuable antitumor agents such as Taxol[®],⁷⁷⁻⁸⁰ aminopeptidase inhibitors like bestatin,^{81,82} and recent isolates like the microsclerodermins⁸³ and pedeins⁸⁴ (Figure 2.1). The presence of this moiety and the stereochemistry of the hydroxy as well as the amino group play a vital role in the biological activity of the molecules containing it and as a result they are the target of a variety of synthetic methods.

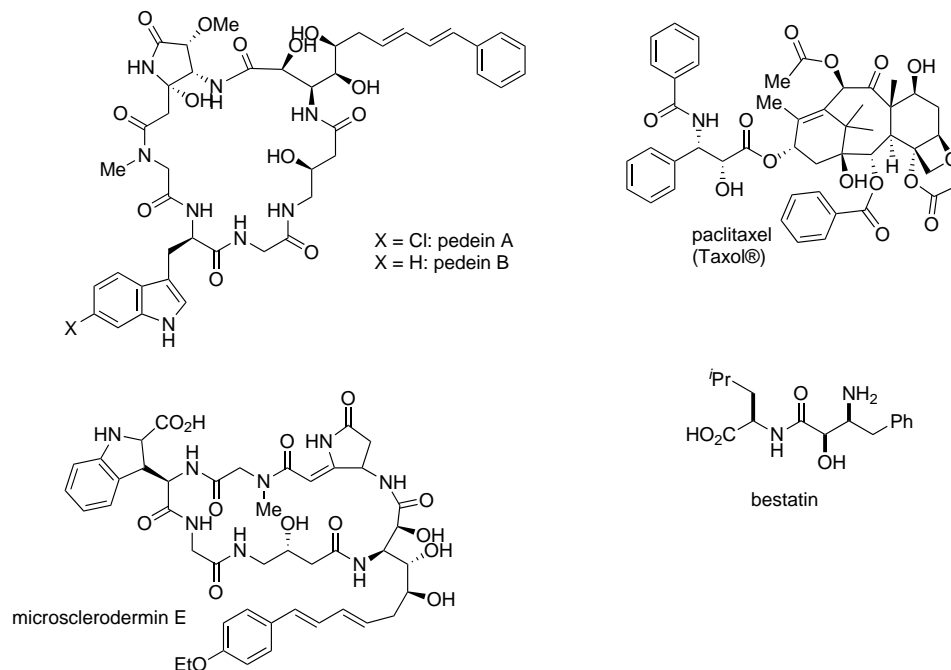
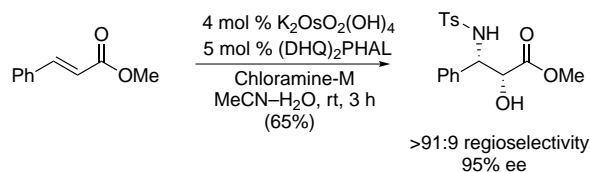


Figure 2.1. Natural products containing *vic*-aminoalcohol fragment.

An addition of the amino and the hydroxy group across a carbon–carbon double bond, commonly known as alkene aminohydroxylation was first described in 1975.⁸⁵ Over 20 years later, catalytic asymmetric aminohydroxylation was reported⁸⁶ and is now one of the most reliable methods for the synthesis of 1,2-aminoalcohols from alkenes. Exclusive formation of only one diastereomer is guaranteed by the stereospecificity of the addition that proceeds through the cyclic intermediate. Typical conditions involve treatment of an olefin with an osmium oxidant, (typically $K_2[OsO_2(OH)_4]$), a chiral ligand, benzyl carbamate as a nitrogen source and the *tert*-butyl hypochlorite in a water–*t*BuOH mixture (Scheme 2.1).⁸⁷

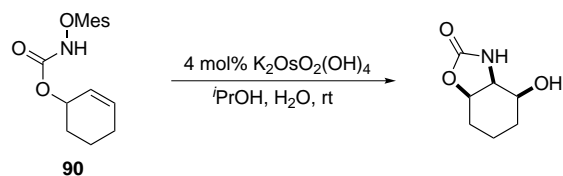
Scheme 2.1. Synthesis of Taxol side chain via Sharpless asymmetric aminohydroxylation.



Regioselectivity is the main drawback of this method, especially for unsymmetrical alkenes. This problem has been somewhat addressed by Donohoe and co-workers by tethering the nitrogen source (such as carbamate) to an allylic alcohol **90** (Scheme 2.2).⁸⁸ However, this

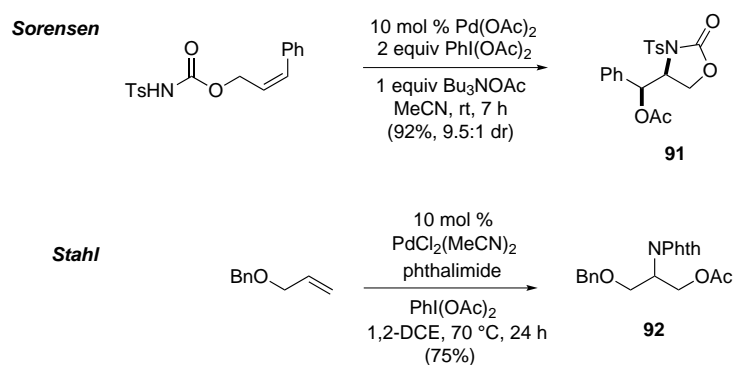
approach limits the scope of aminohydroxylation to allylic alcohols.

Scheme 2.2. Donohoe's intramolecular asymmetric aminohydroxylation.



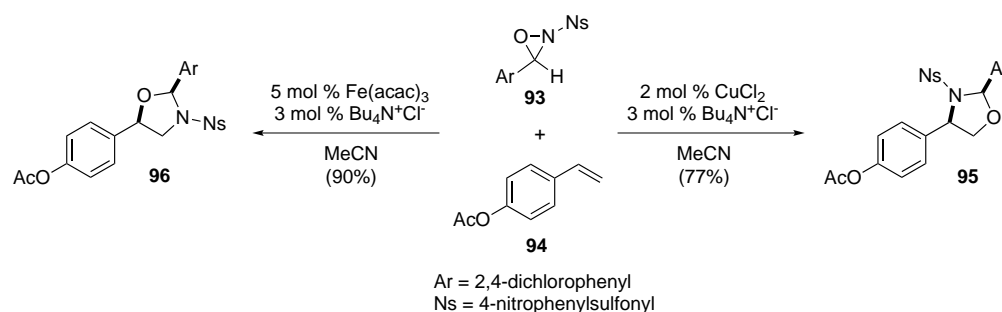
The toxicity of osmium stimulated development of other milder methods and led to discoveries of alternatives, such as palladium catalyzed reactions. An interesting example has been demonstrated by the Sorensen group. Aminoacetoxylation of a range of alkenes with high levels of regio- and stereocontrol can be achieved using a tethered *N*-Ts carbamate as a nitrogen source to give *syn*- (**91**) and *anti*- products in good diastereoselection.⁸⁹ An intermolecular example of the same reaction was reported by Liu and Stahl. Oxidation with $PhI(OAc)_2$ and the phthalimide as a nitrogen source affords 1,2-aminoalcohol derivatives **92** in good yield and regioselectivity (Scheme 2.3).⁹⁰

Scheme 2.3. Aminoacetoxylation approach to *vic*-aminoalcohol derivatives.



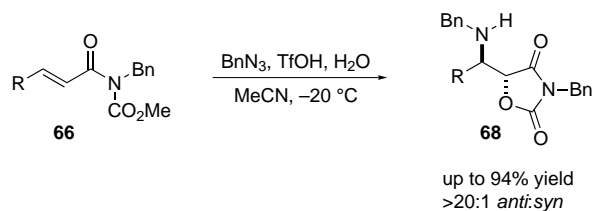
Nitrogen and oxygen can also be installed on a carbon-carbon double bond using a single reagent. Yoon et al. reported a copper(II)-catalyzed regioselective aminohydroxylation of alkenes using the *N*-sulfonyl oxaziridine **93** (Scheme 2.4).^{91,92} Although this method addresses regioselectivity issues associated with Sharpless aminohydroxylation of styrene derivatives, such as **94**, only moderate *cis:trans* selectivity can be achieved. In 2010 the Yoon group reported that by a careful choice of the catalyst, regioselectivity of aminohydroxylation can be controlled. If CuCl₂ is used, 1,3-oxazolidine **95** forms as the major product but under conditions utilizing an iron(III) catalyst, regioisomer **96** dominates (Scheme 2.4).⁹³

Scheme 2.4. Yoon's radical aminohydroxylation using oxaziridines.



A conceptually different approach to olefin functionalization was illustrated by Johnston and co-workers in 2005. Benzyl azide undergoes a Brønsted acid promoted 1,3-dipolar cycloaddition with the α,β -unsaturated imide **66**. Intermediate triazolines can be isolated or fragmented by warming to room temperature which is followed by cyclization of a latent oxygen nucleophile onto an α -diazonium intermediate (see Scheme 1.28, section 1.4) to afford *anti*-oxazolidine dione products **68** with very high dr (Scheme 2.5).⁷² Fragmentation of the triazolone at low temperature can be triggered by use of water as a secondary catalyst.⁷⁴

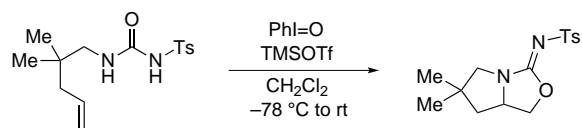
Scheme 2.5. Brønsted acid-promoted formal aminohydroxylation of α,β -unsaturated imides.



Another metal-free oxidative approach to functionalization of alkenes was shown by

Cochran and Michael. Intramolecular oxyamination of olefins with $\text{PhI}=\text{O}$ using a tethered urea as an oxygen and nitrogen source proceeds with high diastereoselection (Scheme 2.6). The strength of the acid catalyst determines the reaction outcome. Strong acids, such as triflic acid, prefer an oxyamination pathway, whereas weak acids yield diamination products.⁹⁴

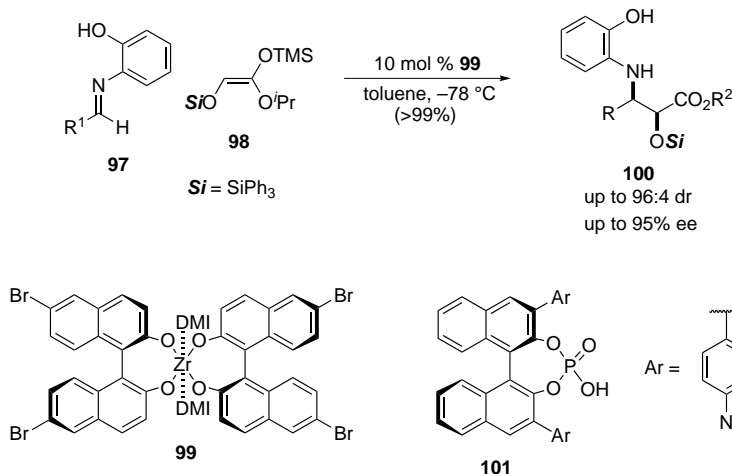
Scheme 2.6. Metal free, acid promoted intramolecular oxyamination.



2.1.2 Vicinal aminoalcohols via C–C bond forming reactions

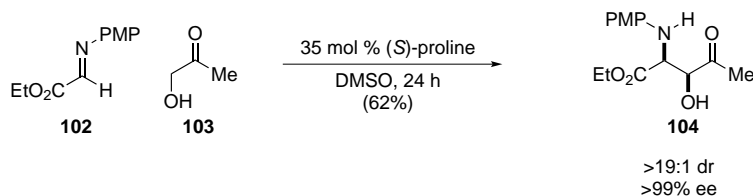
With the advent of asymmetric catalysis, a significant development was achieved in the area of carbon–carbon bond forming reactions between imines and glycolic acid enolates or their equivalents.^{95,96} Early work in the asymmetric glycolate Mannich reaction involved silyl ketene acetals as nucleophiles. In 1998 Kobayashi and co-workers demonstrated the first catalytic diastereo- and enantioselective glycolate Mannich reaction (Scheme 2.7). Metal complex **99** catalyzes addition of the silyl ketene acetal **98** to benzaldimines **97** to form Mannich adducts **100** with very high stereoselection.⁹⁷ A hydroxy group on the imine substituent is needed for effective binding to the catalyst. Later, Akiyama reported that the same reaction can be catalyzed by chiral phosphoric acid **101**. α -Hydroxy- β -amino esters such as **100** form as a single diastereomer in high ee when a large triphenylsilyl group is used (Scheme 2.7).⁹⁸

Scheme 2.7. Kobayashi's asymmetric glycolate Mannich reaction with silyl ketene acetal nucleophiles.



In 2002 List⁹⁹ and Barbas¹⁰⁰ independently showed that L-proline is a very efficient organocatalyst in the direct Mannich reaction. The imino ester **102** in reaction with α -hydroxyacetone (**103**) delivers serine derivative **104** essentially as a single stereoisomer (Scheme 2.8).

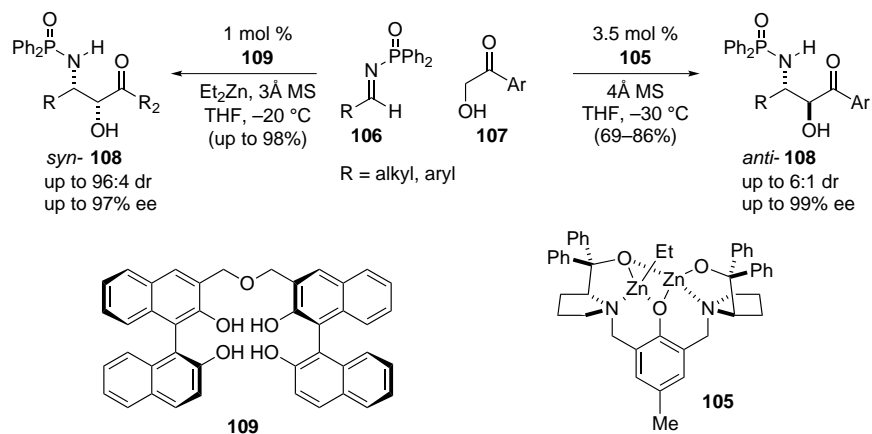
Scheme 2.8. Proline catalyzed direct Mannich reaction of α -hydroxy ketones.



Trost utilized α -hydroxy acetophenone in a direct Mannich reaction catalyzed by dinuclear zinc Lewis acid complex **105**. Phosphinoyl imines **106** react with the hydroxyketone nucleophile **107** to deliver *trans*-adducts **108** with exceptional enantioselection. However, high levels of diastereoselection weren't observed for all substrates. It was also observed that *N*-Boc imines deliver amino alcohol derivatives with the opposite relative stereochemistry.^{101,102} A significant contribution to this field has been brought by Shibasaki and co-workers. Zinc and indium(III) complexes with the linked BINOL ligand **109** were shown to be excellent catalysts in the direct glycolate Mannich reaction.^{103–106} Similar to the observation made by Trost, a correlation between the *syn-anti* stereoselection and the protecting group on the imine nitrogen was noted.¹⁰⁵ Phosphinoyl and tosyl imines yield *syn* adducts,

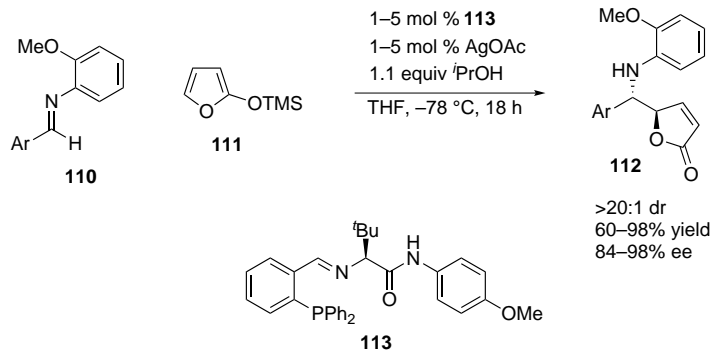
whereas *N*-Boc imines give *anti* products. Reaction conditions tolerate a variety of aryl and alkyl¹⁰⁶ imines as well as glycolate equivalents as nucleophiles and deliver products with good dr and excellent enantioselectivity (Scheme 2.9).

Scheme 2.9. Enantioselective Lewis acid catalyzed glycolate Mannich reactions.



Vicinal aminoalcohols can also be prepared through a vinylogous Mannich reaction. The pioneering work in this area was published by Martin and co-workers in their 1999 publication. They demonstrated vinylogous Mannich reaction of triisopropylsilyloxyfurans with aldimines catalyzed by the (*S*)-BINOL– $\text{Ti}(\text{O}^i\text{Pr})_4$ complex that produces *syn*-aminoalcohol derivatives in up to 44% ee.¹⁰⁷ A vast improvement upon this reaction was brought about by the groups of Hoveyda and Snapper. In presence of AgOAc and amino acid derived phosphine **113**, commercially available siloxyfuran **111** engages with aldimines in an asymmetric vinylogous Mannich reaction.^{108,109} The reaction protocol is very simple and doesn't require anhydrous conditions or solvents (Scheme 2.10). Later the scope of this reaction was extended to alkyl imines formed in situ in a three component reaction between alkyl aldehydes, aniline and siloxyfuran to deliver vinylogous Mannich products as a single diastereomer and often in nearly enantiopure form.¹¹⁰

Scheme 2.10. Hoveyda's silver-catalyzed vinylogous Mannich reaction of siloxyfurans.

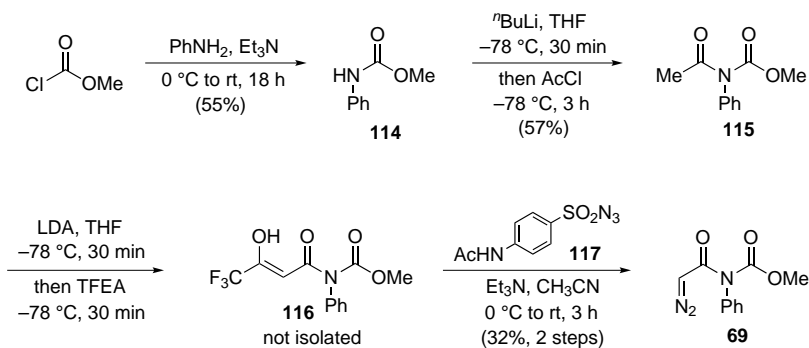


2.2 Diastereoselective Brønsted acid-catalyzed glycolate Mannich reaction

2.2.1 Large scale synthesis of α -diazo imide

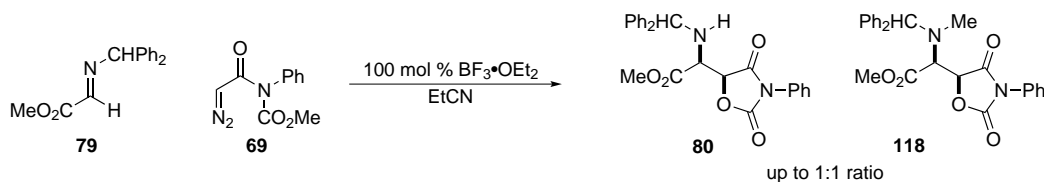
Scheme 2.11 depicts our initial synthesis of the α -diazo imide **69** which is based on the procedure reported by Doyle. It commences with the synthesis of the methyl phenyl-carbamate **114** from aniline and methyl chloroformate in 57% yield after recrystallization. Acetylation of **114** with acetyl chloride delivered *N*-acetyl derivative **115** in 77% yield. The lithium enolate of **115** generated with LDA was reacted with 2,2,2-trifluoroethyl trifluoroacetate (TFEA). The intermediate enol **116** is not purified, and is immediately subjected to the diazo transfer reaction with 4-acetamidobenzenesulfonyl azide (*p*-ABSA) **117** to deliver α -diazo imide **69** in 32% yield over two steps.⁷⁰

Scheme 2.11. Small scale preparation of α -diazo imide **69**



Reaction conditions applied in the reaction of α -diazo imide **69** with imine **79** didn't translate well to other substrates. The main problem was a subsequent reaction that produced *N*-alkyl transfer product **118** next to **80**. We hypothesized that by increasing the size of the carbamate this undesired pathway will be suppressed. Indeed, when α -diazo imide **119** with 2-propyl carbamate was used, *N*-alkyl transfer product was no longer observed (Table 2.1).⁷⁰

Scheme 2.12. Alkyl transfer side reaction of α -diazo imide addition to imines.



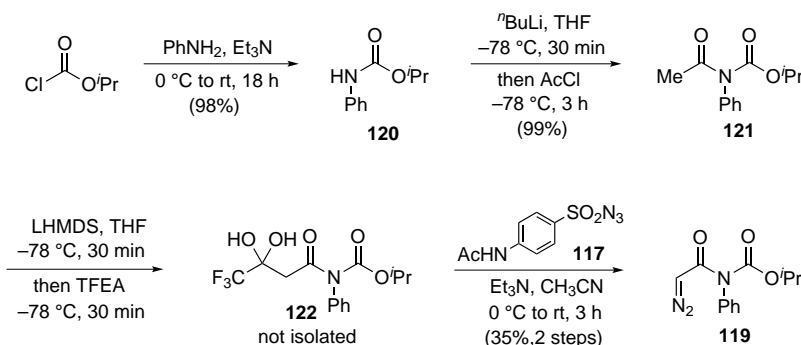
One challenge of large scale preparation of α -diazo imide **69** was the preparation of the active fluorinated intermediate **116**. It is not stable to common purification techniques. Therefore, near complete conversion of precursor **115** must be achieved for the subsequent step to be successful. If unreacted **115** is present after the diazo transfer step, it is impossible to separate it from the diazo product by conventional chromatography techniques. Additionally, purification of **69** required chromatography at 0 °C in order to suppress silica gel promoted decomposition (*vide infra*).

Before investigating the *syn*-glycolate Mannich reaction in more detail, our goal was to establish a reliable preparative protocol for the synthesis of α -diazo imide **119**. The synthesis of acetylated intermediate **121** in nearly quantitative yield without purification was achieved by acylation of aniline with isopropyl chloroformate at room temperature. We established that crystallization of the isopropyl phenyl carbamate (**120**) was not necessary—after aqueous work-up, the purity of the crude product exceeded 97% by gas chromatography. The acetylation reaction proceeds without any sign of side-products but suffers from incomplete conversion at -78 °C. Warming the reaction mixture to room temperature drove the reaction to completion and afforded *N*-acetyl imide **121** in nearly quantitative yield without the need for chromatography (> 97% purity by GC).

A second challenge in the preparation of fluorinated intermediate **122** was overcome by substitution of lithium diisopropylamide with lithium hexamethyldisilazide. Although careful temperature control normally provides full conversion of **121**, attempts to perform this reaction at a scale larger than 25 g were unsuccessful. Straightforward trituration with a nonpolar organic solvent, such as hexanes, effects the removal of **121**, should incomplete

conversion occur in this step. Spectroscopic data of the solid obtained by trituration were in agreement with the hydrate of the trifluoromethyl ketone and not the enol form observed by Doyle (Scheme 2.13).²³

Scheme 2.13. Large scale preparation of α -diazo imide **119**



Although the yield of the diazo transfer remained lower than reported examples, the desired diazo imide can be prepared as a pure crystalline solid, as determined by combustion analysis.¹¹¹ The technique used for purification of the final product also limits the scale of the reaction. We have found that the rate of decomposition of the α -diazo imide during chromatography was slow when silica gel was deactivated with triethylamine. This modification eliminated the use of a custom-made jacketed flash column.

The nucleophilic carbamate moiety of the α -diazo imide is its key innovative feature for cascade reaction development. However, its use is not without complication. As we have shown, nucleophilic additions can be followed by cyclization. But at the same time, under acidic conditions, the α -diazo imide can undergo self-cyclization to oxazolidine dione **123**. When isopropyl 2-diazoacetyl(phenyl)carbamate (**119**) alone is subjected to triflic acid at room temperature, oxazolidine dione **123** forms exclusively (Figure 2.2). Alternatively, when **119** is treated with silica gel in ethyl acetate, carbonate **124** forms as a single product. We postulate that both by-products share the same intermediate, the orthoester **125**.¹¹² After protonation 5-*exo*-tet cyclization leads to an oxonium intermediate which can be trapped in the presence of water. Proton transfer to isopropoxide, collapse of the tetrahedral intermediate and elimination of 2-propanol leads to **123**. If proton transfer occurs to the amide nitrogen instead, collapse of the tetrahedral intermediate affords carbonate **124** (Figure 2.2).

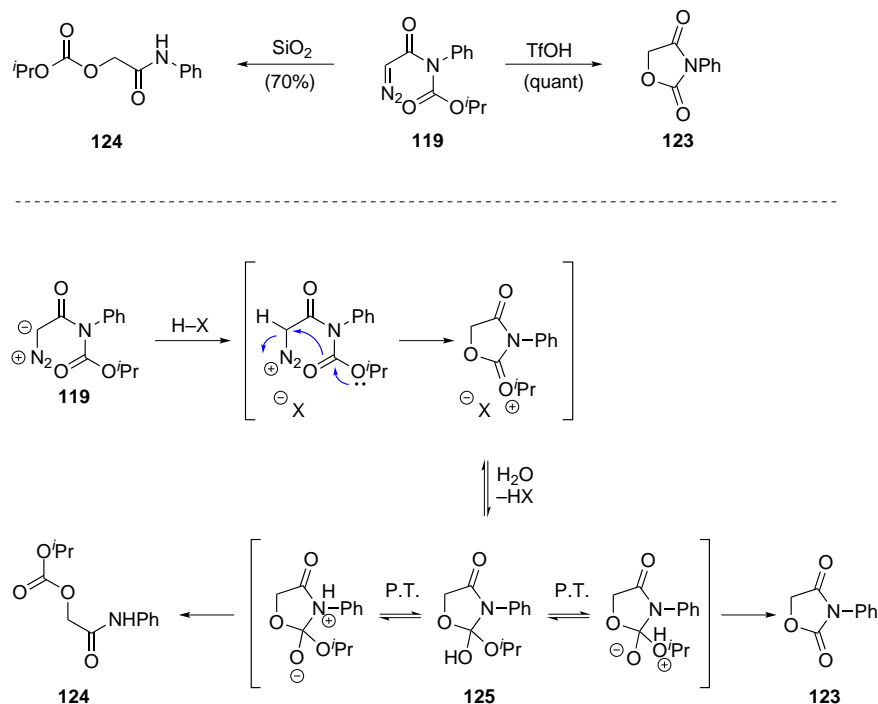


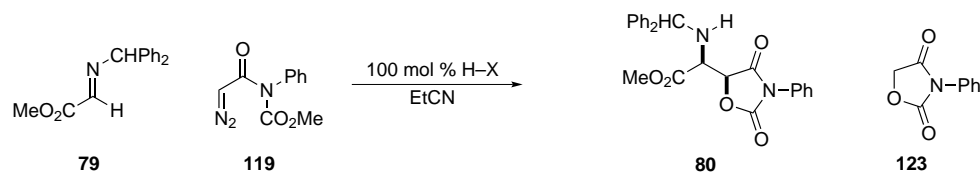
Figure 2.2. Decomposition pathways of α -diazo imide.

2.2.2 Optimization of reaction conditions and substrate scope

Through a series of experiments we established optimal conditions for *syn*-glycolate Mannich reaction of α -diazo imide **119** and imine **79**. A screen of Brønsted acids revealed that acids with pK_a values* below -10 perform best (Table 2.1, entries 1–3). Acids within a pK_a range of -10 to 2 are still able to promote the reaction but at the cost of competitive decomposition of the diazo imide which decreases yield dramatically (entries 4, 5). The diazo imide is slowly converted to oxazolidinone **123** when exposed to a Brønsted acid in the absence of imine (see section 2.2.1). Weak acids (pK_a above 3) were not able to promote the reaction (entries 6–9). Additionally, the rate of α -diazo imide decomposition was also very slow when using weak Brønsted acids such as benzoic acid. Even after 24 h at rt, diazo **119** was still present in the reaction mixture. Although HBF_4 delivered the product in highest yield, TfOH provided an optimal combination of reactivity, availability, convenience (readily dried, distilled, and measured as a liquid), and isolated product yield (entry 2).

We also investigated nitrogen protecting groups on the imine substrate since the nature of this substituent will determine the azomethine proton affinity and the basic character of the nitrogen in the product oxazolidinone. We chose derivatives of 4-chlorobenzaldehyde

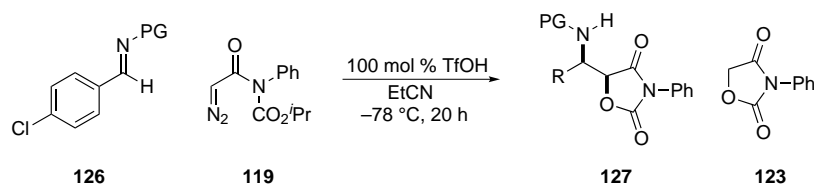
*Values in water.

Table 2.1. *syn*-Glycolate Mannich reaction: Brønsted acid survey.^a

entry	X-H	T (°C)	time (h)	conv (%)	yield ^b (%)
1	HBF ₄	-78	1	100	83
2	TfOH	-78	1	100	76
3	Tf ₂ NH	-78	1	100	71
4	TFA	-78	1	65	42
5	TsOH	-78	1	100	43
6	PhCO ₂ H	rt	24	<5	-
7	AcOH	rt	24	<5	-
8	PPTS	rt	24	<5	-
9	NH ₄ Cl	rt	24	<5	-

^aAll reactions were 0.15 M in imine and used 1.2 equiv of diazo imide. ^bIsolated yield. ^cProduct not isolated (40% conversion measured by ¹H NMR).

126 because it allowed us to prepare a large number of imines. Overall, the benzhydryl group is optimal, delivering product in 59% yield and 10:1 dr (Table 2.2, entry 1). The bulkier trityl group resulted in an imine that is completely unreactive towards diazo **119** (entry 2). Electron rich protecting groups also lower the reactivity of the imine (entries 3, 4 and 6). Phenyl imine exhibited nearly the same conversion and yield as benzhydryl imine (entry 5) but the degree of diazo decomposition was much higher. Full imine conversion and slightly higher yield was observed for *N*-Boc imine but at the cost of diastereoselection (entry 9). These trends suggest a balance between azomethine activation by the nitrogen substituent and the Brønsted acid activating agent. Although a DPM group provides little azomethine polarization it should be readily protonated, succumbing to the full activation potential of the proton. Conversely, a carbamate provides substantial native azomethine polarization. Binding to the proton may be weaker but the combined effect lowers the activation barrier. The reasons for the large difference in diastereoselection, however, are less clear.

Table 2.2. Screen of *N*-protecting group on the imine substrate.^a

entry	PG	conv. (%)	yield (%)	dr ^b (%)	127:123^c
1	Ph ₂ CH	67	59	10:1	>20:1
2	Ph ₃ C	–	–	–	>1:20
3	PhCH ₂	52	19	10:1	1:1
4	PMB	53	22	10:1	1:2
5	Ph	71	50	10:1	1:1
6	PMP	8	4	–	1:10
7	allyl	53	4	–	1:10
8	2-pyridyl	38	15	2:1	1:1
9	Boc	100	16	2:1	4:1
10	Ts	–	–	–	–

^aAll reactions were 0.15 M in imine and used 1.2 equiv of diazo imide. ^bIsolated yield. ^cDetermined by ¹H NMR.

Optimization studies suggest that glyoxal-derived imines are more reactive than simple aldimines. We prepared a series of α -keto imines and employed them in the *syn*-glycolate Mannich reaction as a complement to aryl imines. Substrates **128–134** were synthesized from the corresponding hydrates (Table 2.3). Aryl derivatives were accessed from the oxidation of various aryl methyl ketones (method A). Aliphatic glyoxals were prepared as their hydrates by DMDO oxidation of the corresponding diazoketones according to a reported procedure (method B).¹¹³

Table 2.3. Synthesis of α -keto imines

entry	R	imine	yield (%)	entry	R	imine	yield (%)
1		128	68	5		132	99
2		129	43	6		133	65
3		130	45	7		134	65
4		131	69				

Table 2.4 is representative of the scope of the *syn*-glycolate Mannich reaction. Aryl α -keto imines with both electron rich and electron poor substituents provided oxazolidine dione products with high diastereoselection and good to excellent yield (entries 2–4). Heteroaromatic substrate **131** yielded the adduct with lower diastereoselection at the 6:1 level (entry 5). Diastereoselection was even lower for α -keto imines bearing alkyl substituents (entries 6–8) but this was compensated by the nearly quantitative yield. Characteristic crystallinity of the oxazolidine diones allowed a single diastereomer of **139** to be isolated by recrystallization in 62 % yield without need for chromatography (Scheme 2.14). Lower reactivity was observed across the array of aryl imines (entries 9–13). Despite an extended reaction time (18 hours), yields were generally lower with dr maintained at the 10:1 level.

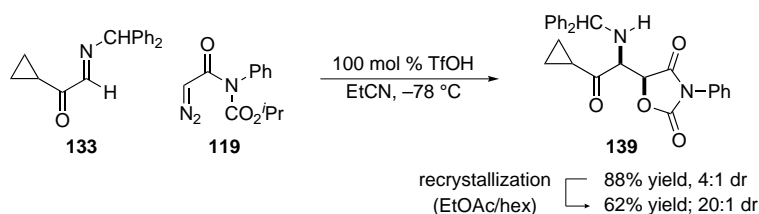
Scheme 2.14. Preparative procedure for the synthesis of the **139**.

Table 2.4. Scope of the *syn*-glycolate Mannich reaction.^a

entry	R	product	time (h)	dr	yield (%)
1		80	1	>20:1	76
2		135	1	>20:1	79
3		136	1	>20:1	81
4		137	1	>20:1	72
5		138	1	6:1	80
6		139	1	4:1	88
7		140	1	4:1	98
8		141	1	1:1	97
9		142	18	10:1	69
10		143	18	10:1	48
11		144	18	10:1	53
12		145	18	10:1	37
13		146	18	10:1	36

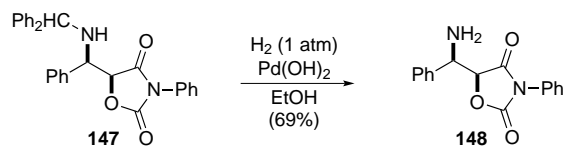
^aAll reactions were 0.15 M in imine and used 1.2 equiv of diazo imide.

^bIsolated yield. ^cDetermined by ¹H NMR.

2.2.3 Functionalization of the oxazolidine dione ring

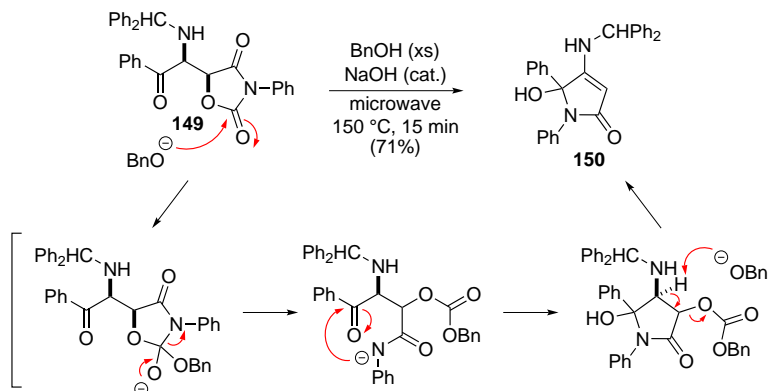
The oxazolidine diones produced by this method are masked α -hydroxy- β -amino acids. In order to access this functional motif, the oxazolidine dione ring has to be hydrolyzed and the diphenylmethyl group removed. Deprotection of the secondary amine can be achieved under mild conditions. Hydrogenation of compound **147** in the presence of palladium(II) hydroxide in ethanol delivers the free amine **148** in 71 % yield (Scheme 2.15).

Scheme 2.15. Hydrogenation of the benzhydryl group.



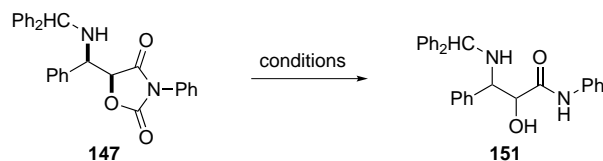
Functionalization of the oxazolidine dione ring proved more challenging. When the oxazolidine dione **149** was treated with a catalytic amount of sodium hydroxide in benzyl alcohol in a microwave reactor, no reaction was observed at 120 °C. After heating for 15 min at 150 °C, the α,β -unsaturated cyclic amide **150** was isolated as a single compound in 51 % yield (Scheme 2.16). A possible mechanism for this reaction is shown in Scheme 2.16 where the carbamate carbonyl might be more reactive toward nucleophiles than the amide carbonyl. Hydrolysis of the carbamate followed by cyclization of the amide nitrogen onto the ketone and subsequent elimination of the carbonate delivers compound **150**, where both stereocenters set during the *syn*-glycolate Mannich reaction are lost.

Scheme 2.16. Preliminary result of oxazolidine dione hydrolysis



When the same conditions were applied toward compound **147**, the desired α -hydroxy amide **151** was observed. Unfortunately, the diastereomeric integrity of the parent molecule was low; nearly a 1:1 ratio of the two diastereomers was isolated (Table 2.5, entry 1). An identical result was obtained when oxazolidine dione **147** was treated with lithium methoxide at room temperature. Full conversion of the substrate was observed after just 15 min, but *syn* stereochemistry wasn't retained (entry 2). The diastereomers were separated and fully characterized to confirm the outcome of the reaction. We hypothesized that prior to nucleophilic attack, a deprotonation–protonation occurs which is responsible for the loss of diastereoselection. Thermal ring opening was also unsuccessful. Heating of **147** in methanol and ethanol in a microwave reactor at 150 °C and 170 °C, respectively, failed to deliver the desired product (entries 3 and 4). Despite full conversion, only decomposition products were observed in the crude reaction mixture when analyzed by ^1H NMR. The same results were obtained when oxazolidine dione was heated at 125 °C in methanol saturated with HCl (entry 5). Heating with benzylamine in the microwave at 100 °C for 1 hour, a conversion of 90 % was determined by NMR analysis but still the final product formed in nearly 1:1 dr (entry 6). A saturated solution of ammonia in methanol at 80 °C delivered aminoalcohol **151** in 2:1 dr (entry 7).

Table 2.5. Opening of oxazolidine dione using alcohol nucleophiles.



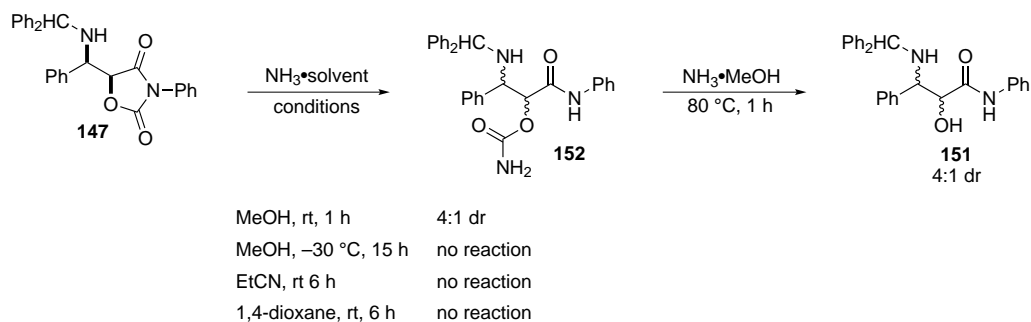
entry	conditions	conv (%)	dr
1	BnOH, NaOH, 150 °C, 15 min	80	1:1
2	MeOH, LiOH, rt, 15 min	100	1:1
3	MeOH, 150 °C, 1 h	100	1:1
4	EtOH, 170 °C, 1 h	100	1:1
5	MeOH, HCl, 125 °C, 1 h	100	1:1
6	BnNH ₂ , 100 °C, 1 h	90	1:1
7	NH ₃ · MeOH, 80 °C, 15 min	80	2:1

When the reaction with ammonia was carried out at room temperature, carbamate **152** in 4:1 dr was the major product together with traces of aminoalcohol **151** (Scheme 2.17). Isolation of **152** was unsuccessful and there is no analytical data to support structure **152**.[†] How-

[†]Our later experience with NH₃ · MeOH conditions showed that the product of oxazolidine dione opening

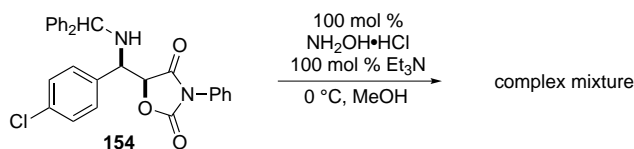
ever, when **152** was subjected to ammonia in methanol at 80 °C for 1 h, the relative amount of **152** decreased significantly and the major product became a 4:1 mixture of aminoalcohol **151**, albeit with incomplete conversion. When the reaction temperature was –30 °C, compound **147** was only sparingly soluble, and no reaction was observed. Use of a polar protic solvent appears to be necessary since reactions with ammonia in other solvents, such as propionitrile and dioxane, resulted in no reaction even at room temperature (Scheme 2.17).

Scheme 2.17. Opening of oxazolidine dione ring using alcohol solution of ammonia.



The potent nucleophilic reactivity of hydroxylamine evident in many transformations is thought to arise as a consequence of the α -effect,^{114,115} a behavior observed in a variety of nucleophiles which possess a heteroatom in the α position to the attacking nucleophilic atom. We hypothesized that hydroxylamine might be a better nucleophile than ammonia and the rate of addition might then dominate over deprotonation. Unfortunately, when **153** was exposed to hydroxylamine only partial conversion was observed and the desired product wasn't observed in the ¹HNMR of the crude reaction mixture (Scheme 2.18).

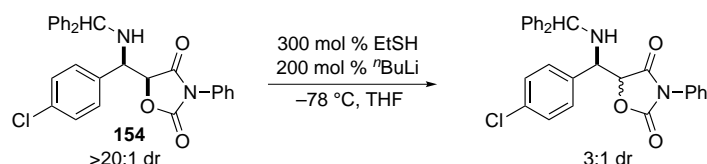
Scheme 2.18. Opening of the oxazolidine dione using more reactive nucleophiles.



is a methyl carbonate, not primary carbamate, see section 3.4.3

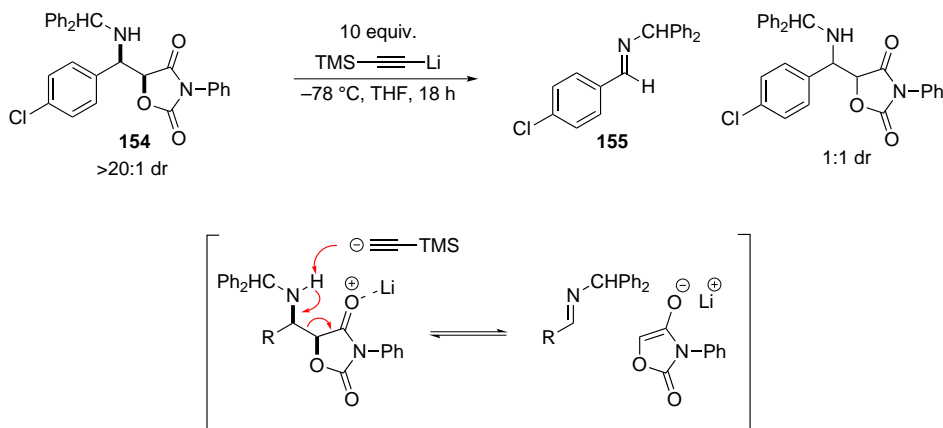
Sulfur nucleophiles provide enhanced nucleophilicity without significant increase in basicity. When diastereomerically pure oxazolidine dione **153** was treated with ethyl thiolate at $-78\text{ }^{\circ}\text{C}$ overnight no ring opening was observed. Although starting material was fully recovered, it was a mixture of both diastereomers in a 3:1 ratio (Scheme 2.19).

Scheme 2.19. Opening of oxazolidine dione with ethyl thiolate.



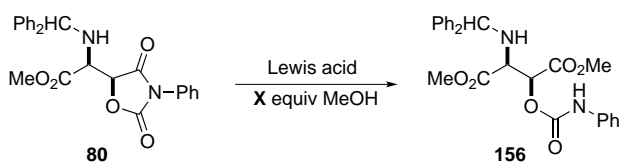
We then turned to carbon nucleophiles but reagents such as methyl magnesium bromide provided a complex mixture of products. In a reaction where **154** was stirred with 10 equiv of TMS lithium acetylide at $-20\text{ }^{\circ}\text{C}$ for 24 h, the ^1H NMR of the crude reaction mixture showed traces of both diastereomers of the starting material and benzhydryl imine **155** as a major product. *retro*-Mannich products have never been observed in diazo **119** additions to imines but this result clearly demonstrates that the retro pathway can operate under certain conditions. A mechanism explaining the outcome of the reaction is shown in Scheme 2.20.

Scheme 2.20. Opening of oxazolidine dione with lithium acetylide.



Clearly, the Brønsted basicity of the reagents used, as well as a potential *retro*-Mannich pathway, is responsible for a decrease in the diastereomeric ratio during the ring opening of oxazolidine dione. We therefore turned to Lewis acid activation of the oxazolidine dione ring towards milder nucleophiles such as methanol. A screen of various Lewis acids is presented in Table 2.6. When oxazolidine dione **80** was exposed to methanol in the presence of 200 mol % of titanium(IV) isopropoxide, 30 % conversion to the diester **156** was observed (entry 1). Increased amounts of titanium reagent as well as higher reaction temperatures didn't improve conversion (entries 2 and 3). Shortly after titanium(IV) tetraisopropoxide is added to the reaction mixture, a copious amount of white precipitate forms. We hypothesized that in the presence of a large excess of methanol, solid titanium(IV) tetramethoxide forms, and the Lewis acid is in fact removed from the reaction medium. Application of $\text{Ti}(\text{O}^i\text{Pr})_4$ in THF with 50 equivalents of methanol was unsuccessful (entry 4). Aluminum Lewis acids are considered to have relatively similar reactivity to titanium Lewis acids but when aluminum-based reagents of varying Lewis basicity were evaluated, no sign of product was observed (entries 5–7).

Table 2.6. Lewis acid-assisted opening of oxazolidine dione ring.

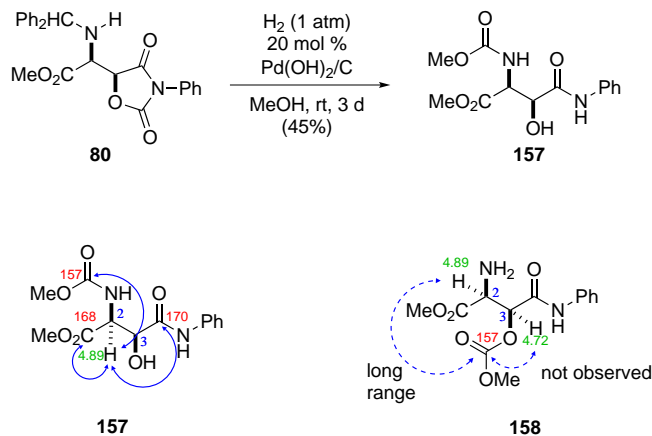


entry	Lewis Acid	x (equiv)	conv ^a (%)
1	200 mol % $\text{Ti}(\text{O}^i\text{Pr})_4$	excess	30 (16)
2	200 mol % $\text{Ti}(\text{O}^i\text{Pr})_4$	excess	30
3	500 mol % $\text{Ti}(\text{O}^i\text{Pr})_4$	excess	30
4	200 mol % $\text{Ti}(\text{O}^i\text{Pr})_4$	50	–
5	100 mol % AlClEt_2	2	–
6	100 mol % AlCl_2Et	2	–
7	100 mol % AlCl_3	2	–

^aMeasured by ^1H NMR.

On one occasion, when hydrogenation of the oxazolidine dione **80** in the presence of 20 mol % of Pearlman's catalyst was carried out for a prolonged period of time (20 h), 15 % conversion to the ring opening product **157** was observed, without any sign of epimerization. Interestingly, when **80** was subjected to the same conditions without a hydrogen source, the reaction didn't take place, suggesting that ring opening occurs after DPM deprotection. This is probably not due to increased reactivity of the primary amine compared to *N*-DPM compound **80**, but simply to relative solubility. Oxazolidine diones have limited solubility in alcohols at room temperature and once the benzydryl group is removed and the oxazolidine dione free base is in solution, the rate of the regioselective methanolysis increases. If the reaction was carried out for 3 days, aminoalcohol **157** is produced in 45 % yield as a single diastereomer. If the reaction is allowed to stir for a longer time, slow decomposition of the product was observed (Scheme 2.21).

Scheme 2.21. Opening of the oxazolidine dione **80** and structural assignment of the methanolysis product.



The *O,N*-acyl transfer product **157** is proposed based on the analysis of the C–H heteronuclear correlations. A new methyl group correlates to the carbonyl carbon at 152 ppm which is more consistent with the structure **157** rather than **158**. The carbonyl shift for both the carbamate and the carbonate cannot be used for the assignment because both are expected in the 150–160 ppm range. However, the HMBC correlation between H2 at 4.89 ppm to all three carbonyl carbons supports structure **157**. Additionally, in structure **158**, correlation between H2 and carbonyl at 157 ppm is unlikely due to the 4 bond distance. Also, lack of correlation between H3 and the carbonate carbon at 157 ppm suggests that structure **158** is not plausible (Scheme 2.21).

2.3 Development of enantioselective glycolate Mannich reaction

2.3.1 Evaluation of chiral Brønsted acids in reactions of α -diazo imide with azomethines

The Brønsted acid catalyzed *syn*-glycolate Mannich reaction is a novel method for the diastereoselective synthesis of *syn*-1,2-amino alcohols. An enantioselective variant of this reaction is a logical extension of this methodology. As it was presented in section 1.2.2 there are many efficient and stereoselective reactions of diazo compounds and azomethines catalyzed by chiral Brønsted acids, and development of the enantioselective glycolate Mannich reaction that utilizes the chiral Brønsted acid catalysts became our next goal.

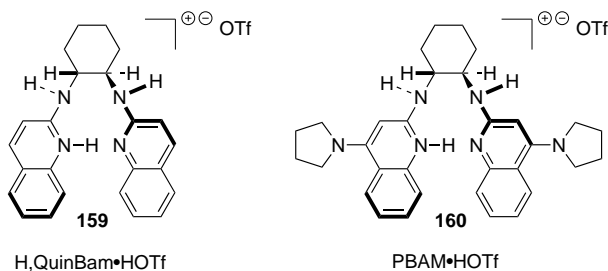
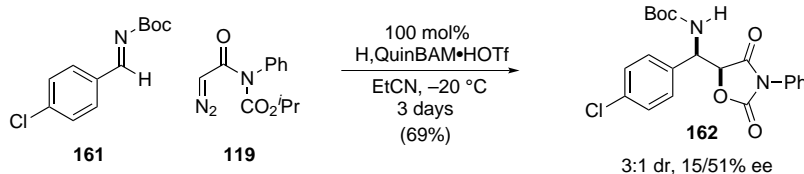


Figure 2.3. Bis(amidinium) (BAM) catalysts for enantioselective aza-Henry reaction.

In reaction of α -diazo imide with *N*-Boc imines we saw a moderate reactivity and diastereoselection when triflic acid was used as a catalyst (Table 2.2, entry 9). We also knew that *N*-Boc imines can be successfully activated towards nucleophilic addition using chiral proton catalysts such as H,QuinBam (**159**) or PBAM (**160**) (Figure 2.3).^{116–118} This prompted us to evaluate chiral Brønsted catalysts in the *syn*-glycolate Mannich reaction. No reaction was observed when benzaldimine **161** was reacted with α -diazo imide **119** in presence of catalyst **159** at -78°C . Reaction was warmed to -20°C and after 3 days 6% of the oxazolidine dione **162** was isolated in 3:1 dr (Scheme 2.22). Enantioselection measured for the major diastereomer was only 15% (51% for the minor diastereomer). Reactions carried out with substoichiometric amount of the catalyst failed to show catalyst turnover.

To gain a broader perspective on the type of organocatalyst needed for glycolate Mannich reaction, we evaluated several popular catalysts based on axially chiral phosphoric acid (**163** and **34**), and chiral thiourea catalysts **164** and **165** (Scheme 2.23). To our disappointment, in all cases no reaction was observed after 18 h at room temperature. Reaction catalyzed by thiourea **165** was carried out in CDCl_3 and observed by ^1H NMR. Throughout reaction time

Scheme 2.22. Glycolate Mannich reaction promoted by chiral Brønsted acid.

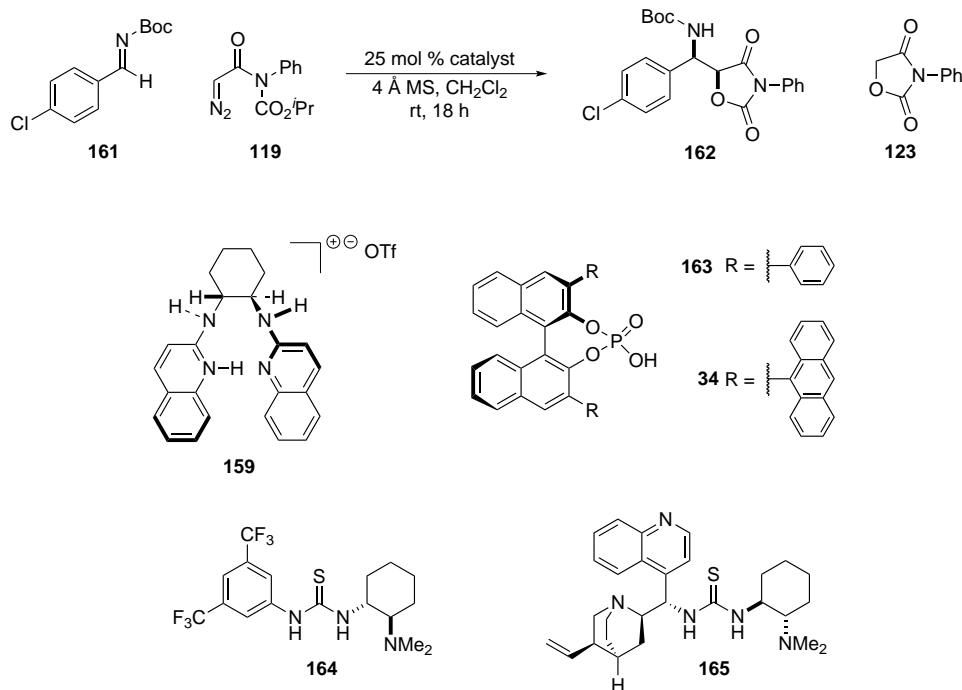


imine and α -diazo imide **119** remained unreacted. This is in agreement with our previous study of the correlation between Brønsted acid strength and reaction outcome (Section 2.2.2). Imine activation can only be achieved with very strong Brønsted acids without significant protonative diazo decomposition. Moderately strong Brønsted acids deliver a mixture of oxazolidinone product **162** and oxazolidinone by-product **123**. Weak acids can neither activate imine nor decompose α -diazo imide. Clearly the thiourea family of catalysts falls into the latter category. The ^1H NMR spectrum of the reaction carried out in CDCl_3 didn't show characteristic singlet at 4.80 ppm corresponding to the methylene protons of compound **123**. Although phosphoric acids **163** and **34** are stronger which is evidenced by presence of the by-product **123** in the ^1H NMR spectrum of the crude reaction mixture, they don't possess sufficient strength to activate the imine towards productive carbon-carbon bond formation. We concluded that Brønsted acid catalyzed enantioselective glycolate Mannich reaction is unlikely to be developed with these acids simply because of the high potential for protonative decomposition of diazo imide **119** that competes with effective azomethine activation. However, it is important to understand that the factors that affect the rate of protonative decomposition remain unclear.

2.3.2 Evaluation of Lewis acids in the *syn*-glycolate Mannich reaction

The results obtained with the chiral Brønsted acids as catalysts were disappointing (section 2.3.1) so in order to extend the area of our search for an effective chiral catalyst we performed a survey of Lewis acidic metal catalysts that could serve as a foundation for the development of an enantioselective reaction. A series of Lewis acids was evaluated in the reaction of the *N*-benzhydryl α -imino ester **79** and α -diazo imide **119**. Although titanium(IV) tetraisopropoxide didn't promote the reaction, more Lewis acidic titanium(IV) tetrachloride delivered *syn*-oxazolidinone dione **80** in 32% yield (Table 2.7, entry 8). Boron trifluoride etherate promoted the reaction to a much higher degree and the product was isolated in 79% yield (entry 9). It is important to note that when the reaction was carried at $-20\text{ }^{\circ}\text{C}$ for 16 h, a mixture of diastereomers was isolated in 93% yield but now in favor of the *anti*-

Scheme 2.23. Chiral Brønsted acid screen



diastereomer (entry 10). It is not clear how the *anti*-diastereomer forms but it appears that the *syn*-stereoisomer is a kinetic product and forms exclusively when reaction time is relatively short (Table 2.7, entry 9). Recently Aggarwal and co-workers proposed that BF₂OTf, generated from BF₃ · OEt₂ and TMSOTf is a stronger Lewis acid than BF₃.¹¹⁹ When we evaluated this reagent in the *syn*-glycolate Mannich reaction, slight enhancement in yield was observed (Table 2.7, entry 11). Aggarwal also proposed that BF₃ · OEt₂, TMSOTf, BF₂OTf and TMSF exist in equilibrium (Figure 2.4) and therefore it is possible that TMSOTf is the active Lewis acid under these conditions. When TMSOTf was used in the reaction, the oxazolidine dione product was isolated in 93% yield (Table 2.7, entry 12). Iron(III) chloride was also an active catalyst but required longer reaction time at room temperature. The reaction catalyzed by copper(II) triflate and indium(III) triflate afforded oxazolidine dione **80** in 65% and 80% yield respectively (entry 14 and 15).

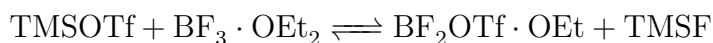
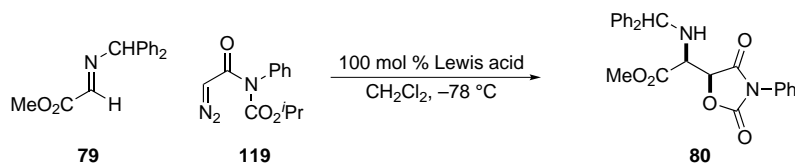


Figure 2.4. Equilibrium reaction between BF₃ · OEt₂ and TMSOTf.

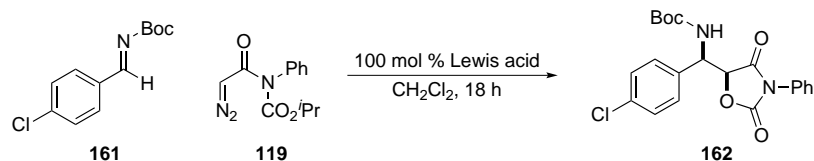
Table 2.7. Evaluation of Lewis acid catalysts in the *syn*-glycolate Mannich reaction.^a

entry	Lewis acid	T (°C)	time (h)	<i>syn:anti</i>	yield ^b (%)
1	AgOTf	rt	6	–	–
2	(CuOTf) ₂ · toluene	rt	24	–	–
3	Sc(OTf) ₃	rt	24	–	–
4	Mg(OTf) ₂	rt	24	–	–
5	Zn(OTf) ₂	rt	24	–	–
6	Yb(OTf) ₃	rt	24	–	–
7	Ti(O ^{<i>i</i>} Pr) ₄	rt	24	–	–
8	TiCl ₄	-78	24	>20:1	32
9	BF ₃ · OEt ₂	-78	1	>20:1	79
10	BF ₃ · OEt ₂	-78	16	1:2	93
11	BF ₂ OTf · OEt ₂	-78	1	>20:1	81
12	TMSOTf	-78	1	>20:1	93
13	FeCl ₃	rt	15	>20:1	72
14	In(OTf) ₃	-78	6	>20:1	80
15	Cu(OTf) ₂	-78	2	>20:1	65

^aAll reactions were 0.15 M in imine and used 1.2 equiv of diazo imide.

^bIsolated yield.

During development of the *syn*-glycolate Mannich reaction, *N*-Boc benzaldimines showed slightly better reactivity towards α-diazo imide **119** but moderate diastereoselection. We decided to also evaluate *N*-Boc imine **161** in Lewis acid catalyzed addition of α-diazo imide **119** (Table 2.8). Lewis acids based on Mg(II), Yb(III), La(III) and Ti(IV) didn't promote the reaction even at room temperature (Table 2.8, entries 1–5). Scandium(III) triflate (entry 6) was able to promote the reaction at -20 °C but the product formed in 1:1 dr. Modest reactivity was observed when the reaction was promoted by BF₃ · OEt₂ and Zn(OTf)₂ which yielded oxazolidine dione in 48 % and 43 % yield, respectively (Table 2.8, entries 7 and 9). Surprisingly, TMSOTf wasn't a better Lewis acid than BF₃ · OEt₂ and delivered the desired product only in 39 % yield and 1:1 dr (entry 8). Copper(II) triflate and indium(III) triflate showed similar activity affording **162** in 59 % and 55 % yield, respectively (Table 2.8).

Table 2.8. Evaluation of Lewis acid catalysts in the *syn*-glycolate Mannich reaction.^a

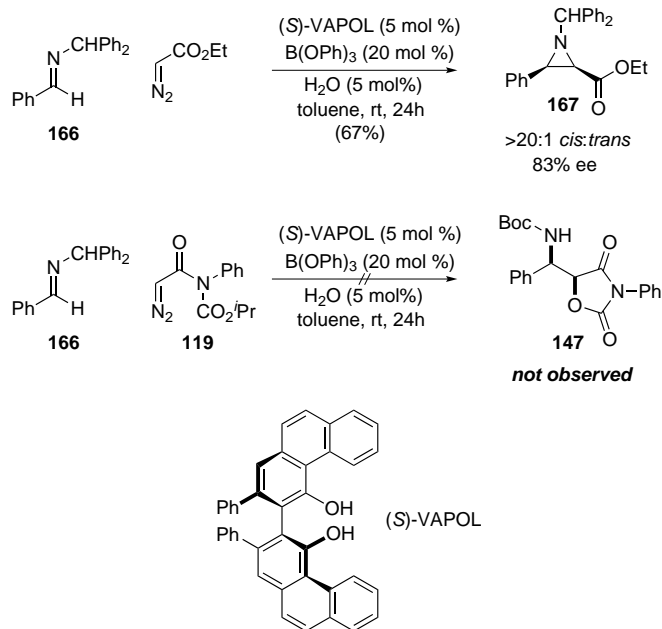
entry	Lewis acid	T (°C)	<i>syn:anti</i>	yield ^b (%)
1	Mg(OTf) ₂	rt	–	–
2	Yb(OTf) ₃	rt	–	–
3	La(OTf) ₃	rt	–	–
4	Ti(O ^{<i>i</i>} Pr) ₄	rt	–	–
5	TiCl ₄	rt	–	–
6	Sc(OTf) ₃	–20	1:1	nd
7	BF ₃ · OEt ₂	–78	3:1	48
8	TMSOTf	–78	1:1	39
9	Zn(OTf) ₂	–78	3:1	43
10	In(OTf) ₃	–78	3:1	59
11	Cu(OTf) ₂	–78	3:1	55

^aAll reactions were 0.15 M in imine and used 1.2 equiv of diazo imide. ^bIsolated yield.

Encouraged by the fact that BF₃ · OEt₂ performed very well in this reaction we decided to employ α -diazo imide in the enantioselective aziridination conditions developed by Antilla and Wulff.^{53,54} Similarities between the α -diazo imide and ethyl diazo acetate suggested that this chemistry might be a good foundation for the development of the asymmetric variant of the *syn*-glycolate Mannich reaction.

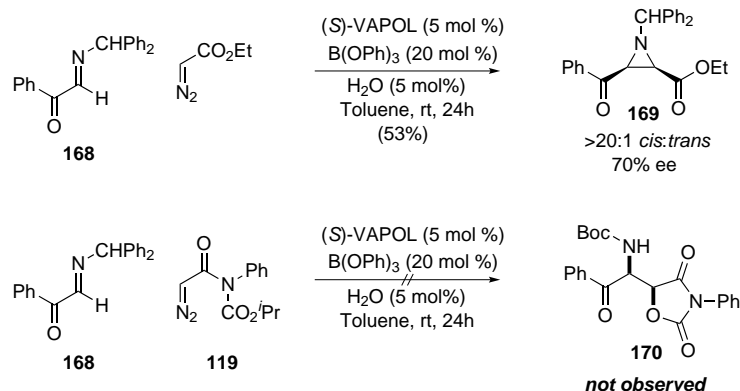
Chiral boron complexes used in this reaction are prepared via a strict protocol. We began with a control experiment to evaluate the degree to which we are able to reproduce the published result. The imine **166** was reacted with ethyl diazoacetate in the presence of the (*S*)-VAPOL–borate Lewis acid (Scheme 2.24) to afford the *cis*-aziridine product **167** in 67% yield and 83% ee (76% yield, 87% ee in original publication⁵⁶). However, when benzaldimine **166** was reacted with α -diazo imide **119** under identical conditions, neither aziridine nor oxazolidine dione **147** was observed in the reaction mixture (Scheme 2.24).

Scheme 2.24. Evaluation of chiral borate complexes in *syn*-glycolate reaction.



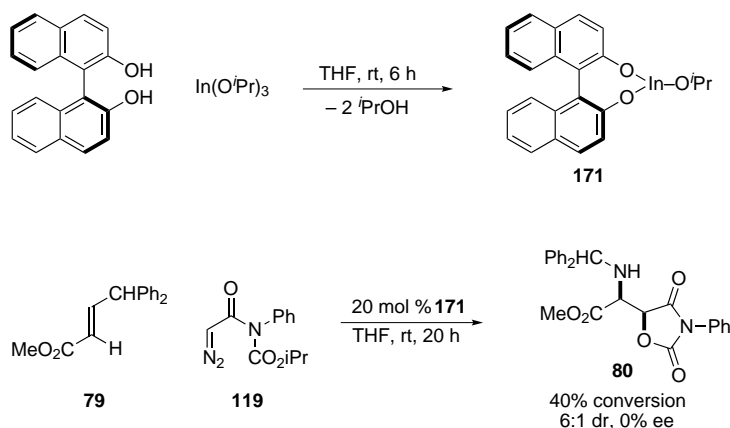
We demonstrated earlier that benzaldimines are substantially less reactive towards α -diazo imide **119** when compared to α -keto imines. It was speculated that low reactivity of the imine resulted in no acquisition of the desired product. To aid the reactivity of the electrophile, we turned our attention to α -keto imine **168**. When reacting **168** with ethyl diazo acetate in presence of a catalytic amount of (*S*)-VAPOL–borate complex, the corresponding *cis*-aziridine **169** forms in 53 % yield and moderate enantioselection (70 % ee, Scheme 2.25). However, when imine **168** was reacted with the α -diazo imide under otherwise identical reaction conditions, the reaction returned only starting materials. Additionally, no reactivity was observed when the reaction mixture was heated to reflux. It is important to note, however, that α -diazo imide **119** appears to be relatively stable under elevated temperatures since only partial decomposition was evident from the ^1H NMR spectrum.

Scheme 2.25. Evaluation of chiral borate complexes in the *syn*-glycolate reaction with glyoxal imines.



Inspired by work of Shibasaki in the area of the Lewis acid-catalyzed asymmetric direct glycolate Mannich¹⁰³ reaction and with our finding that indium is a competent Lewis acid for our reaction (Table 2.7), we turned our attention to indium-based Lewis acids for the development of the diastereo- and enantioselective *syn*-glycolate Mannich reaction. Indium–BINOL or indium–VAPOL complexes prepared from indium(III) triflate catalyzed the reaction to the same extent as In(OTf)₃. The obtained product, however, was racemic. We attribute this partly to the complex preparation procedure. It is possible that upon mixing In(OTf)₃ with the BINOL ligand, triflic acid is generated and can serve as the actual catalyst. On this basis, we hypothesized that indium(III) triisopropoxide should be first mixed with the BINOL ligand, followed by evacuation of the isopropanol under high vacuum and high temperature to generate InOⁱPr–BINOL complex **171** (Scheme 2.26).

Scheme 2.26. Evaluation of indium(III)–BINOL complexes in the *syn*-glycolate reaction.



When such a complex was evaluated as the catalyst in the addition of α -diazo imide to *N*-benzhydryl α -imino ester **79**, the reaction was very sluggish and only 40 % conversion to the product was observed after 20 h (Scheme 2.26). This supported our hypothesis about the nature of the acid catalyst. It seems that in the InO^{*i*}Pr–BINOL complex, Lewis acidity of indium is significantly reduced and the product forms as a racemate. This suggests that the chiral environment around indium metal doesn't provide facial discrimination for an enantioselective reaction. Also, no reaction was observed when *N*-Boc benzaldimine **161** was reacted with α -diazo imide in the presence of complex **171**.

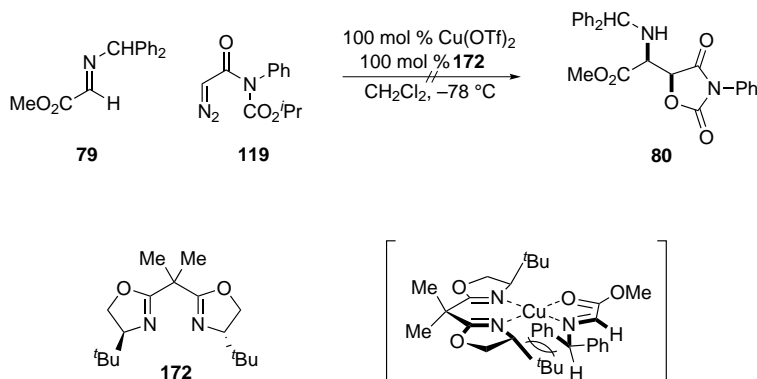
2.3.3 Glycolate Mannich reaction catalyzed by chiral Cu(II)–BOX complexes

There are several reasons for the extensive use of copper Lewis acids in stereoselective transformations: 1) well established and easily predictable coordination geometry about the metal, 2) availability, 3) two oxidation states with two distinct reactivity profiles, and moderate Lewis acidity that can be tuned with a choice of ligands and counter-ions. Copper(II) complexes usually adopt a square planar, square pyramidal, or trigonal bipyramidal geometry, whereas Cu(I) complexes prefer the tetrahedral geometry.¹²⁰ Literature accounts suggest that copper(II)-based catalysts operate as Lewis acid promoters in a very similar manner as boron trifluoride.¹²¹ This similarity appears to be true in the case of our reaction (Table 2.7, entry 9 and 15).

Among privileged ligands for asymmetric synthesis, bis(oxazoline) **172** is widely recognized as a broadly effective chiral ligand for copper(II) salts. Encouraged by the results obtained with Cu(OTf)₂, we wanted to evaluate copper(II) complexes with ligand **172**. We chose iminoester **79**, a substrate that was most reactive in the *syn*-glycolate reaction with a hypothesis that the imine nitrogen, along with the ester carbonyl, will engage in bidentate complexation to the copper center. Unfortunately, no product was observed when copper(II)–**172** complex was used as catalyst. It seems that in presence of bis(oxazoline), the azomethine nitrogen can no longer bind to copper. This could be attributed to steric (large DPM group) or electronic (electron-poor imine) effects. After analyzing the molecular model, we believe that despite involvement of the oxygen of the ester carbonyl in bidentate chelation with copper, the benzhydryl substituent on the imine nitrogen is too sterically demanding to keep the substrate bound to the catalyst as it is shown in Scheme 2.27.

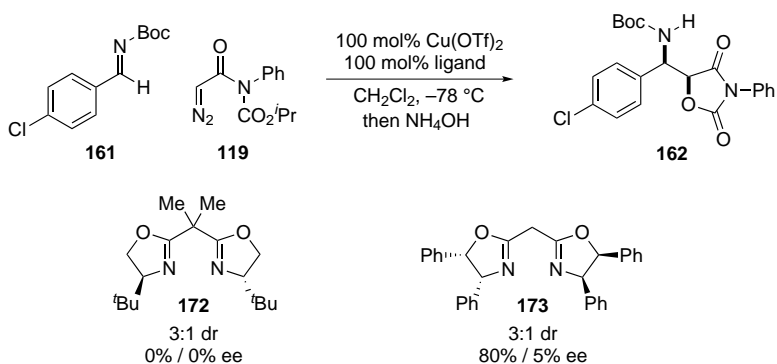
Our previous studies suggest that imine activation can be achieved only for a limited group of substrates. Similar performance of *N*-Boc imines in Cu(OTf)₂ promoted the glycolate Mannich reaction, indicating that the *N*-Boc benzaldimine **161** might be a better substrate for α -diazo imide **119** in the presence of the copper(II)–bis(oxazoline) complex.

Scheme 2.27. Preliminary results of Cu(II)–bis(oxazoline) catalyzed glycolate Mannich reaction of benzhydryl imines.



Although the structure *N*-Boc benzaldimine **161** does not provide additional Lewis base character that could coordinate to the metal center, the steric bulk of *tert*-butyl carbamate might be beneficial for enantioselection. Contrary to the *N*-DPM imine, the *N*-Boc imine reacted with the diazoalkane in the presence of the copper complex with ligand **172** and delivered oxazolidinone **162** as a 2:1 mixture of diastereomers in 30 % yield. Unfortunately, chiral HPLC analysis established that both diastereomers were racemates. Conversely, when carrying this reaction out with bis(oxazoline) **173**, the product was acquired in substantial ee. The major diastereomer formed in 80 % ee; the minor was nearly racemic (Scheme 2.28).

Scheme 2.28. Preliminary results of Cu(II)–bis(oxazoline) catalyzed glycolate Mannich reaction of *N*-Boc benzaldimines.



Ligand **173** not only differed from **172** in capacity towards asymmetric induction, they also behaved differently in this particular reaction. The complex with ligand **172** provided a green color throughout the reaction and upon quench and work-up, the copper was successfully washed away. Characteristic signals for the ligand were observed in ¹H NMR spectrum

of the crude reaction mixture. As for the case of ligand **173**, the solution was green prior to addition of the substrate. Upon addition of the imine and α -diazo imide, the reaction mixture turned brown and eventually purple. The substance responsible for the purple tint was not water soluble nor separable from the product by chromatography. Evidence of the paramagnetic broadening of the proton NMR spectrum suggested that colored impurities might be the result of residual copper. Additionally, recovery of the ligand from the reaction was fruitless.

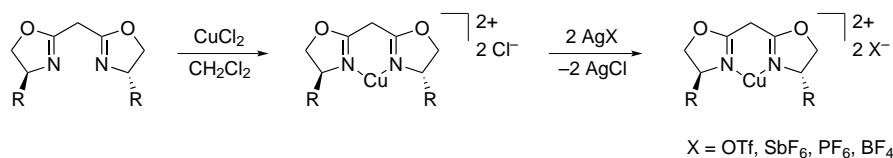
Intrigued by this result we decided to use ligand **173** in substoichiometric amount to avoid high concentration of the by-product and aid purification. However, when 30 mol % of the $[\text{Cu}(\text{Ph}_2\text{BoxH})](\text{OTf})_2$ was used, the concentration of the purple byproduct remained relatively high and the product had to be purified twice by silica gel chromatography. Despite this effort, the faint purple color persisted.

Chiral HPLC analyses were often inconsistent. The purest fractions after silica gel chromatography that contained only the major diastereomer gave ee values up to 95 %. However, combined fractions containing both diastereomers were determined provided the major diastereomer in only 82 % ee. Oxazolidine diones are only slightly soluble in ethanol and since HPLC samples are prepared in an ethanol–hexanes solution, solubility became an issue. We hypothesized that during HPLC sample preparation, racemic oxazolidine dione **162** crystallizes, thereby enriching the mother liquor in one enantiomer. Enantiomeric excess values for the newly formed crystals were low. When the sample was dissolved in hot ethanol and analyzed immediately after cooling to room temperature, consistent ee values were obtained. For reproducibility and accuracy, HPLC samples were prepared in hot ethanol, cooled to room temperature, immediately injected onto the chiral HPLC, and analyzed before any crystallization could occur.

Literature suggests that the role of the counter-ion in the active copper–bis(oxazoline) complex is as important as the structure of the ligand. Combination of the substituents on the oxazoline ring with the nature of the anion imposes a degree of distortion from copper's native square planar geometry, which influences the orientation of substrates inside the chiral environment of the complex. A more dissociated counter-ion can increase the relative Lewis acidity of the copper metal, e.g., copper(II) acetate is less Lewis acidic than copper(II) trifluoroacetate. Additionally, formation of the naked copper Lewis acid is important in transformations that require strong activation of the substrate or the reagent by Lewis acid. For example, when the counter-ions are chlorine, bromine, tetrafluoroborate (BF_4) or triflate TfO, they do not dissociate very easily upon addition of moderately strong Lewis basic donors (ligands). Complete dissociation is observed when the counter-ions are non-coordinating, such as SbF_6 .¹²²

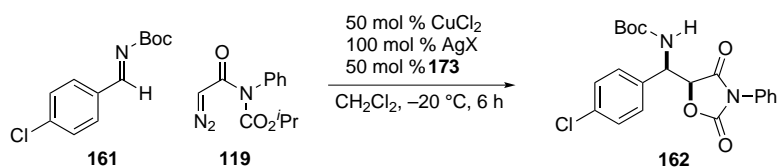
Copper(II) triflate is commercially available, yet copper(II) salts with other counter-ions have to be prepared *in situ* by anion exchange between a CuCl_2 complex and a silver salt of the desired counter-ion. Silver chloride precipitate is removed and the Cu(II)–ligand complex with counter-ion of choice remains in solution (Scheme 2.29).

Scheme 2.29. Preparation of bis(oxazoline) complexes with different counterions.



Stereoselection in α -diazo imide additions to *N*-Boc benzaldimines clearly depends on the counter-ion. Trifluoromethanesulfonate and tetrafluoroborate (Table 2.9, entry 1 and 2) provided the oxazolidine dione product **162** in higher enantioselection (50 % ee and 49 % ee) than non-coordinating hexafluorophosphate (31 % ee) and hexafluoroantimonate (9 % ee) counter-ions. Since the geometry of the transition state may be different for each counter-ion, strongly coordinating ligands can therefore provide a geometry that will result in a higher degree of enantioselection.

Table 2.9. Correlation between enantioselection and the counter-ion for copper.^a



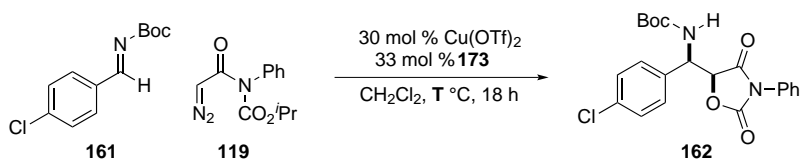
entry	X	dr	ee (%)
1	TfO	3:1	50
2	BF_4	3:1	49
3	PF_6	3:1	31
4	SbF_6	3:1	9

^aAll reactions were 0.15 M in imine and used 1.2 equiv of diazo imide. The isolated yields were low (20 %–30 %)

For enantioselective reactions, the selectivity for one enantiomer over the other is typically related indirectly to temperature. When a reaction is under kinetic control, the energy difference between the transition states determines the relative rates of the two competing reactions and thereby also the ratio of the products formed. For a kinetically controlled process, the product ratio can be calculated from the free energy differences between the transition states or, vice versa.¹²³ If experimentally determined enantioselection is close to theoretically estimated values over a range of temperatures it is reasonable to assume that the same two reaction pathways are operating over the temperature range. Energy profile studies are carried out to reveal background reactions which is usually evidenced by sudden drop in enantioselectivity.

The temperature profile for the *syn*-glycolate reaction is shown in Table 2.10. According to the Arrhenius equation¹²³ two diastereomeric transition states differ by 2.81 kcal/mol (70% ee at -78°C). The same free energy difference at -40°C and -20°C corresponds to 62% ee and 58% ee, respectively, which is close to the values obtained experimentally (Table 2.10, entries 4 and 5). This suggests that lower enantioselection observed at higher temperatures is not due to a nonselective reaction pathway.

Table 2.10. Temperature profile of the reaction catalyzed by copper(II)-bis(oxazoline) **166** complex.^a

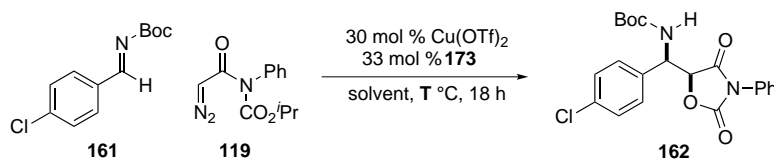


entry	T °C	ee ^b (%)	ee ^c (%)
1	-78	75	–
2	-60	70	70
3	-50	67	–
4	-40	66	62
5	-20	59	58

^aAll reactions were 0.15 M in electrophile and used 1.2 equiv of diazo imide. ^bMeasured by chiral HPLC. ^cValues predicted using Arrhenius equation and correlation tables (ref. 111).

Addition of α -diazo imide to *N*-Boc imines appears to be insensitive to the solvent used with one exception (Table 2.11). When the reaction was carried out in propionitrile, enantioselection dropped dramatically. As a polar and strongly coordinating solvent, propionitrile is a competitive ligand for copper(II) which leads to nearly racemic product (Table 2.10, entry 1). Dichloromethane is the optimal solvent for this transformation delivering product in 75 % ee (entry 2). When the reaction was carried out in 1,2-dichloroethane at $-20\text{ }^{\circ}\text{C}$, the enantiomeric excess was 75 % (Table 2.11, entry 6) which is similar to CH_2Cl_2 at $-78\text{ }^{\circ}\text{C}$. However, when the same reaction was carried out at $-35\text{ }^{\circ}\text{C}$, only 60 % ee was observed. This is probably due to the fact that at temperatures close to the melting point of the solvent ($-35\text{ }^{\circ}\text{C}$), the reaction mixture becomes viscous and lowers the selectivity.

Table 2.11. Copper-bis(oxazoline) catalyzed glycolate Mannich reaction: solvent screen.^a



entry	solvent	T $^{\circ}\text{C}$	ee ^b (%)
1	EtCN	-78	5
2	CH_2Cl_2	-78	75
3	THF	-78	60
4	Et_2O	-78	nd
5	CH_3NO_2	-20	60
6	1,2-DCE	-20	75
7	1,2-DCE	-35	60
8	toluene	-20	60
9	CH_2Cl_2 - CH_3NO_2 (9:1)	-78	53

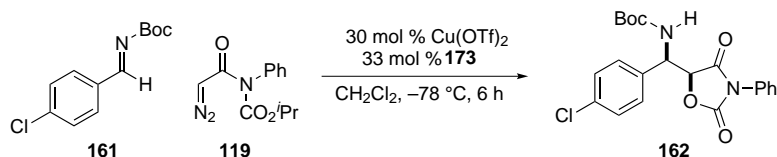
^aAll reactions were 0.15 M in imine and used 1.2 equiv of diazo imide. A typical yield oscillated around 20 %

^bMeasured by chiral HPLC.

The inconsistent ee values observed during optimization studies suggested that the method for reaction termination might influence enantioselection. To evaluate this hypothesis the reaction of the benzaldimine **161** with α -diazo imide in the presence of 30 mol % of copper-**173** complex was quenched by addition of different reagents (Table 2.12). The reaction quenched with satd aq NaHCO_3 delivered the product in reduced enantioselection (63 % ee, entry 1) and when pyridine was used, the product was formed in 75 % ee (Table 2.12, entry 2). We were surprised that the reaction quenched by a solution of HCl in methanol resulted in decomposition with only traces of product identified in the crude reaction mixture (Table 2.12,

entry 3). When the reaction was allowed to warm to room temperature after reacting for 20 h at $-78\text{ }^{\circ}\text{C}$, enantioselection of the oxazolidine dione was determined to be 70 % (entry 4) which suggests that once the reaction is complete, no racemization occurs upon warming.

Table 2.12. Correlation between enantioselection reaction termination protocol.^a



entry	quench	ee (%)
1	NaHCO_3	63
2	pyridine	75
3	HCl/MeOH	– ^b
4	warm to rt	70

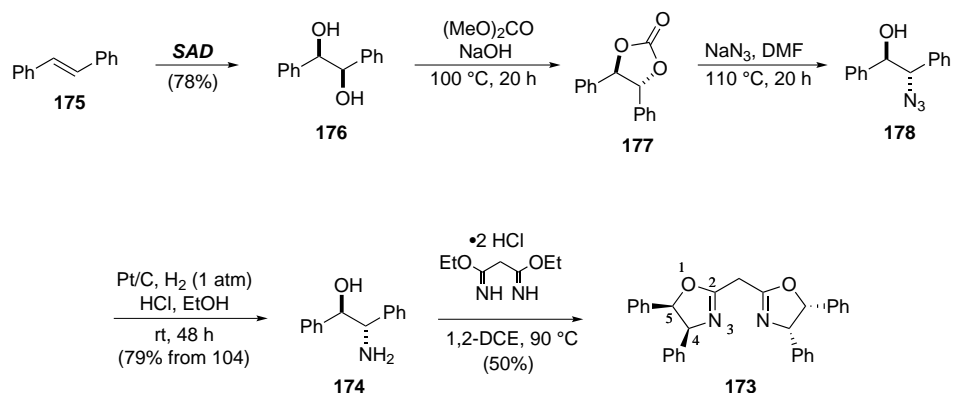
^aAll reactions were 0.15 M in imine and used 1.2 equiv of diazo imide.

^bDecomposition.

We then searched for the ligand that might provide a higher level of reactivity, diastereo- and enantioselection. We planned to evaluate derivatives of bis(oxazoline) ligand **173** that are both commercially available and prepared in the laboratory. Preliminary studies suggested that substitution of the carbon that connects the two oxazoline rings is important, as well as substitution at the 5-position of the oxazoline (cf. **173**, Scheme 2.30).

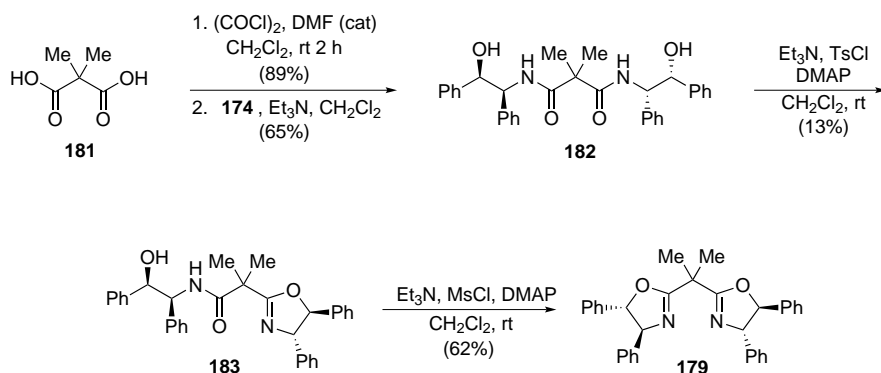
A common intermediate for the derivatives of the Ph_2BoxH ligand **173** is the optically pure 2-amino-1,2-diphenylethanol (**174**). The synthesis commences with a Sharpless asymmetric dihydroxylation (SAD) of the *trans*-stilbene (**175**) using osmium(IV) tetroxide, dihydroquinidine 4-chlorobenzoate as a ligand and NMO as a co-oxidant to arrive at enantiopure *R,R*-(+)-1,2-diphenylethane-1,2-diol (**176**) in 78 % yield after recrystallization. Diol **176** was converted to the cyclic carbonate **177** which was then opened with sodium azide. Resulting azido alcohol **178** was reduced to the amine to give the aminoalcohol **174** in 79 % yield over 3 steps.^{124–126} Condensation of **174** with the diethylmalonimidate hydrochloride yielded bis(oxazoline) ligand **173** in 50 % yield (Scheme 2.30).¹²⁷

Scheme 2.30. Synthesis of bis(oxazoline) **166**.



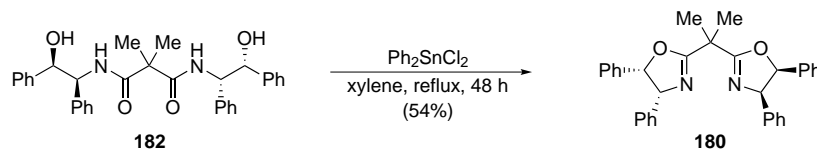
To evaluate the relationship between ligand reactivity and substitution at the carbon bridging two oxazoline rings, we prepared *trans*- and *cis*-Ph₂BoxMe ligands (cf. **179** and **180**, Scheme 2.31). Commercially available 2,2-dimethylmalonic acid (**181**) was converted to the acid chloride and then reacted with aminoalcohol **174** to deliver symmetric amidoalcohol **182** in 65 % yield. Cyclization according to the conditions reported by Evans and co-workers¹²⁸ didn't deliver the *trans*-diphenyl bis(oxazoline) **179** and only the unreacted diamide **182** and partially cyclized derivative **183** were isolated. Treatment of the compound **183** with methanesulfonyl chloride in the presence of triethylamine and DMAP in dichloromethane at room temperature afforded ligand **179** in 62 % yield (Scheme 2.31).

Scheme 2.31. Synthesis of bis(oxazoline) **172**.



The derivative that has two phenyl substituents in a *cis*-relationship was prepared according to the procedure published by Desimoni.¹²⁹ Diamide **182** was subjected to thermal dehydration in presence of diphenyl tin dichloride. The cyclization proceeded smoothly and delivered the bis(oxazoline) **180** in 54 % yield (Scheme 2.32).

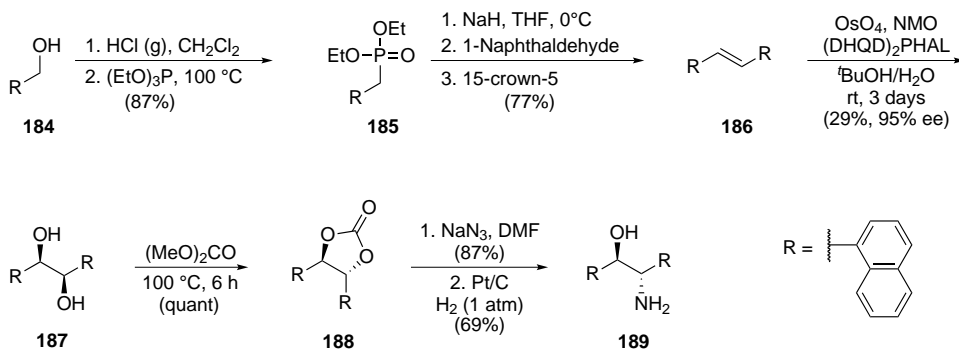
Scheme 2.32. Synthesis of bis(oxazoline) **173**.



Results obtained with complex **173** (when compared to **172**) suggest that the substitution at the 5-position of the oxazoline is necessary for high ee (Scheme 2.28). We hypothesized that a larger substituent in positions 4- and 5- would increase enantioselection. To test this hypothesis, a ligand with a 1-naphthyl substituent in 4- and 5- positions was prepared in a similar manner to **173**.

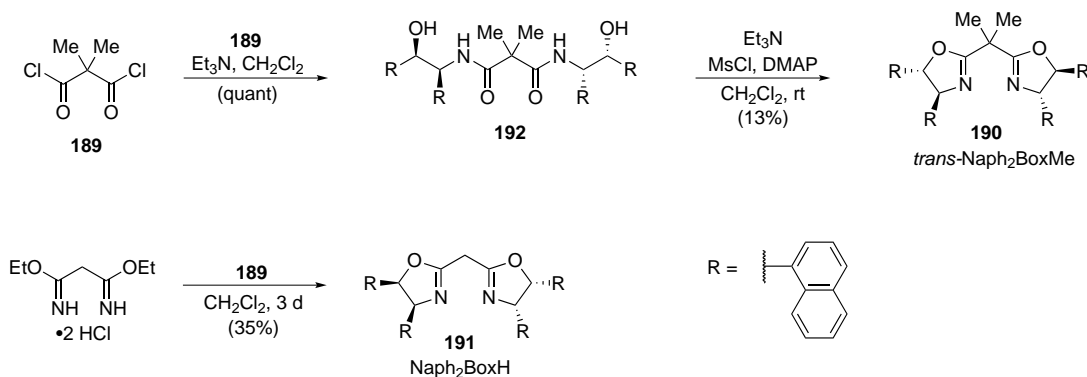
The olefin needed for the Sharpless asymmetric dihydroxylation (SAD) was synthesized from 1-naphthalenemethanol (**184**) which was converted to primary chloride using HCl gas in dichloromethane, followed by Arbuzov reaction with triethyl phosphite to deliver phosphonate ester **185** in 87% overall yield over two steps. Phosphonate **185** was then reacted with 1-naphthaldehyde in a Wadsworth–Emmons reaction to provide the (*E*)-1,2-di(naphthalen-1-yl)ethene (**186**) in 77% yield. Under Sharpless asymmetric dihydroxylation conditions, diol **187** suffered from oxidative cleavage to the 1-naphthaldehyde, low substrate conversion and low enantioselection that was increased by fractional crystallization but at the expense of yield (29% yield and 95% ee after recrystallization). This compound was then subjected to dimethyl carbonate in the presence of a catalytic amount of NaOH while slight vacuum was applied to evacuate the methanol by-product and drive the reaction to completion. The resulting cyclic carbonate **188** was opened with sodium azide to give the corresponding azide in 87% yield. Hydrogenation of the azide to the free amine delivered the desired aminoalcohol **189** in 60% yield (3 steps) and 95% ee (Scheme 2.33).

Scheme 2.33. Synthesis of the 1-naphthyl substituted aminoalcohol.



Synthesis of *trans*-¹Naph₂BoxMe **190** and ¹Naph₂BoxH **191** was accomplished via the same route as 4,5-diphenyl derivatives **173** and **179**. Synthesis of diamide **192** was very efficient and the product was used without further purification. However, cyclization of **192** to **190** suffered from low conversion and delivered multiple products. Only a small amount of the ligand was isolated after extensive chromatography. Cyclization of **189** with diethyl malonimidate hydrochloride was also very sluggish. Only partial conversion to **191** was completed after 3 days at rt and afforded bis(oxazoline) in 35 % yield.

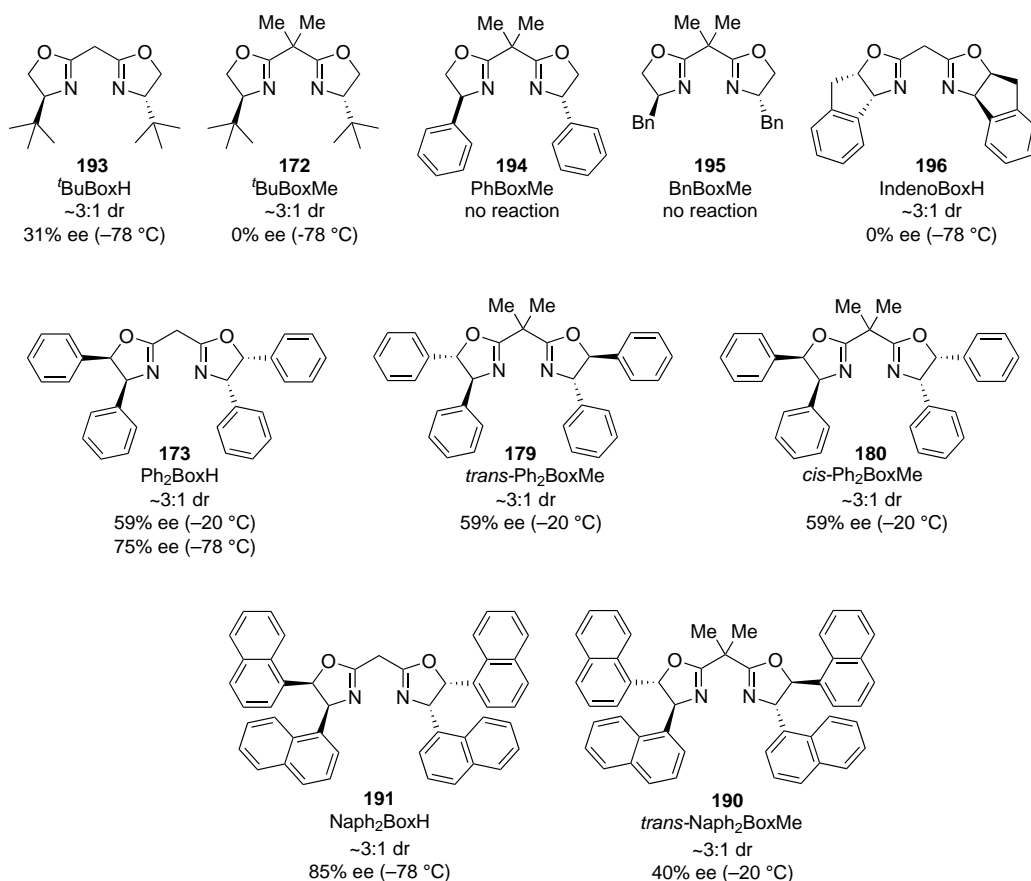
Scheme 2.34. Synthesis of 1-naphthyl substituted bis(oxazolines).



Prepared bis(oxazolines) **173**, **179**, **180**, **190** and **191** together with commercially available ligands **172**, **193–196** were tested in the *syn*-glycolate Mannich reaction (Scheme 2.35). The behavior of ligands having two methyl substituents on the bridging carbon, **179**, **180**, **190** and **172** was significantly different from ligands without substitution; the former were far less reactive. Reactions catalyzed by **179** and **180** had to be carried out at -20°C . Additionally, substitution of the bridging carbon appears to influence enantioselection as well. *tert*-Butyl substituted ligand **193** delivered oxazolidine dione in 31 % ee but bis(oxazoline) **172** with a substituted bridge gave racemic product. Results for the diphenyl substituted ligands **173**, **179** and **180** suggest that a substituent at the 5 position is necessary for reactivity and enantioselection (**173** and **179**). However, there is no clear correlation between relative stereochemistry of the phenyl substituents on the oxazoline, because ligands **173**, **179** and **180** delivered oxazolidine dione in 59 % ee at -20°C . Increased steric bulk appears to help in enantioselection. When bis(oxazoline) **197** with two 1-naphthyl substituents was used as a ligand, oxazolidine dione formed in 85 % ee. A derivative of this ligand with substituted bridge was far inferior. *trans*-¹Naph₂BoxMe **190** was able to promote the reaction but higher reaction temperature (-20°C) was required and oxazolidine dione product formed in only 40 % ee. Throughout this series of ligands, diastereoselection remained practically constant,

forwarding a hypothesis that the catalyst only activates imine towards carbon–carbon bond formation and diastereoselective cyclization to oxazolidine dione is not influenced by the acid catalyst.

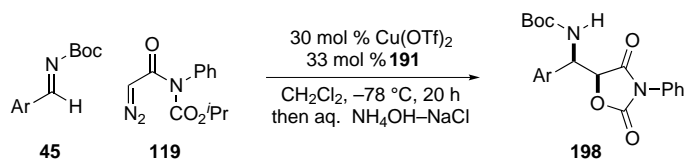
Scheme 2.35. Survey of various bis(oxazoline) ligands in the copper(II) catalyzed glycolate Mannich reaction.



The copper(II) complex with ligand **191** was used to survey the scope of the enantioselective glycolate Mannich reaction (Table 2.13). Unfortunately, the high enantioselectivity observed for 4-chlorobenzaldimine **161** was not general for all substrates. Isolated yields of products were less than satisfactory with only one product forming in yield higher than 50%. Imine derived from 2-naphthaldehyde afforded oxazolidine dione in 55% yield and 78% ee (Table 2.13, entry 4). Generally, reactions of α -diazo imide with *N*-Boc imines in presence of chiral copper(II)–bis(oxazoline) ligands suffered from a low level of reproducibility in terms of enantioselectivity. Reaction on the model substrate, *N*-Boc imine **161** (entry 2), showed that enantioselectivity can be as low as 55% and as high as 85% but most generally oscillating around 70%. Excessive purification lowered the yield of the product, due to a purple colored

side-product formed in all reactions that were catalyzed by complexes of bis(oxazolines) with the unsubstituted bridge.

Table 2.13. Substrate scope of the enantioselective glycolate Mannich.^a



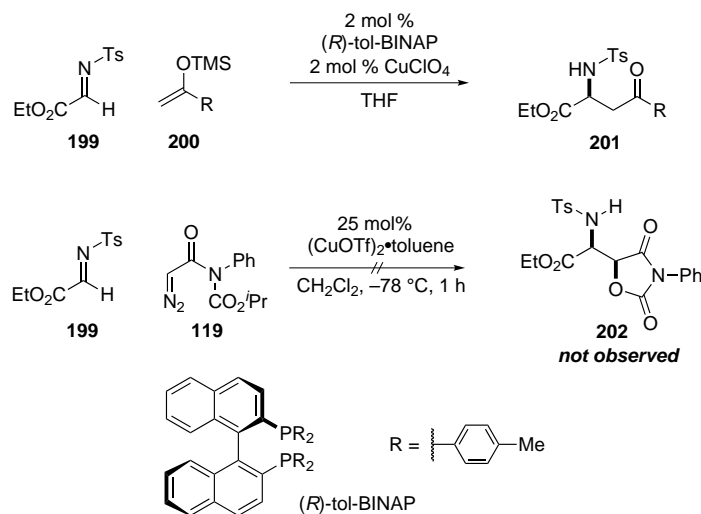
entry	R	yield ^b (%)	dr ^c	ee (%)
1		45	3:1	70
2		48	3:1	55–85
3		39	2:1	70
4		55	2:1	78

^aAll reactions were 0.15 M in imine and used 1.2 equiv of diazo imide. ^bCombined isolated yield for both diastereomers. ^cMeasured by ¹H NMR.

2.3.4 New reactivity of α -diazo imide in presence of copper(I) catalysts

Limited success of the copper(II) catalyzed *syn*-glycolate Mannich reaction, mainly due to low reactivity of *N*-Boc benzaldimines towards α -diazo imide **119**, motivated us to search for a more reactive catalyst. It is often assumed that reactions of diazoalkanes with imines catalyzed by copper(I) catalysts involve diazo decomposition and the resulting metalcarbene reacts with the imine. An azomethine ylide intermediate can then afford aziridine as illustrated in Figure 1.2 (Section 1.2).⁴⁷ Copper(I) can also act as a Lewis acid but unlike copper(II) that coordinates in square planar geometry, copper(I) adopts a tetrahedral geometry. Lectka and co-workers demonstrated that copper(I)-(R)-tol-BINAP complex is an excellent catalyst for the diastereo- and enantioselective alkylation of α -imino esters, such as **199**, with enolsilane nucleophiles (Scheme 2.36). When we employed α -diazo imide **119** in the reaction with tosyl α -imino ester **199** in presence of 25 mol % of the copper(I) triflate-toluene complex, only decomposition products were observed and no desired oxazolidinone **202** was seen in the ¹H NMR of the crude reaction mixture (Scheme 2.36).

Scheme 2.36. Lewis acid activation of imines using copper(I) complexes.



During optimization studies for the *syn*-glycolate Mannich reaction, copper(I) triflate did not deliver any identifiable products (section 2.3.2, Table 2.7, entry 2). However, during these investigations we discovered that the quality of CuOTf is crucial to the success of the reaction. When the same reaction was repeated using a fresh (CuOTf)₂·toluene catalyst, the *cis*-aziridine imide **203** was identified in the reaction mixture together with the vinylogous carbamate **204** (Scheme 2.37). Interestingly, only 10 mol% of the catalyst (20 mol% in copper) was required for the full conversion and no sign of the oxazolidine dione **80** was observed (Scheme 2.37). This was the first time that addition occurred selectively to *cis*-aziridine without evidence of intramolecular cyclization to oxazolidine dione. This suggests that the copper(I) catalyst is able to activate the imine towards α -diazo imide, but is unable to promote aziridine opening to oxazolidine dione. Also, the presence of the vinylogous carbamate **204** byproduct suggests that the reaction operates via Lewis acid-catalyzed addition of the diazoalkane to azomethine^{48,49} rather than through a metallocarbene intermediate.

The observation of *N*-DPM *cis*-aziridine **203** in this reaction suggests that the stereoselectivity of the carbon–carbon bond formation is different than the one proposed for Brønsted acid promoted *syn*-glycolate Mannich reaction (see section 1.4.4). We advocate an *anti* addition of diazo **119** to imine when triflic acid is an azomethine activator, but the reaction catalyzed by Cu(I) seems to go through the *syn*-amino diazonium intermediate* (Figure 2.5).

*See section 1.4 for discussion

Scheme 2.37. Copper(I) aziridination of imines using α -diazo imide.

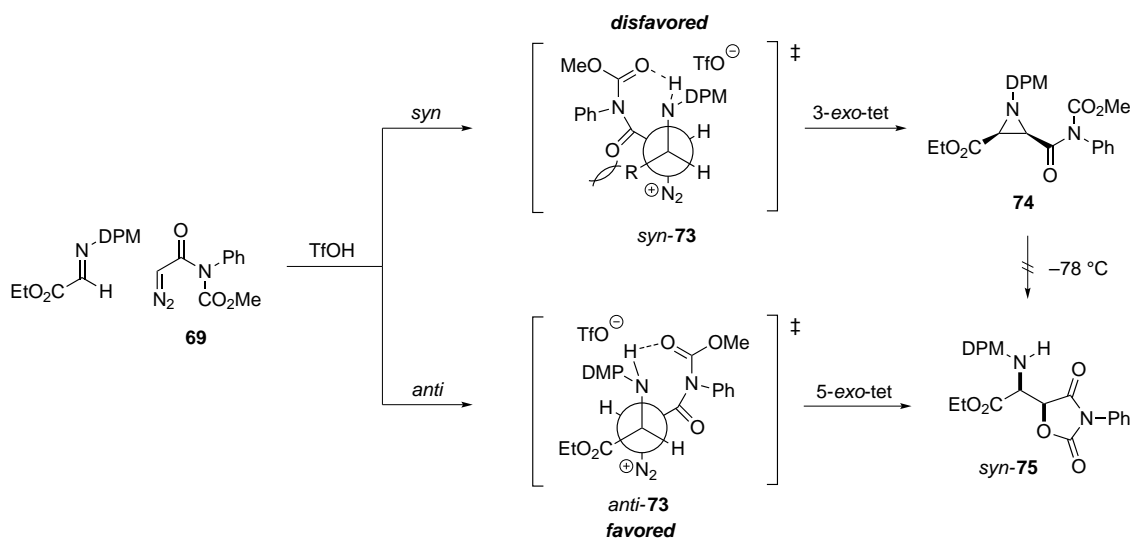
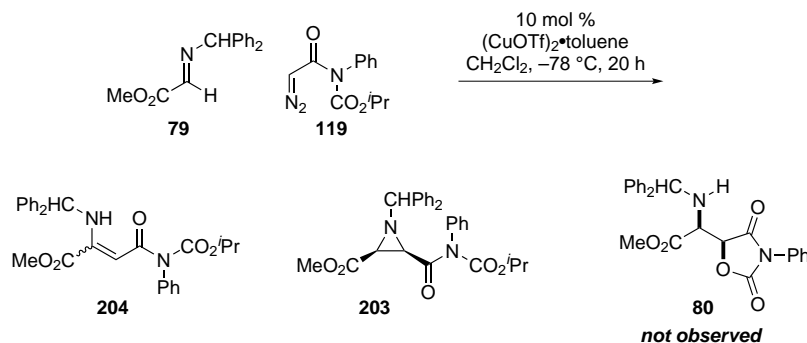
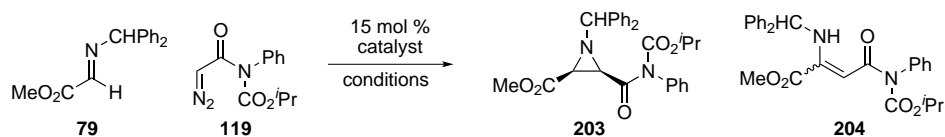


Figure 2.5. Origin of stereoselectivity in Brønsted acid-promoted diazo-azomethine reactions.

The reaction of imine **79** with α -diazo imide does not seem to be influenced by metal counterion. Copper(I) triflate and tetrakis(acetonitrile) copper(I) perchlorate catalyze the reaction to the same extent (Table 2.14, entry 1 and 2). Although the former afforded aziridine in slightly higher yield, the ratio of **203** to **204** remained unchanged. Although lowering the reaction temperature significantly increased chemoselectivity, a fair number of side-products were observed. Chemoselectivity seems also to be a function of the solvent with trifluoromethyl benzene being optimal solvent in terms of chemoselectivity (entry 5). Despite high conversion and selectivity, reactions in polar solvents delivered complex mixtures (Table 2.14, entries 6–8).

Table 2.14. Optimization of the copper(I) catalyzed reaction of α -diazo imide with *N*-DPM imines.^a



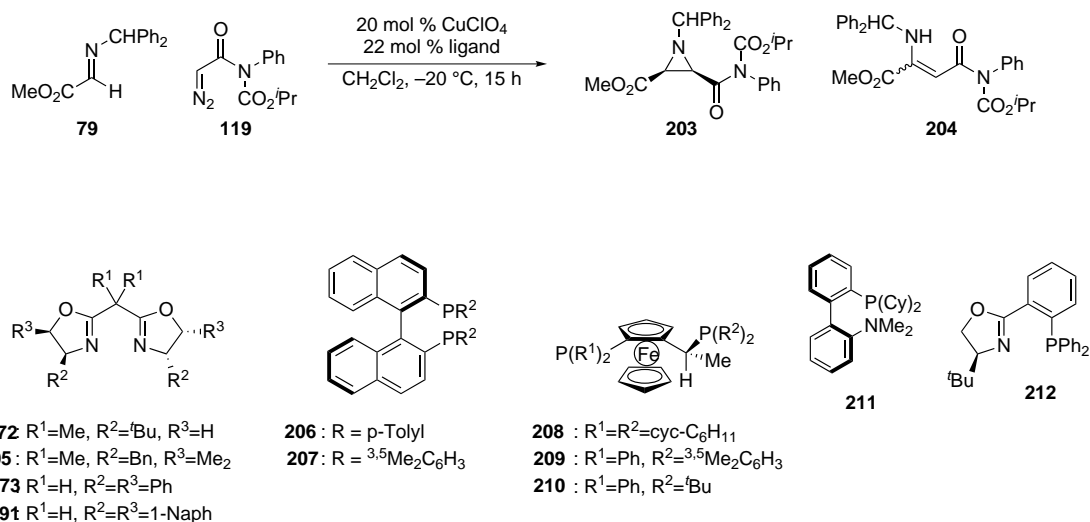
entry	catalyst	solvent	T celsius	time (h)	203:204 ^b	conv (%)
1	(CuOTf) ₂ · toluene	CH ₂ Cl ₂	-20	6	63:37	90 (49) ^c
2	CuClO ₄ · 4 MeCN	CH ₂ Cl ₂	-20	15	61:39	90
3	CuClO ₄ · 4 MeCN	CH ₂ Cl ₂	-78	20	91:9	80 ^d
4	CuClO ₄ · 4 MeCN	toluene	-20	15	85:15	90
5	CuClO ₄ · 4 MeCN	PhCF ₃	-20	15	95:5	90
6	CuClO ₄ · 4 MeCN	THF	-20	15	88:12	90
7	CuClO ₄ · 4 MeCN	Et ₂ O	-20	15	88:12	90
8	CuClO ₄ · 4 MeCN	EtCN	-20	15	60:40	85

^aAll reactions were 0.10 M in electrophile and used 1.2 equiv of diazo imide. ^bSubstrate conversion was calculated from ¹H NMR of the crude reaction mixture. ^cIsolated yield. ^dSignificant amount of unknown side-products.

Our ultimate goal was to achieve enantioselective reactions with diazo imide **119**. One advantage of copper(I) Lewis acids over the copper(II) counterparts lays in their affinity to a broader range of ligands. Chiral phosphine and diamine ligands, together with bis(oxazolines), are often used to prepare chiral copper(I) catalysts for stereoselective reactions. It is commonly observed that metal complexes are weaker Lewis acids than metal salts and our results confirm this trend.¹²⁰ A survey of an array of different ligands is presented in Scheme 2.38. We identified that the aziridination can proceed in up to 20% conversion and only up to 29% ee albeit with high chemoselectivity towards *cis*-aziridine. Longer reaction times and higher catalyst loading didn't improve the yield.

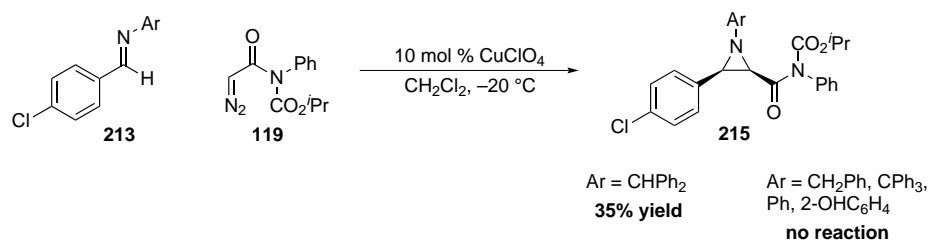
After discovery of the novel reactivity of α -diazo imide towards *N*-DPM imines in reactions catalyzed by copper(I), we suspected that this behavior might be more general and applicable to a wider group of imines with different nitrogen substituents. The Brønsted acid catalyzed reaction worked only for the narrow set of *N*-benzhydryl imines. Again we picked derivatives based on 4-chlorobenzaldehyde since they are easier to prepare. Results demonstrate a strong dependence of the reaction on the nitrogen protecting group not only in terms of reactivity but also the chemoselectivity.

Scheme 2.38. Lewis acid activation of imines using copper(I) complexes.



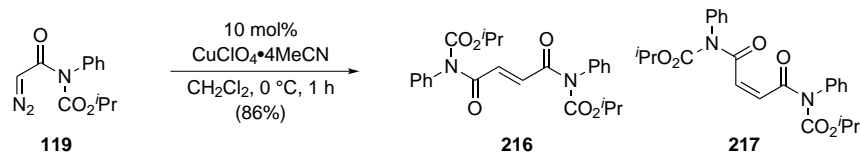
Aryl *N*-DPM imines behave similarly to imino ester **79** but are much less reactive. Despite low conversion, high chemoselectivity for *cis*-aziridine **215** was observed (35 % yield). Increasing (*N*-Tr) and reducing (*N*-Bn) the number of phenyl rings relative to the benzhydryl group resulted in no reaction. The same effect was observed for the *N*-phenyl and *N*-(2-hydroxy)phenyl group (Scheme 2.39).

Scheme 2.39. Copper(I) promoted α -diazo imide dimerization.



In instances when azomethine was unreactive towards the α -diazo imide, a significant amount of the α -diazo imide homocoupling products **216** and **217** was observed (Scheme 2.40). When the reaction was carried out without imine, *E*- and *Z*-olefin **216** and **217** were isolated in 86 % combined yield as a nearly 1:1 mixture. We did not observe homocoupling products in reactions catalyzed by triflic acid, even in slow reactions with aryl aldimines. The only byproduct was the oxazolidine dione **123**. Following this observation we retrospectively analyzed copper(II) catalyzed additions to *N*-Boc aldimines and many reactions contained **216** and **217** as by-products.

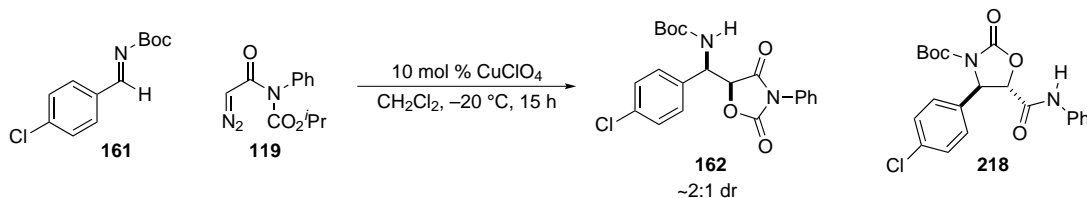
Scheme 2.40. Copper(I) promoted α -diazo imide dimerization.



2.3.5 Exploration of α -diazo imide–copper(I) system

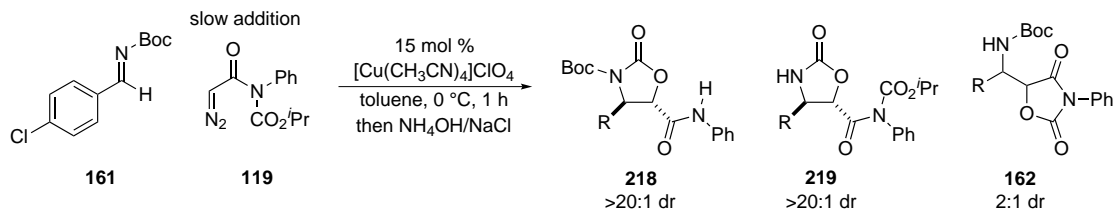
Radically different reactivity was observed for *N*-Boc, *N*-Ts and *N*-silyl imines. The reaction between *N*-Boc benzaldimine **161** and α -diazo imide in presence of copper(I) perchlorate proceeded very quickly. After gas evolution ceased (ca. 15 min) at room temperature, nearly full conversion was observed by ^1H NMR. Oxazolidine dione **162** (ca. 2:1 dr) was present together with *N*-Boc oxazolidinone **218** (Scheme 2.41).

Scheme 2.41. Reactivity of *N*-Boc imines and α -diazo imide in presence of copper(I) catalysts.



Encouraged by this result we decided to explore the new and unique reactivity of *N*-Boc imines with α -diazo imide **119**. To suppress homocoupling of **119**, the solution of the diazo in toluene was added to the solution of the *N*-Boc 4-chlorobenzaldimine **161** via automated syringe pump over a period of 30 min. After quench with the saturated aqueous solution of ammonium chloride in brine (2:1), the reaction mixture was analyzed by ^1H NMR. The spectrum showed three products **218**, **219**, and **162** in 67:6:27 ratio, respectively (Scheme 2.42).

Scheme 2.42. Result of slow addition of α -diazo imide to *N*-Boc imines in the presence of copper(I) catalyst.



The observed products presumably are derived from the diazonium intermediate *anti*-**220** (Figure 2.6). The carbon–carbon bond formation is followed by the acyl transfer that gives intermediate **221**. Cyclization of the isopropyl carbamate produces oxazolidinone **218** as the major product; the alternative oxazolidinone **222** was not observed (Figure 2.6, pathway c). It is worth mentioning that the rate of the acyl transfer appears to be higher than aziridination because no aziridine products were observed. Competitive to the acyl transfer is a direct cyclization of the aminodiazonium **220**. If the Boc group participates in this process, oxazolidinone **219** formation will result (pathway a). Alternatively, if the isopropyl carbamate oxygen displaces dinitrogen, *syn*-oxazolidine dione **162** (pathway b) is formed. The *syn*-diastereomer of the minor product, oxazolidine dione **162**, is derived from *syn* C–C bond formation and direct cyclization, which is highly unfavored.

Stereochemistry of the oxazolidinone ring has been assigned as *trans*, analogous to known examples,¹⁰² and confirmed by NOE. We suggest that stereoselectivity for *trans*-**218** is due to the fact that the *anti*-aminodiazonium intermediate **220** experiences less steric stress compared to the *syn* intermediate.

The outcome of this reaction depends on the way it is terminated. Our initial conditions required quenching with the solution of ammonium hydroxide in brine, in which case the oxazolidinone **219** forms in very small amounts (Table 2.15, entry 1). When the reaction was quenched with aqueous EDTA or pyridine, oxazolidinones **218** and **219** formed in nearly equal amounts but with slightly higher conversion for the latter (Table 2.15, entry 2 and 4). The relative amount of compound **219** compared to oxazolidinone **218** increased when the reaction was quenched with aq HCl (entry 3). When the reaction was not quenched, but instead filtered through a pad of silica gel, products **218** and **219** dominated and formation of the oxazolidine dione **162** was not significant (Table 2.15, entry 5). Filtration through a pad of neutral alumina resulted in a mixture that contained predominantly *N*-Boc product **218**, albeit with lower conversion (entry 6). However, in this case, diazo addition and stirring time was shorter which suggested that product **218** and **219** are the kinetic and thermodynamic product, respectively. This hypothesis was supported by further experiments

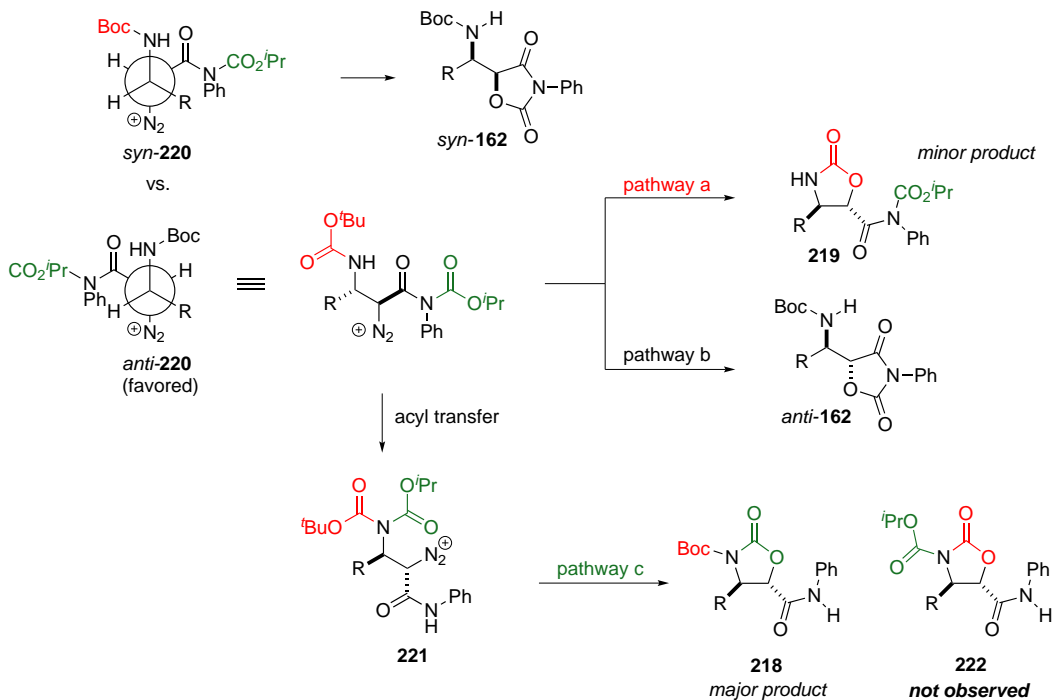
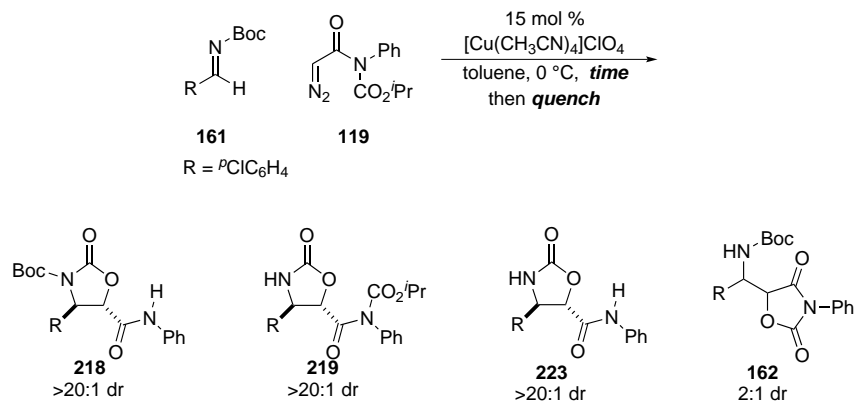


Figure 2.6. Mechanistic pathways of the α -aminodiazonium formed from *N*-Boc imine and α -diazo imide.

when reactions quenched by filtration through silica gel after 30 min, 1, 3, and 18 h clearly show that early in the reaction, oxazolidinone **218** dominates but with time the ratio of products reverses and favors product **219**. Applying a protocol later developed for *N*-Ts imines (quench with 100 mol % of triflic acid, *vide infra*) resulted in *N*-Boc removal and the *N*-H oxazolidinone **223** was isolated in 53 % yield. When the reaction was carried out in polar solvents, higher amounts of the oxazolidinone dione were observed in comparison to nonpolar solvents such as toluene. No correlation was found between the ratio of products and the reaction temperature, concentration or catalyst loading. A set of substrates was subjected to optimized reaction conditions (entry 7) but high chemoselectivity towards a single product couldn't be obtained and yields oscillated around 35 % for *N*-Boc oxazolidinones of type **218**.

Table 2.15. Correlation between reaction termination protocol and product outcome.^a

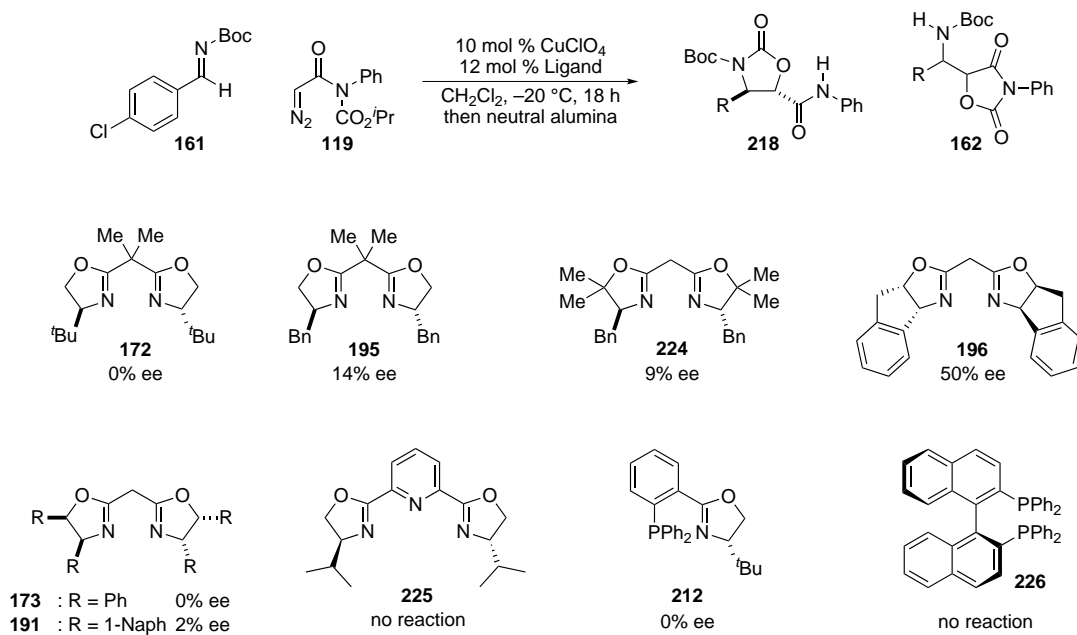


entry	quench	time (h)	conv ^b (%)	218:219:162^b
1	NH ₄ OH/NaCl	1	>95	67:6:27
2	EDTA	1	83	44:37:19
3	HCl	1	88	37:55:8
4	pyridine	1	>95	47:34:19
5	silica gel	1	>90	54:38:8
6	neutral alumina	1	79	92:7:1
7 ^c	silica gel	0.5	80	85:3:12
8 ^c	silica gel	3	>90	27:63:10
9 ^c	silica gel	18	>95	22:67:12
10	TfOH	1	>90	– ^d

^aAll reactions were 0.10 M in imine and 1.2 equiv of diazo imide was added via syringe pump over 30 min. ^bEstimated from ¹H NMR. ^c4-Methoxybenzalimine was used as a substrate. ^d*N*-Boc deprotected oxazolidinone **223** was observed as a major product.

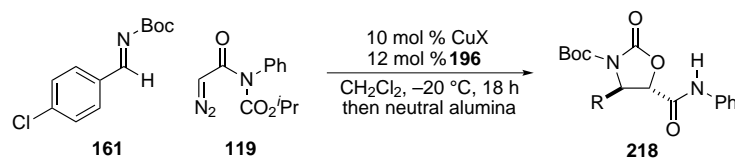
Although the synthesis of **218** was not our initial goal, this reaction is an interesting example of diazo reactivity. To determine if this reaction can be carried out enantioselectively, a series of chiral ligands was evaluated. Ligands **172**, **173** and **212** delivered product as racemates. Slight enantioselection was observed for bis(oxazolines) **195**, **224** and **191**. Moderate enantioselection was delivered by ligand **196** (50% ee). Application of PyBOX **225** and axially chiral phosphine **226** resulted in no reaction.

Scheme 2.43. Evaluation of chiral copper(I) complexes



Dependence of enantioselection upon counterion was then assessed for ligand **196**. Neither triflate nor hexafluoroantimonate were able to positively influence the enantioselection. In both instances the oxazolidinone product formed in low enantioselection (Table 2.16).

Table 2.16. Correlation between enantioselection and counterion

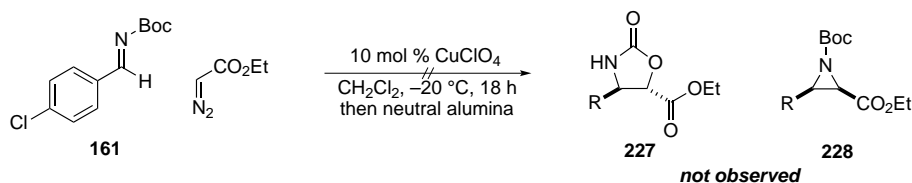


entry	X	ee (%)
1	ClO ₄	48
2	TfO	34
3	SbF ₆	40

^aAll reactions were 0.15 M in imine and used 1.2 equiv of diazo imide.

We expected to see compound **227** as a major product of reaction of imine **161** with ethyl diazoacetate. After addition of the diazo compound, the Boc group is the only ester that can cyclize onto the diazonium carbon. When we performed this control experiment neither **227** nor aziridine **228** was observed by ^1H NMR. Clearly, the difference in reactivity between ethyl diazoacetate and α -diazo imide is substantial.

Scheme 2.44. Control reaction of ethyl diazoacetate with *N*-Boc imines in the presence of copper(I) catalyst.



N-Tosyl imines also revealed new reactivity towards α -diazo imide. The reaction of the *N*-tosyl benzaldimine **229** with α -diazo imide is quite fast. After ca. 15 min nitrogen evolution is no longer observed and a complex mixture of products is present by ^1H NMR (Figure 2.7, spectrum a). Attempts to isolate a single compound from the crude reaction mixture were unsuccessful. To our surprise, when 100 mol % of triflic acid was added to the reaction prior to the quench, ^1H NMR showed oxazolidinone **230** as the only product with a small amount of 4-chlorobenzaldehyde and *p*-toluenesulfonamide as minor side-products (spectrum b). Although diastereoselection was negligible, we were struck by the chemoselectivity of the overall reaction, knowing how complicated the mixture is prior to addition of triflic acid. We established that optimal conditions for this transformation involve 10 mol % of the copper(I) catalyst in dichloromethane with slow addition of the α -diazo imide followed by treatment with 100 mol % of triflic acid, and the oxazolidinone can be isolated in 82 % yield albeit as a 1.2:1 mixture of diastereomers.

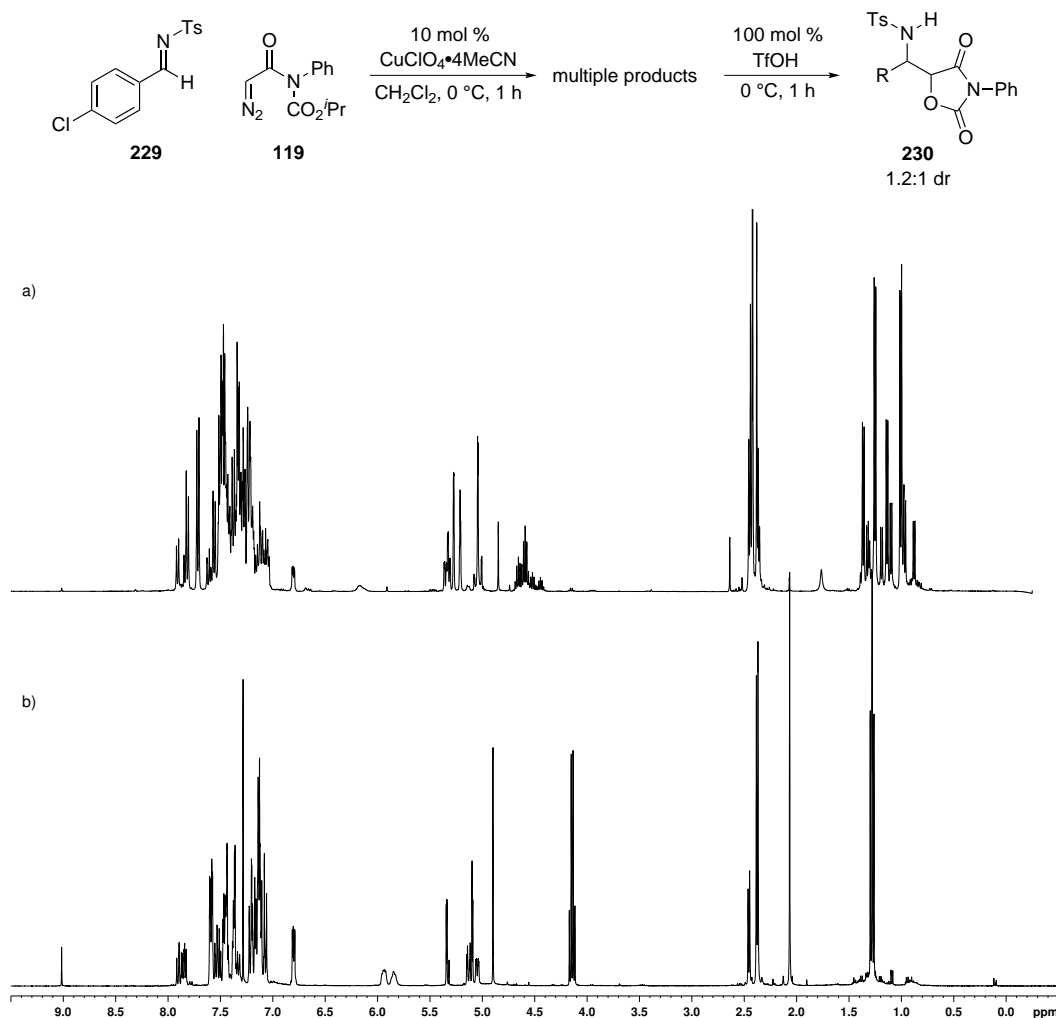


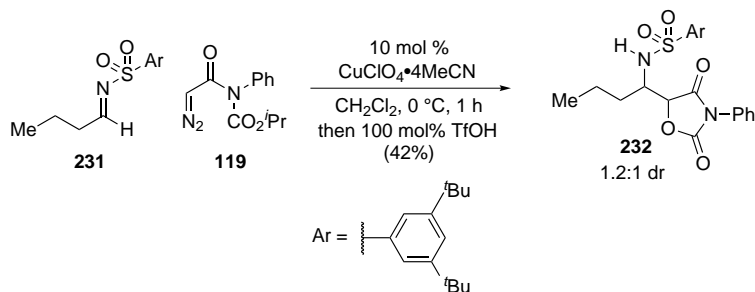
Figure 2.7. Brønsted acid promoted formation of *N*-Ts oxazolidinone **230**. (a) ^1H NMR (CDCl_3) spectrum of the crude reaction mixture without addition of triflic acid (b) ^1H NMR (CDCl_3) spectrum of the crude reaction mixture after addition of triflic acid.

We knew that triflic acid is not able to promote addition of diazo **119** to imine **229** (see section 2.2.2, Table 2.2) but it was not clear if the reaction occurs only under copper(I) catalysis, or perhaps copper(II) is also able to catalyze reaction to oxazolidinone. When 10 mol% of $\text{Cu}(\text{OTf})_2$ was used as a catalyst at 0°C for 3 h, oxazolidinone **230** was observed in the crude reaction mixture only in trace amounts among multiple unidentified side-products. A second control experiment revealed that, like in case of *N*-Boc imine, no reaction was observed with ethyl diazoacetate.

We hypothesized that diastereoselection could be increased by use of a sterically demanding aryl sulfonamide as the protecting group for the imine nitrogen. Reaction of the 3,5-di(*tert*-butyl)phenyl sulfonamide protected imine **231** derived from the butyraldehyde

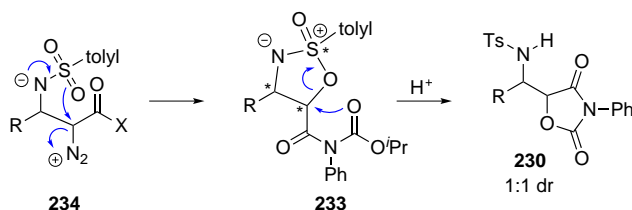
under optimized conditions delivered oxazolidine dione **232** in moderate yield but without improvement in diastereoselection (Scheme 2.45). Although our hypothesis turned out to be false, it is important to note that the reaction conditions seem to tolerate alkyl imines which is promising as reactions with alkyl imines are not as well developed as reactions with aldimines.

Scheme 2.45. Glycolate Mannich reaction with bulky sulfonyl alkyl imines.



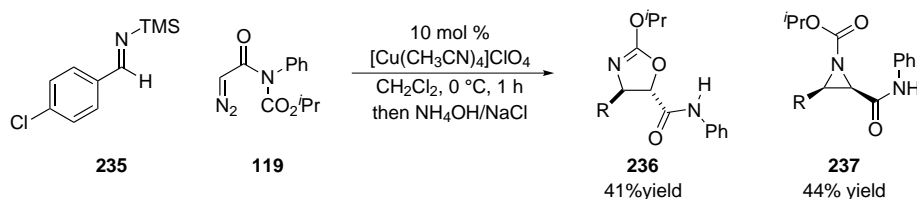
To explain the reaction outcome we propose a cyclic sulfonimide intermediate **233** as a precursor to the oxazolidine dione in reaction of the *N*-tosyl imines catalyzed by copper(I). Addition of the diazo nucleophile results in the formation of the *vic*-amino diazonium intermediate **234**. Cyclization of the sulfonamide oxygen onto diazonium carbon leads to the cyclic sulfonimide **233**. The stereogenic sulfur atom increases the number of possible stereoisomers. This might explain the multiple products observed in the ¹H NMR spectrum before addition of triflic acid. Sensitivity of the cyclic sulfonimide **233** towards Brønsted acids is not surprising. Treatment with TfOH causes sulfonimide ring opening that is followed by the oxazolidine dione ring formation to arrive at the structure **230** where the stereocenter at sulfur no longer exists.

Scheme 2.46. Postulated mechanism of formation of *N*-Ts glycolate Mannich products.



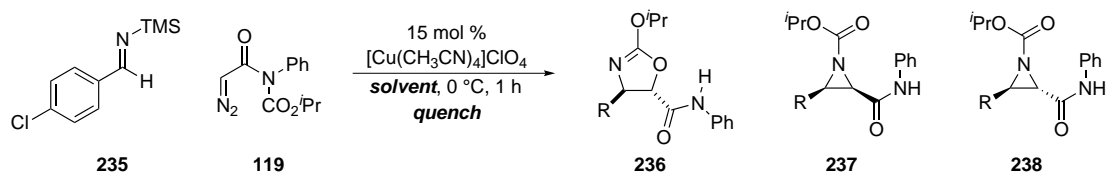
Even more puzzling was the result of the α -diazo imide addition to the trimethylsilyl imine **235**. The reaction produced very cleanly two major products in 1.5:1.0 ratio. Although ^1H NMR of the minor product suggested an aziridine product, the resonances for the methine doublets were shifted downfield and appeared at 3.93 and 3.53 ppm (3.51 and 2.83 ppm for *N*-DPM aziridine). After isolation and full characterization, we assigned oxazoline **236** and aziridine **237** as products of this reaction (41 % and 44 % yield respectively, Scheme 2.47)

Scheme 2.47. The outcome of the reaction of α -diazo imide with *N*-TMS imine.



Our experience with the *N*-Boc imine under copper(I) catalysis (Table 2.15) suggested that this reaction might also be sensitive to the solvent and the way it is terminated. Our hypothesis turned out to be true. Filtration through a pad of neutral alumina reversed the ratio of the products with *cis*-aziridine being the major product (Table 2.17, entry 2). In deuterated chloroform the ratio favoring *cis*-aziridine was the highest observed and **236** was isolated in 70% yield (Table 2.17, entry 3). In acetonitrile the reaction didn't occur because the catalyst was not soluble in this solvent (entry 4). A reaction carried out in hexanes produced the *cis*-aziridine exclusively but suffered from low conversion, the reaction mixture was not homogeneous in this case (entry 5). In toluene almost an equal amount of *trans*-aziridine **238** formed next to the *cis*-isomer but oxazoline was still the major product (Table 2.17, entry 6). A clear example of the effect of the quench is shown in entries 7 and 8. Reaction in trifluoromethylbenzene delivers both products in nearly 1:1 ratio when filtered through alumina but strongly favors oxazoline **236** when filtered through silica gel.

Table 2.17. Solvent and quench-dependent product distribution in α -diazo imide addition to silyl imines.^a



entry	solvent	quench	236:237:238 ^b	yield (%) ^c
1	CH ₂ Cl ₂	NH ₄ OH/NaCl	60:38:2	–
2	CH ₂ Cl ₂	neutral alumina	36:61:3	–
3	CDCl ₃	neutral alumina	20:72:8	70
4	CH ₃ CN	neutral alumina	–	–
5	hexanes	neutral alumina	5:90:5 ^d	–
6	toluene	neutral alumina	55:28:17	–
7	PhCF ₃	neutral alumina	44:54:2	–
8	PhCF ₃	silica gel	89:7:3	55

^aAll reactions were 0.15 M in imine and used 1.2 equiv of diazo imide.

^bEstimated from ¹H NMR of the crude reaction mixture. ^cIsolated yield.

^dReaction mixture was not homogeneous and unreacted diazo and aldehyde were major products.

The following mechanism might explain the outcome of the reaction (Figure 2.8). Tetrahedral coordination geometry of the copper(I) catalyst allows for binding of the imine nitrogen and both carbonyl oxygens of the diazo imide (**A**). Carbon–carbon bond formation is followed by acyl transfer from the diazo to the imine nitrogen to give structure **C**. Carbamate anion collapse triggers *N*–*O* transfer of the silyl group to afford the diazonium intermediate **239** which can cyclize to give aziridine or oxazoline. A correlation between reaction quench and the ratio between oxazoline **236** and *cis*-aziridine **237** and the fact that the reaction is terminated after nitrogen evolution is complete, suggests that transformation of **239** to either **236** or **237** is probably not as straightforward as it is depicted in Figure 2.8.

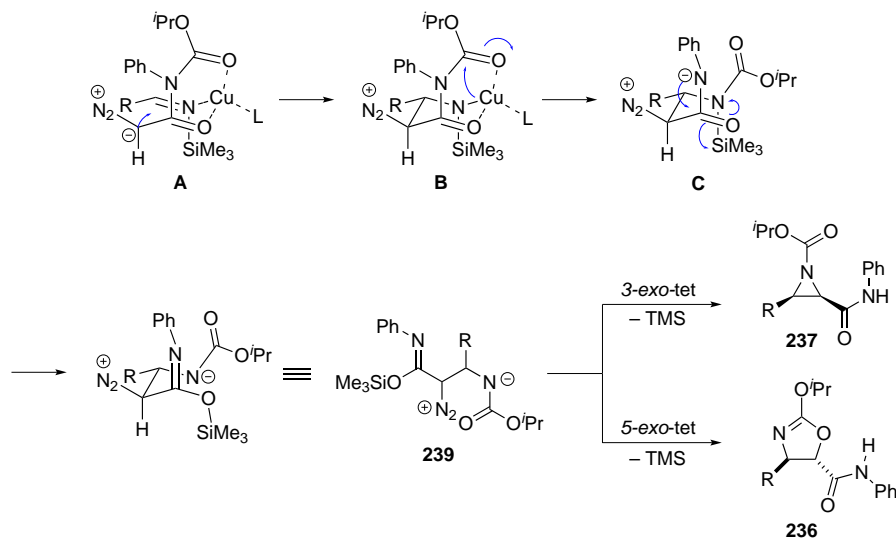
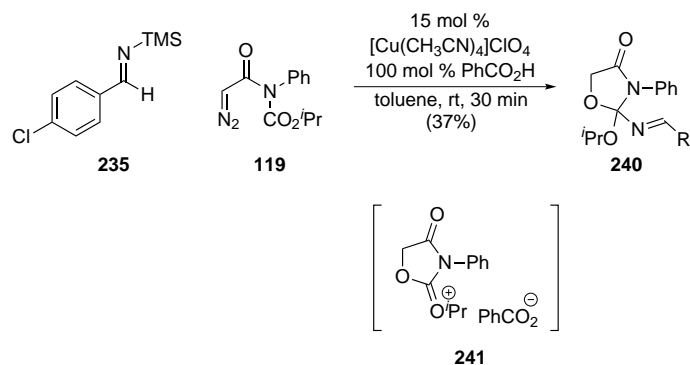


Figure 2.8. Postulated mechanism for the formation of **236** and **237**.

Among imines evaluated in reactions with α -diazo imide, the nucleophilicity of the silyl imine nitrogen is relatively high when compared to *N*-Boc, *N*-Ts or even *N*-DPM. The evidence that supports this hypothesis was obtained when we tried to influence the reaction outcome by use of a weak Brønsted acid, such as benzoic acid as an additive. In this case, a new compound formed and no sign of the expected oxazoline or aziridine was present in the ^1H NMR spectrum. The new compound had two characteristic doublets at 4.66 and 4.56 ppm as well as a sharp singlet at 8.62 ppm. The coupling constant of the doublets was quite high (14.3 Hz) which suggested a diastereotopic methylene group. Based on analysis of HSQC and HMBC correlations we proposed structure **240** to be the product. Compound **240** is probably a result of the addition of the imine nitrogen to the oxonium intermediate **241** (Scheme 2.48). As it was the case with *N*-Boc and *N*-Ts imines, no reaction was observed with EDA.

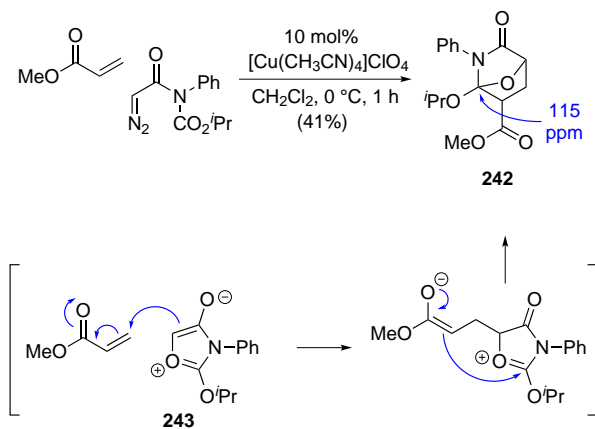
One of the key questions we had about the reaction of α -diazo imide with *N*-silyl imines was whether the reaction is Lewis acid catalyzed, or does it involve diazo decomposition to a metalcarbene. The latter hypothesis is consistent with the observation of the diazo homocoupling products. We carried out a control experiment in which we employed α -diazo imide in a cyclopropanation reaction with the excess of methyl acrylate under otherwise identical conditions (Scheme 2.49). The product, what at first appeared to be the expected cyclopropane, was the orthoester **242**. The key correlations that allowed us to elucidate the structure of compound **242** were heteronuclear correlations to the quaternary carbon at 115 ppm. The methine protons as well as diastereotopic methylene protons show HMBC correlation to the resonance at 115 ppm. We suggest that the product is a result of a Michael

Scheme 2.48. Reaction of α -diazo imide with *N*-TMS imine in the presence of a proton source.



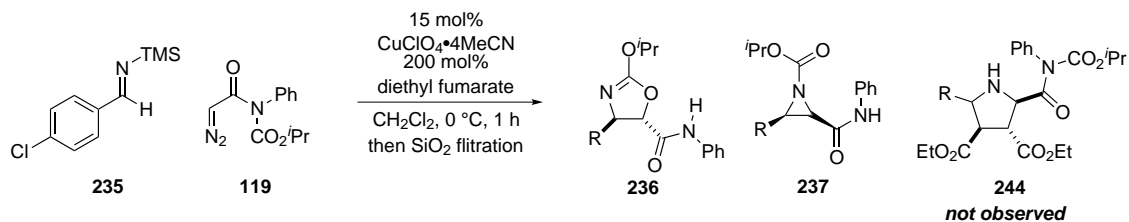
addition of the oxonium ylide **243** to the methyl acrylate followed by the addition of the enolate to the carbamate oxocarbenium to give **242**. Alternatively, compound **242** can arise from a cycloaddition between the methyl acrylate and the oxonium ylide **243** (Scheme 2.49).

Scheme 2.49. Attempted cyclopropanation with the α -diazo imide.



The reaction of *N*-TMS imine with the α -diazo imide in the presence of dipolarophiles such as diethyl fumarate is a test for the presence of azomethine ylide in the reaction.⁴⁷ When α -diazo imide **119** was reacted with the imine **235** in the presence of a 2 fold excess of diethyl fumarate, only oxazoline **236** and aziridine **237** were observed in the ^1H NMR spectrum of the crude reaction mixture. The absence of a pyrrolidine of type **244** suggests that intermediacy of an azomethine ylide as noted by Jacobsen⁴⁷ is unlikely (Scheme 2.50).

Scheme 2.50. Control experiment for the formation of an azomethine ylide.



2.3.6 Summary and conclusions

In this chapter we presented the development of a highly diastereoselective Brønsted acid-promoted addition of α -diazo imide **119** to *N*-DPM imines. This reaction is a viable alternative to glycolate additions to imines in cases where diastereoselection is a challenge. By use of the novel α -diazo imide reagent, diastereoselectivity of aminoalcohol formation is controlled by intramolecular oxygen delivery.

We also explored asymmetric reactions of the α -diazo imide with various azomethine electrophiles. We found that certain copper(II)–bis(oxazoline) complexes allow for the formation of *N*-Boc oxazolidinone diones in good enantiomeric excess and moderate dr.

Reactions catalyzed by copper(I) catalysts revealed new reactivity of the α -diazo imide. The reaction with *N*-DPM imines produces aziridines **203** that do not cyclize further to oxazolidinone dione. The reactivity of *N*-silyl and *N*-sulfonyl imines follows new pathways, not observed under Brønsted acid catalysis.

CHAPTER 3

Progress towards the total synthesis of (+)-zwittermicin A

3.1 Background

3.1.1 Isolation, structural assignment and biological activity

Understanding of plant protection at the molecular level is an important endeavor that brings together efforts from disciplines such as agricultural and environmental sciences, microbiology, and chemistry. Through a mutual relationship with microbes, plants receive protection from diseases by small molecules which are an attractive source for researchers to discover new biologically active compounds.

Bacillus cereus UW85 was shown to suppress diseases in a variety of plants.^{130–133} In one study, it was the only strain of 700 tested that reduced alfalfa seedling mortality caused by *Phytophthora megasperma* f. sp. *medicaginis* to 0%.¹³⁰ *Bacillus cereus* UW85 also suppresses diseases of tobacco,¹³¹ cucumber,¹³² and peanuts¹³³ caused by pathogenic fungi.

(+)-Zwittermicin A (**245**) was identified as a secondary metabolite produced by *Bacillus cereus* UW85 that is responsible for the aforementioned biological activity.^{134,135} It has a broad spectrum of activity, inhibiting certain gram-positive, gram-negative, and eukaryotic microorganisms.¹³⁶ It also potentiates the insecticidal activity of the protein toxin produced by *Bacillus thuringiensis*, increasing mortality of insects that are typically recalcitrant to killing, such as gypsy moths reared on willow leaves.^{130,137,138}

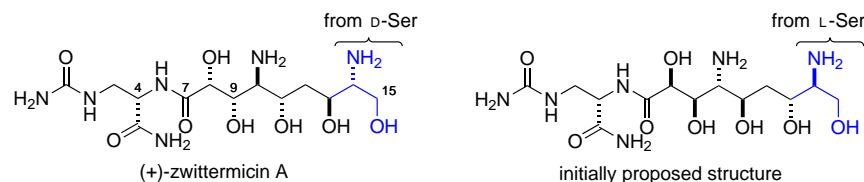


Figure 3.1. (+)-Zwittermicin A

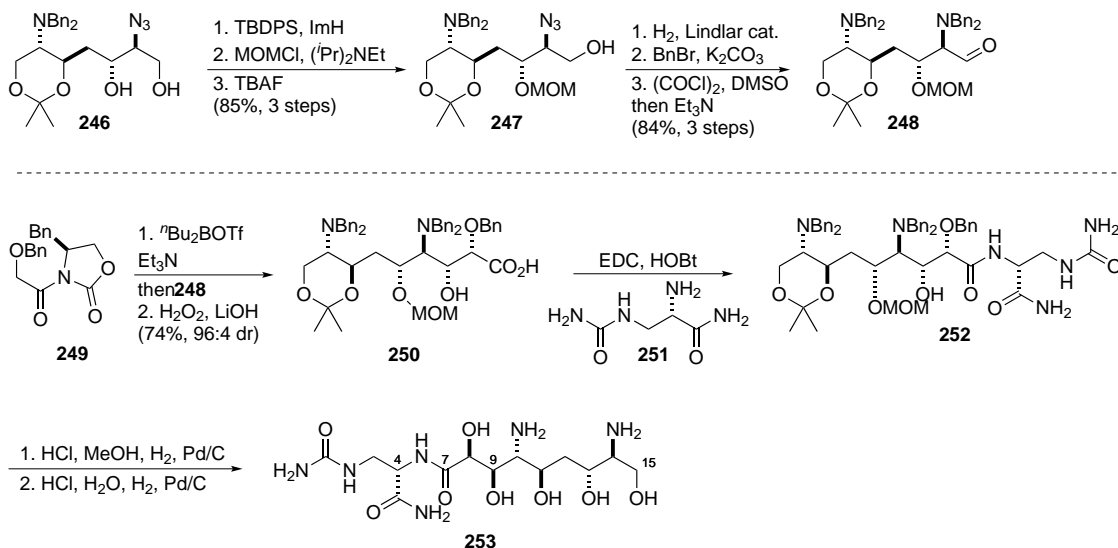
When isolation and structural elucidation of **245** was disclosed in 1994,¹³⁴ only the relative stereochemistry of the C8–C10 fragment was proposed. The complete relative and absolute configuration was first speculated about in 2007 by Rogers and Molinski.¹³⁹ Pairwise ¹³C NMR chemical shift difference analysis of six diastereomeric 2,6-diamino-1,3,5,7-

heptatetraols allowed for the relative stereochemistry of the C9–C15 portion of **245** to be established. The absolute stereochemistry of this fragment was proposed based on biosynthetic grounds. It was assumed that the starting unit for the non-ribosomal peptide synthetase (NRPS)–polyketide synthase (PKS) megasynthase is L-Ser and the absolute stereochemistry at C14 is the same as in the amino acid. The stereochemistry of the remaining C1–C4 fragment was established by amide hydrolysis and derivatization of natural **245** and comparison to a known amino acid *S*-albizziine.

3.1.2 Revision of the absolute stereochemistry

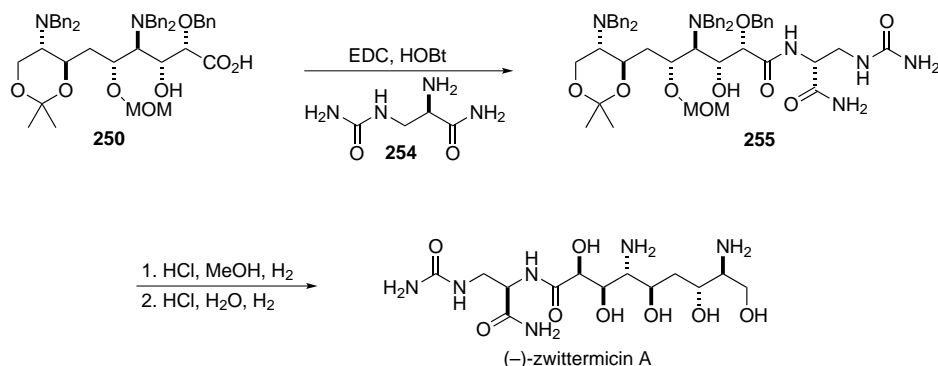
To confirm the proposed structural and stereochemical assignment, Molinski and co-workers pursued a total synthesis of the natural product. The synthesis starts from azidodiol **246**, which was prepared from L-Ser as part of the NMR studies. The terminal alcohol was protected as a TBDPS ether, the secondary alcohol was protected as a MOM ether, and the TBDPS group was removed to give **247** in 85% over 3 steps. Azide **247** was hydrogenated, the free amine was benzylated, and the primary alcohol was oxidized to give aldehyde **248**. Compound **248** was employed in a diastereoselective Evan's aldol addition of the chiral glycolate auxiliary **249** to give, after hydrolysis, carboxylic acid **250** in 74% and 96:4 dr. Coupling of acid **250** with amine **251** and global deprotection yielded (–)-**253** (Scheme 3.1). Although the ¹H NMR spectrum of the C10–C15 fragment of **253** was almost identical to the natural sample of **245**, a pronounced difference occurred at H8. Also, the specific rotation of (–)-**253** was of opposite sign and of larger magnitude than for natural (+)-**245**.

Scheme 3.1. Synthesis of the initially proposed stereoisomer of zwittermicin A.



To resolve this discrepancy, compound **250** was coupled with **254**, the enantiomer of **251**, to give adduct **255**. Global deprotection of compound **255** afforded (–)-**245**, the enantiomer of the isolated natural product. The specific rotation of (–)-**245** was opposite in sign and equal in magnitude to natural (+)-zwittermicin A (Scheme 3.2).¹⁴⁰

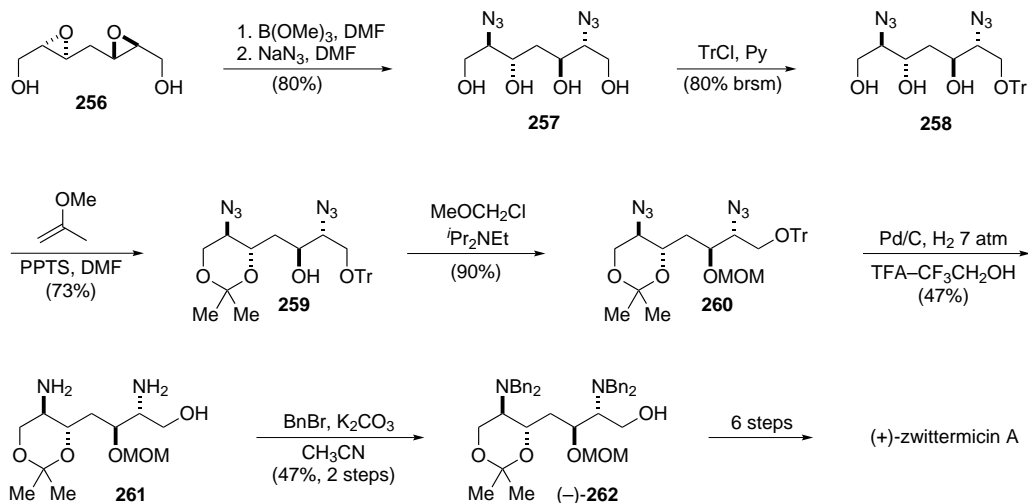
Scheme 3.2. Synthesis of zwittermicin A enantiomer



These findings suggested that the assignment of the relative stereochemistry of the C10–C15 fragment was correct and the mismatch resulted from the inversion of all configurations in the diaminopolyol–carboxylate moiety of (–)-**253**. This result refuted the original hypothesis on the origin of stereochemistry at C14 and now suggests that D-Ser rather than L-Ser is incorporated during biosynthesis.

A formal total synthesis of (+)-zwittermicin A (**245**) was recently accomplished by the Molinski group.¹⁴¹ The C9–C15 portion of (+)-**245** was prepared in a two-directional approach from the known bis(epoxide) **256**.¹⁴² Double Miyashita-type opening¹⁴³ of the epoxide afforded bis(azide) **257** in 80% yield. Compound **257** was desymmetrized by placing a trityl group on the terminal alcohol to get to **258** in 69% yield. The 1,3-diol was converted to acetonide **259**, followed by protection of the secondary alcohol as a MOM ether. Simultaneous removal of the trityl group and reduction of both azides was accomplished by hydrogenation to give diamine **261** that was protected as a dibenzylamine using benzyl bromide (Scheme 3.3). A formal synthesis of (+)-zwittermicin (**245**) can be achieved by utilizing **262** instead of **247** in a synthetic path depicted in Scheme 3.1.

Scheme 3.3. Formal Total Synthesis of (+)-Zwittermicin A



3.1.3 Biosynthesis

The aminopolyol chain of (+)-zwittermicin A (ZmA) may imply that it is a product of carbohydrate metabolism, but it is in fact a polyketide. Emmert and co-workers first suggested in 2004 that the biosynthesis of zwittermicin A arises from a non-ribosomal peptide synthetase (NRPS)–polyketide synthase (PKS) megasynthase.¹⁴⁴ This hypothesis was recently validated by Kevany and co-workers, who characterized the complete zwittermicin A biosynthesis gene cluster from *Bacillus cereus* UW85.¹⁴⁵ In order to explain the formation of the terminal amide group,¹⁴⁶ they suggested that **245** is initially produced as part of a larger metabolite that is processed twice, resulting in formation of the natural product and two additional metabolites.

Based on analysis of the NRPS/PKS components and other enzymes encoded by the biosynthesis gene cluster, Kevany and colleagues proposed the following biosynthesis (Figure 3.2).¹⁴⁵ The *zmaO* module of the NRPS/PKS megasynthase activates L-Asn, condenses it with a fatty acid, and epimerizes the L-Asn to D-Asn to form the fatty acyl-D-Asn-*S*-*zmaO* intermediate. The next five NRPS/PKS modules form the backbone of zwittermicin A by condensing the fatty acyl-D-Asn intermediate with L-Ser, malonate, (2*S*)-aminomalonnate, (2*R*)-hydroxymalonnate, and β -Uda. During the condensation of these precursors, the stereochemistry of the L-Ser unit is changed to D-Ser to result in the stereochemistry of the final product. It is not yet clear how this occurs because an epimerase (E) domain is not found in the NRPS module that incorporates L-Ser. However, the module immediately upstream of the L-Ser-associated module contains an E domain. The growing fatty acyl-peptide/polyketide is extended by an additional amino acid, L-Ala, to form a covalently

linked intermediate on the second PCP domain of zmaB. At this stage, the backbone of ZmA has a fatty acyl-D-Asn at its N terminus and L-Ala at its C terminus, both of which must be removed to make the antibiotic. The authors propose that the fatty acyl-D-Asn intermediate is released by oxidation by zmaL and removal of the fatty acyl-D-Asn piece by zmaM which leads to **245** and two metabolites (Figure 3.2).¹⁴⁵

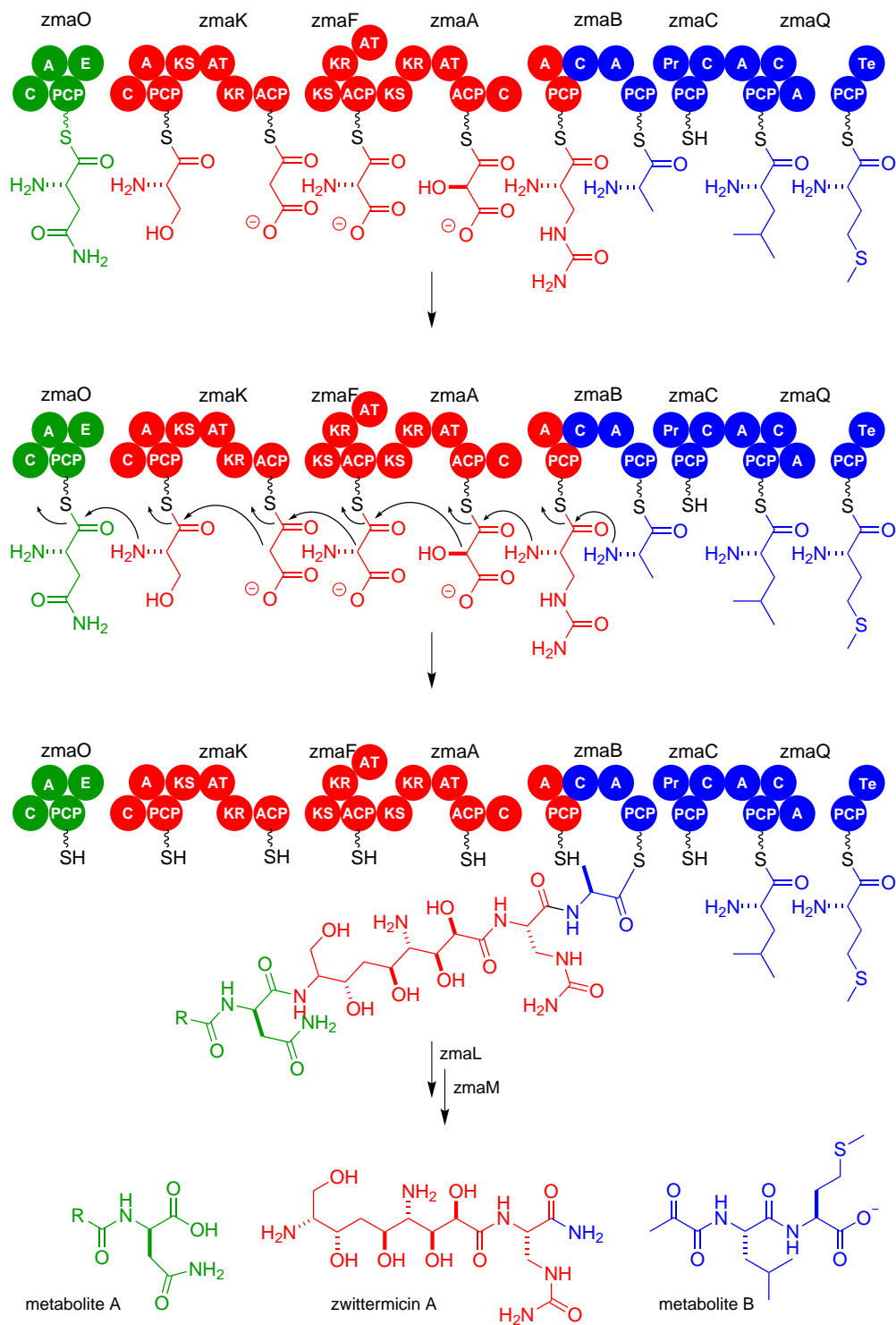


Figure 3.2. Proposed biosynthesis of zwittermicin A (adapted from ref. 145)

3.2 Two-directional synthesis

3.2.1 Introduction

Acyclic molecules with underlying symmetry may be approached using a two-directional strategy instead of the more prevalent one-directional strategy. In a linear approach, the synthetic target is built in one direction by homologation of the existing fragment and is most useful for the synthesis of short chains. A one-directional *convergent* strategy is often utilized by chemists for the synthesis of complex natural products that are assembled from smaller fragments. Whenever an underlying element of symmetry is present in the target molecule or fragment, two-directional synthesis may be applied. Performing two structure building transformation simultaneously at chain ends reduces the number of steps required but, depending on the symmetry element, can require a challenging desymmetrization step (Figure 3.3).^{147,148}

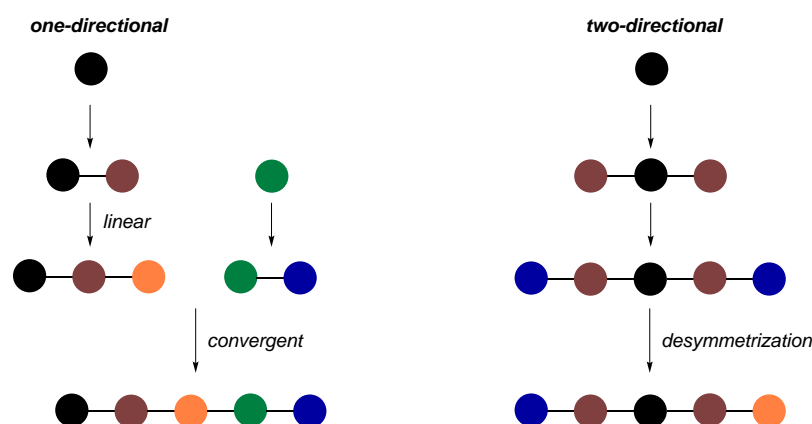
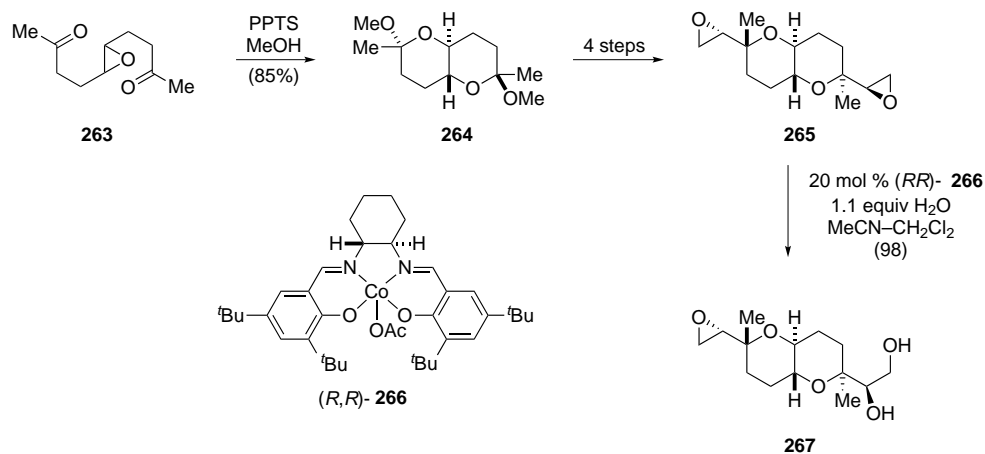


Figure 3.3. General strategies for the synthesis of acyclic compounds.

3.2.2 Two-directional synthesis of natural products

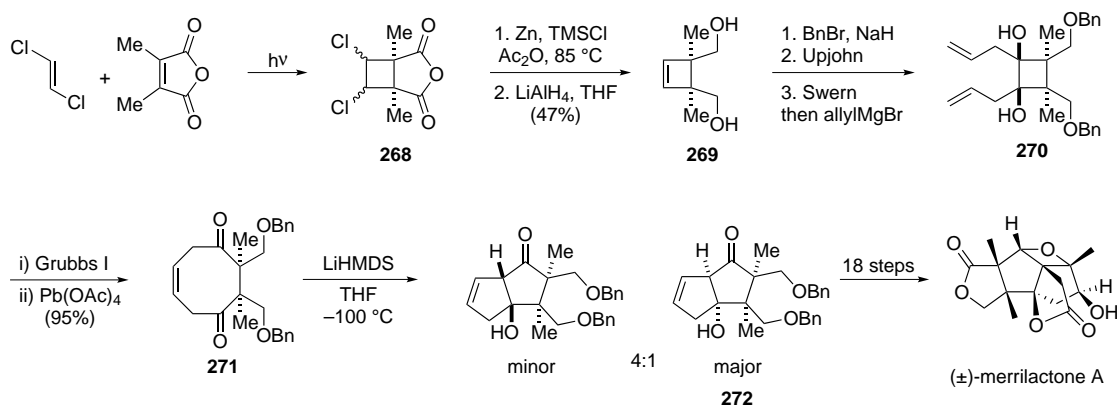
The chemical literature is rich in examples of two-directional synthesis, and early examples have been summarized by Schreiber¹⁴⁷ and Magnuson.¹⁴⁸ In 2004 Nelson demonstrated a two-directional synthesis of compound **267** in a total synthesis of hemibrevetoxin B (Scheme 3.4). The *trans*-epoxydiketone **263** undergoes acid-catalyzed cyclization to give diacetal **264**, which after four additional steps gives centrosymmetric diepoxide **265**. Desymmetrization is achieved via enantioselective epoxide opening with water in a transformation catalyzed by cobalt complex **266**. Diol **267** forms in 98 % yield and 95 % ee.¹⁴⁹

Scheme 3.4. Two-directional synthesis of the intermediate in a total synthesis of hemibrevetoxin B.



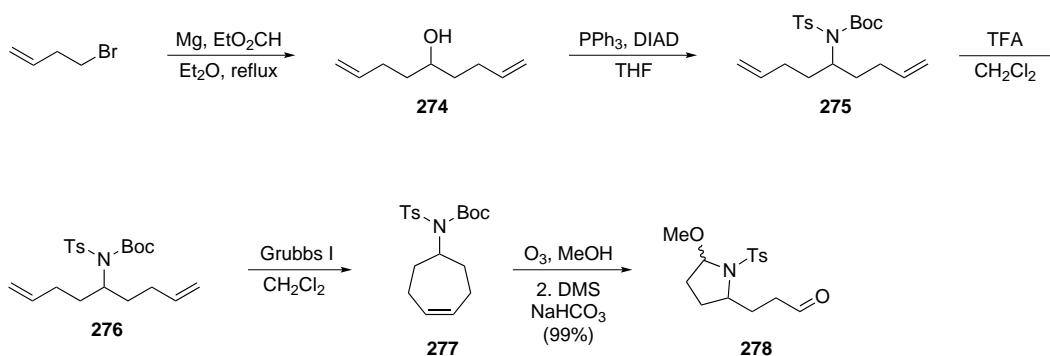
Inoue and co-workers demonstrated an elegant two-directional synthesis of (\pm)-merrilactone A (Scheme 3.5).¹⁵⁰ Photocycloaddition of dichloroethylene and dimethyl maleic anhydride produces dichloride **268**. Further two-directional elaboration affords cyclobutene **269**. After the protection of alcohols as benzyl ethers, an Upjohn dihydroxylation was performed, and the resulting diol was oxidized to a diketone and reacted *in situ* with allyl magnesium bromide to give cyclobutane **270** in 78% overall yield. Treatment of **270** with Grubbs I catalyst at elevated temperature causes cyclooctane ring formation which is followed by addition of $\text{Pb}(\text{OAc})_4$ to deliver key intermediate **271**. At this point desymmetrization was performed via a transannular aldol reaction. Using $\text{LiN}(\text{TMS})_2$ as a base, desired compound **272** forms in 3:1 dr and 85% yield.¹⁵⁰

Scheme 3.5. Two-directional synthesis of merrilactone A.



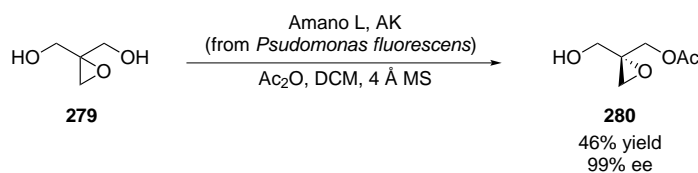
In 2008, Stockmann and co-workers applied a two-directional approach to the formal synthesis of anatoxin-a.¹⁵¹ Starting from 3-butenyl bromide, key aldehyde **278** is prepared in just 6 steps (Scheme 3.6). Double Grignard addition to ethyl formate produces alcohol **274**. The alcohol is converted to *N*-Boc sulfonamide **275** in a Mitsunobu reaction. The Boc group is removed, and bis(alkene) **276** is cyclized to cycloheptene **277** under Grubbs ring closing metathesis conditions. Desymmetrization of the alkene is carried out via ozonolysis and *in situ* addition of the sulfonamide nitrogen to form hemiaminal **278**. Elaboration of **278** allows for the formal synthesis of anatoxin-a (Scheme 3.6).¹⁵¹

Scheme 3.6. Assembly of an intermediate for a formal synthesis of anatoxin-a.



Enzymatic reactions are often utilized for desymmetrization. High specificity of enzymes for substrates allows for selective transformations in cases where conventional reagents give a statistical mixture of products (Scheme 3.7).¹⁵² Simple *meso*-diol **279** can be desymmetrized and resolved in an enzymatic reaction with acetic anhydride to give essentially enantiopure acetate **280** as shown in Scheme 3.7.¹⁵³

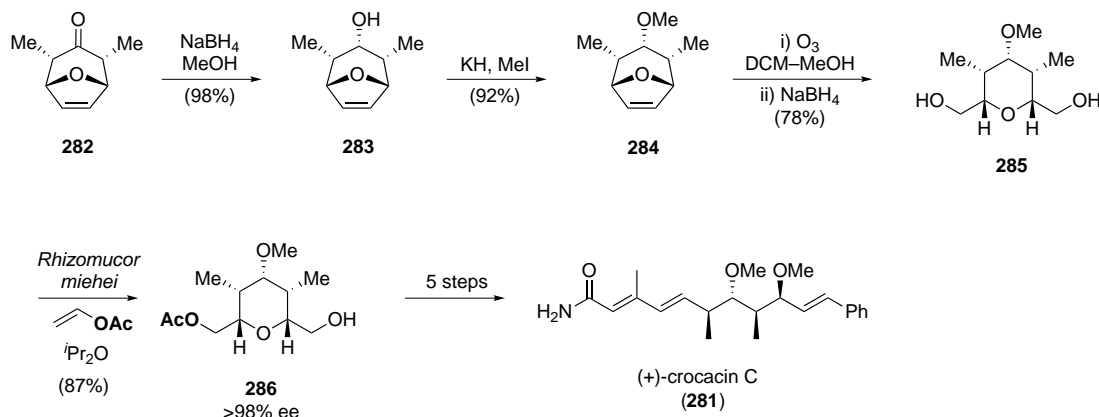
Scheme 3.7. Enzymatic desymmetrization–resolution of *meso*-epoxides.



An example of synthetic utility of enzymes in two-directional synthesis was disclosed by the Pons group in their the total synthesis of (+)-crocacin C (**281**).¹⁵⁴ The oxabicyclo **282**¹⁵⁵ was reduced diastereoselectively, and the resulting alcohol **283** was etherified using methyl iodide. Ether **284** was subjected to ozonolysis with reductive work-up, which gave *meso*-diol

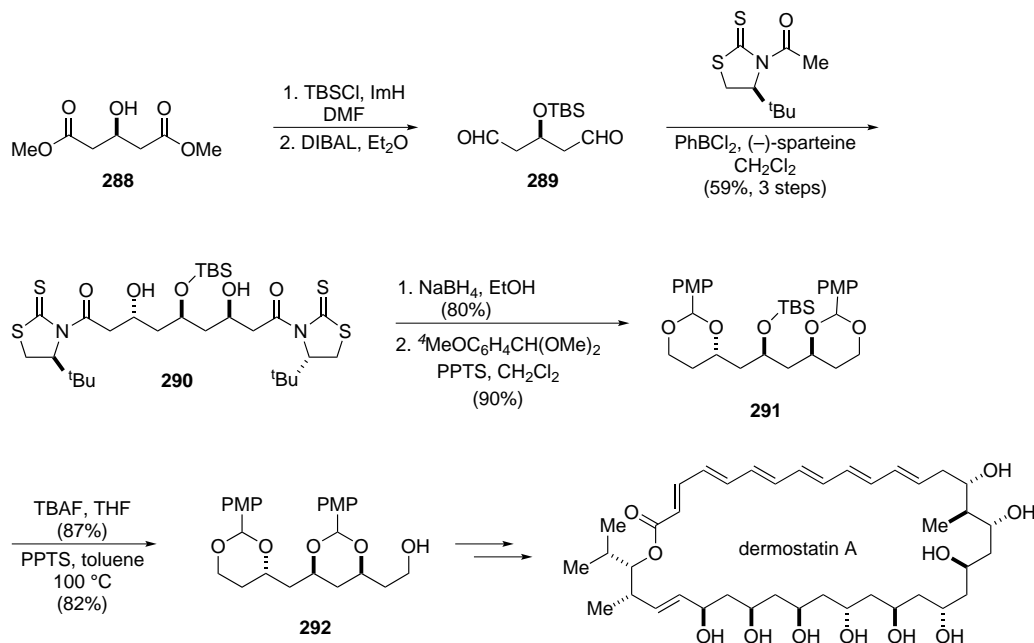
285 in 70 % over three steps. Desymmetrization was performed using *Rhizomucor miehei* in the presence of vinyl acetate in diisopropyl ether giving acetate **286** in 87 % yield and over 98 % ee. This desymmetrization protocol unmasked five contiguous stereogenic centers in a single operation (Scheme 3.8).¹⁵⁴

Scheme 3.8. Enzymatic desymmetrization en route to (+)-crocacin C.



In 2011, Sammakia and co-workers utilized this approach in their synthesis of dermostatin A (Scheme 3.9).¹⁵⁶ Starting with glutarate ester **288**, alcohol protection followed by reduction of the ester provided the bis(aldehyde) **289**. Desymmetrization was achieved via a diastereoselective acetate aldol reaction with *N*-acetylthiazolidinethione that provided product **290** as a single diastereomer in 70 % yield. Reductive removal of the auxiliary and protection of the resulting 1,3-diol as the *p*-anisaldehyde dimethyl acetal gave compound **291**. The termini of *pseudo-C*₂ symmetric compound **291** were differentiated via acetal group migration. The central alcohol was deprotected with TBAF and then treated with PPTS in toluene at 100 °C. Only the group that provided *syn*-acetal migrated during this reaction, to yield key intermediate **292** for the completion of the synthesis of dermostatin A.¹⁵⁶

Scheme 3.9. Synthesis of the *pseudo*- C_2 -symmetric bisacetal en route to dermostatin A.

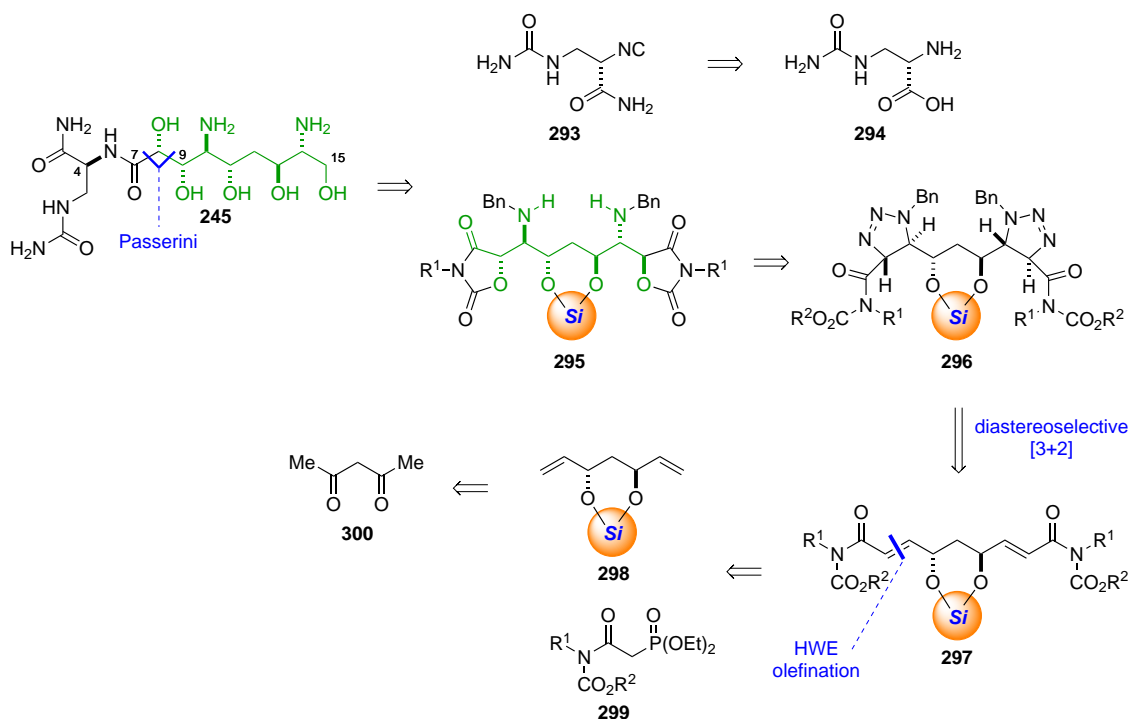


3.2.3 Approach to (+)-zwittermicin A via a two-directional azide–alkene cycloaddition

In our synthesis of (+)-zwittermicin A, we plan to use the amide functionality at C7 for the main retrosynthetic disconnection. A Passerini reaction will be used to bring together two fragments and form the amide as well as the secondary alcohol at C8. The isonitrile (**293**) required for this step will carry all necessary functional groups for maximum convergence. It will be derived from the known amino acid L-albizziine (**294**). Bis(oxazolidine dione) **295** represents a masked form of the aldehyde needed for the Passerini reaction and has all stereocenters of the C9–C15 aminopolyol chain.

A stereoselective approach to **295** is the main pillar of our strategy. Taking advantage of the *pseudo*- C_2 -symmetry of the C9–C15 chain of zwittermicin A, we will establish terminal aminoalcohols in a bidirectional approach. Bis(oxazolidine dione) **295** will come from a stereospecific fragmentation of bis(triazoline) **296**. Compound **296** will be formed using a triflic acid-promoted Huisgen cycloaddition reaction between bis(imide) **297** and benzyl azide. Diastereoselectivity of this transformation will be controlled by the protecting group at the central *anti*-1,3-diol. Bis(imide) **297** will be synthesized via a Horner–Wadsworth–Emmons reaction between the aldehyde derived from **298** and imidophosphonate **299**. Compound **298** will be prepared asymmetrically from pentane-2,4-dione **300** using published procedures.

Scheme 3.10. Retrosynthetic analysis



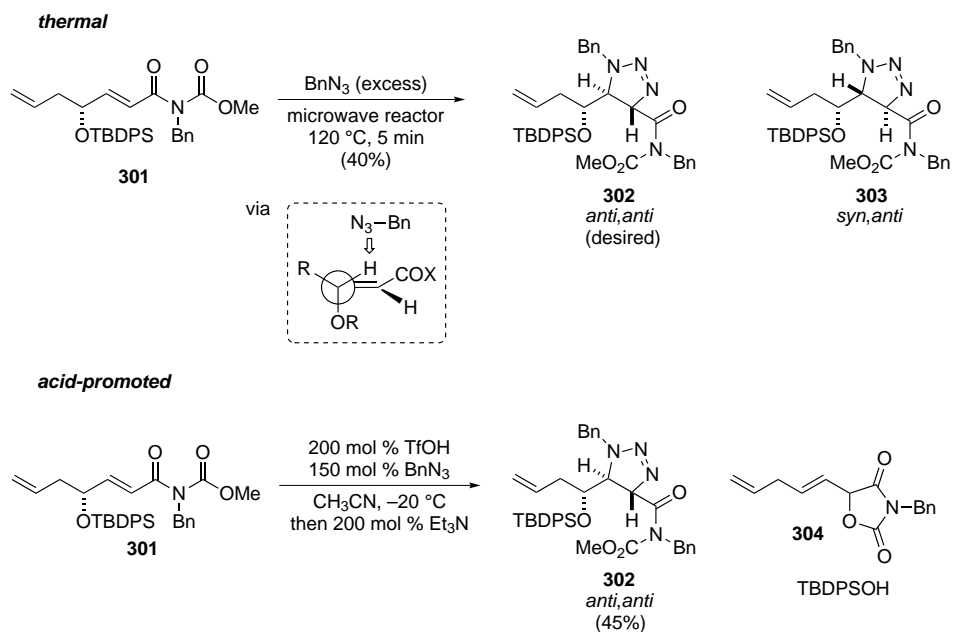
3.3 Previous work

3.3.1 Diastereoselective azide–alkene reaction: a model study

We began investigation of substrate-controlled diastereoselection in the Brønsted acid-promoted azide–alkene reactions by studying a reaction of **301** and benzyl azide.⁷³ This chiral non-racemic imide was equipped with the TBDPS group to provide the necessary bulk for a substrate-controlled diastereoselective [3+2] cycloaddition. Reaction under thermal conditions delivered modest yield and diastereoselection for the desired *anti,anti*-triazoline (**302**) over the *syn,anti* diastereomer (**303**) (Scheme 3.11). Stereoselectivity originates from the arrangement of the C–O bond orthogonal to the π -plane as observed in stereoselective addition reactions of organocuprates¹⁵⁷ to α,β -unsaturated esters.¹⁵⁸

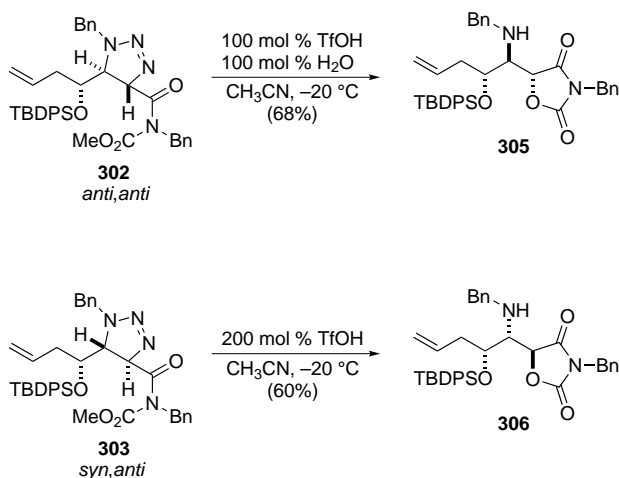
Although the bulky TBDPS ether influences the selectivity of the reaction, further lowering of the reaction temperature to increase dr is not practical for thermal reactions. On the other hand, activation of the imide by Brønsted acid operates at an acceptable rate at temperatures as low as $-20\text{ }^{\circ}\text{C}$. Using triflic acid in acetonitrile at $-20\text{ }^{\circ}\text{C}$, the same reaction proceeded with exceptional selectivity and delivered the desired *anti,anti*-triazoline (**302**) in 40% yield, albeit with nearly equal amounts of S_N2' elimination product **304** (Scheme 3.11).

Scheme 3.11. Substrate-controlled diastereoselectivity in [3+2] cycloaddition



Selectivity was confirmed by NMR (1D and 2D) analysis of both **302** and **303** as well as their fragmentation products, oxazolidine diones **305** and **306** respectively (Scheme 3.12).⁷³ This procedure which involves [3+2] Huisgen cycloaddition and acid-promoted triazoline fragmentation in separate steps avoids the possibility of S_N2' product formation.

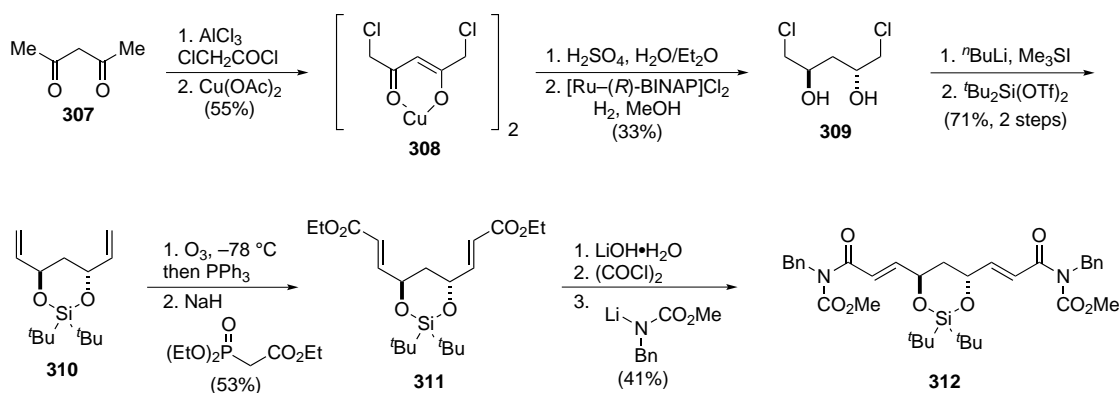
Scheme 3.12. Diastereoselectivity in acid-promoted reaction



3.3.2 Synthesis of bis(imide) **312**

Synthesis of the key substrate for the [3+2] cycloaddition reaction, bis(imide) **312**, commences with preparation of (2*R*,4*R*)-1,5-dichloropentane-2,4-diol (**309**) according to a known literature procedure.¹⁵⁹ First, 1,3-pentane dione (**307**) is subjected to a reversible acetylation reaction and the product, 1,5-dichloropentane-2,4-dione, is trapped as copper(II) complex **308** in 55 % yield. Treatment of **308** with sulfuric acid revealed the 1,3-dione, which was subjected to asymmetric Noyori reduction to yield diol **309** in 40 % yield.¹⁵⁹ Conversion of **309** to bis(alkene) **310** was achieved in 71 % yield in two steps. A reaction of **310** with a large excess of dimethylsulfonium methylide¹⁶⁰ was followed by protection of the 1,3-diol as a di-*tert*-butylsilyl ether.¹⁶¹ Aldehyde obtained by ozonolysis of **310** was immediately reacted with the stabilized phosphonate ester anion in a Horner–Wadsworth–Emmons reaction to give **311** in 53 % yield. Ethyl ester **311** was saponified, converted to the corresponding acid chloride, and coupled with the lithium benzyl(methoxycarbonyl)amide to yield desired bis(imide) **312** in 41 % yield (Scheme 3.13).

Scheme 3.13. Preparation of the di(*tert*-butyl)silyl bis(imide).

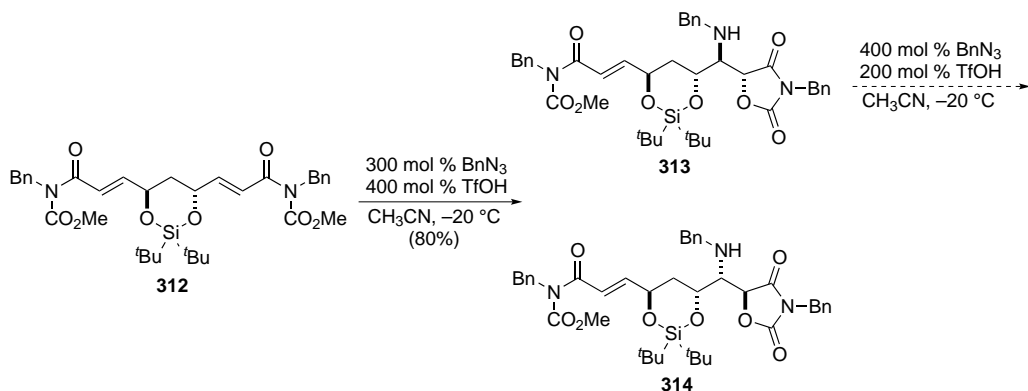


The attempt to obtain a bis(triazoline) from **312** via Brønsted acid-promoted [3+2] cycloaddition with benzyl azide was unsuccessful. The major product was a 5:1 mixture of *anti-anti*- and *syn-anti*-oxazolidine dione, **313** and **314** respectively, where only half of the imide reacted*. When **313** was resubjected to the reaction conditions with a large excess of benzyl azide, no further reaction was observed (Scheme 3.14).

An alternative approach to the bis(triazoline) is a reaction of **312** with benzyl azide under thermal conditions. We observed full conversion of bis(imide) **312** after a reaction in neat benzyl azide at 100 °C for 1 h in the microwave reactor. Similar to our prior experience,

*For a complete nOe conformational analysis of the products see: ref 73

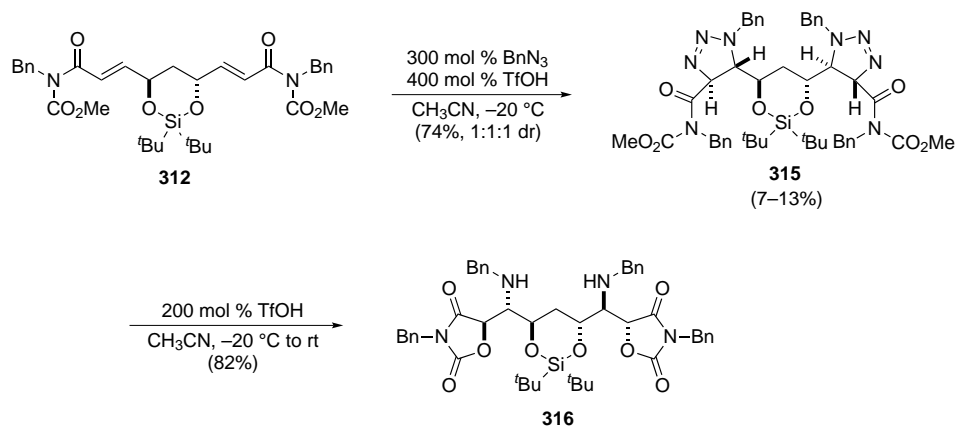
Scheme 3.14. Attempted Two-Directional Triflic Acid-Catalyzed [3+2] Reaction



the reaction was not selective. We obtained a statistical mixture of three diastereomeric triazolines in 74% yield. Extensive chromatography was necessary to isolate bis(triazoline) **315** but the isolated yield was significantly diminished (13%). The relative stereochemical identity of the product was confirmed by analysis of NOE correlations.

With **315** in hand, we tested the triflic acid-promoted triazoline fragmentation–cyclization reaction to **316**. Compound **315** was treated with TfOH in acetonitrile at rt for several hours and provided bis(oxazolidone) **316** in 82% yield. Analysis of the NOE correlations provided evidence that the relative stereochemistry of **316** is *anti,anti* as in zwittermicin A (Scheme 3.15).

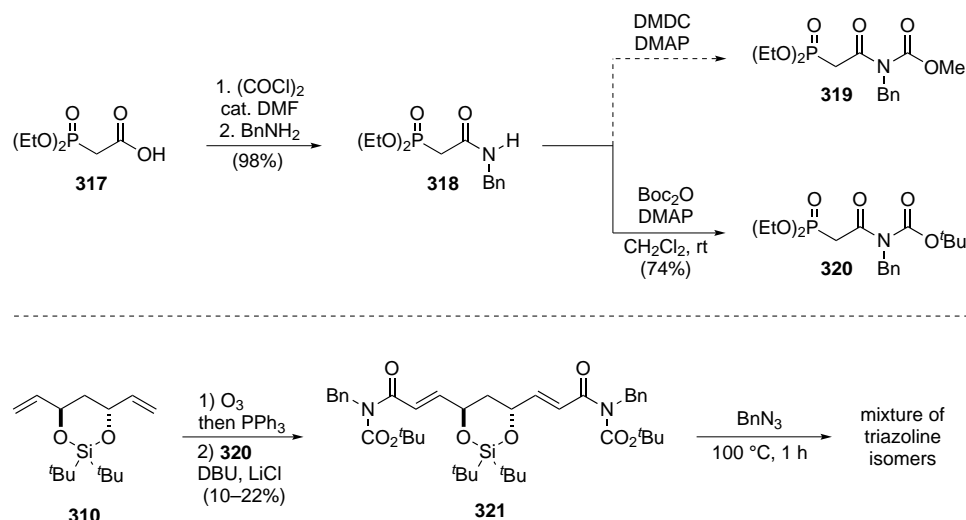
Scheme 3.15. Thermal Two-Directional [3+2] Reaction



To shorten the synthesis of the bis(imide), a Horner–Wadsworth–Emmons reaction with imidophosphonate **320** was pursued. Phosphonate **320** can be easily prepared from diethylphosphonoacetic acid **317** in three steps. Conversion of **317** to the acid chloride and

a reaction with benzylamine yields amidophosphonate **318** in nearly quantitative yield. An attempt to install a methyl ester using dimethyl dicarbonate (DMDC) and DMAP was unsuccessful but the same reaction with Boc anhydride proceeded smoothly and afforded bis(imide) **321** in 74% yield. Although a variety of protocols was applied, the yield of the ozonolysis–olefination sequence with imidophosphonate **320** was very low (10–22%) and required extensive chromatographic purification of product **321** (Scheme 3.16).

Scheme 3.16. Horner–Wadsworth–Emmons reaction with *tert*-butyl imidophosphonate.



A seemingly insignificant change of the ester functional group (methyl to *tert*-butyl) in the bis(imide) caused a serious problem. Nearly identical reactivity and selectivity was observed for bis(imide) **321** in the microwave-assisted reaction with benzyl azide. Unfortunately, chromatographic purification of the desired *anti,anti*-bis(triazoline) proved to be difficult and we were unable to obtain a pure sample using conventional chromatography techniques.

3.3.3 Summary of previous work

This work provided evidence that the bis(oxazolidine dione) is a viable intermediate in the synthesis of zwittermicin A. The fragmentation–cyclization of *anti,anti*-triazoline **315** proceeds as planned and provides an intermediate with the required relative stereochemistry of zwittermicin A. However, there are several challenges that need to be addressed before the synthesis of the natural product can be pursued further. The synthesis of the key intermediates, bis(imide) **312** and bis(triazoline) **315**, is far from efficient. The overall yield of the transformation of **310** to **315** (6 steps) is ca. 2%. The Brønsted acid-catalyzed aminohydrox-

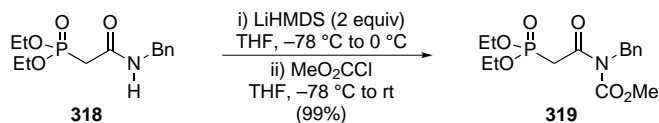
ylation reaction is diastereoselective, but only one half of the bis(imide) molecule engages in the reaction. On the other hand, both alkenes react in a microwave-assisted [3+2] reaction of **312** with benzyl azide, but the reaction is neither chemo- nor diastereoselective. Isolation of **315** is laborious and low yielding.

3.4 Results and discussion

3.4.1 Optimization of the synthesis of bis(imide) **312**

Before approaching the problem of diastereoselectivity in bis(triazoline) formation we needed to establish a more convergent and better yielding route to **312**. We first focused our efforts on the optimization of the Horner–Wadsworth–Emmons reaction, specifically the synthesis of the imidophosphonate methyl ester **319**. Our previous attempts at an acyl transfer from dimethyl dicarbonate to the amidophosphonate **318** were unsuccessful (Section 3.3). We were pleased to observe a nearly quantitative conversion of **318** to **319** when the lithium amide of **318**, generated with 2 equiv of LiHMDS, was acylated with methyl chloroformate (Scheme 3.17).

Scheme 3.17. Synthesis of the imidophosphonate.

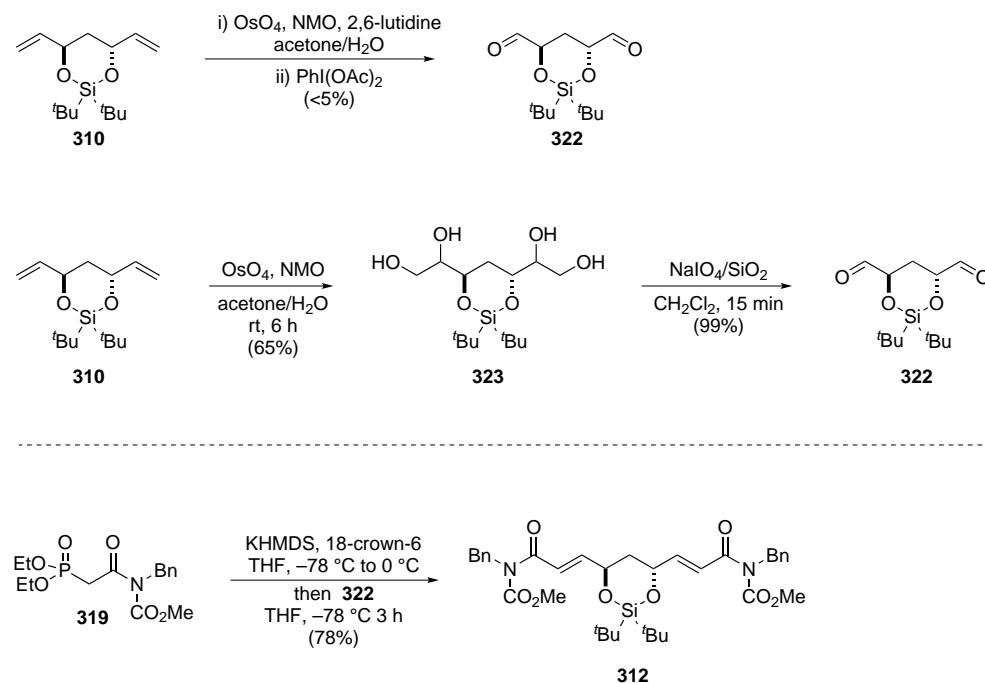


To improve the formation of **312** we turned to examination of ozonolysis of **310**. Although full consumption of the alkene was observed after 30 min at $-78\text{ }^\circ\text{C}$ we were unable to isolate the bis(aldehyde) **322**. Various work-up procedures gave rise to ill-defined multicomponent reaction mixtures, while only small amounts of the aldehyde functionality was observed in the ^1H NMR spectrum.

With identification of the problematic step, we moved to implement a dihydroxylation–diol cleavage protocol to access the bis(aldehyde) **322**. First we evaluated a one-pot procedure developed by Nicolaou and co-workers¹⁶² that employs $\text{PhI}(\text{OAc})_2$ in presence of 2,6-lutidine to cleave the diol *in situ* after dihydroxylation with catalytic OsO_4 and NMO. Although we observed clean conversion to the aldehyde, the product was not compatible with silica gel chromatography and only a trace amount of **322** was obtained. As a solution to this problem we turned to a two-step procedure. Dihydroxylation of **310** gave compound

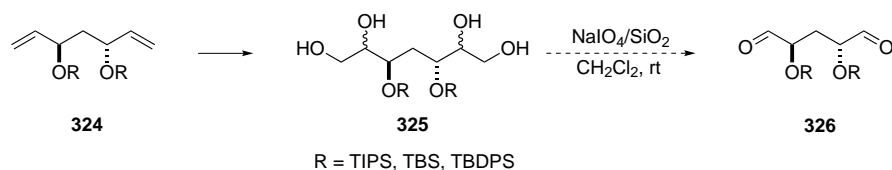
323 as a mixture of diastereomers in 65 % yield. With the preparation of **323** accomplished, Johnson-Lemieux oxidation¹⁶³ was undertaken using the protocol developed by Zhong and Shing.¹⁶⁴ The reaction with silica gel-supported NaIO₄ delivered bis(aldehyde) **322** in quantitative yield without need for chromatography. Crude **322** was reacted with a large excess of the potassium anion of imidophosphonate **319** in presence of 18-crown-6 (Scheme 3.18). The desired bis(imide) **312** was obtained in 78 % yield as an *E,E*-isomer.

Scheme 3.18. Improved synthesis of the bis(imide) **312**



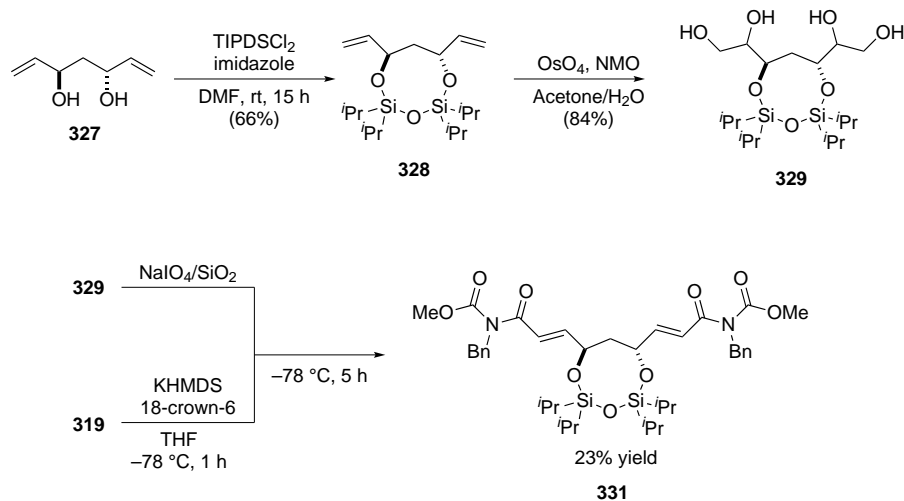
With this more convergent route to **312** in hand, we were able to fully address the question of reactivity and selectivity of the [3+2] cycloaddition reaction. We hypothesized that by modifying the 1,3-diol protecting group we would be able to obtain the desired reactivity and selectivity. Our initial plan was to use an acyclic bis(silyl ether) protection of 1,3-diol, but such alkenes were unstable under ozonolysis conditions. With the improved preparation, we revisited acyclic silyl derivatives **324**. Although dihydroxylation proceeded without complication, the resulting polyols (**325**) didn't afford the corresponding aldehydes **326** when subjected to oxidative cleavage. Silyl protected polyols (**325**) with varying degree of steric bulk yielded complex reaction mixtures when subjected to NaIO₄ (Scheme 3.19). At this point it became clear to us that the central 1,3-diol had to be protected as a cyclic silyl ether, with the belief that conformational constraint and added steric hindrance might lower the nascent aldehyde reactivity.

Scheme 3.19. Unsuccessful synthesis of acyclic silyl ether aldehydes.



Low reactivity and selectivity with bis(imide) **312** can be attributed to two factors, the size of the siloxane ring and size of the substituent on the silicon atom. The first hypothesis can be addressed by incorporation of the 1,3-diol into an 8-membered ring by reaction with TIPDSCl₂ (1,3-dichloro-1,1,3,3-tetraisopropyldisiloxane) in DMF in the presence of imidazole. This protecting group was originally developed for the selective protection of nucleosides.^{165,166} In contrast to the 6-membered DTBS ring (compound **312**), the TIPDS ring is more flexible and might improve the reactivity and selectivity of the bis(imide) in the cycloaddition reaction. The reaction of diol **327** with TIPDSCl₂ was straightforward and afforded the product **328** in 66 % yield. Upjohn dihydroxylation delivered polyol **329** (in 84 % yield) that was subjected to oxidative cleavage with NaIO₄ · SiO₂ and immediately reacted with the anion of the imidophosphonate **330** generated with KHMDS and 18-crown-6. We were disappointed to see very low yield (23 %) of the desired bis(imide) **331** (Scheme 3.20).

Scheme 3.20. Preliminary synthesis of the TIPDS bis(imide).



A careful analysis of the mass balance of this reaction revealed that a major by-product of this reaction is phosphonate **334** (Figure 3.4). We speculated that formation of *trans*-oxaphosphetane **332** is slow (Figure 3.4, path A) and the competitive acyl transfer occurs

(path B) to give phosphonate carbonate **333**, which produces compound **334** upon methyl carbonate elimination (Figure 3.4). The proton, carbon and phosphorus NMR as well as mass spectrometry data were in agreement with the proposed structure (**334**).

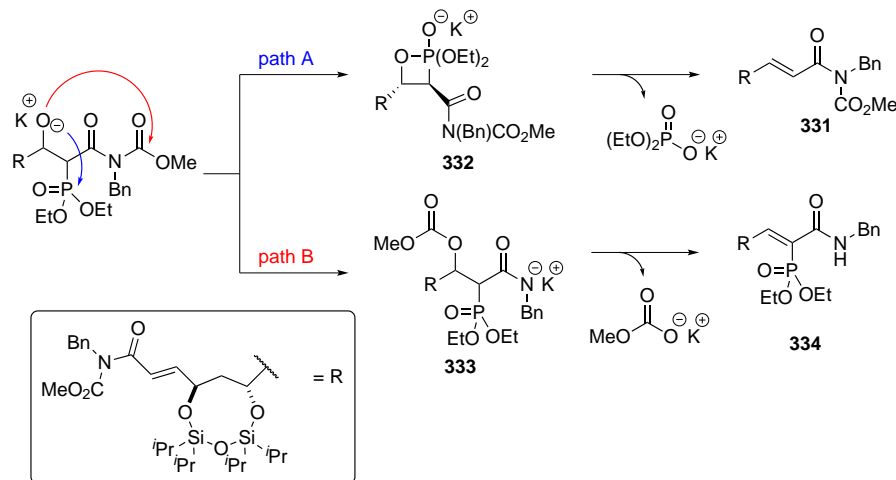
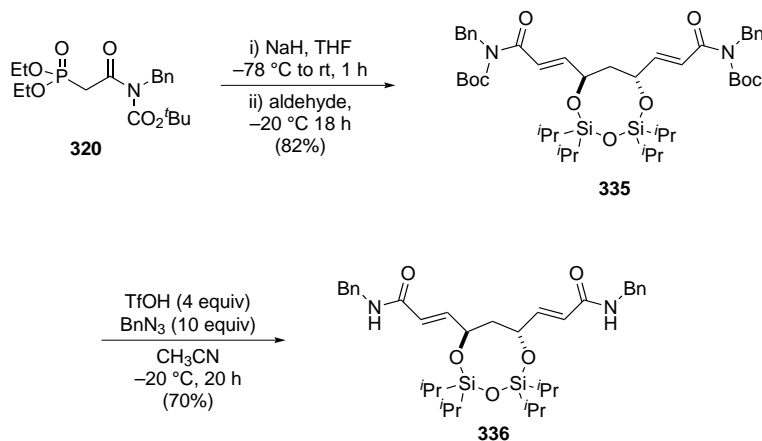


Figure 3.4. Mechanism of the competitive acyl transfer during Horner-Wadsworth-Emmons reaction

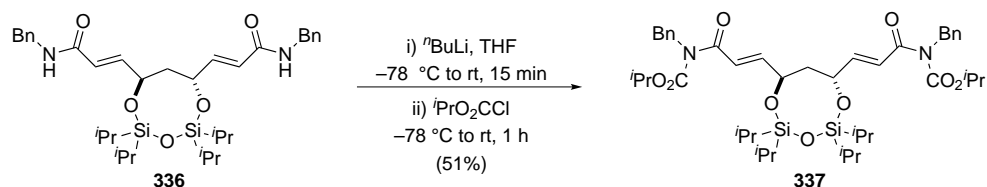
To address this problem, we increased the steric demand of the ester group to limit the rate of the undesired acyl transfer. Bis(imide) **335** was prepared in 82% yield when imidophosphonate **320** was used. Unfortunately, when we reacted **335** with benzyl azide, we observed gas evolution immediately after addition of triflic acid. The bis(amide) **336** was isolated as the only product (Scheme 3.21) which suggests that removal of the Boc group is significantly faster than [3 + 2] reaction with benzyl azide, even at -20°C .

It became clear to us that the bulky ester does increase the yield of the Horner-Wadsworth-Emmons reaction by limiting the pathway to elimination, however it should not be acid-labile. Therefore, we hypothesized that the isopropyl ester, while providing steric bulk, would not as easily succumb to decomposition. Instead of preparing the imidophosphonate required for the Horner-Wadsworth-Emmons reaction, we could test this hypothesis by preparing bis(imide) **337** through acylation of **336**. Compound **336** was treated with two equivalents of $n\text{BuLi}$ followed by addition of isopropyl chloroformate to arrive at **337** in 51% yield (Scheme 3.22).

Scheme 3.21. Removal of the *N*-Boc group during Brønsted acid-promoted reaction with benzyl azide.



Scheme 3.22. Synthesis of the isopropyl bis(imide).



3.4.2 Studies of facial discrimination in the acid-promoted azide–olefin cycloaddition

We then investigated diastereoselectivity of the cycloaddition as a function of size of the cyclic silyl group. We began with a thermal reaction of the bis(imide) **312**. After 45 min at 100 °C under microwave irradiation in neat benzyl azide, all three stereoisomers formed nonselectively (1:2:1 ratio) (Table 3.1). The desired 2,3-*anti* diastereomer **315a** was separated and the relative stereochemistry was assigned through a spectroscopic study (NOESY).⁷³ Although the overall yield was satisfactory, purification of the desired 2,3-*anti*/2',3'-*anti* diastereomer **315a** was cumbersome.

We then turned our attention to triflic acid-promoted triazoline formation. When imide **312** was reacted with BnN₃ in the presence of triflic acid at -20 °C in acetonitrile, again, all three bis(triazolines) were isolated in 67% yield (Table 3.1, entry 2). In this experiment, however, the 2,3-*syn* diastereomer **315b** was favored and the desired **315a** formed as a minor product. We found that a change of the carbamate functionality from Me to ⁱPr slightly improves selectivity but delivered mostly undesired bis(triazolines) **339b** and **339c** (entry 3) in 54% combined yield with the desired **339a** forming in trace amounts. Bis(imide) **340**

with a smaller diisopropyl silyl ring, decomposed under the reaction conditions providing the mixture of triazolines in only 7% yield* (Table 3.1, entry 4).

Table 3.1. Substrate-Controlled Double (3+2) Cycloaddition

entry	alkene	<i>Si</i>	R	conditions	product	a:b:c	yield %
1	312		Me	A	315	1:2:1	72
2	312		Me	B	315	1:2.5:5.4	67
3	338		<i>i</i> Pr	B	339	1:9:9	54
4	340		<i>i</i> Pr	B	341	ND	7
5	331		Me	B	342	18:1:1	27
6	337		<i>i</i> Pr	B	343	18:1:1	79

^a Conditions A: BnN₃ (neat), microwave 100 °C, 1 h; Conditions B: TfOH (5 eq), BnN₃ (10 eq) MeCN 0.2 M, 20 °C, 18 h. ^b Ratio of products was measured by ¹H NMR analysis of the crude reaction mixture. ^c Combined isolated yield. ^d ND = not determined due to signal overlap by ¹H NMR.

Our original expectation was that the siloxane protected 1,3-*anti*-diol would assume a twist-boat conformation in order to maintain its two alkene substituents in a *pseudo*-equatorial arrangement (**A**, Figure 3.5). We reasoned that expansion of the ring from six to eight members through the formation of a disiloxanylidene derivative might better achieve

*The ratio could not be determined from the ¹H NMR spectrum

this goal by providing greater flexibility around the oxygen-substituted edge (**B**, Figure 3.5). Accordingly, the 8-membered ring methyl carbamate **331** incorporating a tetraisopropoxydisiloxanylidene group^{167,168} (TIPDS) was prepared. Not only did bis(imide) **331** provide the bis(triazoline) with high diastereoselection (Table 3.1, entry 5), it favored the desired *anti,anti*-**342a** in 30 % yield. Introduction of the isopropyl carbamate in bis(imide) **337** led to a significant increase in the yield of the 2,3-*anti* bis(triazoline) **343a** (79 %) without loss of diastereoselection (Table 3.1, entry 6).

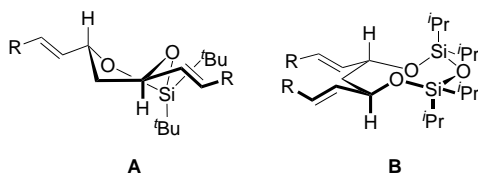
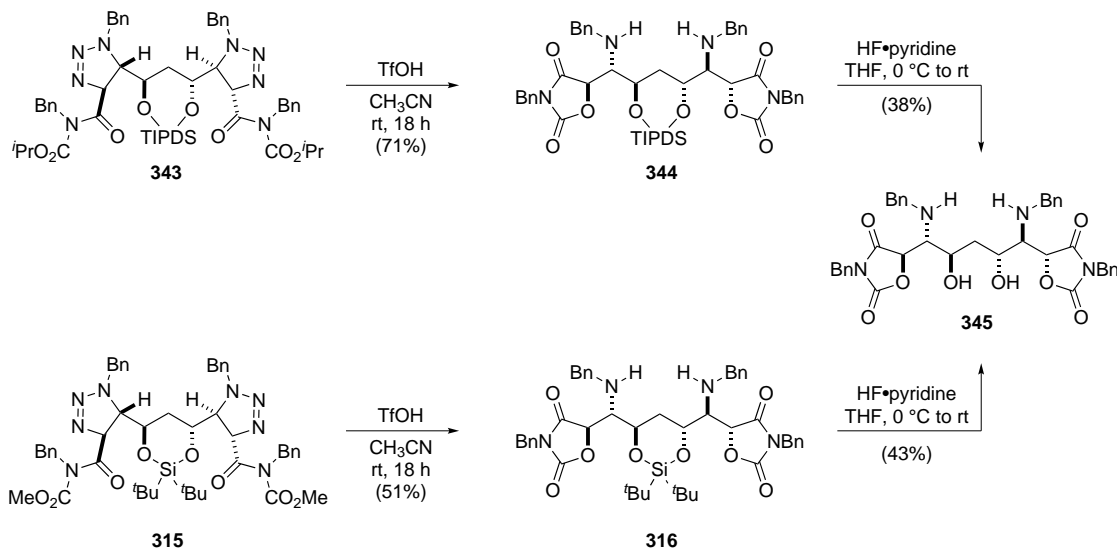


Figure 3.5. Depictions of the likely major conformations of the siloxane (A) and disiloxane (B) rings.

The relative stereochemistry of the TIPDS-protected bis(triazoline) **343** was confirmed by comparison to previously assigned⁷³ *anti,anti*-bis(oxazolidine dione) **316**. The bis(triazoline) **343** was treated with triflic acid at room temperature and gave the bis(oxazolidine dione) **344** in 71 % yield. The silyl group in compound **316** and **344** was removed in the reaction with HF · pyridine and both bis(oxazolidine dione) substrates converged at the diol **345** (Scheme 3.23).

Scheme 3.23. Confirmation of the relative stereochemistry of TIPDS bis(oxazolidine dione).



3.4.3 Functionalization of the bis(oxazolidine dione)

With efficient access to the key bis(oxazolidine dione), we attempted functionalization of the compound **344** in preparation for the Passerini coupling. Unfortunately, as in our previous studies (see section 2.2.3), hydrolytic opening of the oxazolidine dione ring was challenging (Table 3.2). Compound **344** was treated with KOH in 1,4-dioxane only to return the unreacted starting material after 1 h at rt (entry 1), extending the reaction time led to decomposition (entry 2). No reactivity was observed for LiOH in methanol–water mixture at room temperature (entry 3) and use of more nucleophilic lithium hydroperoxide led to decomposition (entry 4). Conditions that allowed for methanolysis of the oxazolidine dione in *syn*-glycolate Mannich products (i.e. Pd(OH)₂, H₂, MeOH) also did not provide the desired product (entry 5). The heterogeneous hydroxide reagent (Me₃SnOH) was not reactive towards the oxazolidine dione, even at elevated temperatures (entry 6). The oxazolidine dione **344** was not compatible with strong protic hydrolysis conditions (entry 7), mild hydride reduction (entry 8) or Lewis acid-promoted addition of methanol (entry 9).

Table 3.2. Functionalization of the bis(oxazolidine dione) **345**.

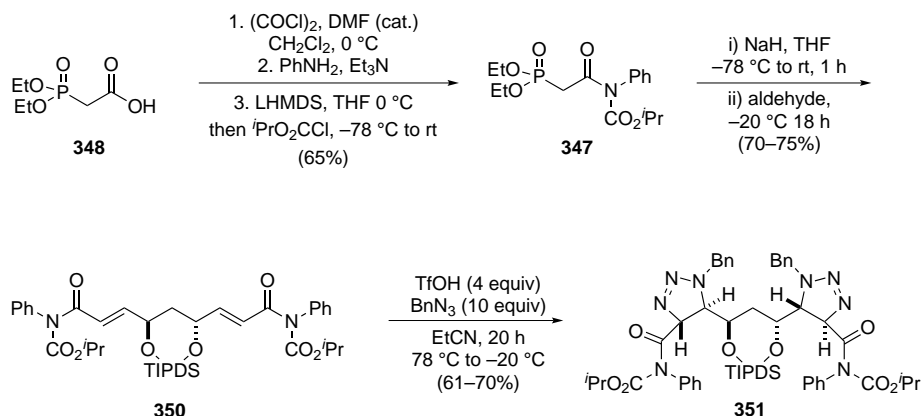
entry	conditions	result
1	KOH, 1,4-dioxane, rt	no reaction
2	KOH, 1,4-dioxane, rt	decomposition
3	LiOH, MeOH–H ₂ O, rt	no reaction
4	LiOH, H ₂ O ₂ , THF, H ₂ O	decomposition
5	Pd(OH) ₂ , H ₂ , MeOH, rt	no reaction
6	Me ₃ SnOH, 1,2-DCE, 78 °C	no reaction
7	HCl, MeOH, H ₂ O	decomposition
8	DIBAL, THF, rt	no reaction
9	Ti(O ^{<i>i</i>} Pr) ₄ , methanol	no reaction

Unsuccessful functionalization of compound **344** was attributed to the low electrophilicity of oxazolidine dione carbonyls caused by the electron-rich benzyl substituent. We hypothesized that by changing the benzyl group to a phenyl substituent, which was successfully functionalized previously in our *syn*-glycolate chemistry, we can increase the reactivity of the oxazolidine dione. The synthesis of the *N*-phenyl bis(oxazolidine dione) **346** was carried out according to the optimized route. The imidophosphonate **347** was synthesized in two steps from diethylphosphonoacetic acid (**348**) as described in Section 3.4.1. We found a simple protocol for an efficient Horner–Wadsworth–Emmons reaction that avoided use of the expensive 18-crown-6 reagent. Deprotonation of the imidophosphonate **347** with sodium hydride in THF at room temperature followed by addition of aldehyde **349** was found to provide the desired bis(imide) **350** with similar efficiency (70–75 %). The electronic effect of the phenyl group was revealed during the [3+2] cycloaddition reaction, where we observed higher reactivity towards the benzyl azide. The reaction was complete in 6 h and provided the desired bis(triazoline) **351** in 70 % yield[†] (Scheme 3.24).

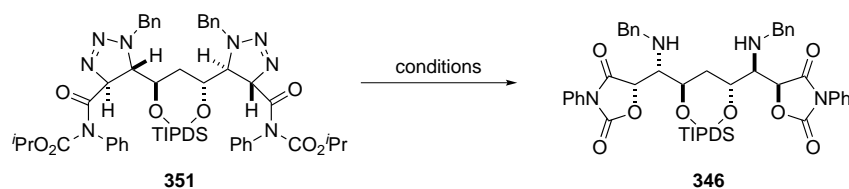
What was beneficial for reactivity in the azide–alkene reaction, proved to be detrimental in fragmentation of the bis(triazoline) **351**. Under standard conditions, 2 equivalents of TfOH in acetonitrile at rt, conversion of **351** to **346** was very sluggish. After 48 h, a considerable amount of bis(triazoline) was still present together with the product **346** and partially converted triazoline (Table 3.3, entry 1). Attempts to accelerate the reaction rate by addition of water⁷⁴ caused decomposition. When the reaction was carried out in propionitrile at elevated temperature (55–60 °C), full conversion was achieved after 6 h but these harsh conditions contributed to decomposition which lowered isolated yields (20–40 %) (Table 3.3, entry 2). The reaction in toluene at 50 °C saw even higher degree of decomposition (entry 3). Surprisingly, less acidic methanesulfonic acid, promoted the reaction and full conversion was observed after only 15 min at room temperature. The ¹H NMR spectrum of the

[†]The key cycloaddition reaction can be carried out at 20 g scale without loss of yield or diastereoselectivity.

Scheme 3.24. Synthesis of the *N*-Ph substituted bis(triazoline).



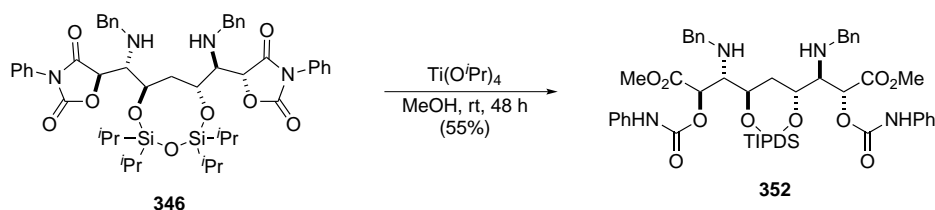
crude reaction mixture was very clean but the isolated yield was much lower than expected (Table 3.3, entry 4). Similar conversion was observed when the reaction was quenched with water (entry 5) or aqueous base (entry 7). When the reaction was quenched with aqueous HCl, no bis(oxazolidinone) **346** was obtained (entry 6). The attempt to purify the reaction mixture directly without aqueous work-up met with limited success, as only 10% of compound **346** was obtained (entry 8). We hypothesized that when methanesulfonic acid is not washed away during work-up, the $\text{CH}_3\text{SO}_3\text{H}$ salt of the product is too polar for chromatographic purification. Indeed, when the reaction mixture was filtered through a small pad of silica gel and eluted extensively with ethyl acetate, 40–65% yield of the product was obtained in a pure form (Table 3.3, entry 9). However, this procedure was not practical on a large scale since a large volume of ethyl acetate was necessary for purification. We then established an optimal procedure in which the reaction is performed using 4 equivalents of $\text{TsOH} \cdot \text{H}_2\text{O}$ in dichloromethane at room temperature. The excess acid is neutralized by addition of solid sodium bicarbonate, and the reaction mixture is filtered, concentrated, and purified by chromatography to give the product in 86–90% yield (Table 3.3, entry 10)

Table 3.3. Optimization of fragmentation of the bis(triazoline) to bis(oxazolidine dione).

entry	acid (equiv)	solvent	T (°C)	time (h)	quench	conversion ^a (%)	yield ^{b,c} (%)
1	TfOH (3)	EtCN	23	18	aq NaHCO ₃	25	nd
2	TfOH (3)	EtCN	50	5	aq NaHCO ₃	95	40
3	TfOH (4)	toluene	50	5	aq NaHCO ₃	90	>20
4	MsOH (3)	EtCN	23	0.25	aq NaHCO ₃	>95	52
5	MsOH (3)	EtCN	23	0.50	H ₂ O	>95	nd
6	MsOH (3)	EtCN	23	0.50	aq HCl	—	—
7	MsOH (3)	EtCN	23	0.50	aq NaOH	>95	nd
8	MsOH (3)	EtCN	23	0.25	SiO ₂	>95	10
9	TsOH · H ₂ O (3)	CH ₂ Cl ₂	23	1	SiO ₂	>95	40–65
10	TsOH · H ₂ O (4)	CH ₂ Cl ₂	23	1	solid NaHCO ₃	>95	86–90

^aMeasured by ¹H NMR. ^bIsolated yield. ^cnd = not determined.

With an optimized procedure for the synthesis of the compound **346** we returned to the investigation of conditions for opening the oxazolidine dione rings. The conditions utilizing a mild heterogeneous hydroxide, as described in Section 2.2.3, did not afford the desired product, and more conventional hydroxide- or alkoxide-based reagents caused decomposition or epimerization. Again, we turned our attention to Lewis acid activation of the oxazolidine dione carbonyls toward alcohol nucleophiles. When the strong Lewis acid TiCl₄ was used in methanol, no reaction occurred. However, a stoichiometric amount of a milder Ti(O^{*i*}Pr)₄ in methanol, gave 55 % yield of bis(ester)[‡] **352** after 2 days at room temperature (Scheme 3.25).

Scheme 3.25. Lewis acid-promoted opening of the bis(oxazolidine dione) **347**.

[‡]The chemoselectivity towards the amide carbonyl is consistent with our previous observations (see chapter 2, section 2.2.3)

Gratifyingly, the crystalline nature of the bis(ester) **352** allowed us to corroborate our assignment of the relative stereochemistry[§] that was established during the alkene-azide cycloaddition reaction (Figure 3.6, Figure 3.7).

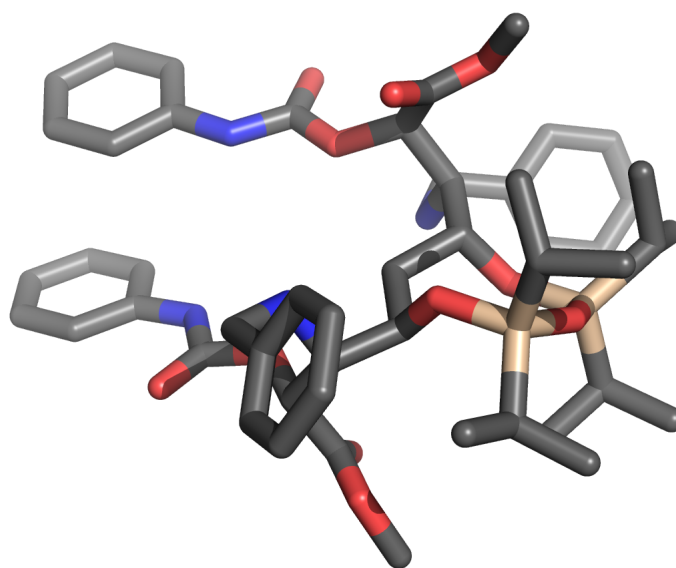


Figure 3.6. Perspective view of the disiloxane view in bis(ester) **352**.

[§]Assignment by NOE correlations was completed by Dr. Ki Bum Hong. See ref. 73

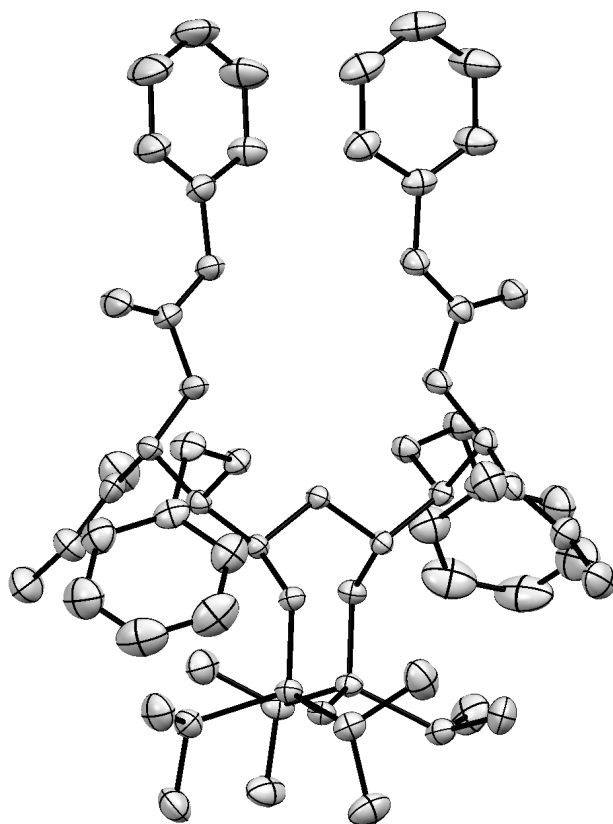
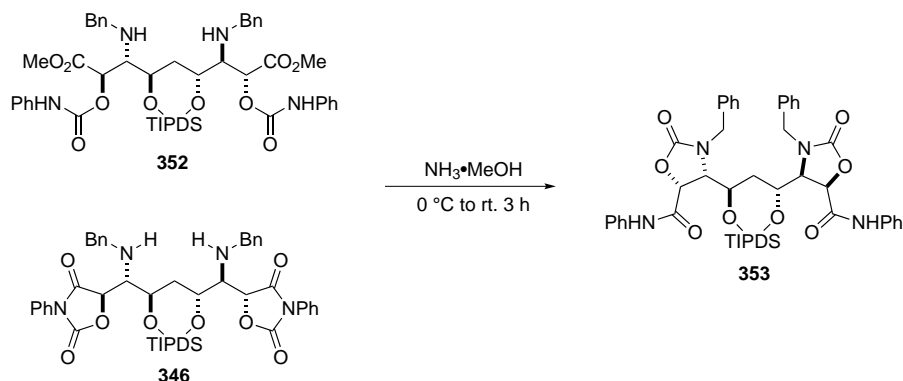


Figure 3.7. The X-ray structure of the bis(ester) **352**.

Unfortunately, this reaction suffered from irreproducibility and low conversion of the starting material even at prolonged reaction times. This was complicated by the fact that the product **352** could not be separated from substrate **346** by chromatography, and modification of the reaction conditions (temperature, concentration, Lewis acid) did not improve this situation. We hypothesized that we could subject compound **352** to hydrolysis to cleave the carbamate group and the resulting alcohol product might be easily separable from bis(oxazolidinone) **346**. Treatment of a sample containing 75 % of compound **352** and 25 % of **346** with aqueous HCl, at reflux for 12 h, caused decomposition. When the same material was subjected to a methanol solution of ammonia, very slow conversion was observed. Although the reaction was not selective (more than one product observed by TLC), it was interesting to see that both bis(ester) **352** and bis(oxazolidinone) **346** were consumed. In fact, when pure bis(oxazolidinone) **346** was subjected to the same reaction conditions the same major component was observed. The product of both reactions was assigned as the bis(oxazolidinone) **353** using heteronuclear correlations of the methylene protons of the benzyl group to the carbamate carbonyl carbon (Scheme 3.26).

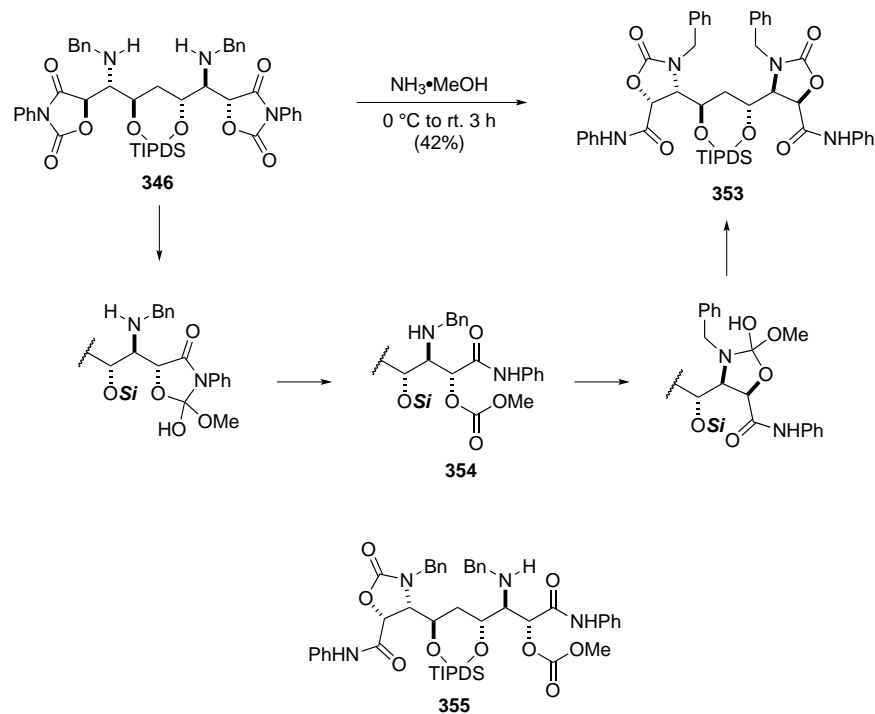
Scheme 3.26. Base promoted cyclization to bis(oxazolidinone).



We postulate that the product **353** arrives from a methoxide attack on the carbamate carbonyl to give methyl carbonate **354**. Under basic conditions, *N*-benzyl amine attacks the carbonate to form the oxazolidinone ring (Scheme 3.27). This mechanism is supported by the intercepted intermediate **355** that can be isolated in small quantities (8 % yield) from the same reaction. The 1D and 2D NMR spectra are in agreement with the proposed structure. The key correlation that allowed for the assignment of **355** was the HMBC correlation of the methyl group to the carbonate carbonyl at 161 ppm (Scheme 3.27). If it were a part of the ester group, the shift of the corresponding carbon would be higher, around 170 ppm like in compound **352**. The convergence of **352** and **346** to **353** also suggests that ammonia in

methanol establishes an equilibrium from **352** to **346**

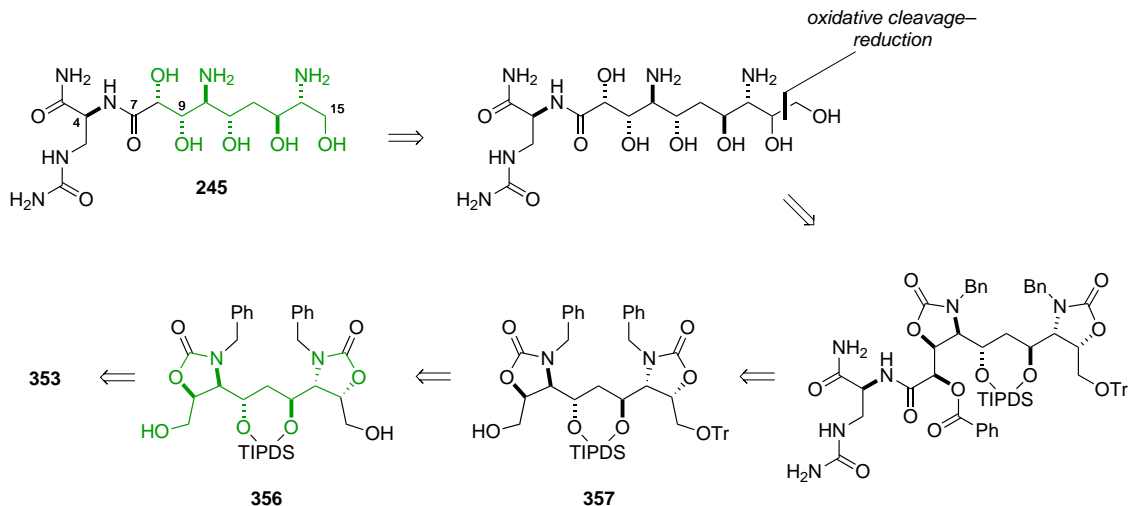
Scheme 3.27. Mechanism of the base-promoted isomerization of **347**.



3.4.4 Desymmetrization and synthesis of the aldehyde for Passerini coupling

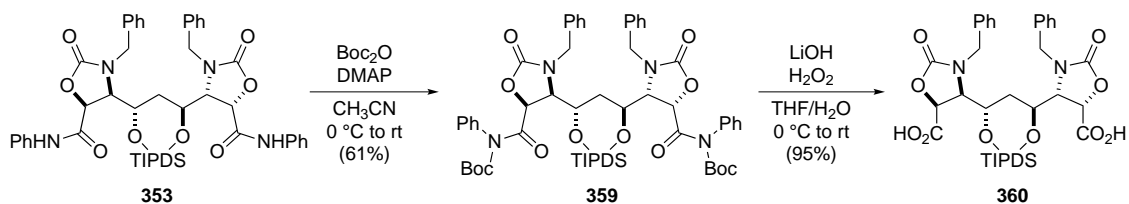
The base-promoted isomerization of the bis(oxazolidinone) **346** to bis(amide) **353** not only released the termini of the molecule for further functionalization but also protected the secondary amine in the same reaction. In preparation for the Passerini reaction we directed our efforts toward two goals, desymmetrization and removal of one of the terminal carbons. When compared with the C9-C15 fragment of zwittermicin A, bis(amide) **353** has an additional carbon, so a strategy was devised in which the desymmetrization will be performed on the bis(alcohol) **356** by monoprotection. The remaining alcohol in compound **357** could be oxidized to aldehyde **358** and coupled with the isonitrile **293** in a Passerini reaction. The terminal carbon could be removed at the late stage of the synthesis by oxidative cleavage–reduction sequence (Scheme 3.28).

Scheme 3.28. A strategy for desymmetrization and removal of C16 carbon.



With compound **353** in hand, we attempted a hydrolysis of the phenyl amide by the nitrosation–hydrolysis sequence published by Evans and co-workers.^{169,170} Unfortunately, reaction of bis(amide) **353** with NaNO_2 produced complex mixtures. The alternative activation of the amide by conversion to an *N*-Boc carbamate proceeded smoothly and delivered **359** in 61 % yield. The saponification with lithium hydroperoxide in THF– H_2O mixture at 0°C was very facile and delivered the bis(carboxylic acid) **360** in 95 % yield without purification (Scheme 3.29).

Scheme 3.29. Preparation of bis(carboxylic acid) **361**.




Handling of carboxylic acid **360** was challenging due to its high affinity to silica gel, rendering this compound incompatible with conventional chromatography purification techniques. Therefore the bis(carboxylic acid) **360** was converted to the corresponding bis(ester) **361** to aid purification by treatment of **360** with an ethereal solution of diazomethane (99 % yield).

Preparation of the bis(alcohol) **356** was not straightforward. Treatment of the bis(ester) with LiAlH_4 or RedAl in THF at -78°C for 4 h produced a complex mixture (Table 3.4,

entries 1 and 2). The same result was observed when bis(carboxylic acid) was treated with borane–THF complex (entry 3). No reaction was observed when the bis(ester) **362** was reacted with DIBAL, even at room temperature (entry 4). We were pleased to see very clean and efficient reaction with sodium borohydride in methanol at room temperature that yielded the desired bis(alcohol) **356** in 92 % isolated yield (Table 3.4, entry 5).

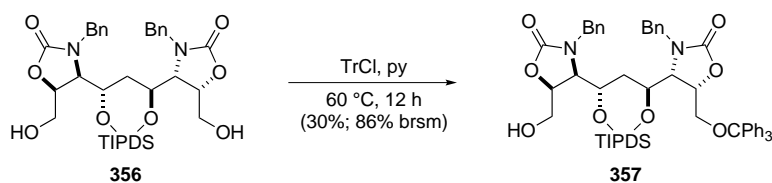
Table 3.4. Optimization of the reduction of bis(ester).



entry	R	conditions	yield ^b (%)
1	OMe	LiAlH ₄ , THF, –78 °C, 4 h	—
2	OMe	RedAl, THF, –78 °C, 4 h	—
3	OH	BH ₃ · THF, THF, rt, 6 h	—
4	OMe	DIBAL, THF, rt, 6 h	—
5	OMe	NaBH ₄ , MeOH, rt, 1 h	92

Compound **356** was reacted with a substoichiometric amount of trityl chloride in pyridine at 60 °C for 12 h and provided the desymmetrized alcohol* **357** in 30 % yield (86 % brsm). With the compound **357** we were ready to explore the key Passerini reaction that will bring the aminopolyol and isonitrile fragments together (Scheme 3.30).

Scheme 3.30. Desymmetrization of alcohol **357**.




Oxidation of alcohol **357** was problematic. Treatment of **357** with 2.1 equiv of Dess–Martin periodinane in CH₂Cl₂ at room temperature delivered a complex mixture following a standard aqueous work-up¹⁷¹ (Table 3.5, entry 1). Extending the reaction time did not improve the outcome of the reaction (entry 2). We saw much higher reactivity when a con-

*Initially, bis(alcohol) **356** was monoprotected as a TBS ether but we later found that a conversion to a trityl ether gives us more control over the conversion to the bisprotected compound.

trolled amount of water was added to the reaction¹⁷² but no aldehyde was observed in the ¹H NMR of the crude reaction mixture (entry 3). When an equimolar amount of DMP was used and the reaction was diluted with diethyl ether and filtered, about 60% conversion was estimated by proton NMR analysis (entry 4). Catalytic *N*-oxide radical-based oxidation conditions (TEMPO/PhI(OAc)₂) consumed **357** within 1 h, but delivered a product of overoxidation, as did Ley oxidation (entry 6). Among activated DMSO methods, we evaluated Parikh–Doering and Swern oxidation conditions. When alcohol **357** was treated with 3 equiv of SO₃ · pyridine complex in DMSO–CH₂Cl₂, no reaction was observed even after 20 h (entry 7). Under the standard Swern oxidation conditions, no product was observed whenever aqueous work-up was performed (entry 8). Relatively clean conversion to the aldehyde **363** was observed when the reaction was diluted with ether, filtered, and concentrated (entry 9). Attempts to purify the aldehyde by chromatography were fruitless. It was apparent that aldehyde **363** is sensitive to water and/or air so it was used in a subsequent step without work-up or purification.

Table 3.5. Survey of oxidation conditions for the synthesis of aldehyde **364**.



entry	reagent	equiv	work-up	conv ^a (%)
1	DMP	2.1	aqueous	— ^b
2	DMP	2.1	aqueous	— ^b
3	DMP ^c	2.1	aqueous	— ^b
4	DMP	1.0	filtration	60
5	TEMPO/PhI(OAc) ₂	2.1	filtration	— ^d
6	TPAP/NMO	2.0	filtration	— ^d
7	SO ₃ · pyridine	1.0	filtration	no reaction
8	(COCl) ₂ , DMSO	3.0	aqueous	— ^b
9	(COCl) ₂ , DMSO	3.0	filtration	60–80

^aEstimated by ¹H NMR analysis of the crude reaction mixture. ^bReaction resulted in a complex mixture. ^cWet dichloromethane was used as solvent.

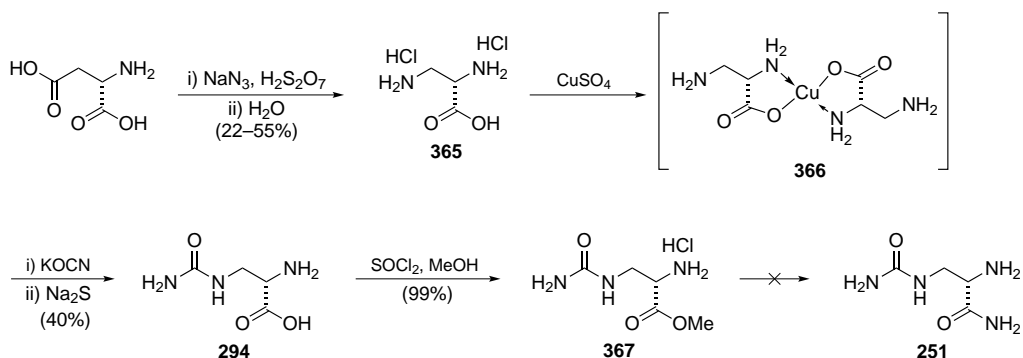
^dOveroxidation to carboxylic acid occurred.

3.4.5 Synthesis of the isonitrile fragment

As outlined in section 3.2.3, for the most convergent approach, the isonitrile fragment should be functionalized with a urea and a primary amide. Although the isonitrile **293** has no precedence in the literature, amine **251** has been previously prepared by Rogers and Molinski.¹⁴⁰ Modification of the amine by formylation and dehydration should provide the isonitrile **364**. The synthesis of **251** commences with the preparation of L-1,3-diaminopropionic acid (**365**) (L-DAP) from L-Asp as described by Rao.¹⁷³ (Scheme 3.31). The Schmidt reaction of L-Asp afforded L-DAP in 71 % yield which was then subjected to copper(II) sulfate in water at pH 5 to chelate the carboxylate and secondary amine to form **366**. The primary amine of the complex **366** was selectively reacted with potassium cyanate in water at 58 °C while maintaining pH 5 using HCl.^{174–177} After the reaction, decomplexation by treatment with sodium sulfide and copper(II) sulfide gave albizziine (**294**) as the only product.

Attempts to convert the carboxylic acid of **294** to a primary amide failed. Preparation of the mixed anhydride and treatment with ammonium hydroxide returned only the starting material, most likely due to the insolubility of **294** in THF. We then treated **294** with thionyl chloride in refluxing methanol which returned the methyl ester **367** quantitatively. Unfortunately, treatment with either ammonia in methanol or ammonium hydroxide didn't provide the desired primary amide **251**.

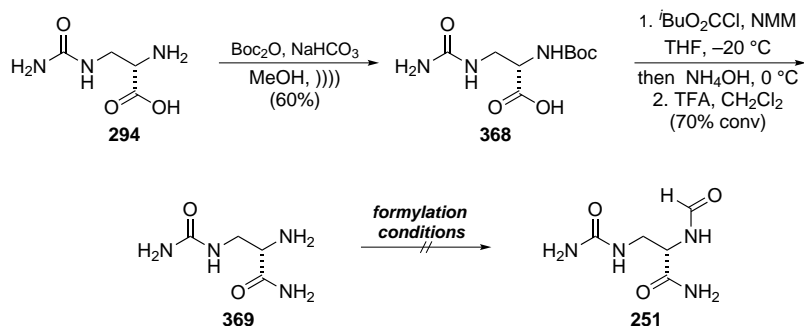
Scheme 3.31. Synthesis of albizziine-derived isonitrile



Following the protocol used by Molinski and co-workers¹⁷⁸ in their synthesis of zwittermicin A, we temporarily protected the secondary amine with a Boc group. Sonication of albizziine in methanol in the presence of Boc_2O and solid NaHCO_3 gave **368** in 60 % yield. Formation of the mixed anhydride, followed by addition of ammonium hydroxide provided the primary amide **369** in 70 % conversion. This material was treated with trifluoroacetic

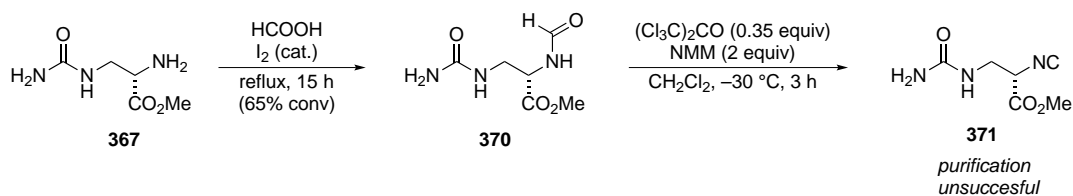
acid and the secondary amine was liberated. Compound **369** was then subjected to several formylation conditions which unfortunately didn't deliver the desired *N*-formyl precursor to the isonitrile.

Scheme 3.32. Synthesis of albizziine amide-derived isonitrile



Formylation of the amine in compound **367** also proved to be difficult. Several literature procedures were evaluated^{179–182} but none of them allowed for high conversion of **367**. On one occasion,¹⁸⁰ 65% conversion to **370** was achieved and this mixture was subjected to dehydration conditions developed by Danishefsky and co-workers.¹⁸³ Although the crude reaction mixture contained isonitrile, as evidenced by a characteristic IR stretch at 2250 cm^{-1} , purification of the desired compound **371** was unsuccessful.

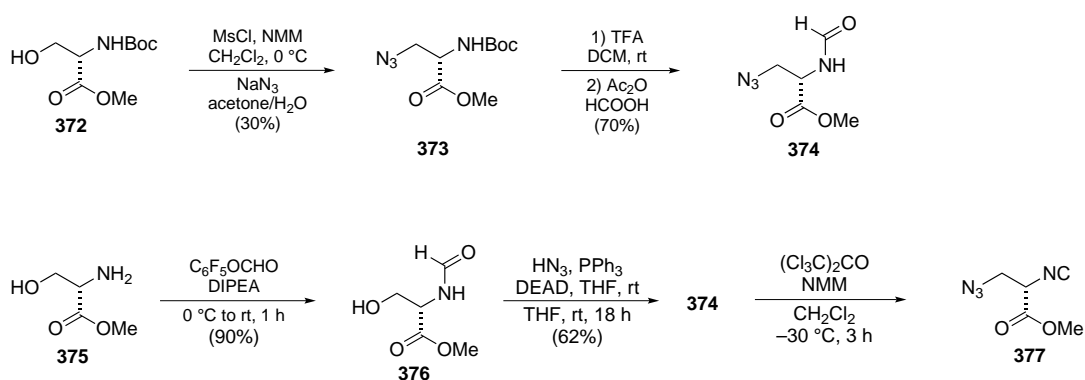
Scheme 3.33. Synthesis of albizziine methyl ester-derived isonitrile



We hypothesized that the terminal urea functional group is not compatible with dehydration conditions. To overcome this difficulty we proceeded to synthesize isonitrile **377**, where the terminal amine is prepared from an azide. Commercially available *N*-Boc serine methyl ester **372** was converted to the mesylate and then subjected to sodium azide in DMF at rt. This reaction provided the desired azide **373** in 30% yield with mesylate elimination product as the major component. Deprotection of **373** with TFA and subsequent treatment with acyl formate provided the formamide **374** in 70% yield over two steps. A more convenient route to **374** can be achieved from L-serine methyl ester. Formamide formation of

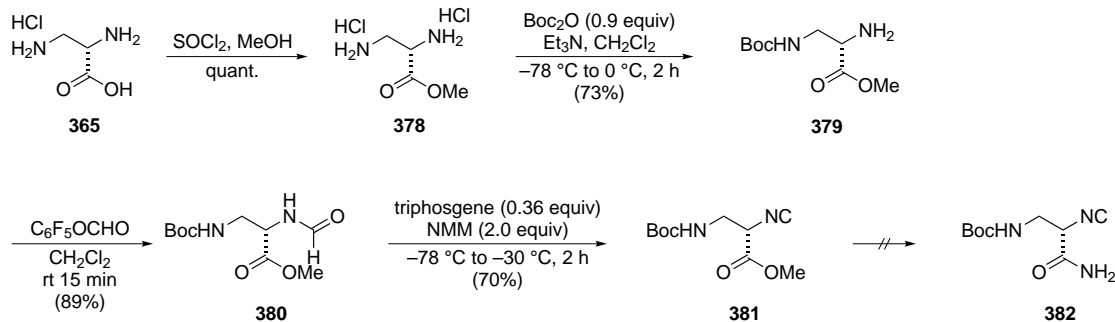
commercially available **375** using formic acid anhydride¹⁸⁴ was sluggish. A more reactive formyl group donor, pentafluorophenyl formate,¹⁸⁵ afforded the formyl derivative **376** in 90 % yield. Mitsunobu displacement of the terminal alcohol using hydrazoic acid in the presence of PPh₃ and DEAD afforded the desired azide **374** in 62 % yield. Dehydration of **374** was also problematic. Although respectable levels of conversion to the desired isonitrile **377** could be achieved, purification was problematic as the product decomposed during aqueous work-up or chromatography. An attempt to use crude isonitrile **377** in the Passerini reaction with benzaldehyde was unsuccessful.

Scheme 3.34. Synthesis of albizziine methyl ester-derived isonitrile



After exploring the synthesis of isonitrile **293** it became clear to us that protection of the primary amine in the isonitrile fragment could not be avoided.¹⁶⁷ L-DAP (**365**) was converted to methyl ester **378**. The primary amine was selectively protected using Boc₂O and triethylamine in dichloromethane, as described by Egbertson and co-workers,¹⁸⁶ and the secondary amine **379** was formylated using pentafluorophenyl formate to give formamide **380** in 89 % yield. Dehydration of **380** proceeded smoothly and afforded the desired isonitrile **381** in 70 % yield. Direct conversion of the methyl ester to primary amide **382** was unsuccessful. Therefore, this functional group will be modified after the Passerini coupling.

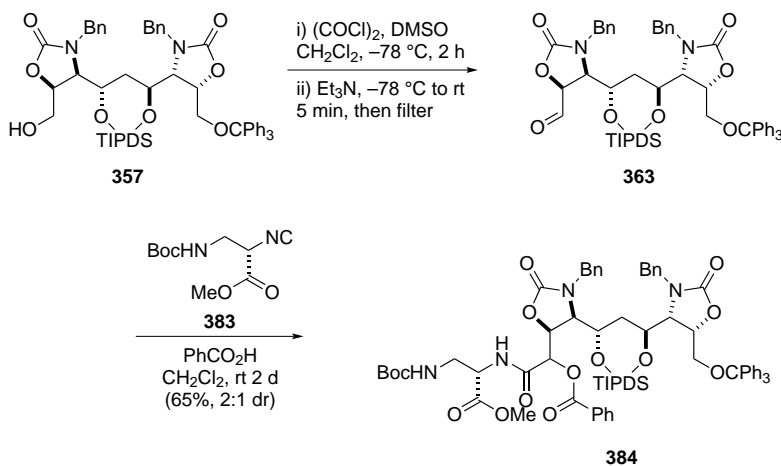
Scheme 3.35. Synthesis of DAP methyl ester-derived isonitrile



3.4.6 First generation synthesis of the Passerini adduct and its functionalization

The next desired step was a key Passerini reaction that brings together the aminopolyol fragment and the isonitrile **383**. As described in the previous section, alcohol **357** was oxidized to aldehyde **363** by Swern oxidation[†] and immediately reacted with isonitrile **383** and benzoic acid. After 2 days at room temperature, the desired Passerini adduct **384** formed in 65% yield as an inseparable mixture of diastereomers in 2:1 ratio (Scheme 3.36). We anticipate that further functionalization will allow for the separation of diastereomers, and stereochemical identity will be assigned later by comparison to the natural product.

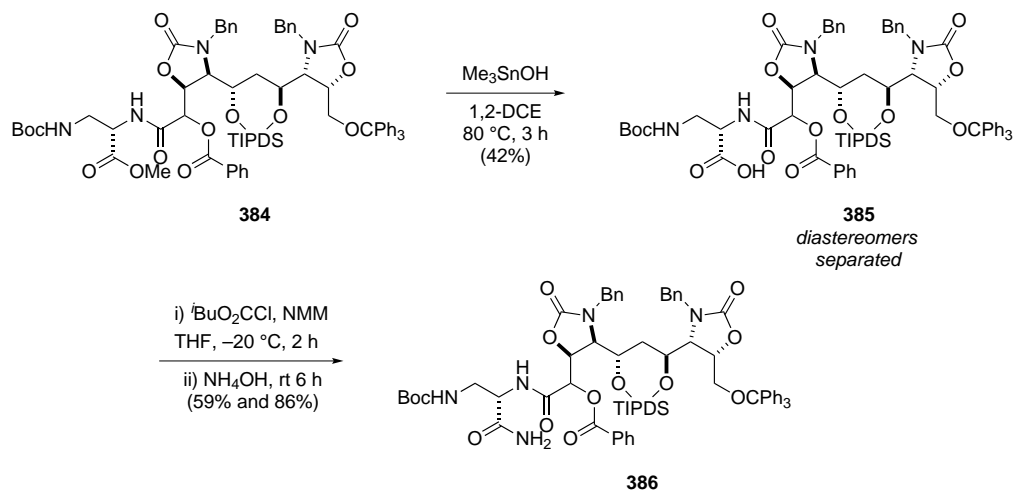
Scheme 3.36. Synthesis of the first generation Passerini adduct.



[†]We found that longer activation time was crucial to reproducibility and conversion.

The next task was functional group manipulation of the western fragment of adduct **384**. Direct transformation of the methyl ester in compound **384** to a primary amide was unsuccessful. In our preliminary attempts at a direct CO₂Me to CONH₂ conversion[‡] using ammonium hydroxide in toluene at 80 °C returned the starting material. Other conditions, including ammonia in methanol and NH₄OH in THF–water at 100 °C in a microwave resulted in decomposition. We then pursued a two-step sequence in which the methyl ester is saponified and then activated to be converted to an amide. Standard hydrolysis protocols such as K₂CO₃ or LiOH in methanol were effective at saponifying the methyl ester and cleaving the benzoate but erosion of dr was observed. Due to high acidity of the proton in α position to the amide, we decided to rely on a selective methyl ester hydrolysis method developed for compounds prone to epimerization.¹⁸⁷ Methyl ester **384** was reacted with trimethyltin hydroxide in 1,2-dichloromethane at 80 °C for 3 h to give the corresponding carboxylic acid (**385**) in 42 % combined yield, and the diastereomers could now be separated by HPLC (25 % and 17 % yield respectively). Next, each diastereomer was converted to a mixed anhydride in reaction with isobutyl chloroformate and *N*-methylmorpholine followed by ammonium hydroxide. This reaction afforded the corresponding amide diastereomers **386** in 86 % and 59 % yield respectively (Scheme 3.37).

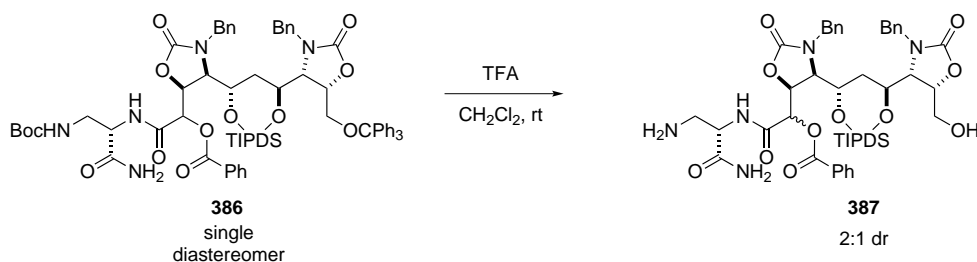
Scheme 3.37. Functionalization of the Passerini adduct: transformation of a methyl ester to primary amide.



[‡]Reactions were carried out on a TBS protected adduct.

Next we pursued deprotection of the terminal amine and attachment of the urea moiety. Carbamate **386** was treated with TFA in CH_2Cl_2 at room temperature in order to cleave the Boc group as well as remove the trityl ether. After purification, what looked as a single compound by HPLC was in fact a 2:1 mixture of diastereomers of compound **387**. We hypothesized that under acidic conditions, the α position to the amide undergoes epimerization (Scheme 3.38).

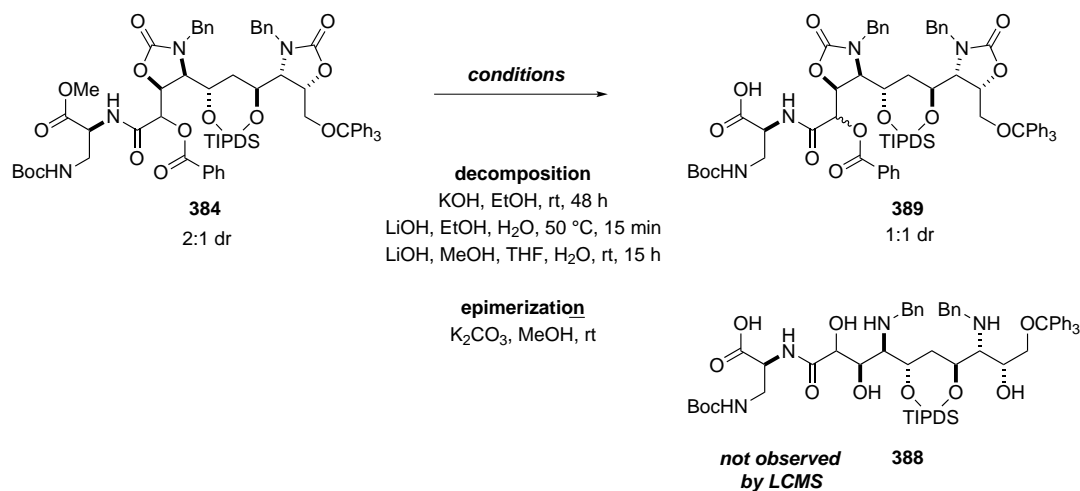
Scheme 3.38. Removal of the Boc and trityl groups.



To solve this problem we conducted the functionalization in a different order. We planned to remove the benzoate ester and hydrolyze the oxazolidinone rings before removing the Boc and trityl groups. Despite the fact that strongly basic conditions promote epimerization, we attempted a global hydrolysis of Passerini adduct **384** to determine if methyl ester, benzoate and oxazolidinone can be hydrolyzed in a single reaction to give compound **388**. A number of hydroxide- and alkoxide-based conditions were used but without much success. Even though some were effective at removing the benzoate ester to give **389**, oxazolidinone rings were not reactive under these conditions and reactions at elevated temperature caused decomposition (Scheme 3.39).

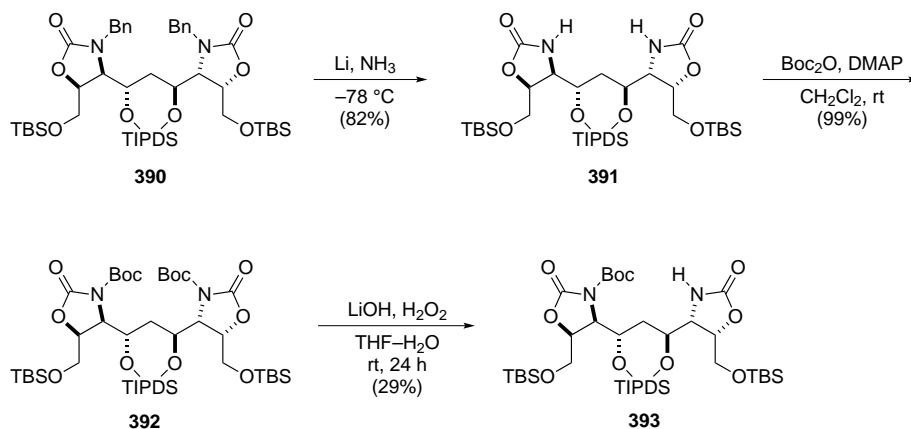
It became evident that oxazolidinone rings with *N*-benzyl substituent might not be sufficiently electrophilic for mild hydrolysis to occur. On the other hand, application of harsher conditions leads to decomposition. We wanted to explore the reactivity of oxazolidinones towards hydrolysis using a model based on the C_2 -symmetric compound **390**. In order to increase the electrophilicity of the oxazolidinone carbonyl, the benzyl group was replaced with a Boc group. Birch reduction efficiently removed the benzyl substituent and gave bis(carbamate) **391** in 82% yield. Compound **392** was synthesized in nearly quantitative yield by reacting **391** with Boc_2O and DMAP in dichloromethane (Scheme 3.40). When compound **392** was treated with Cs_2CO_3 in methanol at 60°C or K_2CO_3 at room temperature, decomposition occurred. Use of lithium hydroperoxide in $\text{THF-H}_2\text{O}$ led to partial conversion at room temperature after 20 h. The main product was identified as desym-

Scheme 3.39. Global hydrolysis of the Passerini adduct.



metrized compound **393** that arises from *N*-Boc oxazolidinone ring opening where the resulting secondary alcohol attacks the *tert*-butyl carbamate to form **393** after elimination of *tert*-butanol (Scheme 3.40). Although we obtained an undesired product, our hypothesis about low electrophilicity of the *N*-Bn oxazolidinone ring was further confirmed.

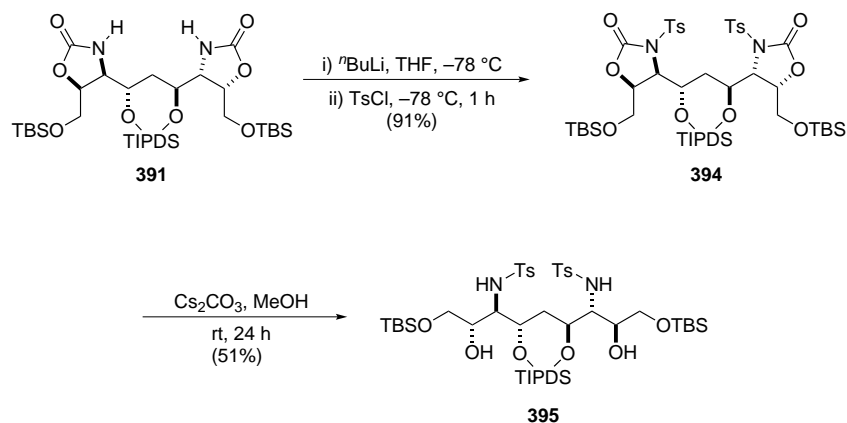
Scheme 3.40. Undesired opening–cyclization of *N*-Boc bis(oxazolidinone).



To prevent recyclization after hydrolysis, we pursued an *N*-Ts derivative of **391**. Treatment of bis(carbamate) **391** with ⁿBuLi followed by 4-toluenesulfonyl chloride[§] delivered bis(sulfonamide) **394** in 91 % yield. When compound **394** was reacted with Cs₂CO₃ in methanol at room temperature for 24 h, the desired acyclic aminopolyol **395** was isolated in 51 % yield (Scheme 3.41)

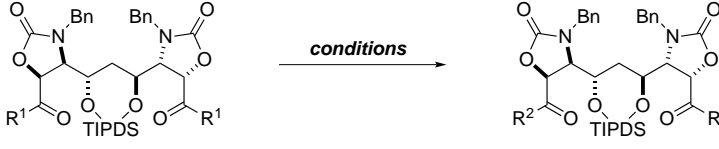
[§]We found that high yields are only obtained when freshly recrystallized tosyl chloride is used.

Scheme 3.41. Successful hydrolysis of *N*-Ts derivative **395**.



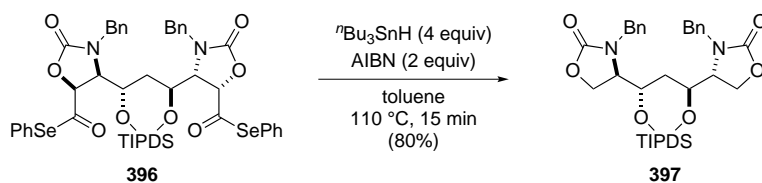
3.4.7 Studies towards the desymmetriation and decarbonylation

It was apparent that the late stage removal of the carbon at C16 will be more challenging than we originally anticipated. Our alternative plan was to achieve desymmetrization and decarbonylation before the Passerini reaction, preferentially, at the bis(carboxylic acid) stage. A direct desymmetrization by decarbonylation was met with limited success as the stoichiometry of product formation from **360** was difficult to control. Activation of the bis(carboxylic acid) as an acid chloride followed by addition of *tert*-butyl hydroperoxide and pyridine returned the starting material (Table 3.6, entry 1). Attempts to prepare the *tert*-butyl perester via DCC or EDC coupling were also fruitless (entries 2, 3); activation and *in situ* Barton decarbonylation gave the same result (Table 3.6, entry 4). Preparation of the bis(selenoester) **396** required significant optimization. Treatment of **359** with benzeneselenenol and triethylamine at $50\text{ }^\circ\text{C}$ returned the starting material, as did the reaction with the lithium phenyl selenide (entries 5 and 6, respectively). We first observed the product when the bis(carboxylic acid) **360** was reacted with diphenyl diselenide and tributyl phosphine in dichloromethane at room temperature, but the reaction stalled at about 40% conversion and the product decomposed during purification (Table 3.6, entry 7). A reasonable conversion was seen when the acid chloride of **360** was treated with benzeneselenenol and triethylamine. The bis(selenoester) **396** is highly prone to hydrolysis which was observed during chromatographic purification and is probably the main factor that lowers the isolated yield (21%, entry 8).

Table 3.6. Synthesis of the symmetric phenylselenoester.


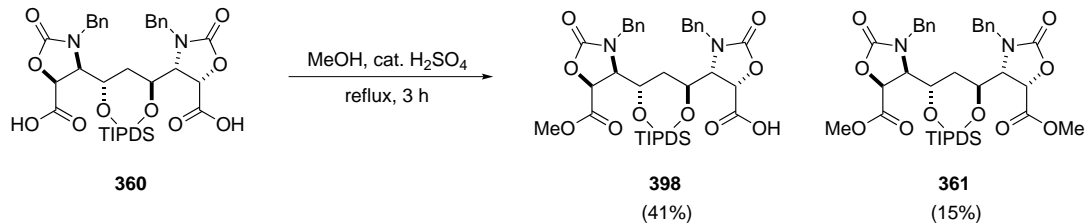
entry	R	conditions	yield ^b (%)
1	Cl	^t BuOOH, pyridine	—
2	OH	^t BuOOH, DCC, ⁱ Pr ₂ EtN	—
3	OH	^t BuOOH, EDC, ⁱ Pr ₂ EtN	—
4	Cl	Barton salt, toluene, hv, 100 °C	—
5	N(Ph)Boc	PhSeH, Et ₃ N, DMF, 50 °C	—
6	N(Ph)Boc	PhSeH, LHMDS, THF, rt	—
7	OH	PhSeSePh, ⁿ Bu ₃ P, CH ₂ Cl ₂ , rt	5
8	Cl	PhSeH, Et ₃ N, rt, 30 min	21

With compound **396** in hand we tested the radical decarbonylation conditions. Although the reaction of **396** with 1 equiv of ⁿBu₃SnH and 1 equiv of AIBN in toluene at 110 °C was very fast (full conversion after 30 min) the main product was bis(carboxylic acid) **360**. To ensure that the reaction operates under strictly anhydrous conditions, the selenoester was dried over P₂O₅ under vacuum, dry toluene and freshly recrystallized AIBN were used. After only 10 min of reaction, full conversion of the bis(selenoester) **396** was achieved and the bis(oxazolidinone) **397** formed in 80 % yield (Scheme 3.42).

Scheme 3.42. Radical decarbonylation of the bis(selenoester) **397**.

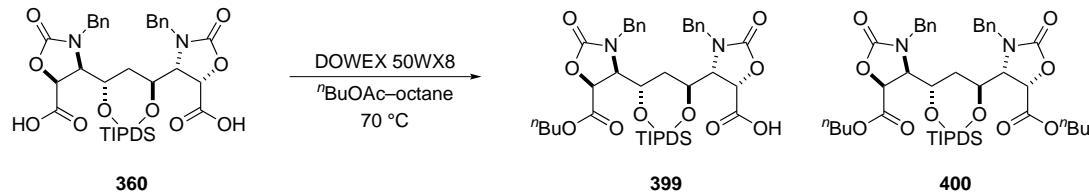
With a successful removal of the C16 carbon we turned our attention to desymmetrization of the bis(carboxylic acid) through a selective formation of monoester **398**. We were able to obtain the monoester via Fischer esterification in refluxing methanol, but the process was labor intensive. The reaction was stopped at ca. 60 % conversion when formation of bis(ester) **361** was observed (Scheme 3.43). The mixture of both products and unreacted starting material was separated by preparative HPLC as conventional chromatography was ineffective. Very low selectivity and yield (41 %) prompted us to investigate other monoesterification methods.

Scheme 3.43. Fischer esterification of the bis(carboxylic acid).



Monoesterification of simple dicarboxylic acids can be selectively achieved via corresponding cyclic anhydrides. Long dicarboxylic acids can be monoprotected in the reaction with diazomethane^{188,189} or dimethyl sulfate¹⁹⁰ by monocarboxylate chemisorption on alumina. Methods utilizing phase-transfer catalysis have also been reported,¹⁹¹ and enzyme-based methods for monoalkylation of dicarboxylic acids have experienced an increased interest among organic chemists.¹⁹² Nishiguchi and co-workers reported a highly selective monoesterification of dicarboxylic acids with 4–14 carbon chains. Transesterification catalyzed by the DOWEX 50WX2 resin (50–100 mesh) is achieved in an alkane–HCO₂ⁿBu mixture at high temperature. The rate of monoesterification of diacids was found to be much higher than that of the monocarboxylic acids because it mostly happens in the water layer surrounding the DOWEX resin (ca. 50 % water by weight).^{193,194}

We hypothesized that by applying Nishiguchi’s conditions we can obtain better selectivity towards the monoester. When dicarboxylic acid **360** was reacted in 1:10 mixture of *n*-butyl acetate and octane at 70 °C in presence of the DOWEX resin for 1 h, we measured 60 % conversion and ca. 5:1 ratio of monoester **399** to bis(ester) **400** (Table 3.7, entry 1). After 2 h, the conversion increased to 70 % but only the amount of the diester increased. However, the ratio of components after preparative HPLC didn’t match the amounts we observed when we analyzed the reaction mixture. The overall conversion was lower (62 %) and the ratio of the monoester to diester was 6.5:1 (entry 2). This confirms Nishiguchi’s claim that the dicarboxylic acid is mainly in the water layer surrounding the resin. Our analysis of the reaction mixture was limited to the organic layer that is clearly enriched in the ester components. Following the findings reported by Nishiguchi and co-workers, we hypothesized that we can achieve better yield and selectivity by reducing the amount of the resin and decreasing the amount of ⁿBuOAc in octane. After 1 h the ratio between the diacid, monoester and diester was 44:40:16, respectively (entry 3). Although the ratio of the diester increased with time (entry 4) we continued the reaction for total of 4 hours. At that point, HPLC analysis of the reaction mixture (organic layer) showed 9:35:55 ratio. Once the resin was filtered and washed with methanol, the ratio was 41:42:17 (Table 3.7), entry 5).

Table 3.7. Selective monoesterification promoted by DOWEX ion-exchange resin.^a

entry	resin (g/mmol)	time (h)	<i>n</i> BuOAc–octane	360:399:400 ^a
1	4	1	1:10	42:51:7
2		2		29:50:21 (62:33:5) ^b
3	2	1	1:20	44:40:16
4		2		23:44:33
5		4		9:35:55 (41:42:17) ^b

^aDetermined by HPLC analysis of the reaction mixture. ^bDetermined by analysis of the reaction mixture after the work-up during preparative HPLC.

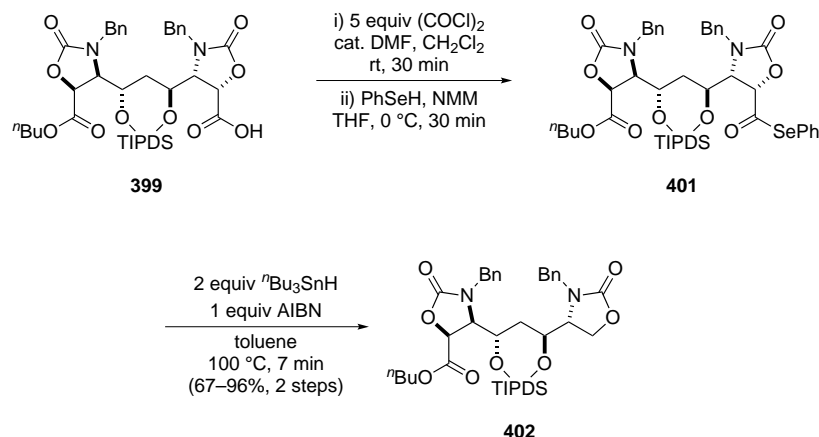
Further optimization of this protocol established that if the reaction is performed in an *n*-butyl formate–toluene mixture with 2 g of the resin per mmol of substrate, the desired *n*-butyl ester **399** can be isolated in 57 % yield. We also found that careful column chromatography using a mixture of AcOH–MeOH–CH₂Cl₂ (gradient 1:2:97 to 1:8:91 and then 1:20:79) as solvent allows for preparative purification of monoester **399** without the need for multiple HPLC runs.

3.4.8 Second generation synthesis of the Passerini adduct

With an efficient strategy for desymmetrization and decarbonylation in hand, we pursued a synthesis of the Passerini adduct with C16 removed. Monoester **399** was transformed into a selenoester by first reaction with oxalyl chloride and catalytic DMF in dichloromethane at rt. The crude acid chloride was added to a solution of benzeneselenol[¶] and 4-methylmorpholine at 0 °C and provided corresponding selenoester **401**. Compound **401** was not isolated, but after extensive drying over P₂O₅ under vacuum, was treated with 2 equiv of ⁿBu₃SnH and 1 equiv of freshly recrystallized AIBN in toluene at 100 °C. After 7 min the reaction was complete by TLC, and column chromatography of the concentrated reaction mixture gave desired ester **402** in 67–96 % over 2 steps (Scheme 3.44).

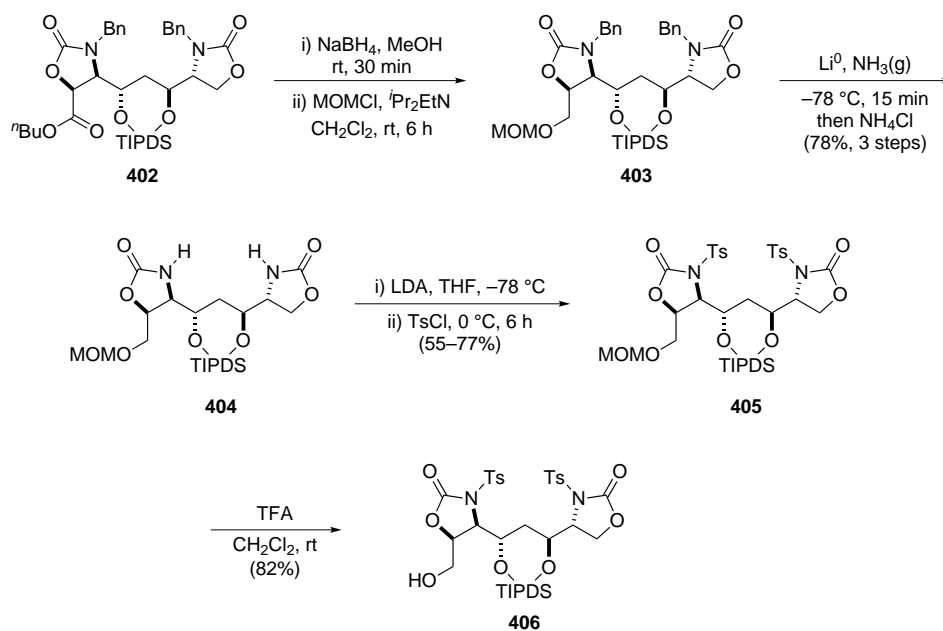
[¶]We found that the order of addition is important for high conversion.

Scheme 3.44. Preparation and decarbonylation of the selenoester **402**.



In preparation for the Passerini reaction, the ester **402** was reduced with NaBH_4 in methanol and the resulting alcohol was protected as a MOM ether with MOMCl and $^i\text{Pr}_2\text{NEt}$. Birch reduction of **403** efficiently removed both benzyl groups and afforded the bis(carbamate) **404** in 78% over 3 steps. Next, deprotonation with LDA followed by addition of freshly recrystallized tosyl chloride afforded the *N*-Ts derivative **405** in 77% yield. The removal of the MOM group was achieved in 82% yield by reaction with 60% TFA in DCM at rt to give **406** (Scheme 3.45).

Scheme 3.45. Elaboration of the monoester **403**.



Again, the oxidation of the alcohol turned out to be a challenge. A series of oxidation conditions was evaluated and the results are presented in Table 3.8. Dess–Martin oxidation and activated DMSO methods (Swern, Parikh–Doering) resulted in decomposition (entries 1–3). Excess PCC in dichloromethane in the presence of Celite did not react after 12 h but upon addition of activated molecular sieves, conversion of the starting material was observed but to decomposition products (entry 4, 5). A stoichiometric amount of TPAP in CH₂Cl₂ at room temperature consumed the starting material in only 15 min but returned the product of overoxidation which was confirmed by LCMS analysis (entry 6). TEMPO oxidation also resulted in production of the corresponding carboxylic acid when excess bleach was used (entry 7). Use of stoichiometric amount of Ca(OCl)₂¹⁹⁵ showed only 5 % conversion after 1 h at rt (entry 8). More exotic oxidation methods, RuCl₂(PPh₃)₃ in benzene or AgCO₃ · Celite did not engage in a reaction with the alcohol **406** (entry 9, 10).

Table 3.8. Survey of oxidation conditions for the synthesis of the aldehyde **408**.

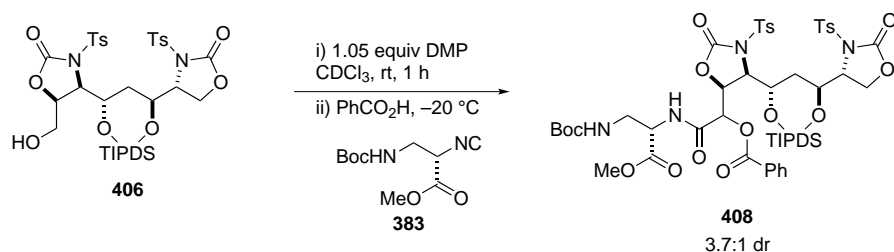
entry	conditions	result
1	DMP, CH ₂ Cl ₂ , rt, aqueous work-up	decomposition
2	SO ₃ · pyridine, DMSO, rt	decomposition
3	(COCl) ₂ , DMSO, ⁱ Pr ₂ EtN, CH ₂ Cl ₂	decomposition
4	PCC, Celite, CH ₂ Cl ₂ , rt, 12 h	no reaction
5	PCC, Celite, 4 Å MS, CH ₂ Cl ₂ , rt, 8 h	decomposition
6	TPAP (1 equiv), CH ₂ Cl ₂ , rt, 15 min	overoxidation
7	TEMPO, bleach, KBr, NaHCO ₃ , rt, 30 min	overoxidation
8	TEMPO, Ca(OCl) ₂ , CH ₂ Cl ₂ –NaHCO ₃ , rt, 1 h	ca 5 % conv.
9	RuCl ₂ (PPh ₃) ₃ , benzene, rt, 12 h	no reaction
10	AgCO ₃ · Celite, benzene, reflux, 12 h	no reaction

To gain more insight into the decomposition pathway we performed the Dess–Martin reaction in CDCl₃ and followed the reaction by ¹H NMR. To our amazement, the reaction proceeded very smoothly and selectively. After 5 min, already 50 % conversion to **407** was observed by ¹H NMR analysis (Figure 3.8, spectrum B). The reaction was complete after 15 min (Figure 3.8, spectrum C) and the reaction mixture did not change composition even after an additional 3 h (spectrum D). This experiment showed very clearly that problems with oxidation of **406** are correlated with exposure to water and/or air. To the NMR tube containing aldehyde **407** was added 12 equiv of benzoic acid which did not affect the aldehyde.

Addition of PhCO₂H was followed by addition of 2 equiv of isonitrile **383** and at the time when the ¹H NMR spectrum was acquired (ca. 5 min) the reaction was already complete with the Passerini adduct **408** (1.6:1 dr) as the major product (Figure 3.8, spectrum E). This shows very high reactivity of the aldehyde **407**. Normally, Passerini reactions require long reaction times, even at room temperature,¹⁹⁶ but in our case, aldehyde **407** is significantly more reactive but this comes at a cost of sensitivity to decomposition.

With this study we established a very straightforward protocol for the synthesis of the Passerini adduct **408**. The alcohol **406** is treated with 1.05 equiv of Dess–Martin periodinane in CDCl₃ at rt. After 1 h to the reaction is added 10–15 equiv of benzoic acid and the reaction mixture is cooled to –78 °C. The isonitrile **383** (1.5 equiv) is then added in one portion and the reaction is warmed to –20 °C. With this protocol, 3.7:1 ratio of diastereomers of the adduct **408** is obtained in 50 % isolated yield (Scheme 3.46).

Scheme 3.46. One-pot oxidation and Passerini coupling.



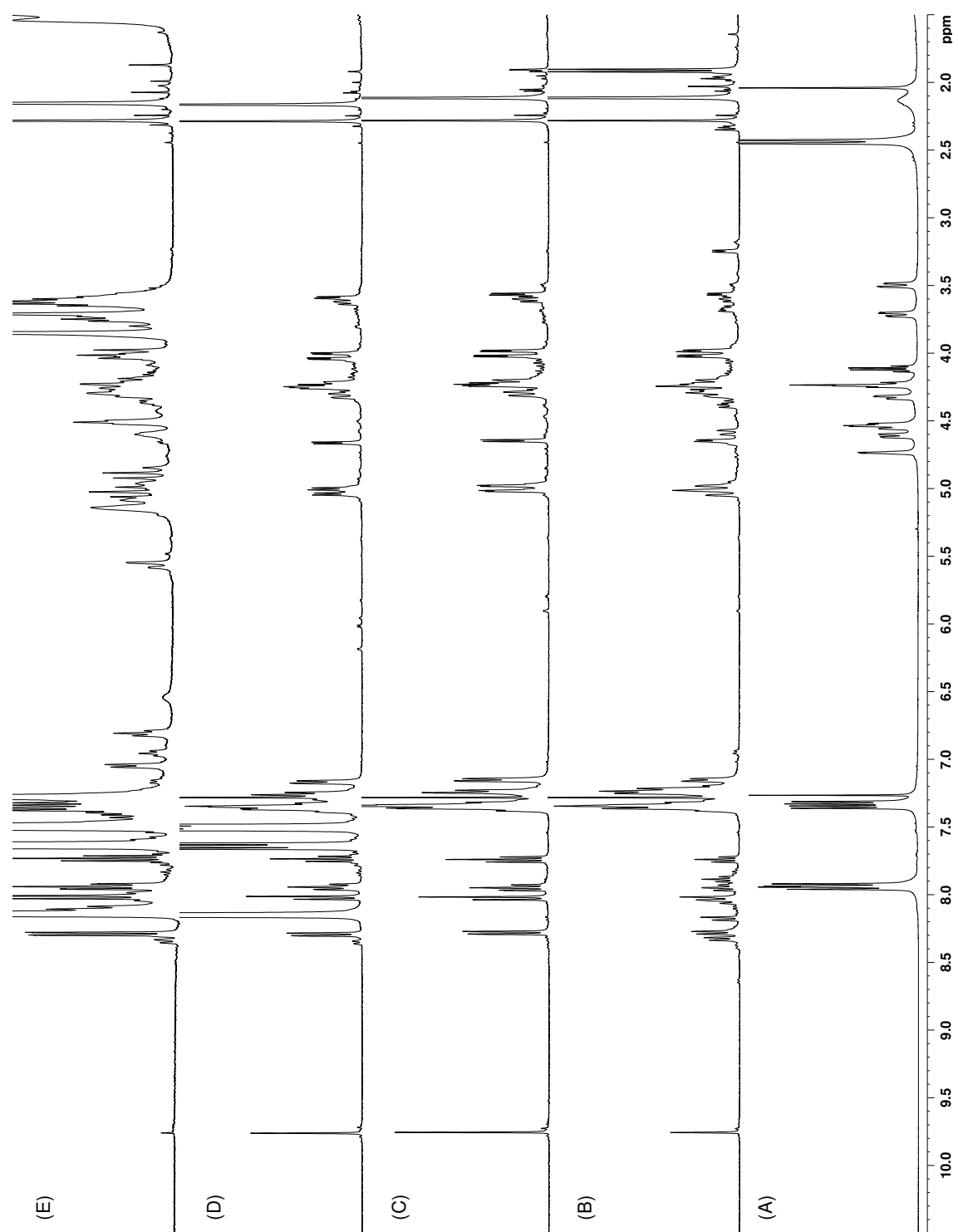
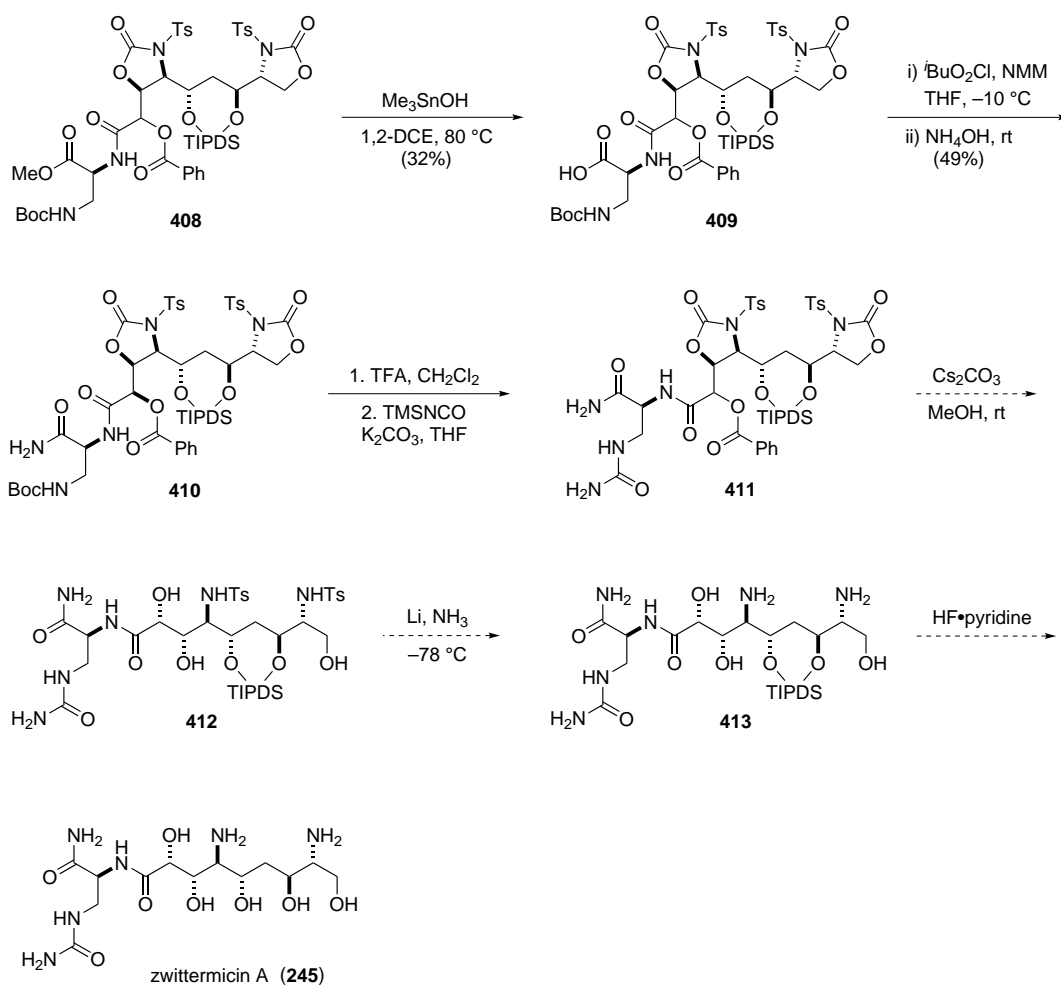


Figure 3.8. Dess–Martin oxidation of **406** followed by ^1H NMR. (A) Alcohol **406**; (B) Reaction mixture after 5 min; (C) reaction mixture after 15 min; (D) reaction mixture after addition of PhCO_2H ; (E) reaction mixture after addition of isonitrile **383**.

3.4.9 The end game strategy

The proposed sequence for the elaboration of adduct **408** starts with saponification of the methyl ester with trimethyltin hydroxide to give terminal acid **409**. Activation of the carboxylic acid as a mixed anhydride, followed by treatment with aqueous ammonia will provide primary amide **410**. After removal of the Boc group, the resulting terminal amine will be reacted with trimethylsilyl isocyanate to provide the terminal urea functionality in compound **411**. Treatment of compound **411** with Cs₂CO₃ in methanol will cleave the benzoate group as well as open the oxazolidinone rings. The 4-toluenesulfonamide substituent in compound **412** will be removed by Birch reduction¹⁹⁷ to give the aminopolyol **413**. Finally, treatment of **413** with HF · pyridine complex will remove the TIPDS group and afford the (+)-zwittermicin A **245** (Scheme 3.47). As described in earlier sections, many of these operations has been performed successfully on various intermediates. An unknown aspect, however, is the identity of the favored epimer in the conversion of **406** to **408**. Should the major diastereomer be a precursor to *epi*-zwittermicin A, an additional substitution step will be added to the end game outlined. Alternatively, the Passerini coupling can be performed at room temperature to increase the amount of the minor diastereomer.

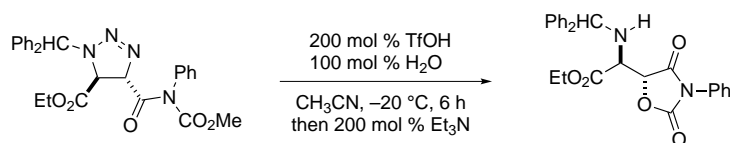
Scheme 3.47. End-game strategy for the synthesis of zwittermicin A.



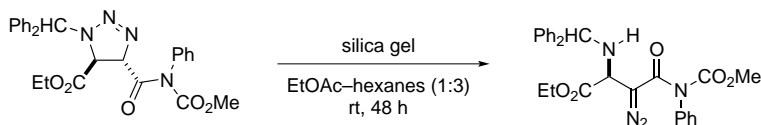
APPENDIX A

Experimental Section

Compounds relevant to Chapter 1

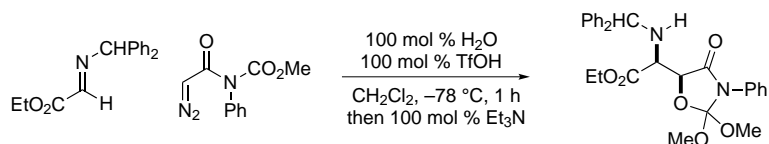


Oxazolidine dione *anti*-75. To a cold ($-20\text{ }^{\circ}\text{C}$) solution of triazoline (50.0 mg, 100 μmol) in acetonitrile (500 μL) was added TfOH (18 μL , 200 μmol) followed by water (1.8 μL , 100 μmol) and the solution was stirred at $-20\text{ }^{\circ}\text{C}$ for 6 h. The reaction was quenched with triethylamine (28 μL , 200 μmol) and concentrated to a yellow oil that was purified using flash chromatography (SiO_2 , 10–20% ethyl acetate in hexanes) to afford the oxazolidine dione as a colorless oil (34 mg, 78%). $R_f = 0.25$ 20% (EtOAc/hexanes); IR (film) 3328, 3058, 3017, 2982, 1821, 1751 cm^{-1} ^1H NMR (400 MHz, CDCl_3) δ 7.49–7.22 (m, 15H), 5.28 (d, $J = 2.5$ Hz, 1H), 5.09 (d, $J = 4.6$ Hz, 1H), 4.33 (dq, $J = 10.8, 7.2$ Hz, 1H), 4.25 (dd, $J = 10.8, 7.2$ Hz, 1H), 3.98 (dd, $J = 8.4, 2.5$ Hz, 1H), 2.75 (dd, $J = 8.4, 4.6$ Hz, 1H), 1.29 (t, $J = 7.2$ Hz, 3H); ^{13}C NMR (100 MHz, CDCl_3) ppm 169.7, 169.0, 154.2, 142.7, 141.8, 130.8, 129.5, 129.3, 129.1, 129.0, 128.7, 128.6, 128.5, 127.7, 127.6, 127.58, 127.55, 127.3, 127.2, 125.6, 125.5, 80.4, 66.2, 62.5, 59.2, 14.1; HRMS (ESI): Exact mass calcd for $\text{C}_{26}\text{H}_{24}\text{N}_2\text{NaO}_5$ $[\text{M} + \text{Na}]^+$ 467.1583, found 467.1581.

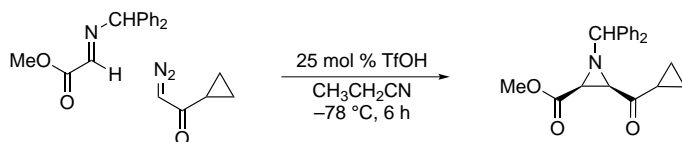


α -Diazoamine 76. A slurry of silica gel (2 g) and triazoline (64 mg, 130 μmol) in hexanes–ethyl acetate (3:1, (3 mL)) was stirred for 48 h at rt and then filtered, concentrated, and purified using flash chromatography (SiO_2 , 20% ethyl acetate in hexanes) to afford the α -diazoamine as a yellow oil (38 mg, 59%). $R_f = 0.33$ 20% (EtOAc/hexanes); IR (film) 3334, 3028, 2956, 2096, 1736, 1665 cm^{-1} ^1H NMR (400 MHz, CDCl_3) δ 7.40–7.20 (m, 13H), 7.15 (d, $J = 7.8$ Hz, 2H), 4.97 (s, 1H), 4.25 (s, 1H), 4.21 (dq, $J = 10.7, 7.2$ Hz, 1H), 4.17 (dq, $J = 10.7, 7.2$ Hz, 1H), 3.80 (s, 3H), 2.70 (br s, 1H), 1.25 (t, $J = 7.2$ Hz, 3H); ^{13}C NMR (100 MHz, CDCl_3) ppm 169.9, 166.1, 154.0, 142.8,

142.0, 129.2, 128.7, 128.5, 127.9, 127.5, 127.4, 127.3, 64.4, 62.0, 56.2, 53.9, 14.1; HRMS (ESI): Exact mass calcd for $C_{27}H_{27}N_4O_5$ $[M + H]^+$ 487.1981, found 487.1968.

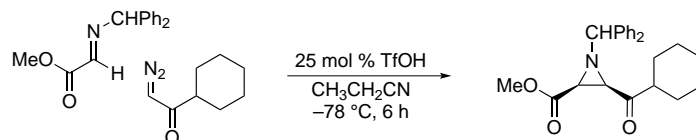


Orthoamide 78. To a cold solution ($-78\text{ }^\circ\text{C}$) of imine (26.7 mg, 100 μmol) and α -diazo imide (26.3 mg, 120 μmol) in dichloromethane (500 μL) was added TfOH (9 μL , 100 μmol), and the solution was stirred at $-78\text{ }^\circ\text{C}$ for 1 h. The reaction was quenched with satd aq NaHCO_3 and extracted with ethyl acetate. The organic layers were dried and concentrated, and the resulting solid was purified using flash chromatography (SiO_2 , 10% ethyl acetate in hexanes) to afford the orthoamide as a colorless oil (6.4 mg, 13%). $R_f = 0.22$ 20% (EtOAc/hexanes); IR (film) 3448, 2962, 2935, 2894, 2860, 1739 cm^{-1} ^1H NMR (600 MHz, CDCl_3) δ 7.60 (dd, $J = 8.7, 2.1$ Hz, 1H), 7.45 (d, $J = 7.5$ Hz, 1H), 7.44 (d, $J = 7.1$ Hz, 1H), 7.40–7.38 (m, 3H), 7.35–7.24 (m, 7H), 7.21–7.17 (m, 2H), 5.02 (s, 1H), 4.90 (d, $J = 2.7$ Hz, 1H), 4.26 (dq, $J = 10.6, 2.6$ Hz, 2H), 3.87 (dd, $J = 11.8, 2.6$ Hz, 1H), 3.41 (s, 3H), 3.38 (s, 3H), 2.72 (dd, $J = 12.0, 2.0$ Hz, 1H), 1.30 (t, $J = 7.1$ Hz, 3H); ^{13}C NMR (150 MHz, CDCl_3) ppm 171.5, 168.1, 144.3, 141.9, 133.8, 129.1, 128.5, 128.3, 127.8, 127.3, 127.2, 127.1, 127.0, 124.7, 121.2, 79.3, 64.9, 61.4, 59.1, 51.7, 51.1, 14.2; HRMS (ESI): Exact mass calcd for $C_{28}H_{30}N_2NaO_6$ $[M + \text{Na}]^+$ 513.2002, found 513.1995.

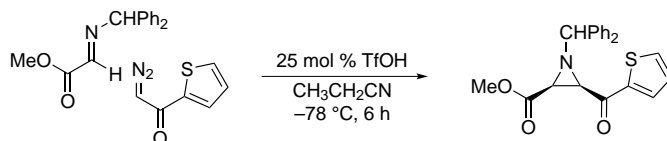


Methyl 1-benzhydryl-3-(cyclopropanecarbonyl)aziridine-2-carboxylate (81). To a solution of the imine (115 mg, 454 μmol) and diazoketone (60 mg, 540 μmol) in propionitrile (1.5 mL) at $-78\text{ }^\circ\text{C}$ was added triflic acid (10.0 μL , 114 μmol). The reaction mixture was stirred at $-78\text{ }^\circ\text{C}$ for 6 h and then was quenched with satd aq sodium bicarbonate. The mixture was extracted with ethyl acetate and the combined organic layers were washed with brine, dried and concentrated. The resulting oil was purified using flash chromatography (SiO_2 , 20% ethyl acetate in hexanes) to afford the aziridine as a white solid (133 mg, 88%). Mp 116–117 $^\circ\text{C}$; $R_f = 0.33$ (20% EtOAc/hexanes); IR (film) 3062, 1748, 1688, 1453 cm^{-1} ; ^1H NMR (500 MHz, CDCl_3) δ 7.55 (d, $J = 7.8$ Hz, 2H), 7.49 (d, $J = 7.8$ Hz, 2H), 7.37–7.29 (m, 4H), 7.28–7.23 (m, 2H), 3.87 (s, 1H), 3.71 (s, 3H), 2.75 (d, $J = 7.1$ Hz, 1H), 2.73 (d, $J = 7.1$ Hz, 1H), 2.60–2.51 (m, 1H), 1.09–1.00 (m, 1H), 0.95–0.82 (m, 3H); ^{13}C NMR (125 MHz, CDCl_3) 205.6, 167.8, 141.7, 141.5, 128.57, 128.55, 127.6, 127.4, 127.3,

127.0, 77.2, 52.3, 50.7, 45.0, 18.3, 12.4, 11.3 ppm; HRMS (ESI): Exact mass calcd for $C_{21}H_{21}NNaO_3$ $[M+Na]^+$ 358.1414, found 358.1419.

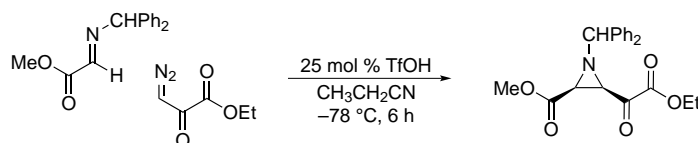


Methyl 1-benzhydryl-3-(cyclohexanecarbonyl)aziridine-2-carboxylate (82). To a solution of the imine (97.2 mg, 384 μ mol) and diazoketone (70.0 mg, 460 μ mol) in propionitrile (1.2 mL) at -78°C was added triflic acid (8.0 μ l, 90 μ mol). The reaction mixture was stirred at -78°C for 6 h and then was quenched with satd aq sodium bicarbonate. The mixture was extracted with ethyl acetate, and the combined organic layers were washed with brine, dried and concentrated. The resulting oil was purified using flash chromatography (SiO_2 , 10–25% ethyl acetate in hexanes) to afford the aziridine as a white solid (121 mg, 83%). Mp $154\text{--}156^\circ\text{C}$; $R_f = 0.20$ (10% EtOAc/hexanes); IR (film) 3062, 1742, 1700, 1450 cm^{-1} ; $^1\text{H NMR}$ (500 MHz, CDCl_3) δ 7.51 (d, $J = 7.6\text{ Hz}$, 2H), 7.43 (d, $J = 7.3\text{ Hz}$, 2H), 7.35 (d, $J = 7.5\text{ Hz}$, 2H), 7.31 (d, $J = 7.9\text{ Hz}$, 2H), 7.28–7.22 (m, 2H), 3.77 (s, 1H), 3.70 (s, 3H), 2.89 (tt, $J = 11.5, 3.0\text{ Hz}$, 1H), 2.73 (d, $J = 6.9\text{ Hz}$, 1H), 2.61 (d, $J = 6.9\text{ Hz}$, 1H), 1.71 (m, 1H), 1.59 (m, 2H), 1.46 (m, 1H), 1.38–1.14 (m, 2H), 1.13–0.95 (m, 3H), 0.71 (ddd, $J = 15.6, 12.2, 3.7\text{ Hz}$, 1H); $^{13}\text{C NMR}$ (125 MHz, CDCl_3) 208.8, 168.5, 141.7, 141.4, 128.6, 128.5, 127.9, 127.8, 127.3, 126.8, 109.4, 77.6, 52.4, 49.1, 47.5, 44.7, 28.4, 26.3, 26.0, 25.8, 25.04 ppm; HRMS (ESI): Exact mass calcd for $C_{24}H_{27}NNaO_3$ $[M+Na]^+$ 400.1883, found 400.1889.

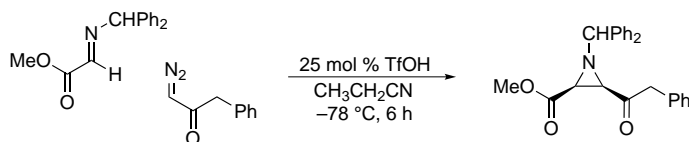


Methyl 1-benzhydryl-3-(thiophene-2-carbonyl)aziridine-2-carboxylate (83). To a solution of the imine (85.5 mg, 318 μ mol) and diazoketone (58.0 mg, 380 μ mol) in propionitrile (1.0 mL) at -78°C was added triflic acid (7.0 μ l, 80 μ mol). The reaction mixture was stirred at -78°C for 6 h and then was quenched with satd aq sodium bicarbonate. The mixture was extracted with ethyl acetate and the combined organic layers were washed with brine, dried and concentrated. The resulting oil was purified using flash chromatography (SiO_2 , 15–30% ethyl acetate in hexanes) to afford the aziridine as a pale yellow solid (97 mg, 81%). Mp $172\text{--}173^\circ\text{C}$; $R_f = 0.28$ (20% EtOAc/hexanes); IR (film) 3087, 3062, 1747, 1660, 1452 cm^{-1} ; $^1\text{H NMR}$ (500 MHz, CDCl_3) δ 7.60

(d, $J = 4.6$ Hz, 1H), 7.57 (d, $J = 7.7$ Hz, 2H), 7.50 (d, $J = 7.5$ Hz, 2H), 7.46 (d, $J = 3.9$ Hz, 1H), 7.38–7.33 (m, 2H), 7.33–7.28 (m, 4H), 6.96 (dd, $J = 4.5, 4.2$ Hz, 1H), 3.97 (s, 1H), 3.66 (s, 3H), 3.25 (d, $J = 6.7$ Hz, 1H), 2.82 (d, $J = 6.7$ Hz, 1H); ^{13}C NMR (125 MHz, CDCl_3) 185.3, 167.8, 142.3, 141.3, 141.2, 134.5, 133.6, 128.7, 128.6, 128.0, 127.9, 127.8, 127.5, 127.2, 77.8, 52.3, 48.0, 45.0 ppm; HRMS (ESI): Exact mass calcd for $\text{C}_{22}\text{H}_{19}\text{NNaO}_3\text{S}$ $[\text{M}+\text{Na}]^+$ 400.0978, found 400.0974.

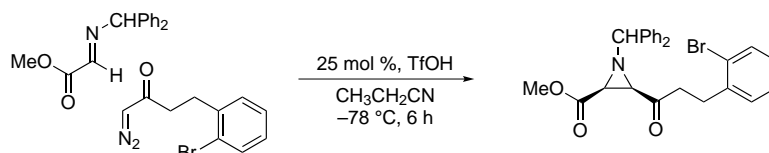


Methyl 1-benzhydryl-3-(2-ethoxy-2-oxoacetyl)aziridine-2-carboxylate (85). To a solution of the imine (127 mg, 500 μmol) and diazoketone (85.0 mg, 600 μmol) in propionitrile (1.6 mL) at -78 $^\circ\text{C}$ was added triflic acid (11.0 μl , 120 μmol). The reaction mixture was stirred at -78 $^\circ\text{C}$ for 6 h and then was quenched with satd aq sodium bicarbonate. The mixture was extracted with ethyl acetate and the combined organic layers were washed with brine, dried and concentrated. The resulting oil was purified using flash chromatography (SiO_2 , 10–30 % ethyl acetate in hexanes) to afford the aziridine as a white solid (88 mg, 48 %). Mp 98–100 $^\circ\text{C}$; $R_f = 0.29$ (20 % EtOAc/hexanes); IR (film) 3062, 1733, 1452 cm^{-1} ; ^1H NMR (500 MHz, CDCl_3) δ 7.50 (d, $J = 7.9$ Hz, 2H), 7.48 (d, $J = 8.0$ Hz, 2H), 7.34–7.29 (m, 4H), 7.27–7.22 (m, 2H), 4.29 (dq, $J = 10.8, 7.1$ Hz, 1H), 4.25 (dq, $J = 10.7, 7.2$ Hz, 1H), 3.95 (s, 1H), 3.70 (s, 3H), 3.31 (d, $J = 6.7$ Hz, 1H), 2.89 (d, $J = 6.7$ Hz, 1H), 1.31 (t, $J = 7.1$ Hz, 3H); ^{13}C NMR (125 MHz, CDCl_3) 186.4, 167.1, 160.0, 141.1, 128.6, 128.5, 127.6, 127.3, 127.2, 77.2, 62.6, 52.6, 46.6, 45.9, 13.8 ppm; HRMS (ESI): Exact mass calcd for $\text{C}_{21}\text{H}_{21}\text{NNaO}_5$ $[\text{M}+\text{Na}]^+$ 390.1312, found 390.1311.

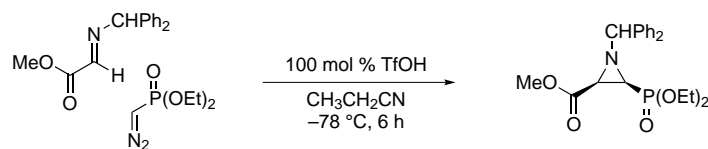


Methyl 1-benzhydryl-3-(2-phenylacetyl)aziridine-2-carboxylate (86). To a solution of the imine (152 mg, 600 μmol) and diazoketone (160 mg, 720 μmol) in propionitrile (2.0 mL) at -78 $^\circ\text{C}$ was added triflic acid (13.0 μl , 150 μmol). The reaction mixture was stirred at -78 $^\circ\text{C}$ for 6 h and then was quenched with satd aq sodium bicarbonate. The mixture was extracted with ethyl acetate and the combined organic layers were washed with brine, dried and concentrated. The resulting oil was purified using flash chromatography (SiO_2 , 10 % ethyl acetate in hexanes) to afford the aziridine as a white solid (175 mg, 67 %). Mp 159–160 $^\circ\text{C}$; $R_f = 0.36$ (20 % EtOAc/hexanes); IR (film) 3062,

1743, 1716 cm^{-1} ; ^1H NMR (500 MHz, CDCl_3) δ 7.57 (d, $J = 7.5$ Hz, 2H), 7.52 (d, $J = 7.2$ Hz, 2H), 7.43–7.36 (m, 4H), 7.36–7.22 (m, 5H), 7.05 (d, $J = 7.0$ Hz, 2H), 4.24 (d, $J = 17.4$ Hz, 1H), 3.87 (s, 1H), 3.75 (s, 3H), 3.68 (d, $J = 17.3$ Hz, 1H), 2.81 (d, $J = 6.9$ Hz, 1H), 2.73 (d, $J = 6.9$ Hz, 1H); ^{13}C NMR (125 MHz, CDCl_3) 203.4, 168.4, 141.7, 141.3, 133.8, 129.7, 128.8, 128.6, 128.3, 128.0, 127.8, 127.5, 126.9, 126.7, 77.3, 52.5, 49.8, 47.2, 45.0 ppm; HRMS (ESI): Exact mass calcd for $\text{C}_{25}\text{H}_{23}\text{NNaO}_3$ $[\text{M}+\text{Na}]^+$ 408.1576, found 408.1565. Anal calcd for $\text{C}_{25}\text{H}_{23}\text{NO}_3$: C, 77.90; H, 6.01; N, 3.65; found: C, 78.13; H, 6.01; N, 3.65.



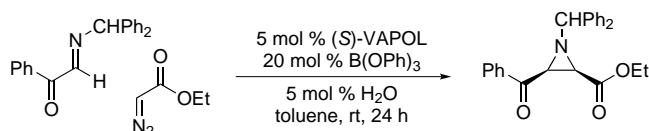
Aziridine (87). To a solution of the imine (38.0 mg, 150 μmol) and diazoketone (45.6 mg, 180 μmol) in propionitrile (0.5 mL) at -78°C was added triflic acid (3.5 μl , 150 μmol). The reaction mixture was stirred at -78°C for 6 h and then was quenched with satd aq sodium bicarbonate. The mixture was extracted with ethyl acetate and the combined organic layers were washed with brine, dried and concentrated. The resulting oil was purified using flash chromatography (SiO_2 , 18% ethyl acetate in hexanes) to afford the aziridine as a yellow oil (45.0 mg, 67%). $R_f = 0.25$ (10% EtOAc /hexanes); IR (film) 3062, 3028, 2952, 2848, 1745, 1708, 1636, 1599, 1567, 1494, 1471, 1453 cm^{-1} ; ^1H NMR (400 MHz, CDCl_3) δ 7.53–7.49 (m, 3H), 7.43 (d, $J = 7.0$ Hz, 2H), 7.35–7.15 (m, 8H), 7.06 (dd, $J = 7.8, 1.8$ Hz, 1H), 3.79 (s, 1H), 3.67 (s, 3H), 3.20–3.12 (m, 1H), 2.92–2.81 (m, 2H), 2.78–2.66 (m, 3H); ^{13}C NMR (100 MHz, CDCl_3) 205.0, 168.2, 141.6, 141.3, 140.3, 132.6, 130.5, 128.7, 128.6, 127.9, 127.7, 127.6, 127.37, 127.42, 126.8, 124.4, 77.5, 52.4, 49.8, 44.9, 40.5, 29.4 ppm; HRMS (ESI): Exact mass calcd for $\text{C}_{26}\text{H}_{24}\text{BrNaNO}_3$ $[\text{M}+\text{Na}]^+$ 500.0837, found 500.0850.



Methyl 1-benzhydryl-3-(diethoxyphosphoryl)aziridine-2-carboxylate (88).

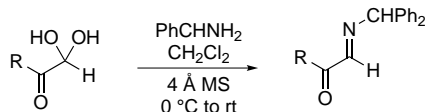
To a solution of the imine (45.1 mg, 178 μmol) and diazophosphonate (38.0 mg, 213 μmol) in propionitrile (0.6 mL) at -78°C was added triflic acid (16 μl , 180 μmol). The reaction was slowly warmed to -20°C , stirred for 18 h, and then was quenched with satd aq sodium bicarbonate. The mixture was extracted with ethyl acetate and the combined organic layers were washed with brine, dried and concentrated. The resulting oil was purified using flash chromatography (SiO_2 , 48:50:2 ethyl

acetate–hexanes–methanol) to afford the aziridine as a white solid (65.8 mg, 92 %). Mp 110–111 °C; $R_f = 0.24$ (48:50:2 ethyl acetate–hexanes–methanol); IR (film) 3462, 3062, 3028, 2953, 2929, 1852, 1753, 1637, 1600, 1494, 1477, 1453 cm^{-1} ; ^1H NMR (400 MHz, CDCl_3) δ 7.57 (d, $J = 7.4$ Hz, 2H), 7.41 (ddd, $J = 8.3, 1.9, 1.5$ Hz, 2H), 7.33–7.21 (m, 6H), 4.03–3.88 (m, 3H), 3.84–3.74 (m, 1H), 3.77 (s, 3H), 3.69 (s, 1H), 2.64 (dd, $J = 7.2, 5.3$ Hz, 1H), 2.15 (dd, $J = 17.0, 7.2$ Hz, 1H), 1.21 (dd, $J = 7.1, 7.0$ Hz, 3H), 1.12 (dd, $J = 7.2, 7.0$ Hz, 3H); ^{13}C NMR (100 MHz, CDCl_3) 167.5 (d, $J = 2.8$ Hz), 141.5, 141.3, 128.43, 128.42, 128.0, 127.7, 127.3, 127.2, 78.8 (d, $J = 6.0$ Hz), 62.7 (d, $J = 6.4$ Hz), 62.4 (d, $J = 5.9$ Hz), 52.3, 43.3 (d, $J = 5.5$ Hz), 39.9, 37.7, 16.2 (d, $J = 7.3$ Hz), 16.1 (d, $J = 7.3$ Hz) ppm; HRMS (ESI): Exact mass calcd for $\text{C}_{21}\text{H}_{26}\text{NaNNO}_5\text{P}$ $[\text{M}+\text{Na}]^+$ 426.1446, found 426.1436.

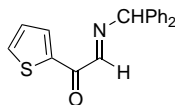


(2*R*,3*S*)-ethyl 1-benzhydryl-3-benzoylaziridine-2-carboxylate (414). A 25 mL flask (Schlenk with a Teflon valve) containing a stir bar was flame-dried and cooled under argon. To the flask was added (*S*)-VANOL (13.5 mg, 29 μmol) and triphenylborate (29 mg, 100 μmol). Under an argon flow, dry toluene (1.0 mL) was added to dissolve the two reagents, and this was followed by the addition of water (0.5 μL , 25 μmol). The Teflon valve was closed and the flask was heated at 80 °C for 1 h. The threaded Teflon valve was opened to gradually apply high vacuum (0.1 mmHg) to remove the solvent. The vacuum was maintained for a period of 30 min at a temperature of 80 °C. The flask was then filled with argon and the catalyst mixture was allowed to cool to room temperature. To the flask containing the catalyst was first added aldimine (145 mg, 500 μmol) and then dry toluene (1 mL). Ethyl diazoacetate (63 μL , 600 μmol) was added via syringe, the Teflon valve was closed, and the reaction mixture was stirred at room temperature for 24 h. The mixture was then diluted with hexanes (15 mL) and transferred to a (100 mL) round-bottomed flask. The reaction flask was rinsed twice with dichloromethane (5 mL), and the rinse was added to the round-bottom flask and the solution was concentrated. Crude aziridine was purified by trituration to give the desired aziridine as a clear oil (101 mg, 53 %). The optical purity was determined to be 70 % ee by HPLC analysis (Chiralcel OD-H, 10 % $i\text{PrOH}$ –hexanes, 0.70 mL min^{-1} , $t_r(\text{major}) = 23.4$ min, $t_r(\text{minor}) = 17.1$ min. $R_f = 0.25$ (10 % EtOAc/hexanes); IR (film) 3462, 3062, 3028, 2953, 2929, 1852, 1753, 1637, 1600, 1494, 1477, 1453 cm^{-1} ; ^1H NMR (400 MHz, CDCl_3) δ 7.75 (d, $J = 8.1$ Hz, 2H), 7.59 (d, $J = 7.3$ Hz, 4H), 7.51 (dd, $J = 7.5, 7.3$ Hz, 1H), 7.37–7.27 (m, 8H), 4.12 (q, $J = 7.1$ Hz, 2H), 3.99 (s, 1H), 3.34 (d, $J = 6.7$ Hz, 1H), 2.85 (d, $J = 6.9$ Hz, 1H), 1.12 (t, $J = 7.1$ Hz, 3H); ^{13}C NMR (100 MHz, CDCl_3) 192.2, 167.6, 141.6, 141.6, 136.0, 133.2, 129.0, 128.6, 128.5, 128.4, 127.9, 127.7, 127.4, 127.3, 77.9, 61.2, 47.9, 45.0, 13.9 ppm; HRMS (ESI): Exact mass calcd for $\text{C}_{25}\text{H}_{23}\text{NNaO}_3$ $[\text{M}+\text{Na}]^+$ 408.1576, found 408.1585.

Compounds relevant to Chapter 2

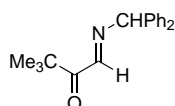


General procedure for the synthesis of benzhydryl imines. Imines were prepared by condensation of the corresponding hydrate¹¹³ with diphenylmethanimine (1 equiv) using 4 Å MS in dichloromethane at 0 °C and warmed to rt. Solution was filtered through Celite and concentrated. Unless otherwise stated the imine was recrystallized from toluene–petroleum ether.



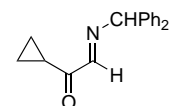
(Benzhydrylimino)-1-(thiophen-2-yl)ethanone (131). The hydrate (1.25 g, 7.90 mmol) was treated with diphenylmethanimine (1.36 mL, 7.9 mmol) according to the general procedure. The reaction was stirred for 1 h and concentrated to light yellow oil. Column chromatography (SiO₂, 20 % ethyl acetate in hexanes) of the residue provided the title compound as light brown solid which was recrystallized from hexanes to give brown crystals (0.66 g, 69 %).

Mp 71–74 °C; *R_f* = 0.20 (10 % EtOAc/hexanes); IR (film) 3085, 3061, 3027, 2867, 1632, 1599 cm⁻¹; ¹H NMR (400 MHz, CDCl₃) δ 8.32 (dd, *J* = 3.8, 1.0 Hz, 1H), 8.07 (s, 1H), 7.77 (dd, *J* = 5.0, 1.2 Hz, 1H), 7.44–7.43 (m, 4H), 7.40–7.35 (m, 4H), 7.31–7.28 (m, 2H), 7.18 (dd, *J* = 4.8, 4.0 Hz, 1H), 5.69 (s, 1H); ¹³C NMR (100 MHz, CDCl₃) 182.2, 142.2, 138.5, 136.7, 136.0, 128.7, 128.5, 127.7, 127.5, 78.2 ppm; HRMS (ESI): Exact mass calcd for C₁₉H₁₅NNaOS [M+Na]⁺ 328.0772, found 328.0772.



1-(Benzhydrylimino)-3,3-dimethylbutan-2-one (132). The hydrate (1.00 g, 7.57 mmol) was treated with diphenylmethanimine (1.3 mL, 7.6 mmol) according to the general procedure. The reaction was stirred for 1 h and concentrated to clear oil (2.09 g, 99 %). IR (film) 3298, 3061, 3028, 2968, 2879, 1683 cm⁻¹; ¹H NMR (400 MHz, CDCl₃) δ 7.38 (s, 1H), 7.18 (d, *J* = 4.4 Hz, 8H), 7.30–7.24 (m, 2H), 5.49 (s, 1H) 1.38 (s, 9H); ¹³C NMR (100 MHz, CDCl₃)

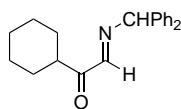
205.7, 158.8, 142.5, 128.6, 127.3, 78.6, 43.8, 26.7 ppm; HRMS (ESI): Exact mass calcd for C₁₉H₂₁NO [M+H]⁺ 280.1705, found 280.1696.



2-(Benzhydrylimino)-1-cyclopropylethanone (133). The hydrate (670 mg, 5.8 mmol) was treated with diphenylmethanimine (1.0 mL, 5.8 mmol) according to the general procedure. The reaction was stirred for 1 h and concentrated to clear oil and recrystallized from hexanes to give colorless crystals (990 mg, 65 %). Mp 64–66 °C; IR (film) 3085, 3061, 3027, 3007, 2865, 1683 cm⁻¹; ¹H NMR (400 MHz, CDCl₃) δ 7.80 (s, 1H), 7.37–7.27 (m, 10H),

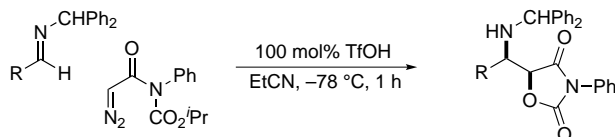
5.66 (s, 1H), 3.14 (dddd, *J* = 4.8, 4.7, 1.1, 1.0 Hz, 1H), 1.20–1.16 (m, 2H), 1.08–1.03 (m, 2H); ¹³C NMR (100 MHz, CDCl₃) 201.2, 159.8, 142.1, 128.6, 127.6, 127.4, 77.4, 15.7, 12.6 ppm; HRMS

(ESI): Exact mass calcd for C₁₈H₁₈NO [M+H]⁺ 264.1388, found 264.1395.

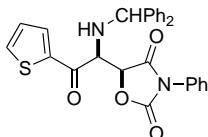


2-(Benzhydrylimino)-1-cyclopropylethanone (134).

The hydrate (298 mg, 1.88 mmol) was treated with diphenylmethanamine (325 μ L, 1.89 mmol) according to the general procedure. The reaction was stirred for 1 h and concentrated to light yellow solid and recrystallized from hexanes to give colorless crystals (397 mg, 65 %). Mp 50–51 °C; IR (film) 3061, 2930, 2854, 1691 cm⁻¹; ¹H NMR (400 MHz, CDCl₃) δ 7.69 (s, 1H), 7.37–7.27 (m, 10H), 5.60 (s, 1H), 3.49 (br, 1H), 1.88 (m, 2H), 1.82 (m, 2H), 1.44–1.33 (m, 4H), 1.27–1.22 (m, 1H); ¹³C NMR (100 MHz, CDCl₃) 204.8, 159.0, 142.2, 128.7, 127.5, 127.5, 77.5, 44.4, 28.5, 25.9, 25.6 ppm; HRMS (ESI): Exact mass calcd for C₂₁H₂₂NO [M-H]⁺ 304.1701, found 304.1682.

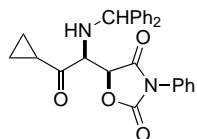


General procedure for the *syn*-glycolate Mannich reaction. To a cold –78 °C solution of the imine (1.0 equiv) and α -diazo imide (1.2 equiv) in propionitrile (0.15 M) was added dry TfOH (1.0 equiv), and the solution was stirred at –78 °C. The reaction was quenched with satd aq NaHCO₃ and extracted with ethyl acetate. The organic layers were dried, concentrated, and the resulting solid was purified by silica gel flash chromatography.



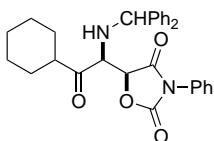
***syn*-Oxazolidinone dione 138.** Imine (46 mg, 150 μ mol) was treated with α -diazo imide (44 mg, 180 μ mol) and dry TfOH (13 μ L, 150 μ mol) according to the general procedure and stirred for 1 h. Purified by flash chromatography (SiO₂, 15–25 % ethyl acetate in hexanes) to afford the oxazolidinone dione as colorless oil (57 mg, 80 %). R_f = 0.14 (20 % EtOAc/hexanes); IR (film) 3063, 3027, 2926, 1824, 1750, 1711, 1665, 1597 cm⁻¹; ¹H NMR (400 MHz, CDCl₃) δ 7.89 (dd, *J* = 5.0, 0.8 Hz, 1H),

7.61 (dd, *J* = 3.8, 0.7 Hz, 1H), 7.59–7.54 (m, 2H), 7.54–7.48 (m, 3H), 7.39–7.11 (m, 10H), 7.17 (dd, *J* = 4.8, 3.9 Hz, 1H), 5.21 (d, *J* = 2.4 Hz, 1H), 4.90 (d, *J* = 3.8 Hz, 1H), 4.71 (dd, *J* = 11.2, 2.4 Hz, 1H), 3.24 (dd, *J* = 11.2, 3.4 Hz, 1H); ¹³C NMR (100 MHz, CDCl₃) 188.8, 169.8, 153.8, 142.7, 141.4, 141.1, 135.8, 133.1, 130.8, 129.4, 129.3, 129.0, 129.0, 128.6, 128.6, 128.5, 127.7, 127.6, 127.5, 127.2, 125.7, 125.5, 79.1, 67.6, 65.3, 61.0 ppm; HRMS (CI): Exact mass calcd for C₂₈H₂₃N₂O₄S [M+H]⁺ 483.1373, found 483.1368.



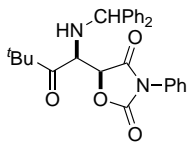
***syn*-Oxazolidinone dione 139.** Imine (132 mg, 500 μ mol) was treated with α -diazo imide (148 mg, 600 μ mol) and dry TfOH (44 μ L, 500 μ mol) according to the general procedure and stirred for 1 h. Purified by flash chromatography (SiO₂, 10–20 % ethyl acetate in hexanes) to afford the

oxazolidine dione as colorless oil (215 mg, 98 %) which was recrystallized from 10 % EtOAc in hexanes to give colorless crystals (136.5 mg, 62 %). Mp 167–168 °C; $R_f = 0.23$ (20 % EtOAc/hexanes); IR (film) 3406, 3027, 2923, 1820, 1748, 1707, 1598 cm^{-1} ; ^1H NMR (400 MHz, CDCl_3) δ 7.57–7.49 (m, 2H), 7.49–7.43 (m, 3H), 7.37–7.20 (m, 10H), 5.34 (d, $J = 1.6$ Hz, 1H), 4.86 (d, $J = 4.6$ Hz, 1H), 4.17 (dd, $J = 10.1, 1.7$ Hz, 1H), 2.99 (dd, $J = 10.1, 4.7$ Hz, 1H), 1.98 (m, 1H), 1.24–1.17 (m, 1H), 1.17–1.09 (m, 1H), 1.07–0.96 (m, 2H); ^{13}C NMR (100 MHz, CDCl_3) 205.8, 170.1, 154.0, 142.7, 141.7, 130.8, 129.4, 129.0, 128.6, 128.5, 127.5, 127.3, 125.7, 78.5, 65.6, 64.8, 18.8, 12.6, 11.5 ppm; HRMS (ESI): Exact mass calcd for $\text{C}_{27}\text{H}_{24}\text{N}_2\text{O}_4$ $[\text{M}]^+$ 440.1736, found 440.1756.

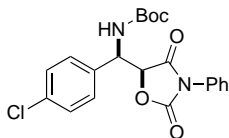


***syn*-Oxazolidine dione 140.** Imine (46 mg, 150 μmol) was treated with α -diazo imide (44 mg, 180 μmol) and dry TfOH (13 μL , 150 μmol) according to the general procedure and stirred for 1 h. Purified by flash chromatography (SiO_2 , 5–15 % ethyl acetate in hexanes) to afford the oxazolidine dione as colorless oil (215 mg, 98 %) which was recrystallized from 10 % EtOAc in hexanes to give colorless crystals (70.0 mg, 97 %).

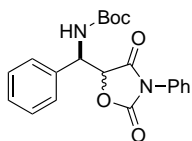
$R_f = 0.37$ (20 % EtOAc/hexanes); IR (film) 2930, 2854, 1820, 1750, 1712, 1598 cm^{-1} ; ^1H NMR (400 MHz, CDCl_3) δ 7.56–7.23 (m, 15H), 5.18 (d, $J = 2.6$ Hz, 1H), 4.81 (d, $J = 4.8$ Hz, 1H), 4.11 (d, $J = 10.1$ Hz, 1H), 3.06 (dd, $J = 10.1, 5.7$ Hz, 1H), 2.52 (m, 1H), 1.85–1.12 (m, 10H); ^{13}C NMR (100 MHz, CDCl_3) 208.6, 170.2, 153.9, 142.4, 141.8, 130.8, 129.4, 129.0, 128.6, 128.5, 127.5, 127.5, 125.7, 78.0, 65.8, 62.7, 47.5, 28.8, 27.7, 25.5, 25.4, 25.1 ppm; HRMS (ESI): Exact mass calcd for $\text{C}_{30}\text{H}_{31}\text{N}_2\text{O}_4$ $[\text{M}+\text{H}]^+$ 483.2278, found 483.2228.



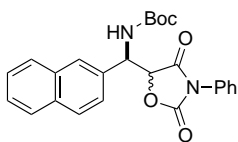
syn-Oxazolidine dione 141. Imine (43 mg, 150 μmol) was treated with α -diazo imide (45 mg, 180 μmol) and dry TfOH (13 μL , 150 μmol) according to the general procedure and stirred for 1 h. Purified by flash chromatography (SiO_2 , 15–25% ethyl acetate in hexanes) to afford the oxazolidine dione as colorless oil (59.5 mg, 88%). $R_f = 0.29$ (20% EtOAc/hexanes); IR (film) 3308, 3028, 2967, 1824, 1771, 1708, 1598 cm^{-1} ; ^1H NMR (500 MHz, CDCl_3) δ 7.55–7.21 (m, 15H), 5.11 (d, $J = 3.6$ Hz, 1H), 4.93 (d, $J = 5.6$ Hz, 1H), 4.27 (dd, $J = 9.9, 3.4$ Hz, 1H), 2.88 (dd, $J = 10.0, 5.6$ Hz, 1H), 1.17 (s, 9H); ^{13}C NMR (125 MHz, CDCl_3) 211.4, 170.1, 154.3, 142.4, 141.8, 129.3, 129.0, 128.7, 128.6, 127.7, 127.6, 127.6, 127.3, 125.8, 77.1, 66.0, 60.2, 44.0, 26.9 ppm; HRMS (ESI): Exact mass calcd for $\text{C}_{28}\text{H}_{29}\text{N}_2\text{O}_4$ $[\text{M}+\text{H}]^+$ 457.2122, found 457.2067.



syn-Oxazolidine dione 162. Imine (24.0 mg, 100 μmol) was treated with α -diazo imide (29.7 mg, 120 μmol) and dry TfOH (8.8 μL , 100 μmol) according to the general procedure and stirred for 6 h at -20°C . The resulting oil (3:1 dr, ^1H NMR) was purified by flash chromatography (SiO_2 , 5–20% ethyl acetate in hexanes) to afford the oxazolidine dione as colorless oil (30 mg, 72%). Chiral HPLC analysis (Chiralcel OD-H, 30% i PrOH–hexanes, 0.70 mL min^{-1} , $t_r(\text{d1e1}) = 11.2$ min, $t_r(\text{d1e2}) = 11.8$ min, $t_r(\text{d2e1}) = 28.2$ min, $t_r(\text{d2e2}) = 41.2$ min. *Major diastereomer:* Colorless solid; Mp 213–214 $^\circ\text{C}$; $R_f = 0.35$ (20% EtOAc/hexanes); IR (film) 3361, 2978, 2933, 1819, 1746, 1598, 1503, 1456, 1407 cm^{-1} ; ^1H NMR (400 MHz, CDCl_3) δ 7.46–7.36 (m, 5H), 7.32 (d, $J = 8.5$ Hz, 2H), 7.10 (dd, $J = 8.4, 1.5$ Hz, 2H), 5.58 (d, $J = 8.9$ Hz, 1H), 5.44 (d, $J = 7.0$ Hz, 1H), 5.17 (d, $J = 3.3$ Hz, 1H), 1.43 (s, 9H); ^{13}C NMR (150 MHz, CDCl_3) 170.0, 154.5, 153.4, 134.9, 134.0, 130.0, 129.4, 129.2, 129.2, 128.5, 125.4, 81.0, 79.3, 53.4, 28.2 ppm; HRMS (ESI): Exact mass calcd for $\text{C}_{21}\text{H}_{21}\text{ClNaN}_2\text{O}_5$ $[\text{M}+\text{Na}]^+$ 439.1037, found 439.1054.

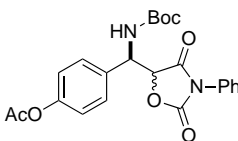


syn-Oxazolidine dione 415. Imine (103 mg, 500 μmol) was treated with α -diazo imide (98.9 mg, 400 μmol) and dry TfOH (36 μL , 400 μmol) according to the general procedure and stirred for 6 h at -20°C . The resulting oil (2:1 dr, ^1H NMR) was purified by flash chromatography (SiO_2 , 5–20% ethyl acetate in hexanes) to afford the oxazolidine dione as colorless oil (78.1 mg, 51%). Chiral HPLC analysis (Chiralcel OD-H, 20% i PrOH–hexanes, 0.70 mL min^{-1} , $t_r(\text{d1e1}) = 11.6$ min, $t_r(\text{d1e2}) = 13.8$ min, $t_r(\text{d2e1}) = 18.0$ min, $t_r(\text{d2e2}) = 69.3$ min. $R_f = 0.33$ (25% EtOAc/hexanes); IR (film) 3354, 3034, 2977, 2930, 1821, 1746, 1599, 1502, 1455, 1455 cm^{-1} ; ^1H NMR (600 MHz, CDCl_3) δ 7.42–7.31 (m, 16H), 7.07 (d, $J = 7.4$ Hz, 2H), 6.77–6.75 (m, 2H), 5.62 (d, $J = 8.3$ Hz, 1H), 5.46–5.44 (m, 3H), 5.35 (br, 1H), 5.19 (d, $J = 3.4$ Hz, 1H), 1.47 (s, 9H), 1.44 (s, 9H); ^{13}C NMR (150 MHz, CDCl_3) 170.1, 168.8, 154.7, 153.5, 130.2, 130.0, 129.3, 129.20, 129.23, 129.1, 129.0, 128.9, 128.8, 128.6, 128.5, 128.2, 127.7, 127.1, 125.6, 80.8, 80.7, 79.6, 79.5, 55.8, 54.1, 28.3, 28.2 ppm;



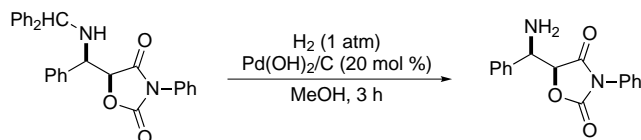
syn-Oxazolidine dione 416. To an oven-dried vial with stir bar was added imine (51.1 mg, 200 μmol), copper(II) triflate (36.2 mg, 100 μmol) and propionitrile (1.5 mL). The solution was cooled to -78°C and solution of α -diazo imide (54.4 mg, 220 μmol) in dichloromethane (0.5 mL) was added via cannula and the solution was stirred at -20°C for 6 h.

The reaction was then quenched with NH_4OH in brine (2:1) and extracted with ethyl acetate. The organic layers were dried, concentrated, and the resulting oil (1.4:1 dr by ^1H NMR) was purified by flash chromatography (SiO_2 , 10–25 % ethyl acetate in hexanes) to afford (48.1 mg, 55 %) of the oxazolidine dione as colorless oil. An analytical sample of the major diastereomer was obtained by chromatography (SiO_2 , 10 % ethyl acetate in hexanes). Chiral HPLC analysis (Chiralcel AD, 10 % $i\text{PrOH}$ –hexanes, 1.0 mL min^{-1} , $t_r(\text{d1e1}) = 32.0$ min, $t_r(\text{d1e2}) = 36.0$ min, $t_r(\text{d2e1}) = 44.2$ min, $t_r(\text{d2e2}) = 53.2$ min. $R_f = 0.31$ (25 % EtOAc/hexanes); IR (film) 3345, 3060, 2980, 2934, 1823, 1749, 1598, 1503, 1457 cm^{-1} ; ^1H NMR (600 MHz, CDCl_3) δ 7.87–7.82 (m, 4H), 7.52–7.50 (m, 2H), 7.44–7.41 (m, 1H), 7.23–7.16 (m, 3H), 6.60–6.57 (m, 2H), 5.56–5.51 (m, 3H), 1.48 (s, 9H); ^{13}C NMR (150 MHz, CDCl_3) 154.7, 153.6, 133.3, 133.0, 130.7, 129.8, , 129.2, 129.09, 129.12, 128.4, 128.2, 127.6, 127.4, 126.9, 126.8, 125.4, 124.6, 81.0, 80.9, 55.9, 28.3 ppm; HRMS (ESI): Exact mass calcd for $\text{C}_{25}\text{H}_{24}\text{NaN}_2\text{O}_5$ $[\text{M}+\text{Na}]^+$ 455.1583, found 455.1585.

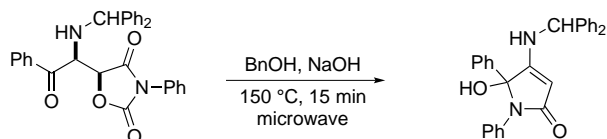


syn-Oxazolidine dione 417. To an oven-dried vial with stir bar was added imine (52.7 mg, 200 μmol), copper(II) triflate (36.2 mg, 100 μmol) and propionitrile (1.5 mL). The solution was cooled to -78°C and solution of α -diazo imide (54.4 mg, 220 μmol) in dichloromethane (0.5 mL) was added via cannula and the solution was stirred at -20°C for 6 h.

The reaction was then quenched with NH_4OH in brine (2:1) and extracted with ethyl acetate. The organic layers were dried, concentrated, and the resulting oil (1.4:1 dr by ^1H NMR) was purified by flash chromatography (SiO_2 , 10–25 % ethyl acetate in hexanes) to afford (48.1 mg, 55 %) of the oxazolidine dione as colorless oil. An analytical sample of the major diastereomer was obtained by chromatography (SiO_2 , 15 % ethyl acetate in hexanes). Chiral HPLC analysis (Chiralcel IA, 10 % $i\text{PrOH}$ –hexanes, 1.0 mL min^{-1} , $t_r(\text{d1e1}) = 28.6$ min, $t_r(\text{d1e2}) = 36.4$ min, $t_r(\text{d2e1}) = 42.3$ min, $t_r(\text{d2e2}) = 53.2$ min. $R_f = 0.27$ (25 % EtOAc/hexanes); IR (film) 3363, 2979, 2934, 1819, 1754, 1711, 1607, 1598, 1504 cm^{-1} ; ^1H NMR (600 MHz, CDCl_3) δ 7.45–7.39 (m, 3H), 7.27 (d, $J = 8.0$ Hz, 2H), 7.21 (d, $J = 8.0$ Hz, 2H), 7.11 (d, $J = 7.7$ Hz, 2H), 5.55 (d, $J = 8.4$ Hz, 1H), 5.43 (d, $J = 7.8$ Hz, 1H), 5.19 (d, $J = 3.3$ Hz, 1H), 2.37 (s, 9H), 1.45 (s, 9H); ^{13}C NMR (150 MHz, CDCl_3) 170.2, 170.2, 154.7, 153.6, 138.8, 130.3, 129.6, 129.3, 129.1, 127.0, 125.6, 80.7, 79.6, 53.9, 28.2, 21.1 ppm; HRMS (ESI): Exact mass calcd for $\text{C}_{23}\text{H}_{24}\text{NaN}_2\text{O}_7$ $[\text{M}+\text{Na}]^+$ 463.1481, found 463.1486.

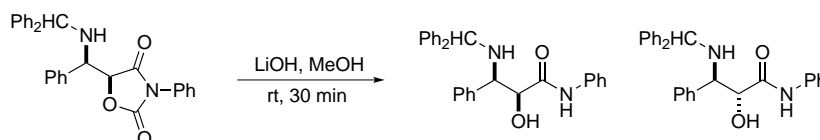


***syn*-5-(amino(phenyl)methyl)-3-phenyloxazolidine-2,4-dione (418).** To a solution of oxazolidinone dione (123 mg, 123 μmol) in ethanol (1.0 mL) and ethyl acetate (1.0 mL) was added Pd(OH)₂ (23 mg, 12 μmol , 20 % wt. on carbon). The flask was put under an atmosphere of hydrogen and the solution was stirred at ambient temperature for 5 h. The reaction was filtered through Celite, concentrated, and the resulting solid was purified by chromatography (SiO₂, 30 % ethyl acetate in hexanes) to afford the amine as a clear oil (24.1 mg, 69 %). $R_f = 0.1$ (30 % EtOAc/hexanes); IR (film) 3388, 3062, 1815, 1744, 1598, 1502 cm^{-1} ; ¹H NMR (600 MHz, CDCl₃) δ 7.47–7.39 (m, 7H), 7.37–7.34 (m, 1H), 7.30–7.28 (m, 2H), 5.08 (d, $J = 2.5$ Hz, 1H), 4.58 (br, 1H), 2.83 (br, 2H); ¹³C NMR (150 MHz, CDCl₃) 170.9, 154.3, 130.7, 129.3, 129.1, 129.0, 128.9, 128.3, 128.1, 127.4, 126.6, 125.7, 125.6, 82.7, 56.0 ppm; HRMS (ESI): Exact mass calcd for C₁₆H₁₂NO₃ [M–NH₃]⁺ 266.0817, found 266.0594.



4-(Benzhydrylamino)-5-hydroxy-1,5-diphenyl-1*H*-pyrrol-2(5*H*)-one (150).

To a microwave vial (0.5 mL) was added benzyl alcohol (0.5 mL), sodium hydroxide (1.0 mg, 25 μmol) and oxazolidinone dione (50.0 mg, 105 μmol). The vial was sealed and heated in the microwave at 150 °C for 15 min. The reaction mixture was cooled, poured into water, and layers were separated. The organic layer was dissolved in ethyl acetate, washed with water, dried and concentrated to an oil that was purified using flash chromatography (SiO₂, 20 % ethyl acetate in hexanes) to afford the amide as a clear oil (133 mg, 88 %). $R_f = 0.21$ (25 % EtOAc/hexanes); IR (film) 3403, 3199, 3061, 3029, 2924, 2853, 1664, 1533, 1600, 1495 cm^{-1} ; ¹H NMR (600 MHz, CDCl₃) δ 7.74 (dd, $J = 8.5, 0.8$ Hz, 2H), 7.46 (dd, $J = 8.5, 1.2$ Hz, 2H), 7.30–7.19 (m, 11H), 7.03–6.99 (m, 3H), 6.75 (dd, $J = 5.8, 2.1$ Hz, 2H), 6.65 (s, 1H), 4.80 (d, $J = 4.6$ Hz, 1H), 4.60 (d, $J = 4.4$ Hz, 1H), 4.34 (s, 1H); ¹³C NMR (150 MHz, CDCl₃) 173.6, 164.9, 140.9, 139.5, 137.2, 137.2, 128.6, 128.4, 128.3, 128.2, 127.9, 127.8, 127.3, 126.6, 125.8, 124.0, 123.3, 91.8, 88.4, 62.3 ppm; HRMS (CI): Exact mass calcd for C₂₉H₂₄N₂O₂ [M]⁺ 432.1838, found 432.1832.

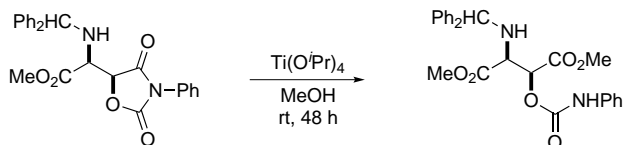


4-(Benzhydrylamino)-5-hydroxy-1,5-diphenyl-1*H*-pyrrol-2(5*H*)-one (151).

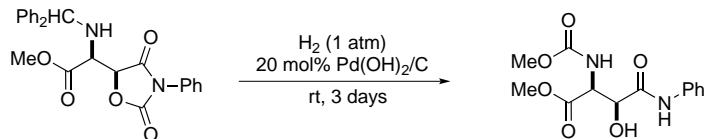
To a solution of oxazolidinone dione (123 mg, 123 μmol) in methanol 1.0 mL was added a saturated solution of lithium hydroxide in methanol (200 μL). The solution was stirred at rt for 30 min, poured into water, and extracted with ethyl acetate. The combined organic layers were dried and concentrated to give a yellow oil (1:1 ratio of diastereomers by ^1H NMR). The residue was purified by flash chromatography (SiO_2 , 10% ethyl acetate in hexanes) to afford the *syn*-diastereomer as a clear oil (8.2 mg, 35%) and anti diastereomer as a clear oil (7.2 mg, 31%).

syn-product: $R_f = 0.18$ (20% EtOAc/hexanes); IR (film) 3362, 3060, 3026, 2922, 2851, 1663, 1599, 1532, 1493 cm^{-1} ; ^1H NMR (600 MHz, CDCl_3) δ 8.55 (br s, 1H), 7.50 (d, $J = 7.8$ Hz, 2H), 7.37–7.33 (m, 6H), 7.30–7.24 (m, 9H), 7.23–7.20 (m, 2H), 7.13 (dd, $J = 7.3, 7.3$ Hz, 1H), 4.74 (s, 1H), 4.26 (d, $J = 4.1$ Hz, 1H), 4.15 (d, $J = 4.1$ Hz, 1H), amine N–H and alcohol O–H not observed; ^{13}C NMR (150 MHz, CDCl_3) 169.9, 143.2, 142.3, 140.0, 137.0, 128.6, 128.4, 128.3, 128.2, 127.9, 127.8, 127.3, 124.8, 119.7, 74.4, 63.9, 61.8 ppm; HRMS (ESI): Exact mass calcd for $\text{C}_{28}\text{H}_{26}\text{NaN}_2\text{O}_2$ $[\text{M}+\text{Na}]^+$ 445.1892, found 445.1904.

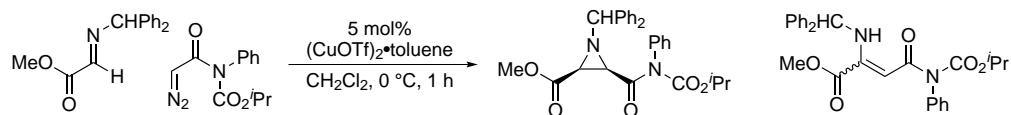
anti-product: $R_f = 0.15$ (20% EtOAc/hexanes); IR (film) 3366, 3060, 3027, 2922, 2851, 1665, 1599, 1531, 1493 cm^{-1} ; ^1H NMR (600 MHz, CDCl_3) δ 8.73 (br s, 1H), 7.39–7.22 (m, 19H), 7.13–7.09 (m, 1H), 4.80 (s, 1H), 4.40 (d, $J = 6.3$ Hz, 1H), 4.08 (d, $J = 6.7$ Hz, 1H), 3.74 (br s, 1H), amine N–H not observed; ^{13}C NMR (150 MHz, CDCl_3) 169.6, 143.2, 142.1, 138.1, 136.9, 128.9, 128.8, 128.7, 128.6, 128.2, 128.0, 127.7, 127.5, 127.3, 127.1, 124.5, 120.1, 73.3, 63.8, 62.6 ppm; HRMS (ESI): Exact mass calcd for $\text{C}_{28}\text{H}_{26}\text{NaN}_2\text{O}_2$ $[\text{M}+\text{Na}]^+$ 445.1892, found 445.1870.



***syn*-Methyl 2-amino(2,4-dioxo-3-phenyloxazolidin-5-yl)acetate (156).** To a solution of oxazolidinone dione (20.0 mg, 46.0 μmol), in methanol (0.5 mL) was added titanium(IV) tetraisopropoxide (26 μL , 92 μmol). The solution was stirred at room temperature for 4 h, poured into water and extracted with ethyl acetate. The combined organic layers were dried and concentrated to give a yellow residue which was purified using flash chromatography (SiO_2 , 20% ethyl acetate in hexanes) affording the title compound as a clear oil (3.4 mg, 16%). $R_f = 0.35$ (20% EtOAc/hexanes); IR (film) 3343, 3061, 3028, 2953, 2924, 2852, 1745, 1602, 1537, 1501 cm^{-1} ; ^1H NMR (600 MHz, CDCl_3) δ 7.32 (d, $J = 7.2$ Hz, 2H), 7.28 (d, $J = 7.2$ Hz, 2H), 7.27 (d, $J = 7.2$ Hz, 2H), 7.24–7.20 (m, 6H), 7.18–7.12 (m, 2H), 6.99 (dd, $J = 7.65, 7.20$ Hz, 1H), 6.78 (br s, 1H), 5.45 (d, $J = 2.5$ Hz, 1H), 4.83 (s, 1H), 3.78 (d, $J = 2.6$ Hz, 1H), 3.72 (s, 3H), 3.70 (s, 3H), 2.50 (br s, 1H); ^{13}C NMR (150 MHz, CDCl_3) 171.5, 167.9, 151.6, 143.7, 141.8, 137.1, 129.0, 128.6, 128.4, 127.8, 127.6, 127.3, 127.2, 123.9, 118.6, 73.7, 65.1, 59.2, 52.6, 52.4 ppm; HRMS (ESI): Exact mass calcd for $\text{C}_{26}\text{H}_{27}\text{N}_2\text{O}_6$ $[\text{M}+\text{H}]^+$ 463.1869, found 463.1869.



***syn*-Aminoalcohol (157).** Oxazolidinone dione (100 mg, 232 μmol) was suspended in methanol (2.0 mL) and $\text{Pd}(\text{OH})_2$ (33 mg, 23 μmol , 20 % wt. on carbon) was added in one portion. The flask was put under an atmosphere of hydrogen and the solution was stirred at ambient temperature for 3 d. It was then filtered through Celite and concentrated. The residue was dissolved in ethyl acetate, washed with satd NH_4Cl , dried, and concentrated. The residue was purified using flash chromatography (SiO_2 , 50 % ethyl acetate in hexanes) to afford amido alcohol (30.9 mg, 45 %) as colorless solid. Mp 146–148 $^\circ\text{C}$; R_f = 0.14 (50 % EtOAc/hexanes); IR (film) 3341, 2955, 2924, 2851, 1723, 1600, 1537 cm^{-1} ; ^1H NMR (600 MHz, CDCl_3) δ 8.66 (s, 1H), 7.53 (d, J = 8.4 Hz, 2H), 7.32 (dd, J = 8.4, 7.2 Hz, 2H), 7.13 (dd, J = 7.6, 7.2 Hz, 1H), 5.87 (d, J = 8.0 Hz, 1H), 4.99 (br, 1H), 4.89 (dd, J = 9.4, 2.6 Hz, 1H), 4.72 (dd, J = 6.6, 2.6 Hz, 1H), 3.77 (s, 3H), 3.66 (s, 3H); ^{13}C NMR (150 MHz, CDCl_3) 170.9, 169.0, 157.7, 136.8, 129.0, 124.9, 120.0, 72.7, 56.5, 53.0, 52.9 ppm; HRMS (ESI): Exact mass calcd for $\text{C}_{13}\text{H}_{16}\text{N}_2\text{NaO}_6$ $[\text{M}+\text{Na}]^+$ 319.0901, found 319.0895.

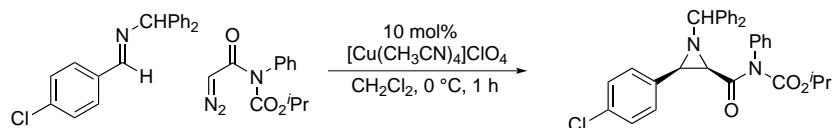


Aziridine 203 and vinylogous amide 204. Copper(I) triflate (2:1 complex with toluene, 8.0 mg, 15 μmol) was dissolved in dichloromethane (1.7 mL) and stirred at room temperature for 15 min. The clear yellow catalyst solution was cooled to -78°C , and a solution of the imine (76.0 mg, 300 μmol) in CH_2Cl_2 (300 μL) was added via cannula, followed by a solution of diazoimide (1.0 M in dichloromethane, 330 μL , 330 μmol) via syringe. The solution was stirred at -78°C for 1 h, warmed to -20°C , and then stirred for 18 h. A satd solution of NaHCO_3 (1.0 mL) was added and stirring continued for 30 min at rt. The layers were separated, and the aqueous layer was extracted with dichloromethane. The combined organic layers were washed with 1.0 M NH_4OH and brine, dried with MgSO_4 , and concentrated to an oil that was purified using flash chromatography (SiO_2 , 20 % ethyl acetate in hexanes) affording aziridine as colorless solid (68.7 mg, 49 %). A second chromatography (SiO_2 , 30 % ethyl acetate in hexanes) afforded the vinylogous amide as colorless solid (20.3 mg, 22 %).

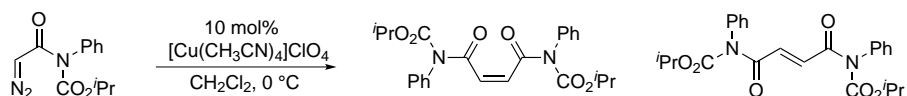
Aziridine: Mp 158–160 $^\circ\text{C}$; R_f = 0.39 (25 % EtOAc/hexanes); IR (film) 3063, 3029, 2984, 2952, 1747, 1597, 1492 cm^{-1} ; ^1H NMR (600 MHz, CDCl_3) δ 7.66 (d, J = 7.6 Hz, 2H), 7.47 (d, J = 7.0 Hz, 2H), 7.40 (d, J = 7.2 Hz, 1H), 7.39 (d, J = 7.6 Hz, 1H), 7.35 (d, J = 7.2 Hz, 1H), 7.33 (d, J = 2.7 Hz, 1H), 7.32 (d, J = 3.0 Hz, 2H), 7.30 (d, J = 3.2 Hz, 1H), 7.25 (dd, J = 8.4, 7.4 Hz, 1H), 7.22 (dd, J = 7.6, 7.4 Hz, 1H), 7.12 (dd, J = 7.5, 1.5 Hz, 2H), 4.92 (dq, J = 6.3, 6.2 Hz, 1H), 4.11 (s, 1H),

3.73 (s, 3H), 3.51 (d, $J = 6.7$ Hz, 1H), 2.83 (d, $J = 6.7$ Hz, 1H), 1.14 (d, $J = 6.2$ Hz, 3H), 1.13 (d, $J = 6.2$ Hz, 3H); ^{13}C NMR (150 MHz, CDCl_3) 168.7, 168.2, 153.4, 141.7, 141.6, 137.3, 128.8, 128.4, 128.3, 128.2, 128.0, 127.7, 127.5, 127.4, 127.2, 76.7, 71.3, 52.4, 48.3, 43.9, 21.4, 21.3 ppm; HRMS (ESI): Exact mass calcd for $\text{C}_{28}\text{H}_{28}\text{NaN}_2\text{O}_5$ $[\text{M}+\text{Na}]^+$ 495.1890, found 495.1888. Anal calcd for $\text{C}_{28}\text{H}_{28}\text{N}_2\text{O}_5$: C, 71.16; H, 5.98; N, 5.93; found: C, 70.90; H, 5.92; N, 5.91.

Vinylogous amide: Mp 174.0–176.5 °C; $R_f = 0.22$ (25 % EtOAc/hexanes); IR (film) 3317, 3062, 3029, 2981, 2932, 1731, 1681, 1600, 1546, 1497 cm^{-1} ; ^1H NMR (600 MHz, CDCl_3) δ 9.38 (br, 1H), 7.67 (d, $J = 7.6$ Hz, 2H), 7.42 (d, $J = 7.5$ Hz, 1H), 7.41 (d, $J = 7.7$ Hz, 1H), 7.27–7.26 (m, 4H), 7.21 (ddd, $J = 7.5, 2.1, 2.1$ Hz, 1H), 7.19–7.06 (m, 6H), 6.94 (s, 1H), 6.06 (br, 1H), 4.97–4.88 (m, 1H), 3.64 (s, 3H), 1.09–0.81 (m, 6H); ^{13}C NMR (150 MHz, CDCl_3) 164.6, 162.1, 137.4, 134.2, 129.2, 128.3, 127.4, 124.8, 119.8, 71.0, 67.9, 52.7, 21.5 ppm; HRMS (ESI): Exact mass calcd for $\text{C}_{28}\text{H}_{28}\text{NaN}_2\text{O}_5$ $[\text{M}+\text{Na}]^+$ 495.1890, found 495.1887.



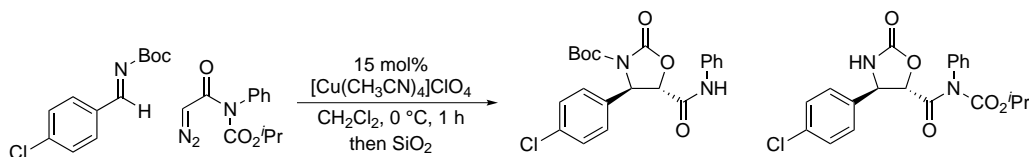
Aziridine 215. A suspension of tetrakis(acetonitrile) copper(I) perchlorate (6.5 mg, 20 μmol) and imine (61.2 mg, 200 μmol) in dichloromethane (1.0 mL) was stirred at rt for 1 h until no solid was observed. The reaction was then cooled to 0 °C, treated with diazo imide (60.0 mg, 243 μmol) in dichloromethane (1.0 mL) slowly via syringe, and stirred at 0 °C for 2 h. A solution of NH_4OH – NaCl 2:1 (2 mL) was then added, and the solution was vigorously stirred for 5 min. The layers were separated and the aqueous layer was extracted with dichloromethane. The combined organic extracts were dried, concentrated, and purified using flash chromatography (SiO_2 , 10–25 % ethyl acetate in hexanes) to afford the aziridine as a yellow oil (39.8 mg, 25 %). $R_f = 0.46$ (25 % EtOAc/hexanes); IR (film) 3063, 3028, 2982, 2924, 2852, 1737, 1597, 1591 cm^{-1} ; ^1H NMR (400 MHz, CDCl_3) δ 7.75 (d, $J = 7.4$ Hz, 2H), 7.50 (d, $J = 7.4$ Hz, 2H), 7.42 (d, $J = 8.3$ Hz, 2H), 7.36 (d, $J = 7.4$ Hz, 1H), 7.34 (d, $J = 7.7$ Hz, 1H), 7.31–7.24 (m, 8H), 7.21–7.17 (m, 1H), 6.51–6.49 (m, 2H), 4.92 (septet, $J = 6.4$ Hz, 1H), 4.13 (s, 1H), 3.68 (d, $J = 7.0$ Hz, 1H), 3.33 (d, $J = 7.0$ Hz, 1H), 1.12 (dd=, $J = 5.8$ Hz, 3H), 1.11 (dd=, $J = 5.8$ Hz, 3H); ^{13}C NMR (100 MHz, CDCl_3) 168.4, 153.2, 142.8, 142.5, 137.2, 134.3, 133.1, 128.8, 128.8, 128.4, 128.1, 127.9, 127.9, 127.4, 127.4, 127.3, 127.1, 77.2, 71.1, 52.0, 47.0, 21.46, 21.37 ppm; HRMS (ESI): Exact mass calcd for $\text{C}_{32}\text{H}_{29}\text{ClNaN}_2\text{O}_3$ $[\text{M}+\text{Na}]^+$ 547.1759, found 547.1746.



***E*-Alkene 216 and *Z*-Alkene 217.** To a suspension of tetrakis(acetonitrile) copper(I) perchlorate (6.5 mg, 20 μ mol) in dichloromethane (1.0 mL) was added a solution of diazo imide (49.5 mg, 200 μ mol) in dichloromethane (1.0 mL) via syringe over a 10 min period. The reaction was stirred at 0 °C, and once gas evolution ceased (ca. 1 h), the reaction mixture was concentrated. The resulting oil was purified using flash chromatography (SiO₂, 10–20 % ethyl acetate in hexanes) to afford the (*Z*)-olefin as a clear oil (9.2 mg, 21 %). A second chromatography (SiO₂, 25 % ethyl acetate in hexanes) afforded the (*E*)-olefin as colorless crystals (10.9 mg, 25 %).

(*Z*)-Alkene: $R_f = 0.30$ (25 % EtOAc/hexanes); IR (film) 3064, 2963, 2926, 2854, 1738, 1732, 1698, 1694, 1682, 1596 cm⁻¹; ¹H NMR (600 MHz, CDCl₃) δ 7.40–7.34 (m, 3H), 7.20–7.19 (m, 2H), 6.83 (s, 1H), 4.98 (septet, $J = 6.2$ Hz, 1H), 1.16 (d, $J = 6.2$ Hz, 6H); ¹³C NMR (150 MHz, CDCl₃) 168.0, 153.4, 137.4, 130.6, 129.0, 128.4, 128.2, 71.5, 21.5 ppm; HRMS (ESI): Exact mass calcd for C₂₄H₂₆NaN₂O₆ [M+Na]⁺ 461.1683, found 461.1673.

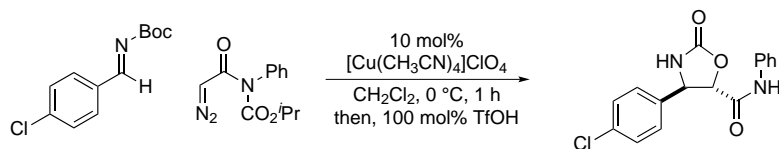
(*E*)-Alkene: Mp 211–213 °C; $R_f = 0.34$ (25 % EtOAc/hexanes); IR (film) 2983, 2920, 2850, 1732, 1685, 1492 cm⁻¹; ¹H NMR (600 MHz, CDCl₃) δ 7.68 (s, 1H), 7.42 (dd, $J = 7.8, 7.2$ Hz, 2H), 7.37 (ddd, $J = 7.7, 1.5, 1.3$ Hz, 1H), 7.14 (d, $J = 7.6$ Hz, 2H), 5.03 (septet, $J = 6.3$ Hz, 1H), 1.20 (d, $J = 6.4$ Hz, 6H); ¹³C NMR (150 MHz, CDCl₃) 166.9, 153.3, 137.6, 134.2, 129.1, 128.3, 128.1, 71.9, 21.5 ppm; HRMS (ESI): Exact mass calcd for C₂₄H₂₆NaN₂O₆ [M+Na]⁺ 461.1683, found 461.1678. Anal calcd for C₂₄H₂₆N₂O₆: C, 65.73; H, 5.98; N, 6.39. Found: C, 65.63; H, 5.93; N, 6.35.



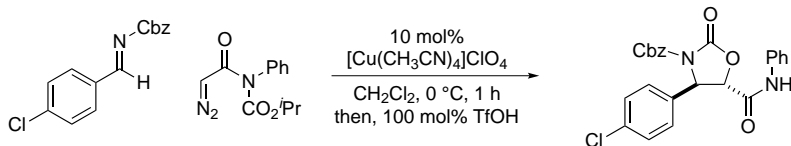
***N*-Boc oxazolidinone 218 and oxazolidinone 219.** A solution of the imine (28.0 mg, 120 μ mol) and tetrakis(acetonitrile) copper(I) perchlorate (5.0 mg, 18 μ mol) in dichloromethane (700 μ L) was stirred at rt for 10 min. The resulting yellow solution was cooled to –78 °C, a solution of α -diazo imide (37.1 mg, 150 μ mol) in dichloromethane (300 μ L) was added via cannula, and the solution was slowly warmed to –20 °C and stirred for 6 h. The reaction mixture was filtered through a pad of silica gel (5 g), eluted with ethyl acetate, and concentrated prior to flash chromatography (SiO₂, 25 % ethyl acetate in hexanes) to afford the *N*-Boc oxazolidinone **419** as a white solid (25.0 mg, 50 %). A second chromatography (SiO₂, 25–50 % ethyl acetate in hexanes) afforded *N*-H oxazolidinone as a white solid, (11.0 mg, 23 %).

***N*-Boc oxazolidinone 218:** Mp 166–168 °C; $R_f = 0.35$ (25 % EtOAc/hexanes); IR (film) 3328, 2981, 2933, 1822, 1749, 1691, 1600, 1543, 1493 cm⁻¹; ¹H NMR (400 MHz, CDCl₃) δ 8.45 (s, 1H), 7.64 (dd, $J = 1.9, 1.0$ Hz, 1H), 7.61 (dd, $J = 2.1, 1.1$ Hz, 1H), 7.42–7.30 (m, 6H), 7.18 (ddd, $J = 7.4, 7.4, 1.1, 1.0$ Hz, 1H), 5.50 (d, $J = 4.4$ Hz, 1H), 4.67 (d, $J = 4.4$ Hz, 1H), 1.30 (s, 9H); ¹³C NMR (100 MHz, CDCl₃) 165.4, 150.6, 147.8, 129.4, 129.1, 127.1, 125.5, 120.3, 85.0, 77.4, 61.3,

27.6 ppm; HRMS (ESI): Exact mass calcd for $C_{21}H_{21}ClNaN_2O_5$ $[M+Na]^+$ 439.1037, found 0.0000. **N-H oxazolidinone 219**: Mp 183–184 °C; $R_f = 0.05$ (25 % EtOAc/hexanes); IR (film) 3312, 2984, 2934, 1769, 1736, 1596, 1493 cm^{-1} ; 1H NMR (600 MHz, $CDCl_3$) δ 7.44–7.37 (m, 7H), 7.13–7.11 (m, 2H), 5.89 (br, 1H), 5.76 (d, $J = 4.0$ Hz, 1H), 5.14 (dd, $J = 4.0, 0.9$ Hz, 1H), 4.95 (sept, $J = 6.3$ Hz, 1H), 1.14 (d, $J = 6.0$ Hz, 3H), 1.13 (d, $J = 6.0$ Hz, 3H); ^{13}C NMR (150 MHz, $CDCl_3$) 170.1, 157.9, 153.1, 137.7, 136.8, 134.8, 129.2, 128.6, 128.0, 127.9, 81.6, 72.5, 58.3, 21.5, 21.3 ppm; HRMS (ESI): Exact mass calcd for $C_{20}H_{19}ClNaN_2O_5$ $[M+Na]^+$ 425.0880, found 425.0880.

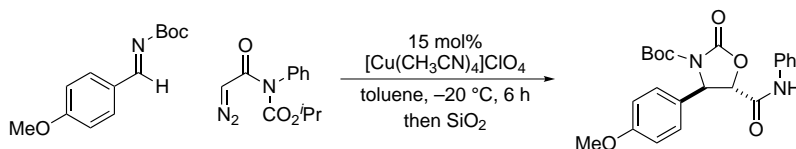


Oxazolidinone 223. A solution of $[Cu(CH_3CN)_4]ClO_4$ (6.5 mg, 20 μ mol) and the imine (48.0 mg, 200 μ mol) in dichloromethane (1.5 mL) was stirred at rt for 1 h. The resulting yellow solution was cooled to 0 °C, a solution of α -diazo imide (62.0 mg, 250 μ mol) in dichloromethane (500 μ L) was added via cannula, and the solution was slowly warmed to 0 °C and stirred for 1 h. This mixture was treated with triflic acid (18 μ L, 200 μ mol) via syringe in one portion, and the reaction was warmed to rt and stirred for 1 h prior to quenching with NH_4OH -brine (2:1). The aqueous layer was extracted with dichloromethane and the combined organic extracts were dried, concentrated, and purified using flash chromatography (SiO_2 , 10–30 % ethyl acetate in hexanes) to afford the product as a white solid (33.2 mg, 52 %). Mp 224–225 °C; $R_f = 0.10$ (25 % EtOAc/hexanes); IR (film) 3319, 1770, 1682, 1600, 1543, 1492 cm^{-1} ; 1H NMR (400 MHz, $DMSO-d_6$) δ 10.3 (br, 1H), 8.56 (br, 1H), 7.60 (d, $J = 8.0$ Hz, 2H), 7.48 (d, $J = 8.3$ Hz, 2H), 7.40 (d, $J = 8.5$ Hz, 2H), 7.34 (d, $J = 7.7$ Hz, 1H), 7.32 (d, $J = 7.8$ Hz, 1H), 7.11 (dd, $J = 7.1, 5.0$ Hz, 1H), 4.98 (d, $J = 5.0$ Hz, 1H), 4.80 (d, $J = 5.3$ Hz, 1H); ^{13}C NMR (100 MHz, $CDCl_3$) 168.1, 159.1, 140.7, 139.4, 134.7, 130.5, 130.5, 130.0, 126.2, 121.9, 82.1, 59.6 ppm; HRMS (ESI): Exact mass calcd for $C_{15}H_{13}ClNaN_2O$ $[M+Na]^+$ 339.0512, found 339.0493.

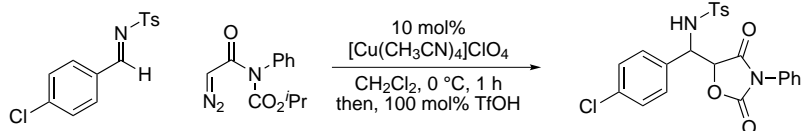


Oxazolidinone 236. A solution of tetrakis(acetonitrile) copper(I) perchlorate and the imine (54.7 mg, 200 μ mol) in CH_2Cl_2 (1.5 mL) was stirred at rt for 1 h. The resulting yellow solution was cooled to 0 °C, a solution of α -diazo imide (62.0 mg, 250 μ mol) in dichloromethane (500 μ L) was

added via cannula, and the solution was slowly warmed to 0 °C and stirred for 1 h. This mixture was treated with triflic acid (18.0 μL, 200 μmol) via syringe in one portion, and the reaction was warmed to rt and stirred for 1 h prior to quenching with NH₄OH–brine (2:1). The aqueous layer was extracted with dichloromethane and the combined organic extracts were dried, concentrated, and purified using flash chromatography (SiO₂, 10–30 % ethyl acetate in hexanes) to afford the product as a colorless solid (43.9 mg, 49 %). Mp 224–225 °C; R_f = 0.11 (25 % EtOAc/hexanes); IR (film) 3329, 3063, 1825, 1748, 1690, 1600, 1543, 1494 cm⁻¹; ¹H NMR (400 MHz, DMSO-*d*₆) δ 8.23 (s, 1H), 7.58 (d, *J* = 7.6 Hz, 2H), 7.42–7.24 (m, 9H), 7.19 (dd, *J* = 7.6, 7.5 Hz, 1H), 7.09 (dd, *J* = 7.6, 1.5 Hz, 2H), 5.58 (d, *J* = 4.2 Hz, 1H), 5.21 (d, *J* = 12.1 Hz, 1H), 5.06 (d, *J* = 12.0 Hz, 1H), 4.71 (d, *J* = 4.0 Hz, 1H); ¹³C NMR (100 MHz, CDCl₃) 165.0, 150.1, 149.4, 136.9, 136.1, 135.0, 133.9, 129.6, 129.4, 129.3, 129.2, 128.7, 128.6, 128.5, 128.3, 127.2, 125.6, 125.5, 120.3, 77.7, 69.2, 61.0 ppm; HRMS (ESI): Exact mass calcd for C₂₃H₁₉ClNaN₂O₃ [M+Na]⁺ 473.0880, found 473.0883.



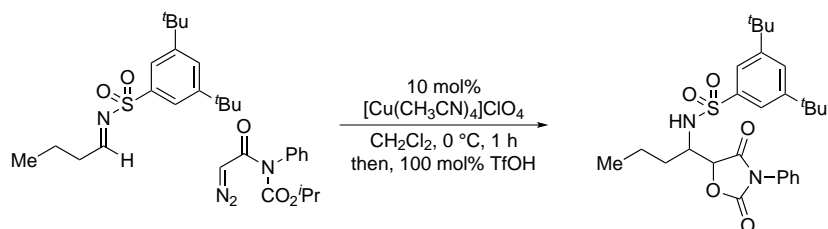
Oxazolidinone 420. A solution of [Cu(CH₃CN)₄]ClO₄ (4.8 mg, 15 μmol) and the imine (24.7 mg, 100 μmol) in toluene (0.7 mL) was stirred at rt for 10 min. The resulting yellow solution was cooled to –78 °C, a solution of α-diazo imide (30.9 mg, 125 μmol) in toluene 300 μL was added via cannula, and the solution was slowly warmed to –20 °C and stirred for 6 h. The reaction mixture was filtered through a pad of silica gel (5 g), eluted with ethyl acetate, and concentrated prior to flash chromatography (SiO₂, 25 % ethyl acetate in hexanes) to afford the amide as a white solid (17.0 mg, 41 %). Mp 164–166 °C; R_f = 0.15 (25 % EtOAc/hexanes); IR (film) 3322, 2980, 2935, 1821, 1731, 1689, 1602, 1546, 1515, 1500, 1494 cm⁻¹; ¹H NMR (600 MHz, CDCl₃) δ 8.58 (s, 1H), 7.67 (d, *J* = 7.7 Hz, 2H), 7.37 (d, *J* = 7.7 Hz, 1H), 7.35 (d, *J* = 8.0 Hz, 1H), 7.31 (dd, *J* = 3.0, 2.1 Hz, 1H), 7.29 (dd, *J* = 2.7, 2.1 Hz, 1H), 7.18 (dd, *J* = 7.5, 7.4 Hz, 1H), 6.95 (dd, *J* = 2.8, 2.3 Hz, 1H), 6.93 (dd, *J* = 2.7, 2.2 Hz, 1H), 5.47 (d, *J* = 4.4 Hz, 1H), 4.72 (d, *J* = 4.4 Hz, 1H), 3.83 (s, 3H), 1.30 (s, 9H); ¹³C NMR (100 MHz, CDCl₃) 165.7, 159.8, 151.0, 148.0, 136.5, 131.1, 128.9, 127.0, 125.2, 120.4, 114.4, 84.4, 77.9, 61.6, 55.3, 27.5 ppm; HRMS (ESI): Exact mass calcd for C₂₂H₂₈N₃O₆ [M+Na]⁺ 430.1978, found 430.1985. Anal calcd for C₂₂H₂₄N₂O₆: C, 64.05; H, 5.87; N, 6.79. Found: C, 63.77; H, 5.79; N, 6.77.



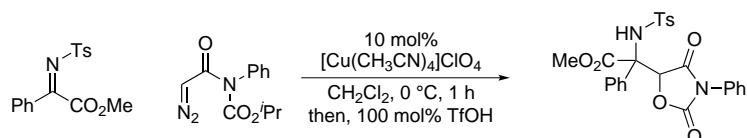
Oxazolidinone dione 230. A solution of the imine (59 mg, 200 μmol) and tetrakis(acetonitrile) copper(I) perchlorate (6.5 mg, 20 μmol) in CH_2Cl_2 (1.5 mL) was stirred at rt for 1 h. The resulting yellow solution was cooled to 0 $^\circ\text{C}$, a solution of α -diazo imide (60.0 mg, 240 μmol) in dichloromethane (500 μL) was added via automated syringe pump over 1 h, and the resulting yellow solution was treated with triflic acid (18.0 μL , 200 μmol) via syringe in one portion, and the reaction was warmed to rt and stirred for 1 h prior to quenching with NH_4OH -brine (2:1). prior to quenching with NH_4OH -brine (2:1). The aqueous layer was extracted with dichloromethane and the combined organic extracts were dried, concentrated, and purified using flash chromatography (SiO_2 , 25 % ethyl acetate in hexanes) to afford the sulfonamide as a yellow solid (78.2 mg, 83 %, 1:1 dr by ^1H NMR). The analytical samples for both diastereomers were obtained by flash chromatography (SiO_2 , 10–25 % ethyl acetate in hexanes).

Diastereomer 1: Yellow solid; Mp 195–200 $^\circ\text{C}$; $R_f = 0.22$ (25 % EtOAc/hexanes); IR (film) 3271, 3068, 2963, 1819, 1748, 1598, 1504, 1494 cm^{-1} ; ^1H NMR (600 MHz, CDCl_3) δ 7.55 (d, $J = 8.3$ Hz, 2H), 7.41–7.39 (m, 3H), 7.15 (dd, $J = 8.5, 1.6$ Hz, 2H), 7.12 (d, $J = 3.4$ Hz, 1H), 7.11 (d, $J = 2.3$ Hz, 1H), 7.09 (m, 1H), 7.08 (m, 2H), 7.06 (s, 1H), 6.03 (br, 1H), 5.11 (d, $J = 2.8$ Hz, 1H), 5.06 (d, $J = 2.8$ Hz, 1H), 2.33 (s, 3H); ^{13}C NMR (150 MHz, CDCl_3) 169.4, 153.5, 143.9, 136.8, 134.9, 133.1, 130.1, 129.5, 129.3, 129.2, 129.0, 128.5, 127.0, 125.6, 80.3, 56.3, 21.4 ppm; HRMS (ESI): Exact mass calcd for $\text{C}_{23}\text{H}_{20}\text{ClN}_2\text{O}_5\text{S}$ $[\text{M}+\text{H}]^+$ 471.0776, found 471.0774.

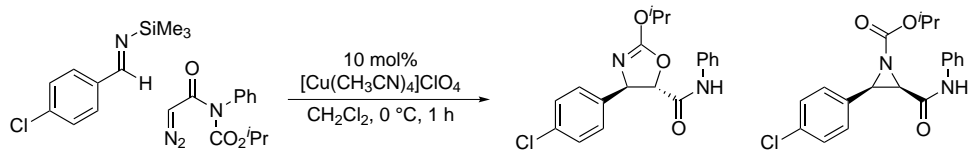
Diastereomer 2: Yellow solid; Mp 177–178 $^\circ\text{C}$; $R_f = 0.17$ (25 % EtOAc/hexanes); IR (film) 3271, 3068, 2963, 1819, 1748, 1598, 1504, 1494 cm^{-1} ; ^1H NMR (600 MHz, CDCl_3) δ 7.58 (d, $J = 8.3$ Hz, 2H), 7.36–7.34 (m, 3H), 7.18–7.17 (m, 1H), 7.16 (dd, $J = 2.3, 2.0$ Hz, 1H), 7.14 (d, $J = 8.0$ Hz, 2H), 7.06 (dd, $J = 2.5, 1.7$ Hz, 1H), 7.05 (dd, $J = 2.5, 1.7$ Hz, 1H), 6.79–6.78 (m, 2H), 5.82 (br, 1H), 5.36 (d, $J = 2.9$ Hz, 1H), 5.04 (d, $J = 2.7$ Hz, 1H), 2.36 (s, 3H); ^{13}C NMR (150 MHz, CDCl_3) 168.2, 153.1, 144.1, 136.6, 135.4, 130.6, 129.8, 129.7, 129.4, 129.4, 129.3, 129.1, 129.0, 127.0, 125.4, 81.3, 57.4, 21.4 ppm; HRMS (ESI): Exact mass calcd for $\text{C}_{23}\text{H}_{20}\text{ClN}_2\text{O}_5\text{S}$ $[\text{M}+\text{H}]^+$ 471.0776, found 471.0774.



Oxazolidine dione 232. A suspension of the imine (64.7 mg, 200 μmol) and tetrakis(acetonitrile) copper(I) perchlorate (6.5 mg, 20 μmol) in CH_2Cl_2 (1.5 mL) was stirred at rt for 1 h. The resulting yellow solution was cooled to 0 $^\circ\text{C}$, a solution of α -diazo imide (61.8 mg, 250 μmol) in dichloromethane (500 μL) was added via automated syringe pump over 1 h, and the resulting yellow solution was treated with triflic acid (18 μL , 200 μmol) via syringe in one portion, and the reaction was warmed to rt and stirred for 30 min prior to quenching with NH_4OH -brine (2:1). The aqueous layer was extracted with dichloromethane and the combined organic extracts were dried, concentrated, and purified using flash chromatography (SiO_2 , 25 % ethyl acetate in chloroform) to afford the sulfonamide as a yellow solid (42.0 mg, 42 %, 1.0:0.8 dr by ^1H NMR). *Data for both diastereomers:* Mp 182–188 $^\circ\text{C}$; R_f = 0.38 (25 % EtOAc/hexanes); IR (film) 3429, 2963, 2872, 1818, 1749, 1599, 1503, 1458 cm^{-1} ; ^1H NMR (600 MHz, CDCl_3) δ 7.74 (d, J = 1.8 Hz, 2H), 7.70 (d, J = 1.8 Hz, 2H), 7.64 (dd, J = 1.7, 1.7 Hz, 1H), 7.63 (dd, J = 1.7, 1.7 Hz, 1H), 7.48–7.39 (m, 6H), 7.35–7.33 (m, 2H), 7.22–7.21 (m, 2H), 5.03 (d, J = 2.4 Hz, 1H), 4.94 (d, J = 9.8 Hz, 1H), 4.84 (d, J = 2.0 Hz, 1H), 4.84 (d, J = 8.3 Hz, 1H), 4.04–3.99 (m, 1H), 3.87–3.83 (m, 1H), 1.61–1.53 (m, 2H), 1.46–1.40 (m, 2H), 1.40–1.22 (m, 38H) 1.20–1.13 (m, 1H), 1.09–1.00 (m, 1H), 0.75 (dd, J = 7.3, 7.3 Hz, 3H), 0.68 (dd, J = 7.3, 7.3 Hz, 3H); ^{13}C NMR (150 MHz, CDCl_3) 169.7, 169.3, 154.1, 153.5, 152.5, 152.4, 139.6, 139.0, 130.4, 129.4, 129.3, 129.1, 129.0, 127.3, 127.1, 125.8, 125.5, 121.3, 121.2, 81.3, 79.7, 54.0, 53.5, 35.2, 35.2, 31.2, 18.7, 18.5, 13.3, 13.1 ppm; HRMS (ESI): Exact mass calcd for $\text{C}_{27}\text{H}_{40}\text{N}_3\text{O}_5\text{S}$ $[\text{M}+\text{NH}_4]^+$ 518.2689, found 518.2535.



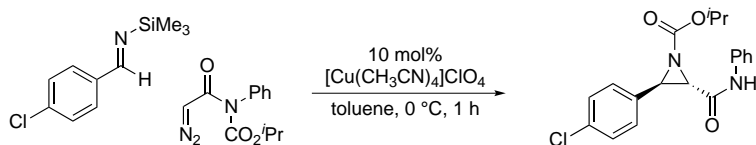
Oxazolidine dione 421. A suspension of the imine (45.5 mg, 143 μmol) and tetrakis(acetonitrile) copper(I) perchlorate (7.4 mg, 22 μmol) in CH_2Cl_2 (0.7 mL) was stirred at rt for 1 h. The resulting yellow solution was cooled to 0 $^\circ\text{C}$ and a solution of α -diazo imide (44.5 mg, 180 μmol) in dichloromethane (300 μL) was added via automated syringe pump over 15 min. The resulting yellow solution was treated with triflic acid (13.0 μL , 150 μmol) via syringe in one portion and the reaction was warmed to rt, stirred for 30 min, and concentrated. The resulting oil was purified using flash chromatography (SiO_2 , 5–10 % ethyl acetate in chloroform) to afford the sulfonamide as a clear oil (52.5 mg, 75 %, 2.3:1 dr by ^1H NMR). *Major diastereomer:* R_f = 0.09 (25 % EtOAc/hexanes); IR (film) 3282, 3066, 2955, 1821, 1754, 1598 cm^{-1} ; ^1H NMR (400 MHz, CDCl_3) δ 7.47–7.36 (m, 5H), 7.30–7.20 (m, 5H), 7.18–7.13 (m, 2H), 7.10–7.06 (m, 2H), 6.23 (s, 1H), 6.15 (s, 1H), 3.66 (s, 3H), 2.36 (s, 3H); ^{13}C NMR (100 MHz, CDCl_3) 168.6, 168.4, 152.9, 143.3, 137.8, 131.2, 130.4, 129.3, 129.3, 129.3, 129.16, 129.19, 129.1, 128.3, 128.1, 127.0, 125.6, 78.7, 68.5, 53.9, 21.4 ppm; HRMS (ESI): Exact mass calcd for $\text{C}_{25}\text{H}_{22}\text{NaN}_2\text{O}_7\text{S}$ $[\text{M}+\text{Na}]^+$ 517.1045, found 517.1046.



Oxazoline 236 and aziridine 237. A suspension of the tetrakis(acetonitrile) copper(I) perchlorate (7.4 mg, 22 μmol) in dichloromethane (2.0 mL) was cooled to 0 °C and the imine (53 μL , 250 μmol) was added via syringe. The solution was stirred for 15 min at 0 °C and a solution of α -diazo imide (74.2 mg, 300 μmol) in dichloromethane (500 μL) was added via syringe and the reaction was stirred at 0 °C for 1 h. The reaction mixture was filtered through a pad of silica gel (10 mL), eluted with ethyl acetate, and concentrated prior to flash chromatography (SiO_2 , 10 % ethyl acetate in hexanes) to afford oxazoline as a clear oil that solidified on standing (39.0 mg, 44 %). A second flash chromatography (SiO_2 , 25 % ethyl acetate in hexanes) afforded *cis*-aziridine as a yellow solid (37.0 mg, 39 %).

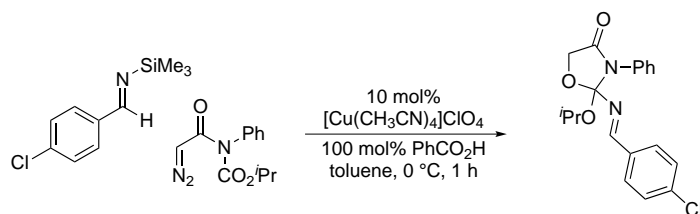
Oxazoline 236: Mp 108–109 °C; R_f = 0.55 (25 % EtOAc/hexanes); IR (film) 3396, 3315, 3061, 2983, 1673, 1601, 1537, 1492 cm^{-1} ; ^1H NMR (600 MHz, CDCl_3) δ 8.08 (s, 1H), 7.60 (d, J = 7.5 Hz, 2H), 7.42 (d, J = 8.5 Hz, 2H), 7.38–7.34 (m, 4H), 7.18 (dd, J = 7.6, 7.5 Hz, 1H), 5.34 (d, J = 6.4 Hz, 1H), 5.09 (sept, J = 6.3 Hz, 1H), 4.74 (d, J = 6.4 Hz, 1H), 1.49 (d, J = 6.2 Hz, 3H), 1.45 (d, J = 6.3 Hz, 3H); ^{13}C NMR (150 MHz, CDCl_3) 167.6, 160.2, 140.7, 136.5, 133.6, 129.2, 128.8, 127.7, 125.2, 120.1, 84.0, 76.4, 70.6, 21.8, 21.7 ppm; HRMS (ESI): Exact mass calcd for $\text{C}_{19}\text{H}_{19}\text{ClNaN}_2\text{O}_3$ $[\text{M}+\text{Na}]^+$ 381.0976, found 381.0980.

Aziridine 237: Mp 144–145 °C; R_f = 0.55 (25 % EtOAc/hexanes); IR (film) 3316, 3061, 2983, 2937, 1728, 1686, 1599, 1532, 1496 cm^{-1} ; ^1H NMR (400 MHz, CDCl_3) δ 7.71 (s, 1H), 7.36 (d, J = 8.8 Hz, 2H), 7.28 (dd, J = 2.3, 2.0 Hz, 1H), 7.26 (dd, J = 2.5, 1.9 Hz, 1H), 7.23 (m, 1H), 7.23–7.19 (m, 3H), 7.07 (ddd, J = 7.0, 1.6, 1.6 Hz, 1H), 5.03 (sept, J = 6.2 Hz, 1H), 3.94 (d, J = 7.0 Hz, 1H), 3.54 (d, J = 7.1 Hz, 1H), 1.34 (d, J = 6.3 Hz, 3H), 1.34 (d, J = 6.2 Hz, 3H); ^{13}C NMR (100 MHz, CDCl_3) 163.3, 160.8, 136.0, 134.4, 131.3, 129.0, 128.9, 128.8, 128.7, 124.9, 120.2, 77.2, 71.8, 44.4, 44.3, 21.7 ppm; HRMS (ESI): Exact mass calcd for $\text{C}_{19}\text{H}_{19}\text{ClNaN}_2\text{O}_3$ $[\text{M}+\text{Na}]^+$ 381.0976, found 381.0968.

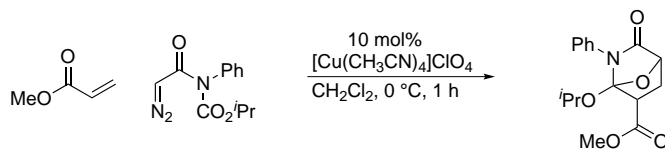


***trans*-Aziridine 238.** A suspension of the tetrakis(acetonitrile) copper(I) perchlorate (24.5 mg, 75.0 μmol) in toluene (2.0 mL) was cooled to 0 °C and the imine (160 μL , 750 μmol) was added via syringe. The solution was stirred for 15 min at 0 °C and the α -diazo imide (123.6 mg, 500.0 μmol) was added in one portion, and stirring was continued for 1 h. The reaction mixture was filtered through a pad of neutral alumina (10 mL), eluted with ethyl acetate, and concentrated prior to flash

chromatography (SiO₂, 10 % ethyl acetate in hexanes) to afford oxazoline as a clear oil (6.9 mg, 4 %). *R_f* = 0.07 (10 % EtOAc/hexanes); IR (film) 3145, 3060, 2982, 2933, 1697, 1602, 1552, 1495 cm⁻¹; ¹H NMR (600 MHz, CDCl₃) δ 7.97 (s, 1H), 7.53 (d, *J* = 7.9 Hz, 2H), 7.34–7.30 (m, 4H), 7.24–7.26 (m, 2H), 7.13 (dd, *J* = 7.4, 7.4 Hz, 1H), 4.92 (sept, *J* = 6.2 Hz, 1H), 3.86 (d, *J* = 2.5 Hz, 1H), 3.30 (d, *J* = 2.6 Hz, 1H), 1.27 (d, *J* = 6.2 Hz, 3H), 1.05 (d, *J* = 6.3 Hz, 3H); ¹³C NMR (150 MHz, CDCl₃) 163.7, 159.2, 137.0, 134.6, 132.7, 129.1, 128.9, 128.2, 124.9, 119.8 ppm; HRMS (ESI): Exact mass calcd for C₁₉H₁₉ClNaN₂O₃ [M+Na]⁺ 381.0976, found 381.0984.



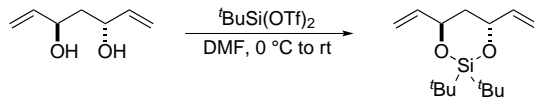
Orthoamide 240. A suspension of the CuClO₄ · 4 MeCN (9.6 mg, 30 μmol) in toluene (1.0 mL) was cooled to 0 °C and the imine (64 μL, 300 μmol) was added via syringe followed by benzoic acid (24.4 mg, 300 μmol). The yellow solution was stirred for 15 min at 0 °C and the α-diazo imide (49.4 mg, 300 μmol) was added in one portion, and stirring was continued for 1 h. The reaction mixture was concentrated prior to flash chromatography (SiO₂, 10 % ethyl acetate in hexanes with 2 % Et₃N) to afford the title compound as a clear oil (37.7 mg, 21 %). *R_f* = 0.20 (25 % EtOAc/hexanes); IR (film) 3066, 2976, 2871, 1731, 1645, 1595, 1572, 1498 cm⁻¹; ¹H NMR (600 MHz, CDCl₃) δ 8.60 (s, 1H), 7.76 (d, *J* = 8.5 Hz, 2H), 7.63 (d, *J* = 7.7 Hz, 2H), 7.41 (d, *J* = 8.4 Hz, 2H), 7.39 (d, *J* = 8.0 Hz, 2H), 7.28 (t, *J* = 7.4 Hz, 1H), 4.65 (d, *J* = 14.3 Hz, 1H), 4.43 (d, *J* = 14.2 Hz, 1H), 4.14 (sept, *J* = 6.2 Hz, 1H), 1.30 (d, *J* = 6.1 Hz, 3H), 1.03 (d, *J* = 6.2 Hz, 3H); ¹³C NMR (150 MHz, CDCl₃) 168.7, 160.7, 138.4, 134.3, 133.1, 130.6, 129.1, 128.8, 127.1, 125.4, 118.8, 67.8, 67.3, 24.0, 23.1 ppm;



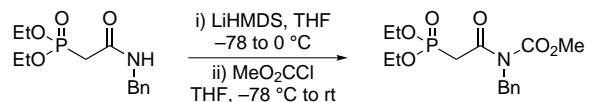
Orthoamide 242. A suspension of the CuClO₄ · 4 MeCN (6.5 mg, 20 μmol) in CH₂Cl₂ (2.0 mL) was cooled to 0 °C and the methyl acrylate (360 μL, 4.0 mmol) was added via syringe. The solution was stirred for 5 min at 0 °C and a solution of the α-diazo imide (74.2 mg, 300 μmol) in dichloromethane (500 μL) was added via automated syringe pump over 1 h. The resulting solution was concentrated and purified using flash chromatography (SiO₂, 10–25 % ethyl acetate in hexanes) to afford the

adduct as a white solid (51 mg, 41 %). Mp 133–135 °C; $R_f = 0.30$ (25 % EtOAc/hexanes); IR (film) 2979, 2950, 1744, 1698, 1599, 1496 cm^{-1} ; ^1H NMR (600 MHz, CDCl_3) δ 7.49–7.47 (m, 2H), 7.42–7.39 (m, 2H), 7.19 (dddd, $J = 7.4, 7.3, 1.0, 1.0$ Hz, 1H), 4.83 (d, $J = 5.8$ Hz, 1H), 4.26 (sept, $J = 6.2$ Hz, 1H), 3.81 (s, 3H), 3.42 (dd, $J = 8.4, 4.7$ Hz, 1H), 2.68 (ddd, $J = 12.7, 5.7, 4.7$ Hz, 1H), 2.08 (dd, $J = 12.7, 8.4$ Hz, 1H), 1.23 (d, $J = 6.1$ Hz, 3H), 0.84 (d, $J = 6.3$ Hz, 3H); ^{13}C NMR (150 MHz, CDCl_3) ppm 171.0, 170.3, 134.9, 128.9, 125.2, 120.6, 115.7, 75.3, 71.6, 52.4, 49.0, 31.3, 23.5, 22.4; HRMS (ESI): Exact mass calcd for $\text{C}_{16}\text{H}_{19}\text{NaNO}_5$ $[\text{M}+\text{Na}]^+$ 328.1161, found 328.1169.

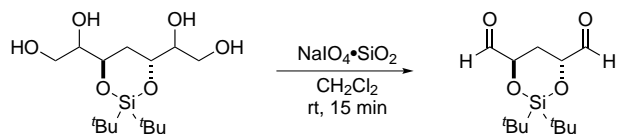
Compounds relevant to Chapter 3



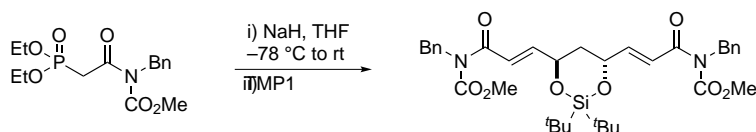
(4*R*,6*R*)-2,2-Di-*tert*-butyl-4,6-divinyl-1,3,2-dioxasilinane (310). To a solution of the diol (2.75 g, 21.5 mmol) in DMF (12 mL) at 0 °C was added *t*BuSi(OTf)₂ (7.0 mL, 22 mmol). The mixture was warmed to rt, stirred for 18 h and then poured onto a silica gel column and eluted with 5 % ethyl acetate in hexanes (ca. 500 mL) to give the desired product as a clear oil (5.25 g, 91 %). $[\alpha]_{\text{D}}^{20} +11.4$ (*c* 3.50, CHCl₃); $R_f = 0.70$ (30 % EtOAc/hexanes); IR (film) 3014, 2963, 2859, 1645, 1474 cm⁻¹; ¹H NMR (400 MHz, CDCl₃) δ 5.91 (ddd, *J* = 17.2, 10.8, 5.2 Hz, 1H), 5.29 (ddd, *J* = 17.2, 1.6, 1.6 Hz, 1H), 5.10 (ddd, *J* = 10.8, 1.6, 1.6 Hz, 1H), 4.64–4.59 (m, 1H) 1.88 (t, *J* = 3.2 Hz, 1H), 1.00 (s, 9H); ¹³C NMR (100 MHz, CDCl₃) ppm 140.5, 114.0, 70.7, 39.8, 27.2, 21.1; HRMS (ESI): Exact mass calcd for C₁₅H₂₇O₂Si [M-H]⁺ 267.1775, found 267.1775.



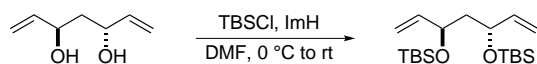
Methyl benzyl(2-(diethoxyphosphoryl)acetyl)carbamate (319). To a solution of HMDS (23.0 mL, 110 mmol) in THF (130 mL) at -78 °C was added *n*-butyllithium (2.5 M in hexanes, 44 mL, 110 mmol) via syringe. The solution was warmed to 0 °C, stirred for 15 min, and then cooled to -78 °C. A solution of the amidophosphonate (14.3 g, 50.0 mmol) was added in one portion. The solution was warmed to 0 °C, (15 min), cooled to -78 °C and then methyl chloroformate (4.7 mL, 60 mmol) was added via syringe and the solution was slowly warmed to rt. The reaction was quenched with satd aq ammonium chloride and extracted with diethyl ether. The combined organic layers were dried and concentrated to give the imidophosphonate as a yellow oil (17.2 g, 99 %) and was used without further purification. $R_f = 0.45$ (50 % EtOAc/hexanes); IR (film) 3482, 2984, 1740, 1695 cm⁻¹; ¹H NMR (600 MHz, CDCl₃) δ 7.32–7.22 (m, 5H), 4.95 (s, 2H), 4.12 (dq, *J* = 15.0, 7.0 Hz, 4H), 3.83 (d, *J* = 22.3 Hz, 2H), 3.81 (s, 3H), 1.28 (t, *J* = 7.0 Hz, 6H); ¹³C NMR (100 MHz, CDCl₃) ppm 167.4 (d, *J* = 6.8 Hz, 155.0, 137.1, 128.3, 127.7, 127.3, 62.5 (d, *J* = 6.8 Hz), 54.0, 47.6, 37.2 (d, *J* = 132 Hz), 16.2 (d, *J* = 6.4 Hz); ³¹P NMR (162 MHz, CDCl₃, δ): 22.5; HRMS (ESI): Exact mass calcd for C₁₅H₂₂NNaO₆P [M+Na]⁺ 366.1082, found 366.1099.



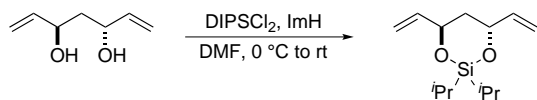
(4*R*,6*R*)-2,2-Di-*tert*-butyl-1,3,2-dioxasilinane-4,6-dicarbaldehyde (322). To a suspension of the silica gel-supported NaIO₄ (1.00 g) in CH₂Cl₂ (5 mL) at rt was added crude polyol (90 mg, 270 μmol) in one portion. The slurry was stirred for 15 min, filtered through Celite, washed with chloroform and concentrated to give the aldehyde as clear oil (72 g, 99%) which was used without further purification. $R_f = 0.35$ (5% MeOH/CHCl₃); IR (film) 2962, 2935, 2894, 2860, 2810, 1742 cm⁻¹; ¹H NMR (600 MHz, CDCl₃) δ 9.75 (s, 1H), 4.38 (t, $J = 5.7$ Hz, 1H), 2.25 (t, $J = 5.7$ Hz, 1H), 1.06 (s, 9H); ¹³C NMR (150 MHz, CDCl₃) ppm 201.9, 75.2, 29.1, 26.9, 21.2; HRMS (ESI): Exact mass calcd for C₁₃H₂₅O₄Si [M+H]⁺ 273.1517, found 273.1519.



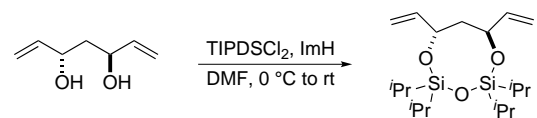
Bisimide 312. To a solution of the KHMDS (0.5 M in toluene, 2.3 mL, 890 μmol) and 18-crown-6 (235 mg, 890 μmol) in THF (2 mL) at 0 °C was added imidophosphonate (306 mg, 1.15 mmol) and the solution was stirred at 0 °C for 1 h. The solution was cooled to -78 °C and the solution of the aldehyde (40 mg, 150 μmol) in tetrahydrofuran (0.5 mL) was added via cannula. The resulting yellow solution was stirred for 3 h at -78 °C and quenched with satd aq NH₄Cl warmed to rt and concentrated. The reaction mixture was diluted with ethyl acetate, the layers were separated and the aqueous layer was extracted with ethyl acetate. The combined organic layers were washed with brine, dried and concentrated and the resulting yellow oil was purified using flash chromatography (SiO₂, 10–20% ethyl acetate in hexanes) to afford the bis-imide as clear oil (75.4 mg, 78%). $[\alpha]_D^{20} -32.4$ (c 0.73, CHCl₃); $R_f = 0.35$ (20% EtOAc/hexanes); IR (film) 3032, 2934, 3859, 1730, 1683, 1634, 1561 cm⁻¹; ¹H NMR (400 MHz, CDCl₃) δ 7.31–7.23 (m, 5H), 7.17 (dd, $J = 14.9, 1.6$ Hz, 1H), 6.98 (dd, $J = 15.0, 4.1$ Hz, 1H), 4.97 (s, 2H), 4.87–4.83 (m, 1H), 3.80 (s, 3H), 2.04 (dd, $J = 5.4, 4.1$ Hz, 1H), 1.06 (s, 9H); ¹³C NMR (100 MHz, CDCl₃) ppm 168.0, 154.9, 148.6, 137.5, 128.4, 127.7, 127.3, 123.1, 69.5, 53.8, 47.7, 38.6, 27.1, 21.2; HRMS (ESI): Exact mass calcd for C₃₅H₄₆N₂NaO₈Si [M+Na]⁺ 673.2921, found 673.2923.



Bis(silyl ether) 422. To a solution of the diol (2.50 g, 19.5 mmol) and imidazole (4.0 g, 60 mmol) in DMF (20 mL) at 0 °C was added TBSCl (9.0 g, 60 mmol). The mixture was warmed to rt, stirred for 4 h and then poured onto a silica gel column and eluted with 5 % ethyl acetate in hexanes (ca. 500 mL) to give the desired product as a clear oil (6.75 g, 97 %). $[\alpha]_D^{20} -7.3$ (*c* 2.40, CHCl₃); $R_f = 0.40$ (10 % EtOAc/hexanes); IR (film) 2956, 2929, 2887, 2857 cm⁻¹; ¹H NMR (400 MHz, CDCl₃) δ 5.81 (ddd, *J* = 17.0, 10.5, 7.4 Hz, 1H), 5.12 (br d, *J* = 17.0 Hz, 1H), 5.03 (d, *J* = 10.5 Hz, 1H), 4.18 (dt, *J* = 6.8, 6.6 Hz, 1H), 1.69 (dd, *J* = 6.5, 6.4 Hz, 1H), 0.89 (s, 9H), 0.06 (s, 3H), 0.03 (s, 3H); ¹³C NMR (100 MHz, CDCl₃) ppm 141.9, 114.1, 71.3, 47.3, 25.9, 18.2, -3.9, -4.7; HRMS (ESI): Exact mass calcd for C₁₉H₄₁O₂Si₂ [M+H]⁺ 357.2640, found 357.2650.

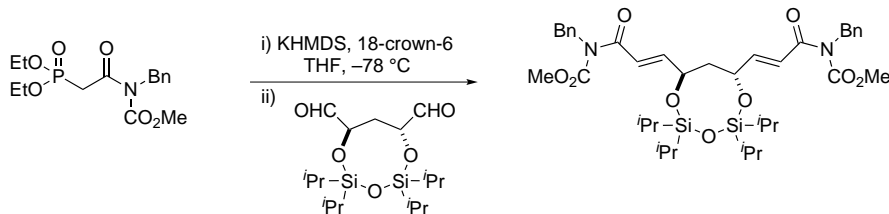


(4*R*,6*R*)-2,2-Diisopropyl-4,6-divinyl-1,3,2-dioxasilinane (423). To a solution of the diol (256 mg, 2.00 mmol) and imidazole (410 mg, 6.00 mmol) in DMF (1 mL) at 0 °C was added DIPSCl₂ (556 mg, 3.00 mmol). The mixture was warmed to rt and stirred for 6 h and then poured onto a silica gel column and eluted with 2 % ethyl acetate in hexanes (ca. 200 mL) to give the desired product as a clear oil (303 mg, 63 %). $[\alpha]_D^{20} -14.0$ (*c* 0.15, CHCl₃); $R_f = 0.28$ (hexanes); IR (film) 3080, 3013, 2945, 2895, 2868 cm⁻¹; ¹H NMR (400 MHz, CDCl₃) δ 5.92 (ddd, *J* = 16.8, 10.6, 5.1 Hz, 1H), 5.32 (ddd, *J* = 17.0, 1.5, 1.5 Hz, 1H), 5.14 (ddd, *J* = 10.4, 1.4, 1.4 Hz, 1H), 4.64 (m, 1H), 1.89 (t, *J* = 5.2 Hz, 1H), 1.07–1.02 (m, 7H); ¹³C NMR (100 MHz, CDCl₃) ppm 140.2, 114.3, 70.6, 40.6, 16.9, 16.8, 13.5; HRMS (ESI): Exact mass calcd for C₁₃H₂₅O₂Si [M+H]⁺ 241.1618, found 241.1610.

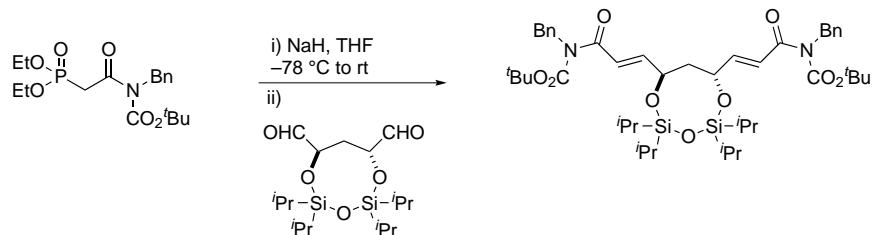


(6*S*,8*S*)-2,2,4,4-Tetraisopropyl-6,8-divinyl-1,3,5,2,4-trioxadisilocane (328). To a solution of the diol (1.00 g, 7.81 mmol) in DMF (10 mL) at 0 °C was added diisopropylsilyl bis(triflate) (4.7 mL, 16 mmol) over 5 min. Reaction was warmed to rt and stirred for 20 h. Reaction mixture was poured into water (50 mL) and the resulting solution was extracted with ethyl acetate. The combined organic layers were washed with 5 % aq LiCl, dried and concentrated. The resulting oil was purified using flash chromatography (SiO₂, 2–5 % ethyl acetate in hexanes) to afford the alkene

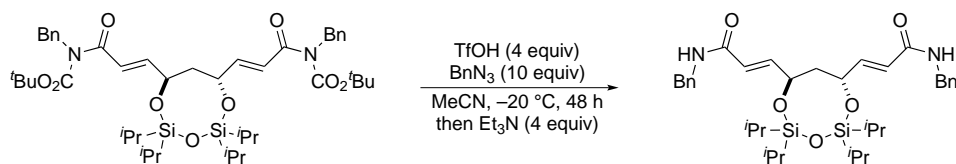
as a clear oil (1.75 g, 60%). $[\alpha]_D^{20} -13.1$ (*c* 0.35, CHCl_3); $R_f = 0.31$ (hexanes); IR (film) 2944, 2895, 2868, 1465, 1402 cm^{-1} ; $^1\text{H NMR}$ (400 MHz, CDCl_3) δ 5.88 (ddd, $J = 17.1, 10.5, 4.9$ Hz, 1H), 5.25 (dd, $J = 17.1, 1.7, 1.7$ Hz, 1H), 5.05 (dd, $J = 10.5, 1.6, 1.6$ Hz, 1H), 4.49 (m, 1H), 1.55 (dd, $J = 5.7, 5.6$ Hz, 1H), 1.10–0.93 (m, 14H); $^{13}\text{C NMR}$ (150 MHz, CDCl_3) ppm 140.8, 113.1, 68.4, 44.7, 17.4, 17.4, 17.3, 17.2, 13.4, 12.8; HRMS (ESI): Exact mass calcd for $\text{C}_{19}\text{H}_{39}\text{O}_3\text{Si}_2$ $[\text{M}+\text{H}]^+$ 371.2450, found 371.2432.



Bisimide 331. To a solution of KHMDS (2.5 g, 12 mmol) and 18-crown-6 (3.3 g, 12 mmol) in THF (80 mL) at $0\text{ }^\circ\text{C}$ was added imidophosphonate (4.3 g, 12 mmol) and the solution was stirred at $0\text{ }^\circ\text{C}$ for 1 h. The resulting yellow suspension was cooled to $-78\text{ }^\circ\text{C}$. In a separate flask, to a suspension of silica gel-supported $^{164}\text{NaIO}_4$ (10.0 g) in CH_2Cl_2 at rt was added polyol **329** (1.10 g, 1.51 mmol) in one portion. The slurry was stirred for 15 min, filtered through Celite, washed with chloroform and concentrated. The resulting crude aldehyde was diluted with THF (5 mL) and was added to the cold suspension of the imidophosphonate via cannula. The reaction mixture was stirred for 3 h at $-78\text{ }^\circ\text{C}$, quenched with satd aq NH_4Cl , warmed to rt, and concentrated. The residue was diluted with ethyl acetate, the layers were separated, and the aqueous layer was extracted with ethyl acetate. The combined organic layers were washed with brine, dried, concentrated and the resulting yellow oil was purified using flash chromatography (SiO_2 , 10–25% ethyl acetate in hexanes) to afford the bisimide as a clear oil (410 mg, 22%). $[\alpha]_D^{20} -0.9$ (*c* 13.50, CHCl_3); $R_f = 0.61$ (25% EtOAc/hexanes); IR (film) 3034, 2946, 2867, 1740, 1685, 1639 cm^{-1} ; $^1\text{H NMR}$ (400 MHz, CDCl_3) δ 7.33–7.21 (m, 5H), 7.14 (dd, $J = 15.1, 1.6$ Hz, 1H), 7.01 (dd, $J = 15.1, 3.9$ Hz, 1H), 4.97 (d, $J = 15.4$ Hz, 1H), 4.94 (d, $J = 15.3$ Hz, 1H), 4.72 (m, 1H), 3.79 (s, 3H), 1.66 (dd, $J = 8.4, 5.8$ Hz, 1H), 1.12–0.99 (m, 14H); $^{13}\text{C NMR}$ (100 MHz, CDCl_3) ppm 167.5, 167.4, 155.0, 137.1, 128.3, 127.7, 127.3, 62.5, 62.4, 54.0, 47.6, 37.6, 36.7, 16.3, 16.2; HRMS (ESI): Exact mass calcd for $\text{C}_{39}\text{H}_{56}\text{N}_2\text{O}_9\text{Si}_2$ $[\text{M}+\text{Na}]^+$ 753.3597, found 753.3609.

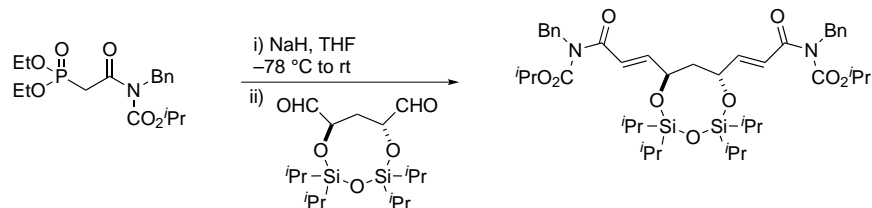


Bisimide 335. To a solution of the imidophosphonate (701 mg, 1.82 mmol) in tetrahydrofuran (10 mL) at $-78\text{ }^{\circ}\text{C}$ was added sodium hydride (44 mg, 1.8 mmol). The solution was warmed to rt, stirred for 15 min, cooled to $-78\text{ }^{\circ}\text{C}$ and the solution of the aldehyde **349** (194 mg, 374 μmol) in tetrahydrofuran (5 mL) was added via cannula. The reaction was warmed to $-20\text{ }^{\circ}\text{C}$ stirred for 18 h and quenched with water (1 mL). The reaction mixture was concentrated and diluted with ethyl acetate. The aqueous layer was extracted with ethyl acetate and the combined organic layers were dried and concentrated. The resulting yellow oil was purified using flash chromatography (SiO_2 , 10% ethyl acetate in hexanes) to afford the bisimide as a colorless oil (360 mg, 83%). $[\alpha]_{\text{D}}^{20} -25.1$ (c 24.50, CHCl_3); $R_f = 0.35$ (10% EtOAc/hexanes); IR (film) 3065, 3033, 2945, 2867, 1732, 1682, 1641, 1496 cm^{-1} ; ^1H NMR (400 MHz, CDCl_3) δ 7.30–7.18 (m, 5H), 7.06 (dd, $J = 14.9, 1.5$ Hz, 1H), 6.95 (dd, $J = 15.0, 3.4$ Hz, 1H), 4.90 (d, $J = 14.9$ Hz, 1H), 4.86 (d, $J = 15.0$ Hz, 1H), 4.75–4.66 (m, 1H), 1.67 (dd, $J = 8.1, 4.9$ Hz, 1H), 1.39 (s, 9H), 1.10–0.97 (m, 14H); ^{13}C NMR (100 MHz, CDCl_3) ppm 168.4, 152.9, 148.1, 138.1, 128.3, 127.5, 127.0, 122.6, 83.2, 67.2, 47.8, 42.9, 27.8, 17.4, 17.2, 13.2, 12.8; HRMS (ESI): Exact mass calcd for $\text{C}_{45}\text{H}_{68}\text{N}_2\text{NaO}_9\text{Si}_2$ $[\text{M}+\text{Na}]^+$ 859.4361, found 859.4404.

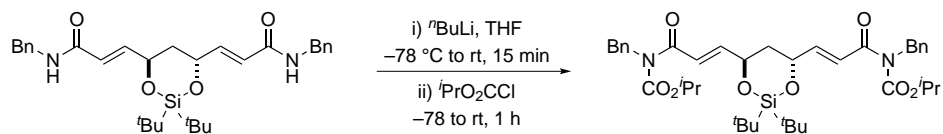


Acrylamide 336. To a solution of the bisimide (450 mg, 538 μmol) and benzyl azide (585 mg, 5.15 mmol) in acetonitrile (4.0 mL) at $-20\text{ }^{\circ}\text{C}$ was added triflic acid (220 μL , 2.50 mmol). The reaction was stirred at $-20\text{ }^{\circ}\text{C}$ for 18 h and then quenched with triethylamine (360 μL , 2.6 μmol) and warmed to rt. The reaction mixture was extracted with ethyl acetate and the combined organic layers were washed with brine, dried and concentrated. The resulting yellow solid was purified using flash chromatography (SiO_2 , 50% ethyl acetate in hexanes) to afford the bis(amide) as a white powder (241 mg, 70%). $[\alpha]_{\text{D}}^{20} -28.5$ (c 0.17, CHCl_3); $R_f = 0.38$ (50% EtOAc/hexanes); IR (film) 3268, 3065, 3031, 2944, 2894, 1671, 1633, 1552 cm^{-1} ; ^1H NMR (400 MHz, CDCl_3) δ 7.34–7.35 (m, 5H), 6.89 (dd, $J = 15.0, 3.6$ Hz, 1H), 6.87 (dd, $J = 15.0, 1.5$ Hz, 1H), 6.02 (t, $J = 5.7$ Hz, 1H), 4.65 (m, 1H), 4.53 (dd, $J = 14.7, 5.8$ Hz, 1H), 4.45 (dd, $J = 14.7, 5.6$ Hz, 1H), 1.57 (ddd, $J = 13.8, 8.1, 8.1$ Hz, 1H), 1.08–0.90 (m, 14H); ^{13}C NMR (100 MHz, CDCl_3) ppm 165.4, 146.1,

138.1, 128.7, 127.8, 127.5, 121.6, 66.9, 43.7, 43.2, 17.4, 17.3, 17.2, 17.2, 13.2, 12.7; HRMS (ESI): Exact mass calcd for $C_{35}H_{53}N_2O_5Si_2$ $[M+H]^+$ 637.3493, found 637.3523.

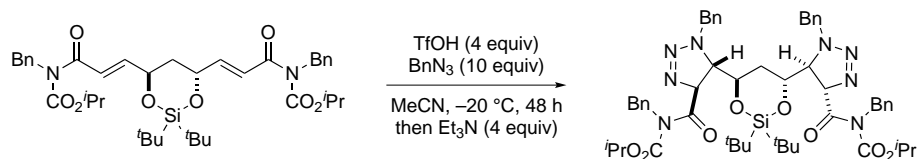


Bisimide 337. To a solution of the imidophosphonate (2.50 g, 6.70 mmol) in tetrahydrofuran (20 mL) at $-78\text{ }^\circ\text{C}$ was added sodium hydride (180 mg, 6.7 mmol). The solution was warmed to $0\text{ }^\circ\text{C}$, stirred for 30 min, cooled to $-78\text{ }^\circ\text{C}$, and then treated with a solution of aldehyde (prepared¹⁶⁴ from 736 mg, 1.68 mmol of tetraol **329**) in tetrahydrofuran (5 mL) was added via cannula. The reaction was warmed to $-20\text{ }^\circ\text{C}$ stirred for 18 h and quenched with satd NH_4Cl . The reaction mixture was concentrated, diluted with ethyl acetate, separated, and the aqueous layer was extracted further with ethyl acetate. The combined organic layers were washed with brine, dried and concentrated. The yellow residue was purified using flash chromatography (SiO_2 , 10–20% ethyl acetate in hexanes) to afford the bisimide as a colorless oil (1.09 g, 80%). $[\alpha]_D^{20}$ -20.2 (c 0.44, CHCl_3); $R_f = 0.69$ (25% EtOAc /hexanes); IR (film) 3033, 2945, 2893, 2867, 1732, 1682, 1639, 1495 cm^{-1} ; ^1H NMR (400 MHz, CDCl_3) δ 7.32–7.20 (m, 5H), 7.15 (dd, $J = 15.1, 1.5$ Hz, 1H), 7.00 (dd, $J = 15.0, 4.0$ Hz, 1H), 4.99 (sept, $J = 6.3$ Hz, 1H), 4.95 (s, 2H), 4.73 (m, 1H), 1.69 (ddd, $J = 13.8, 8.0, 8.0$ Hz, 1H), 1.23 (d, $J = 6.2$ Hz, 3H), 1.22 (d, $J = 6.3$ Hz, 3H), 1.15–0.85 (m, 14H); ^{13}C NMR (100 MHz, CDCl_3) ppm 168.3, 153.7, 148.7, 137.9, 128.2, 127.7, 127.1, 122.5, 71.1, 67.2, 47.6, 43.0, 21.6, 17.3, 17.2, 17.2, 13.2, 12.7; HRMS (ESI): Exact mass calcd for $C_{43}H_{64}N_2NaO_9Si_2$ $[M+Na]^+$ 831.4048, found 831.4023.



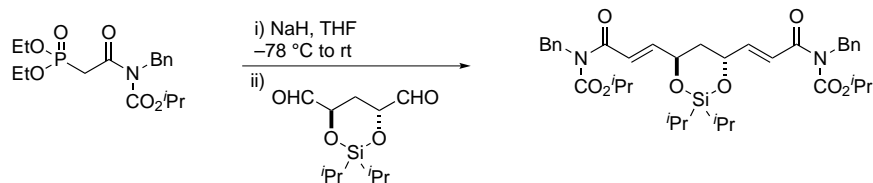
Bisimide 338. A solution of the bis(amide) (65.0 mg, 121 μmol) in THF (1.0 mL) was cooled to $-78\text{ }^\circ\text{C}$ and *n*-butyllithium (2.5 M in hexanes, 120 μL , 304 μmol) was added via syringe. The brown solution was stirred for 30 min and isopropyl chloroformate (1.0 M in toluene, 360 μL , 360 μmol) was added via syringe. The reaction was warmed to rt, stirred for additional 30 min and then quenched with aq satd NH_4Cl . The aqueous layer was extracted with ethyl acetate and the combined organic layers were dried and concentrated. The residue was purified using flash chromatography (SiO_2 ,

15% ethyl acetate in hexanes) to afford the desired product as a colorless oil (52.7 mg, 62%). $[\alpha]_{\text{D}}^{20}$ -23.2 (c 0.25, CHCl_3); $R_f = 0.55$ (25% EtOAc/hexanes); IR (film) 3033, 2934, 3858, 1732, 1683, 1637, 1559 cm^{-1} ; ^1H NMR (400 MHz, CDCl_3) δ 7.33–7.21 (m, 5H), 7.16 (dd, $J = 15.1, 1.7$ Hz, 1H), 6.97 (dd, $J = 15.1, 4.2$ Hz, 1H), 4.98 (sept, $J = 6.45$ Hz, 1H), 4.95 (s, 2H), 4.87–4.83 (m, 1H), 2.05 (dd, $J = 5.4, 5.3$ Hz, 1H), 1.22 (d, $J = 6.3$ Hz, 3H), 1.20 (d, $J = 6.3$ Hz, 3H), 1.06 (s, 9H); ^{13}C NMR (100 MHz, CDCl_3) ppm 168.3, 153.8, 147.9, 137.8, 128.3, 127.8, 127.2, 123.4, 77.3, 77.2, 77.0, 76.7, 71.2, 69.6, 47.6, 38.7, 27.0, 21.6, 21.6, 21.1; HRMS (ESI): Exact mass calcd for $\text{C}_{39}\text{H}_{53}\text{N}_2\text{NaO}_8\text{Si}$ $[\text{M}-\text{H}]^+$ 705.3571, found 705.3569.



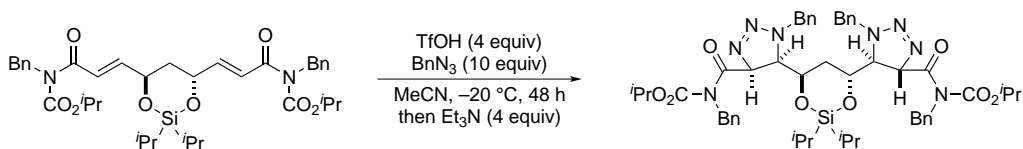
Bis(triazoline) 339. The imide (48.4 mg, 68.5 μmol) was treated with benzyl azide (91.1 mg, 685 μmol) according to the general procedure and purified using flash column chromatography (SiO_2 , 30% ethyl acetate in hexanes) to afford the triazoline mixture (1:9:9) as a yellow oil (36.0 mg, 54%).

Data for the 2,3-*syn*/2',3'-*syn* bis(triazoline): $[\alpha]_{\text{D}}^{20}$ $+92.8$ (c 0.75, CHCl_3); $R_f = 0.20$ (50% Et_2O /hexanes); IR (film) 3064, 3032, 2932, 2858, 1740, 1692 cm^{-1} ; ^1H NMR (600 MHz, CDCl_3) δ 7.31–7.12 (m, 10H); 6.40 (d, $J = 9.6$ Hz, 1H); 5.03 (sept, $J = 6.4$ Hz, 1H); 5.00 (d, $J = 15.4$ Hz, 1H); 4.90 (d, $J = 15.2$ Hz, 1H); 4.86 (d, $J = 15.2$ Hz, 1H); 4.58 (d, $J = 15.6$ Hz, 1H); 4.17 (ddd, $J = 10.4, 5.1, 5.1$ Hz, 1H); 3.85 (dd, $J = 9.1, 4.7$ Hz, 1H); 1.54 (t, $J = 5.6$ Hz, 1H); 1.26 (d, $J = 6.3$ Hz, 3H); 1.17 (d, $J = 6.3$ Hz, 3H); 0.92 (s, 9H); ^{13}C NMR (150 MHz, CDCl_3) ppm 169.9, 153.7, 137.2, 135.6, 128.7, 128.4, 128.0, 127.8, 127.5, 127.3, 82.0, 71.9, 67.9, 62.5, 53.0, 48.2, 33.2, 27.0, 21.7, 21.4, 21.3; HRMS (ESI): Exact mass calcd for $\text{C}_{53}\text{H}_{69}\text{N}_8\text{O}_8\text{Si}$ $[\text{M}+\text{H}]^+$ 973.5008, found 973.4994.

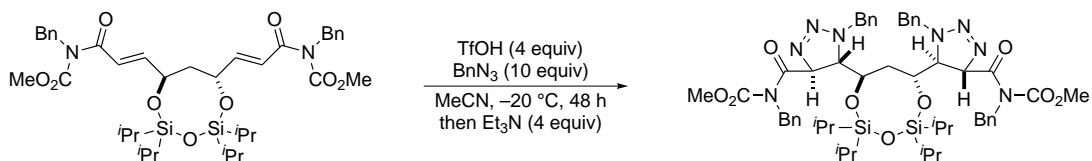


Bisimide 340. To a solution of the imidophosphonate (700 mg, 1.88 mmol) in tetrahydrofuran (2.0 mL) at -78°C was added sodium hydride (50 mg, 2.1 mmol). The solution was warmed to 0°C , stirred for 30 min, cooled to -78°C and a solution of aldehyde (prepared¹⁶⁴ from 128 mg, 415 μmol of the corresponding tetraol) in tetrahydrofuran (2 mL) was added via cannula. The

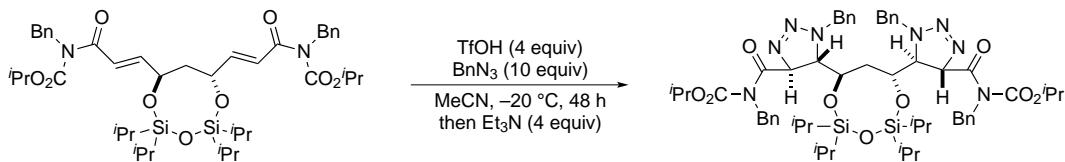
reaction was warmed to $-20\text{ }^{\circ}\text{C}$ stirred for 6 h and quenched with satd NH_4Cl . The reaction mixture was concentrated and diluted with ethyl acetate, separated, and the aqueous layer was extracted further with ethyl acetate. The combined organic layers were washed with brine, dried and concentrated. The resulting yellow oil was purified using flash chromatography (SiO_2 , 10–15 % ethyl acetate in hexanes) to afford the Bisimide as a colorless oil (181 mg, 64 %). $[\alpha]_{\text{D}}^{20} -23.5$ (c 0.61, CHCl_3); $R_f = 0.66$ (25 % EtOAc /hexanes); IR (film) 3033, 2981, 2944, 2866, 1732, 1682, 1639, 1496 cm^{-1} ; ^1H NMR (400 MHz, CDCl_3) δ 7.36–7.22 (m, 5H), 7.17 (dd, $J = 15.0, 1.8$ Hz, 1H), 6.95 (dd, $J = 15.0, 4.2$ Hz, 1H), 4.98 (sept, $J = 6.5$ Hz, 1H), 4.95 (s, 2H), 4.87 (ddd, $J = 5.2, 4.1, 1.8$ Hz, 1H), 2.03 (dd, $J = 5.6, 5.2$ Hz, 1H), 1.29–1.20 (m, 7H), 1.11–0.99 (m, 6H); ^{13}C NMR (100 MHz, CDCl_3) ppm 168.3, 153.8, 147.7, 137.9, 128.6, 128.3, 127.8, 127.2, 123.6, 71.3, 69.4, 47.6, 39.3, 22.1, 21.6, 21.6, 16.8, 16.7, 13.4 ppm; HRMS (ESI): Exact mass calcd for $\text{C}_{37}\text{H}_{50}\text{N}_2\text{NaO}_8\text{Si}$ $[\text{M}+\text{Na}]^+$ 701.3234, found 701.3215.



Bis(triazoline) 341. To a solution of the bisimide **340** (80.0 mg, 118 μmol) and benzyl azide (160 mg, 1.2 mmol) in acetonitrile (500 μL) at $-20\text{ }^{\circ}\text{C}$ was added triflic acid (52 μL , 590 μmol) and the solution was stirred at $-20\text{ }^{\circ}\text{C}$ for 18 h. The reaction was quenched with triethylamine (83 μL , 590 μmol) and warmed to rt. The reaction mixture was poured into water and extracted with ethyl acetate. The combined organic layers were washed with brine, dried and concentrated. The resulting brown oil was purified using flash chromatography (SiO_2 , 50 % ethyl acetate in hexanes) to afford the triazoline as a yellow oil (8 mg, 7 %). $R_f = 0.28$ (50 % Et_2O /hexanes); IR (film) 3064, 3032, 2943, 2866, 1813, 1741, 1687, 1604 cm^{-1} ; ^1H NMR (600 MHz, CDCl_3) δ 7.31–7.15 (m, 18H), 7.10–7.07 (m, 2H), 6.30 (d, $J = 9.6$ Hz, 1H), 6.02 (d, $J = 9.6$ Hz, 1H), 5.30 (d, $J = 15.3$ Hz, 1H), 5.08–5.00 (m, 2H), 4.97 (d, $J = 15.1$ Hz, 1H), 4.88 (d, $J = 9.6$ Hz, 1H), 4.81 (d, $J = 15.5$ Hz, 1H), 4.61 (d, $J = 15.2$ Hz, 1H), 4.50 (d, $J = 15.2$ Hz, 1H), 4.29–4.25 (m, 1H), 4.05 (dd, $J = 9.6, 5.5$ Hz, 1H), 3.85 (dd, $J = 9.4, 4.1$ Hz, 1H), 3.82 (dd, $J = 10.0, 1.3$ Hz, 1H), 1.28–0.78 (m, 30H); ^{13}C NMR (150 MHz, CDCl_3) ppm 170.02, 169.98, 153.9, 153.7, 137.32, 137.29, 135.7, 135.4, 128.8, 128.7, 128.6, 128.5, 128.4, 128.3, 128.0, 127.83, 127.75, 127.6, 127.4, 127.3, 127.2, 82.0, 81.3, 72.0, 71.9, 67.7, 66.4, 62.6, 62.2, 53.2, 52.7, 48.3, 48.1, 35.6, 33.6, 29.7, 21.8, 21.7, 21.4, 21.3, 17.5, 17.44, 17.43, 16.9, 16.8, 16.6, 16.5, 13.9, 13.04, 12.98; HRMS (ESI): Exact mass calcd for $\text{C}_{51}\text{H}_{64}\text{N}_8\text{NaO}_8\text{Si}$ $[\text{M}+\text{Na}]^+$ 945.4695, found 945.4741.

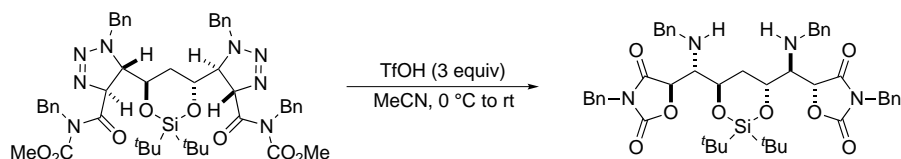


Triazoline 342. To a solution of the bisimide (410 mg, 540 μmol) and benzyl azide (665 mg, 5.00 mmol) in CH_3CN (2.0 mL) at -20°C was added triflic acid (200 μL , 2.20 mmol) and the solution was stirred at -20°C for 40 h. The reaction was quenched with triethylamine (300 μL , 2.20 mmol) and warmed to rt. The reaction mixture was poured into water and extracted with ethyl acetate. The combined organic layers were washed with brine, dried and concentrated. The resulting brown oil was purified using flash chromatography (SiO_2 , 25% ethyl acetate in hexanes) to afford the triazoline as yellow oil (150 mg, 27%). $[\alpha]_{\text{D}}^{20} +56.9$ (c 0.23, CHCl_3); $R_f = 0.37$ (25% EtOAc /hexanes); IR (film) 3031, 2945, 2866, 1740, 1691, 1496 cm^{-1} ; ^1H NMR (600 MHz, CDCl_3) δ 7.26–7.18 (m, 8H), 7.10–7.08 (m, 2H), 6.08 (d, $J = 10.2$ Hz, 1H), 5.28 (d, $J = 15.4$ Hz, 1H), 4.95 (d, $J = 15.2$ Hz, 1H), 4.86 (d, $J = 15.2$ Hz, 1H), 4.49 (d, $J = 15.4$ Hz, 1H), 4.24 (ddd, $J = 7.8, 5.9, 1.5$ Hz, 1H), 3.82 (dd, $J = 10.2, 1.4$ Hz, 1H), 3.79 (s, 3H), 1.20 (dd, $J = 8.1, 5.7$ Hz, 1H), 1.07–1.08 (m, 6H), 1.01–0.96 (m, 4H), 0.90–0.85 (m, 4H); ^{13}C NMR (150 MHz, CDCl_3) ppm 169.9, 154.9, 137.0, 135.3, 128.6, 128.5, 128.0, 127.8, 127.3, 127.3, 81.3, 66.1, 62.3, 54.0, 52.7, 48.2, 36.2, 17.5, 17.5, 17.4, 16.9, 13.9, 12.6; HRMS (ESI): Exact mass calcd for $\text{C}_{53}\text{H}_{70}\text{N}_8\text{NaO}_9\text{Si}_2$ $[\text{M}+\text{Na}]^+$ 1041.4702, found 1041.4757.

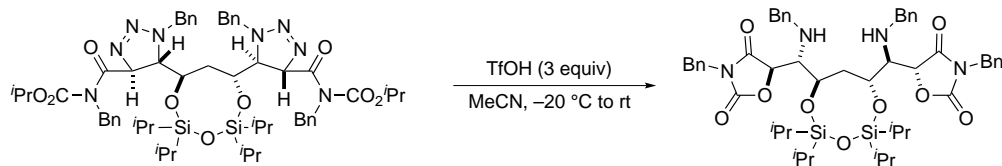


Triazoline 343. To a solution of the bisimide **337** (35 mg, 43 μmol) and benzyl azide (57 mg, 430 μmol) in acetonitrile (200 μL) at -20°C was added triflic acid (19 μL , 210 μmol) and the solution was stirred at -20°C for 3 h. The reaction was quenched with triethylamine (30 μL , 220 μmol) and warmed to rt. The reaction mixture was poured into water and extracted with ethyl acetate. The combined organic layers were washed with brine, dried and concentrated. The resulting brown oil was purified using flash chromatography (SiO_2 , 25% ethyl acetate in hexanes) to afford the triazoline as yellow oil (34.9 mg, 75%). $[\alpha]_{\text{D}}^{20} +132.9$ (c 0.85, CHCl_3); $R_f = 0.50$ (25% EtOAc /hexanes); IR (film) 3064, 3032, 2943, 2866, 1734, 1685, 1496 cm^{-1} ; ^1H NMR (400 MHz, CDCl_3) δ 7.28–7.16 (m, 8H), 7.13–7.07 (m, 2H), 6.03 (d, $J = 9.9$ Hz, 1H), 5.32 (d, $J = 15.6$ Hz, 1H), 5.03 (sept, $J = 6.3$ Hz, 1H), 4.98 (d, $J = 15.1$ Hz, 1H), 4.82 (d, $J = 15.1$ Hz, 1H), 4.51 (d, $J = 15.6$ Hz, 1H), 4.33–4.25 (m, 1H), 3.83 (dd, $J = 10.5, 1.5$ Hz, 1H); 1.29 (d, $J = 6.3$ Hz, 3H), 1.23 (dd, $J = 8.1, 5.8$ Hz, 1H), 1.17 (d, $J = 6.3$ Hz, 3H), 1.12–0.80 (m, 14H); ^{13}C NMR (100 MHz,

CDCl₃) ppm 170.0, 153.8, 137.3, 135.4, 128.6, 128.3, 128.0, 127.7, 127.4, 127.1, 81.2, 77.2, 71.9, 66.4, 62.2, 52.7, 48.1, 35.6, 21.8, 21.3, 17.5, 17.4, 17.4, 16.8, 13.8, 12.5; HRMS (ESI): Exact mass calcd for C₅₇H₇₈N₈NaO₉Si₂ [M+Na]⁺ 1097.5328, found 1097.5304.

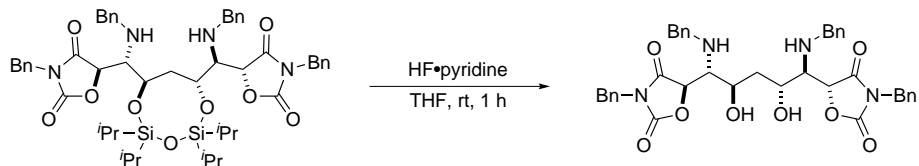


Bis(oxazolidine dione) 316 To a solution of triazolone (125 mg, 136 μ mol) in acetonitrile (500 μ L) at 0 °C was added triflic acid (26 μ L, 300 μ mol) via syringe. The solution was slowly warmed to rt and stirred for 15 h and then quenched with triethylamine (42 μ L, 300 μ mol). The reaction mixture was poured into water and extracted with ethyl acetate. The combined organic layers were washed with brine, dried and concentrated. The resulting yellow oil was purified using flash chromatography (SiO₂, 25 % ethyl acetate in hexanes) to afford the bis(oxazolidine dione) as a yellow oil (58 mg, 51 %) [α]_D²⁰ -49.3 (*c* 1.5, CHCl₃); R_f = 0.30 (25 % EtOAc/hexanes); IR (film) 3341, 3031, 2931, 2857, 1815, 1735, 1496 cm⁻¹; ¹H NMR (600 MHz, CDCl₃) δ 7.46–7.38 (m, 3H); 7.33–7.15 (m, 7H); 4.69 (d, *J* = 4.0 Hz, 1H); 4.68 (s, 2H); 4.49 (ddd, *J* = 11.0, 4.9, 4.9 Hz, 1H); 3.91 (d, *J* = 12.6 Hz, 1H); 3.75 (d, *J* = 12.6 Hz, 1H); 3.07 (dd, *J* = 5.5, 4.1 Hz, 1H); 1.97 (dd, *J* = 5.8, 4.8 Hz, 1H); 1.92 (brs, 1H); 0.98 (s, 9H); ¹³C NMR (150 MHz, CDCl₃) ppm 171.8, 155.2, 139.5, 134.6, 129.0, 128.9, 128.8, 128.73, 128.67, 128.6, 128.5, 128.4, 128.3, 127.2, 79.5, 69.7, 62.8, 53.6, 43.7, 33.9, 27.1, 21.2; HRMS (ESI): Exact mass calcd for C₄₇H₅₇N₄O₈Si [M+H]⁺ 833.3946, found 833.3946.

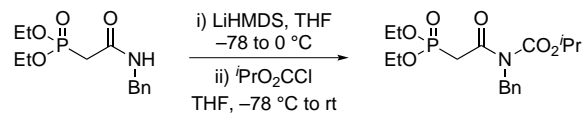


Bis(oxazolidine dione) 344. To a solution of triazolone (150 mg, 145 μ mol) in acetonitrile (1.0 mL) at -20 °C was added triflic acid (40 μ L, 450 μ mol) via syringe. The solution was slowly warmed to rt and stirred for 10 h and then quenched with triethylamine (63 μ L, 450 μ mol). The reaction mixture was poured in to water and extracted with ethyl acetate. The combined organic layers were washed with brine, dried and concentrated. The resulting yellow oil was purified using flash chromatography (SiO₂, 20 % ethyl acetate in hexanes) to afford the bis(oxazolidine dione) as a yellow oil (96 mg, 71 %) [α]_D²⁰ 25.1 (*c* 7.10, CHCl₃); R_f = 0.38 (25 % EtOAc/hexanes); IR (film) 3064, 3031, 2945, 2867, 1815, 1738, 1496 cm⁻¹; ¹H NMR (600 MHz, CDCl₃) δ 7.38–7.36 (m, 2H), 7.28–7.21 (m, 6H), 7.14–7.12 (m, 2H), 4.94 (d, *J* = 4.3 Hz, 1H), 4.68 (d, *J* = 14.5 Hz, 1H), 4.65

(d, $J = 14.6$ Hz, 1H), 4.31 (ddd, $J = 7.5, 5.2, 5.2$ Hz, 1H), 3.81 (d, $J = 13.0$ Hz, 1H), 3.73 (d, $J = 13.0$ Hz, 1H), 3.13 (d, $J = 4.5, 4.6$ Hz, 1H), 1.86 (dd, $J = 7.6, 5.7$ Hz, 1H), 1.09–0.98 (m, 14H) N-H peak was not observed; ^{13}C NMR (150 MHz, CDCl_3) ppm 171.4, 155.1, 139.4, 134.6, 129.0, 128.9, 128.8, 128.6, 128.6, 128.4, 128.3, 128.2, 127.2, 79.9, 68.0, 63.6, 53.2, 43.6, 36.8, 17.6, 17.5, 17.4, 17.2, 13.6, 12.8; HRMS (ESI): Exact mass calcd for $\text{C}_{51}\text{H}_{67}\text{N}_4\text{O}_9\text{Si}_2$ $[\text{M}+\text{H}]^+$ 935.4446, found 935.4454.

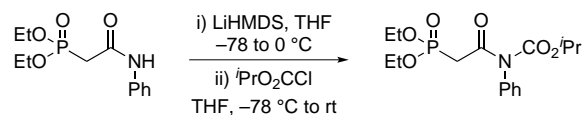


Bis(oxazolidinone dione) 345. To a solution of the bis(oxazolidinone dione) (100 mg, 107 μmol) in tetrahydrofuran (500 μL , 123 μmol) was added HF–pyridine (70:30 by wt., 65 μL) and the reaction was stirred at rt for 1 h. The reaction mixture was poured into water and extracted with dichloromethane. The combined organic layers were dried, concentrated and purified using flash chromatography (SiO_2 , 50–70 % ethyl acetate in hexanes) to afford the diol as a colorless oil (28 mg, 38 %). $[\alpha]_{\text{D}}^{20} -30.0$ (c 0.54, CHCl_3); $R_f = 0.45$ (50 % EtOAc/hexanes); IR (film) 3482, 3031, 2924, 1811, 1732 cm^{-1} ; ^1H NMR (400 MHz, CDCl_3) δ 7.38–7.34 (m, 2H), 7.28–7.22 (m, 6H), 7.18–7.13 (m, 2H), 4.95 (d, $J = 2.0$ Hz, 1H), 4.61 (d, $J = 15.2$ Hz, 1H), 4.57 (d, $J = 15.2$ Hz, 1H), 3.81 (d, $J = 12.5$ Hz, 1H), 3.76 (ddd, $J = 11.0, 5.7, 5.7$ Hz, 1H), 3.67 (d, $J = 12.8$ Hz, 1H), 3.05 (dd, $J = 9.1, 2.0$ Hz, 1H), 1.80 (dd, $J = 5.6, 5.3$ Hz, 1H), 1.70 (br. 2H); ^{13}C NMR (100 MHz, CDCl_3) ppm 172.5, 155.9, 138.6, 134.5, 128.7, 128.7, 128.6, 128.5, 128.2, 127.5, 79.3, 68.9, 62.4, 52.4, 43.7, 41.0; HRMS (ESI): Exact mass calcd for $\text{C}_{39}\text{H}_{41}\text{N}_4\text{O}_8$ $[\text{M}+\text{H}]^+$ 693.2924, found 693.2953.

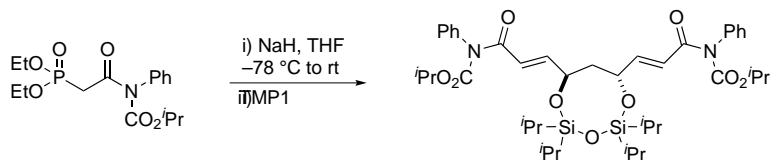


Isopropyl benzyl(2-(diethoxyphosphoryl)acetyl)carbamate (424). To a solution of hexamethyldisilazane (9.67 mL, 59.9 mmol) in THF (50 mL) at -78°C was added *n*-butyllithium (2.5 M in hexanes, 12.5 mL, 59.8 mmol) via syringe. The solution was warmed to 0°C , stirred for 15 min, and then cooled to -78°C . A solution of the amidophosphonate (7.76 g, 27.2 mmol) was added in one portion. The solution was warmed to 0°C (15 min), cooled to -78°C and then isopropyl chloroformate (1.0 M in toluene, 41 mL) was added via syringe and the solution was slowly warmed to rt. The reaction was quenched with satd aq ammonium chloride and concentrated. The yellow residue was diluted with ethyl acetate and layers were separated. The aqueous layer was extracted

with ethyl acetate, and the combined organic layers were dried and concentrated. The residue was purified using flash chromatography (SiO₂, 50 % ethyl acetate in hexanes) to afford the imidophosphonate as a yellow oil (4.02 g, 40 %). $R_f = 0.25$ (50 % EtOAc/hexanes); IR (film) 3031, 2983, 2936, 1734, 1695 cm⁻¹; ¹H NMR (400 MHz, CDCl₃) δ 7.27–7.18 (m, 5H), 4.95 (septet, $J = 6.2$ Hz, 1H), 4.91 (s, 2H), 4.09 (dq, $J = 15.0, 7.1$ Hz, 4H), 3.82 (d, $J = 22$ Hz, 2H), 1.25 (t, $J = 7.0$ Hz, 6H), 1.19 (d, $J = 6.3$ Hz, 6H); ¹³C NMR (100 MHz, CDCl₃) ppm 167.6 (d, $J = 6.4$ Hz), 153.8, 137.4, 128.2, 127.7, 127.2, 71.6, 62.4 (d, $J = 130$ Hz), 47.4, 37.1 (d, $J = 133.3$ Hz), 36.4, 21.5, 16.2 (d, $J = 6.4$ Hz); ³¹P NMR (162 MHz, CDCl₃, δ): 21.7; HRMS (ESI): Exact mass calcd for C₁₇H₂₆NNaO₆P [M+Na]⁺ 394.1395, found 394.1405.

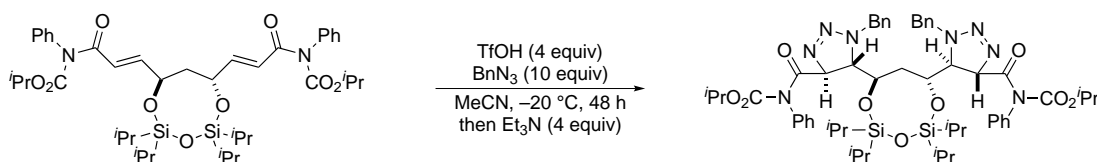


Isopropyl (2-(diethoxyphosphoryl)acetyl)(phenyl)carbamate (347). To a solution of hexamethyldisilazane (2.40 mL, 11.6 mmol) in THF (20 mL) at -78 °C was added *n*-butyllithium (2.5 M in hexanes, 4.70 mL, 11.7 mmol) via syringe. The solution was warmed to 0 °C, stirred for 30 min and then cooled to -78 °C. Amidophosphonate (1.57 g, 5.79 mmol) was added in one portion and the solution was warmed to 0 °C and stirred for 30 min. The reaction mixture was cooled to -78 °C, isopropyl chloroformate (1.0 M in toluene, 8.7 mL, 8.7 mmol) was added via syringe and the solution was slowly warmed to rt. The reaction was quenched with water (1.0 mL), concentrated, and the residue was purified using flash chromatography (SiO₂, 25 % ethyl acetate in hexanes) to afford the imidophosphonate as a brown oil (1.66 g, 86 %). $R_f = 0.50$ (EtOAc); IR (film) 3473, 3065, 2984, 2936, 1738, 1732, 1713, 1698, 1651, 1596, 1538 cm⁻¹; ¹H NMR (400 MHz, CDCl₃) δ 7.30–7.28 (m, 3H), 7.09 (dd, $J = 6.6, 1.6$ Hz, 2H), 4.95 (sept, $J = 6.1$ Hz, 1H), 4.21 (dq, $J = 8.0, 7.3$ Hz, 4H), 3.94 (d, $J = 21.8$ Hz, 2H), 1.37 (d, $J = 7.2$ Hz, 6H), 1.35 (d, $J = 7.1$ Hz, 6H); ¹³C NMR (100 MHz, CDCl₃) ppm 167.7 (d, $J = 6.5$ Hz), 153.6, 138.0, 128.9, 128.0, 71.5, 62.5 (d, $J = 6.5$ Hz), 36.8 (d, $J = 130$ Hz), 21.3, 16.2 (d, $J = 6.5$ Hz); ³¹P NMR (162 MHz, CDCl₃, δ): 20.4; HRMS (ESI): Exact mass calcd for C₁₆H₂₄NNaO₆P [M+Na]⁺ 380.1239, found 380.1236. Anal calcd for C₁₃H₂₄NO₆P: C, 53.76; H, 6.77; N, 4.06; found C, 52.92; H, 6.85; N, 4.10.

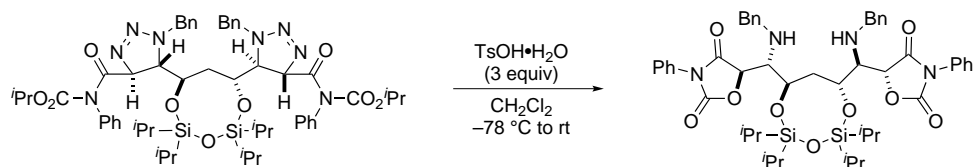


Bisimide 350. To a solution of the imidophosphonate **347** (815 mg, 2.28 mmol) in tetrahydrofuran (10 mL) at -78 °C was added sodium hydride (55 mg, 2.3 mmol). The solution was warmed

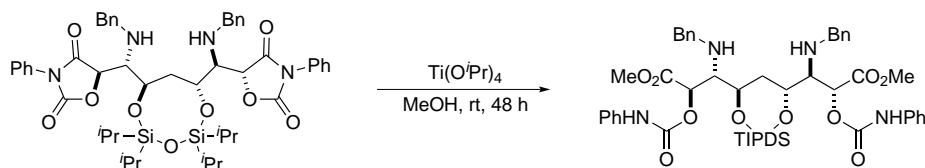
to 0 °C, stirred for 15 min, cooled to -78 °C and then treated with a solution of aldehyde **349** (prepared¹⁶⁴ from 250 mg, 570 μmol of tetraol **329**) in tetrahydrofuran (5 mL) was added via canula. The reaction was warmed to -20 °C stirred for 18 h and quenched with satd NH₄Cl. The reaction mixture was concentrated, diluted with ethyl acetate, separated, and the aqueous layer was extracted further with ethyl acetate. The combined organic layers were washed with brine, dried and concentrated. The resulting yellow oil was purified using flash chromatography (SiO₂, 10–20 % ethyl acetate in hexanes) to afford the bisimide as a colorless oil (327 mg, 73 %). $[\alpha]_D^{20} +3.4$ (*c* 0.89, CHCl₃); *R_f* = 0.53 (25 % EtOAc/hexanes); IR (film) 3065, 3074, 2945, 2894, 2868, 1767, 1736, 1696, 1642, 1642 cm⁻¹; ¹H NMR (400 MHz, CDCl₃) δ 7.42–7.32 (m, 3H), 7.14–7.11 (m, 2H), 7.02 (dd, *J* = 15.3, 3.6 Hz, 1H), 6.81 (dd, *J* = 1.6, 1.6 Hz, 1H), 5.01 (sept, *J* = 6.2 Hz, 1H), 4.70–4.60 (m, 1H), 1.61 (dd, *J* = 8.2, 5.6 Hz, 1H), 1.20 (d, *J* = 3.1 Hz, 3H), 1.18 (d, *J* = 3.1 Hz, 3H), 1.09–0.85 (m, 14H); ¹³C NMR (100 MHz, CDCl₃) ppm 170.3, 153.4, 138.1, 135.3, 129.0, 128.7, 128.7, 128.2, 128.2, 128.1, 128.1, 127.8, 80.9, 71.8, 65.9, 62.4, 52.7, 36.5, 21.6, 21.3, 17.6, 17.5, 17.5, 17.4, 16.9, 14.0, 12.6; HRMS (ESI): Exact mass calcd for C₄₁H₆₀N₂NaO₉Si₂ [M+Na]⁺ 803.3735, found 803.3746. Anal calcd for C₄₁H₆₀N₂O₉Si₂: C, 63.05; H, 7.75; N, 3.59; found C, 63.30; H, 7.60; N, 3.57.



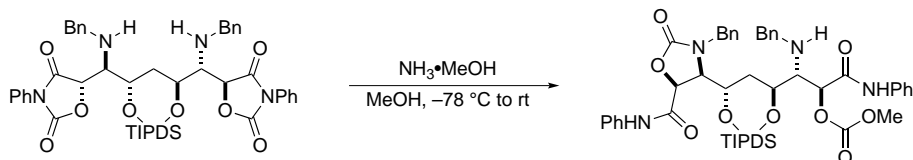
Bis(triazoline) 351. To a solution of the bisimide **350** (400 mg, 500 μmol) and benzyl azide (665 mg, 5.00 mmol) in acetonitrile (2.5 mL) at -20 °C was added triflic acid (220 μL, 2.5 mmol) and the solution was stirred at -20 °C for 6 h. The reaction was quenched with triethylamine (450 μL 2.5 mmol) and warmed to rt. The reaction mixture was poured into water and extracted with ethyl acetate. The combined organic layers were washed with brine, dried and concentrated. The brown residue was purified using flash chromatography at 0 °C (SiO₂, 10–30 % ethyl acetate in hexanes) to afford the triazoline as a yellow oil (358 mg, 68 %). $[\alpha]_D^{20} 114.2$ (*c* 10.10, CHCl₃); *R_f* = 0.38 (25 % EtOAc/hexanes); IR (film) 3063, 3030, 2942, 2867, 1710 cm⁻¹; ¹H NMR (600 MHz, CDCl₃) δ 7.38–7.24 (m, 6H), 7.20 (d, *J* = 7.6 Hz, 2H), 7.11 (ddd, *J* = 6.8, 1.6, 1.6 Hz, 2H), 6.08 (d, *J* = 10.1 Hz, 1H), 5.31 (d, *J* = 15.4 Hz, 1H), 5.05 (septet, *J* = 6.3 Hz, 1H), 4.54 (d, *J* = 15.5 Hz, 1H), 4.31–4.25 (m, 1H), 3.89 (dd, *J* = 9.2, 1.0 Hz, 1H), 1.27–1.22 (m, 4H), 1.18 (d, *J* = 6.2 Hz, 3H), 1.12–0.81 (m, 14H); ¹³C NMR (150 MHz, CDCl₃) ppm 170.3, 153.4, 138.1, 135.3, 129.0, 128.7, 128.7, 128.2, 128.2, 128.1, 128.1, 127.8, 80.9, 71.8, 65.9, 62.4, 52.7, 36.5, 21.6, 21.3, 17.6, 17.5, 17.5, 17.4, 16.9, 14.0, 12.6; HRMS (ESI): Exact mass calcd for C₅₅H₇₄N₈NaO₉Si₂ [M+Na]⁺ 1069.5015, found 1069.5051.



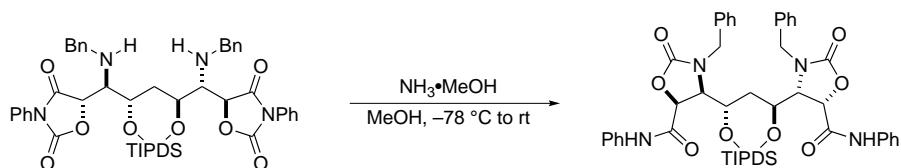
Bis(oxazolidinone dione) 346. To a solution of triazoline (12.00 g, 11.46 μmol) in dichloromethane (120 mL) at $-78\text{ }^\circ\text{C}$ was added toluenesulfonic acid monohydrate (8.72 g, 45.8 mmol) via syringe. The solution was slowly warmed to rt, stirred for 1 h. To the reaction mixture was added solid NaHCO_3 (3.85 g, 45.8 mmol) and stirring was continued for 1 h at rt. Celite (ca. (10 g) was added and the reaction mixture was filtered through a pad of Celite, the filter cake was washed with CH_2Cl_2 and the resulting solution was concentrated. The resulting green oil was purified using flash chromatography (SiO_2 , 25 % ethyl acetate in hexanes) to afford the bis(oxazolidinone) as a yellow oil (10.0 g, 96 %). $[\alpha]_{\text{D}}^{20}$ 14.1 (*c* 0.92, CHCl_3); R_f = 0.30 (25 % EtOAc/hexanes); IR (film) 3029, 2945, 2867, 1817, 1746, 1598, 1502 cm^{-1} ; ^1H NMR (400 MHz, CDCl_3) δ 7.50–7.17 (m, 10H), 5.11 (d, J = 3.8 Hz, 1H), 4.40 (ddd, J = 7.4, 5.2, 5.2 Hz, 1H), 3.96 (d, J = 13.0 Hz, 1H), 3.85 (d, J = 13.0 Hz, 1H), 3.27 (dd, J = 4.6, 4.4 Hz, 1H), 1.96 (dd, J = 7.0, 6.3 Hz, 1H), 1.61 (brs, 1H), 1.07–1.00 (m, 14H); ^{13}C NMR (100 MHz, CDCl_3) 170.7, 154.2, 139.4, 130.8, 129.3, 128.9, 128.5, 128.3, 127.3, 125.7, 79.7, 68.0, 64.3, 53.6, 17.6, 17.5, 17.4, 17.3, 13.6, 12.9 ppm; HRMS (ESI): Exact mass calcd for $\text{C}_{49}\text{H}_{62}\text{N}_4\text{NaO}_9\text{Si}_2$ $[\text{M}+\text{Na}]^+$ 929.4134, found 929.4128.



Bis(ester) 352. To a suspension of bis(oxazolidinone) (31 mg, 34 μmol) in anhydrous methanol (500 μL) was added titanium(IV) isopropoxide (31 μL , 100 μmol) and the suspension was stirred at rt for 48 h. The reaction mixture was poured into water and extracted with dichloromethane. The combined organic layers were washed with brine, dried and concentrated. The residue was purified using flash chromatography (SiO_2 , 0.5–1 % methanol in chloroform) to afford the product as a clear oil (18.2 g, 55 %). $[\alpha]_{\text{D}}^{20}$ -13.9 (*c* 0.72, CHCl_3); R_f = 0.12 (0.5 % MeOH/ CHCl_3); IR (film) 3304, 3197, 3132, 3061, 3028, 2946, 2893, 2867, 1738, 1602, 1556 cm^{-1} ; ^1H NMR (600 MHz, CDCl_3) δ 8.12 (brs, 1H) 7.37–7.16 (m, 9H), 6.99 (t, J = 7.4 Hz, 1H), 5.44 (d, J = 4.6 Hz, 1H), 4.14 (ddd, J = 8.1, 5.2, 2.3 Hz, 1H), 3.96 (d, J = 13.3 Hz, 1H), 3.85 (d, J = 13.5 Hz, 1H), 3.74 (s, 3H), 3.31 (dd, J = 4.6, 2.5 Hz, 1H), 2.07 (dd, J = 6.8, 6.6 Hz, 1H), 1.96 (br, 1H), 1.04–0.96 (m, 9H), 0.92–0.86 (m, 5H); ^{13}C NMR (150 MHz, CDCl_3) ppm 170.3, 152.8, 138.9, 137.9, 128.8, 128.6, 128.4, 128.3, 128.1, 127.3, 123.2, 118.7, 70.8, 68.2, 61.3, 52.4, 51.2, 33.9, 17.4, 17.3, 17.3, 17.1, 13.2, 12.5; HRMS (ESI): Exact mass calcd for $\text{C}_{51}\text{H}_{70}\text{N}_4\text{NaO}_{11}\text{Si}_2$ $[\text{M}+\text{Na}]^+$ 993.4458, found 993.4620.

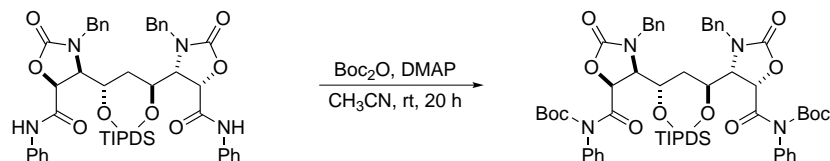


Bis(amide) 355. To a suspension of bis(oxazolidinone) (1.20 g, 1.30 mmol) in anhydrous methanol (50 mL) was added a saturated solution of ammonia in methanol (5.0 mL). The reaction was warmed to rt and stirred for 18 h. The solution was concentrated and purified using flash chromatography (SiO₂, 10–35% ethyl acetate in hexanes) to afford the product as a colorless oil (97.7 mg, 8%). $[\alpha]_D^{20}$ 16.1 (*c* 3.31, CHCl₃); R_f = 0.30 (25% EtOAc/hexanes); IR (film) 3312, 3062, 2928, 2866, 1752, 1685, 1600, 1530 cm⁻¹; ¹H NMR (400 MHz, CDCl₃) δ 9.06 (s, 1H), 8.12 (s, 1H), 7.62 (d, *J* = 8.0 Hz, 2H), 7.56 (d, *J* = 8.0 Hz, 2H), 7.41–7.28 (m, 9H), 7.21–7.06 (m, 6H), 6.99 (dd, *J* = 7.5, 7.3 Hz, 1H), 6.76 (br, 1H), 4.95 (d, *J* = 15.0 Hz, 1H), 4.84 (dd, *J* = 9.9, 9.7 Hz, 1H), 4.76 (d, *J* = 14.6 Hz, 1H), 4.64 (dd, *J* = 7.0, 2.4 Hz, 1H), 4.54 (d, *J* = 5.4 Hz, 1H), 4.17 (d, *J* = 14.6 Hz, 1H), 4.14 (d, *J* = 10.9 Hz, 1H), 3.95 (d, *J* = 15.1 Hz, 1H), 3.85 (dd, *J* = 8.9, 2.2 Hz, 1H), 3.75 (s, 3H), 3.52–3.43 (m, 3H), 1.39 (dd, *J* = 13.0, 12.9 Hz, 1H), 1.29–0.99 (m, 23H), 0.97–0.78 (m, 5H), 0.22 (dd, *J* = 12.9, 12.4 Hz, 1H); ¹³C NMR (100 MHz, CDCl₃) 171.0, 166.8, 160.1, 156.3, 137.4, 136.6, 136.3, 134.6, 130.0, 129.2, 129.0, 128.3, 128.2, 127.83, 127.78, 125.1, 124.4, 120.0, 119.6, 77.2, 73.6, 71.7, 65.9, 65.7, 64.7, 62.5, 55.0, 53.8, 46.3, 35.9, 29.7, 17.8, 17.7, 17.4, 17.29, 17.27, 17.25, 16.7, 14.2, 14.1, 13.8, 13.4, 12.9, 12.5, ppm; HRMS (ESI): Exact mass calcd for C₅₀H₆₇N₄O₁₀Si₂ [M+H]⁺ 939.4396, found 939.4413.

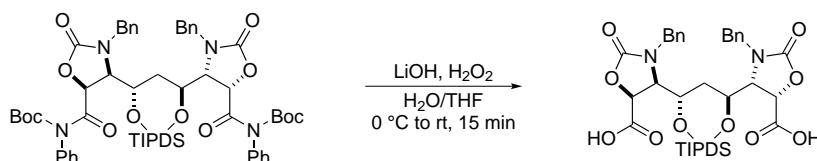


Bis(amide) 353. To a suspension of bis(oxazolidinone) (120 mg, 130 μmol) in anhydrous methanol (10 mL) was added a saturated solution of ammonia in methanol (1.0 mL). The reaction was warmed to rt and stirred for 18 h. The solution was concentrated and purified using flash chromatography (SiO₂, 25–35% ethyl acetate in hexanes) to afford the product as a colorless oil (81 mg, 67%). $[\alpha]_D^{20}$ -79.7 (*c* 1.85, CHCl₃); R_f = 0.25 (25% EtOAc/hexanes); IR (film) 3331, 3063, 2945, 2867, 1760, 1688, 1601 cm⁻¹; ¹H NMR (600 MHz, CDCl₃) δ 8.19 (s, 1H), 7.51 (d, *J* = 8.4 Hz, 2H), 7.34 (d, *J* = 7.6 Hz, 1H), 7.33 (d, *J* = 7.8 Hz, 1H), 7.29–7.22 (m, 3H), 7.18–7.14 (m, 3H), 4.94 (d, *J* = 15.5 Hz, 1H), 4.85 (d, *J* = 4.8 Hz, 1H), 4.39–4.34 (m, 1H), 4.11 (d, *J* = 15.3 Hz, 1H), 3.89 (d, *J* = 5.0 Hz, 1H), 1.66 (dt, *J* = 14.6, 8.8 Hz, 1H), 1.18–0.82 (m, 14H); ¹³C NMR (150 MHz, CDCl₃) ppm 170.7, 154.2, 139.4, 130.8, 129.3, 128.9, 128.5, 128.3, 127.3, 125.7, 79.7, 68.0, 64.3,

53.6, 34.4, 17.6, 17.5, 17.4, 17.3, 13.6, 12.9; HRMS (ESI): Exact mass calcd for C₄₉H₆₃N₄O₉Si₂ [M+H]⁺ 907.4134, found 907.4100.

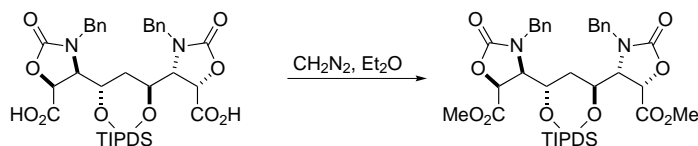


Bis(imide) 359. To a solution of the amide (271 mg, 299 μ mol) in CH₃CN (1.2 mL) at 0 °C was added Boc₂O (655 mg, 3.00 mmol) followed by 4-DMAP (185 mg, 1.50 mmol) and the reaction was stirred at rt for 20 h. The reaction mixture was concentrated and purified using flash chromatography (SiO₂, 30–60% ethyl acetate in hexanes) to afford the product as a yellow oil (201 mg, 61%). [α]_D²⁰ –49.2 (*c* 1.14, CHCl₃); R_f = 0.45 (50% EtOAc/hexanes); IR (film) 3065, 3033, 2944, 2894, 2867, 1775, 1727 cm⁻¹; ¹H NMR (400 MHz, CDCl₃) δ 7.43–7.33 (m, 3H), 7.32–7.24 (m, 3H), 7.23–7.17 (m, 2H), 6.96–6.89 (m, 2H), 5.69 (d, *J* = 2.9 Hz, 1H), 5.05 (d, *J* = 15.1 Hz, 1H), 4.57 (ddd, *J* = 6.6, 1.5, 1.5 Hz, 1H), 4.26 (d, *J* = 15.4 Hz, 1H), 3.87 (dd, *J* = 3.3, 1.5 Hz, 1H), 1.72 (dt, *J* = 13.6, 8.5 Hz, 1H), 1.32 (s, 9H), 1.20–1.10 (m, 7H), 1.02–0.93 (m, 4H), 0.76 (d, *J* = 7.1 Hz, 3H); ¹³C NMR (100 MHz, CDCl₃) ppm 171.0, 157.7, 152.6, 137.4, 135.7, 129.1, 128.7, 128.3, 127.8, 127.6, 84.3, 73.4, 68.8, 61.9, 47.4, 31.2, 27.5, 17.6, 17.54, 17.47, 16.7, 13.3, 12.7; HRMS (ESI): Exact mass calcd for C₅₉H₇₈N₄NaO₁₃Si₂ [M+Na]⁺ 1129.5002, found 1129.5039.

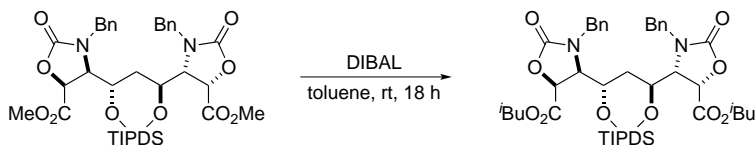


Bis(carboxylic acid) 360. To a solution of the imide (200 mg, 180 μ mol) in THF–H₂O (3:1 v/v, 3.6 mL) at 0 °C was added LiOH (40 mg), followed by H₂O₂ (30% in water, 400 μ L), and the reaction was stirred at rt for 15 min. The reaction was cooled to 0 °C, quenched with solid Na₂SO₃ (1 g) and warmed to rt. Water (5 mL) and ethyl acetate (5 mL) were added and the solution was vigorously stirred for 5 min. The layers were separated and the aqueous layer was acidified to pH 5 with KHSO₄(s). The aqueous layer was extracted with ethyl acetate and the combined organic layers were dried and concentrated to afford the carboxylic acid as a colorless oil (129 mg, 95%). [α]_D²⁰ 28.4 (*c* 0.37, CHCl₃); R_f = 0.32 (10% H₂O/MeCN); IR (film) 3512, 3032, 2946, 2868, 1756, 1497, 1444, 1363 cm⁻¹; ¹H NMR (400 MHz, CDCl₃) δ 7.36–7.21 (m, 3H), 7.12 (d, *J* = 7.8 Hz, 2H), 5.00 (d, *J* = 15.7 Hz, 1H), 4.84 (d, *J* = 4.0 Hz, 1H), 4.70–4.0 (br s, 1H), 4.31 (dd, *J* = 8.1, 6.6 Hz, 1H), 3.89 (d, *J* = 15.7 Hz, 1H), 3.50 (d, *J* = 4.1 Hz, 1H), 1.34 (dt, *J* = 15.0, 8.9 Hz, 1H), 1.18–0.76

(m, 14H); ^{13}C NMR (100 MHz, CD_3OD) ppm 177.1, 161.1, 137.3, 130.9, 130.0, 129.6, 74.3, 65.2, 47.7, 31.7, 18.4, 18.3, 18.0, 17.3, 15.9, 14.1; HRMS (ESI): Exact mass calcd for $\text{C}_{37}\text{H}_{52}\text{N}_2\text{NaO}_{11}\text{Si}_2$ $[\text{M}+\text{Na}]^+$ 779.3007, found 779.2975.

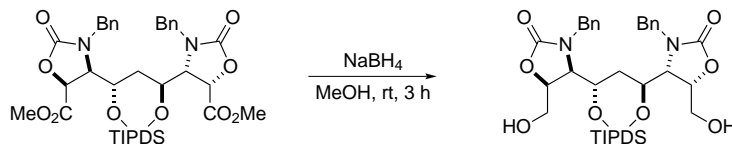


Bis(ester) 361. A solution of bis(carboxylic acid) (132 mg, 175 μmol) in diethyl ether (2 mL) was treated with a solution of diazomethane¹⁹⁸ in diethyl ether (25 mL). The resulting solution was stirred at rt for 18 h and concentrated to afford the bis(ester) as a yellow oil (137 mg, 99 %). $[\alpha]_{\text{D}}^{20} +27.7$ (*c* 0.75, CHCl_3); $R_f = 0.23$ (25 % EtOAc/hexanes); IR (film) 2947, 2868, 1769, 1625 cm^{-1} ; ^1H NMR (400 MHz, CDCl_3) δ 7.39–7.28 (m, 3H), 7.21–7.16 (m, 2H), 5.00 (d, $J = 15.2$ Hz, 1H), 4.74 (d, $J = 4.4$ Hz, 1H), 4.26 (ddd, $J = 13.8, 8.4, 7.8$ Hz, 1H), 3.99 (d, $J = 15.3$ Hz, 1H), 3.73 (s, 3H), 3.54 (dd, $J = 4.8, 1.0$ Hz, 1H), 1.37 (dt, $J = 14.1, 8.8$ Hz, 1H), 1.16–0.81 (m, 14H); ^{13}C NMR (100 MHz, CDCl_3) ppm 169.3, 156.9, 134.7, 128.9, 128.2, 127.6, 70.7, 65.7, 62.0, 52.9, 46.5, 34.5, 17.5, 17.3 (2C), 16.6, 14.0, 12.6; HRMS (ESI): Exact mass calcd for $\text{C}_{39}\text{H}_{56}\text{N}_2\text{NaO}_{11}\text{Si}_2$ $[\text{M}+\text{Na}]^+$ 807.3320, found 807.3301.

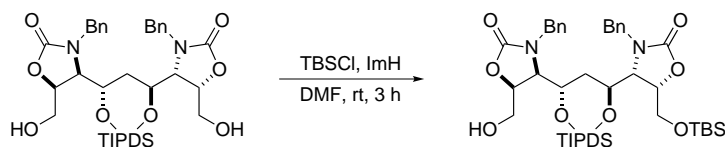


Bis(isobutyl ester) 425. To a solution of the bis(methyl ester) (14.1 mg, 17.9 μmol) in toluene (300 μL) was added DIBAL (1.0 M in toluene, 36 μL , 36 μmol) and the solution was stirred at rt for 18 h. The reaction was quenched by the addition of aq satd Rochelle's salt (1 mL), the layers were separated, and the aqueous layer was extracted with ethyl acetate. The combined organic layers were dried, concentrated and purified using flash chromatography (SiO_2 , 25 % ethyl acetate in hexanes) to afford the bis(isobutyl ester) as a yellow oil (5.1 mg, 33 %). $[\alpha]_{\text{D}}^{20} +30.0$ (*c* 0.54, CHCl_3); $R_f = 0.48$ (25 % EtOAc/hexanes); IR (film) 2960, 2868, 1772 cm^{-1} ; ^1H NMR (600 MHz, CDCl_3) δ 7.35–7.37 (m, 3H), 7.18 (d, $J = 8.2$ Hz, 2H), 5.00 ($J = 15.4$ Hz, 1H), 4.73 (d, $J = 4.4$ Hz, 1H), 4.26 (ddd, $J = 13.8, 8.4, 7.8$ Hz, 1H), 3.99 (d, $J = 15.4$ Hz, 1H), 3.90 (dd, $J = 10.6, 6.6$ Hz, 1H), 3.87 (dd, $J = 10.6, 6.6$ Hz, 1H), 3.54 (d, $J = 4.3$ Hz, 1H), 1.91–1.81 (m, 1H), 1.37 (dt, $J = 13.8, 8.0$ Hz, 1H), 1.15–1.08 (m, 7H), 1.06 (d, $J = 7.7$ Hz, 3H), 0.97 (d, $J = 7.5$ Hz, 3H), 0.91–0.85 (m, 1H), 0.84 (d, $J = 6.7$ Hz, 3H), 0.83 (d, $J = 6.7$ Hz, 3H); ^{13}C NMR (150 MHz, CDCl_3) ppm 169.0, 157.0, 134.8, 129.0, 128.2, 127.7, 72.1, 70.8, 65.9, 62.1, 46.6, 34.6, 27.6, 18.8 (2C), 17.6, 17.4,

16.7, 14.0, 12.6; HRMS (ESI): Exact mass calcd for $C_{45}H_{68}N_2NaO_{11}Si_2$ $[M+Na]^+$ 891.4259, found 891.4265.

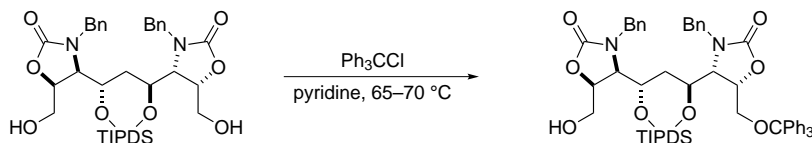


Bis(alcohol) 356. To a suspension of the bis(ester) (32.5 mg, 41.3 μ mol) in anhydrous methanol (600 μ L) at 0 $^{\circ}$ C was added $NaBH_4$ (4.7 mg, 120 μ mol). The reaction was warmed to rt, stirred for 30 min and then quenched by addition of NH_4Cl (200 mg). The reaction mixture was concentrated, diluted with water and extracted with ethyl acetate. The combined organic layers were dried, concentrated and purified using flash chromatography (SiO_2 , 5% methanol in dichloromethane) to afford the product as a colorless oil (27.7 mg, 92%). $[\alpha]_D^{20}$ -20.4 (c 1.26, $CHCl_3$); R_f = 0.20 (5% MeOH/ CH_2Cl_2); IR (film) 3417, 3089, 3064, 3032, 2944, 2894, 2867, 1752, 1738 cm^{-1} ; 1H NMR (600 MHz, $CDCl_3$) δ 7.34–7.29 (m, 2H), 7.29–7.24 (m, 1H), 7.23–7.19 (m, 2H), 4.91 (d, J = 15.1 Hz, 1H), 4.34 (dd, J = 8.9, 4.2 Hz, 1H), 4.14 (ddd, J = 13.7, 7.9, 7.9 Hz, 1H), 4.04 (d, J = 15.3 Hz, 1H), 3.61 (d, J = 12.0 Hz, 1H), 3.48 (d, J = 4.6 Hz, 1H), 3.44 (d, J = 11.9 Hz, 1H), 2.88 (br s, 1H), 1.25 (dt, J = 15.1, 8.7 Hz, 1H), 1.14–0.99 (m, 10H), 0.95–0.91 (m, 3H), 0.87–0.81 (m, 1H); ^{13}C NMR (150 MHz, $CDCl_3$) ppm 158.2, 135.3, 128.8, 128.8, 128.0, 127.9, 74.4, 66.0, 63.4, 60.4, 46.6, 33.9, 17.6, 17.4 (2C), 16.7, 14.1, 12.6; HRMS (ESI): Exact mass calcd for $C_{37}H_{56}N_2NaO_9Si_2$ $[M+Na]^+$ 751.3422, found 751.3451.

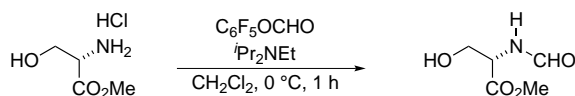


Alcohol 426. A solution of bis(alcohol) (24 mg, 33 μ mol), TBSCl (4.0 mg, 26 μ mol) and imidazole (2.7 mg, 17 μ mol) in DMF (600 μ L) was stirred at rt until TLC analysis showed presence of bis(silyl ether). To the reaction was added aq 5% LiCl (1 mL) and the mixture was extracted with ethyl acetate. The combined organic layers were dried, concentrated, and purified using flash chromatography (SiO_2 , 37% ethyl acetate in hexanes) to afford the desired product as a colorless oil (8.9 mg, 32%). $[\alpha]_D^{20}$ -25.5 (c 2.51, $CHCl_3$); R_f = 0.30 (37% EtOAc/hexanes); IR (film) 3443, 3031, 2945, 2867, 1755 cm^{-1} ; 1H NMR (600 MHz, $CDCl_3$) δ 7.34–7.25 (m, 6H), 7.24–7.21 (m, 4H), 4.94 (d, J = 15.3 Hz, 1H), 4.91 (d, J = 15.2 Hz, 1H), 4.42 (dd, J = 8.9, 4.6 Hz, 1H), 4.19 (dd, J = 10.4, 2.4 Hz, 1H), 4.15–4.05 (m, 4H), 4.03 (d, J = 15.3 Hz, 1H), 3.68 (ddd, J = 12.1, 4.6, 4.6 Hz, 1H), 3.58 (dd, J = 10.5, 3.1 Hz, 1H), 3.50–3.43 (m, 3H), 2.34 (t, J = 5.8 Hz, 1H), 1.26–0.81 (m, 30H),

0.78 (s, 9H), -0.05 (s, 3H), -0.04 (s, 3H); ^{13}C NMR (150 MHz, CDCl_3) ppm 158.0, 157.9, 135.7, 135.2, 128.8 (2C), 128.0 (2C), 127.9 (2C), 74.1, 67.5, 65.5, 63.7, 63.3, 60.6, 60.5, 46.8, 46.6, 33.7, 29.7, 25.7, 18.3, 17.6, 17.4 (2C), 16.8, 16.7, 14.1, 13.8, 12.6 (2C), -5.6 (2C); HRMS (ESI): Exact mass calcd for $\text{C}_{43}\text{H}_{70}\text{N}_2\text{NaO}_9\text{Si}_3$ $[\text{M}+\text{Na}]^+$ 865.4287, found 865.4275.

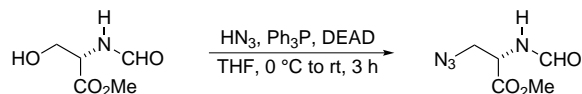


Alcohol 357. A solution of bis(alcohol) (276 mg, 378 μmol) and triphenylmethyl chloride (84.5 mg, 300 μmol) in anhydrous pyridine (2.0 mL) was stirred at $65\text{ }^\circ\text{C}$ – $70\text{ }^\circ\text{C}$ for 8 h. The reaction mixture was poured into 1 M HCl and ethyl acetate (20 mL) was added. The layers were separated and the organic layer was washed with 1 M HCl. The combined aqueous layers were extracted with ethyl acetate, and the organic layers were combined, dried and concentrated. The resulting oil was purified using flash chromatography (SiO_2 , 25–100 % ethyl acetate in hexanes) to afford the desired product as a colorless oil (110 mg, 30 %) and unreacted substrate as a colorless oil (177 mg, 64 %). $[\alpha]_{\text{D}}^{20}$ -26.5 (c 1.50, CHCl_3); R_f = 0.50 (50 % EtOAc/hexanes); IR (film) 3424, 3062, 3030, 2928, 2866, 1753, 1492, 1443 cm^{-1} ; ^1H NMR (400 MHz, CDCl_3) δ 7.39–7.22 (m, 15H), 7.22–7.10 (m, 10H), 4.97 (d, J = 15.3 Hz, 1H), 4.92 (d, J = 15.4 Hz, 1H), 4.38 (dd, J = 9.2, 4.7 Hz, 1H), 4.26 (dd, J = 9.4, 4.8 Hz, 1H), 4.19 (dd, J = 10.0, 3.4 Hz, 1H), 4.05 (d, J = 15.1 Hz, 1H), 4.04 (dd, J = 9.2, 3.8 Hz, 1H), 3.96 (d, J = 15.4 Hz, 1H), 3.53–3.45 (m, 2H), 3.42 (d, J = 4.4 Hz, 1H), 3.35 (ddd, J = 11.2, 5.5, 5.4 Hz, 1H), 3.28 (d, J = 4.8 Hz, 1H), 3.17 (dd, J = 9.2, 6.0 Hz, 1H), 3.05 (dd, J = 10.0, 4.0 Hz, 1H), 1.51 (br s, 2H), 1.30–0.70 (m, 28H); ^{13}C NMR (100 MHz, CDCl_3) ppm 157.9, 143.0, 135.4, 135.3, 128.9, 128.8, 128.5, 128.2, 127.8, 127.2, 87.2, 77.2, 73.8, 73.2, 66.9, 64.9, 63.9, 63.7, 61.2, 60.5, 46.8, 46.4, 34.0, 29.7, 25.8, 17.6, 17.5, 17.46, 17.41, 16.7, 14.2, 13.9, 12.7, 12.5; HRMS (ESI): Exact mass calcd for $\text{C}_{56}\text{H}_{70}\text{N}_2\text{NaO}_9\text{Si}_2$ $[\text{M}+\text{Na}]^+$ 993.4518, found 993.4495.

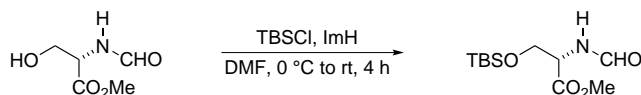


(S)-methyl 2-formamido-3-hydroxypropanoate (376). To a suspension of L-Serine hydrochloride (1.00 g, 6.43 mmol) in CHCl_3 (10 mL) was added pentafluorophenyl formate (980 μL , 7.72 μmol) and Hünig's base (1.12 mL, 6.63 mmol) via syringe. The solution was stirred for 1 h at $0\text{ }^\circ\text{C}$ and concentrated. The residue was purified using flash chromatography (SiO_2 , 50–95 % ethyl acetate in hexanes) to afford the desired product as a clear oil (854 mg, 90 %). $[\alpha]_{\text{D}}^{20}$ $+38.1$ (c 1.00, CHCl_3);

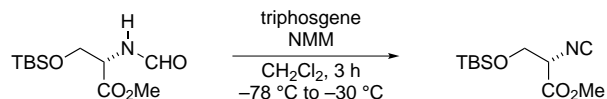
$R_f = 0.25$ (EtOAc); IR (film) 3300, 3031, 2857, 2823, 1748, 1718, 1683, 1669, 1653, 1617, 1558, 1539, 1521, 1516 cm^{-1} ; ^1H NMR (400 MHz, CDCl_3) δ 8.27 (s, 1H), 6.57 (br s, 1H), 5.07 (ddd, $J = 7.6, 3.6, 3.0$ Hz, 1H), 4.00 (dd, $J = 11.5, 2.9$ Hz, 1H), 3.92 (dd, $J = 11.5, 3.4$ Hz, 1H), 3.83 (s, 3H), OH peak was not observed; ^{13}C NMR (100 MHz, CDCl_3) ppm 168.8, 160.6, 53.2, 51.8, 44.8; HRMS (ESI): Decomp.



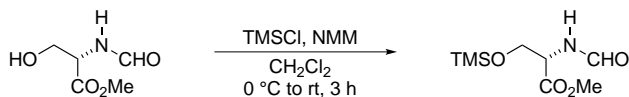
(*S*)-methyl 3-azido-2-formamidopropanoate (374). To a solution of the alcohol (147 mg, 1.00 mmol) and triphenylphosphine (340 mg, 1.20 mmol) in THF at 0 °C was added HN_3 (1.0 M in benzene, 2.0 mL, 2.0 mmol) via syringe. The reaction was stirred at 0 °C for 5 min and DEAD (200 μL , 1.30 mmol) was added dropwise via syringe. The reaction was stirred at 0 °C for 5 min, warmed to rt and stirred for 3 h. The reaction was quenched with satd aq NaHCO_3 , the layers were separated and the aqueous layer was extracted with ethyl acetate, dried and concentrated. The resulting residue was purified using flash chromatography (40–70 % ethyl acetate in hexanes) to afford the desired product as a clear oil (107 mg, 62 %). $[\alpha]_{\text{D}}^{20} +95.7$ (c 5.25, CHCl_3); $R_f = 0.15$ (50 % EtOAc/hexanes); IR (film) 3304, 3036, 2955, 2923, 2875, 2856, 2107, 1744, 1666, 1515 cm^{-1} ; ^1H NMR (400 MHz, CDCl_3) δ 8.26 (s, 1H), 6.65 (br s, 1H), 4.83 (ddd, $J = 7.6, 3.5, 3.4$ Hz, 1H), 3.82 (s, 3H), 3.79 (d, $J = 3.8$ Hz, 2H); ^{13}C NMR (100 MHz, CDCl_3) ppm 169.5, 160.8, 53.1, 52.1, 50.8; HRMS (ESI): Exact mass calcd for $\text{C}_5\text{H}_9\text{N}_4\text{O}_3$ $[\text{M}+\text{H}]^+$ 173.0669, found 173.0664.



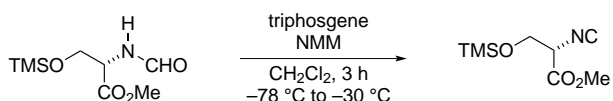
***S*-(methyl 3-((tert-butyldimethylsilyl)oxy)-2-formamidopropanoate (427).** To a solution of the alcohol (200 mg, 1.36 mmol) in DMF (1 mL) at 0 °C was added TBSCl (310 mg, 2.0 mmol) and imidazole (140 mg, 2.0 mmol). The reaction was warmed to rt and stirred for 4 h. The reaction mixture was poured into water and extracted with ethyl acetate. The combined organic layers were dried, concentrated and purified using flash chromatography (SiO_2 , 50 % ethyl acetate in hexanes) to afford the silyl ether as a colorless oil (222 mg, 62 %). $[\alpha]_{\text{D}}^{20} +47.1$ (c 3.08, CHCl_3); $R_f = 0.35$ (50 % EtOAc/hexanes); IR (film) 3314, 3029, 2953, 2933, 2885, 2858, 1750, 1677, 1514, 1468 cm^{-1} ; ^1H NMR (400 MHz, CDCl_3) δ 8.26 (s, 1H), 6.43 (br s, 1H), 4.75 (ddd, $J = 8.4, 2.6, 2.6$ Hz, 1H), 4.08 (dd, $J = 10.2, 2.6$ Hz, 1H), 3.84 (dd, $J = 10.2, 2.9$ Hz, 1H), 3.76 (s, 3H), 0.85 (s, 9H), 0.02 (s, 3H), 0.02 (s, 3H); ^{13}C NMR (100 MHz, CDCl_3) ppm 170.3, 160.6, 63.4, 52.8, 52.5, 25.6, 18.1, -5.6, -5.7; HRMS (ESI): Exact mass calcd for $\text{C}_{10}\text{H}_{20}\text{O}_4\text{N}_1\text{Si}$ $[\text{M}-\text{CH}_3]^-$ 246.1156, found 246.1158.



S-methyl 3-((tert-butyldimethylsilyl)oxy)-2-isocyanopropanoate (428). To a solution of the formamide (60.1 mg, 230 μmol) in dichloromethane (1.0 mL) at rt was added *N*-methylmorpholine (51.0 μL , 460 μmol) and the reaction was cooled to $-78\text{ }^\circ\text{C}$. Triphosgene (24.0 mg, 80.0 μmol) was added in one portion and the reaction was slowly warmed to $-30\text{ }^\circ\text{C}$ and stirred for 3 h. The reaction was quenched with water (at $-30\text{ }^\circ\text{C}$), warmed to rt, and extracted with dichloromethane. The combined organic layers were dried, concentrated to ca. 2 mL and purified using flash chromatography (SiO_2 , 25 % ethyl acetate in hexanes) to afford the isonitrile as a pale yellow oil (35.3 mg, 63 %). $[\alpha]_{\text{D}}^{20} +4.4$ (*c* 1.72, CHCl_3); $R_f = 0.45$ (25 % EtOAc/hexanes); IR (film) 2955, 2887, 2859, 2150, 1763, 1467, 1439 cm^{-1} ; ^1H NMR (400 MHz, CDCl_3) δ 4.34 (dd, $J = 4.7, 4.6$ Hz, 1H), 4.01 (dd, $J = 5.2, 4.1$ Hz, 2H), 3.82 (s, 3H), 0.89 (s, 9H), 0.10 (s, 3H), 0.08 (s, 3H); ^{13}C NMR (100 MHz, CDCl_3) ppm 165.5, 160.8, 63.7, 58.6, 53.3, 25.6, 18.1, $-5.5, -5.6$; HRMS (ESI): Exact mass calcd for $\text{C}_{10}\text{H}_{18}\text{O}_3\text{N}_1\text{Si}$ $[\text{M}-\text{CH}_3]^-$ 228.1050, found 228.1042.

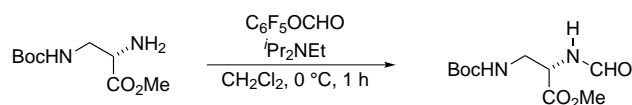


S-methyl 2-formamido-3-((trimethylsilyl)oxy)propanoate (429). To a solution of the alcohol (200 mg, 1.36 mmol) in dichloromethane (7 mL) at $0\text{ }^\circ\text{C}$ was added TMSCl (190 μL , 1.50 mmol) and *N*-methylmorpholine (222 μL , 2.02 mmol). The reaction was warmed to rt and stirred for 3 h. The reaction mixture was concentrated and purified using flash chromatography (SiO_2 , 25 % ethyl acetate in hexanes) to afford the silyl ether as a colorless oil (219 mg, 74 %). $[\alpha]_{\text{D}}^{20} +33.3$ (*c* 1.09, CHCl_3); $R_f = 0.35$ (25 % EtOAc/hexanes); IR (film) 3277, 3028, 2955, 2890, 1753, 1669, 1523, 1440 cm^{-1} ; ^1H NMR (400 MHz, CDCl_3) δ 8.24 (s, 1H), 6.48 (br s, 1H), 4.75 (ddd, $J = 8.5, 2.8, 2.8$ Hz, 1H), 4.04 (dd, $J = 10.4, 2.6$ Hz, 1H), 3.84 (dd, $J = 10.4, 3.1$ Hz, 1H), 3.75 (s, 3H), 0.07 (s, 9H); ^{13}C NMR (100 MHz, CDCl_3) ppm 170.3, 160.6, 62.7, 52.6, 52.5, -0.8 ; HRMS (ESI): Exact mass calcd for $\text{C}_7\text{H}_{14}\text{O}_4\text{N}_1\text{Si}$ $[\text{M}-\text{CH}_3]^-$ 204.0687, found 204.0694.

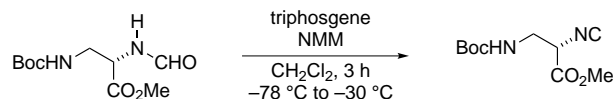


S-methyl 2-isocyano-3-((trimethylsilyl)oxy)propanoate (430). To a solution of the formamide (110 mg, 500 μmol) in dichloromethane (2.5 mL) at rt was added *N*-methylmorpholine

(110 μL , 1.00 mmol) and the reaction was cooled to $-78\text{ }^\circ\text{C}$. Triphosgene (57.0 mg, 190 μmol) was added in one portion and the reaction was slowly warmed to $-30\text{ }^\circ\text{C}$ and stirred for 3 h. The reaction was quenched with water (at $-30\text{ }^\circ\text{C}$), warmed to rt and extracted with ethyl acetate. The combined organic layers were dried, concentrated to ca. 2 mL and purified using flash chromatography (SiO_2 , 25 % ethyl acetate in hexanes) to afford the isonitrile as a pale yellow oil (68 mg, 68 %). $[\alpha]_{\text{D}}^{20} +8.3$ (c 0.93, CHCl_3); $R_f = 0.41$ (25 % EtOAc/hexanes); IR (film) 2958, 2887, 2151, 1762, 1439 cm^{-1} ; ^1H NMR (400 MHz, CDCl_3) δ 4.34 (dd, $J = 4.9, 4.6$ Hz, 1H), 3.98 (d, $J = 4.6$ Hz, 2H), 3.83 (s, 3H), 0.14 (s, 9H); ^{13}C NMR (100 MHz, CDCl_3) ppm 165.4, 160.9, 63.1, 58.6, 53.3, -0.6 ; HRMS (ESI): Exact mass calcd for $\text{C}_7\text{H}_{12}\text{O}_3\text{N}_1\text{Si}$ $[\text{M}-\text{CH}_3]^-$ 186.0581, found 186.0577.

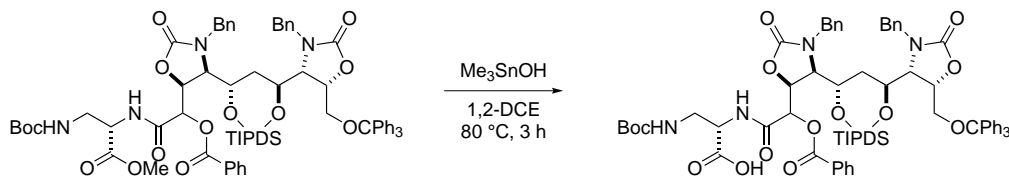


S-methyl 3-((tert-butoxycarbonyl)amino)-2-formamidopropanoate (380). To a solution of the amine (500 mg, 2.30 mmol) in CH_2Cl_2 (3.6 mL) was added pentafluorophenyl formate (600 μL , 2.76 mmol) and Hünig's base (400 μL , 2.30 mmol) via syringe. The solution was stirred for 15 min at $0\text{ }^\circ\text{C}$ and concentrated. The residue was purified using flash chromatography (SiO_2 , 1–5 % methanol in dichloromethane) to afford the desired product as a colorless oil (503 mg, 89 %). $[\alpha]_{\text{D}}^{20} +13.0$ (c 2.24, CHCl_3); $R_f = 0.35$ (4 % MeOH/ CH_2Cl_2); IR (film) 3330, 2978, 1743, 1682, 1517, 1440 cm^{-1} ; ^1H NMR (400 MHz, CDCl_3) δ 8.21 (s, 1H), 7.00 (br s, 1H), 5.03 (dd, $J = 6.2, 5.8$ Hz, 1H), 4.67 (ddd, $J = 6.1, 5.1, 5.0$ Hz, 1H), 3.76 (s, 3H), 3.56 (m, 2H), 1.41 (s, 9H); ^{13}C NMR (100 MHz, CDCl_3) ppm 170.3, 161.2, 156.7, 80.3, 52.8, 52.4, 42.0, 28.2; HRMS (ESI): Exact mass calcd for $\text{C}_{10}\text{H}_{18}\text{O}_5\text{N}_2\text{Na}$ $[\text{M}+\text{Na}]^+$ 269.1113, found 269.1113.



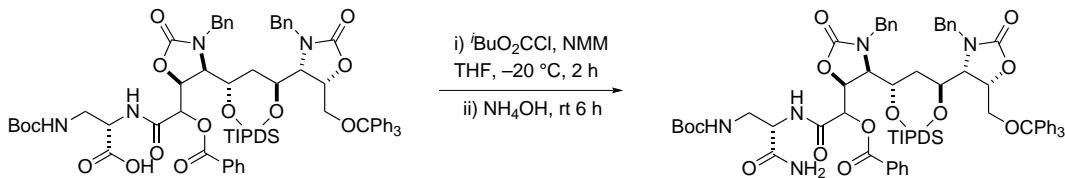
S-methyl 3-((tert-butoxycarbonyl)amino)-2-isocyanopropanoate (381). To a solution of the formamide (203 mg, 824 μmol) in dichloromethane (3.0 mL) at rt was added *N*-methylmorpholine (180 μL , 1.65 mmol) and the reaction was cooled to $-78\text{ }^\circ\text{C}$. Triphosgene (90.5 mg, 305 μmol) was added in one portion and the reaction was slowly warmed to $-30\text{ }^\circ\text{C}$ and stirred for 3 h. The reaction was quenched with water (at $-30\text{ }^\circ\text{C}$), warmed to rt and extracted with ethyl acetate. The combined organic layers were dried, concentrated to ca. 2 mL and purified using flash chromatography (SiO_2 , 25 % ethyl acetate in hexanes) to afford the isonitrile as a pale yellow oil (133 mg, 71 %). $[\alpha]_{\text{D}}^{20} -7.3$ (c 1.30, CHCl_3); $R_f = 0.51$ (25 % EtOAc/hexanes); IR (film) 3363, 2879, 2152, 1756,

1709, 1519, 1441 cm^{-1} ; ^1H NMR (400 MHz, CDCl_3) δ 5.24 (br s, 1H), 4.45 (t, $J = 5.4$ Hz, 1H), 3.78 (s, 3H), 3.68–3.59 (m, 1H), 3.56–3.46 (m, 1H), 1.39 (s, 9H); ^{13}C NMR (100 MHz, CDCl_3) ppm 165.5, 161.0, 155.4, 80.3, 56.2, 53.4, 42.6, 28.1; HRMS (ESI): Exact mass calcd for $\text{C}_{10}\text{H}_{15}\text{O}_4\text{N}_2\text{Si}$ $[\text{M}-\text{H}]^-$ 227.1026, found 227.1028.



Carboxylic acid 385. To a vial containing the methyl ester (50.2 mg, 37.8 μmol) in 1,2-DCE (1 mL) was added trimethyltin hydroxide (20.5 mg, 113 μmol) and the resulting solution was stirred at 70–80 $^\circ\text{C}$ for 4 h. The reaction mixture was cooled, diluted with dichloromethane and washed with a 10% solution of KHSO_4 . The combined aqueous layers were extracted with ethyl acetate and the combined organic layers were dried and concentrated. The resulting yellow oil was dissolved in anhydrous methanol and filtered. The methanol solution was concentrated and purified using preparative HPLC (XBridgeTM Prep C18 5 μm ODBTM 19 \times 150 μm column) using the following program: 10 mL min^{-1} 40 min gradient from 40% buffer A (95% water, 5% acetonitrile, 5 mM NH_4OAc) and 60% buffer B (95% acetonitrile, 5% water, 5 mM NH_4OAc) to 100% buffer B and then 40 min buffer B; t_r (minor diastereomer) = 36.0 min, t_r (major diastereomer) = 38.7 min. Removal of solvent gave the minor diastereomer as a colorless oil (8.4 mg, 17%) and major diastereomer as a colorless oil (12.3 mg, 25%). $[\alpha]_D^{20}$ -40.0 (c 1.23, CHCl_3);

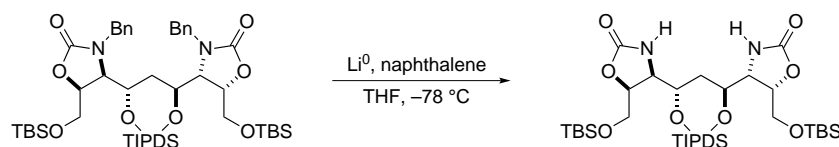
Major diastereomer: IR (film) 3391, 3062, 3032, 2944, 2867, 1741, 1698, 1601, 1525, 1496 cm^{-1} ; ^1H NMR (600 MHz, CDCl_3) δ 8.07 (br d, $J = 3.4$ Hz, 1H), 7.98 (d, $J = 8.0$ Hz, 2H), 7.53 (dd, $J = 8.3, 7.0$ Hz, 1H), 7.37–7.30 (m, 7H), 7.28–7.19 (m, 12H), 7.16 (d, $J = 7.5$ Hz, 2H), 7.13 (d, $J = 7.5$ Hz, 1H), 7.11 (d, $J = 7.8$ Hz, 1H), 7.04 (br d, $J = 7.0$ Hz, 1H), 6.99 (br dd, $J = 7.5, 7.0$ Hz, 1H), 6.89 (br s, 2H), 5.28 (m, 2H), 5.01 (br s, 1H), 4.97 (d, $J = 15.5$ Hz, 1H), 4.86 (d, $J = 15.5$ Hz, 1H), 4.48 (br d, $J = 4.1$ Hz, 1H), 4.29 (br d, $J = 4.4$ Hz, 1H), 4.22 (d, $J = 9.6$ Hz, 1H), 4.17 (d, $J = 15.3$ Hz, 1H), 3.98 (d, $j = 9.8$ Hz, 1H), 3.90 (d, $J = 15.3$ Hz, 1H), 3.67 (m, 1H), 3.62 (br s, 1H), 3.52 (m, 1H), 3.49 (br s, 1H), 3.33 (dd, $J = 10.1, 4.7$ Hz, 1H), 2.97 (dd, $J = 10.5, 3.5$ Hz, 1H), 1.34 (s, 9H), 1.28–1.20 (m, 2H), 1.11 (d, $J = 7.2$ Hz, 3H), 1.08 (d, $J = 7.3$ Hz, 3H), 1.07–0.96 (m, 11H), 0.95–0.85 (m, 6H), 0.80 (m, 1H), 0.75–0.66 (m, 4H), carboxylic acid OH was not observed; ^{13}C NMR (150 MHz, CDCl_3) ppm 171.0, 166.8, 164.8, 158.8, 157.5, 157.3, 143.1, 135.4, 134.4, 133.8, 130.4, 128.7, 128.5, 128.3, 128.0, 127.9, 127.7, 127.6, 127.1, 87.1, 80.5, 73.6, 73.5, 73.2, 67.7, 65.3, 63.5, 60.8, 60.0, 55.0, 47.0, 46.2, 41.3, 33.0, 28.1, 28.0, 17.63, 17.58, 17.5, 17.39, 17.36, 16.7, 16.6, 14.2, 13.6, 12.5, 12.4; HRMS (ESI): Exact mass calcd for $\text{C}_{72}\text{H}_{88}\text{N}_4\text{NaO}_{15}\text{Si}_2$ $[\text{M} + \text{Na}]^+$ 1327.5682, found 1327.5653.



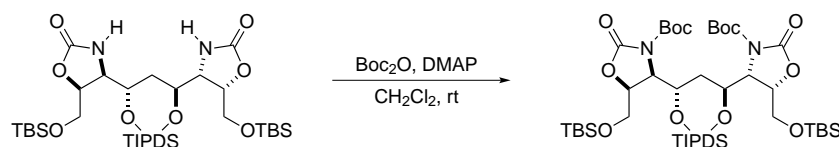
Amide 386. A solution of the carboxylic acid (8.4 mg, 6.4 μmol) in THF (300 μL) was cooled to 0 °C and NMM (2.2 μL , 19 μmol) was added via syringe. The reaction mixture was cooled to -20 °C and $t\text{-BuO}_2\text{CCl}$ (3.0 μL , 23 μmol) was added via syringe. The reaction was stirred at -15 °C for 2 h and then NH_4OH (28–30 %, 20 μL) was added via syringe and the reaction was warmed to rt and stirred for additional 6 h. The reaction was quenched with satd aq NH_4Cl and the resulting mixture was extracted with ethyl acetate. The combined organic layers were dried, concentrated, and the residue was dissolved in anhydrous methanol. The methanol solution was concentrated and purified using preparative HPLC (XBridgeTM Prep C18 5 μm ODBTM 19 \times 150 μm column) using the following program: 10 mL min^{-1} 40 min gradient from 40 % buffer A (95 % water, 5 % acetonitrile, 5 mM NH_4OAc) and 60 % buffer B (95 % acetonitrile, 5 % water, 5 mM NH_4OAc) to 100 % buffer B and then 40 min buffer B; t_r = 59.7 min. Removal of solvent gave the desired amide as a colorless oil (5.0 mg, 59 %). $[\alpha]_D^{20}$ -49.2 (c 0.50, CHCl_3); IR (film) 3338, 3061, 3032, 2945, 2867, 1746, 1681, 1520, 1445 cm^{-1} ; ^1H NMR (600 MHz, CDCl_3) δ 10.11 (br s, 1H), 8.65 (d, J = 5.0 Hz, 1H), 8.17 (d, J = 8.3 Hz, 2H), 7.65 (ddd, J = 7.5, 1.2, 1.2 Hz, 1H), 7.49 (d, J = 8.0 Hz, 1H), 7.47 (d, J = 7.8 Hz, 1H), 7.38–7.27 (m, 12H), 7.26–7.16 (m, 13H), 6.79 (br s, 1H), 5.77 (br s, 1H), 5.30 (br s, 1H), 5.20 (dd, J = 6.2, 5.9 Hz, 1H), 4.92 (d, J = 15.3 Hz, 1H), 4.82 (d, J = 14.8 Hz, 1H), 4.48 (m, 1H), 4.33 (br d, J = 4.6 Hz, 1H), 4.27 (d, J = 12.0 Hz, 1H), 4.18 (d, J = 15.3 Hz, 1H), 4.10 (br s, 1H), 4.09 (d, J = 15.0 Hz, 1H), 3.99 (d, J = 11.5 Hz, 1H), 3.70 (br s, 1H), 3.59 (m, 2H), 3.29 (dd, J = 9.9, 4.8 Hz, 1H), 3.04 (dd, J = 10.5, 4.0 Hz, 1H), 1.66 (dd, J = 12.8, 12.0 Hz, 2H), 1.41 (s, 9H), 1.15 (d, J = 7.4 Hz, 3H), 1.11 (d, J = 7.3 Hz, 3H), 1.07 (d, J = 7.6 Hz, 3H), 1.05–0.95 (m, 11H), 0.94 (m, 3H), 0.83 (m, 1H), 0.72 (br s, 4H); ^{13}C NMR (150 MHz, CDCl_3) ppm 171.7, 166.0, 165.3, 158.4, 157.9, 157.2, 143.2, 135.6, 134.5, 134.0, 130.3, 128.8, 128.7, 128.7, 128.51, 128.48, 128.3, 128.2, 128.0, 127.9, 127.7, 127.1, 87.1, 80.5, 75.3, 74.1, 73.5, 67.8, 64.6, 63.7, 61.6, 60.9, 55.7, 47.1, 46.9, 42.3, 20.5, 17.62, 17.59, 17.47, 17.40, 17.36, 16.68, 16.66, 14.2, 13.6, 12.5; HRMS (ESI): Exact mass calcd for $\text{C}_{72}\text{H}_{89}\text{N}_5\text{NaO}_{14}\text{Si}_2$ $[\text{M} + \text{Na}]^+$ 1326.5842, found 1326.5819.

The same reaction performed on the second (major) diastereomer of the carboxylic acid (12.1 mg, 9.2 μmol) using (3.0 μL , 27 μmol) of NMM, (4 μL , 30 μmol) of $t\text{-BuO}_2\text{CCl}$ and (30 μL) of NH_4OH in (300 μL) of THF afforded the amide as a colorless oil (10.5 mg, 86 %) after HPLC. $[\alpha]_D^{20}$ -53.2 (c 10.5, CHCl_3); ^1H NMR (500 MHz, CDCl_3) δ 8.44 (d, J = 5.7 Hz, 1H), 8.12 (d, J = 7.7 Hz, 2H), 7.65 (dd, J = 7.5, 7.2 Hz, 1H), 7.49 (dd, J = 7.8, 7.7 Hz, 2H), 7.33 (d, J = 7.6 Hz, 6H), 7.28–7.18 (m, 10H), 7.18–7.08 (m, 6H), 7.06 (dd, J = 8.6, 6.7 Hz, 1H), 6.96 (dd, J = 7.6, 7.3 Hz, 2H), 6.71 (br s, 1H), 5.48 (br s, 1H), 5.25 (br dd, J = 6.1, 5.9 Hz, 1H), 4.96–4.86 (m, 3H), 4.45 (m, 1H), 4.28–4.19 (m, 2H), 4.14 (d, J = 0 Hz, 1H), 3.99 (m, 1H), 3.95 (d, J = 14.9 Hz, 1H), 3.63 (br d, J = 3.9 Hz, 1H), 3.60–3.46 (m, 3H), 3.29 (dd, J = 10.6, 4.8 Hz, 1H), 3.00 (dd, J = 10.3, 3.9 Hz,

1H), 1.20 (s, 9H), 1.14–1.09 (m, 6H), 1.08–0.98 (m, 12H), 0.97–0.088 (m, 6H), 0.83 (m, 2H), 0.74 (s, 4H), downfield amide N–H was not observed; ¹³C NMR (125 MHz, CDCl₃) ppm 171.4, 166.8, 165.6, 158.1, 157.8, 157.0, 143.1, 135.4, 134.7, 134.0, 130.6, 128.7, 128.6, 128.5, 128.1, 128.0, 127.9, 127.74, 127.69, 127.2, 87.2, 80.2, 73.8, 73.5, 72.9, 67.8, 65.0, 63.7, 60.9, 60.1, 55.6, 47.1, 46.3, 42.5, 33.1, 28.0, 17.7, 17.6, 17.5, 17.43, 17.36, 17.34, 16.7, 14.3, 13.7, 12.6, 12.4;

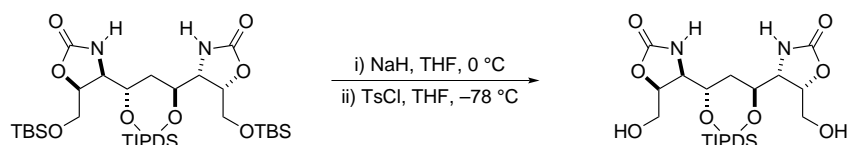


Bis(carbamate) 391. To a suspension of lithium powder (6.6 mg, 940 μ mol) in anhydrous THF (1 mL) was added naphthalene (0.8 mg, 6.0 μ mol). The suspension was vigorously stirred at rt for 30 min and then cooled to -78 °C and stirred for additional 30 min until solution turned dark brown. A solution of carbamate (30.0 mg, 31.3 μ mol) in THF (500 μ L) was added via cannula and the reaction was stirred at -78 °C for 2 h. The reaction was quenched by slow addition of satd aq NH₄Cl and warmed to rt and diluted with ethyl acetate. The layers were separated and the aqueous layer was extracted with ethyl acetate. The combined organic layers were dried, concentrated and the resulting oil was purified using flash chromatography (SiO₂, 30–50 % ethyl acetate in hexanes) to afford the title compound as colorless oil (19.7 mg, 81 %). $[\alpha]_D^{20}$ -23.0 (*c* 3.28, CHCl₃); R_f = 0.27 (40 % EtOAc/hexanes); IR (film) 3265, 3155, 2948, 2865, 1756 cm^{-1} ; ¹H NMR (400 MHz, CDCl₃) δ 5.96 (s, 1H), 4.39 (dd, *J* = 4.9, 4.1 Hz, 1H), 3.99 (m, 1H), 3.80 (dd, *J* = 4.7, 4.0 Hz, 1H), 3.75 (dd, *J* = 11.1, 5.3 Hz, 1H), 3.69 (dd, *J* = 11.0, 4.1 Hz, 1H), 1.50 (dt, *J* = 13.9, 8.1 Hz, 1H), 1.50–0.92 (m, 14H), 0.88 (s, 9H), 0.07 (s, 6H); ¹³C NMR (100 MHz, CDCl₃) 158.8, 68.7, 63.7, 58.9, 33.2, 25.7, 18.2, 17.5, 17.3, 17.2, 13.7, 12.8, -5.5 ppm; HRMS (ESI): Exact mass calcd for C₃₅H₇₂N₂NaO₉Si₂ [M+Na]⁺ 799.4213, found 799.4201.

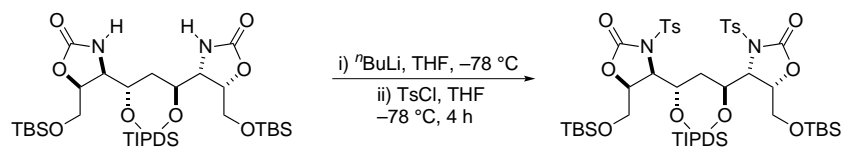


Bis(carbamate) 392. To a solution of the carbamate (30.1 mg, 38.7 μ mol) in DCM 200 μ L at 0 °C was added Boc₂O (84.5 mg, 387 μ mol), followed by DMAP (23.7 mg, 194 μ mol). The solution was warmed to rt and stirred overnight. The reaction mixture was concentrated and the residue was purified using flash chromatography (SiO₂, 10–25 % ethyl acetate in hexanes) to afford the title compound as a colorless oil (42.3 mg, 99 %). $[\alpha]_D^{20}$ 13.4 (*c* 2.12, CHCl₃); R_f = 0.77 (40 % EtOAc/hexanes); IR (film) 2933, 2865, 1800, 1720 cm^{-1} ; ¹H NMR (400 MHz, CDCl₃) δ 4.57 (d,

$J = 3.0$ Hz, 1H), 4.53 (dd, $J = 8.6, 6.3$ Hz, 1H), 4.08 (d, $J = 2.7$ Hz, 1H), 3.80 (dd, $J = 11.2, 4.0$ Hz, 1H), 3.57 (dd, $J = 11.2, 2.2$ Hz, 1H), 1.46 (s, 9H), 1.30 (dt, $J = 13.0, 7.0$ Hz, 1H), 1.07–0.92 (m, 12H), 0.85 (s, 9H), 0.85–0.67 (m, 2H), 0.05 (s, 3H), 0.05 (s, 3H); ^{13}C NMR (100 MHz, CDCl_3) 151.3, 149.9, 83.7, 81.0, 72.5, 65.9, 64.0, 61.2, 36.8, 18.0, 17.5, 17.2, 17.0, 13.7, 12.7, -5.5, -5.6 ppm; HRMS (ESI): Exact mass calcd for $\text{C}_{45}\text{H}_{88}\text{N}_2\text{NaO}_{13}\text{Si}_2$ $[\text{M}+\text{Na}]^+$ 999.5261, found 999.5229.

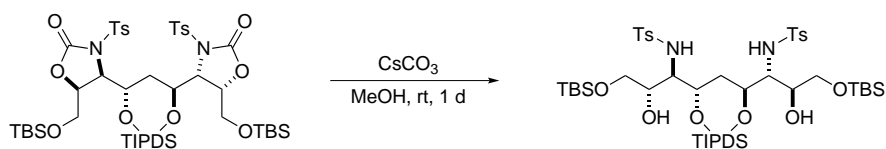


Bis(alcohol) 431. To a solution of the carbamate (52.0 mg, 66.9 μmol) in dimethylformamide (300 μL) at 0 $^\circ\text{C}$ was added sodium hydride (4.8 mg, 200 μmol). The solution was stirred for 30 min and then cooled to -78 $^\circ\text{C}$. Tosyl chloride (37.1 mg, 167 μmol) was added in one portion and the reaction was warmed to rt. The reaction was quenched with water and extracted with ethyl acetate. The combined organic layers were dried, concentrated, and the residue was purified using flash chromatography (SiO_2 , 25% methanol in dichloromethane) to afford the bis(alcohol) as a clear oil (4.2 mg, 11%) $[\alpha]_{\text{D}}^{20} -36.2$ (c 0.82, EtOH); $R_f = 0.23$ (10% MeOH/ CH_2Cl_2); IR (film) 3336, 3288, 3271, 2941, 2927, 2866, 1739, 1658, 1461 cm^{-1} ; ^1H NMR (600 MHz, CD_3OD) δ 4.63 (dd, $J = 8.6, 4.4$ Hz, 1H), 4.60 (br s, 1H), 4.18–4.11 (m, 1H), 3.79–3.72 (m, 2H), 3.62 (dd, $J = 12.1, 4.3$ Hz, 1H), 1.45 (ddd, $J = 13.9, 8.1$ Hz, 1H), 1.19–1.00 (m, 14H), O–H resonances were not observed; ^{13}C NMR (150 MHz, CD_3OD) ppm 161.6, 78.6, 69.5, 64.2, 60.1, 36.6, 18.2, 17.93, 17.89, 17.7, 15.0, 14.2; HRMS (ESI): Exact mass calcd for $\text{C}_{23}\text{H}_{44}\text{N}_2\text{NaO}_9\text{Si}_2$ $[\text{M}+\text{Na}]^+$ 571.2483, found 571.2498.

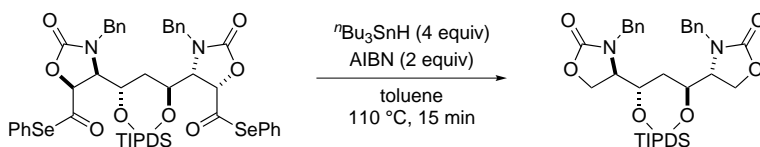


Sulfonamide 394. To a solution of the carbamate (15.5 mg, 20.0 μmol) in tetrahydrofuran (200 μL) at -78 $^\circ\text{C}$ was added *n*-butyllithium (2.5 M in hexanes, 20 μL , 50 μmol) and the solution was stirred for 30 min. *p*-Toluenesulfonyl chloride (8.8 mg, 43 μmol) was added in one portion, the reaction was stirred for 4 h at -78 $^\circ\text{C}$, and then quenched with satd aq NH_4Cl . The reaction mixture was extracted with ethyl acetate, and the combined organic layers were dried and concentrated. The yellow residue was purified using flash chromatography (SiO_2 , 10–25% ethyl acetate in hexanes) to afford the product as a clear oil (19.8 mg, 91%). $[\alpha]_{\text{D}}^{20} -24.4$ (c 1.98, EtOH); $R_f = 0.55$ (50% MeOH/ CH_2Cl_2); IR (film) 3066, 3033, 2848, 2832, 2897, 2864, 1789, 1465 cm^{-1} ; ^1H NMR (600 MHz,

CD₃OD) δ 7.96 (d, $J = 8.3$ Hz, 2H), 7.33 (d, $J = 8.1$ Hz, 2H), 4.68 (dd, $J = 7.5, 4.3$ Hz, 1H), 4.53 (ddd, $J = 14.0, 8.0, 8.0$ Hz, 1H), 4.19 (d, $J = 2.9$ Hz, 1H), 3.56 (d, $J = 4.6$ Hz, 2H), 2.44 (s, 3H), 1.35 (dt, $J = 13.8, 8.0$ Hz, 1H), 1.17–1.08 (m, 6H), 1.00–0.97 (m, 3H), 0.94–0.90 (m, 3H), 0.84 (s, 9H), 0.81–0.75 (m, 2H), 0.03 (s, 3H), –0.05 (s, 3H); ¹³C NMR (150 MHz, CDCl₃) ppm 152.2, 145.6, 135.0, 129.8, 129.7, 128.5, 127.9, 74.0, 68.4, 63.9, 63.4, 37.1, 25.8, 21.7, 18.5, 17.5, 16.9, 13.7, 12.9, –5.4, –5.6; HRMS (ESI): Exact mass calcd for C₄₉H₈₄N₂NaO₁₃S₂Si₄ [M+Na]⁺ 1107.4390, found 1107.4420.

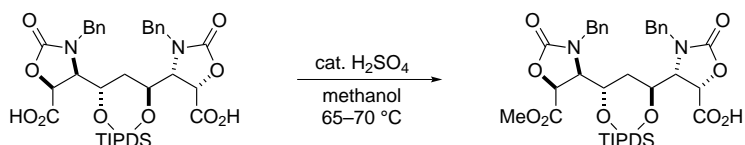


Diol 395. To a vial containing bis(*N*-tosyl carbamate) (9.5 mg, 8.8 μ mol) and Cs₂CO₃ (8.5 mg, 26 μ mol) was added anhydrous methanol (200 μ L), and the reaction was stirred at ambient temperature for 1 day. The reaction was quenched with satd aq NH₄Cl and extracted with ethyl acetate. The combined extracts were dried, concentrated, and purified using flash chromatography (SiO₂, 25–75% ethyl acetate in hexanes) to afford the product as a colorless oil (4.6 mg, 51%). $[\alpha]_D^{20}$ 20.2 (c 0.46, CHCl₃); $R_f = 0.25$ (50% EtOAc/hexanes); IR (film) 3491, 3307, 3032, 2931, 2893, 2864, 1599 cm⁻¹; ¹H NMR (400 MHz, CDCl₃) δ 7.75 (d, $J = 8.1$ Hz, 2H), 7.28 (d, $J = 8.4$ Hz, 2H), 5.18 (d, $J = 7.6$ Hz, 1H), 4.27 (ddd, $J = 8.4, 5.5, 2.8$ Hz, 1H), 3.94 (dd, $J = 7.6, 6.0$ Hz, 1H), 3.27–3.18 (m, 2H), 3.12 (dd, $J = 10.3, 5.7$ Hz, 1H), 3.00 (d, $J = 1.8$ Hz, 1H), 2.41 (s, 3H), 1.61 (dt, $J = 14.0, 8.3$ Hz, 1H), 1.14–0.78 (m, 21H), –0.02 (s, 3H), –0.05 (s, 3H) (N–H and O–H peaks were not observed); ¹³C NMR (125 MHz, CDCl₃) ppm 143.2, 138.3, 129.6, 127.0, 72.1, 70.2, 63.9, 57.4, 37.3, 25.8, 25.7, 21.5, 18.2, 17.5, 17.42, 17.37, 17.2, 13.5, 12.5, –5.49, –5.51; HRMS (ESI): Exact mass calcd for C₄₇H₈₈N₂NaO₁₁S₂Si [M+Na]⁺ 1055.4804, found 1055.4791.

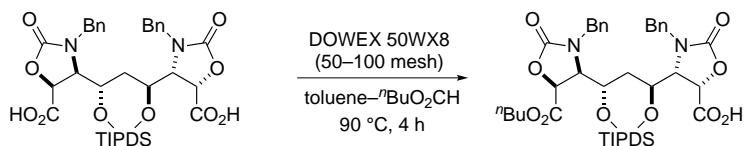


Bis(carbamate) 397. To a solution of the selenoester (9.9 mg, 9.6 μ mol) in toluene (100 μ L) at rt was added ⁿBu₃SnH (10.2 μ L, 38.4 μ mol) and the solution was heated to 100 °C. To a hot reaction mixture was added AIBN (3.1 mg, 19 μ mol) in one portion, and the reaction was stirred at 100 °C for 20 min. The reaction mixture was cooled to rt, concentrated, and purified using flash chromatography (SiO₂, 25–75% ethyl acetate in hexanes) to afford the product as a colorless oil (5.1 mg, 80%). $[\alpha]_D^{20}$ –11.7 (c 0.52, CHCl₃); $R_f = 0.2$ (30% EtOAc/hexanes); IR (film) 2943,

2867, 1452 cm^{-1} ; ^1H NMR (500 MHz, CDCl_3) δ 7.53–7.29 (m, 3H), 7.29–7.17 (m, 2H), 4.98 (d, $J = 15.5$ Hz, 1H), 4.35–4.11 (m, 3H), 4.02 (d, $J = 15.3$ Hz, 1H), 3.63 (dd, $J = 8.8, 4.9$ Hz, 1H), 1.54–0.76 (m, 15H); ^{13}C NMR (125 MHz, CDCl_3) ppm 158.5, 135.5, 128.9, 128.1, 128.0, 66.2, 62.7, 58.2, 46.6, 34.1, 17.6, 17.45, 17.40, 16.8, 14.1, 12.7; HRMS (ESI): Exact mass calcd for $\text{C}_{35}\text{H}_{52}\text{N}_2\text{NaO}_7\text{Si}_2$ $[\text{M} + \text{Na}]^+$ 691.3211, found 691.3212.



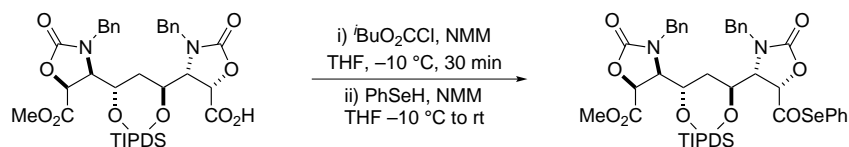
Methyl ester 398. To a solution of the bis(carboxylic acid) (570 mg, 753 μmol) in methanol (5 mL) was added conc. H_2SO_4 (1.0 μL , 18 μmol) and the reaction was heated to reflux and stirred for 6–8 h. The reaction mixture was cooled, concentrated, diluted with ethyl acetate, and washed with water. The combined aqueous layers were extracted with ethyl acetate and the combined extracts were dried and concentrated. The resulting yellow oil was dissolved in anhydrous methanol and filtered. The methanol solution was concentrated and purified using preparative HPLC (XBridgeTM Prep C18 5 μm ODBTM 19 \times 150 μm column) using the following program: 10 mL min^{-1} , 23 min gradient from 77 % buffer A (99.9 % water, 0.1 % TFA) and 23 % buffer B (99.9 % acetonitrile, 0.1 % TFA) to 100 % buffer B and then 5 min buffer B; $t_r(\text{diacid}) = 8.5$ min, $t_r(\text{monoester}) = 16.2$ min, $t_r(\text{diester}) = 23.6$ min. Removal of solvent gave the desired product as a colorless oil (242 mg, 41 %) together with the unreacted bis(carboxylic acid) (110 mg, 19 %) and bis(methyl ester) (90 mg, 15 %); $[\alpha]_{\text{D}}^{20} -28.7$ (c 2.01, CHCl_3); $R_f = 0.50$ (20 % $\text{MeOH}/\text{CH}_2\text{Cl}_2$); IR (film) 3488, 3030, 2947, 2868, 1766, 1439 cm^{-1} ; ^1H NMR (400 MHz, CDCl_3) δ 7.37–7.22 (m, 5H), 7.22–7.10 (m, 5H), 6.90 (br s, 1H), 4.92 (d, $J = 14.8$ Hz, 1H), 4.80 (d, $J = 15.4$ Hz, 1H), 4.66 (d, $J = 3.9$ Hz, 1H), 4.57 (d, $J = 3.4$ Hz, 1H), 4.24 (d, $J = 10.9$ Hz, 1H), 4.19 (d, $J = 11.7$ Hz, 1H), 4.06 (d, $J = 15.4$ Hz, 1H), 4.02 (d, $J = 15.4$ Hz, 1H), 4.71 (d, $J = 3.6$ Hz, 1H), 3.68 (s, 3H), 3.61 (d, $J = 3.9$ Hz, 1H), 1.60 (dd, $J = 13.0, 12.0$ Hz, 1H), 1.40 (dd, $J = 12.6, 12.3$ Hz, 1H), 1.22–0.72 (m, 28H); ^{13}C NMR (150 MHz, CDCl_3) ppm 175.1, 169.5, 158.7, 157.3, 135.2, 134.9, 128.94, 128.89, 128.1, 127.9, 127.6, 127.4, 127.3, 72.9, 71.2, 67.1, 66.0, 63.5, 62.2, 53.0, 46.7, 46.5, 33.8, 20.9, 17.7, 17.6, 17.50, 17.45, 17.4, 17.3, 16.71, 16.68, 14.0, 13.9, 12.7, 12.5; HRMS (ESI): Exact mass calcd for $\text{C}_{38}\text{H}_{55}\text{N}_2\text{O}_{11}\text{Si}_2$ $[\text{M} + \text{H}]^+$ 771.3344, found 771.3376.



Butyl ester 399. To a flask containing bis(carboxylic acid) (1.514 g, 2.00 mmol) and DOWEX 50WX8 (50–100 mesh, 4 g) was added toluene (36 mL) and $n\text{BuO}_2\text{CH}$ (4 mL). The mixture was heated to 90 °C and vigorously stirred for 4 h. The resin was filtered and washed with acetonitrile and ethanol. The resulting solution was concentrated and purified using flash chromatography (SiO_2 , $\text{AcOH-MeOH-CH}_2\text{Cl}_2$, gradient 1:2:97 to 1:8:91 and then 1:20:79) to afford the bis(ester) as a yellow oil (365 mg, 21 %) the mono ester as a yellow oil (933 mg, 57 %), and the bis(carboxylic acid) as a yellow oil (257 mg, 17 %).

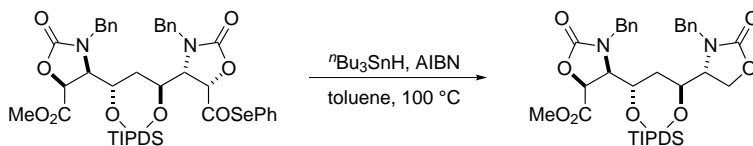
Monoester: $[\alpha]_{\text{D}}^{20} -33.6$ (c 1.48, CHCl_3); $R_f = 0.50$ (20 % $\text{MeOH/CH}_2\text{Cl}_2$); IR (film) 3455, 3065, 3032, 2947, 2869, 1766, 1441 cm^{-1} ; $^1\text{H NMR}$ (400 MHz, CDCl_3) δ 7.38–7.27 (m, 6H), 7.19 (d, $J = 7.3$ Hz, 2H), 7.17 (d, $J = 7.1$ Hz, 2H), 4.98 (d, $J = 15.5$ Hz, 2H), 4.81 (d, $J = 4.5$ Hz, 1H), 4.64 (d, $J = 4.4$ Hz, 1H), 4.30 (d, $J = 10.5$ Hz, 1H), 4.21 (d, $J = 1.1$ Hz, 1H), 4.13 (ddd, $J = 14.9, 10.8, 6.9$ Hz, 1H), 4.09 (ddd, $J = 14.9, 10.8, 6.9$ Hz, 1H), 4.03 (d, $J = 3.2$ Hz, 1H), 3.99 (d, $J = 3.2$ Hz, 1H), 3.62 (d, $J = 4.6$ Hz, 1H), 3.57 (d, $J = 4.0$ Hz, 1H), 2.37 (br, 1H), 1.51 (dt, $J = 13.9, 6.8$ Hz, 2H), 1.40 (m, 2H), 1.25 (dt, $J = 15.2, 7.8$ Hz, 2H), 1.17–0.79 (m, 31H); $^{13}\text{C NMR}$ (100 MHz, CDCl_3) ppm 170.7, 168.8, 157.5, 157.4, 134.7, 134.6, 129.0, 128.9, 128.2, 127.6, 71.2, 70.5, 66.9, 66.1, 65.5, 62.4, 62.1, 46.8, 46.6, 33.9, 30.3, 18.8, 17.51, 17.48, 17.38, 17.36, 17.33, 17.29, 16.6, 14.0, 13.8, 13.5, 12.6; HRMS (ESI): Exact mass calcd for $\text{C}_{41}\text{H}_{60}\text{N}_2\text{NaO}_{11}\text{Si}_2$ $[\text{M}+\text{Na}]^+$ 835.3633, found 835.3636.

Bis(ester): $[\alpha]_{\text{D}}^{20} -34.3$ (c 3.73, CHCl_3); $R_f = 0.95$ (5 % $\text{MeOH/CH}_2\text{Cl}_2$); IR (film) 2930, 2868, 1771, 1496, 1461, 1422 cm^{-1} ; $^1\text{H NMR}$ (400 MHz, CDCl_3) δ 7.37–7.26 (m, 3H), 7.17 (dd, $J = 7.0, 1.2$ Hz, 2H), 5.00 (d, $J = 15.1$ Hz, 1H), 4.71 (d, $J = 4.5$ Hz, 1H), 4.25 (dd, $J = 7.5, 6.2$ Hz, 1H), 4.13 (ddd, $J = 14.9, 10.8, 6.8$ Hz, 1H), 4.09 (ddd, $J = 14.9, 10.8, 6.8$ Hz, 1H), 4.00 (d, $J = 15.4$ Hz, 1H), 3.54 (d, $J = 4.5$ Hz, 1H), 1.53 (m, 2H), 1.36 (dd, $J = 8.3, 5.9$ Hz, 1H), 1.26 (m, 2H), 1.18–1.08 (m, 7H), 1.05 (d, $J = 7.5$ Hz, 3H), 0.96 (d, $J = 7.2$ Hz, 3H), 0.91–0.80 (m, 4H); $^{13}\text{C NMR}$ (100 MHz, CDCl_3) ppm 168.9, 157.2, 134.6, 129.0, 128.2, 127.6, 70.9, 66.1, 65.9, 62.1, 46.6, 34.3, 30.3, 18.8, 17.5, 17.3, 16.6, 14.0, 13.5, 12.6; HRMS (ESI): Exact mass calcd for $\text{C}_{45}\text{H}_{68}\text{N}_2\text{NaO}_{11}\text{Si}_2$ $[\text{M}+\text{Na}]^+$ 891.4261, found 891.4261.

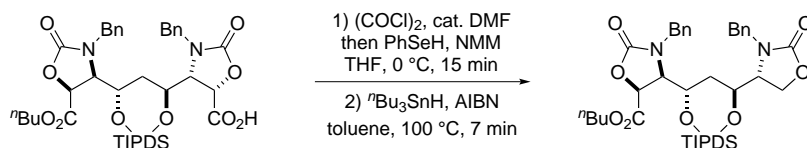


Selenoester 432. To a solution of the carboxylic acid (10.2 mg, 13.2 μmol) in dichloromethane (200 μL) was added *N*-methyl morpholine (4.5 μL , 40 μmol) and the solution was cooled to -10 °C.

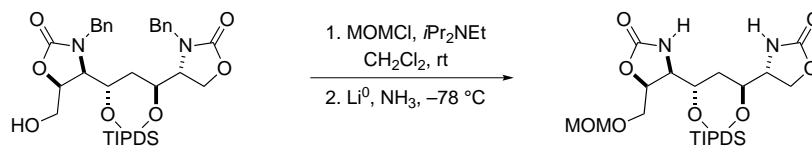
To this solution was added isobutyl chloroformate (5.0 μL , 40 μmol) and the reaction was stirred at -10°C for 30 min. To the reaction mixture was then added *N*-methyl morpholine (4.5 μL , 40 μmol) followed by benzeneselenol (3.0 μL , 26 μmol), and the reaction was warmed to rt and stirred for 1 h. The reaction was quenched with satd aq NH_4Cl , the layers were separated, and the aqueous layer was extracted with dichloromethane. The combined organic layers were dried and concentrated, and the resulting yellow oil was purified using flash chromatography (SiO_2 , 10–50% ethyl acetate in hexanes) to afford the selenoester as a pale yellow oil (5.2 mg, 44%). $[\alpha]_{\text{D}}^{20} -25.4$ (c 0.35, CHCl_3); $R_f = 0.2$ (25% EtOAc/hexanes); IR (film) 3063, 3032, 2946, 2867, 1771, 1714 cm^{-1} ; ^1H NMR (400 MHz, CDCl_3) δ 7.45–7.30 (m, 11H), 7.27 (d, $J = 6.8$ Hz, 2H), 7.18 (d, $J = 6.8$ Hz, 2H), 5.08 (d, $J = 15.5$ Hz, 1H), 5.01 (d, $J = 15.5$ Hz, 1H), 4.79 (d, $J = 4.6$ Hz, 1H), 4.72 (d, $J = 4.1$ Hz, 1H), 4.28 (dd, $J = 8.8, 2.8$ Hz, 1H), 4.25 (dd, $J = 8.8, 2.8$ Hz, 1H), 4.00 (d, $J = 15.5$ Hz, 1H), 3.95 (d, $J = 15.5$ Hz, 1H), 3.68 (s, 3H), 3.52 (dd, $J = 3.8, 0.9$ Hz, 1H), 3.46 (dd, $J = 3.8, 0.9$ Hz, 1H), 1.39–1.29 (m, 2H), 1.18–1.05 (m, 20H) 1.02 (d, $J = 7.6$ Hz, 3H), 1.00 (d, $J = 7.8$ Hz, 3H), 0.93 (m, 2H); ^{13}C NMR (150 MHz, CDCl_3) ppm 204.1, 169.3, 157.0, 156.4, 135.9, 134.6, 134.5, 129.5, 129.4, 129.1, 129.0, 128.4, 128.3, 127.8, 127.6, 124.2, 78.7, 70.5, 65.9, 65.0, 62.3, 62.0, 52.9, 46.7, 46.4, 35.2, 17.6, 17.42, 17.40, 17.37, 16.70, 16.67, 14.2, 14.1, 12.6; HRMS (ESI): Exact mass calcd for $\text{C}_{44}\text{H}_{58}\text{N}_2\text{NaO}_{10}\text{Si}_2\text{Se}$ $[\text{M}+\text{Na}]^+$ 933.2693, found 933.2665.



Ester 433. To a solution of the selenoester (24.9 mg, 27.4 μmol) in toluene (200 μL) at rt was added ⁿBu₃SnH (15 μL , 55 μmol) and the solution was heated to 100 $^\circ\text{C}$. To a hot reaction mixture was added AIBN (4.4 mg, 28 μmol) in one portion, and the reaction was stirred for 20 min at 100 $^\circ\text{C}$. The reaction mixture was cooled to rt, concentrated, and purified using flash chromatography (SiO_2 , 25–75% ethyl acetate in hexanes) to afford the product as a colorless oil (11.5 mg, 58%). $[\alpha]_{\text{D}}^{20} -15.0$ (c 1.15, CHCl_3); $R_f = 0.2$ (25% EtOAc/hexanes); IR (film) 3064, 3031, 2845, 2867, 1760, 1494, 1458, 1438, 1422 cm^{-1} ; ^1H NMR (600 MHz, CDCl_3) δ 7.38–7.27 (m, 6H), 7.23 (d, $J = 7.5$ Hz, 2H), 7.18 (d, $J = 7.5$ Hz, 2H), 5.00 (d, $J = 15.4$ Hz, 1H), 4.97 (d, $J = 15.3$ Hz, 1H), 4.76 (d, $J = 4.5$ Hz, 1H), 4.27 (d, $J = 10.9$ Hz, 1H), 4.23–4.13 (m, 3H), 4.02 (d, $J = 15.1$ Hz, 1H), 3.97 (d, $J = 15.4$ Hz, 1H), 3.73 (s, 3H), 3.63 (ddd, $J = 9.7, 5.4, 1.1$ Hz, 1H), 3.49 (dd, $J = 4.4, 0.7$ Hz, 1H), 1.42–1.36 (m, 1H), 1.18–1.03 (m, 21H), 0.99 (d, $J = 7.6$ Hz, 3H), 0.97 (d, $J = 7.6$ Hz, 3H), 0.90–0.82 (m, 2H); ^{13}C NMR (150 MHz, CDCl_3) ppm 169.5, 158.5, 156.9, 135.5, 134.7, 129.0, 128.9, 128.3, 128.1, 128.0, 127.7, 70.6, 66.1, 65.5, 62.7, 62.1, 58.1, 53.0, 46.6, 46.5, 34.5, 17.59, 17.57, 17.42, 17.37, 16.8, 16.7, 14.10, 14.09, 12.7, 12.6; HRMS (ESI): Exact mass calcd for $\text{C}_{37}\text{H}_{54}\text{N}_2\text{NaO}_9\text{Si}_2$ $[\text{M}+\text{Na}]^+$ 749.3266, found 749.3267.



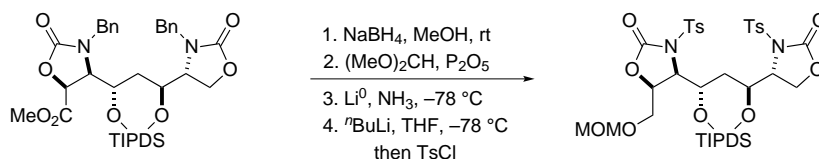
Ester 402. To a solution of the carboxylic acid (812.1 mg, 1.000 mmol) in CH_2Cl_2 (5.00 mL) was added DMF (40 μL , 50 μmol), and the solution was cooled to 0 °C. Oxalyl chloride (430 μL , 5.00 mmol) was added via syringe and the reaction was warmed to rt, stirred for 30 min, and concentrated. In a separate flask, *N*-methyl morpholine (440 μL , 4.00 mmol) was added via syringe, followed by THF (5.00 mL) and benzeneselenol (215 μL , 2.00 mmol). The resulting yellow suspension was stirred at rt for 30 min and cooled to 0 °C. A suspension of the acid chloride in THF (2 mL) was slowly added via cannula. The resulting yellow suspension was stirred at 0 °C for 15 min and then poured into a separatory funnel containing ethyl acetate (100 mL). The resulting solution was washed with satd aq NH_4Cl , and the combined aqueous layers were extracted with ethyl acetate. The combined organic layers were dried and concentrated, and the resulting yellow oil was dried under vacuum over P_2O_5 for 6 h. To a flask containing crude selenoester was added toluene (5.00 mL) and $^t\text{Bu}_3\text{SnH}$ (810 μL , 3.00 mmol) and the solution was heated to 100 °C. AIBN (330 mg, 2.00 mmol) was added in one portion, and the reaction was stirred at 100 °C for 10 min (vigorous gas evolution was observed after ca. 3 min). The reaction was cooled to rt and concentrated, and the residue was purified using flash chromatography (SiO_2 , 15–50 % ethyl acetate in hexanes) to afford the product as a pale yellow oil (515 mg, 67 %). $[\alpha]_{\text{D}}^{20} -25.4$ (c 0.35, CHCl_3); $R_f = 0.2$ (25 % EtOAc/hexanes); IR (film) 3063, 3032, 2946, 2867, 1771, 1714 cm^{-1} ; ^1H NMR (400 MHz, CDCl_3) δ 7.37–7.25 (m, 6H), 7.22 (d, $J = 7.7$ Hz, 2H), 7.17 (d, $J = 7.2$ Hz, 2H), 4.99 (d, $J = 14.7$ Hz, 1H), 4.95 (d, $J = 14.5$ Hz, 1H), 4.68 (d, $J = 4.2$ Hz, 1H), 4.23 (d, $J = 11.1$ Hz, 1H), 4.18 (m, 3H), 4.11 (d, $J = 6.7$ Hz, 1H), 4.09 (d, $J = 7.0$ Hz, 1H), 4.01 (d, $J = 15.0$ Hz, 1H), 3.99 (d, $J = 15.3$ Hz, 1H), 3.61 (dd, $J = 7.5, 7.5$ Hz, 1H), 3.51 (d, $J = 4.4$ Hz, 1H), 1.53 (m, 2H), 1.37 (ddd, $J = 14.4, 11.3, 1.8$ Hz, 1H), 1.31–1.21 (m, 2H), 1.19–1.00 (m, 21H), 1.00–0.91 (m, 6H), 0.90–0.79 (m, 5H); ^{13}C NMR (100 MHz, CDCl_3) ppm 169.0, 158.4, 156.9, 135.4, 134.7, 128.9, 128.8, 128.1, 128.0, 127.9, 127.5, 70.7, 66.0, 65.9, 65.7, 62.5, 62.0, 58.1, 46.5, 34.3, 30.2, 18.8, 17.48, 17.47, 17.33, 17.30, 17.27, 16.7, 16.6, 14.0, 13.9, 13.5, 12.6, 12.5; HRMS (ESI): Exact mass calcd for $\text{C}_{40}\text{H}_{60}\text{N}_2\text{NaO}_9\text{Si}_2$ $[\text{M}+\text{Na}]^+$ 791.3735, found 791.3710.



MOM ether 404. To a solution of the alcohol (490 mg, 700 μmol) in CH_2Cl_2 (1.7 mL at 0 °C) was added DIPEA (905 μL , 7.00 mmol) followed by MOMCl (563 μL , 7.00 mmol). The reaction

was stirred at 0 °C for 1 h and then warmed to rt and stirred for additional 3 h. The reaction was quenched with water and concentrated. The resulting mixture was poured into ether and washed with satd aq NH₄Cl. The combined aqueous layers were extracted with diethyl ether. The combined organic layers were dried and concentrated to give the desired MOM ether (520 mg, 99 %) that was used without further purification.

In a wide tall vial containing lithium (88 mg, 11 mmol), ammonia (ca. 1 mL) was condensed at –78 °C. The resulting deep blue solution was stirred at –78 °C for 1 h. A solution of the MOM ether in THF (200 μL) was added dropwise via syringe and the reaction was stirred at –78 °C for 30 min. The reaction was quenched by addition of solid NH₄Cl and the resulting slurry was allowed to slowly warm to rt. Ethyl acetate (3 mL) was added, and the pH of the aqueous layer was adjusted with solid KHSO₄ to pH 4. The aqueous layer was extracted with ethyl acetate, and the combined organic extracts were dried and concentrated to give the desired product as a colorless solid (301 mg, 76 %), which was used in the next step without further purification. $[\alpha]_D^{20}$ –42.3 (*c* 1.01, CHCl₃); R_f = 0.3 (5 % MeOH/CH₂Cl₂); IR (film) 3280, 3150, 2943, 2867, 1740, 1465, 1412 cm⁻¹; ¹H NMR (400 MHz, CDCl₃) δ 6.57 (s, 1H), 6.51 (s, 1H), 4.64 (s, 2H), 4.54 (dd, *J* = 9.6, 4.7 Hz, 1H), 4.44 (dd, *J* = 9.1, 8.6 Hz, 1H), 4.27 (dd, *J* = 8.8, 5.5 Hz, 1H), 3.99 (m, 2H), 3.87 (ddd, *J* = 9.4, 5.0, 5.0 Hz, 1H), 3.72 (m, 1H), 3.68 (dd, *J* = 4.2, 3.9 Hz, 2H), 3.56 (s, 3H), 1.57 (ddd, *J* = 15.4, 11.2, 2.6 Hz, 1H), 1.46 (ddd, *J* = 15.6, 11.0, 2.6 Hz, 1H), 1.14–0.77 (m, 28H); ¹³C NMR (100 MHz, CDCl₃) ppm 159.9, 159.1, 96.7, 68.7, 68.6, 68.3, 66.5, 59.4, 57.1, 55.5, 34.7, 17.5, 17.3, 17.22, 17.18, 13.8, 13.7, 12.8, 12.7; HRMS (ESI): Exact mass calcd for C₂₄H₄₆N₂NaO₉Si₂ [M + Na]⁺ 585.2640, found 585.2651.

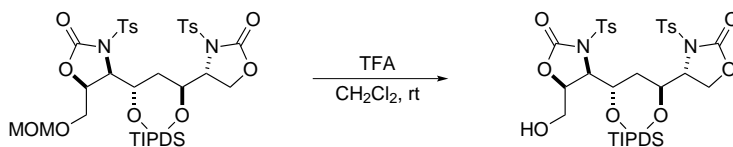


MOM ether 405. To a solution of the ester (47.6 mg, 65.5 μmol) in methanol (1 mL) was added NaBH₄ (7.5 mg, 200 μmol). The reaction was stirred at rt for 30 min, concentrated and diluted with ethyl acetate. The solution was washed with satd aq NH₄Cl, dried and concentrated. The residue was dissolved in CHCl₃ (1 mL) and dimethoxymethane (60 μL, 680 μmol) was added, followed by P₂O₅ (280 mg, 1.0 mmol). The slurry was stirred at rt for 30 min and then poured into ice-cold satd aq Na₂CO₃. The resulting solution was extracted with diethyl ether and the combined organic layers were dried and concentrated to give the product as a colorless oil that was used in the next step without further purification.

In a vial, ammonia (ca. 1 mL) was condensed at –78 °C and lithium (8 mg, 1 mmol) was added. The resulting deep blue solution was stirred at –78 °C for 1 h. A solution of the MOM ether in THF (200 μL) was added dropwise via syringe and the reaction was stirred at –78 °C for 15 min.

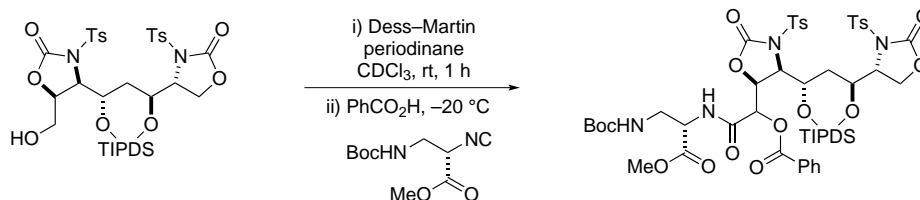
The reaction was quenched by addition of solid NH_4Cl and the resulting slurry was allowed to slowly warm to rt. Ethyl acetate (3 mL) was added, and the pH of the aqueous layer was adjusted with 10% KHSO_4 to pH 4. The aqueous layer was extracted with ethyl acetate, and the combined organic extracts were dried and concentrated to give the desired product as a colorless solid (28.8 mg, 78%), which was used in the next step without further purification.

To a vial containing the carbamate in THF (500 μL) was added $n\text{BuLi}$ (2.5 M in hexanes, 61 μL , 150 μmol), and the solution was stirred at -78°C for 30 min. Tosyl chloride (23.4 mg, 123 μmol) was added in one portion, and the reaction was warmed to 0°C and stirred for 6 h. The reaction was quenched with satd aq NH_4Cl and diluted with ethyl acetate. The layers were separated and the aqueous layer was extracted with ethyl acetate. The combined organic layers were dried and concentrated, and the resulting oil was purified using flash chromatography (SiO_2 , 25–50% ethyl acetate in hexanes) to afford the product as a colorless oil (21.1 mg, 50%). $[\alpha]_{\text{D}}^{20}$ 50.2 (*c* 2.11, CHCl_3); R_f = 0.2 (25% EtOAc/hexanes); IR (film) 2946, 2895, 2868, 1783, 1596, 1493, 1464 cm^{-1} ; ^1H NMR (500 MHz, CDCl_3) δ 7.97 (d, J = 8.6 Hz, 2H), 7.94 (d, J = 9.3 Hz, 2H), 7.36 (d, J = 8.3 Hz, 2H), 7.33 (d, J = 8.3 Hz, 2H), 4.76 (d, J = 2.8 Hz, 1H), 4.61 (dd, J = 11.0, 2.4 Hz, 1H), 4.52 (dd, J = 8.6, 2.8 Hz, 1H), 4.34 (dd, J = 8.6, 2.4 Hz, 1H), 4.28–4.18 (m, 3H), 4.16 (d, J = 3.0 Hz, 1H), 3.62 (dd, J = 11.0, 2.4 Hz, 1H), 3.40 (dd, J = 11.1, 2.3 Hz, 1H), 3.11 (s, 3H), 2.45 (s, 3H), 2.44 (s, 3H), 1.41–1.24 (m, 2H), 1.17–0.99 (m, 24H), 0.97 (d, J = 7.2 Hz, 3H), 0.93–0.81 (m, 2H); ^{13}C NMR (125 MHz, CDCl_3) ppm 152.7, 152.4, 145.8, 145.4, 134.9, 134.7, 129.8, 129.4, 128.7, 128.5, 96.1, 72.8, 68.3, 68.2, 67.7, 63.4, 63.2, 61.3, 55.4, 37.1, 21.70, 21.65, 17.6, 17.50, 17.47, 17.4, 17.0, 13.77, 13.75, 12.8, 12.7; HRMS (ESI): Exact mass calcd for $\text{C}_{38}\text{H}_{58}\text{N}_2\text{NaO}_{13}\text{Si}_2\text{S}_2$ $[\text{M}+\text{Na}]^+$ 893.2817, found 893.2825.

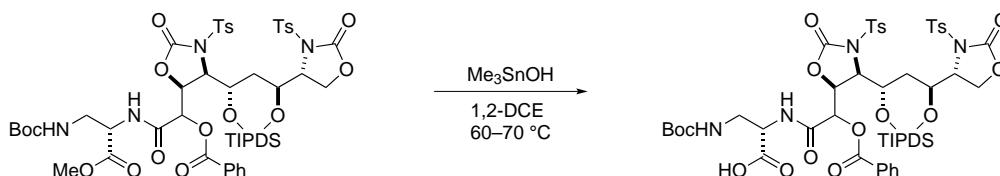


Alcohol 406. To a solution of the alcohol (45.3 mg, 51.9 μmol) in dichloromethane (200 μL) was added trifluoroacetic acid (300 μL). The solution was stirred at rt for 12 h and then concentrated. The residue was purified using flash chromatography (SiO_2 , 75% ethyl acetate in hexanes) to afford the alcohol as a colorless oil (35.4 mg, 82%). $[\alpha]_{\text{D}}^{20}$ +64.0 (*c* 1.71, CHCl_3); R_f = 0.3 (75% EtOAc/hexanes); IR (film) 3549, 3029, 2946, 2894, 2868, 1784, 1596, 1493, 1465 cm^{-1} ; ^1H NMR (500 MHz, CDCl_3) δ 7.95 (d, J = 8.2 Hz, 2H), 7.92 (d, J = 8.2 Hz, 2H), 7.35 (d, J = 8.2 Hz, 2H), 7.32 (d, J = 8.2 Hz, 2H), 4.73 (d, J = 3.0 Hz, 1H), 4.60 (dd, J = 10.8, 3.0 Hz, 1H), 4.53 (m, 2H), 4.32 (dd, J = 9.0, 2.9 Hz, 1H), 4.23 (m, 2H), 3.71 (dd, J = 12.4, 3.5 Hz, 1H), 3.49 (dd, J = 12.2, 2.8 Hz, 1H), 2.44 (s, 3H), 2.42 (s, 3H), 2.12 (br, 1H), 1.35 (m, 2H), 1.20–0.82 (m, 28H); ^{13}C NMR (125 MHz, CDCl_3) ppm 152.8, 152.6, 145.9, 145.7, 134.6, 134.5, 129.8, 129.6, 128.5, 128.4,

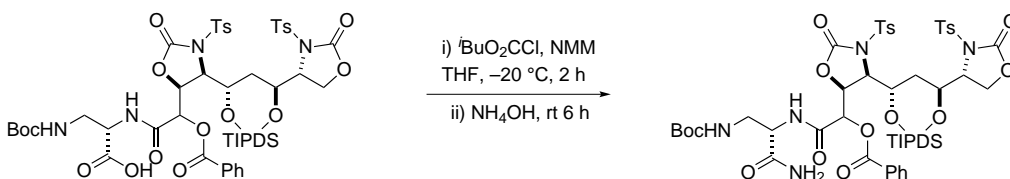
74.3, 68.2, 68.1, 63.3, 63.2, 63.1, 61.2, 37.2, 21.7, 17.50, 17.46, 17.0, 13.8, 12.79, 12.76; HRMS (ESI): Exact mass calcd for $C_{36}H_{54}N_2NaO_{12}Si_2S_2$ $[M+Na]^+$ 849.2554, found 849.2515.



Methyl ester 408. To a flask containing the alcohol (50.2 mg, 60.7 μmol) and Dess–Martin periodinane (27.0 mg, 63.7 μmol) was added $CDCl_3$ (3 mL) at room temperature. The reaction was stirred for 1 h and then benzoic acid (111 mg, 911 μmol) was added in one portion. The reaction was cooled to $-78\text{ }^\circ C$ and the solution of the isonitrile (20.8 mg, 91.0 μmol) in $CDCl_3$ (300 μL) was added via syringe. The reaction was warmed slowly to $-20\text{ }^\circ C$ and stirred for 8 h. A portion of the reaction mixture was analyzed by 1H NMR to determine diastereoselectivity of the reaction (3.7:1 dr). The reaction mixture was warmed to room temperature, concentrated, and the residue was dissolved in diethyl ether. The solution was washed with satd aq $Na_2S_2O_3$ and then with satd aq $NaHCO_3$. The combined aqueous layers were extracted with ether, and the combined organic layers were dried and concentrated. The residue was purified using flash chromatography (SiO_2 , 30–60% ethyl acetate in hexanes) to afford the desired product as a yellow oil (35.6 mg, 50%). IR (film) 3400, 3067, 2947, 2868, 1788, 1434, 1694, 1598, 1520, 1456 cm^{-1} ; 1H NMR (600 MHz, $CDCl_3$) δ 8.09 (dd, $J = 8.5, 1.5$ Hz, 1H), 8.07 (d, $J = 7.6$ Hz, 1H), 8.00–7.96 (m, 2H), 7.80 (d, $J = 8.2$ Hz, 2H), 7.64 (ddd, $J = 7.6, 1.3, 1.2$ Hz, 1H), 7.60 (ddd, $J = 7.4, 1.3, 1.2$ Hz, 1H), 7.49–7.42 (m, 2H), 7.36 (d, $J = 8.2$ Hz, 2H), 7.01 (d, $J = 8.2$ Hz, 2H), 5.51 (d, $J = 2.9$ Hz, 1H), 5.37 (br s, 1H), 4.94 (t, $J = 5.9$ Hz, 1H), 4.66 (dd, $J = 11.5, 1.6$ Hz, 1H), 4.61 (d, $J = 11.3$ Hz, 1H), 4.57 (dd, $J = 7.9, 3.9$ Hz, 1H), 4.47 (m, 1H), 4.39 (d, $J = 3.3$ Hz, 1H), 4.26–4.17 (m, 2H), 3.71 (s, 3H), 3.60–3.49 (m, 2H), 2.45 (s, 3H), 2.30 (s, 3H), 1.49 (ddd, $J = 15.5, 2.3, 2.3$ Hz, 1H), 1.36–1.29 (m, 1H), 1.26 (s, 9H), 1.16–0.79 (m, 28H); ^{13}C NMR (150 MHz, $CDCl_3$) ppm 170.4, 169.6, 165.9, 165.3, 157.1, 152.9, 151.5, 145.7, 145.7, 145.5, 134.6, 134.4, 134.2, 133.6, 130.6, 130.1, 129.9, 129.5, 128.6, 128.45, 128.42, 128.39, 127.6, 80.4, 73.4, 73.2, 68.1, 67.8, 62.8, 62.5, 61.1, 54.7, 52.7, 41.6, 37.0, 28.0, 21.72, 21.70, 17.6, 17.5, 17.4, 17.0, 16.9, 13.9, 13.8, 12.9, 12.8; HRMS (ESI): Exact mass calcd for $C_{53}H_{74}N_4NaO_{18}S_2Si_2$ $[M + Na]^+$ 1197.3876, found 1197.3870.



Carboxylic acid 409. To a vial containing the methyl ester (35.6 mg, 30.0 μmol) in 1,2-DCE (500 μL) was added trimethyltin hydroxide (27.1 mg, 150 μmol) and the resulting solution was stirred at 60–70 °C for 4 h. The reaction mixture was cooled, diluted with dichloromethane and washed with a 10 % solution of aq KHSO_4 . The combined aqueous layers were extracted with ethyl acetate, and the combined organic layers were dried and concentrated. The resulting yellow oil was dissolved in anhydrous methanol and filtered. The methanol solution was concentrated and purified using preparative HPLC (XBridgeTM Prep C18 5 μm ODBTM 19 \times 150 μm column) using the following program: 10 mL min^{-1} 40 min gradient from 40 % buffer A (95 % water, 5 % acetonitrile, 5 mM NH_4OAc) and 60 % buffer B (95 % acetonitrile, 5 % water, 5 mM NH_4OAc) to 100 % buffer B; $t_r = 25.5$ min. Removal of solvent gave the product as a colorless oil (11.5 mg, 32 %). IR (film) 3398, 3067, 2946, 2868, 1788, 1733, 1691, 1598, 1522, 1461 cm^{-1} ; ^1H NMR (600 MHz, CDCl_3) δ 8.27 (br s, 1H), 8.04 (d, $J = 8.1$ Hz, 2H), 7.95 (d, $J = 8.0$ Hz, 2H), 7.80 (d, $J = 8.0$ Hz, 2H), 7.62 (dd, $J = 7.6, 7.5$ Hz, 1H), 7.42 (t, $J = 7.8$ Hz, 2H), 7.34 (d, $J = 8.3$ Hz, 2H), 7.02 (d, $J = 8.1$ Hz, 2H), 5.53 (br d, $J = 2.5$ Hz, 1H), 5.34 (br s, 1H), 5.28 (br s, 1H), 4.61 (d, $J = 12.0$ Hz, 1H), 4.58 (d, $J = 11.8$ Hz, 1H), 4.55 (dd, $J = 8.0, 3.8$ Hz, 1H), 4.43 (br s, 1H), 4.39 (br s, 1H), 4.26 (dd, $J = 9.9, 4.5$ Hz, 1H), 4.20 (dd, $J = 9.1, 8.3$ Hz, 1H), 3.62 (m, 1H), 3.47 (m, 1H), 2.44 (s, 3H), 2.30 (s, 3H), 1.48 (t, $J = 12.6$ Hz, 1H), 1.31 (dd, $J = 12.6, 11.8$ Hz, 1H), 1.22 (s, 9H), 1.13–0.69 (m, 28H) [carboxylic acid proton was not observed]; ^{13}C NMR (150 MHz, CDCl_3) ppm 171.5, 166.5, 165.2, 157.6, 153.0, 151.7, 145.8, 145.6, 134.5, 134.3, 134.2, 130.6, 129.8, 129.5, 128.6, 128.4, 127.5, 80.6, 73.3, 73.0, 68.1, 67.8, 62.75, 62.68, 61.0, 55.2, 41.6, 36.9, 28.0, 21.7, 21.7, 17.6, 17.51, 17.49, 17.4, 17.0, 16.9, 13.8, 13.7, 12.9, 12.7; HRMS (ESI): Exact mass calcd for $\text{C}_{52}\text{H}_{72}\text{N}_4\text{O}_{18}\text{S}_2\text{Si}_2$ [$\text{M} + \text{Na}$]⁺ 1183.3719, found 1183.3678.



Amide 410. A solution of the carboxylic acid (11.5 mg, 10.0 μmol) in THF (300 μL) was cooled to 0 °C and NMM (3.3 μL , 30 μmol) was added via syringe. The reaction mixture was cooled to –20 °C and $t\text{BuO}_2\text{CCl}$ (4.2 μL , 30 μmol) was added via syringe. The reaction was stirred at –15 °C for 2 h and then NH_4OH (28–30 %, 20 μL) was added via syringe and the reaction was warmed to rt and stirred for additional 6 h. The reaction was quenched with satd aq NH_4Cl and the resulting mixture was extracted with ethyl acetate. The combined organic layers were dried, concentrated, and the residue was dissolved in anhydrous methanol. The methanol solution was concentrated and purified using preparative HPLC (XBridgeTM Prep C18 5 μm ODBTM 19 \times 150 μm column) using the following program: 10 mL min^{-1} 30 min gradient from 30 % buffer A (95 % water, 5 %

acetonitrile, 5 mM NH₄OAc) and 70 % buffer B (95 % acetonitrile, 5 % water, 5 mM NH₄OAc) to 100 % buffer B; $t_r = 26.0$ min. Removal of the solvent gave the desired amide as a colorless oil (5.6 mg, 49 %). IR (film) 3360, 3067, 2945, 2868, 1788, 1680, 1598, 1518 cm⁻¹; ¹H NMR (600 MHz, CDCl₃) δ 8.45 (br d, $J = 4.7$ Hz, 1H), 8.08 (d, $J = 8.3$ Hz, 2H), 7.97 (d, $J = 8.3$ Hz, 2H), 7.88 (d, $J = 7.5$ Hz, 2H), 7.64 (t, $J = 7.5$ Hz, 1H), 7.46 (dd, $J = 8.0, 7.5$ Hz, 2H), 7.36 (d, $J = 8.0$ Hz, 2H), 7.13 (d, $J = 8.3$ Hz, 2H), 6.63 (br s, 1H), 5.54 (br s, 1H), 5.29 (m, 2H), 5.24 (dd, $J = 6.5, 6.3$ Hz, 1H), 4.60 (d, $J = 11.8$ Hz, 1H), 4.56 (d, $J = 12.0$ Hz, 1H), 4.52 (dd, $J = 8.0, 3.8$ Hz, 1H), 4.47 (d, $J = 3.3$ Hz, 1H), 4.42 (ddd, $J = 8.5, 3.0, 3.0$ Hz, 1H), 4.24 (dd, $J = 9.8, 4.0$ Hz, 1H), 4.20 (dd, $J = 9.0, 8.5$ Hz, 1H), 3.54 (ddd, $J = 15.1, 6.0, 2.8$ Hz, 1H), 3.44 (ddd, $J = 14.8, 6.3, 6.3$ Hz, 1H), 2.45 (s, 3H), 2.35 (s, 3H), 1.41 (dd, $J = 13.0, 12.3$ Hz, 1H), 1.29 (ddd, $J = 13.8, 2.3, 2.3$ Hz, 1H), 1.21 (s, 9H), 1.16–1.02 (m, 18H), 1.00 (s, 3H), 0.96 (d, $J = 7.3$ Hz, 3H), 0.89 (d, $J = 7.5$ Hz, 3H), 0.70 (m, 1H), ¹³C NMR (150 MHz, CDCl₃) ppm 171.3, 166.2, 166.0, 157.9, 152.8, 151.7, 145.8, 145.8, 134.6, 134.5, 134.4, 130.6, 129.9, 129.6, 128.7, 128.5, 128.4, 127.5, 80.5, 74.1, 73.1, 68.1, 67.9, 62.8, 62.7, 61.1, 55.6, 42.9, 37.0, 28.0, 21.74, 21.71, 17.6, 17.50, 17.49, 17.4, 17.0, 16.9, 13.9, 13.7, 13.0; HRMS (ESI): Exact mass calcd for C₅₂H₇₃N₅NaO₁₇S₂Si₂ [M + Na]⁺ 1182.3879, found 1182.3843.

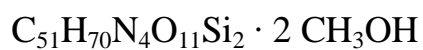
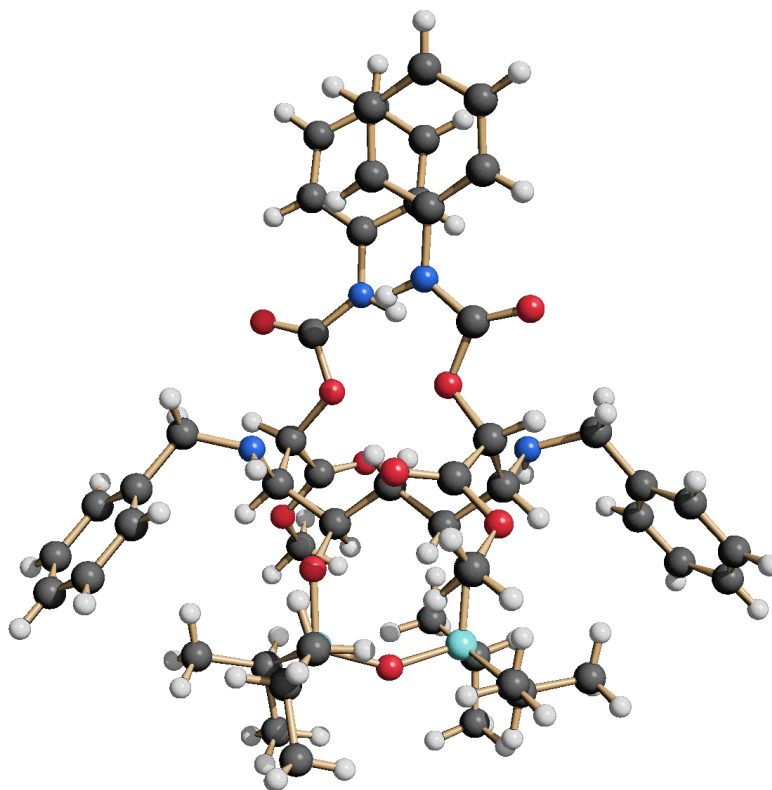
APPENDIX B

X-Ray Crystallography of the compound 345

INDIANA UNIVERSITY DEPARTMENT OF CHEMISTRY

Molecular Structure Center

Report No. 10108



Prepared for
Hubert Muchalski and Professor Jeffrey Johnston

by
M. Pink

November 1, 2010



The sample was submitted by Hubert Muchalski (research group of J. Johnston, Department of Chemistry & Vanderbilt Institute of Chemical Biology, Vanderbilt University). A colorless plate (approximate dimensions $0.23 \times 0.20 \times 0.10 \text{ mm}^3$) was placed onto the tip of a 0.1 mm diameter glass capillary and mounted on a Bruker APEX II Kappa Duo diffractometer equipped with an APEX II detector at 150(2) K.

Data collection

The data collection was carried out using Mo $K\alpha$ radiation (graphite monochromator) with a frame time of 30 seconds and a detector distance of 5.00 cm. A collection strategy was calculated and complete data to a resolution of 0.77 Å with a redundancy of 4 were collected. Five major sections of frames were collected with 0.50° ω and ϕ scans. Data to a resolution of 0.82 Å were considered in the reduction. Final cell constants were calculated from the xyz centroids of 237 strong reflections from the actual data collection after integration (SAINT).¹ The intensity data were corrected for absorption (SADABS).² Please refer to Table 1 for additional crystal and refinement information.

Structure solution and refinement

The polar space group $P2_12_12_1$ was determined based on intensity statistics and systematic absences. The structure was solved using SIR-2004³ and refined with SHELXL-97.⁴ A direct-methods solution was calculated, which provided most non-hydrogen atoms from the E-map. Full-matrix least squares / difference Fourier cycles were performed, which located the remaining non-hydrogen atoms. All non-hydrogen atoms were refined with anisotropic displacement parameters. The hydrogen atoms were placed in ideal positions and refined as riding atoms with relative isotropic displacement parameters with the exception of N and O bound hydrogen atoms. The final full matrix least squares refinement converged to $R1 = 0.0335$ and $wR2 = 0.0621$ (F^2 , all data). The remaining electron density is minuscule and located on bonds.

Structure description

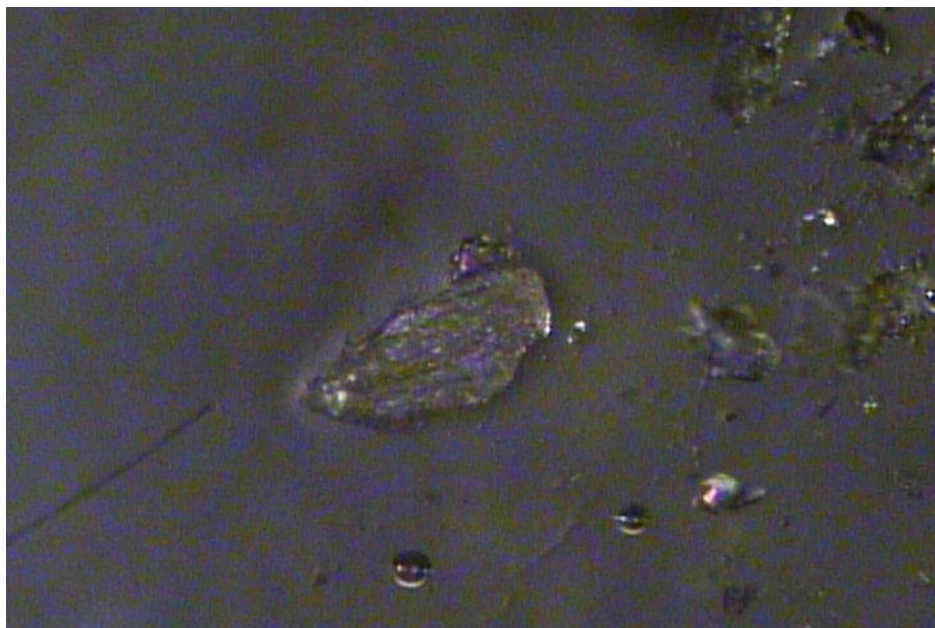
The structure was found as proposed with two solvent molecules per formula unit. The absolute configuration was established by anomalous dispersion effects in the diffraction data; chiral centers have the following configuration: C1, R; C3, R; C4, S; C12, R; C22, S; C30, R. Hydrogen bonding was observed and is listed in the tables.

¹ SAINT, Bruker Analytical X-Ray Systems, Madison, WI, current version.

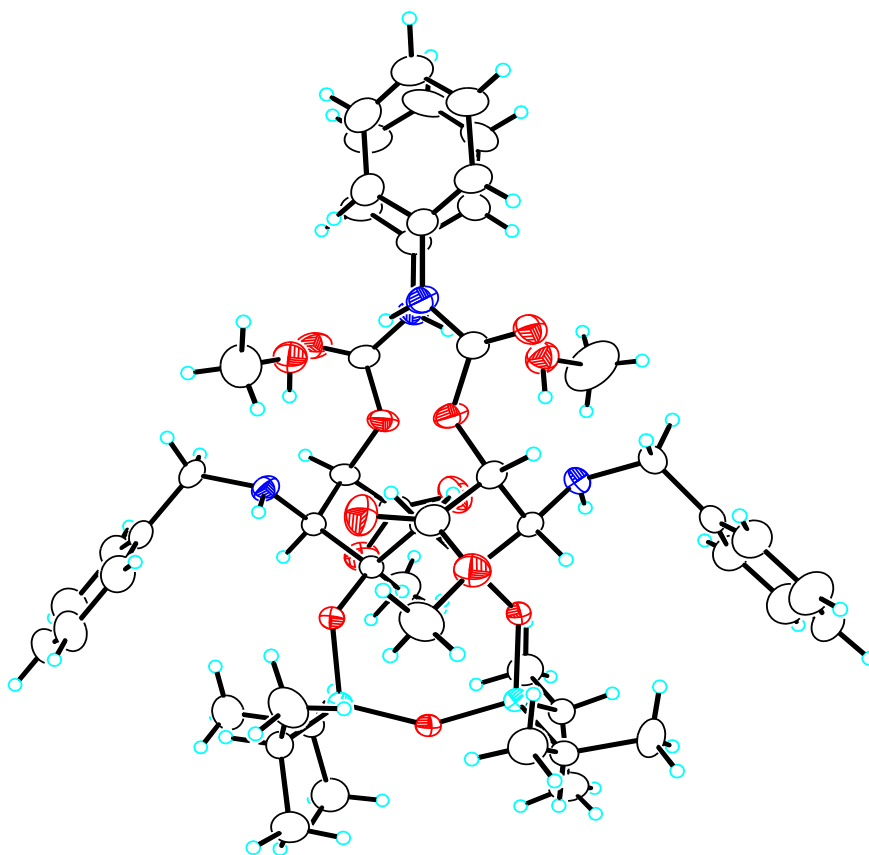
² An empirical correction for absorption anisotropy. R. Blessing, *Acta Cryst.* A51, 33 - 38 (1995).

³ Sir2004, A Program for Automatic Solution and Refinement of Crystal Structures. M. C. Burla, R. Caliandro, M. Carnalli, B. Carrozzini, G. L. Cascarano, L. De Caro, C. Giacovazzo, G. Polidori, R. Sagna. Vers. 1.0 (2004).

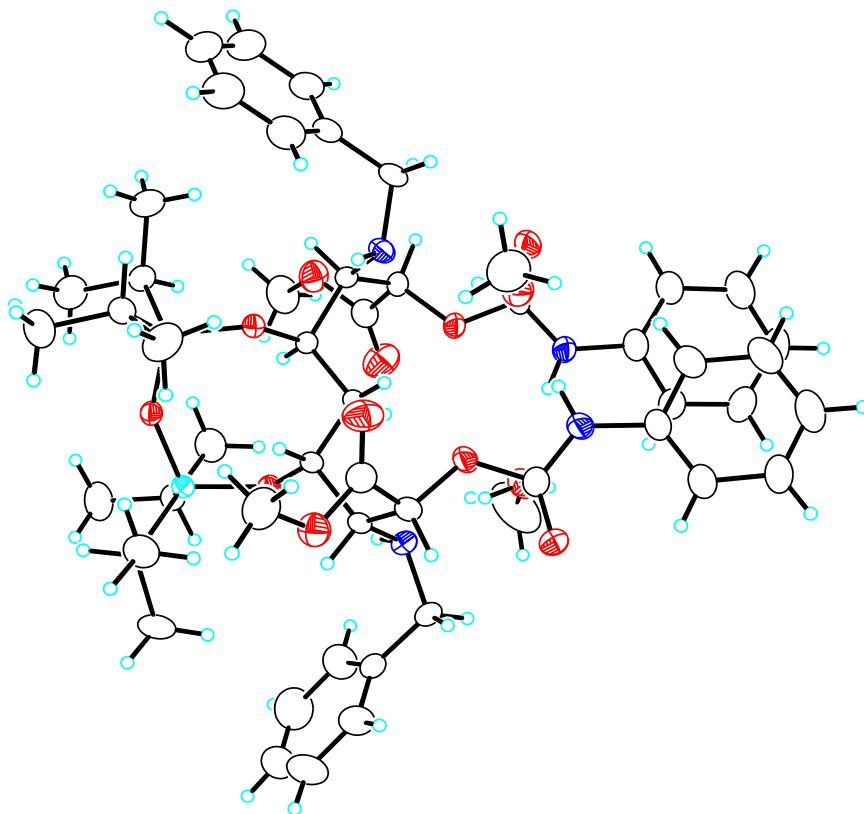
⁴ A short history of *SHELX*. G. M. Sheldrick, *Acta Cryst.* A64, 112 - 122 (2008).



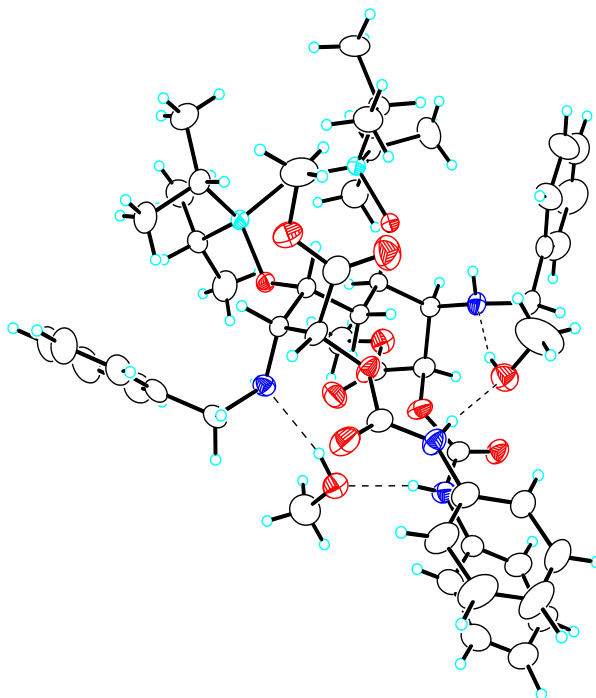
Bulk material.



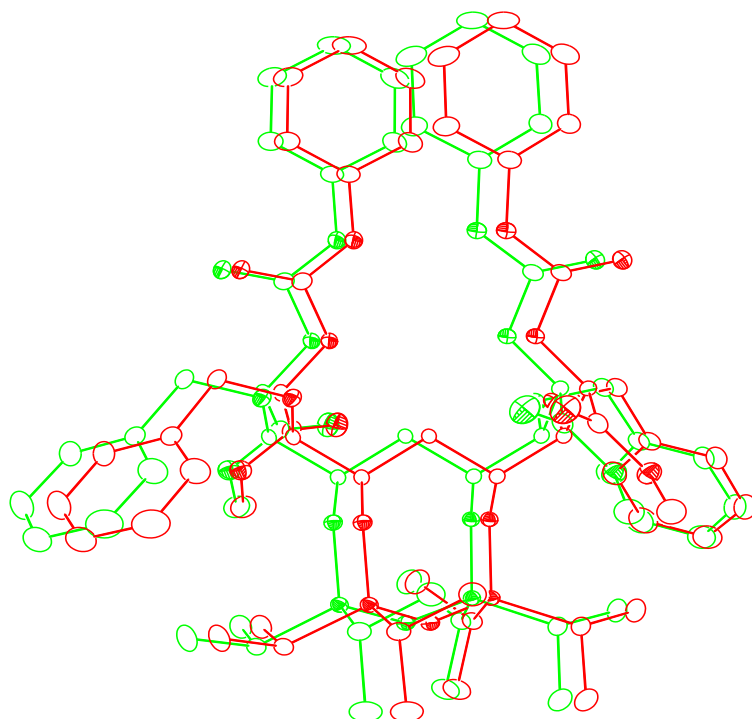
Formula unit.



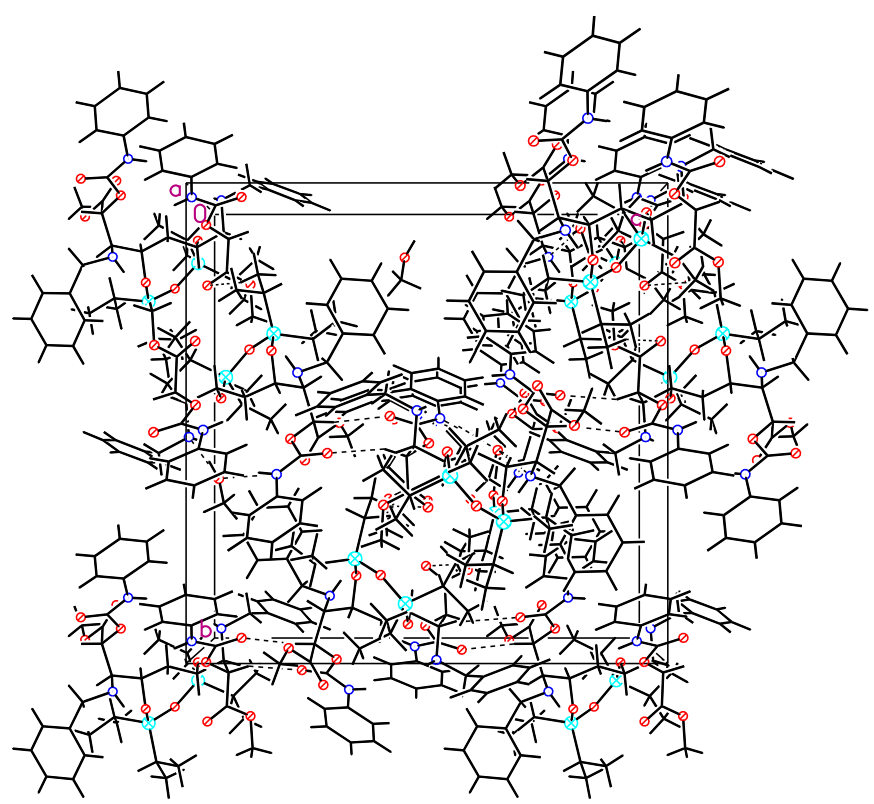
Formula unit, hydrogen atoms and methanol solvent omitted for clarity.



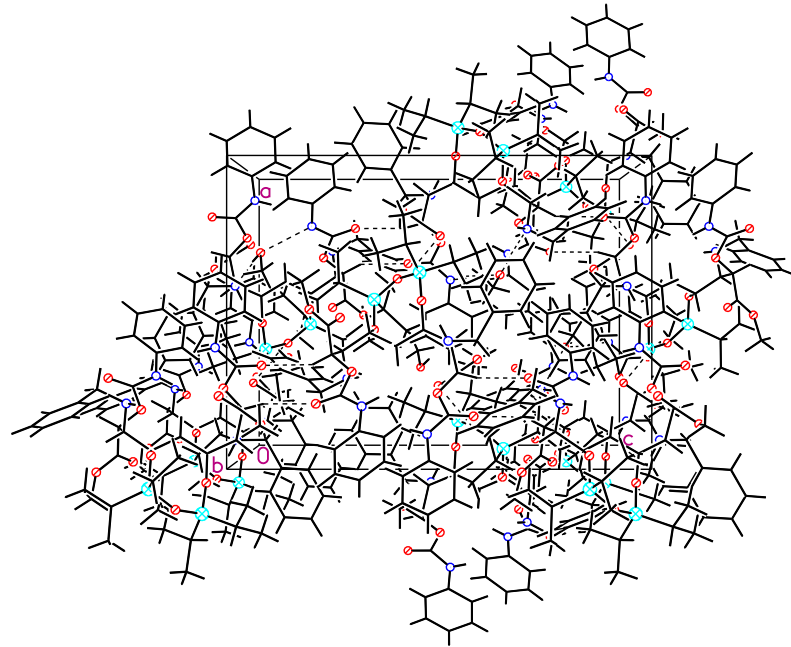
Hydrogen bonding



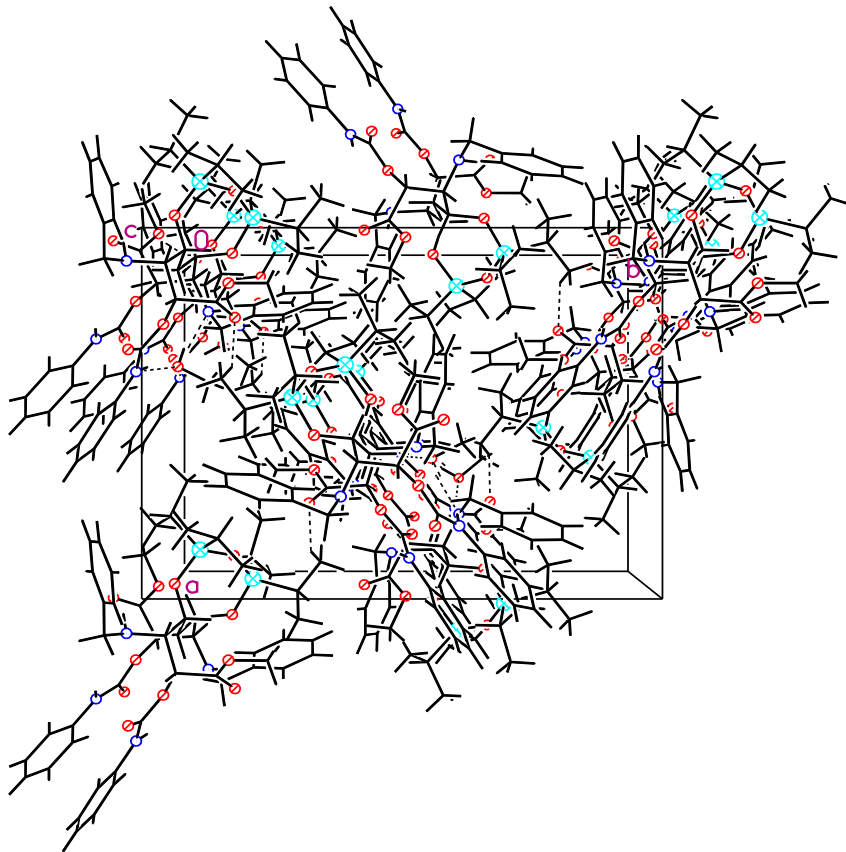
Stereo view.



Cell plot, view along *a*.



Cell plot, view along *b*.



Cell plot, view along *c*.

Table 1. Crystal data and structure refinement for 10108.

Empirical formula	C ₅₃ H ₇₈ N ₄ O ₁₃ Si ₂
Formula weight	1035.37
Crystal color, shape, size	colorless plate, 0.23 × 0.20 × 0.10 mm ³
Temperature	150(2) K
Wavelength	0.71073 Å
Crystal system, space group	Orthorhombic, P2 ₁ 2 ₁ 2 ₁
Unit cell dimensions	a = 14.5176(13) Å □ = 90°. b = 19.5896(18) Å □ = 90°. c = 19.6398(17) Å □ = 90°.
Volume	5585.4(9) Å ³
Z	4
Density (calculated)	1.231 Mg/m ³
Absorption coefficient	0.127 mm ⁻¹
F(000)	2224

Data collection

Diffractionmeter	APEX II Kappa Duo, Bruker
Theta range for data collection	1.47 to 25.07°.
Index ranges	-17 ≤ h ≤ 17, -23 ≤ k ≤ 23, -23 ≤ l ≤ 22
Reflections collected	43241
Independent reflections	9901 [R(int) = 0.0788]
Observed Reflections	7789
Completeness to theta = 25.07°	99.9 %

Solution and Refinement

Absorption correction	Semi-empirical from equivalents
Max. and min. transmission	0.9874 and 0.9713
Solution	Direct methods
Refinement method	Full-matrix least-squares on F ²
Weighting scheme	w = [σ ² F _o ² + AP ²] ⁻¹ , with P = (F _o ² + 2 F _c ²)/3, A = 0.0186
Data / restraints / parameters	9901 / 173 / 679
Goodness-of-fit on F ²	0.902
Final R indices [I > 2σ(I)]	R1 = 0.0335, wR2 = 0.0590
R indices (all data)	R1 = 0.0491, wR2 = 0.0621
Absolute structure parameter	-0.02(7)
Largest diff. peak and hole	0.184 and -0.152 e.Å ⁻³

Goodness-of-fit = [Σ[w(F_o² - F_c²)²]/N_{observns} - N_{params}]^{1/2}, all data.

R1 = Σ(|F_o| - |F_c|) / Σ |F_o|. wR2 = [Σ[w(F_o² - F_c²)²] / Σ [w(F_o²)²]^{1/2}.

Table 2. Atomic coordinates ($\times 10^4$) and equivalent isotropic displacement parameters ($\text{\AA}^2 \times 10^3$) for 10108. U(eq) is defined as one third of the trace of the orthogonalized U_{ij} tensor.

	x	y	z	U(eq)
Si1	-422(1)	2040(1)	8413(1)	22(1)
Si2	-1297(1)	1083(1)	9528(1)	21(1)
O1	570(1)	1633(1)	8423(1)	21(1)
O2	-376(1)	596(1)	9580(1)	22(1)
O3	-1100(1)	1703(1)	8987(1)	22(1)
O4	-93(1)	47(1)	6941(1)	39(1)
O5	168(1)	-786(1)	7699(1)	50(1)
O6	1879(1)	-317(1)	7952(1)	31(1)
O7	2881(1)	-626(1)	7128(1)	43(1)
O8	1547(1)	1726(1)	10922(1)	35(1)
O9	2418(1)	1787(1)	9978(1)	43(1)
O10	2596(1)	410(1)	9960(1)	32(1)
O11	3302(1)	-180(1)	10804(1)	34(1)
N1	2157(1)	1115(1)	7789(1)	26(1)
N2	2935(1)	-1077(1)	8209(1)	30(1)
N3	908(1)	-273(1)	10211(1)	26(1)
N4	3874(1)	-135(1)	9716(1)	30(1)
C1	661(1)	910(1)	8333(1)	20(1)
C2	1074(1)	602(1)	8977(1)	21(1)
C3	566(1)	804(1)	9623(1)	20(1)
C4	1251(1)	804(1)	7690(1)	22(1)
C5	2606(2)	1325(1)	7144(1)	34(1)
C6	2225(2)	1959(1)	6810(1)	32(1)
C7	1891(2)	1937(1)	6156(1)	41(1)
C8	1536(2)	2521(2)	5852(1)	56(1)
C9	1525(2)	3129(1)	6202(1)	59(1)
C10	1863(2)	3158(1)	6851(1)	57(1)
C11	2214(2)	2577(1)	7151(1)	45(1)
C12	1346(2)	60(1)	7467(1)	27(1)
C13	419(2)	-290(1)	7400(1)	32(1)
C14	-973(2)	-251(1)	6781(1)	51(1)
C15	2610(2)	-680(1)	7703(1)	28(1)
C16	3678(2)	-1541(1)	8168(1)	33(1)
C17	3834(2)	-1935(1)	8744(1)	39(1)
C18	4552(2)	-2396(1)	8756(1)	55(1)
C19	5107(2)	-2474(1)	8205(1)	67(1)

C20	4956(2)	-2082(2)	7638(1)	69(1)
C21	4238(2)	-1614(1)	7611(1)	51(1)
C22	961(1)	475(1)	10268(1)	23(1)
C23	892(2)	-626(1)	10874(1)	32(1)
C24	-10(2)	-591(1)	11251(1)	30(1)
C25	-804(2)	-835(1)	10962(1)	47(1)
C26	-1628(2)	-843(2)	11307(2)	66(1)
C27	-1650(2)	-601(2)	11958(2)	72(1)
C28	-882(2)	-337(2)	12254(1)	77(1)
C29	-51(2)	-336(1)	11902(1)	53(1)
C30	1950(1)	692(1)	10436(1)	27(1)
C31	2022(2)	1461(1)	10401(1)	31(1)
C32	1550(2)	2466(1)	10969(1)	45(1)
C33	3274(1)	6(1)	10219(1)	27(1)
C34	4686(2)	-529(1)	9761(1)	30(1)
C35	5162(2)	-633(1)	9152(1)	37(1)
C36	5966(2)	-1008(1)	9148(1)	49(1)
C37	6304(2)	-1279(1)	9743(2)	61(1)
C38	5836(2)	-1167(1)	10345(1)	62(1)
C39	5027(2)	-798(1)	10358(1)	46(1)
C40	-975(2)	1938(1)	7557(1)	30(1)
C41	-414(2)	2320(1)	7013(1)	43(1)
C42	-1993(2)	2150(1)	7522(1)	44(1)
C43	-100(1)	2932(1)	8621(1)	28(1)
C44	616(2)	2969(1)	9187(1)	47(1)
C45	-914(2)	3389(1)	8788(1)	45(1)
C46	-2190(1)	481(1)	9210(1)	28(1)
C47	-3145(2)	807(1)	9139(1)	43(1)
C48	-1900(2)	139(1)	8543(1)	39(1)
C49	-1647(2)	1482(1)	10351(1)	28(1)
C50	-1922(2)	951(1)	10888(1)	48(1)
C51	-942(2)	1974(1)	10640(1)	42(1)
O1S	2030(1)	-1177(1)	9493(1)	38(1)
C1S	1403(2)	-1714(1)	9420(2)	82(1)
O2S	3710(1)	564(1)	8456(1)	38(1)
C2S	4147(2)	1189(1)	8645(1)	58(1)

Table 3. Bond lengths [\AA] and angles [$^\circ$] for 10108.

Si1-O3	1.6354(13)	Si1-O1	1.6467(14)
Si1-C43	1.855(2)	Si1-C40	1.8741(19)
Si2-O3	1.6393(13)	Si2-O2	1.6469(14)
Si2-C46	1.861(2)	Si2-C49	1.864(2)
O1-C1	1.433(2)	O2-C3	1.430(2)
O4-C13	1.343(3)	O4-C14	1.439(3)
O5-C13	1.193(2)	O6-C15	1.368(2)
O6-C12	1.432(2)	O7-C15	1.201(2)
O8-C31	1.338(2)	O8-C32	1.453(3)
O9-C31	1.196(2)	O10-C33	1.361(2)
O10-C30	1.434(2)	O11-C33	1.206(2)
N1-C4	1.462(3)	N1-C5	1.483(2)
N1-H1N	0.865(16)	N2-C15	1.346(2)
N2-C16	1.414(3)	N2-H2N	0.8800
N3-C22	1.471(3)	N3-C23	1.475(2)
N3-H3N	0.848(17)	N4-C33	1.347(2)
N4-C34	1.412(3)	N4-H4N	0.8800
C1-C2	1.524(2)	C1-C4	1.540(2)
C1-H1	1.0000	C2-C3	1.520(2)
C2-H2A	0.9900	C2-H2B	0.9900
C3-C22	1.532(2)	C3-H3	1.0000
C4-C12	1.528(3)	C4-H4	1.0000
C5-C6	1.509(3)	C5-H5A	0.9900
C5-H5B	0.9900	C6-C7	1.374(3)
C6-C11	1.383(3)	C7-C8	1.390(3)
C7-H7	0.9500	C8-C9	1.374(4)
C8-H8	0.9500	C9-C10	1.367(4)
C9-H9	0.9500	C10-C11	1.380(3)
C10-H10	0.9500	C11-H11	0.9500
C12-C13	1.516(3)	C12-H12	1.0000
C14-H14A	0.9800	C14-H14B	0.9800
C14-H14C	0.9800	C16-C21	1.369(3)
C16-C17	1.388(3)	C17-C18	1.379(3)
C17-H17	0.9500	C18-C19	1.359(3)
C18-H18	0.9500	C19-C20	1.370(4)
C19-H19	0.9500	C20-C21	1.390(3)
C20-H20	0.9500	C21-H21	0.9500
C22-C30	1.534(3)	C22-H22	1.0000
C23-C24	1.507(3)	C23-H23A	0.9900
C23-H23B	0.9900	C24-C25	1.371(3)
C24-C29	1.373(3)	C25-C26	1.376(4)

C25-H25	0.9500	C26-C27	1.363(4)
C26-H26	0.9500	C27-C28	1.359(4)
C27-H27	0.9500	C28-C29	1.390(4)
C28-H28	0.9500	C29-H29	0.9500
C30-C31	1.511(3)	C30-H30	1.0000
C32-H32A	0.9800	C32-H32B	0.9800
C32-H32C	0.9800	C34-C39	1.376(3)
C34-C35	1.396(3)	C35-C36	1.379(3)
C35-H35	0.9500	C36-C37	1.375(3)
C36-H36	0.9500	C37-C38	1.381(3)
C37-H37	0.9500	C38-C39	1.380(3)
C38-H38	0.9500	C39-H39	0.9500
C40-C42	1.537(3)	C40-C41	1.537(3)
C40-H40	1.0000	C41-H41A	0.9800
C41-H41B	0.9800	C41-H41C	0.9800
C42-H42A	0.9800	C42-H42B	0.9800
C42-H42C	0.9800	C43-C45	1.519(3)
C43-C44	1.524(3)	C43-H43	1.0000
C44-H44A	0.9800	C44-H44B	0.9800
C44-H44C	0.9800	C45-H45A	0.9800
C45-H45B	0.9800	C45-H45C	0.9800
C46-C48	1.530(3)	C46-C47	1.534(3)
C46-H46	1.0000	C47-H47A	0.9800
C47-H47B	0.9800	C47-H47C	0.9800
C48-H48A	0.9800	C48-H48B	0.9800
C48-H48C	0.9800	C49-C51	1.518(3)
C49-C50	1.535(3)	C49-H49	1.0000
C50-H50A	0.9800	C50-H50B	0.9800
C50-H50C	0.9800	C51-H51A	0.9800
C51-H51B	0.9800	C51-H51C	0.9800
O1S-C1S	1.400(3)	O1S-H1OS	0.95(2)
C1S-H1SA	0.9800	C1S-H1SB	0.9800
C1S-H1SC	0.9800	O2S-C2S	1.429(3)
O2S-H2OS	0.84(3)	C2S-H2SA	0.9800
C2S-H2SB	0.9800	C2S-H2SC	0.9800
O3-Si1-O1	108.82(7)	O3-Si1-C43	112.34(8)
O1-Si1-C43	103.49(8)	O3-Si1-C40	108.55(8)
O1-Si1-C40	109.44(8)	C43-Si1-C40	113.99(9)
O3-Si2-O2	109.16(7)	O3-Si2-C46	111.91(8)
O2-Si2-C46	102.64(8)	O3-Si2-C49	107.40(8)
O2-Si2-C49	114.27(8)	C46-Si2-C49	111.51(9)
C1-O1-Si1	123.96(12)	C3-O2-Si2	127.94(11)
Si1-O3-Si2	148.33(9)	C13-O4-C14	116.02(18)

C15-O6-C12	116.71(15)	C31-O8-C32	115.75(18)
C33-O10-C30	116.97(14)	C4-N1-C5	113.46(16)
C4-N1-H1N	111.8(12)	C5-N1-H1N	107.1(11)
C15-N2-C16	126.59(18)	C15-N2-H2N	116.7
C16-N2-H2N	116.7	C22-N3-C23	113.56(15)
C22-N3-H3N	105.0(12)	C23-N3-H3N	107.6(12)
C33-N4-C34	127.28(18)	C33-N4-H4N	116.4
C34-N4-H4N	116.4	O1-C1-C2	109.06(14)
O1-C1-C4	106.52(14)	C2-C1-C4	114.10(15)
O1-C1-H1	109.0	C2-C1-H1	109.0
C4-C1-H1	109.0	C3-C2-C1	113.44(15)
C3-C2-H2A	108.9	C1-C2-H2A	108.9
C3-C2-H2B	108.9	C1-C2-H2B	108.9
H2A-C2-H2B	107.7	O2-C3-C2	109.93(14)
O2-C3-C22	106.59(14)	C2-C3-C22	113.48(15)
O2-C3-H3	108.9	C2-C3-H3	108.9
C22-C3-H3	108.9	N1-C4-C12	110.73(17)
N1-C4-C1	109.60(15)	C12-C4-C1	114.43(16)
N1-C4-H4	107.3	C12-C4-H4	107.3
C1-C4-H4	107.3	N1-C5-C6	115.99(17)
N1-C5-H5A	108.3	C6-C5-H5A	108.3
N1-C5-H5B	108.3	C6-C5-H5B	108.3
H5A-C5-H5B	107.4	C7-C6-C11	118.4(2)
C7-C6-C5	120.6(2)	C11-C6-C5	120.9(2)
C6-C7-C8	120.4(2)	C6-C7-H7	119.8
C8-C7-H7	119.8	C9-C8-C7	120.2(2)
C9-C8-H8	119.9	C7-C8-H8	119.9
C10-C9-C8	119.9(3)	C10-C9-H9	120.0
C8-C9-H9	120.0	C9-C10-C11	119.7(3)
C9-C10-H10	120.2	C11-C10-H10	120.2
C10-C11-C6	121.4(2)	C10-C11-H11	119.3
C6-C11-H11	119.3	O6-C12-C13	107.69(17)
O6-C12-C4	110.51(15)	C13-C12-C4	112.05(17)
O6-C12-H12	108.8	C13-C12-H12	108.8
C4-C12-H12	108.8	O5-C13-O4	124.2(2)
O5-C13-C12	126.7(2)	O4-C13-C12	109.15(19)
O4-C14-H14A	109.5	O4-C14-H14B	109.5
H14A-C14-H14B	109.5	O4-C14-H14C	109.5
H14A-C14-H14C	109.5	H14B-C14-H14C	109.5
O7-C15-N2	129.1(2)	O7-C15-O6	123.02(19)
N2-C15-O6	107.92(17)	C21-C16-C17	119.7(2)
C21-C16-N2	124.4(2)	C17-C16-N2	115.83(19)
C18-C17-C16	120.1(2)	C18-C17-H17	119.9

C16-C17-H17	119.9	C19-C18-C17	120.5(2)
C19-C18-H18	119.8	C17-C18-H18	119.8
C18-C19-C20	119.4(2)	C18-C19-H19	120.3
C20-C19-H19	120.3	C19-C20-C21	121.3(2)
C19-C20-H20	119.3	C21-C20-H20	119.3
C16-C21-C20	118.9(2)	C16-C21-H21	120.5
C20-C21-H21	120.5	N3-C22-C3	109.71(15)
N3-C22-C30	109.96(17)	C3-C22-C30	114.26(16)
N3-C22-H22	107.5	C3-C22-H22	107.5
C30-C22-H22	107.5	N3-C23-C24	115.27(17)
N3-C23-H23A	108.5	C24-C23-H23A	108.5
N3-C23-H23B	108.5	C24-C23-H23B	108.5
H23A-C23-H23B	107.5	C25-C24-C29	118.5(2)
C25-C24-C23	120.71(19)	C29-C24-C23	120.8(2)
C24-C25-C26	122.0(2)	C24-C25-H25	119.0
C26-C25-H25	119.0	C27-C26-C25	118.6(3)
C27-C26-H26	120.7	C25-C26-H26	120.7
C28-C27-C26	120.9(3)	C28-C27-H27	119.5
C26-C27-H27	119.5	C27-C28-C29	120.0(3)
C27-C28-H28	120.0	C29-C28-H28	120.0
C24-C29-C28	119.9(3)	C24-C29-H29	120.0
C28-C29-H29	120.0	O10-C30-C31	108.00(17)
O10-C30-C22	111.42(16)	C31-C30-C22	109.35(17)
O10-C30-H30	109.3	C31-C30-H30	109.3
C22-C30-H30	109.3	O9-C31-O8	124.8(2)
O9-C31-C30	126.7(2)	O8-C31-C30	108.44(18)
O8-C32-H32A	109.5	O8-C32-H32B	109.5
H32A-C32-H32B	109.5	O8-C32-H32C	109.5
H32A-C32-H32C	109.5	H32B-C32-H32C	109.5
O11-C33-N4	128.0(2)	O11-C33-O10	123.82(19)
N4-C33-O10	108.21(17)	C39-C34-C35	119.7(2)
C39-C34-N4	124.25(19)	C35-C34-N4	116.00(19)
C36-C35-C34	120.1(2)	C36-C35-H35	119.9
C34-C35-H35	119.9	C37-C36-C35	120.2(2)
C37-C36-H36	119.9	C35-C36-H36	119.9
C36-C37-C38	119.4(3)	C36-C37-H37	120.3
C38-C37-H37	120.3	C39-C38-C37	121.2(3)
C39-C38-H38	119.4	C37-C38-H38	119.4
C34-C39-C38	119.4(2)	C34-C39-H39	120.3
C38-C39-H39	120.3	C42-C40-C41	110.27(18)
C42-C40-Si1	114.99(14)	C41-C40-Si1	110.13(15)
C42-C40-H40	107.0	C41-C40-H40	107.0
Si1-C40-H40	107.0	C40-C41-H41A	109.5

C40-C41-H41B	109.5	H41A-C41-H41B	109.5
C40-C41-H41C	109.5	H41A-C41-H41C	109.5
H41B-C41-H41C	109.5	C40-C42-H42A	109.5
C40-C42-H42B	109.5	H42A-C42-H42B	109.5
C40-C42-H42C	109.5	H42A-C42-H42C	109.5
H42B-C42-H42C	109.5	C45-C43-C44	110.23(17)
C45-C43-Si1	113.99(15)	C44-C43-Si1	112.25(15)
C45-C43-H43	106.6	C44-C43-H43	106.6
Si1-C43-H43	106.6	C43-C44-H44A	109.5
C43-C44-H44B	109.5	H44A-C44-H44B	109.5
C43-C44-H44C	109.5	H44A-C44-H44C	109.5
H44B-C44-H44C	109.5	C43-C45-H45A	109.5
C43-C45-H45B	109.5	H45A-C45-H45B	109.5
C43-C45-H45C	109.5	H45A-C45-H45C	109.5
H45B-C45-H45C	109.5	C48-C46-C47	110.69(18)
C48-C46-Si2	111.99(14)	C47-C46-Si2	113.35(15)
C48-C46-H46	106.8	C47-C46-H46	106.8
Si2-C46-H46	106.8	C46-C47-H47A	109.5
C46-C47-H47B	109.5	H47A-C47-H47B	109.5
C46-C47-H47C	109.5	H47A-C47-H47C	109.5
H47B-C47-H47C	109.5	C46-C48-H48A	109.5
C46-C48-H48B	109.5	H48A-C48-H48B	109.5
C46-C48-H48C	109.5	H48A-C48-H48C	109.5
H48B-C48-H48C	109.5	C51-C49-C50	110.34(18)
C51-C49-Si2	114.00(14)	C50-C49-Si2	112.52(15)
C51-C49-H49	106.5	C50-C49-H49	106.5
Si2-C49-H49	106.5	C49-C50-H50A	109.5
C49-C50-H50B	109.5	H50A-C50-H50B	109.5
C49-C50-H50C	109.5	H50A-C50-H50C	109.5
H50B-C50-H50C	109.5	C49-C51-H51A	109.5
C49-C51-H51B	109.5	H51A-C51-H51B	109.5
C49-C51-H51C	109.5	H51A-C51-H51C	109.5
H51B-C51-H51C	109.5	C1S-O1S-H1OS	109.5(15)
O1S-C1S-H1SA	109.5	O1S-C1S-H1SB	109.5
H1SA-C1S-H1SB	109.5	O1S-C1S-H1SC	109.5
H1SA-C1S-H1SC	109.5	H1SB-C1S-H1SC	109.5
C2S-O2S-H2OS	106.7(19)	O2S-C2S-H2SA	109.5
O2S-C2S-H2SB	109.5	H2SA-C2S-H2SB	109.5
O2S-C2S-H2SC	109.5	H2SA-C2S-H2SC	109.5
H2SB-C2S-H2SC	109.5		

Table 4. Anisotropic displacement parameters ($\text{\AA}^2 \times 10^3$) for 10108. The anisotropic displacement factor exponent takes the form: $-2h^2a^*2U11 + \dots + 2hk a^* b^* U12$]

	U11	U22	U33	U23	U13	U12
Si1	20(1)	21(1)	23(1)	3(1)	2(1)	2(1)
Si2	18(1)	22(1)	23(1)	2(1)	2(1)	1(1)
O1	21(1)	20(1)	23(1)	1(1)	2(1)	2(1)
O2	19(1)	22(1)	24(1)	3(1)	1(1)	1(1)
O3	19(1)	21(1)	26(1)	2(1)	0(1)	2(1)
O4	32(1)	45(1)	39(1)	-2(1)	-8(1)	1(1)
O5	57(1)	36(1)	58(1)	7(1)	-7(1)	-9(1)
O6	33(1)	36(1)	23(1)	2(1)	3(1)	17(1)
O7	40(1)	65(1)	25(1)	3(1)	5(1)	22(1)
O8	37(1)	32(1)	37(1)	-4(1)	-1(1)	1(1)
O9	40(1)	49(1)	40(1)	7(1)	-1(1)	-13(1)
O10	23(1)	52(1)	21(1)	2(1)	1(1)	12(1)
O11	35(1)	44(1)	24(1)	5(1)	-1(1)	10(1)
N1	23(1)	32(1)	24(1)	0(1)	4(1)	2(1)
N2	32(1)	31(1)	26(1)	1(1)	2(1)	11(1)
N3	27(1)	26(1)	24(1)	5(1)	-1(1)	2(1)
N4	24(1)	42(1)	24(1)	2(1)	1(1)	5(1)
C1	21(1)	22(1)	18(1)	1(1)	0(1)	3(1)
C2	20(1)	26(1)	16(1)	2(1)	2(1)	5(1)
C3	18(1)	23(1)	18(1)	1(1)	2(1)	0(1)
C4	21(1)	28(1)	18(1)	4(1)	0(1)	3(1)
C5	27(1)	42(2)	32(1)	8(1)	13(1)	2(1)
C6	27(1)	31(1)	37(1)	5(1)	13(1)	-2(1)
C7	45(2)	45(2)	33(1)	3(1)	9(1)	0(1)
C8	65(2)	65(2)	39(1)	14(1)	6(1)	8(2)
C9	64(2)	47(2)	67(2)	25(2)	20(2)	9(2)
C10	70(2)	31(2)	70(2)	2(1)	19(2)	-7(1)
C11	49(2)	41(2)	46(1)	-3(1)	7(1)	-6(1)
C12	27(1)	34(1)	20(1)	1(1)	-1(1)	12(1)
C13	38(2)	31(1)	27(1)	-9(1)	0(1)	6(1)
C14	38(2)	60(2)	55(2)	-14(1)	-10(1)	0(1)
C15	25(1)	30(1)	28(1)	-6(1)	2(1)	6(1)
C16	30(1)	30(1)	38(1)	-8(1)	-3(1)	6(1)
C17	36(2)	35(1)	47(1)	7(1)	2(1)	7(1)
C18	53(2)	47(2)	67(2)	19(1)	2(2)	18(2)

C19	70(2)	62(2)	68(2)	4(2)	4(2)	44(2)
C20	62(2)	91(2)	54(2)	0(2)	16(2)	42(2)
C21	47(2)	69(2)	36(1)	1(1)	5(1)	27(2)
C22	23(1)	31(1)	17(1)	2(1)	4(1)	5(1)
C23	33(1)	39(1)	26(1)	11(1)	0(1)	7(1)
C24	30(1)	29(1)	32(1)	12(1)	4(1)	4(1)
C25	40(2)	44(2)	57(2)	1(1)	5(1)	-6(1)
C26	38(2)	65(2)	95(2)	17(2)	5(2)	-11(2)
C27	52(2)	90(3)	74(2)	39(2)	32(2)	22(2)
C28	74(2)	118(3)	38(2)	12(2)	18(2)	28(2)
C29	50(2)	77(2)	31(1)	6(1)	2(1)	13(2)
C30	24(1)	39(1)	18(1)	1(1)	1(1)	4(1)
C31	23(1)	42(1)	27(1)	0(1)	-8(1)	-2(1)
C32	49(2)	33(2)	52(2)	-7(1)	-11(1)	-3(1)
C33	22(1)	29(1)	30(1)	-2(1)	-5(1)	-1(1)
C34	24(1)	25(1)	42(1)	1(1)	3(1)	1(1)
C35	33(2)	34(1)	44(1)	-3(1)	8(1)	-2(1)
C36	41(2)	42(2)	65(2)	-1(1)	20(1)	3(1)
C37	42(2)	51(2)	91(2)	12(2)	19(2)	18(2)
C38	39(2)	75(2)	71(2)	24(2)	9(1)	24(2)
C39	32(2)	53(2)	51(2)	9(1)	7(1)	12(1)
C40	33(1)	30(1)	27(1)	2(1)	-1(1)	4(1)
C41	51(2)	49(2)	30(1)	10(1)	-1(1)	3(1)
C42	38(2)	54(2)	39(1)	1(1)	-12(1)	1(1)
C43	28(1)	24(1)	32(1)	2(1)	5(1)	0(1)
C44	57(2)	36(2)	48(1)	1(1)	-13(1)	-5(1)
C45	44(2)	31(1)	61(2)	-6(1)	10(1)	3(1)
C46	21(1)	26(1)	37(1)	4(1)	1(1)	-2(1)
C47	24(1)	38(2)	66(2)	-8(1)	-6(1)	-3(1)
C48	34(2)	37(1)	47(1)	-9(1)	-5(1)	-5(1)
C49	30(1)	28(1)	28(1)	4(1)	5(1)	7(1)
C50	56(2)	51(2)	35(1)	9(1)	20(1)	0(1)
C51	49(2)	45(2)	31(1)	-10(1)	0(1)	2(1)
O1S	38(1)	38(1)	39(1)	-3(1)	6(1)	2(1)
C1S	71(2)	69(2)	107(2)	-53(2)	25(2)	-27(2)
O2S	33(1)	43(1)	39(1)	5(1)	-2(1)	1(1)
C2S	48(2)	60(2)	67(2)	6(2)	-12(1)	-14(2)

Table 5. Hydrogen coordinates ($\times 10^4$) and isotropic displacement parameters ($\text{\AA}^2 \times 10^3$) for 10108.

	x	y	z	U(eq)
H1N	2128(12)	1473(8)	8046(8)	5(5)
H2N	2656	-1043	8606	55(8)
H3N	399(13)	-351(9)	10015(8)	8(5)
H4N	3745	37	9313	36(6)
H1	37	708	8256	24
H2A	1068	98	8936	25
H2B	1725	748	9016	25
H3	591	1312	9673	24
H4	942	1056	7311	27
H5A	2557	943	6816	41
H5B	3269	1400	7235	41
H7	1903	1519	5910	49
H8	1300	2500	5401	67
H9	1283	3527	5993	71
H10	1856	3578	7095	68
H11	2453	2601	7601	55
H12	1666	46	7017	32
H14A	-1281	25	6433	76
H14B	-1354	-265	7193	76
H14C	-883	-716	6609	76
H17	3446	-1887	9130	47
H18	4659	-2662	9153	66
H19	5596	-2796	8212	80
H20	5351	-2131	7255	83
H21	4137	-1348	7213	61
H22	561	615	10658	28
H23A	1378	-426	11167	39
H23B	1050	-1112	10800	39
H25	-784	-1003	10508	56
H26	-2170	-1015	11097	79
H27	-2210	-616	12208	87
H28	-913	-153	12701	92
H29	488	-160	12112	63
H30	2110	536	10906	33
H32A	1248	2606	11393	67
H32B	1218	2659	10580	67

H32C	2187	2632	10967	67
H35	4932	-445	8740	45
H36	6286	-1080	8733	59
H37	6855	-1540	9741	74
H38	6075	-1349	10758	74
H39	4708	-729	10775	55
H40	-947	1442	7440	35
H41A	-656	2211	6561	64
H41B	233	2181	7041	64
H41C	-462	2813	7092	64
H42A	-2229	2069	7062	65
H42B	-2049	2636	7633	65
H42C	-2350	1881	7849	65
H43	196	3126	8204	34
H44A	741	3449	9297	71
H44B	1186	2749	9035	71
H44C	382	2735	9593	71
H45A	-696	3855	8872	68
H45B	-1227	3217	9195	68
H45C	-1345	3391	8404	68
H46	-2247	110	9557	33
H47A	-3591	459	8996	64
H47B	-3122	1171	8798	64
H47C	-3334	999	9579	64
H48A	-2382	-180	8397	59
H48B	-1323	-111	8612	59
H48C	-1811	488	8191	59
H49	-2213	1756	10253	34
H50A	-2145	1184	11297	71
H50B	-1385	671	11005	71
H50C	-2411	658	10706	71
H51A	-1193	2192	11049	62
H51B	-797	2324	10300	62
H51C	-380	1724	10759	62
H10S	1738(17)	-805(13)	9719(12)	65(9)
H1SA	828	-1541	9224	123
H1SB	1278	-1917	9866	123
H1SC	1664	-2062	9117	123
H20S	3200(20)	669(14)	8273(13)	78(11)
H2SA	3728	1458	8930	87
H2SB	4303	1449	8234	87
H2SC	4711	1090	8901	87

Table 6. Torsion angles [°] for 10108.

O3-Si1-O1-C1	56.00(14)	C43-Si1-O1-C1	175.65(13)
C40-Si1-O1-C1	-62.48(14)	O3-Si2-O2-C3	43.27(15)
C46-Si2-O2-C3	162.13(14)	C49-Si2-O2-C3	-76.98(15)
O1-Si1-O3-Si2	-10.59(19)	C43-Si1-O3-Si2	-124.58(16)
C40-Si1-O3-Si2	108.44(17)	O2-Si2-O3-Si1	8.00(19)
C46-Si2-O3-Si1	-104.91(17)	C49-Si2-O3-Si1	132.39(16)
Si1-O1-C1-C2	-117.61(15)	Si1-O1-C1-C4	118.81(14)
O1-C1-C2-C3	51.9(2)	C4-C1-C2-C3	170.89(16)
Si2-O2-C3-C2	-112.55(15)	Si2-O2-C3-C22	124.07(14)
C1-C2-C3-O2	58.7(2)	C1-C2-C3-C22	177.99(16)
C5-N1-C4-C12	79.2(2)	C5-N1-C4-C1	-153.65(16)
O1-C1-C4-N1	60.83(19)	C2-C1-C4-N1	-59.6(2)
O1-C1-C4-C12	-174.11(15)	C2-C1-C4-C12	65.5(2)
C4-N1-C5-C6	74.6(2)	N1-C5-C6-C7	-122.1(2)
N1-C5-C6-C11	58.6(3)	C11-C6-C7-C8	-1.1(3)
C5-C6-C7-C8	179.6(2)	C6-C7-C8-C9	0.7(4)
C7-C8-C9-C10	-0.1(4)	C8-C9-C10-C11	0.0(4)
C9-C10-C11-C6	-0.5(4)	C7-C6-C11-C10	1.1(4)
C5-C6-C11-C10	-179.7(2)	C15-O6-C12-C13	109.67(19)
C15-O6-C12-C4	-127.65(18)	N1-C4-C12-O6	56.6(2)
C1-C4-C12-O6	-67.9(2)	N1-C4-C12-C13	176.68(15)
C1-C4-C12-C13	52.2(2)	C14-O4-C13-O5	-4.1(3)
C14-O4-C13-C12	175.64(17)	O6-C12-C13-O5	0.6(3)
C4-C12-C13-O5	-121.1(2)	O6-C12-C13-O4	-179.15(15)
C4-C12-C13-O4	59.1(2)	C16-N2-C15-O7	-1.4(4)
C16-N2-C15-O6	178.96(18)	C12-O6-C15-O7	9.5(3)
C12-O6-C15-N2	-170.85(17)	C15-N2-C16-C21	6.0(4)
C15-N2-C16-C17	-174.7(2)	C21-C16-C17-C18	0.3(4)
N2-C16-C17-C18	-179.1(2)	C16-C17-C18-C19	-0.6(4)
C17-C18-C19-C20	0.9(5)	C18-C19-C20-C21	-1.0(5)
C17-C16-C21-C20	-0.3(4)	N2-C16-C21-C20	179.0(2)
C19-C20-C21-C16	0.6(5)	C23-N3-C22-C3	-155.73(17)
C23-N3-C22-C30	77.8(2)	O2-C3-C22-N3	61.19(19)
C2-C3-C22-N3	-60.0(2)	O2-C3-C22-C30	-174.80(15)
C2-C3-C22-C30	64.1(2)	C22-N3-C23-C24	75.5(2)
N3-C23-C24-C25	58.3(3)	N3-C23-C24-C29	-124.0(2)
C29-C24-C25-C26	-1.3(4)	C23-C24-C25-C26	176.5(2)
C24-C25-C26-C27	0.0(4)	C25-C26-C27-C28	1.9(5)
C26-C27-C28-C29	-2.5(5)	C25-C24-C29-C28	0.7(4)
C23-C24-C29-C28	-177.0(2)	C27-C28-C29-C24	1.2(4)
C33-O10-C30-C31	118.72(18)	C33-O10-C30-C22	-121.16(18)

N3-C22-C30-O10	53.2(2)	C3-C22-C30-O10	-70.6(2)
N3-C22-C30-C31	172.56(15)	C3-C22-C30-C31	48.7(2)
C32-O8-C31-O9	-1.6(3)	C32-O8-C31-C30	179.48(17)
O10-C30-C31-O9	11.9(3)	C22-C30-C31-O9	-109.5(2)
O10-C30-C31-O8	-169.13(15)	C22-C30-C31-O8	69.5(2)
C34-N4-C33-O11	-0.9(4)	C34-N4-C33-O10	178.94(18)
C30-O10-C33-O11	7.7(3)	C30-O10-C33-N4	-172.09(16)
C33-N4-C34-C39	-4.7(3)	C33-N4-C34-C35	176.3(2)
C39-C34-C35-C36	0.5(3)	N4-C34-C35-C36	179.7(2)
C34-C35-C36-C37	-0.3(4)	C35-C36-C37-C38	-0.5(4)
C36-C37-C38-C39	1.0(4)	C35-C34-C39-C38	-0.1(4)
N4-C34-C39-C38	-179.1(2)	C37-C38-C39-C34	-0.7(4)
O3-Si1-C40-C42	48.18(18)	O1-Si1-C40-C42	166.82(15)
C43-Si1-C40-C42	-77.85(18)	O3-Si1-C40-C41	173.49(14)
O1-Si1-C40-C41	-67.87(16)	C43-Si1-C40-C41	47.46(18)
O3-Si1-C43-C45	-50.90(17)	O1-Si1-C43-C45	-168.10(15)
C40-Si1-C43-C45	73.12(17)	O3-Si1-C43-C44	75.33(16)
O1-Si1-C43-C44	-41.88(16)	C40-Si1-C43-C44	-160.65(15)
O3-Si2-C46-C48	60.90(16)	O2-Si2-C46-C48	-56.02(16)
C49-Si2-C46-C48	-178.78(14)	O3-Si2-C46-C47	-65.21(17)
O2-Si2-C46-C47	177.88(15)	C49-Si2-C46-C47	55.12(18)
O3-Si2-C49-C51	-57.61(17)	O2-Si2-C49-C51	63.62(17)
C46-Si2-C49-C51	179.44(15)	O3-Si2-C49-C50	175.77(15)
O2-Si2-C49-C50	-63.00(18)	C46-Si2-C49-C50	52.83(19)

Table 7. Hydrogen bonds for 10108 [\AA and $^\circ$].

D-H...A	d(D-H)	d(H...A)	d(D...A)	\angle (DHA)
N2-H2N...O1S	0.88	1.98	2.850(2)	168.2
N3-H3N...O2	0.848(17)	2.330(17)	2.811(2)	116.4(14)
N4-H4N...O2S	0.88	1.97	2.837(2)	166.4
O1S-H1OS...N3	0.95(2)	1.86(3)	2.788(2)	163(2)
O2S-H2OS...N1	0.84(3)	2.00(3)	2.824(2)	167(3)

checkCIF/PLATON report (basic structural check)

No syntax errors found.
Please wait while processing

[CIF dictionary](#)
[Interpreting this report](#)

Datablock: 10108

Bond precision: C-C = 0.0033 A Wavelength=0.71073
Cell: a=14.5176(13) b=19.5896(18) c=19.6398(17)
alpha=90 beta=90 gamma=90
Temperature: 150 K

	Calculated	Reported
Volume	5585.4(9)	5585.4(9)
Space group	P 21 21 21	P2(1)2(1)2(1)
Hall group	P 2ac 2ab	?
Moiety formula	C51 H70 N4 O11 Si2, 2(C H4 O)	C51 H70 N4 O11 Si2, 2 (C H4 O)
Sum formula	C53 H78 N4 O13 Si2	C53 H78 N4 O13 Si2
Mr	1035.37	1035.37
Dx, g cm-3	1.231	1.231
Z	4	4
Mu (mm-1)	0.127	0.127
F000	2224.0	2224.0
F000'	2225.68	
h,k,lmax	17,23,23	17,23,23
Nref	5470[9904]	9901
Tmin,Tmax	0.971,0.987	0.971,0.987
Tmin'	0.971	

Correction method= MULTI-SCAN
Data completeness= 1.81/1.00 Theta(max)= 25.070
R(reflections)= 0.0335(7789) wR2(reflections)= 0.0621(9901)
S = 0.902 Npar= 679

The following ALERTS were generated. Each ALERT has the format
[test-name](#) [ALERT](#) [alert-type](#) [alert-level](#).
Click on the hyperlinks for more details of the test.

Alert level A

[PLAT222_ALERT_3_A](#) Large Non-Solvent H Uiso(max)/Uiso(min) ... 10.00 Ratio

Alert level C

[PLAT220_ALERT_2_C](#) Large Non-Solvent C Ueq(max)/Ueq(min) ... 3.92 Ratio
[PLAT230_ALERT_2_C](#) Hirshfeld Test Diff for O11 -- C33 .. 5.49 su
[PLAT245_ALERT_2_C](#) U(iso) H1N Smaller than U(eq) N1 by ... 0.02 AngSq
[PLAT245_ALERT_2_C](#) U(iso) H3N Smaller than U(eq) N3 by ... 0.02 AngSq
[PLAT790_ALERT_4_C](#) Centre of Gravity not Within Unit Cell: Resd. # 2
C H4 O

Alert level G

[REFLT03_ALERT_4_G](#) Please check that the estimate of the number of Friedel pairs is correct. If it is not, please give the correct count in the _publ_section_exptl_refinement section of the submitted CIF.
From the CIF: _diffrn_reflns_theta_max 25.07
From the CIF: _reflns_number_total 9901
Count of symmetry unique reflns 5470
Completeness (_total/calc) 181.01%
TEST3: Check Friedels for noncentro structure
Estimate of Friedel pairs measured 4431
Fraction of Friedel pairs measured 0.810
Are heavy atom types Z>Si present yes

[PLAT860_ALERT_3_G](#) Note: Number of Least-Squares Restraints 173
[PLAT720_ALERT_4_G](#) Number of Unusual/Non-Standard Labels 8
[PLAT791_ALERT_4_G](#) Note: The Model has Chirality at C1 (Verify) R
[PLAT791_ALERT_4_G](#) Note: The Model has Chirality at C3 (Verify) R
[PLAT791_ALERT_4_G](#) Note: The Model has Chirality at C4 (Verify) S
[PLAT791_ALERT_4_G](#) Note: The Model has Chirality at C12 (Verify) R
[PLAT791_ALERT_4_G](#) Note: The Model has Chirality at C22 (Verify) S
[PLAT791_ALERT_4_G](#) Note: The Model has Chirality at C30 (Verify) R

1 ALERT level A = In general: serious problem

0 ALERT level B = Potentially serious problem
5 ALERT level C = Check and explain
9 ALERT level G = General alerts; check

0 ALERT type 1 CIF construction/syntax error, inconsistent or missing data
4 ALERT type 2 Indicator that the structure model may be wrong or deficient
2 ALERT type 3 Indicator that the structure quality may be low
9 ALERT type 4 Improvement, methodology, query or suggestion
0 ALERT type 5 Informative message, check

Publication of your CIF in IUCr journals

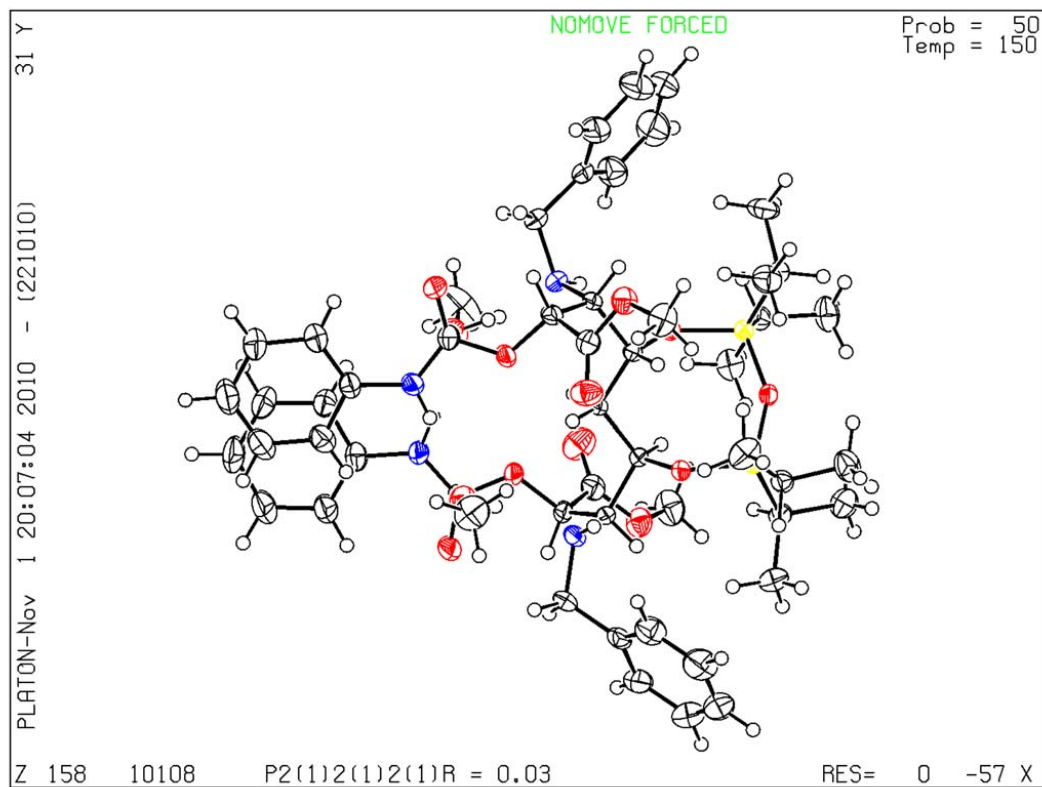
A basic structural check has been run on your CIF. These basic checks will be run on all CIFs submitted for publication in IUCr journals (*Acta Crystallographica*, *Journal of Applied Crystallography*, *Journal of Synchrotron Radiation*); however, if you intend to submit to *Acta Crystallographica Section C* or *E*, you should make sure that [full publication checks](#) are run on the final version of your CIF prior to submission.

Publication of your CIF in other journals

Please refer to the *Notes for Authors* of the relevant journal for any special instructions relating to CIF submission.

PLATON version of 22/10/2010; check.def file version of 11/10/2010

Datablock 10108 - ellipsoid plot



[Download CIF editor \(pubCIF\) from the IUCr](#)
[Download CIF editor \(enCIFer\) from the CCDC](#)
[Test a new CIF entry](#)

APPENDIX C

Spectral data and characterization.

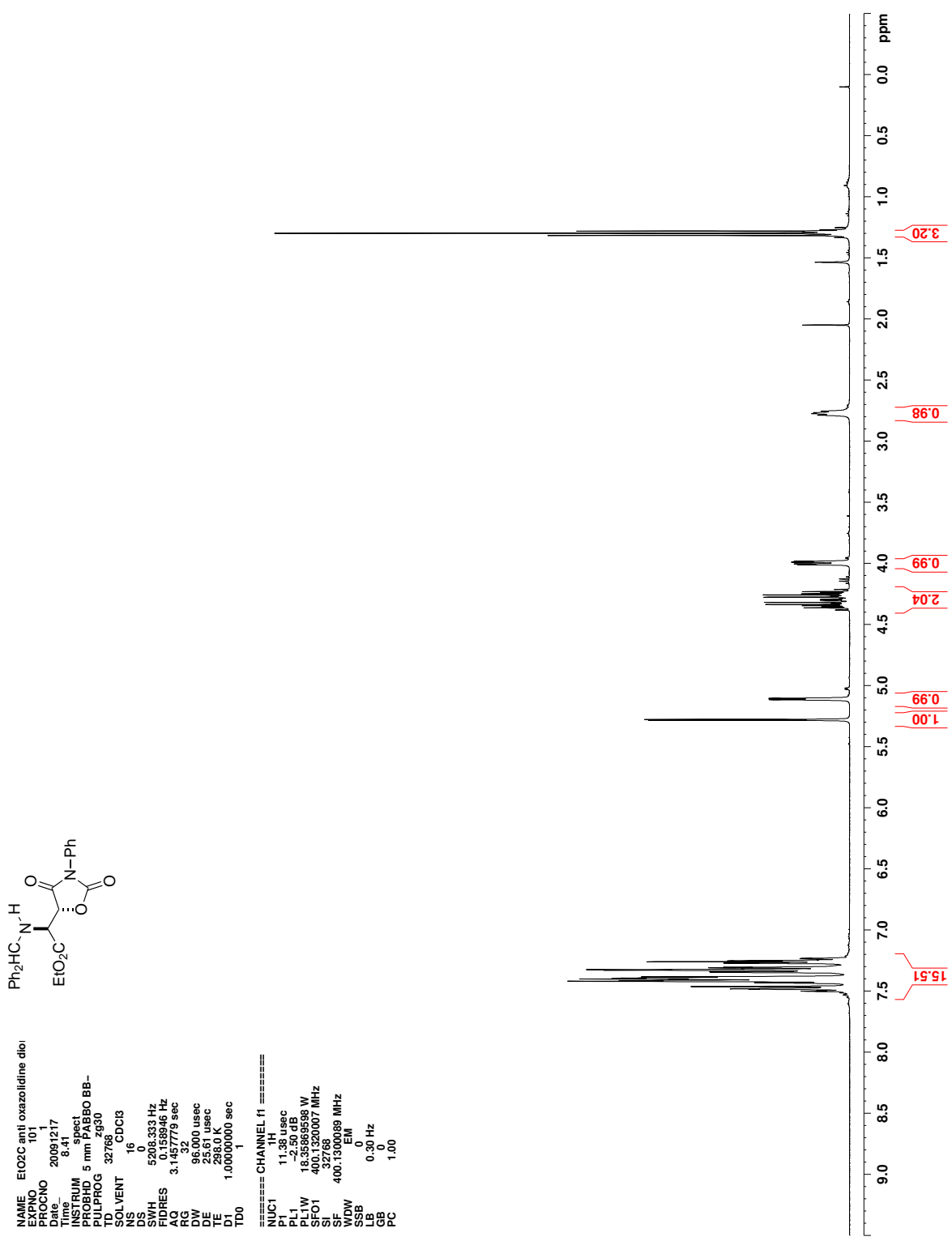


Figure C.1. ¹H NMR (CDCl₃) of 75

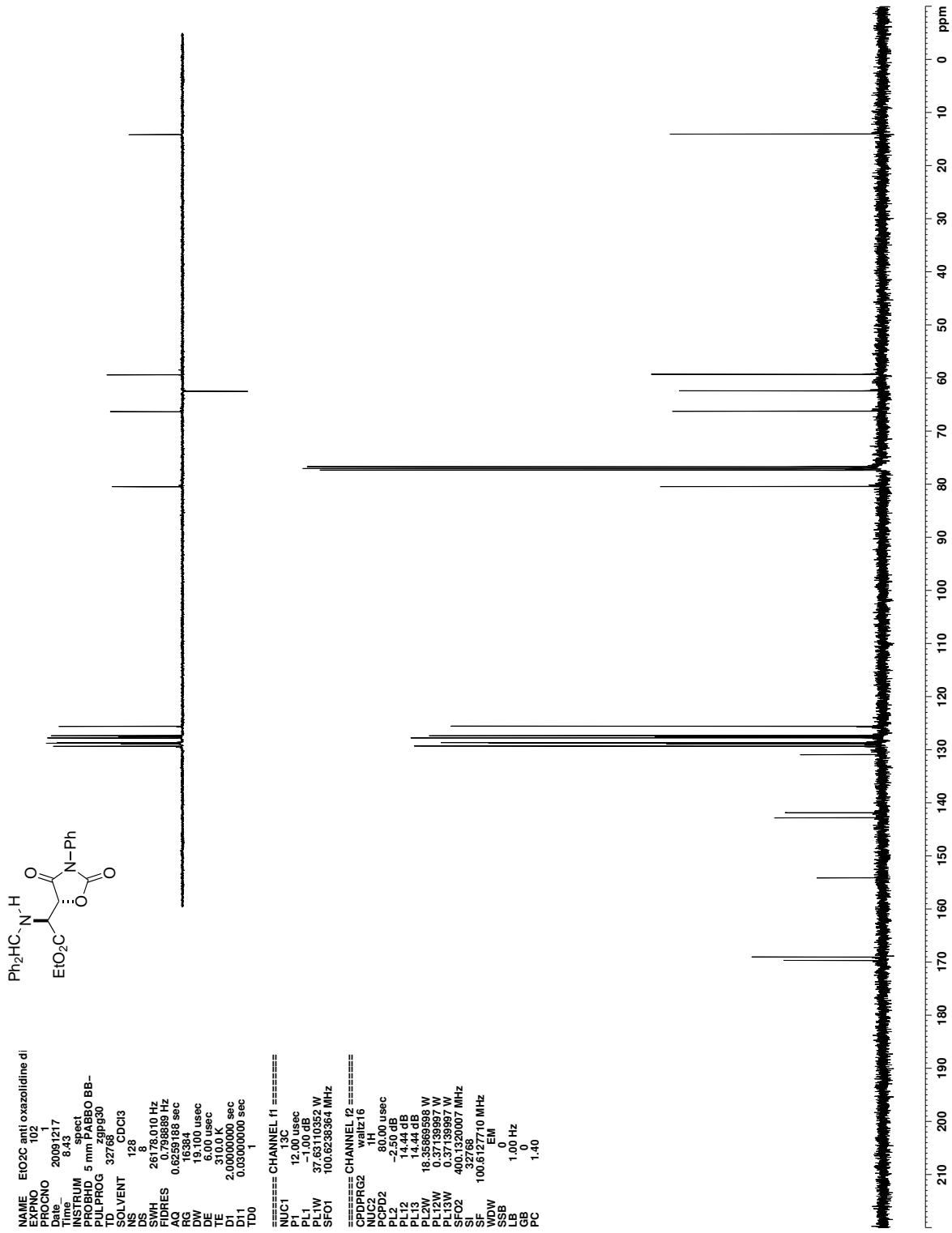


Figure C.2. ¹³C NMR (CDCl₃) of 75

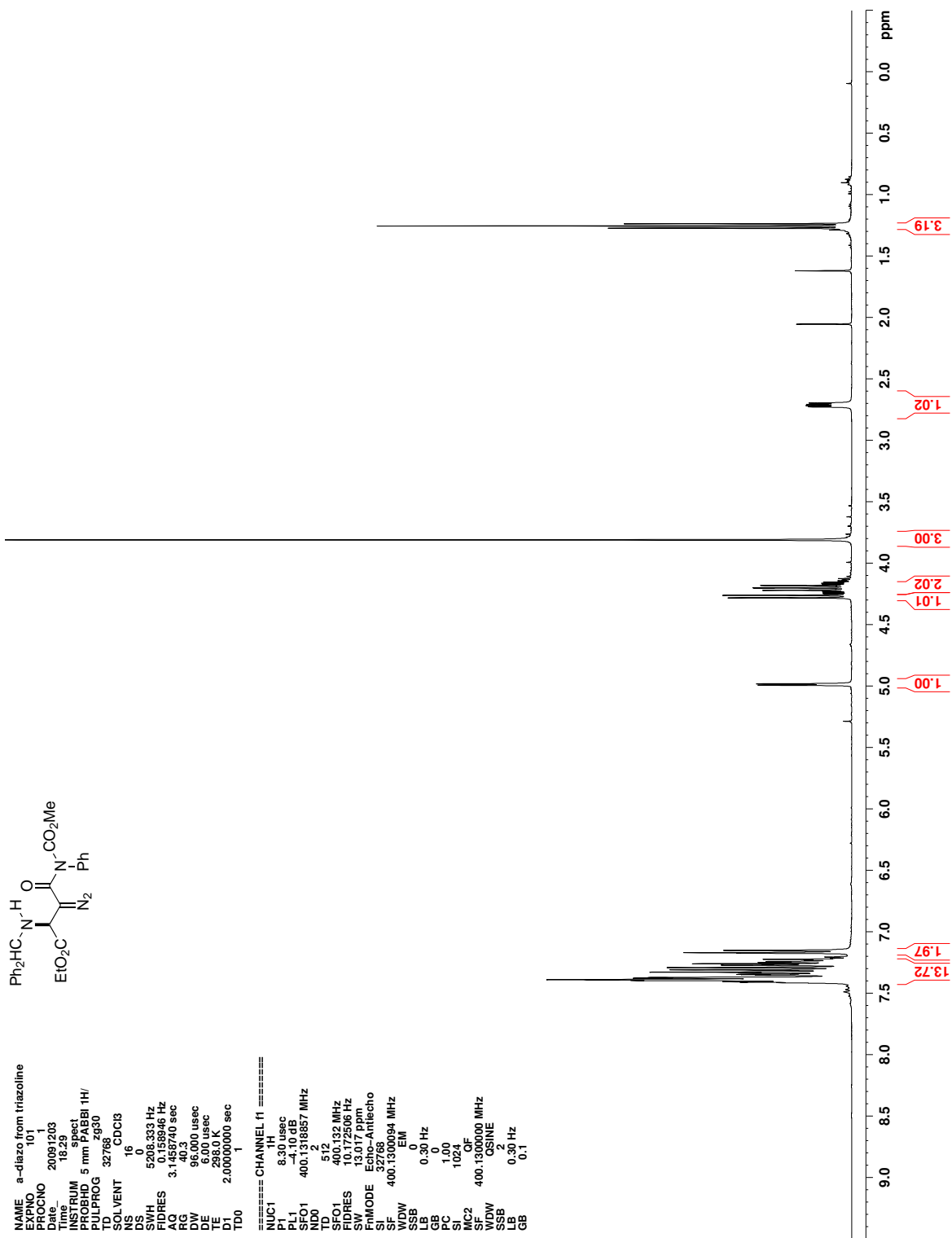


Figure C.3. ^1H NMR (CDCl_3) of 76

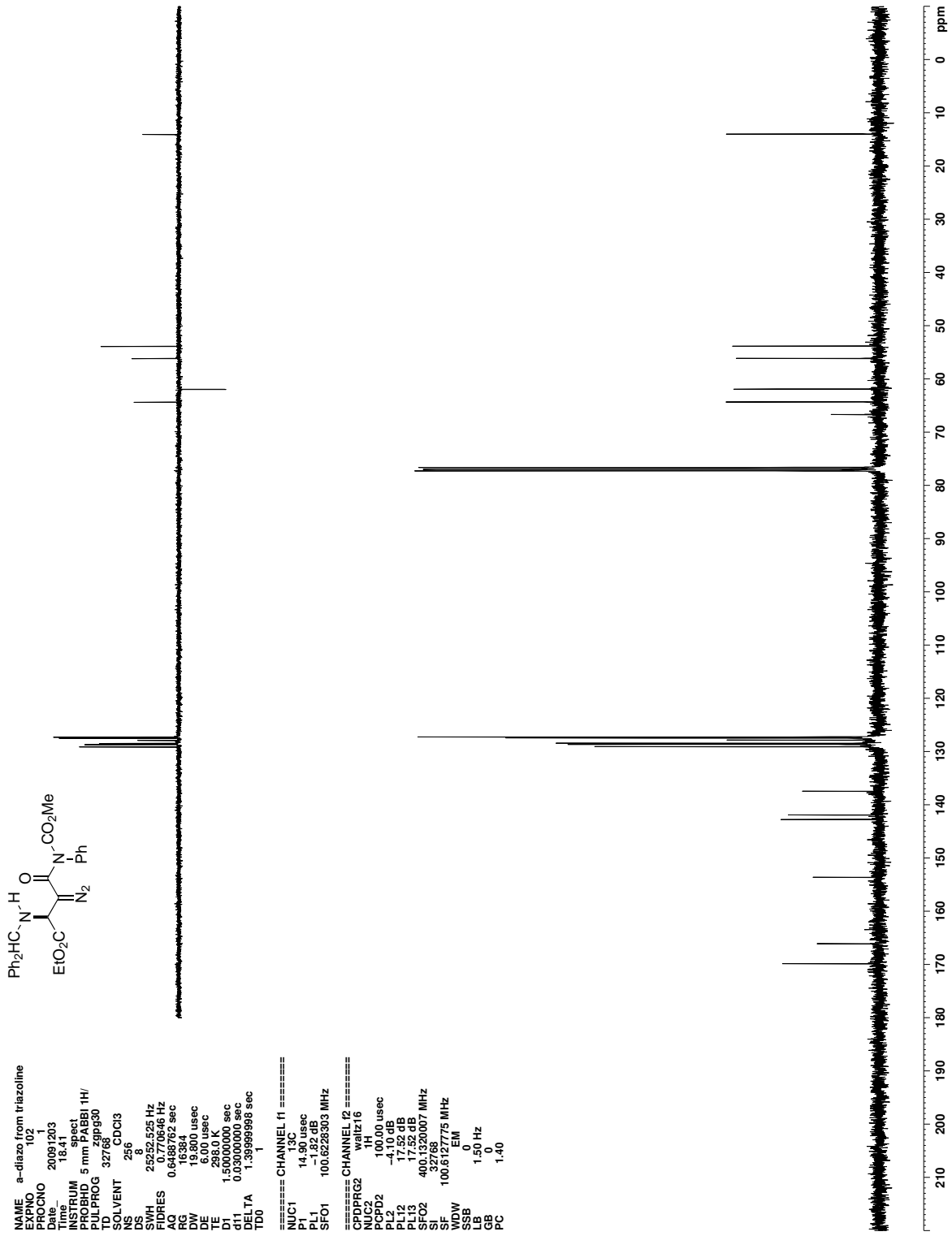


Figure C.4. ^{13}C NMR (CDCl_3) of **76**

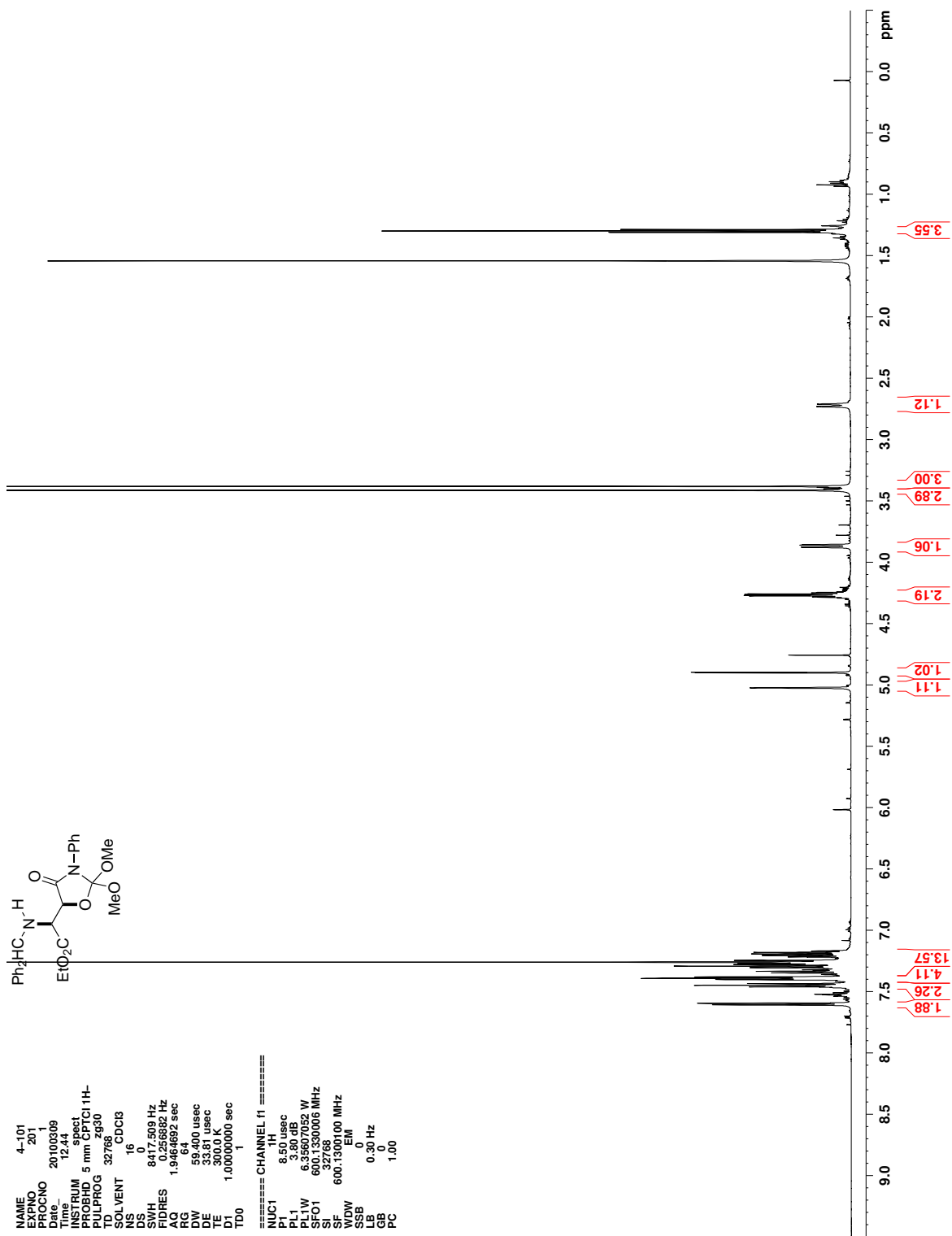


Figure C.5. ^1H NMR (CDCl_3) of 78

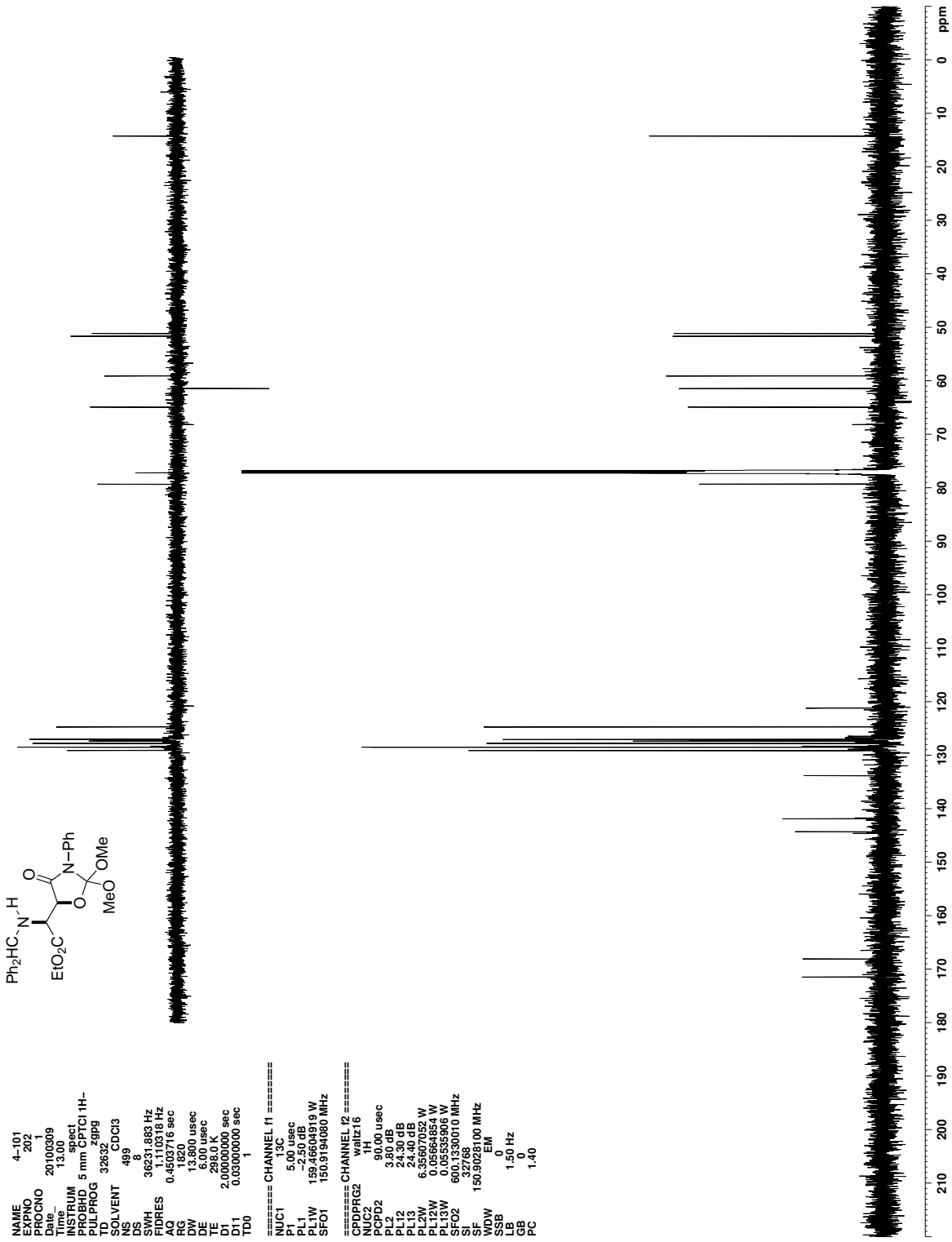


Figure C.6. ¹³C NMR (CDCl₃) of 78

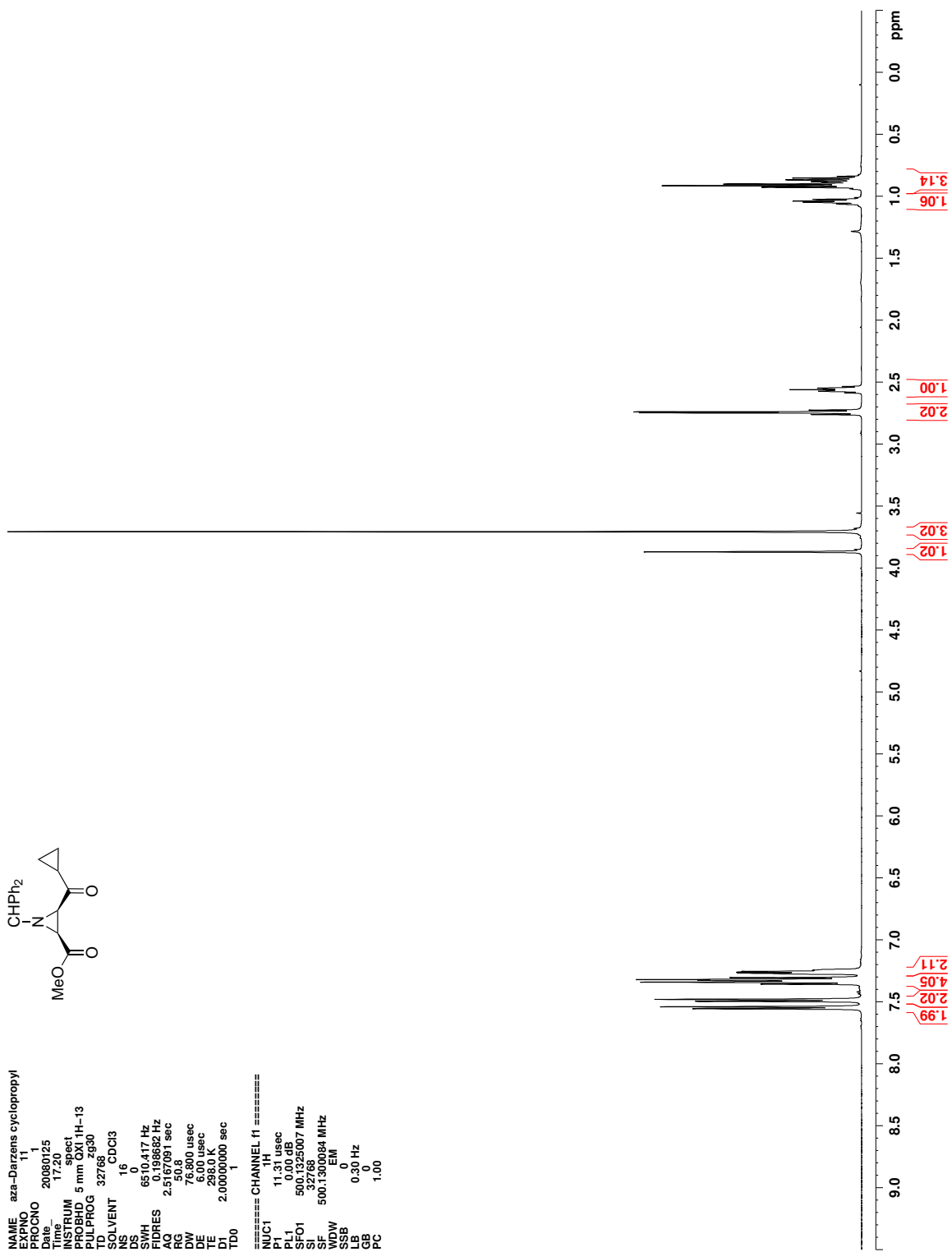


Figure C.7. ^1H NMR (CDCl_3) of **81**

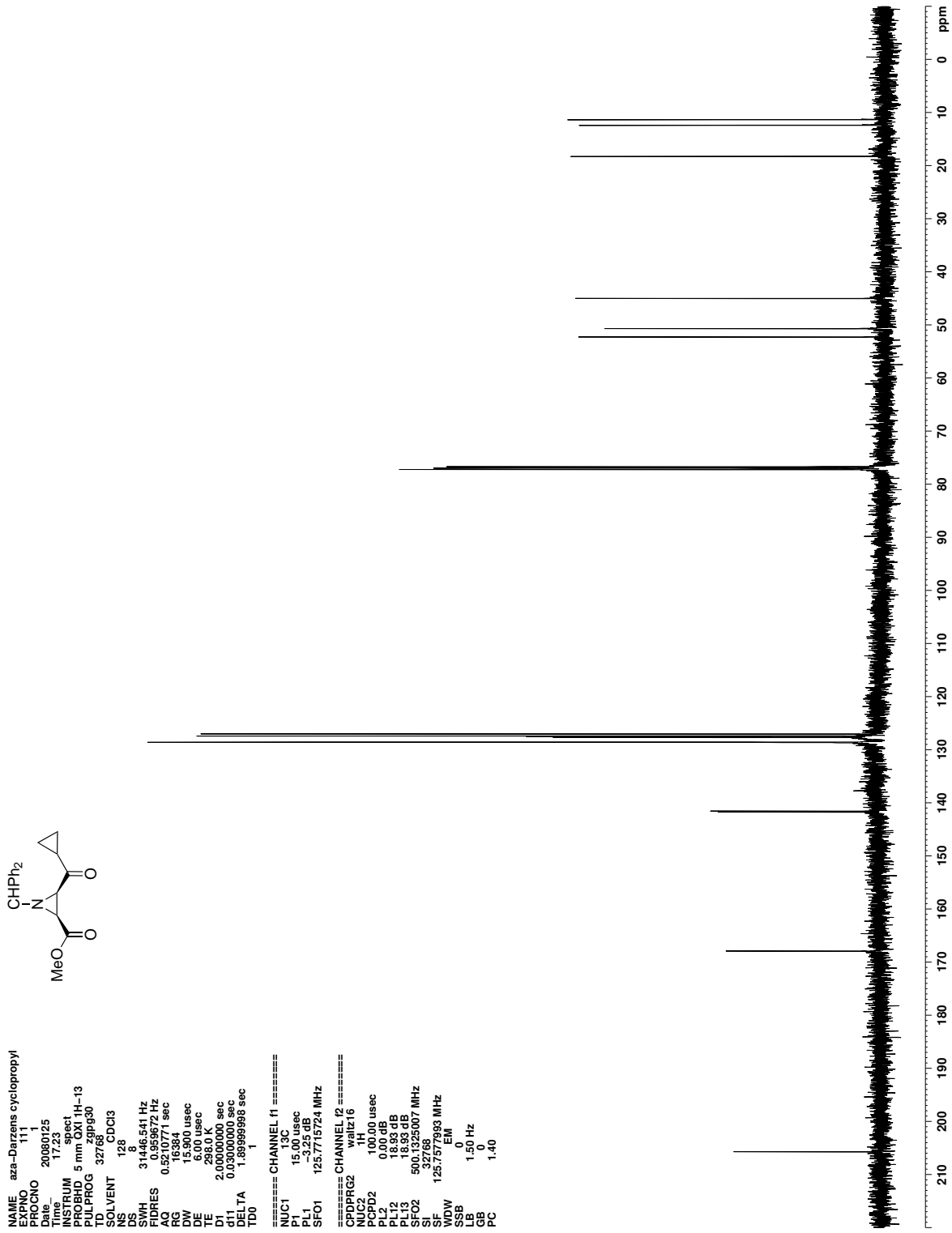


Figure C.8. ¹³C NMR (CDCl₃) of 81

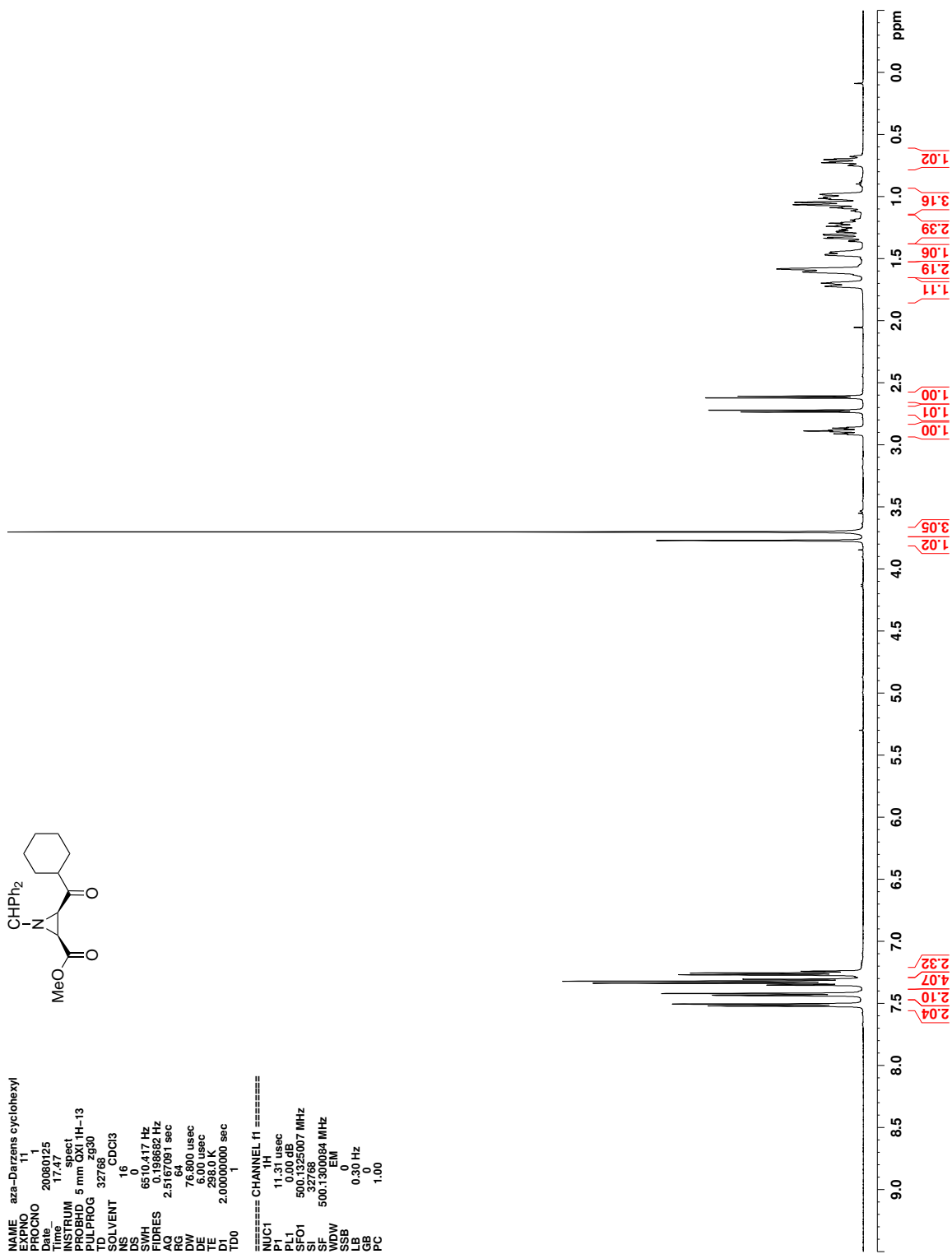
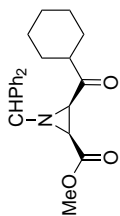


Figure C.9. ^1H NMR (CDCl_3) of **82**



```

NAME az-Darzens cyclohexyl
EXPNO 111
PROCNO 1
Date_ 20080125
Time 17.54
INSTRUM spect
PROBHD 5 mm QXI 1H-13
TD 65536
AQ 0.193672 Hz
RG 327.689930
SOLVENT CDCl3
NS 200
DS 8
SWH 31446.641 Hz
FIDRES 0.193672 Hz
AQRES 0.163847 sec
RG 327.689930
DW 15.900 usec
DE 6.00 usec
TE 298.0 K
D1 2.00000000 sec
d11 0.10000000 sec
DELTA 1.1898998 sec
TD0 1

===== CHANNEL f1 =====
NUC1 13C
P1 15.00 usec
PL1 0.00 dB
SFO1 125.7715724 MHz

===== CHANNEL f2 =====
NUC2 13C
P2 100.00 usec
PL2 0.00 dB
PL12 18.93 dB
PL13 18.93 dB
SFO2 500.1325007 MHz
SF 500.1325007 MHz
WDW EM
SSB 0
LB 1.50 Hz
GB 0
PC 1.40

```

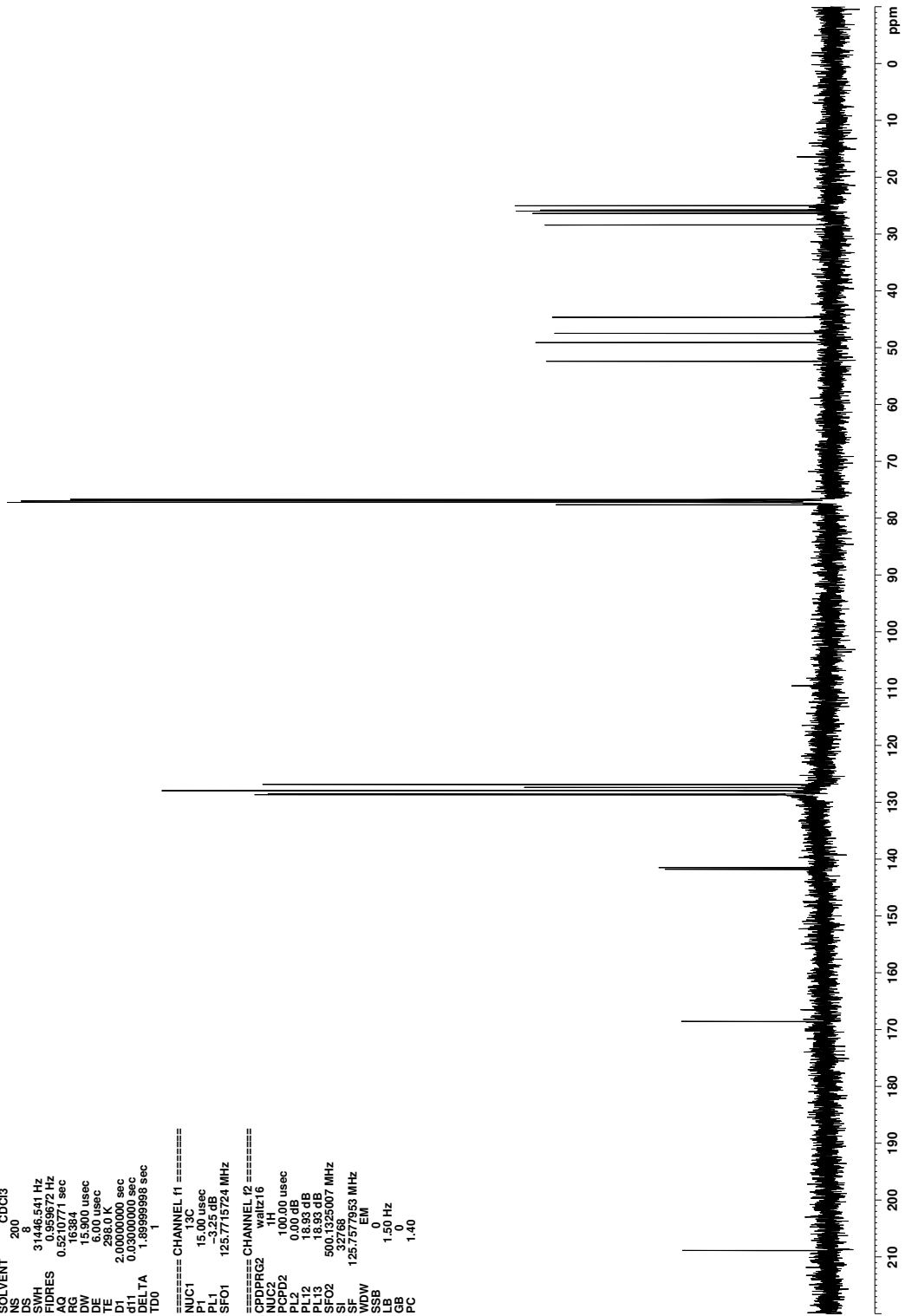


Figure C.10. ^{13}C NMR (CDCl_3) of 82

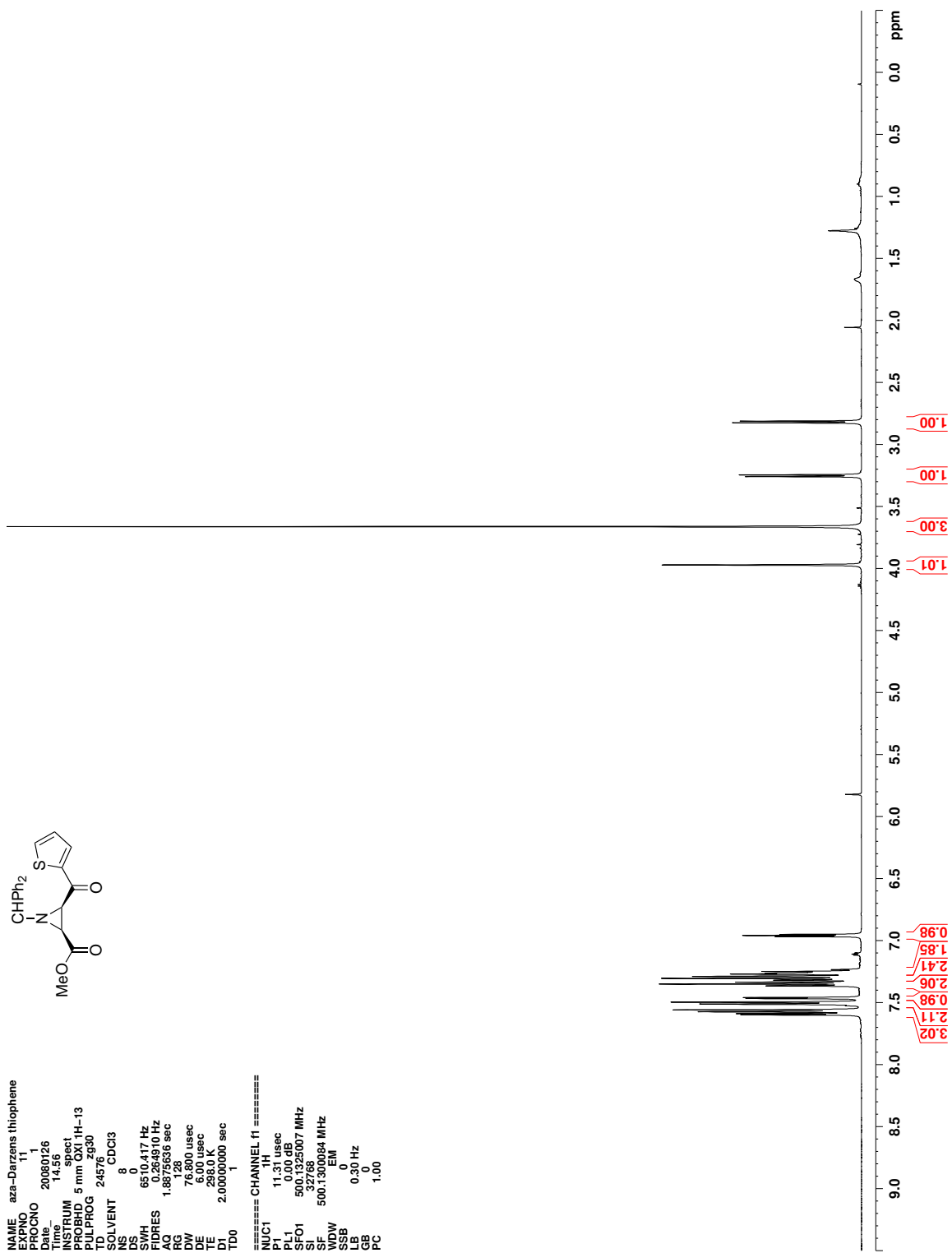
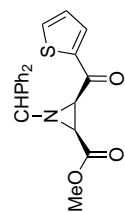


Figure C.11. ^1H NMR (CDCl_3) of **83**



```

NAME      az-Darzens thioephene
PROCNO    111
Date      20080126
Time      15.00
INSTRUM   spect
PROBHD    5 mm QXI 1H-13
TD        32768
SOLVENT   CDCl3
NS        302
DS        8
SWH       31446.641 Hz
FIDRES    0.195972 Hz
AQ        0.5163847 sec
RG        16384
DW        15.900 usec
DE        6.00 usec
TE        298.0 K
D1        2.00000000 sec
d11       0.10000000 sec
DELTA     1.1898998 sec
TD0       1

===== CHANNEL f1 =====
NUC1      13C
P1        15.00 usec
PL1       -2.25 dB
SFO1     125.7715724 MHz

===== CHANNEL f2 =====
CPDPRG2   waltz16
NUC2      13C
P2        100.00 usec
PL2       0.00 dB
PL12     18.93 dB
PL13     18.93 dB
SFO2     500.1325007 MHz
SI        32768
SF        125.7518777 MHz
WDW       EM
SSB       0
LB        1.50 Hz
GB        0
PC        1.40

```

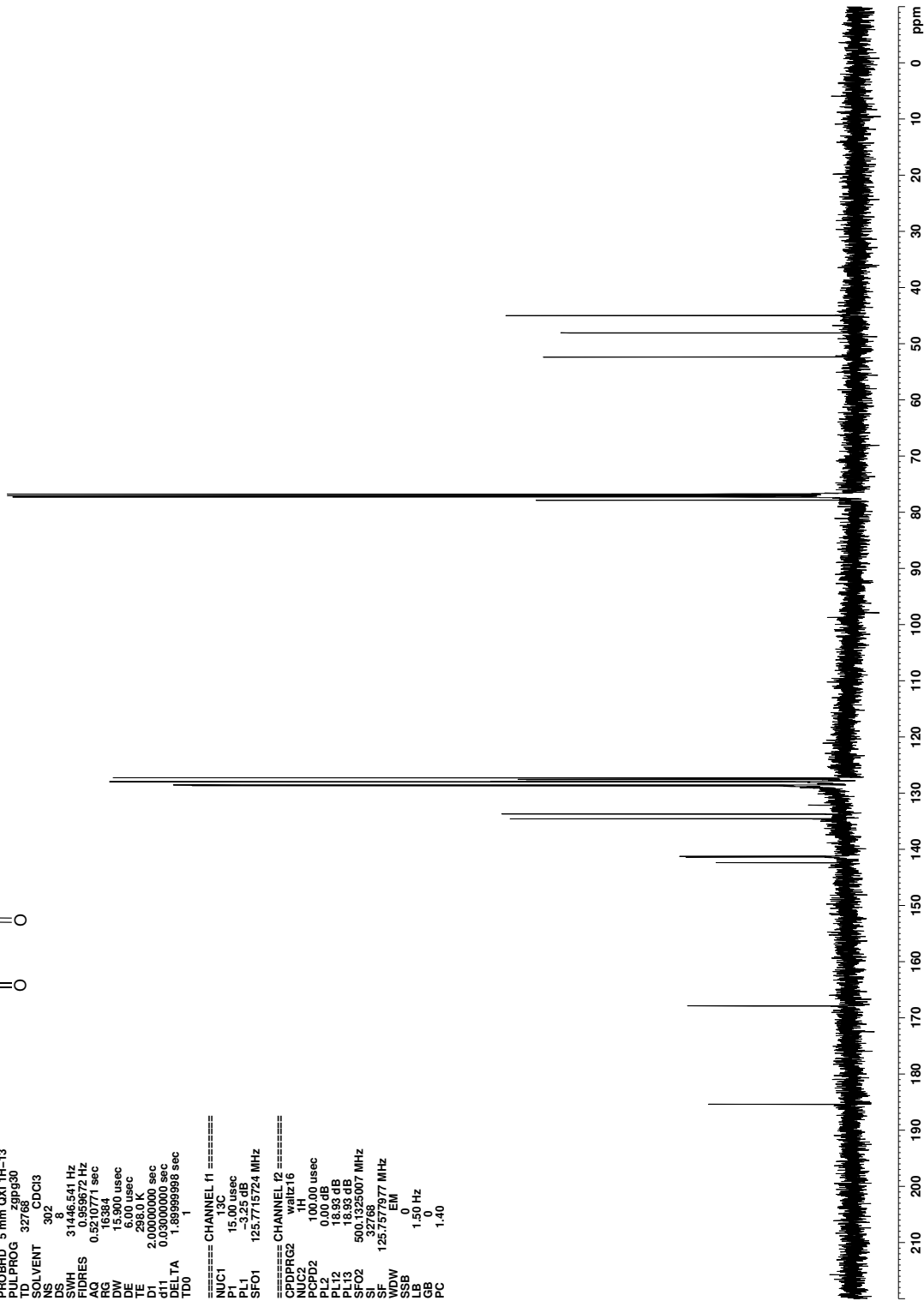


Figure C.12. ¹³C NMR (CDCl₃) of 83

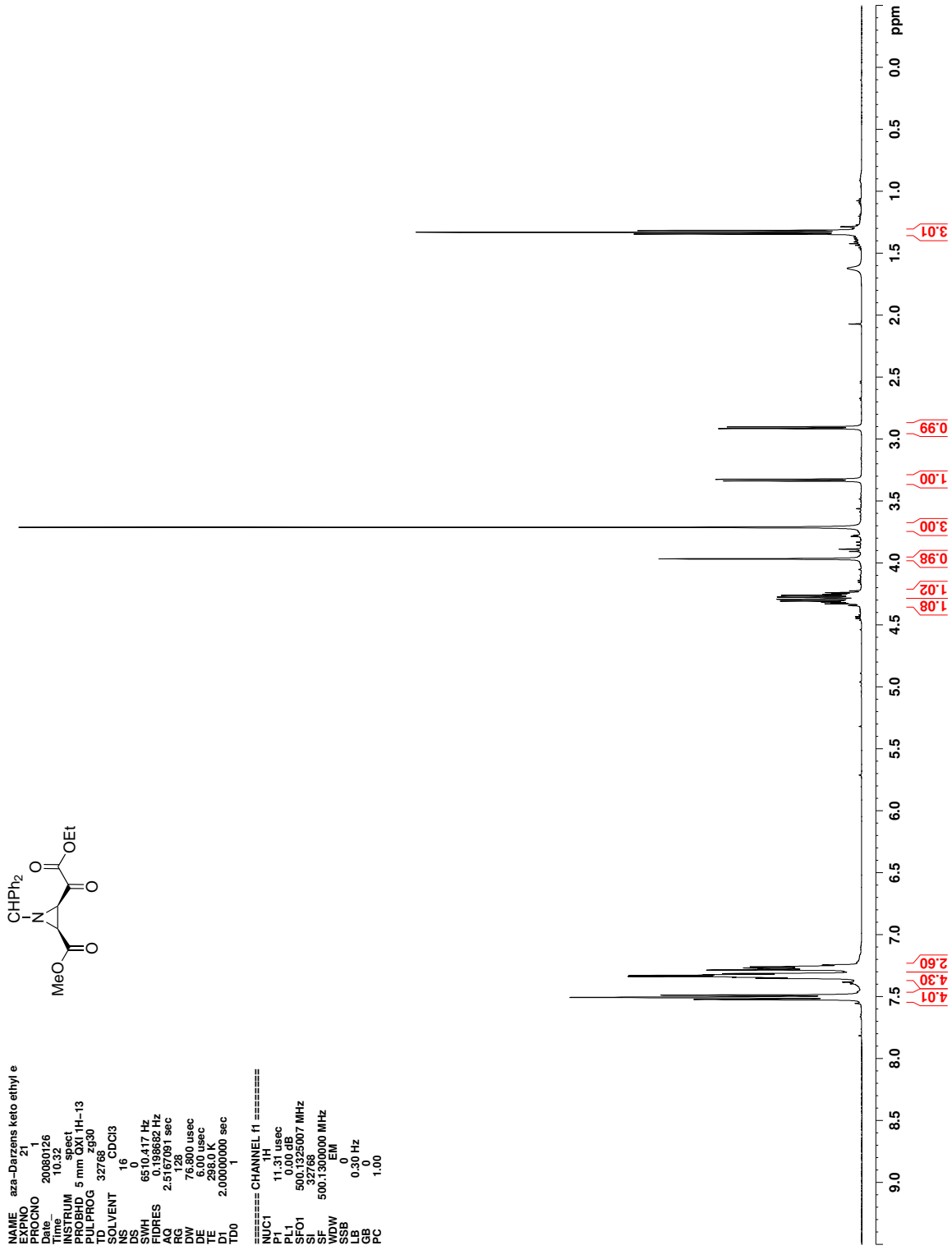
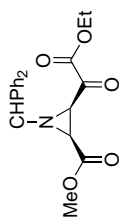


Figure C.13. ¹H NMR (CDCl₃) of 85



```

NAME az-Darzens keto ethyl e
EXPNO 121
PROCNO 121
Date_ 20080126
Time 10.39
INSTRUM spect
PROBHD 5 mm QXI 1H-13
TD 65536
AQ 0.193672 Hz
RG 327.689930
SOLVENT CDCl3
NS 357
DS 8
SWH 31446.641 Hz
FIDRES 0.193672 Hz
AQ 0.193672 Hz
RG 327.689930
DE 15.900 usec
TE 298.0 K
D1 2.0000000 sec
DELTA 1.8999998 sec
TD0 1
===== CHANNEL f1 =====
NUC1 13C
P1 15.00 usec
PL1 0.00 dB
SFO1 125.7715724 MHz
===== CHANNEL f2 =====
CPDPRG2 waltz16
NUC2 13C
P2 100.00 usec
PL2 0.00 dB
PL12 18.93 dB
PL13 18.93 dB
SFO2 500.1325007 MHz
SF 327.689930 MHz
WDW EM
SSB 0
LB 1.50 Hz
GB 0
PC 1.40

```

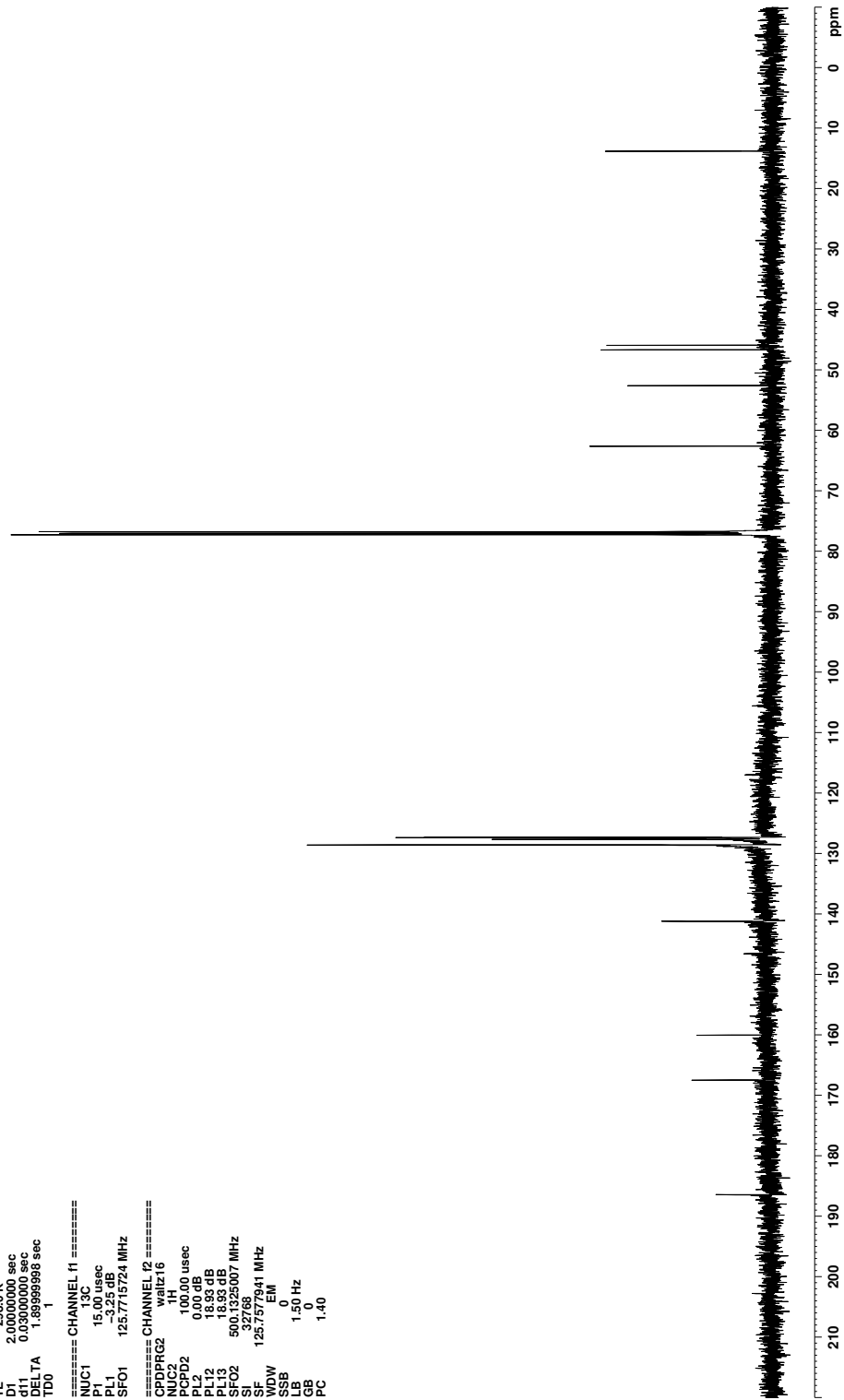


Figure C.14. ¹³C NMR (CDCl₃) of 85

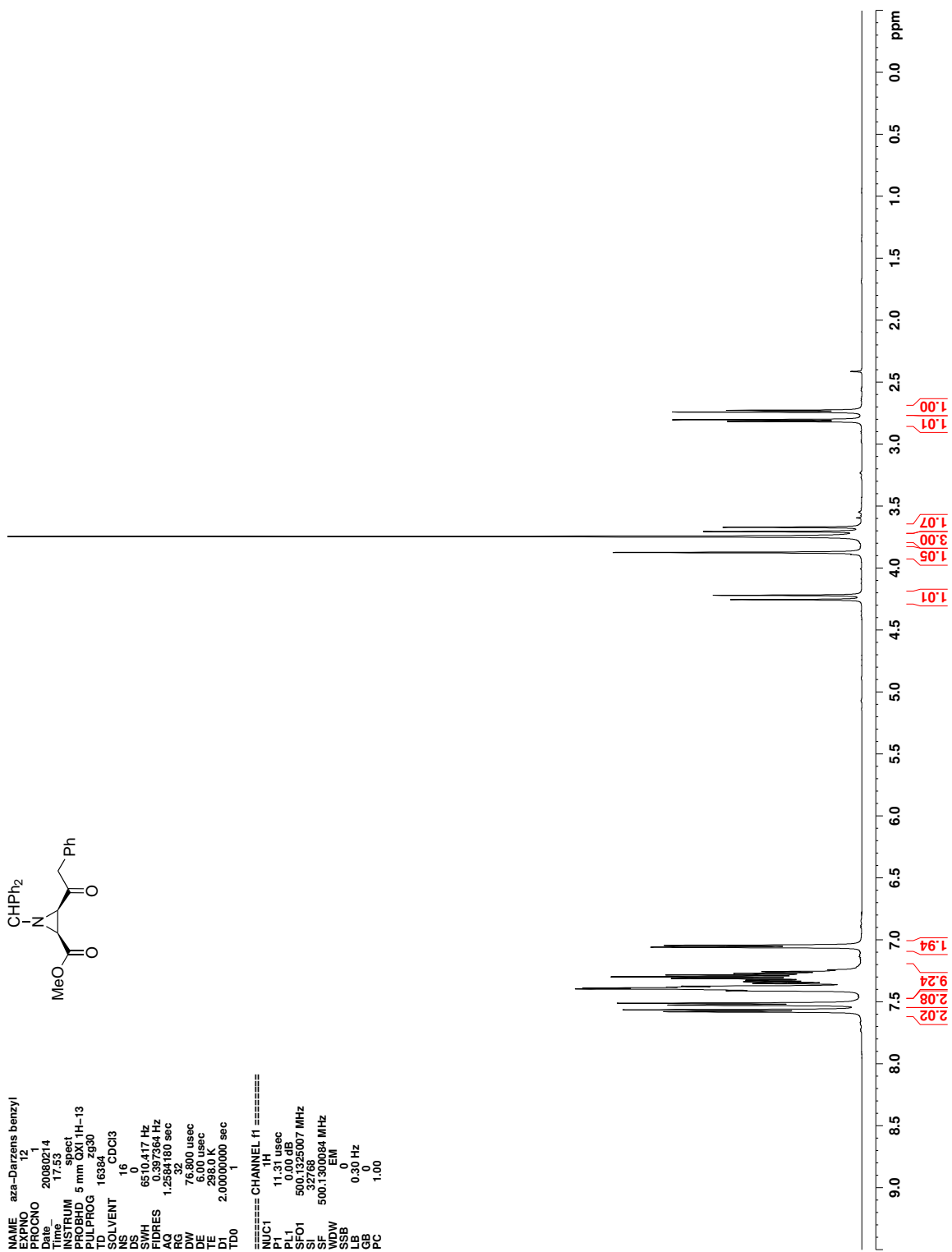


Figure C.15. ^1H NMR (CDCl_3) of **86**

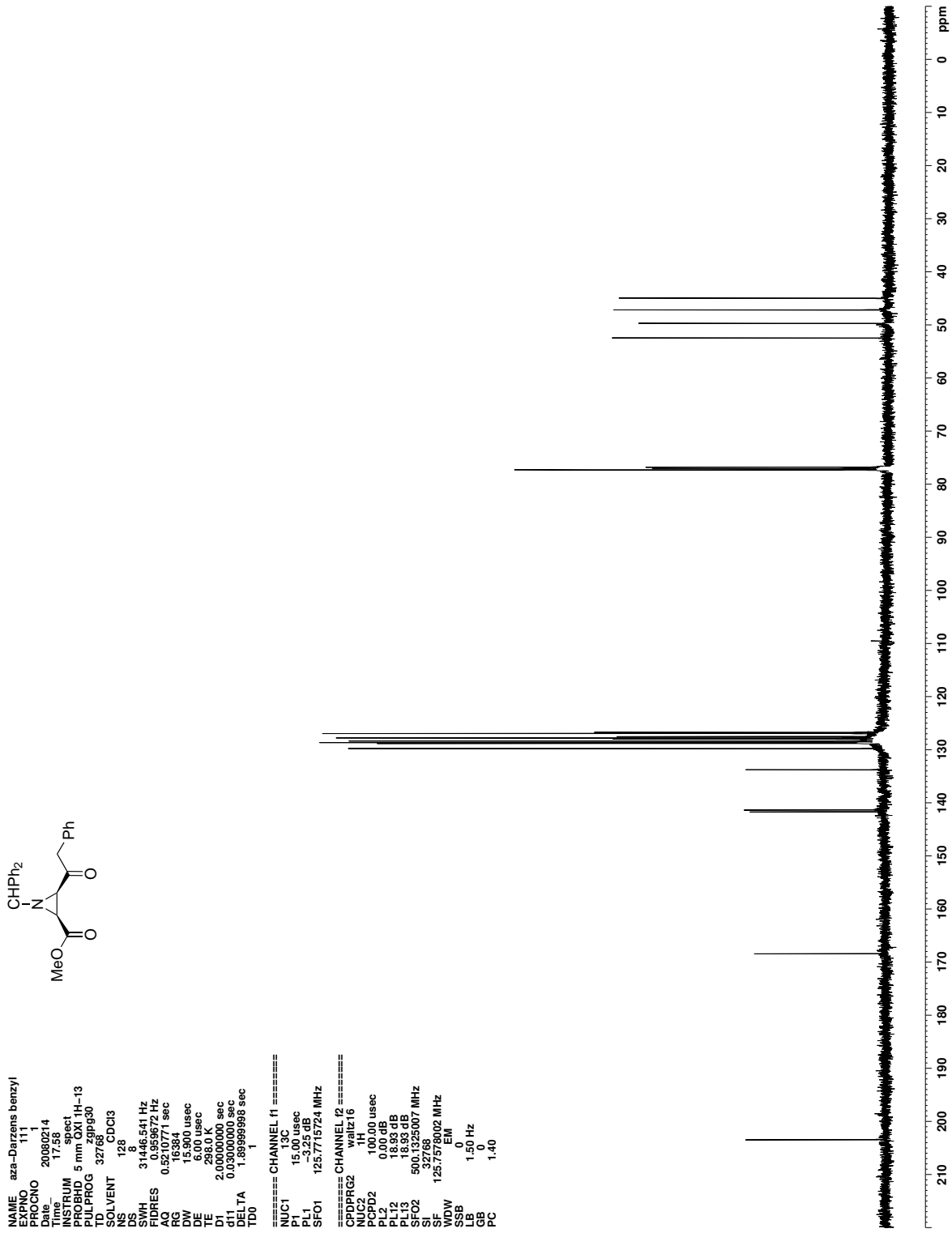


Figure C.16. ¹³C NMR (CDCl₃) of 86

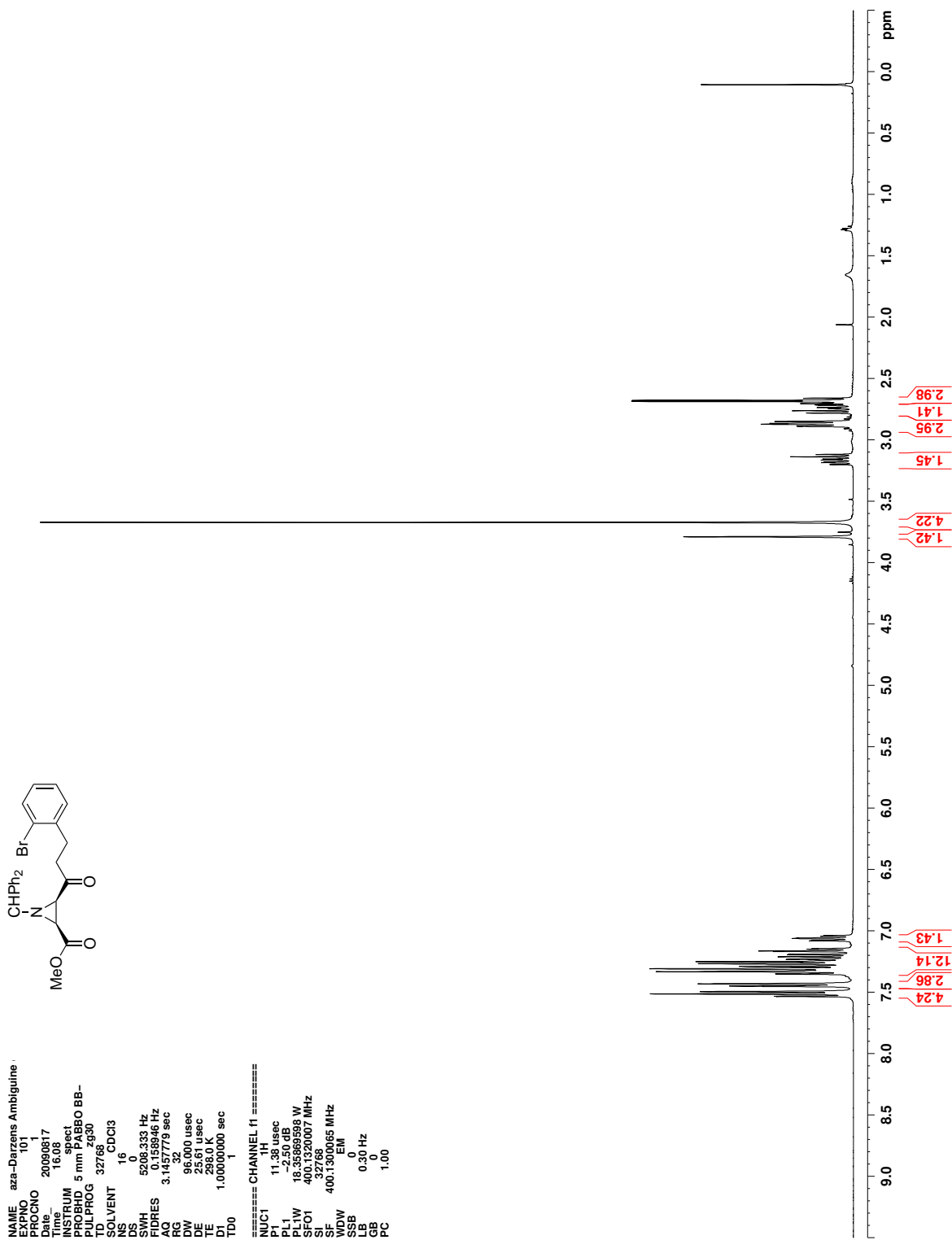


Figure C.17. ^1H NMR (CDCl_3) of 87

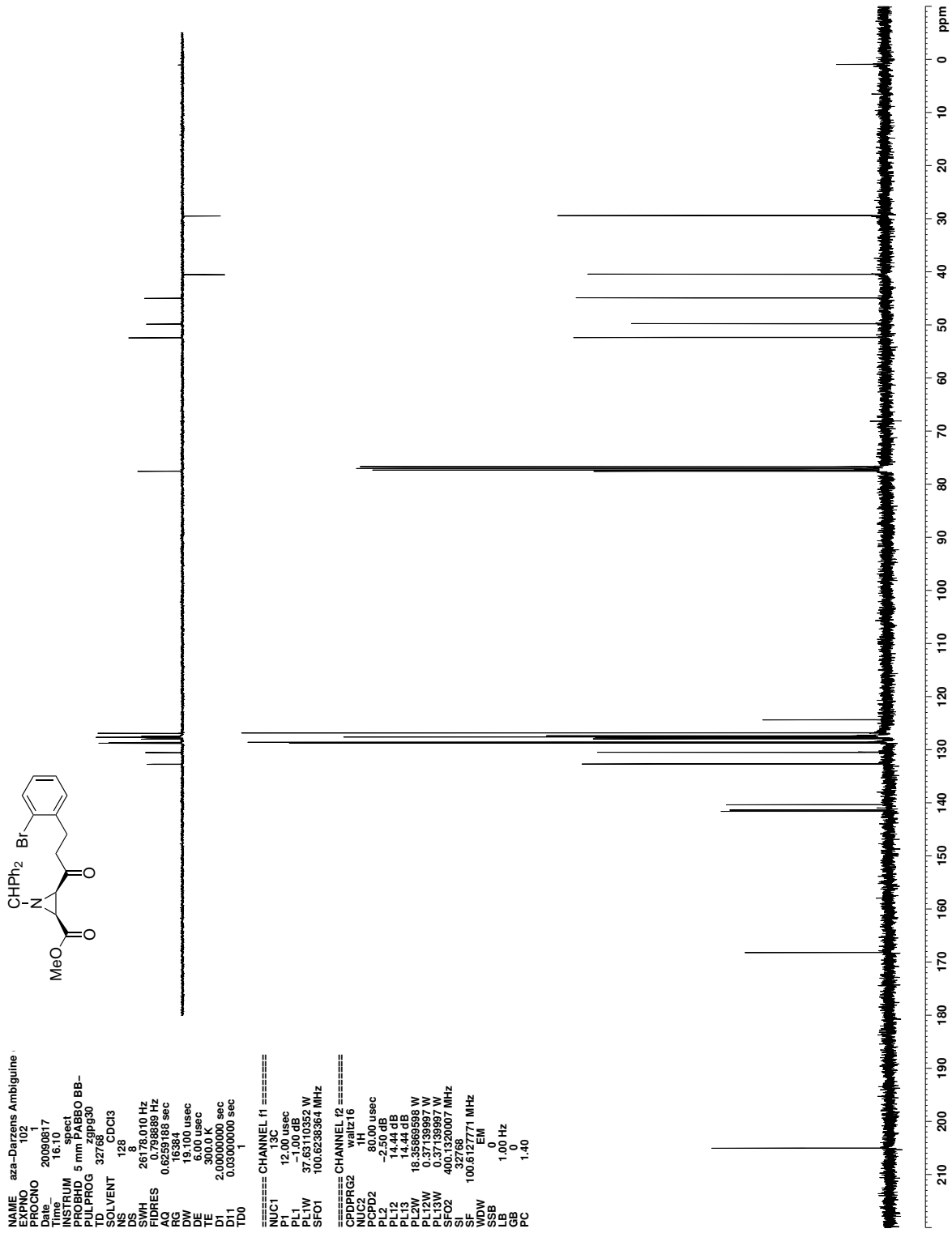


Figure C.18. ¹³C NMR (CDCl₃) of 87

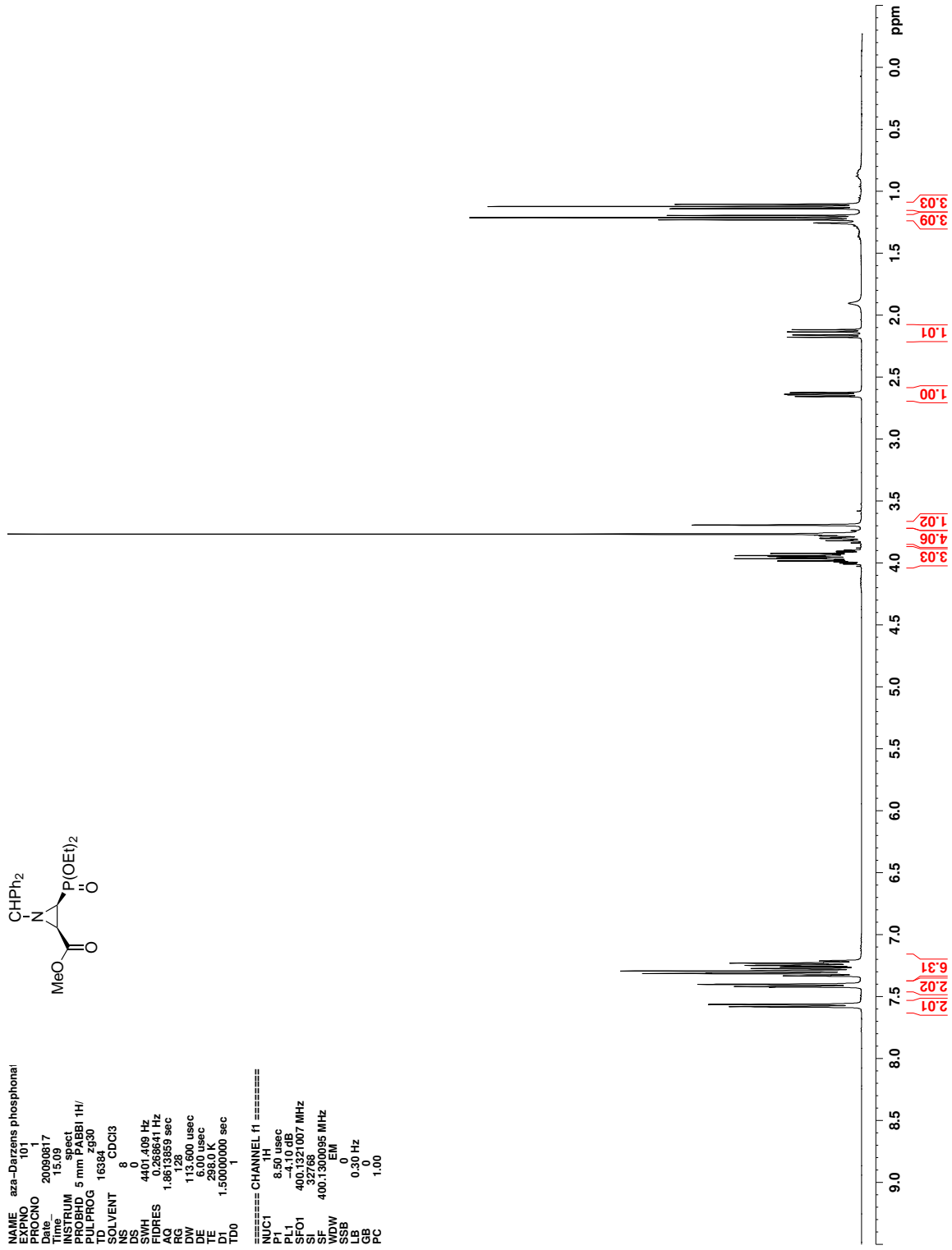


Figure C.19. ¹H NMR (CDCl₃) of 88

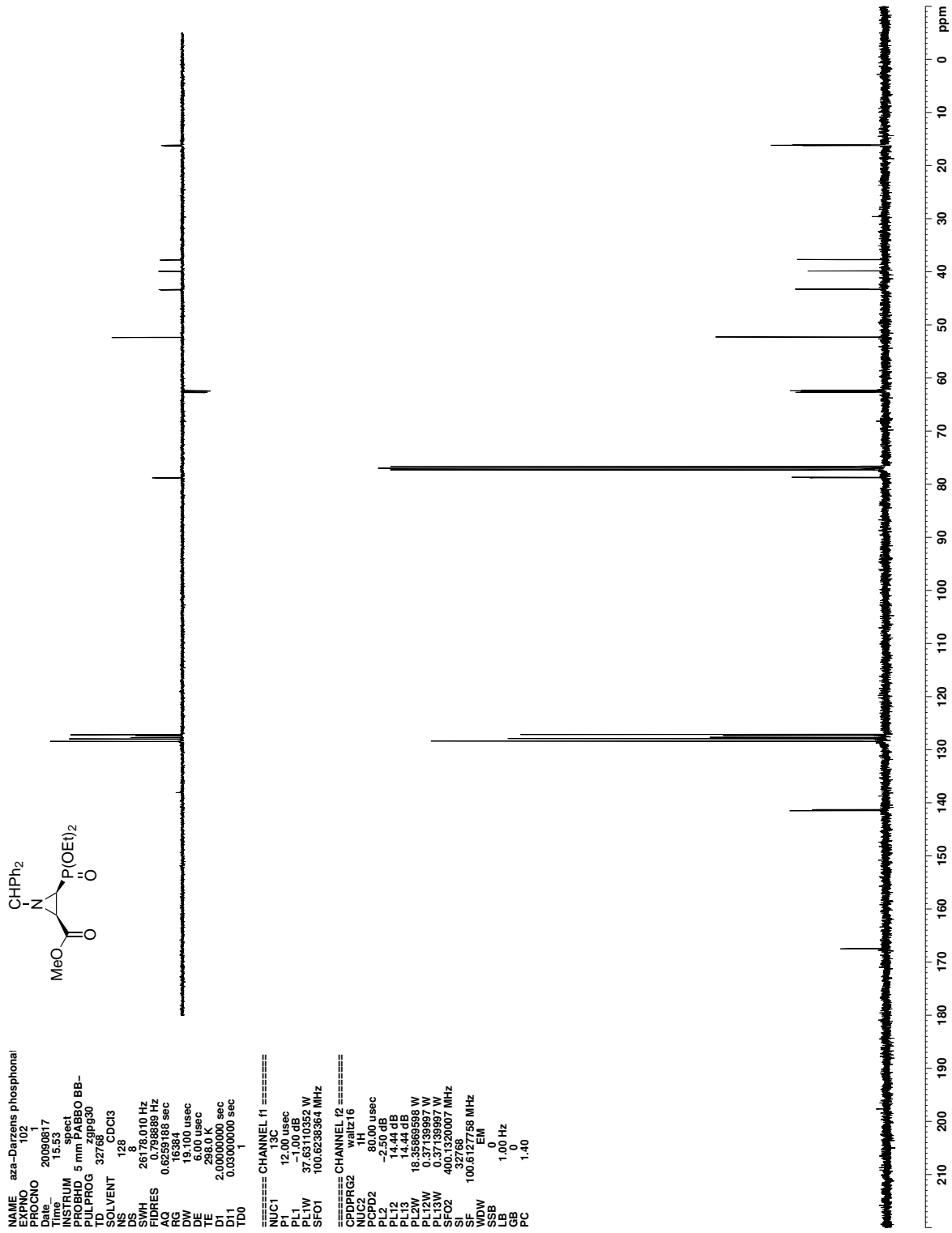
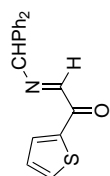


Figure C.20. ¹³C NMR (CDCl₃) of 88



```

NAME      2--099
PROCNO    11
Date_     20071216
Time      12.07
INSTRUM   spect
PROBHD    5 mm PABBO BB-
PULPROG   zg30
TD         65536
SOLVENT   CDCl3
NS         16
DS         0
SWH        5206.333 Hz
FIDRES     0.075473 Hz
AQ         0.0096 sec
RG         32
DW         96.000 usec
DE         6.00 usec
TE         298.0 K
D1         1.00000000 sec
TD0
===== CHANNEL f1 =====
NUC1      1H
P1         11.38 usec
PL1        -2.50 dB
SFO1      400.1300007 MHz
SI         327136
SF         400.1300065 MHz
WDW        EM
SSB        0
LB         0
GB         0
PC         1.00

```

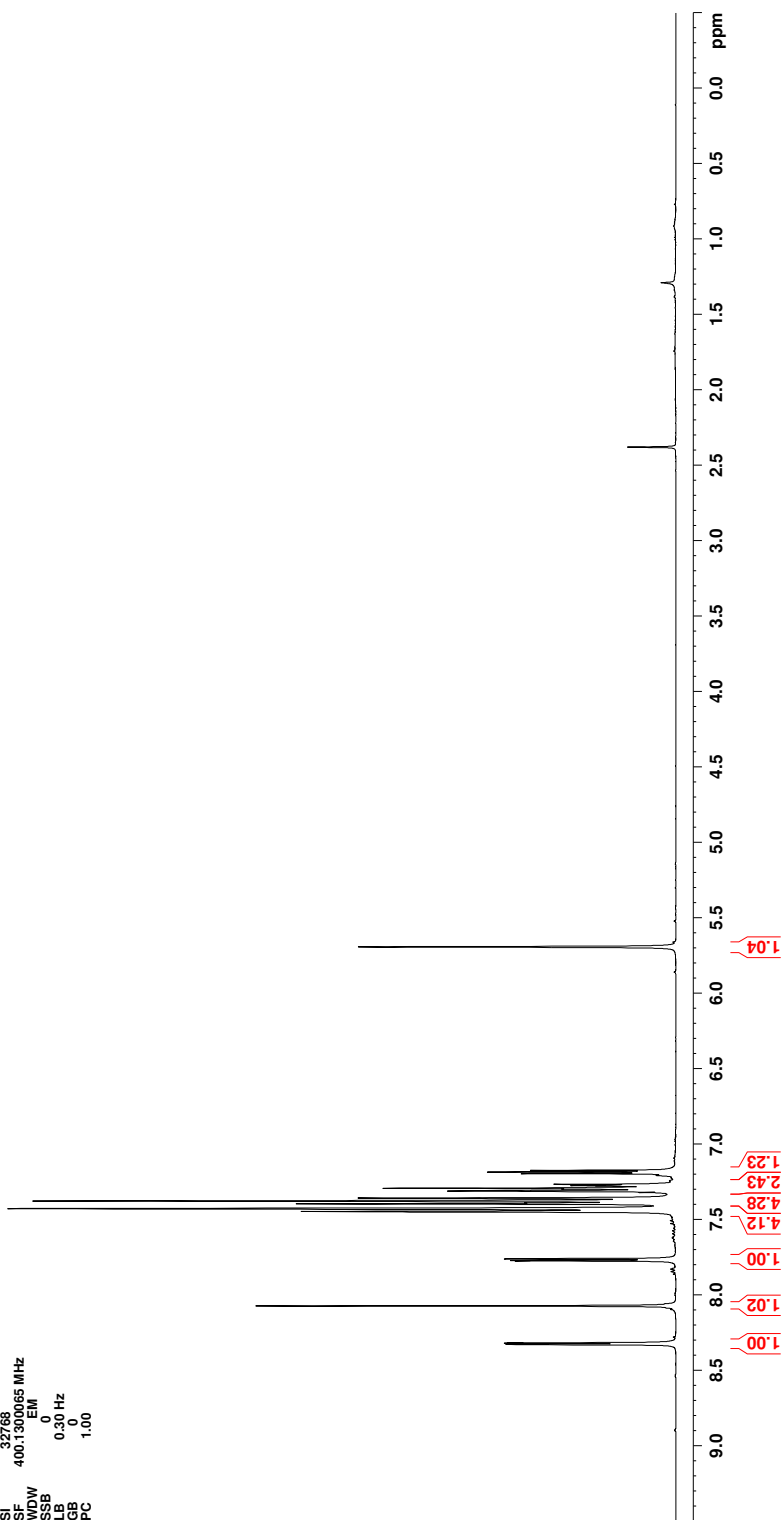


Figure C.21. ¹H NMR (CDCl₃) of 131

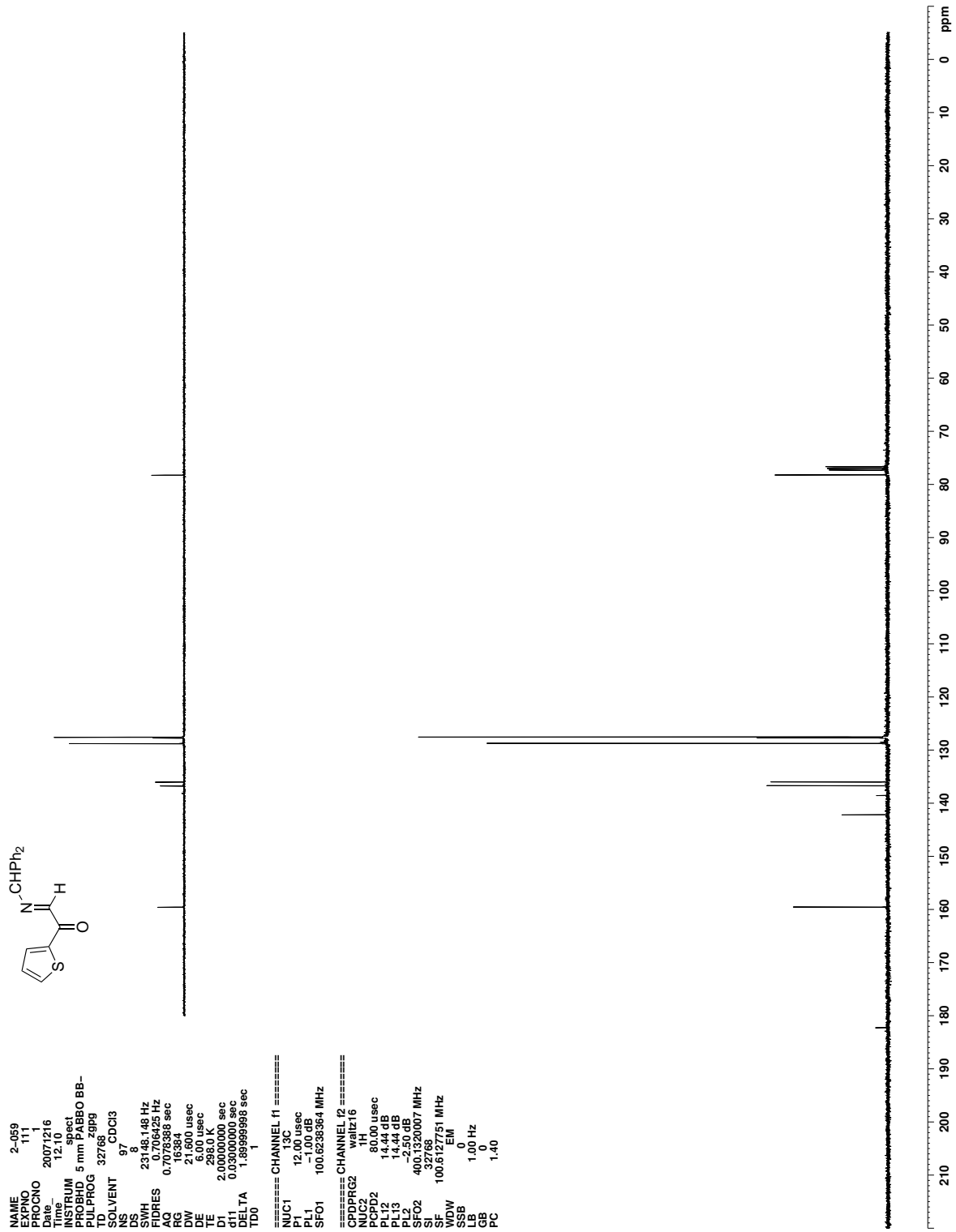


Figure C.22. ^{13}C NMR (CDCl_3) of 131

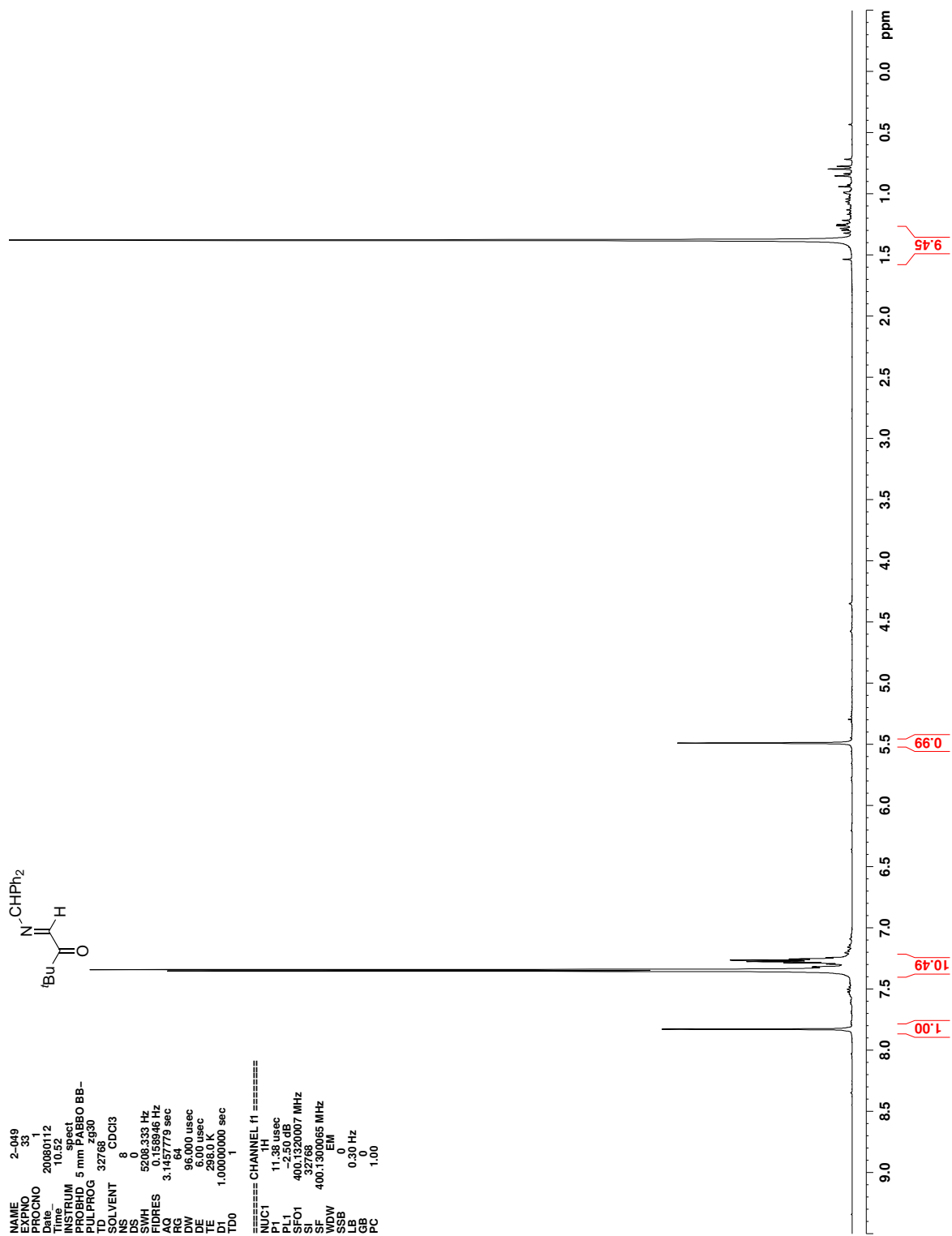


Figure C.23. ^1H NMR (CDCl_3) of 132

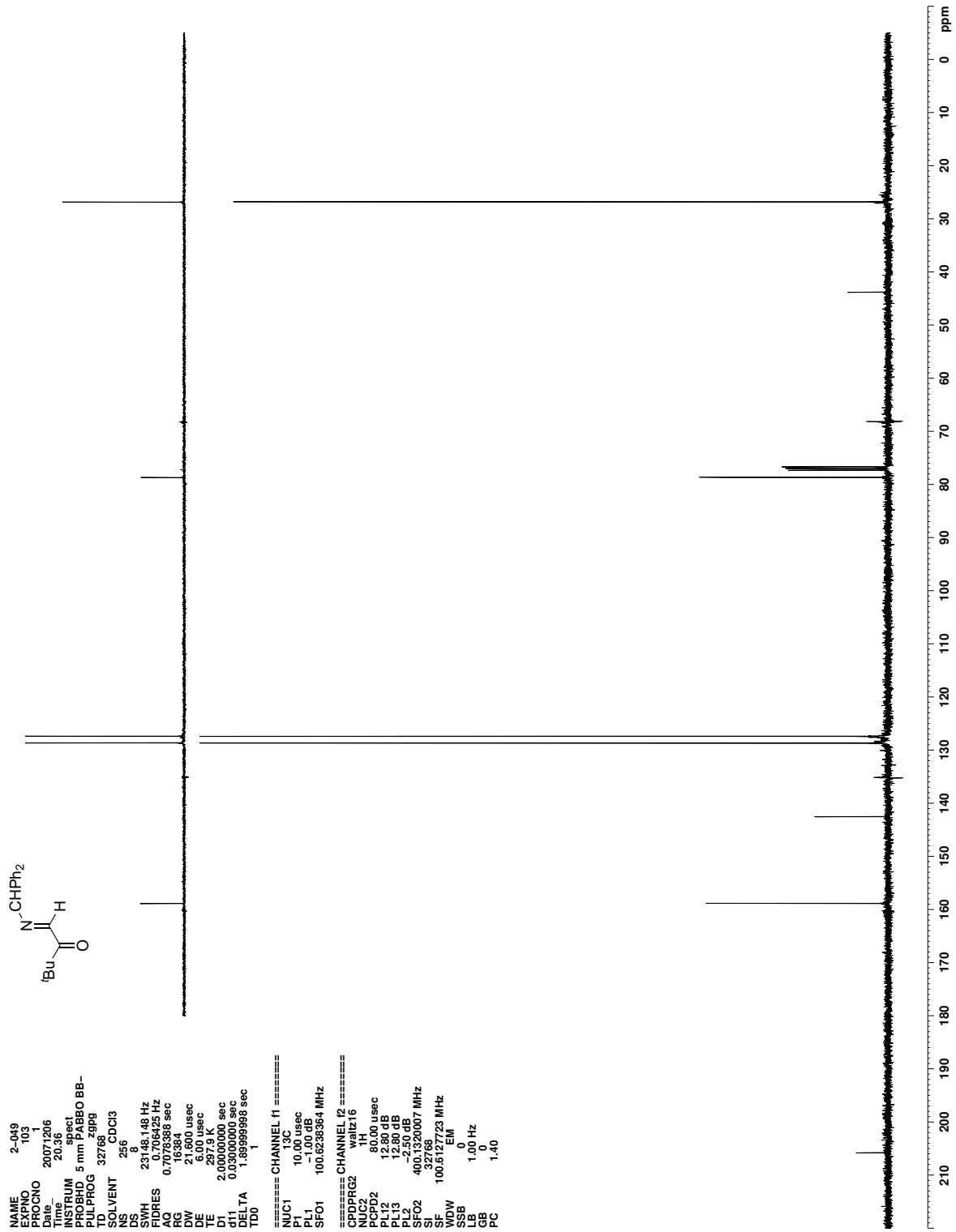


Figure C.24. ^{13}C NMR (CDCl_3) of **132**

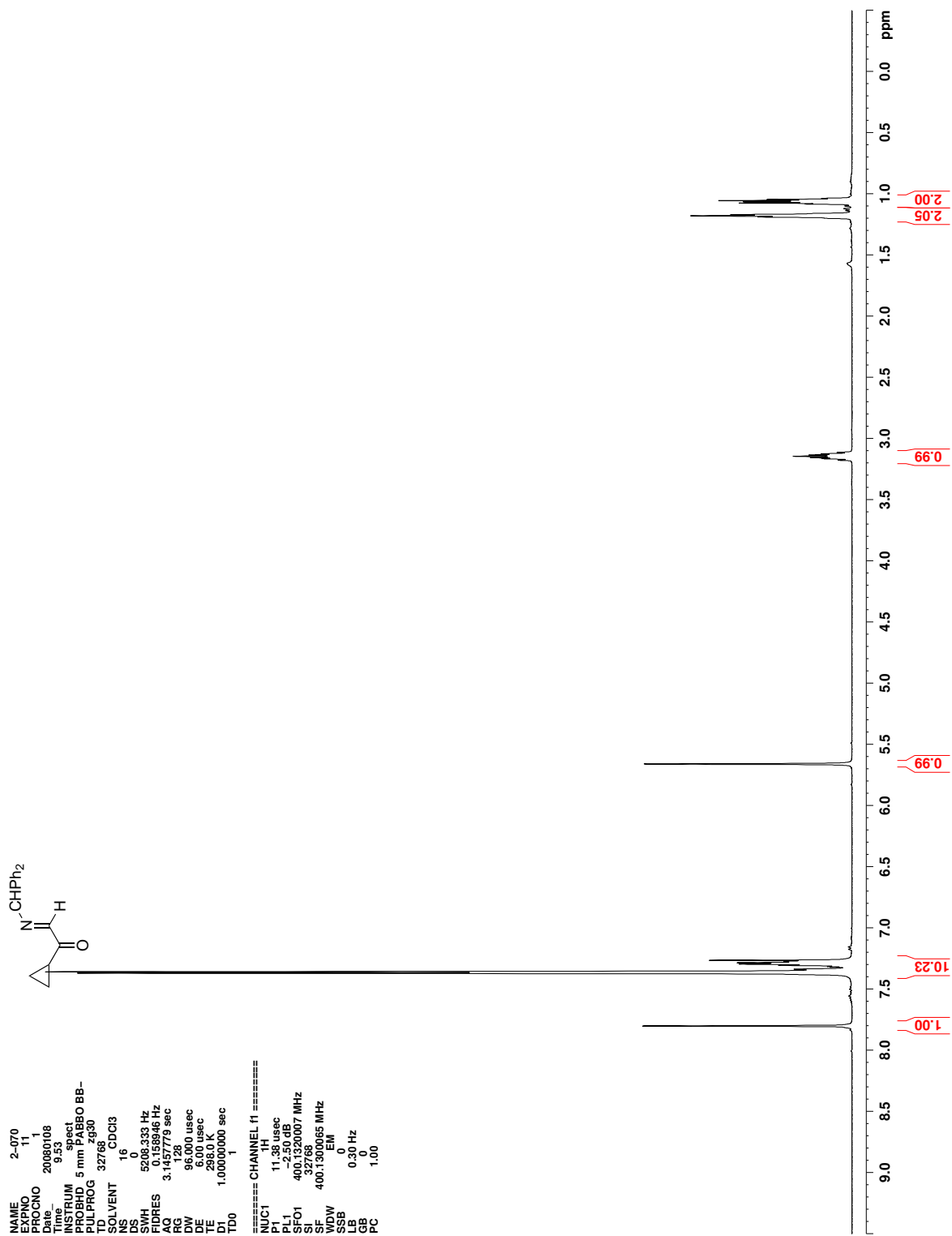


Figure C.25. ^1H NMR (CDCl_3) of 133

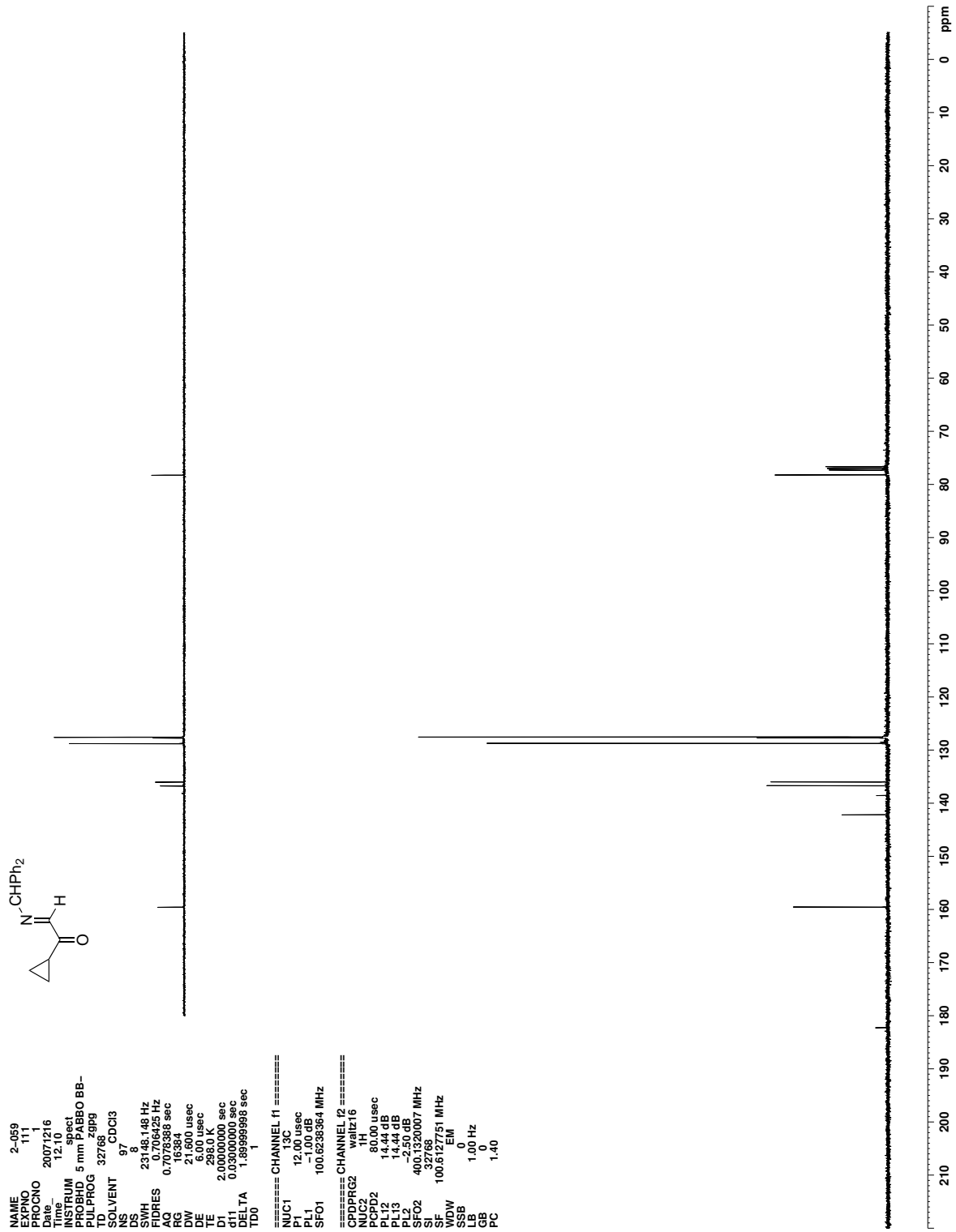


Figure C.26. ^{13}C NMR (CDCl_3) of **133**

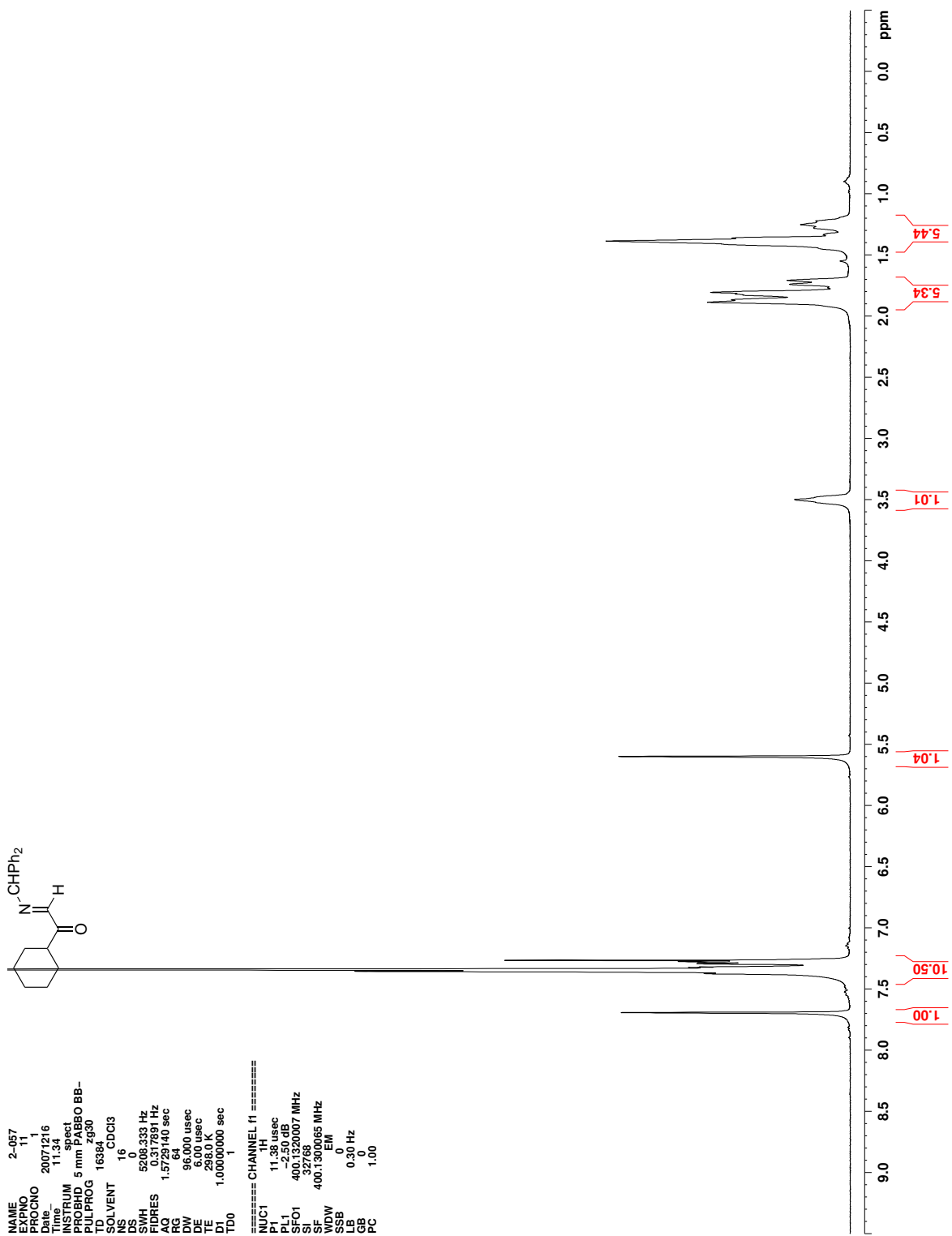


Figure C.27. ^1H NMR (CDCl_3) of 134

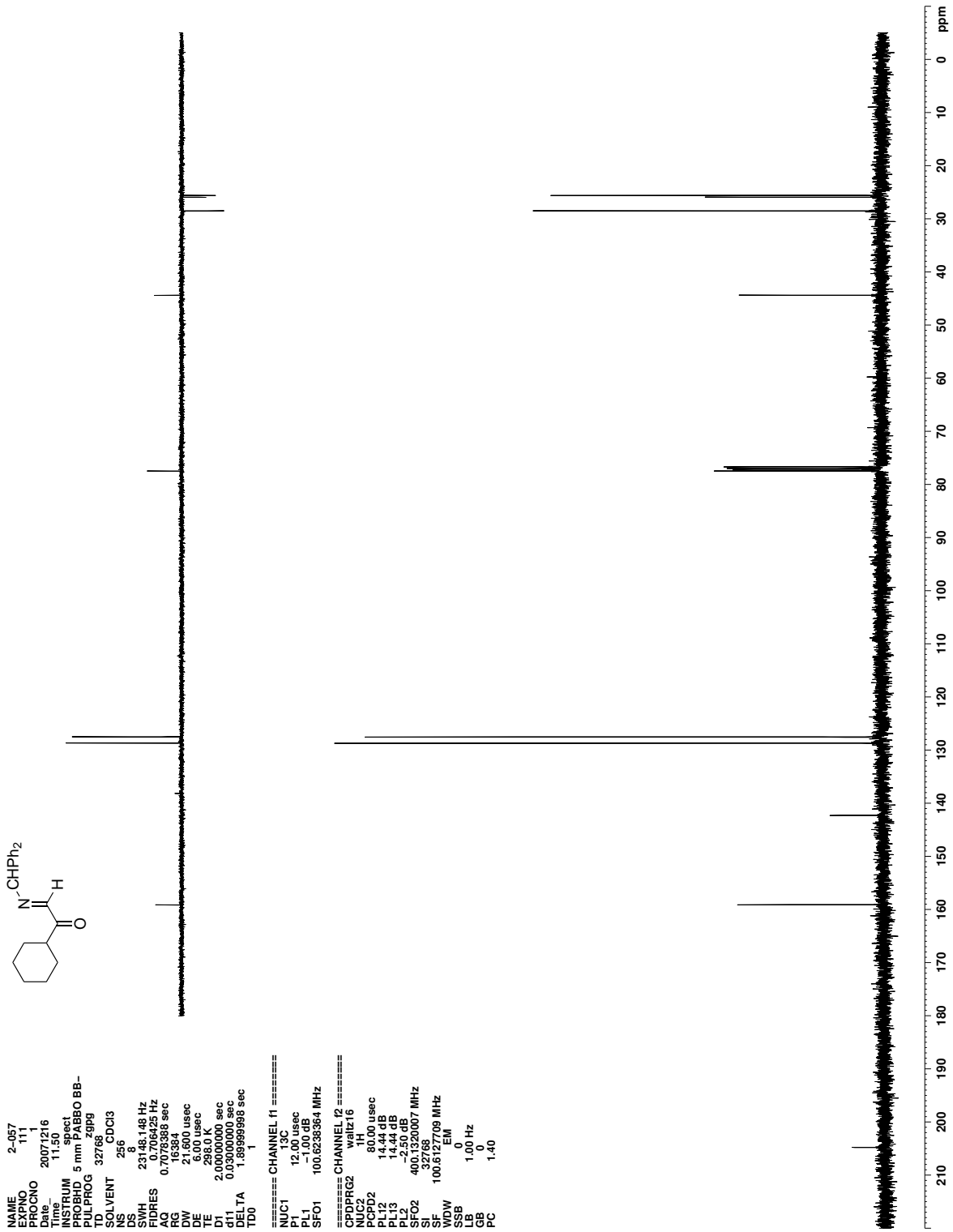
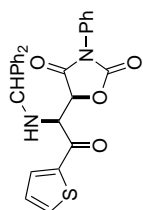


Figure C.28. ^{13}C NMR (CDCl_3) of 134



```

NAME      2-076
EXPNO    1
PROCNO   11
Date_    20080115
Time     11.24
INSTRUM spect
PROBHD   5 mm PABBO BB-
PULPROG zg30
TD       32768
SOLVENT  CDCl3
NS       8
DS       0
SWH      5206.333 Hz
FIDRES   0.152646 Hz
AQ       3.112779 sec
RG       128
DW       96.000 usec
DE       6.00 usec
TE       298.0 K
D1       1.00000000 sec
TD0
===== CHANNEL f1 =====
NUC1     1H
P1       11.38 usec
PL1      -2.50 dB
SFO1     400.1300007 MHz
SI       32768
SF       400.1300065 MHz
WDW      EM
SSB      0
LB       0.30 Hz
GB       0
PC       1.00

```

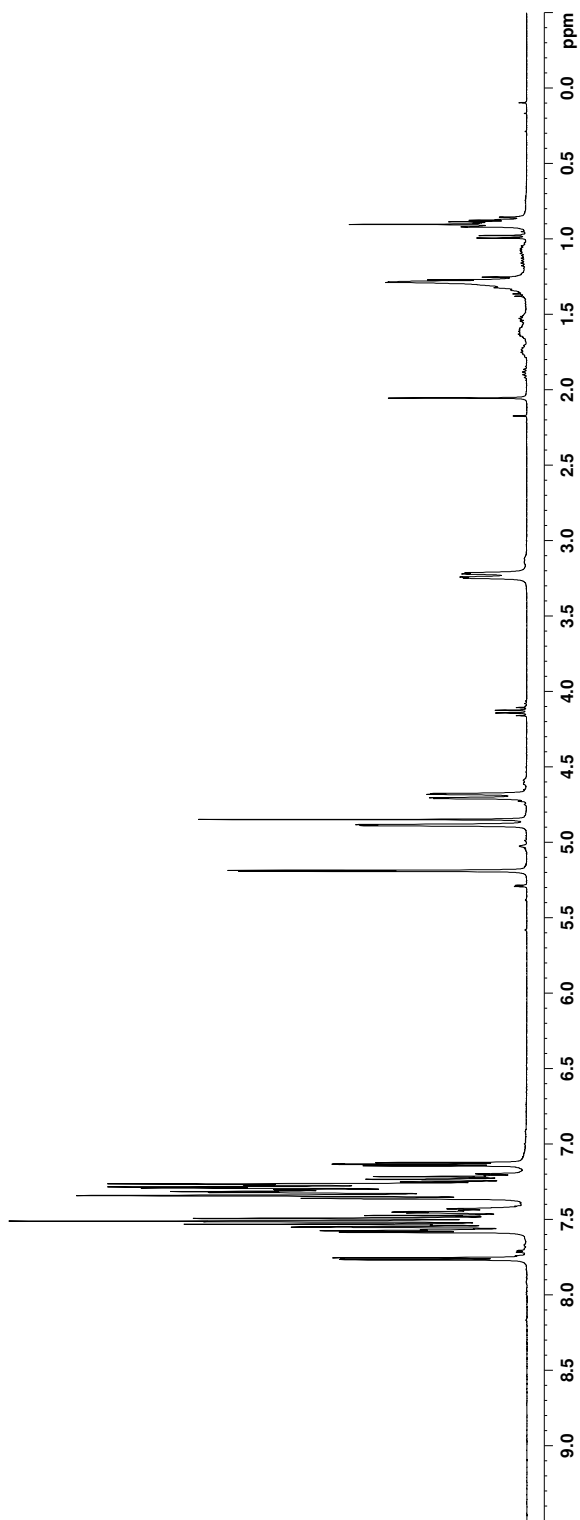


Figure C.29. ¹H NMR (CDCl₃) of 138

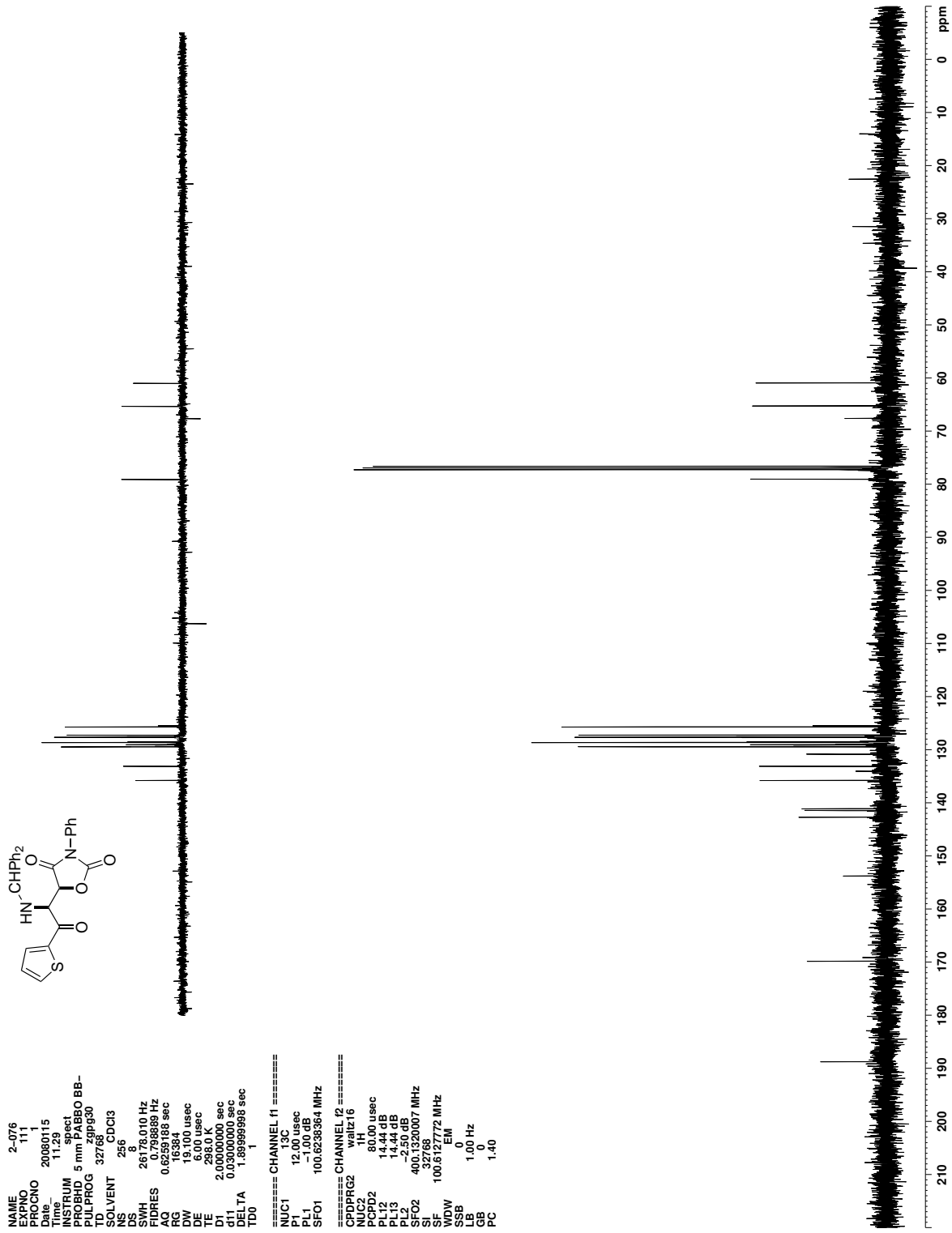


Figure C.30. ¹³C NMR (CDCl₃) of 138

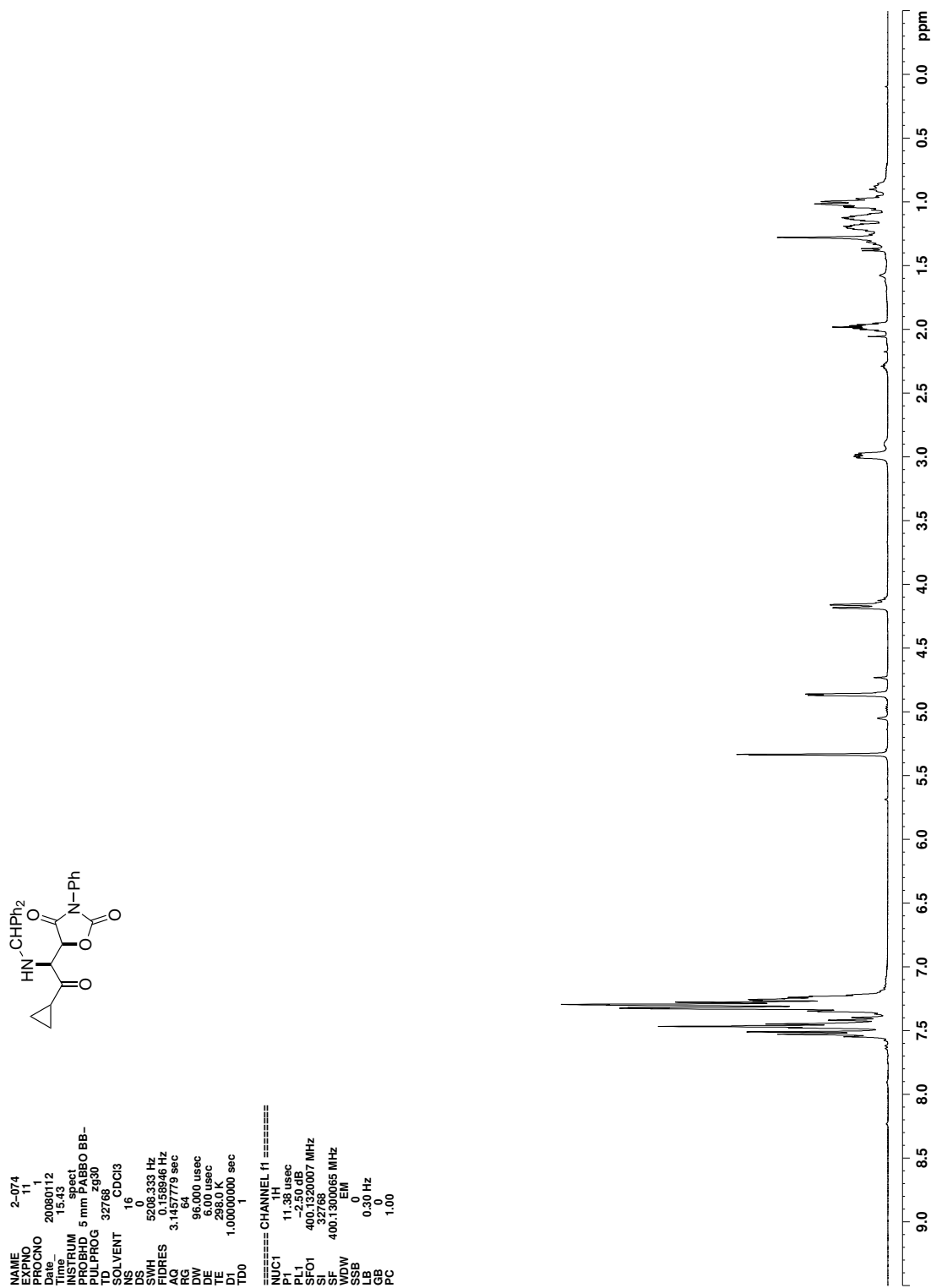


Figure C.31. ¹H NMR (CDCl₃) of 139

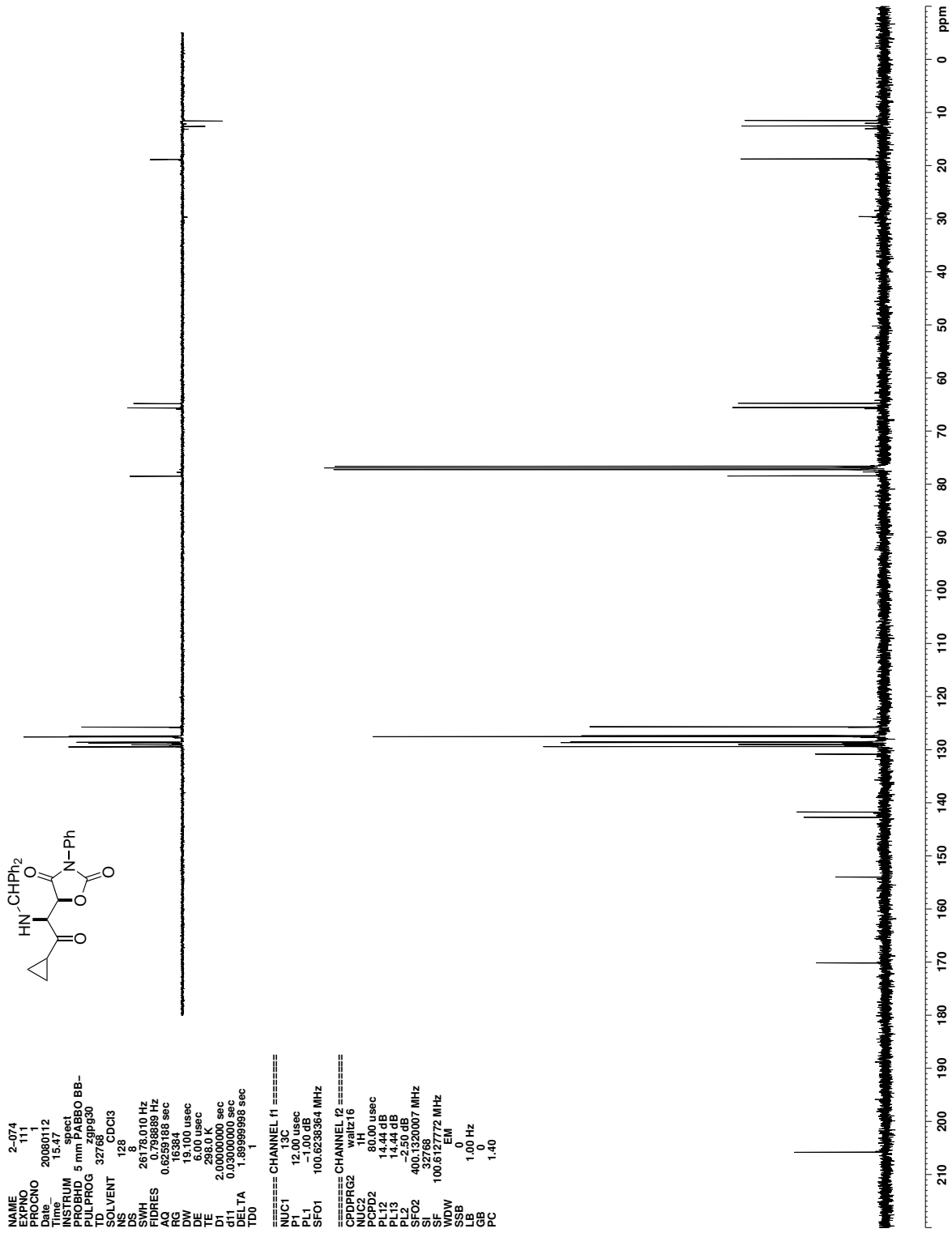


Figure C.32. ^{13}C NMR (CDCl_3) of 139

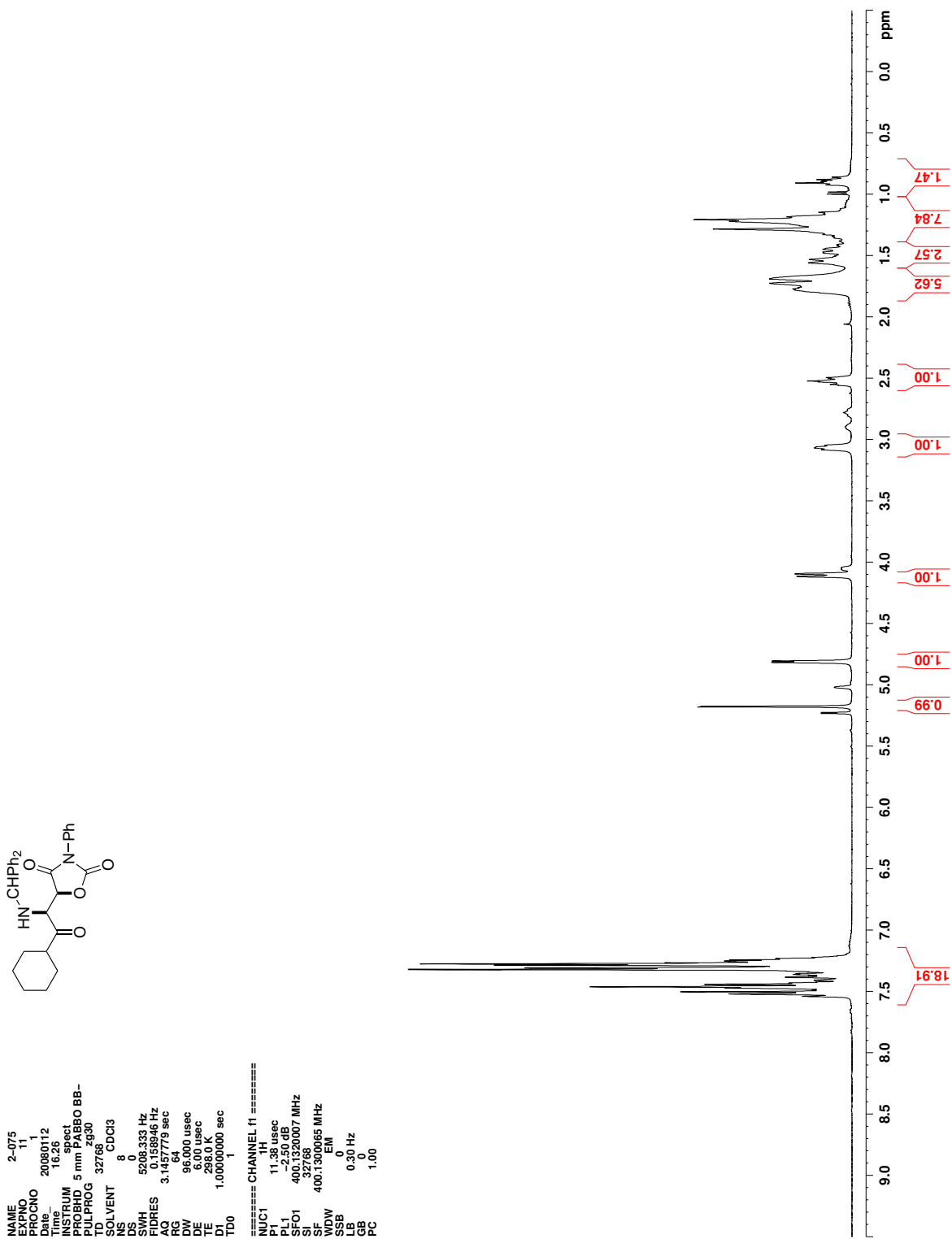


Figure C.33. ^1H NMR (CDCl_3) of 140

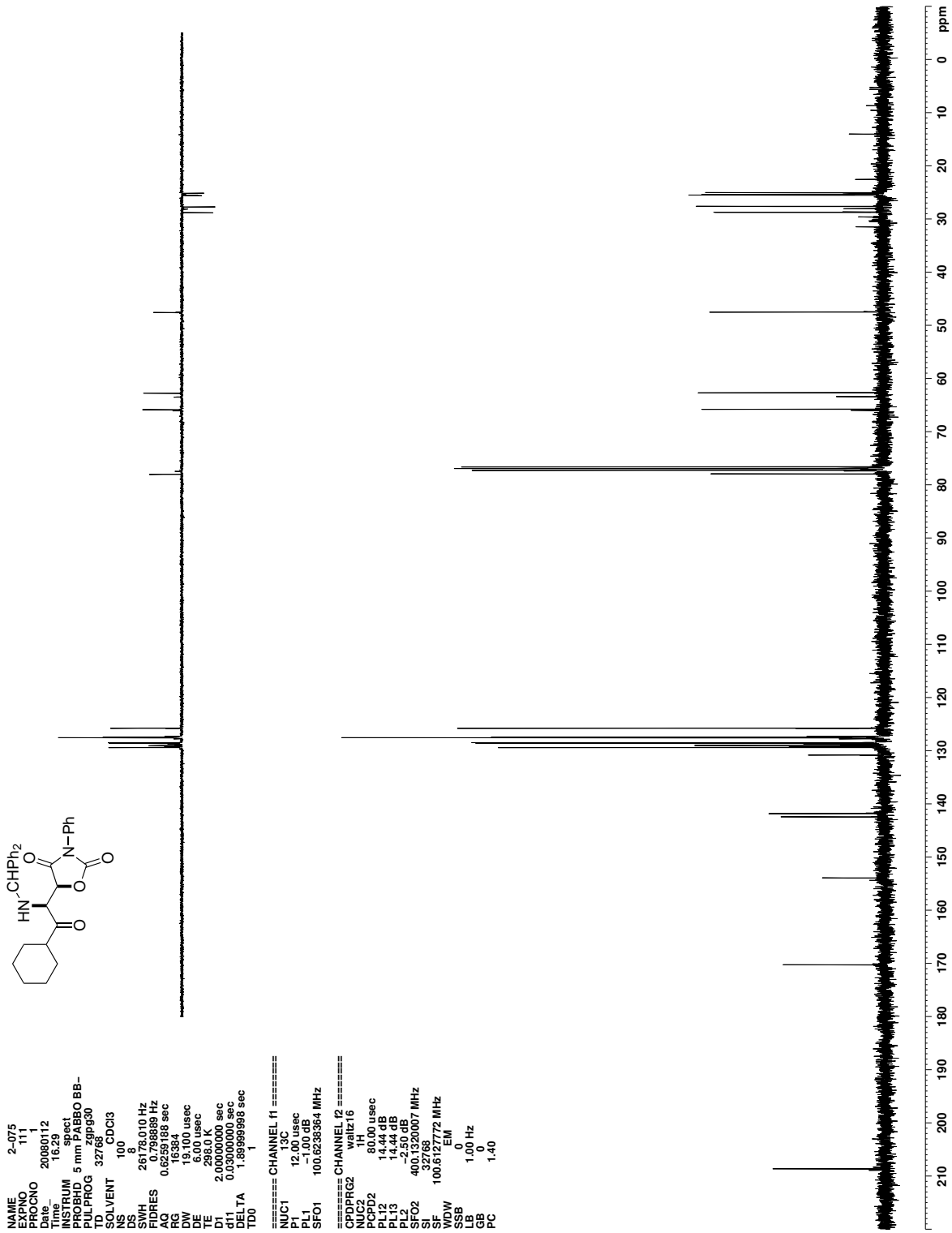


Figure C.34. ^{13}C NMR (CDCl_3) of 140

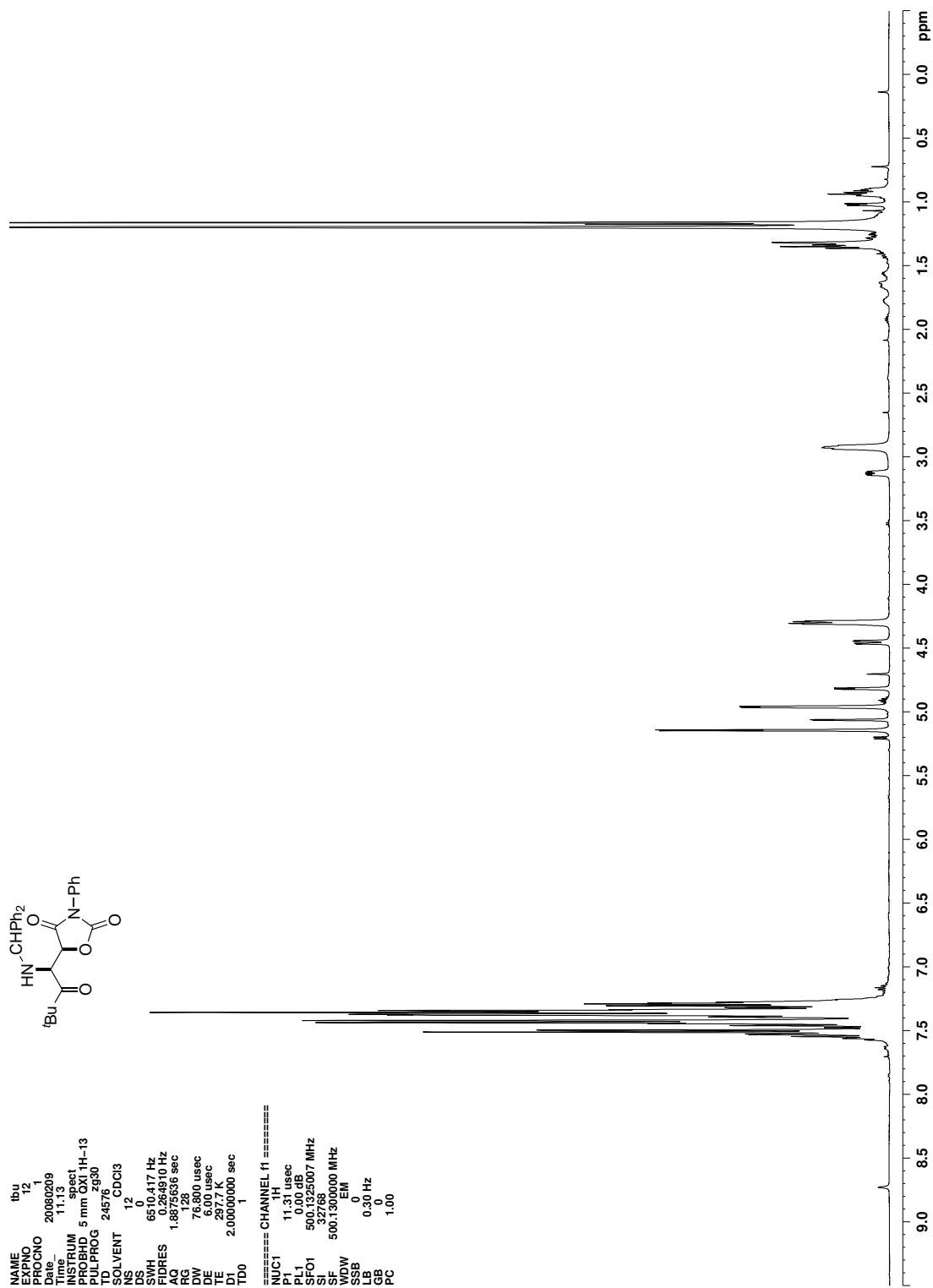


Figure C.35. ^1H NMR (CDCl_3) of 141

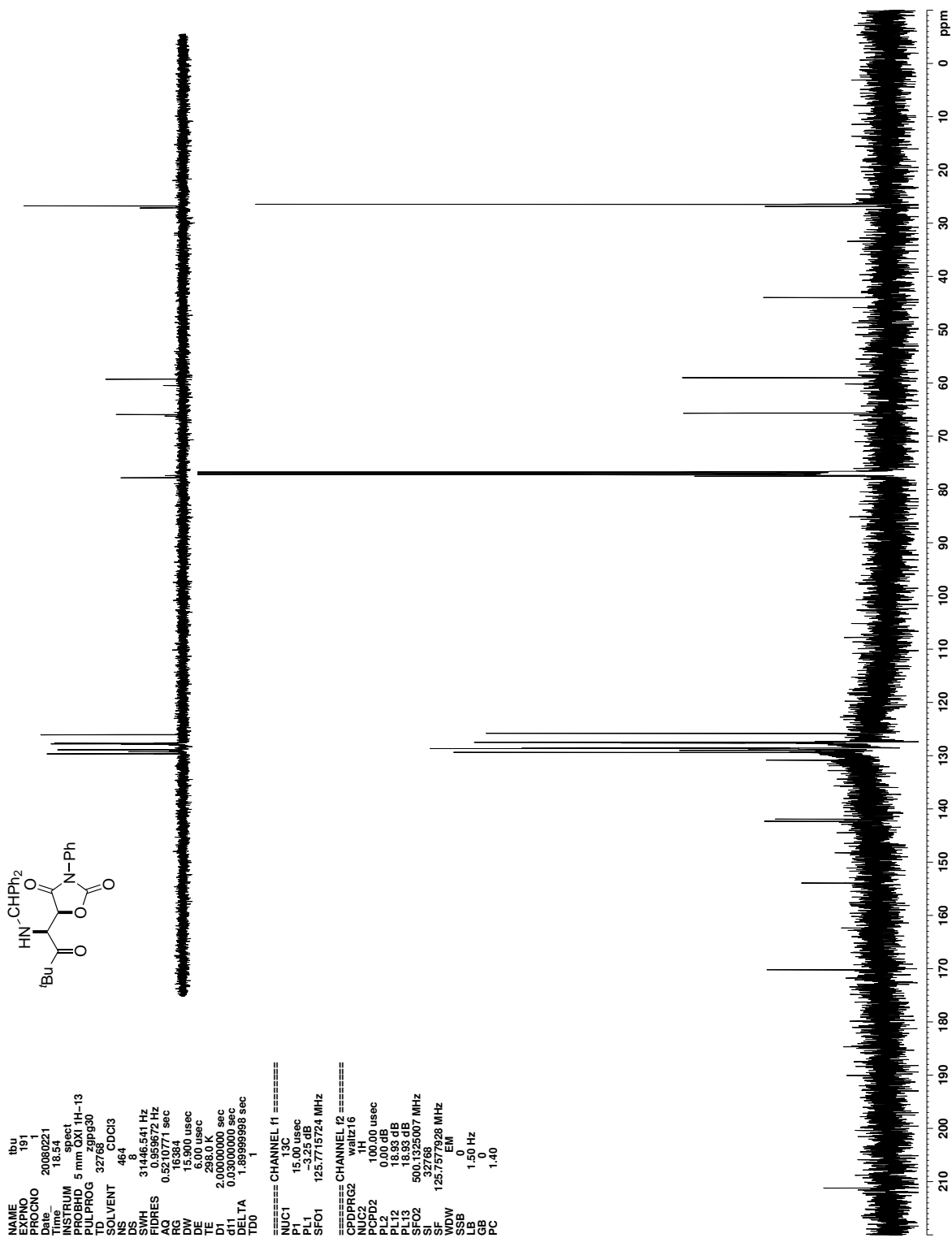


Figure C.36. ^{13}C NMR (CDCl_3) of 141

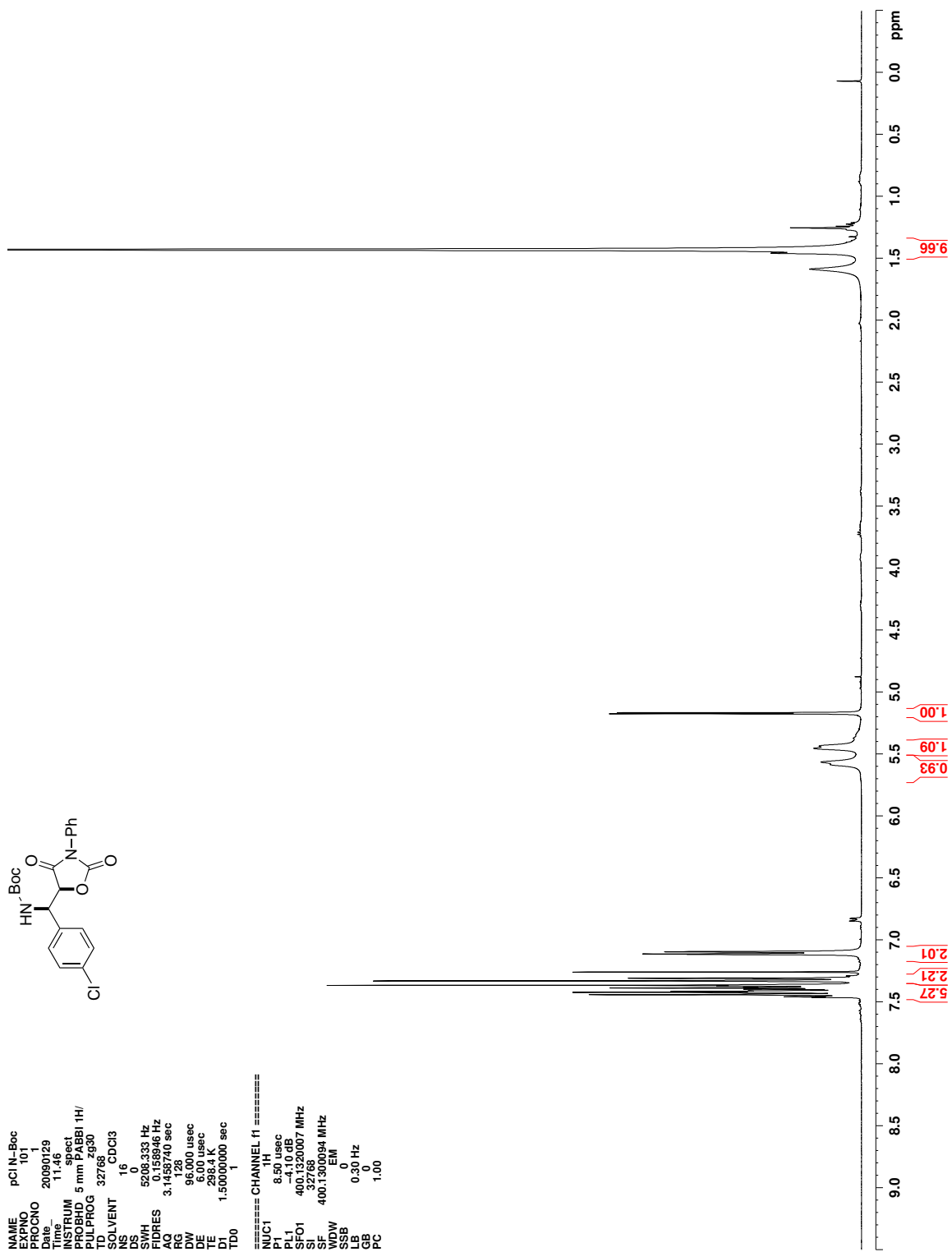


Figure C.37. ^1H NMR (CDCl_3) of 162

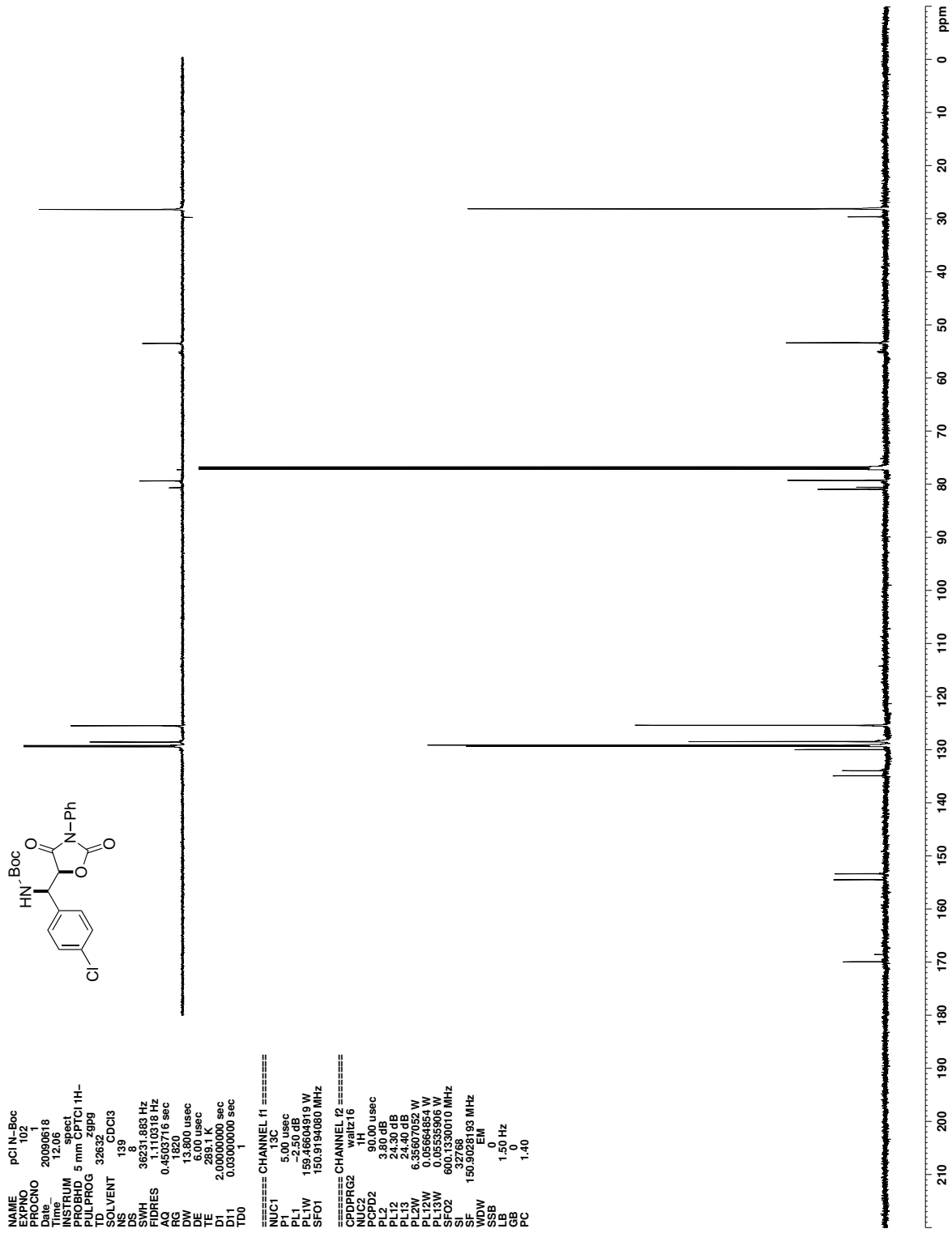


Figure C.38. ¹³C NMR (CDCl₃) of 162

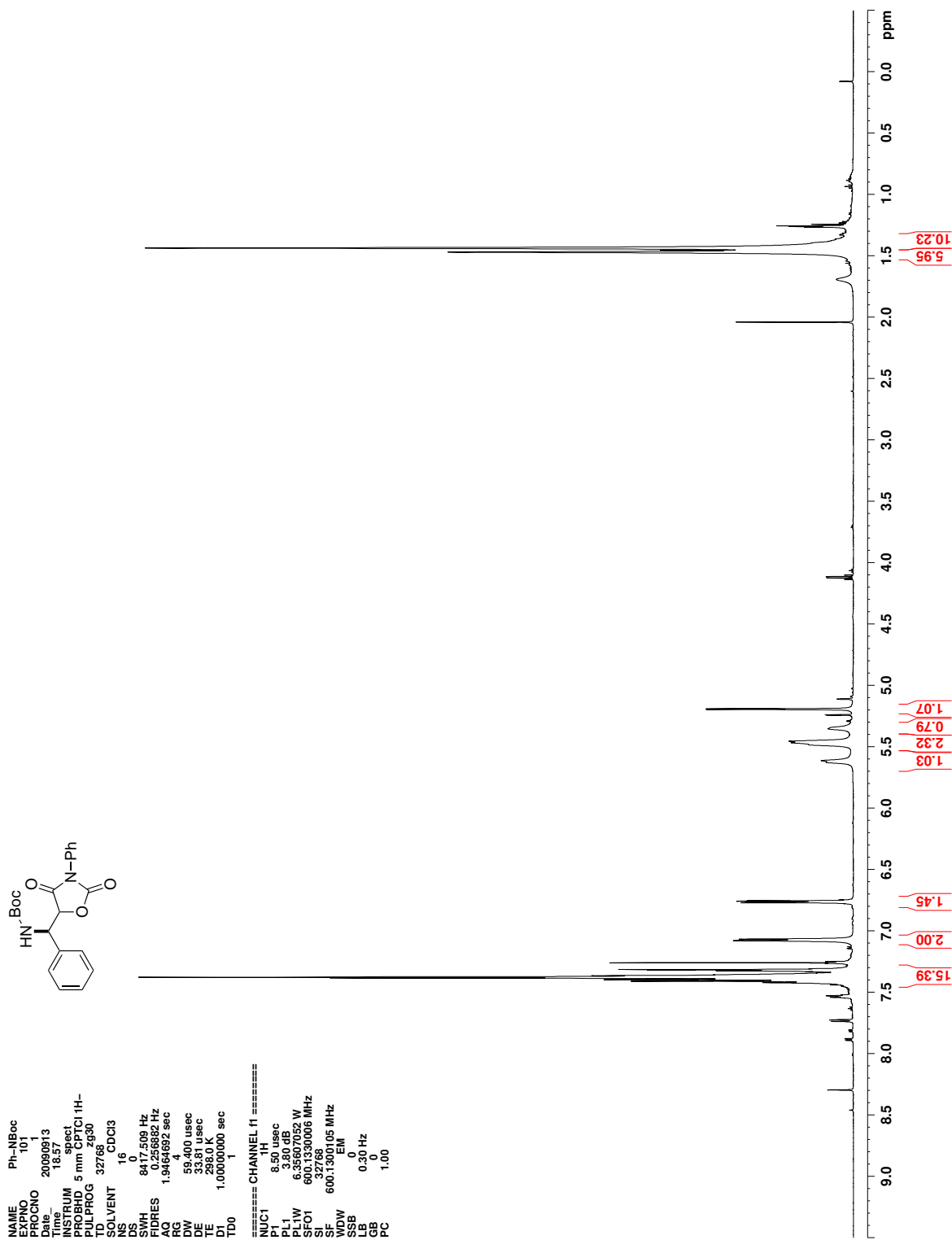


Figure C.39. ^1H NMR (CDCl_3) of 415

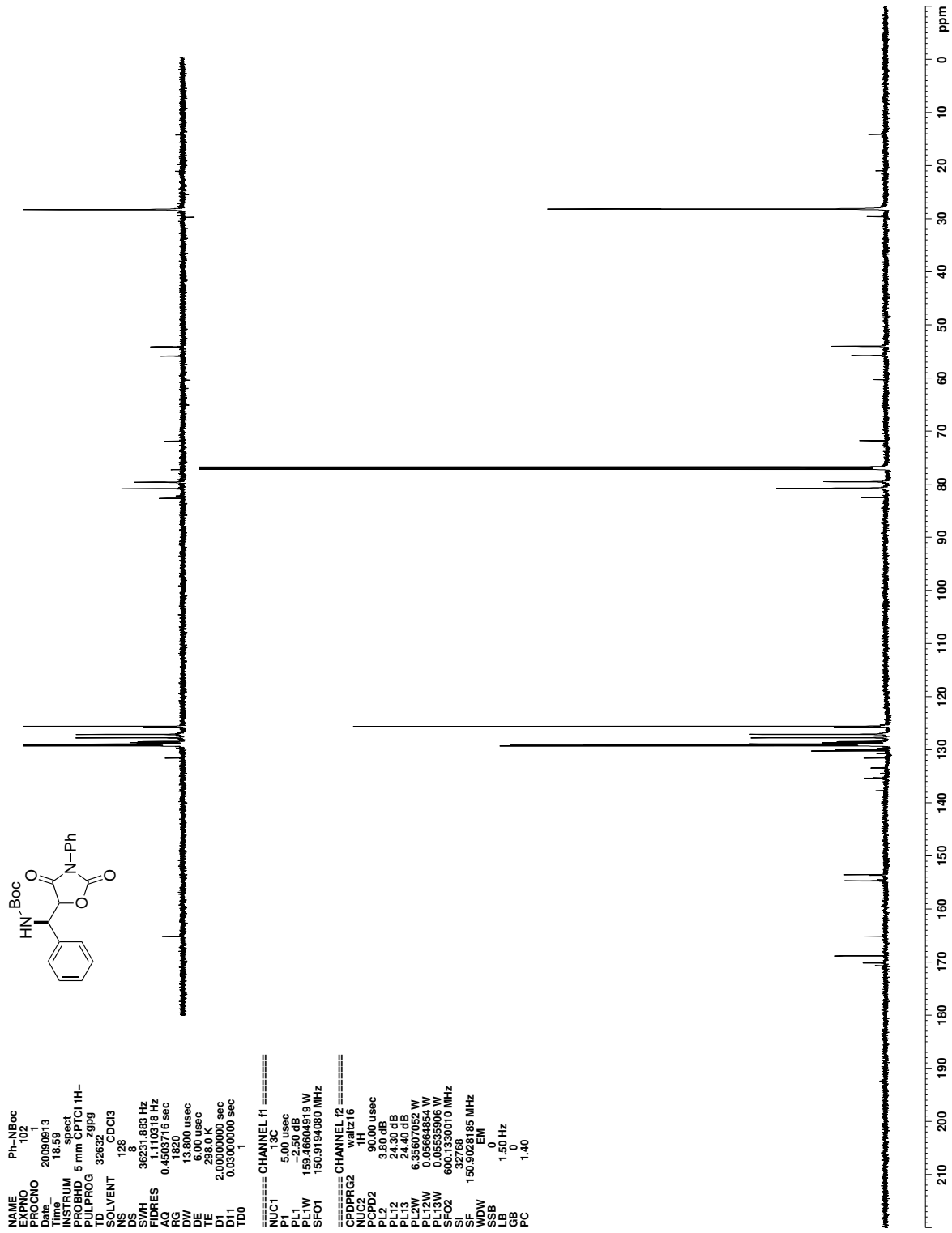


Figure C.40. ¹³C NMR (CDCl₃) of 415

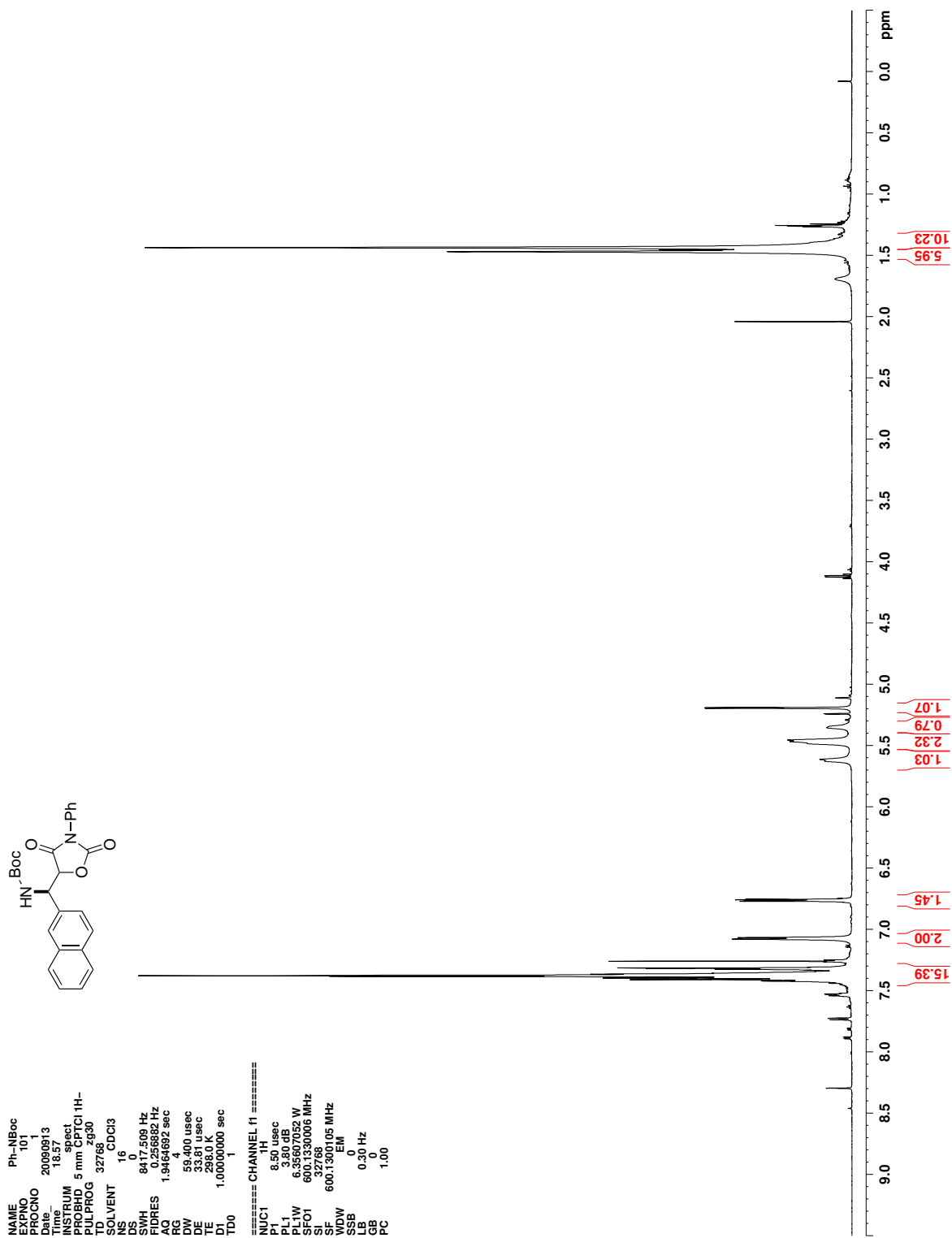


Figure C.41. ^1H NMR (CDCl_3) of 416

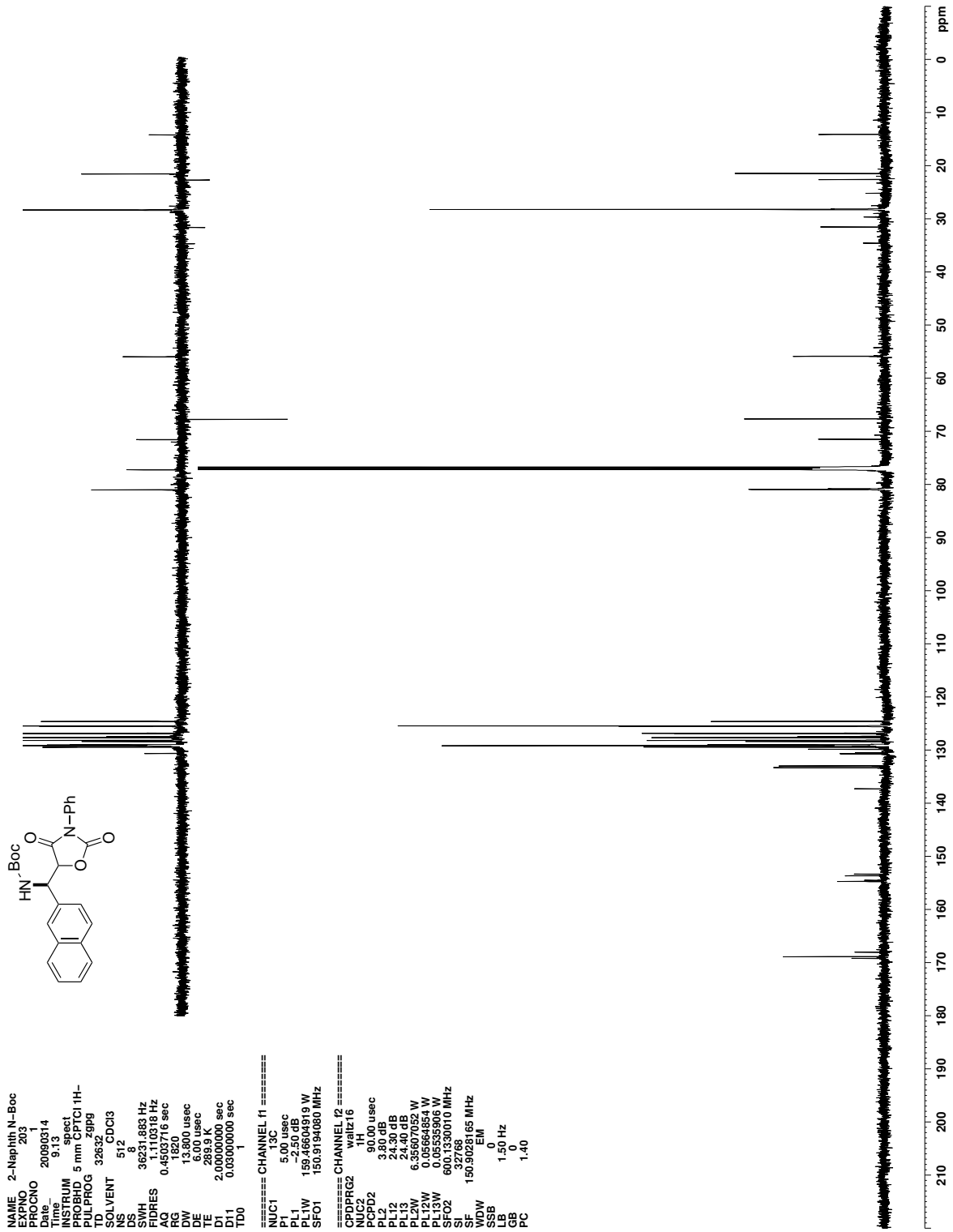


Figure C.42. ^{13}C NMR (CDCl_3) of 416

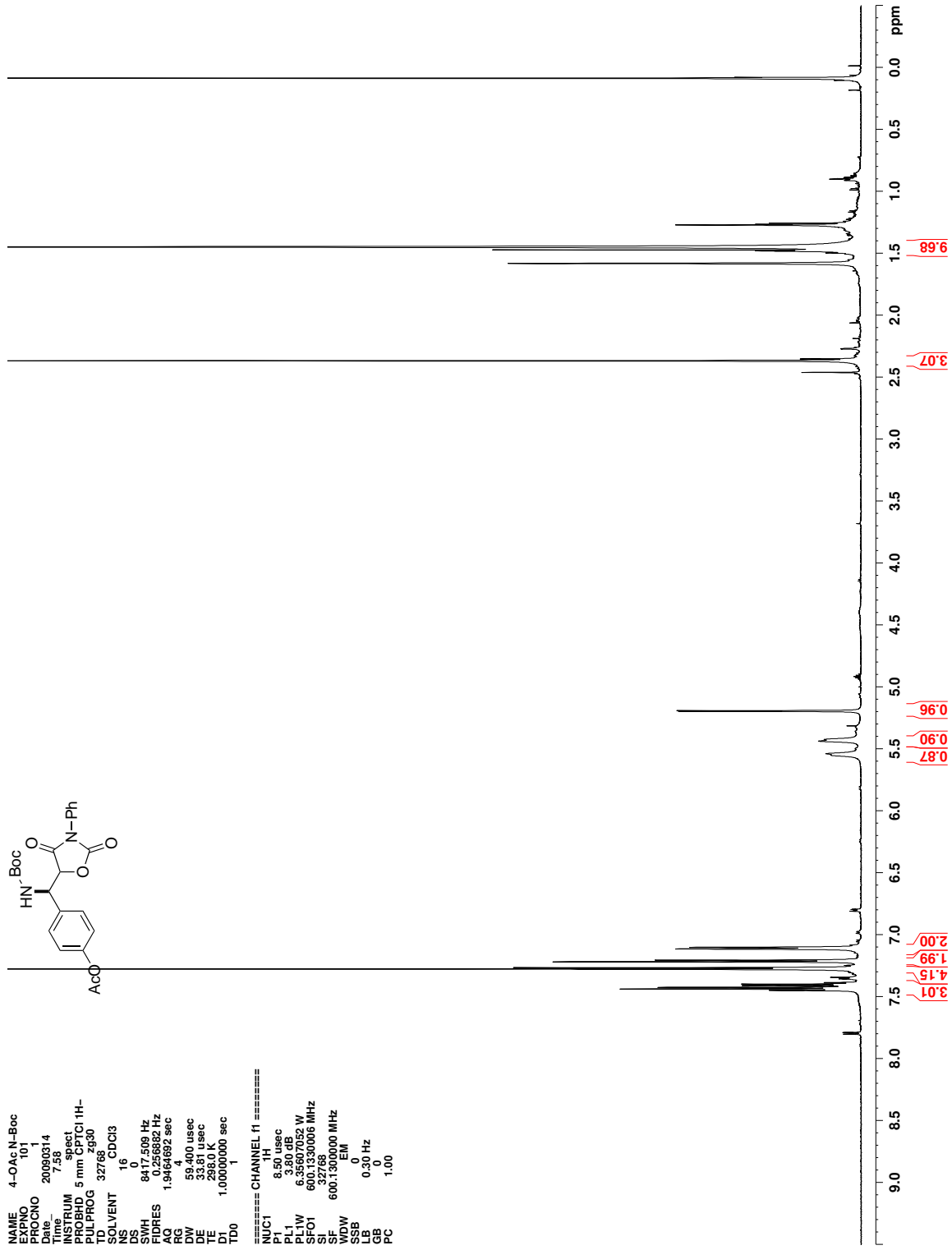


Figure C.43. ¹H NMR (CDCl₃) of 417

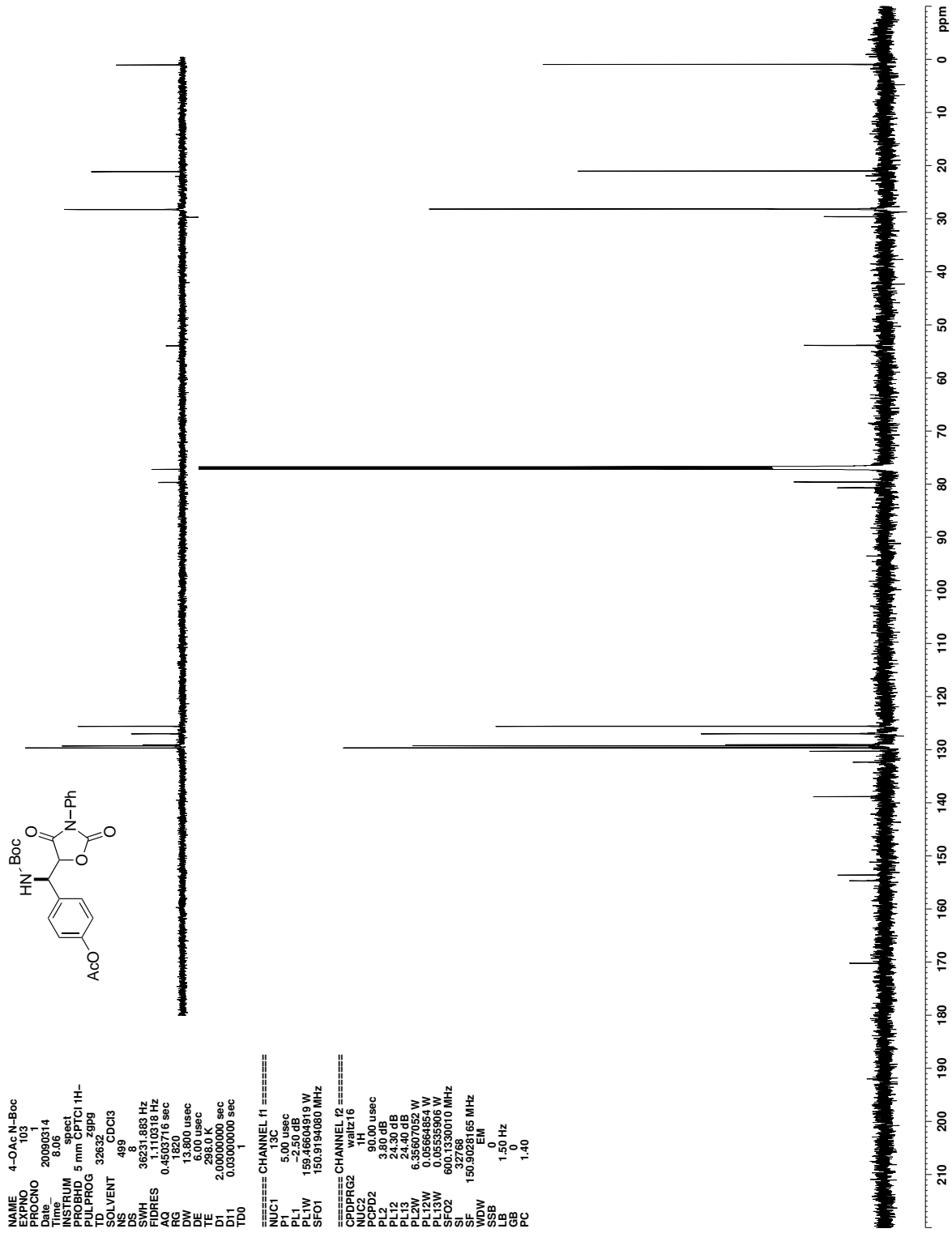


Figure C.44. ¹³C NMR (CDCl₃) of 417

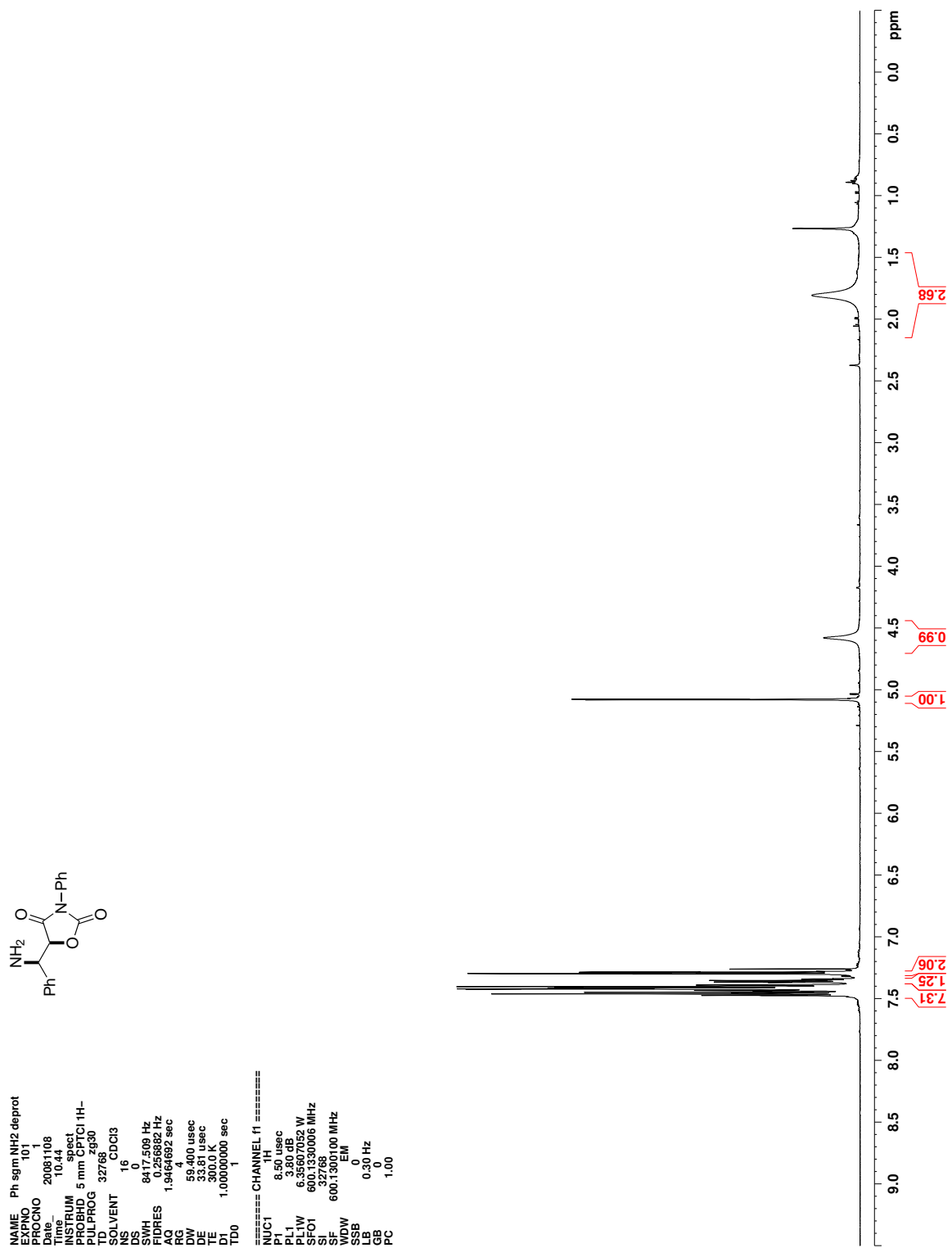


Figure C.45. ¹H NMR (CDCl₃) of 418

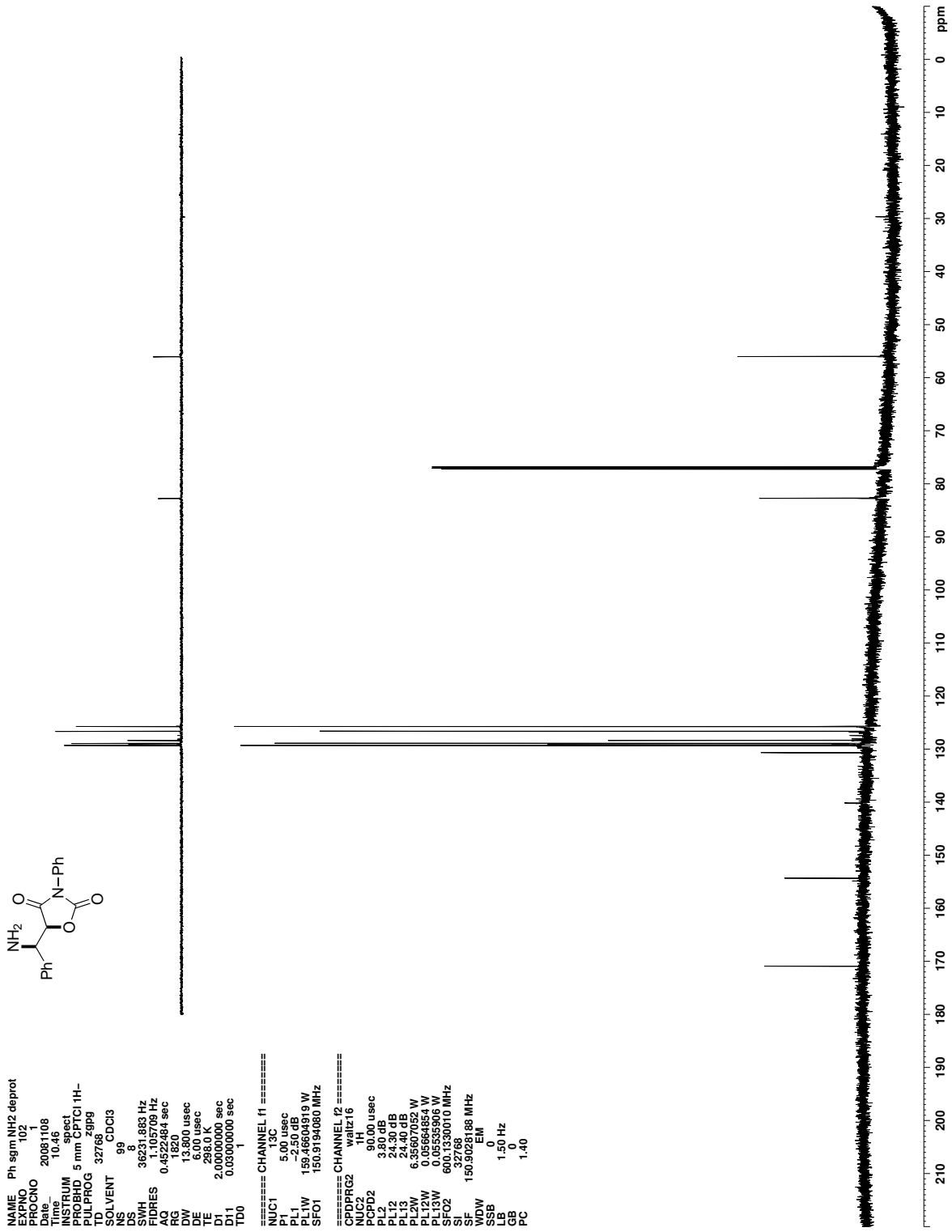
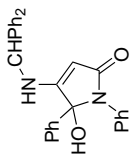


Figure C.46. ^{13}C NMR (CDCl_3) of 418



```

NAME a-keto self cyclized tit
EXPNO 121
PROCNO 121
Date_ 20080827
Time 17.31
INSTRUM spect
PROBHD 5 mm CPTCI 1H-
TD 65536
AQ 0.4520884 sec
RG 1820
DW 13.800 usec
DE 6.00 usec
TE 298.0 K
D1 2.00000000 sec
D11 0.05000000 sec
TD0 1

===== CHANNEL f1 =====
NUC1 13C
P1 5.00 usec
PL1 0.00 dB
PL1W 118.21331373 W
SFO1 150.9194080 MHz

===== CHANNEL f2 =====
CPDPRG2 waltz16
NUC2 13C
PCPD2 90.00 usec
PL2 3.80 dB
PL12 24.30 dB
PL13 24.40 dB
PL2W 6.35607052 W
PL12W 0.05556854 W
PL13W 0.05556854 W
SFO2 600.1330010 MHz
SI 32768
SF 150.9028144 MHz
WDW EM
SSB 0
GB 0
PC 1.40

```

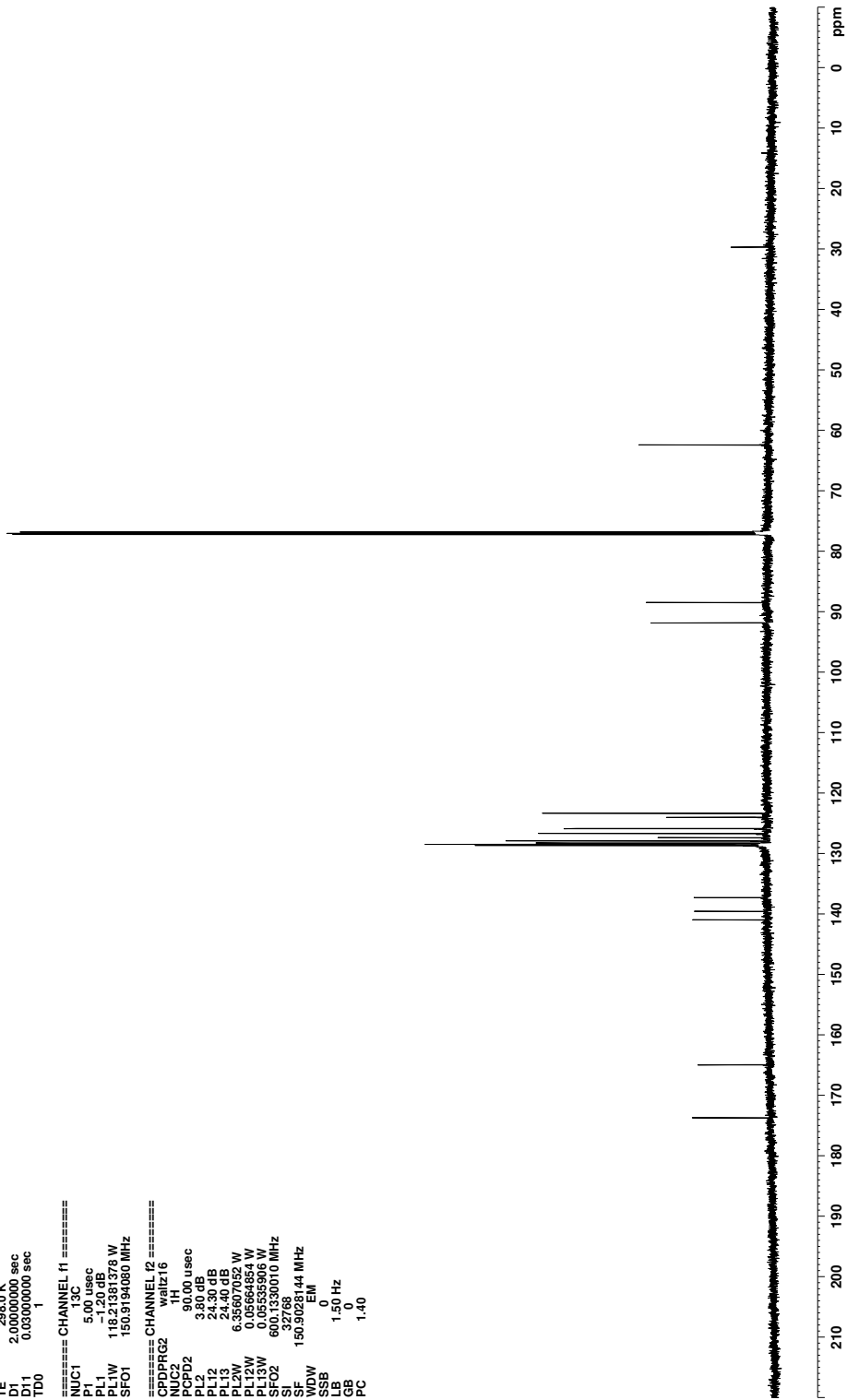


Figure C.48. ^{13}C NMR (CDCl₃) of 150

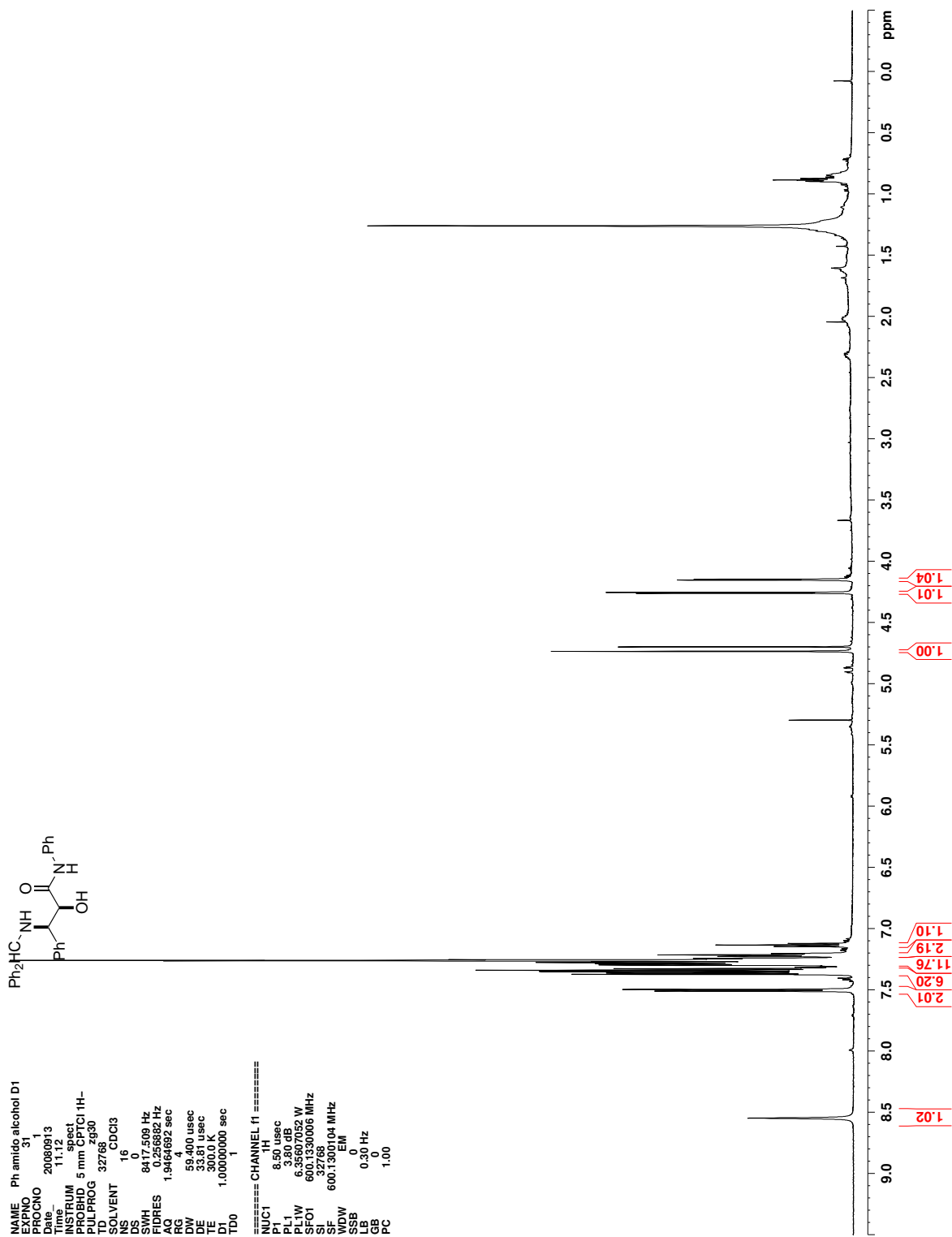


Figure C.49. ^1H NMR (CDCl_3) of 151

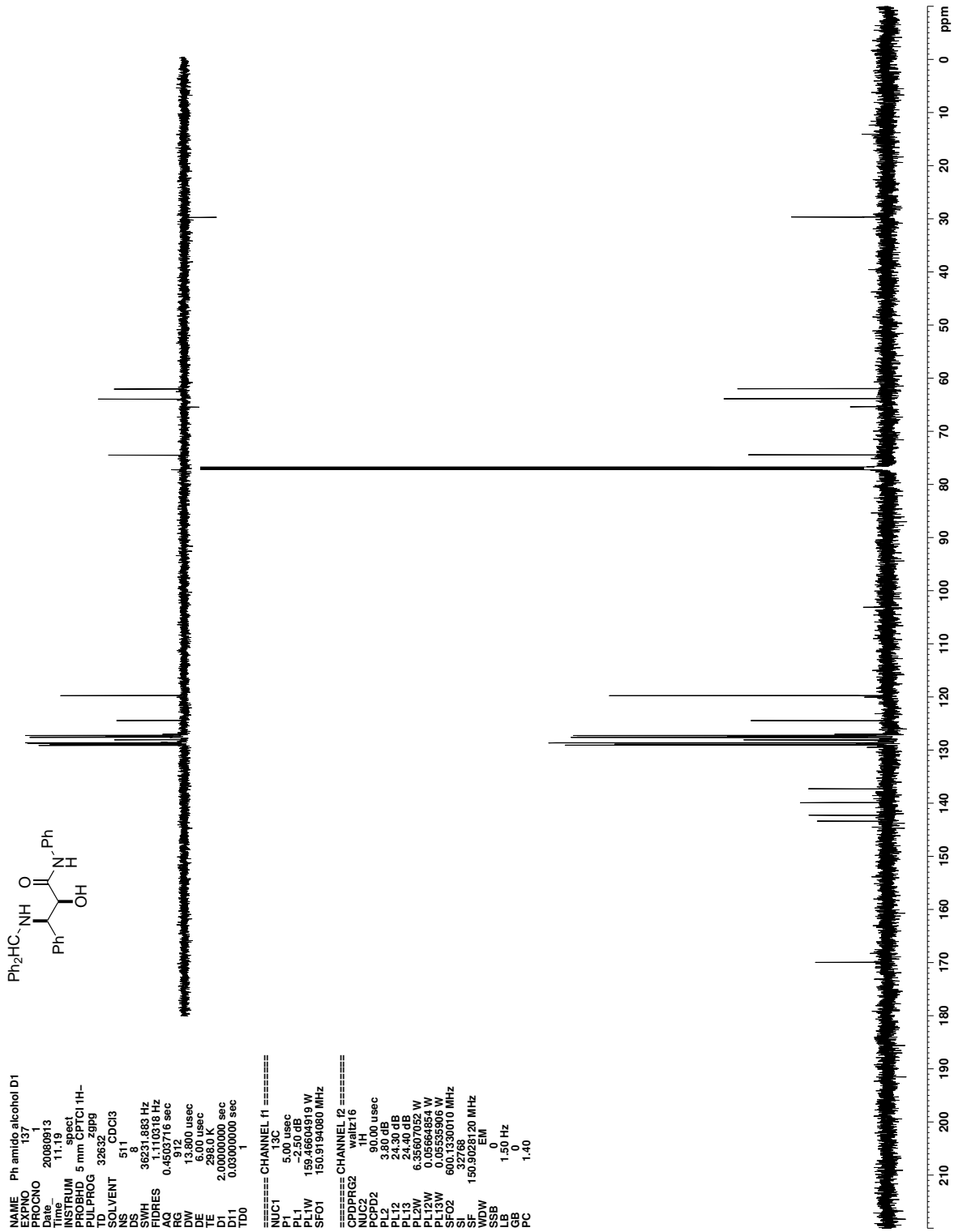


Figure C.50. ^{13}C NMR (CDCl_3) of 151

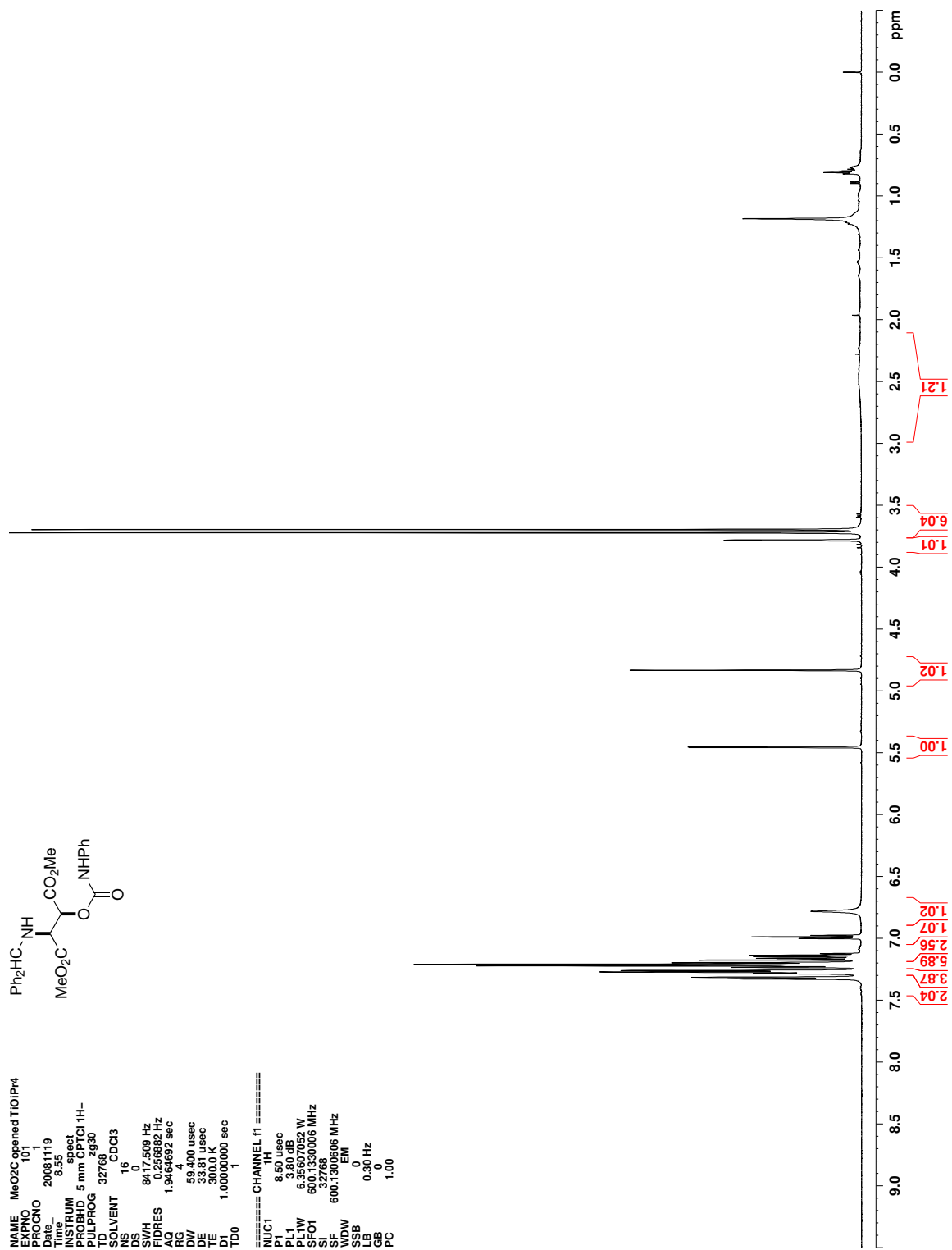


Figure C.51. ^1H NMR (CDCl_3) of 156

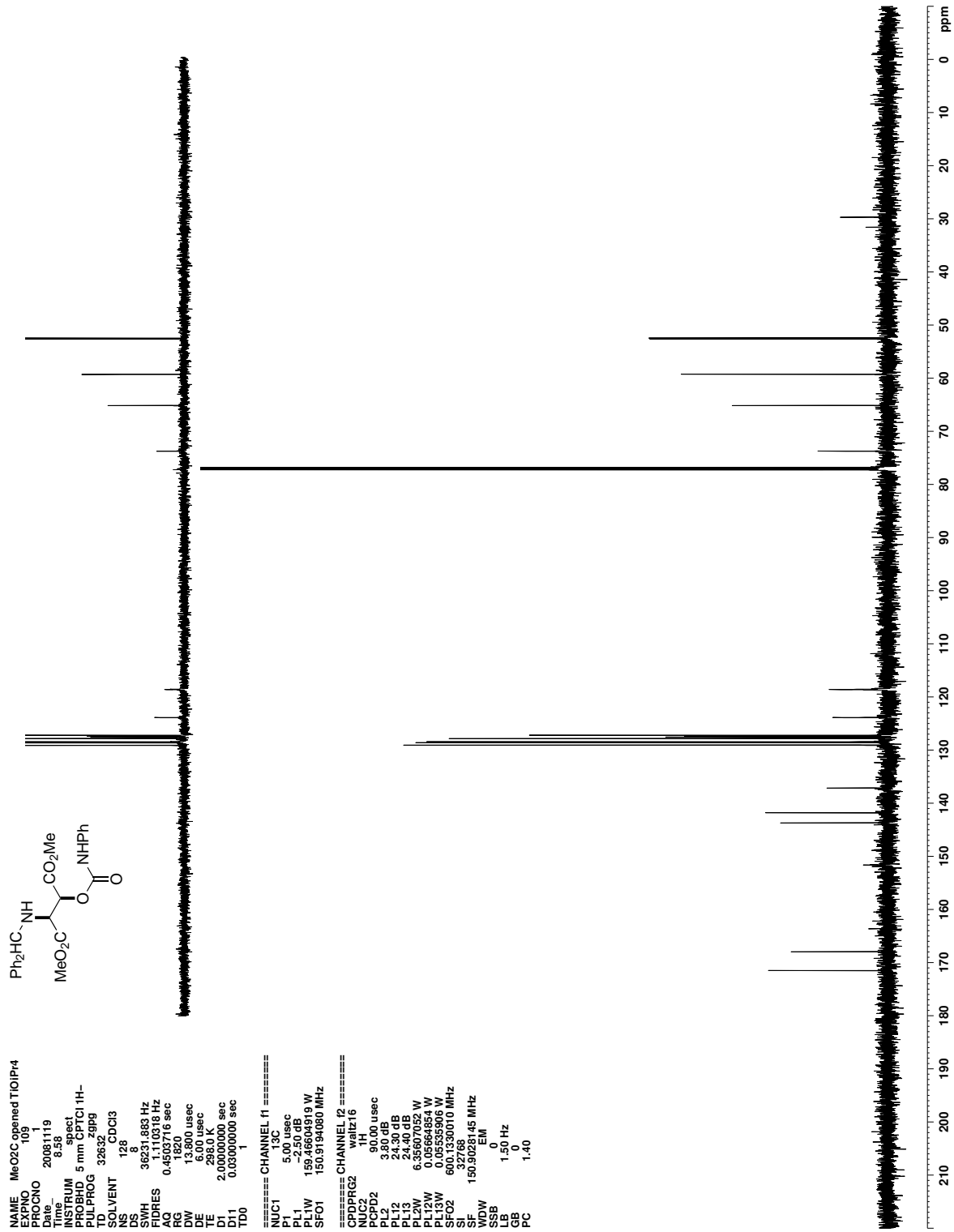


Figure C.52. ^{13}C NMR (CDCl_3) of 156

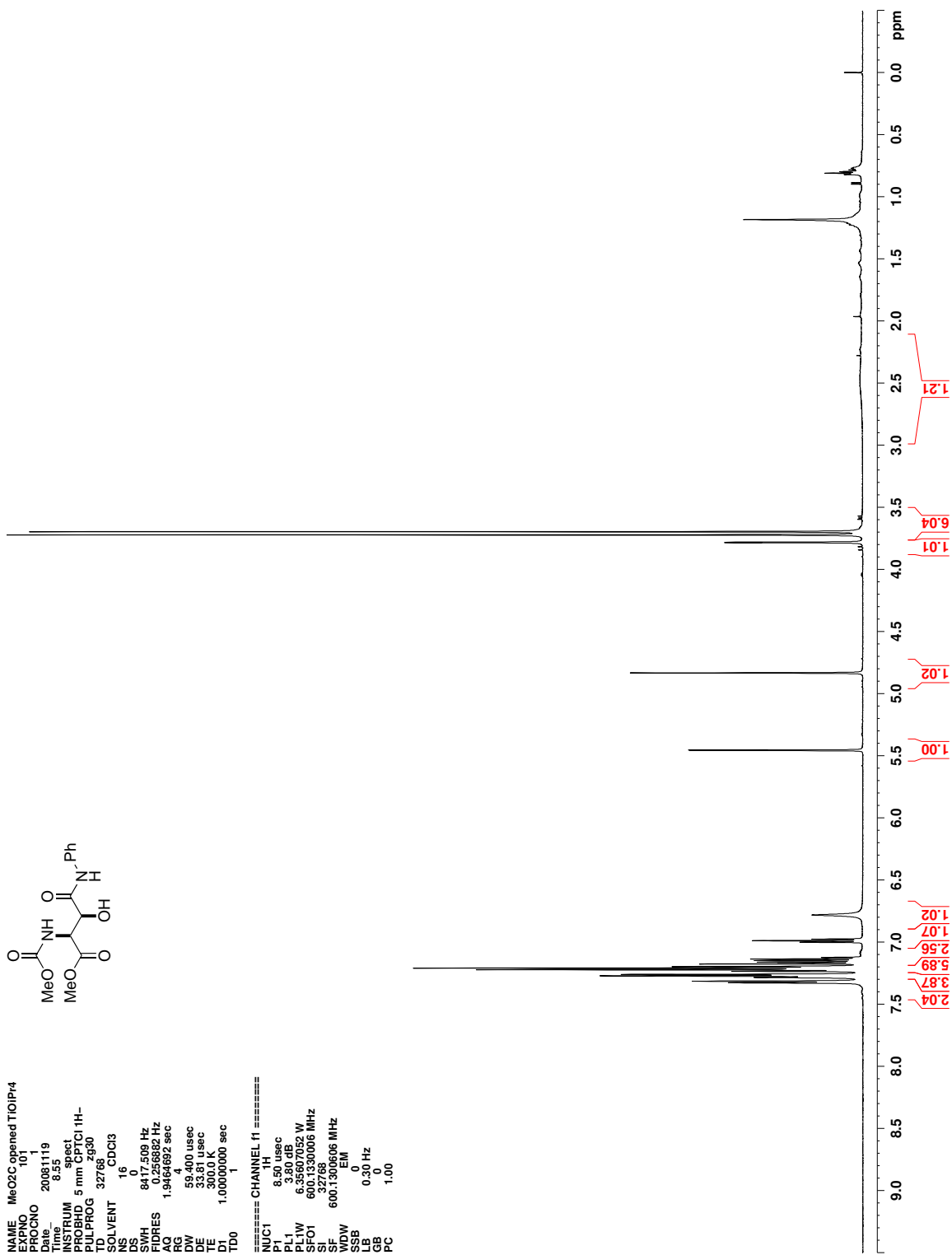


Figure C.53. ^1H NMR (CDCl_3) of 157

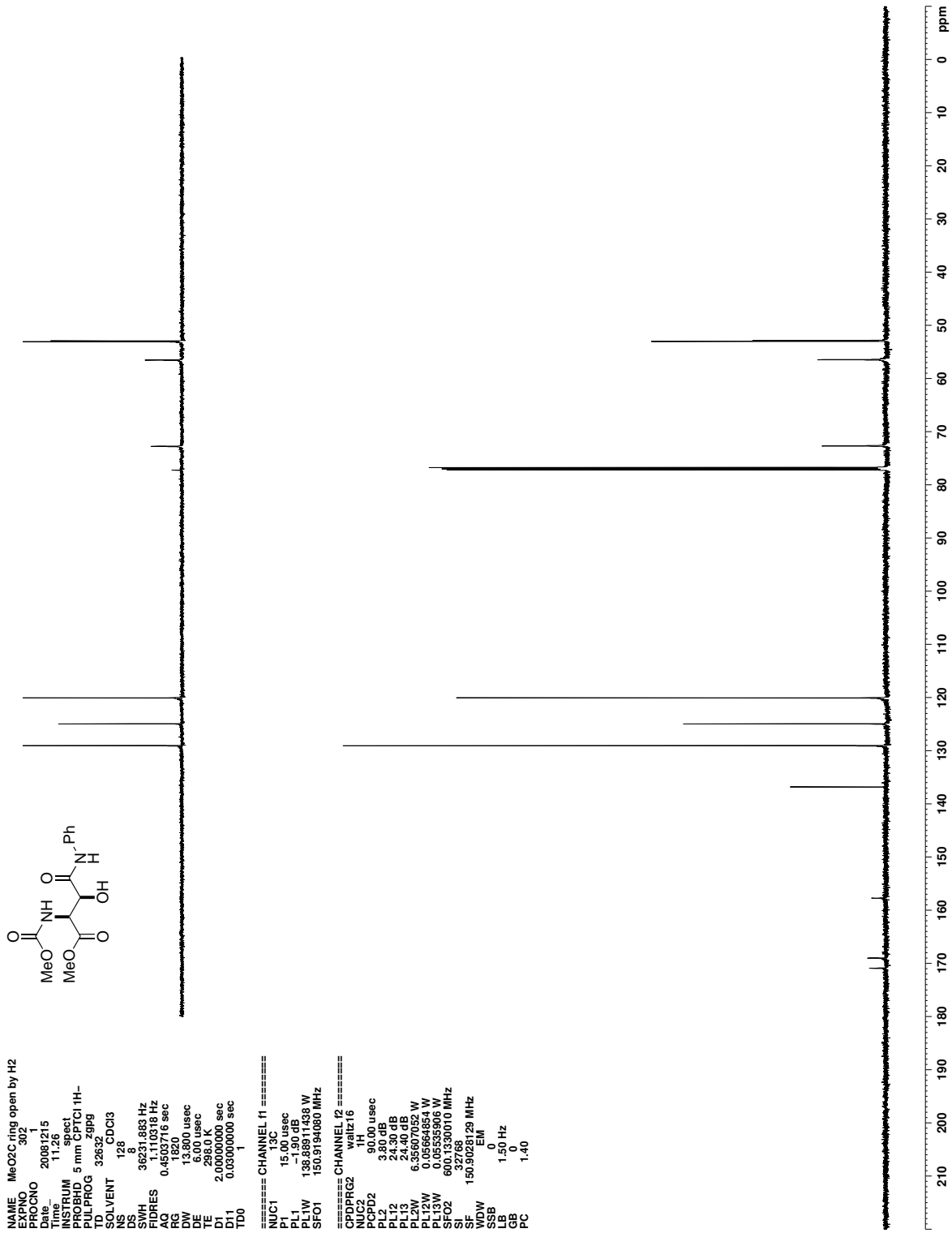


Figure C.54. ^{13}C NMR (CDCl_3) of 157

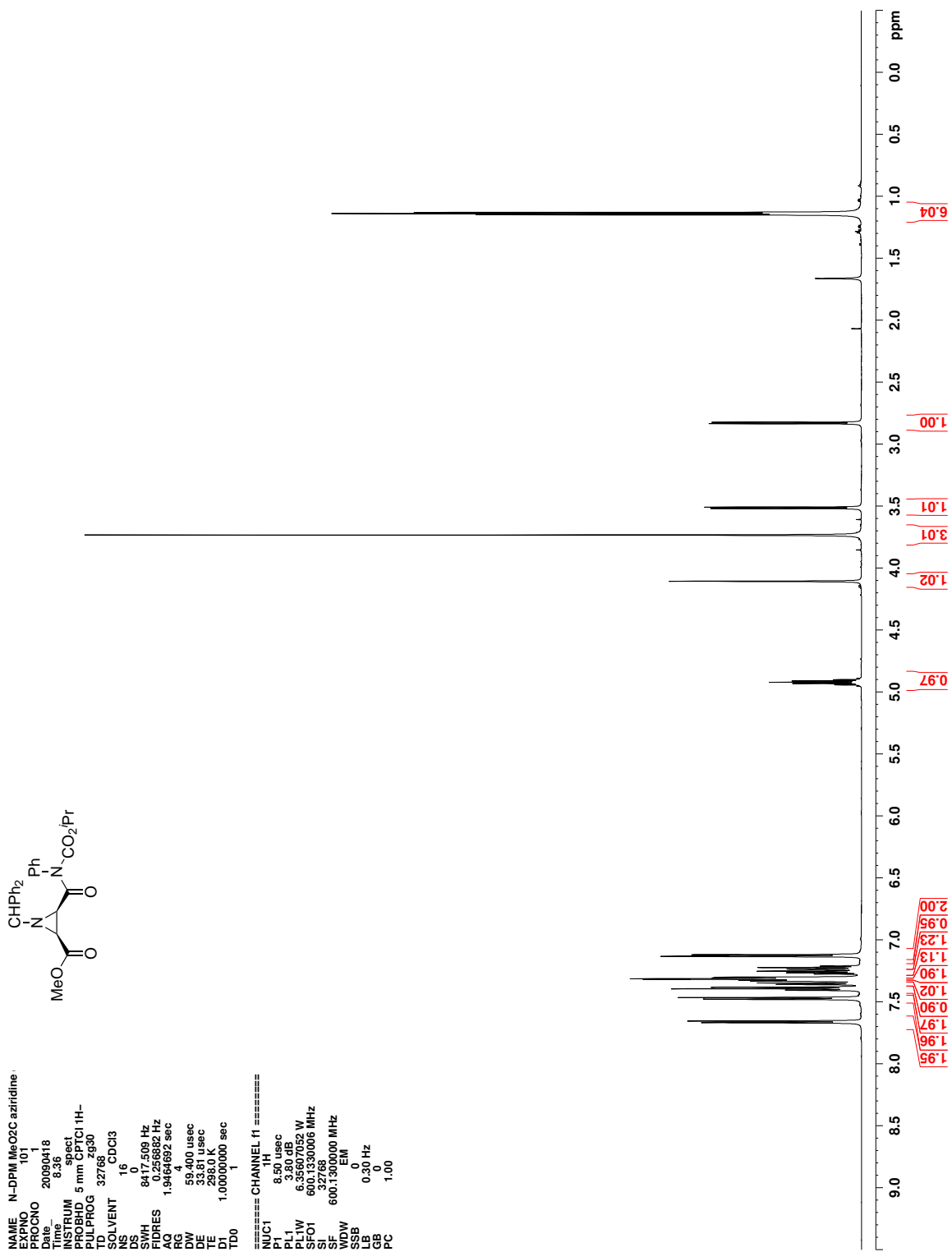


Figure C.55. ^1H NMR (CDCl_3) of **203**

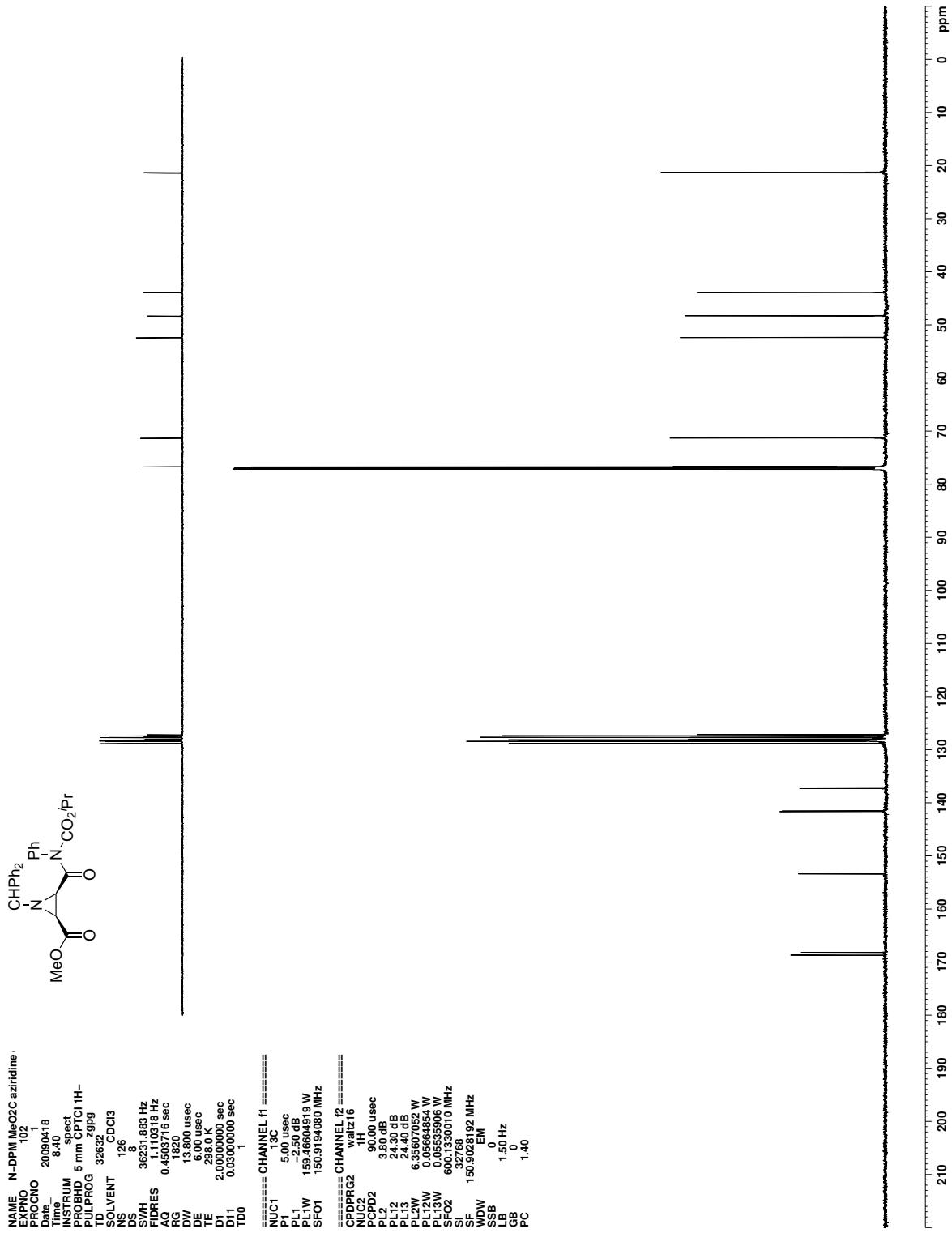


Figure C.56. ¹³C NMR (CDCl₃) of 203

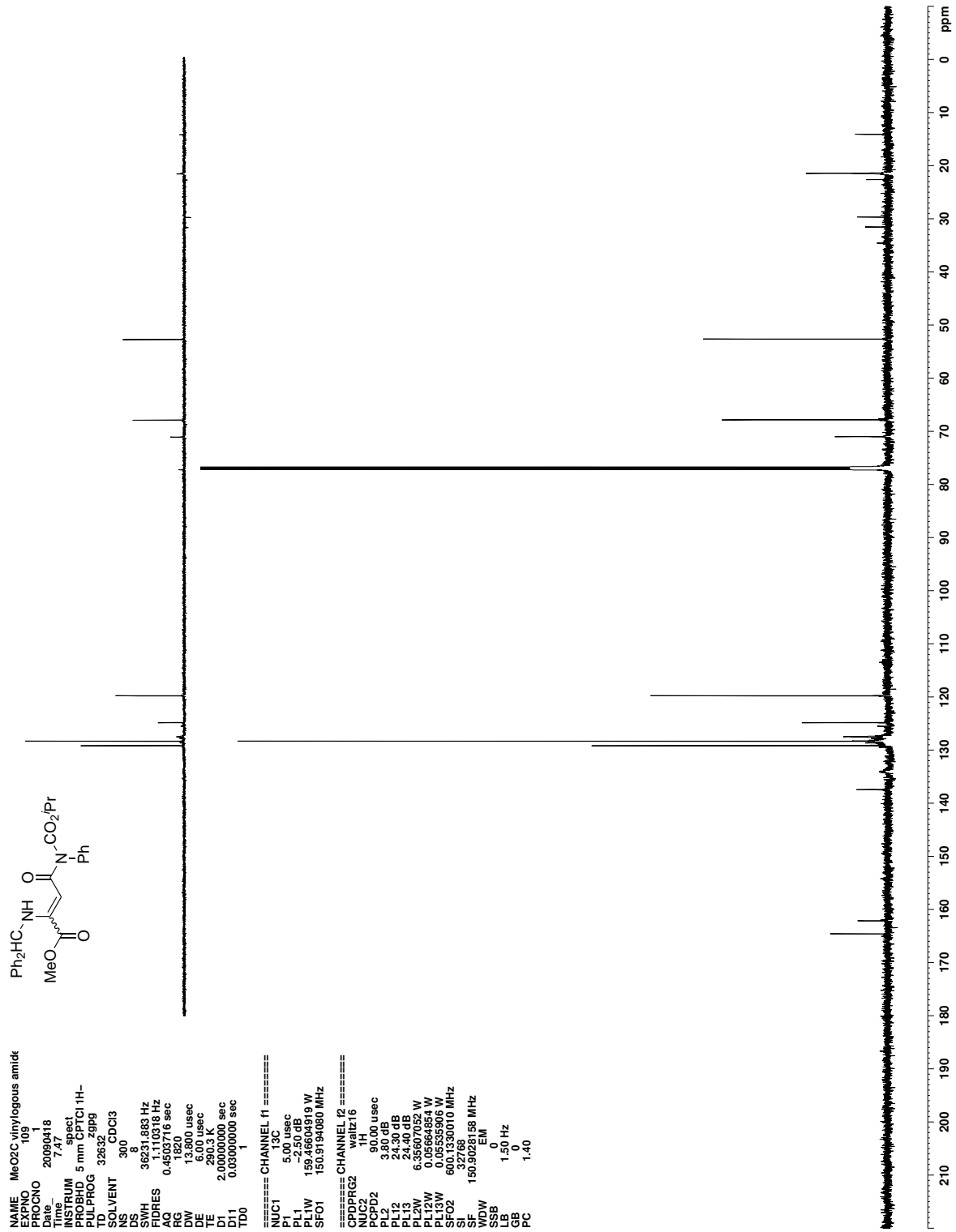


Figure C.58. ^{13}C NMR (CDCl_3) of 204

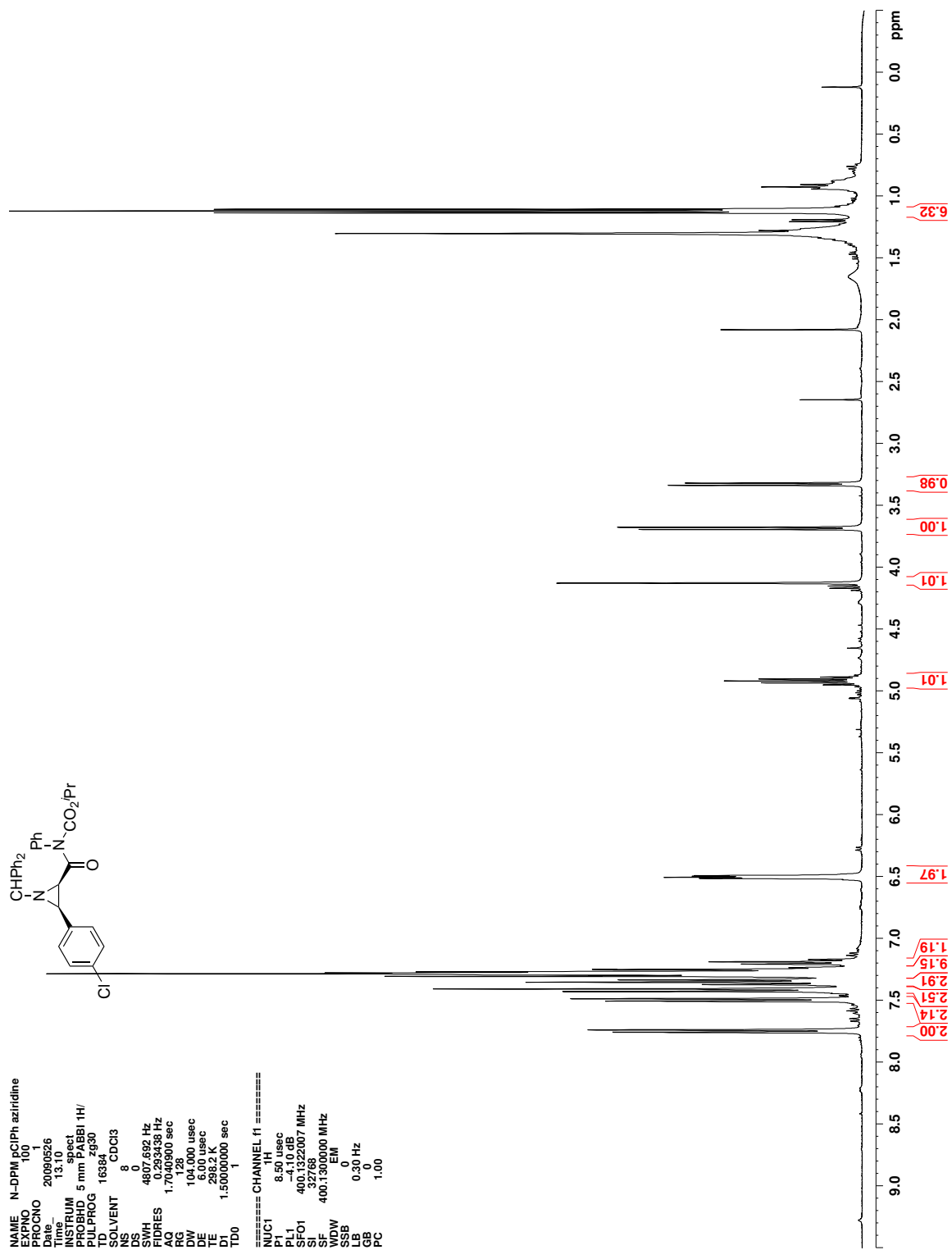


Figure C.59. ^1H NMR (CDCl_3) of 215

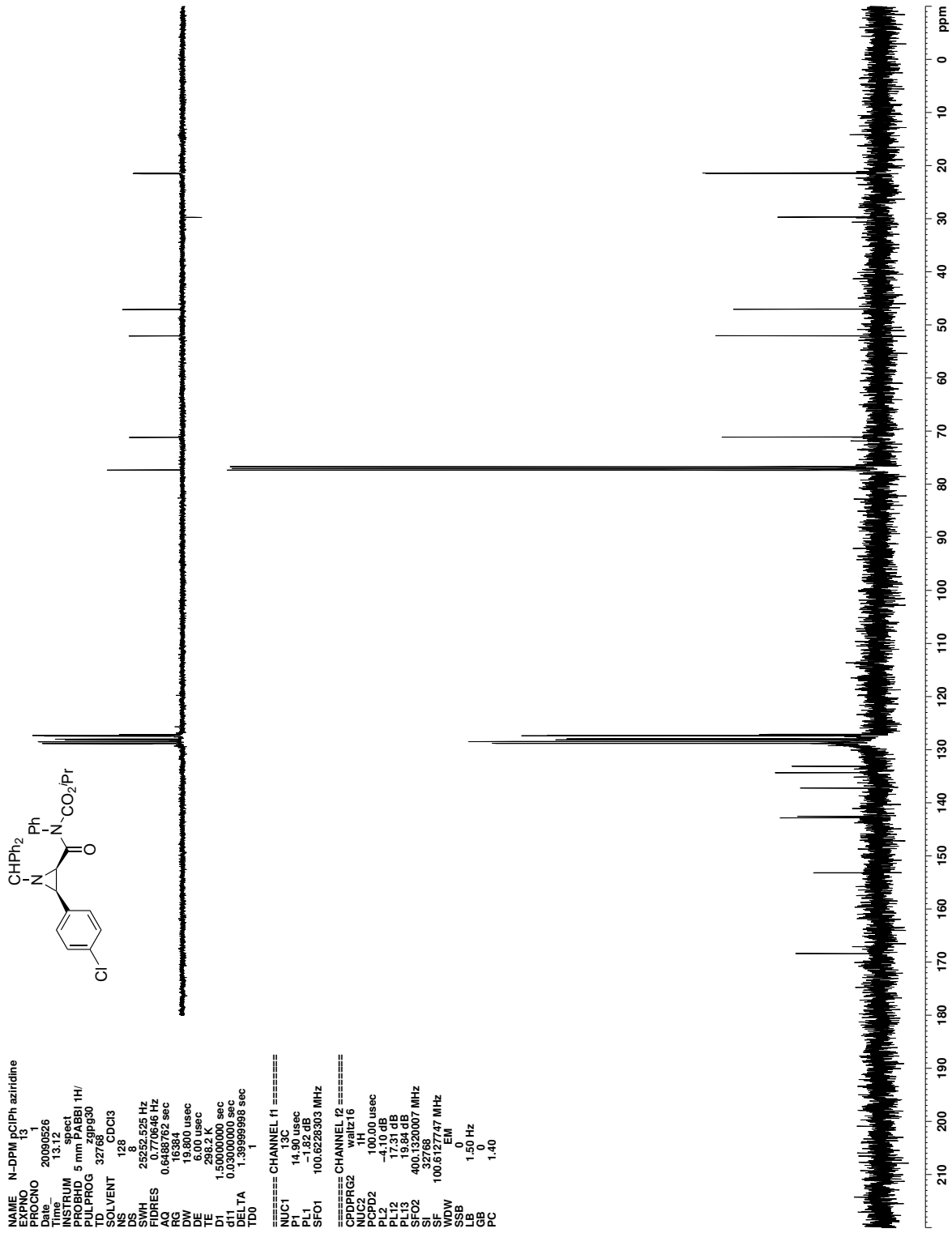


Figure C.60. ^{13}C NMR (CDCl_3) of 215

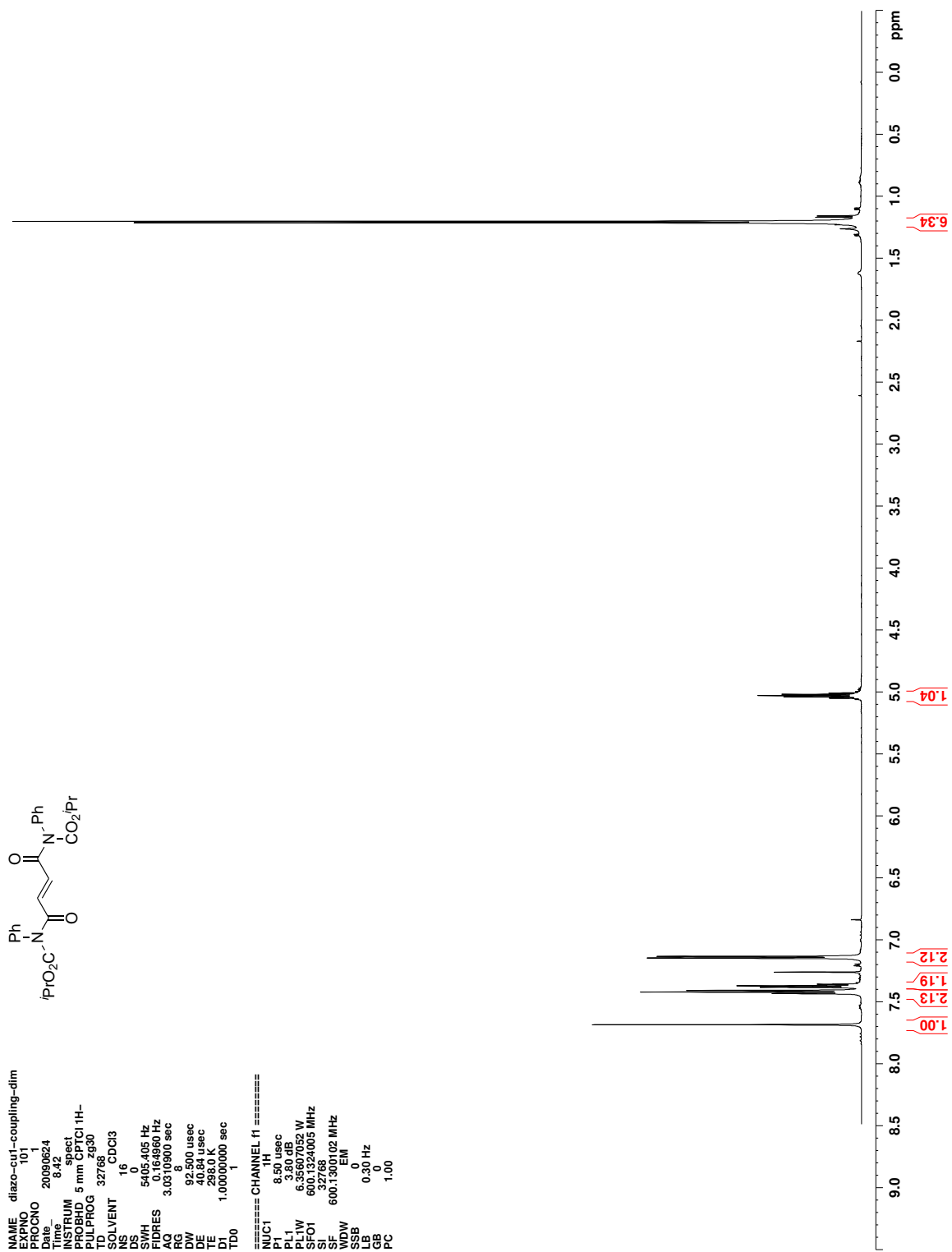


Figure C.61. ^1H NMR (CDCl_3) of 216

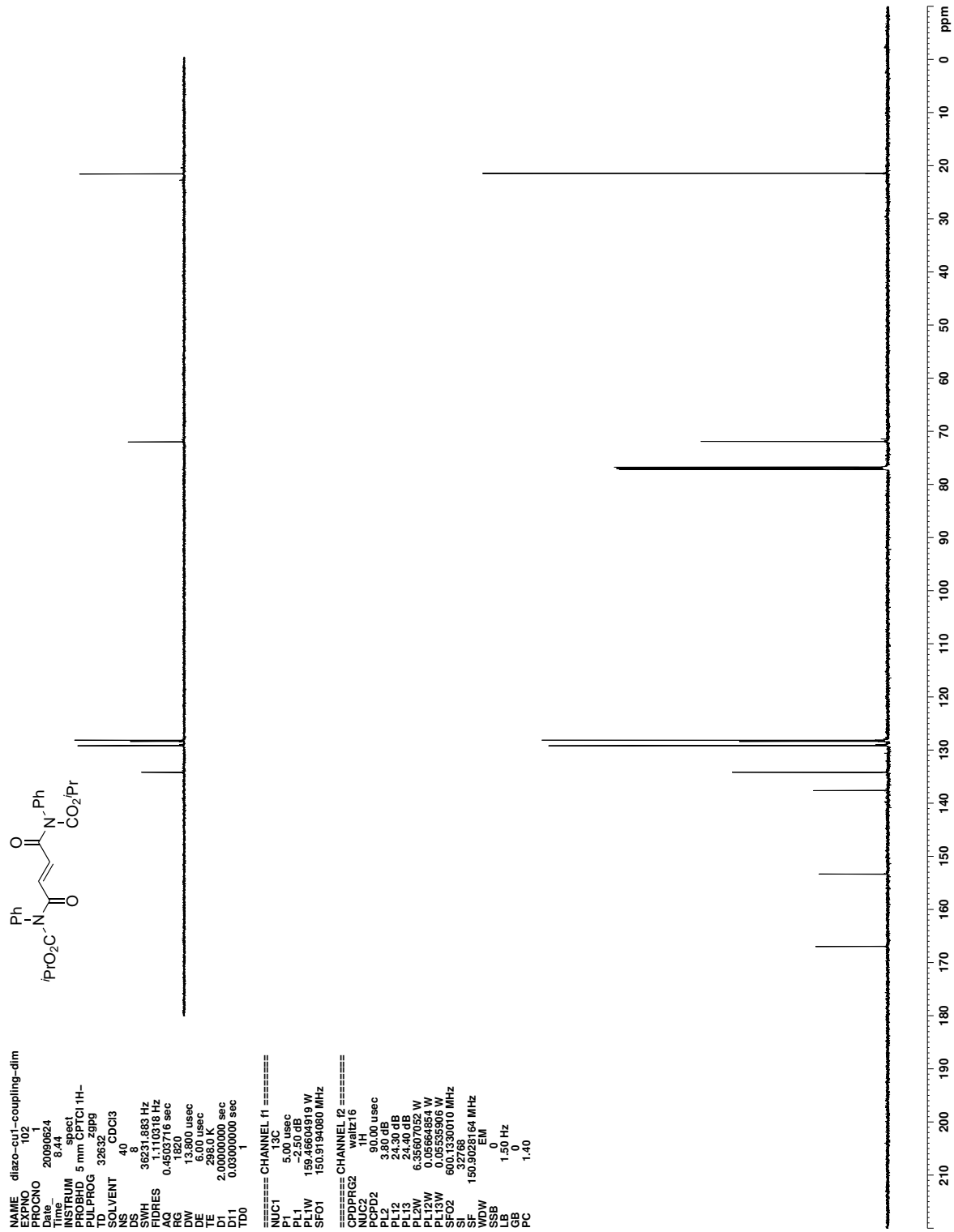


Figure C.62. ^{13}C NMR (CDCl_3) of 216

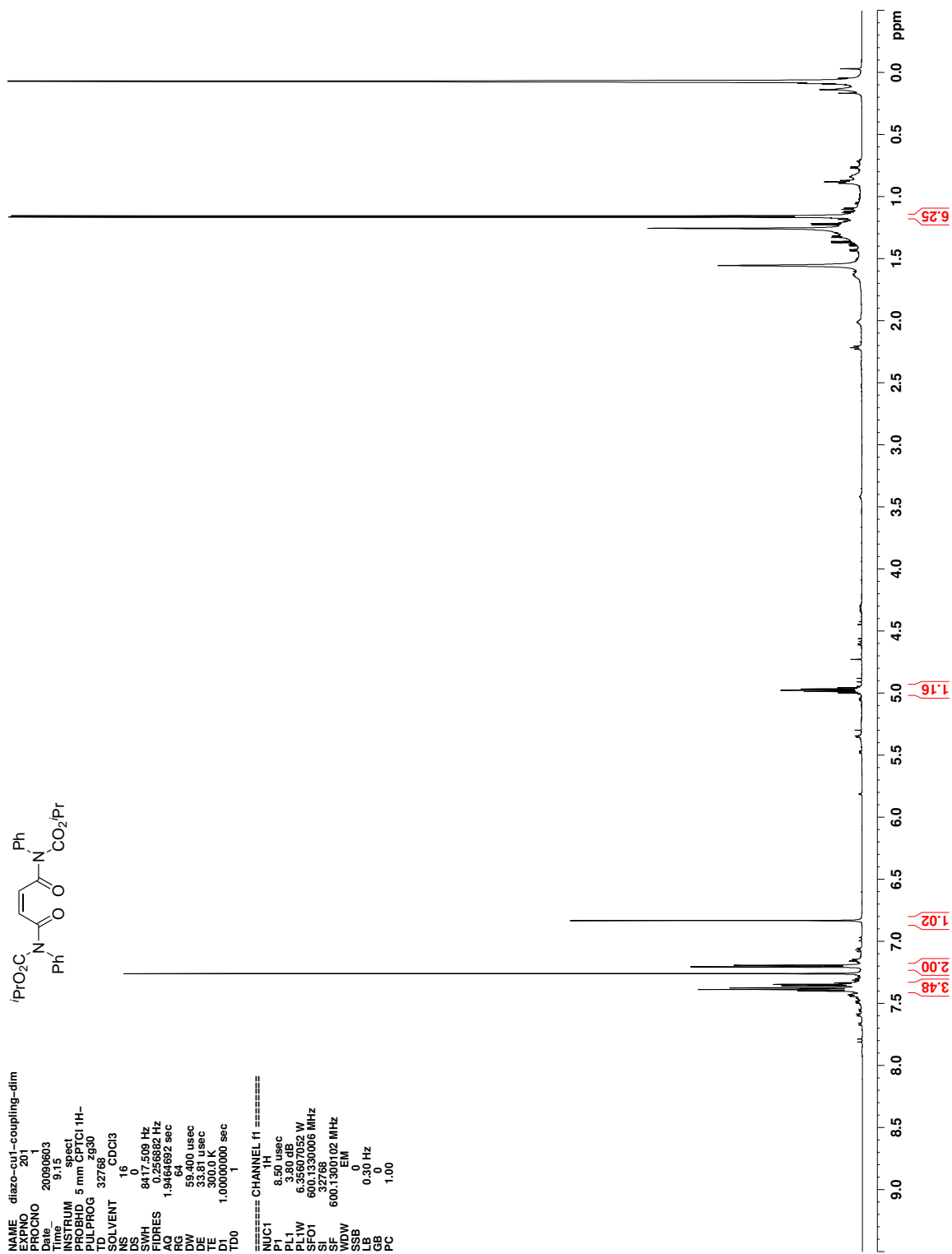


Figure C.63. ^1H NMR (CDCl_3) of **217**

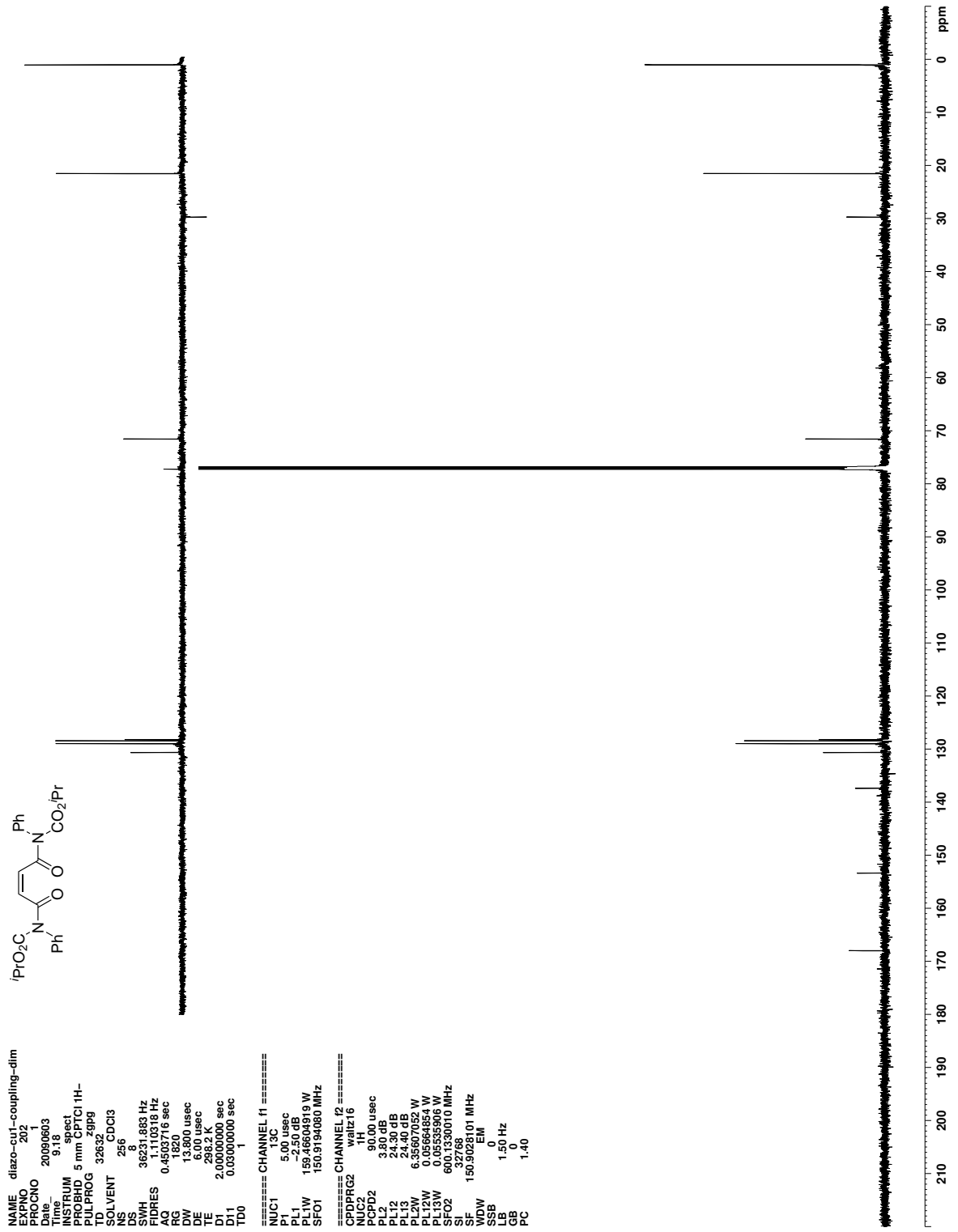


Figure C.64. ¹³C NMR (CDCl₃) of 217

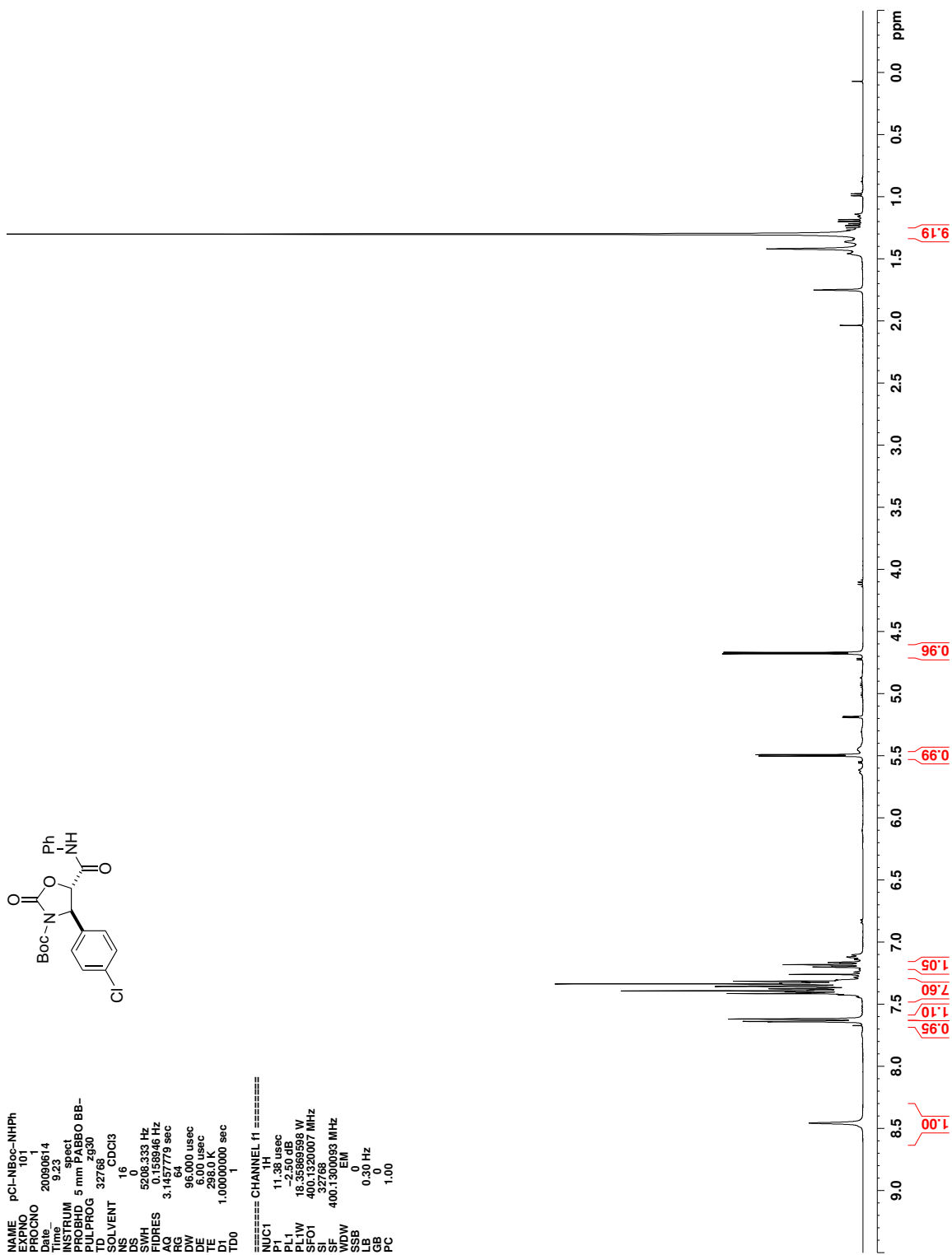


Figure C.65. ^1H NMR (CDCl_3) of 218

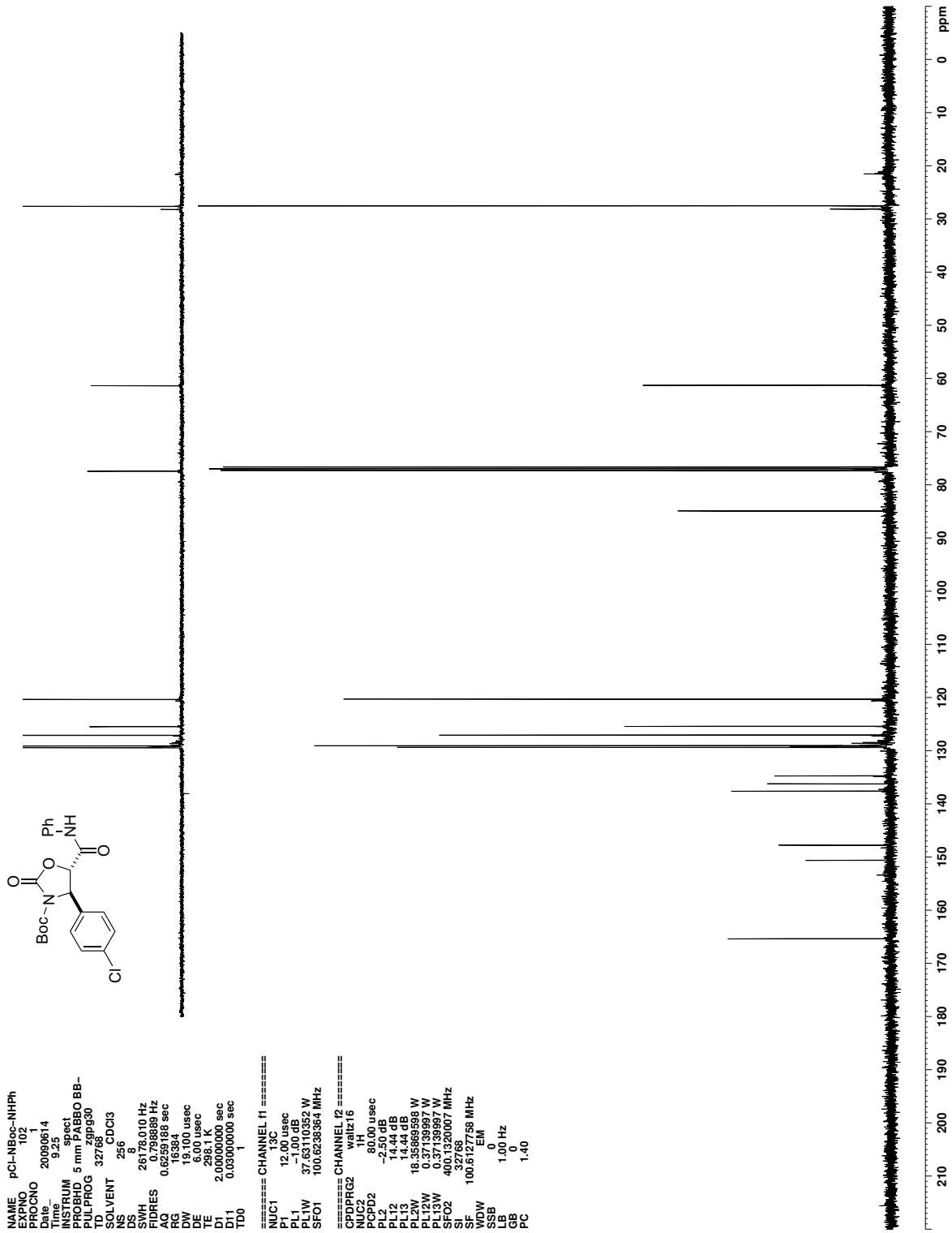


Figure C.66. ^{13}C NMR (CDCl_3) of 218

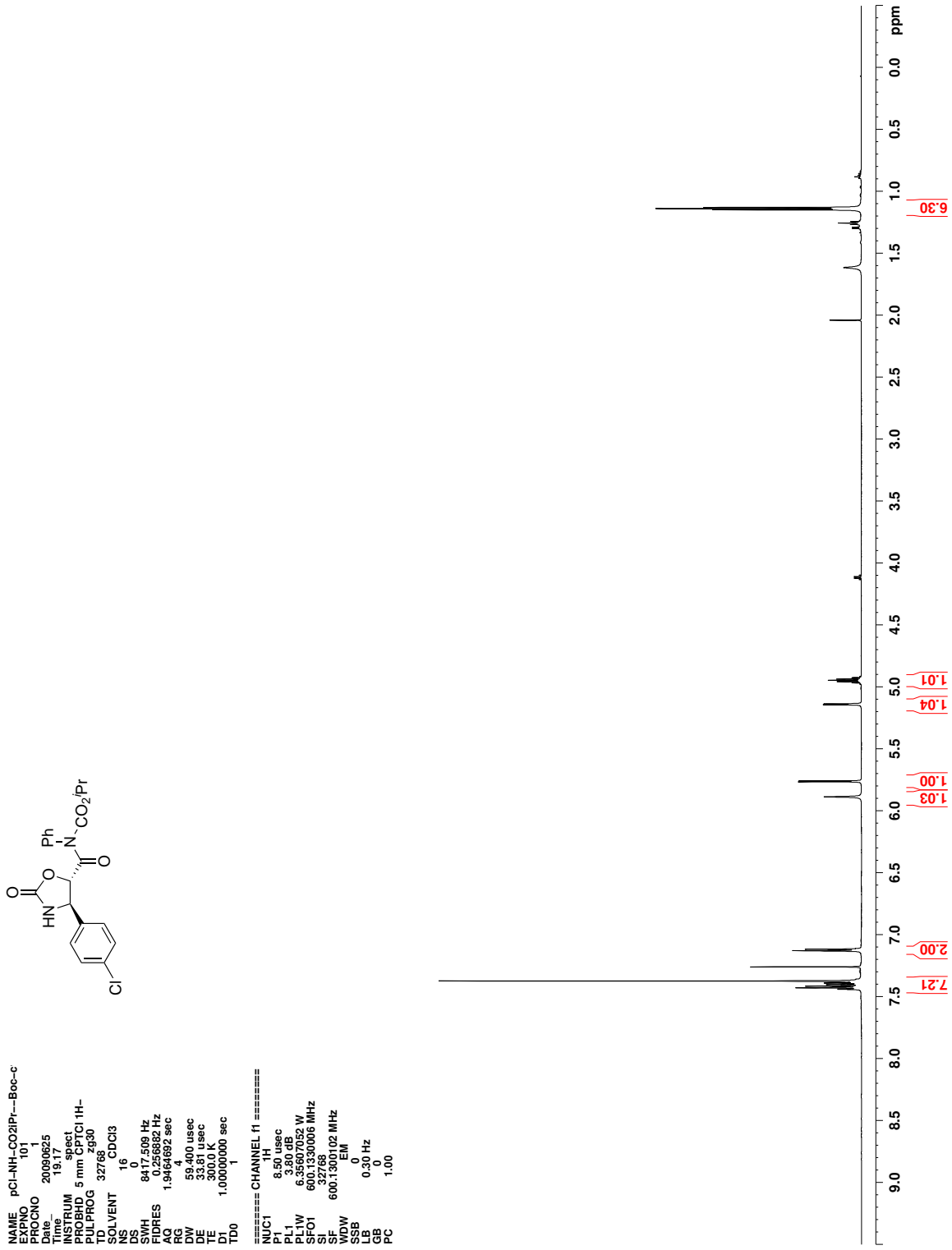


Figure C.67. ¹H NMR (CDCl₃) of 219

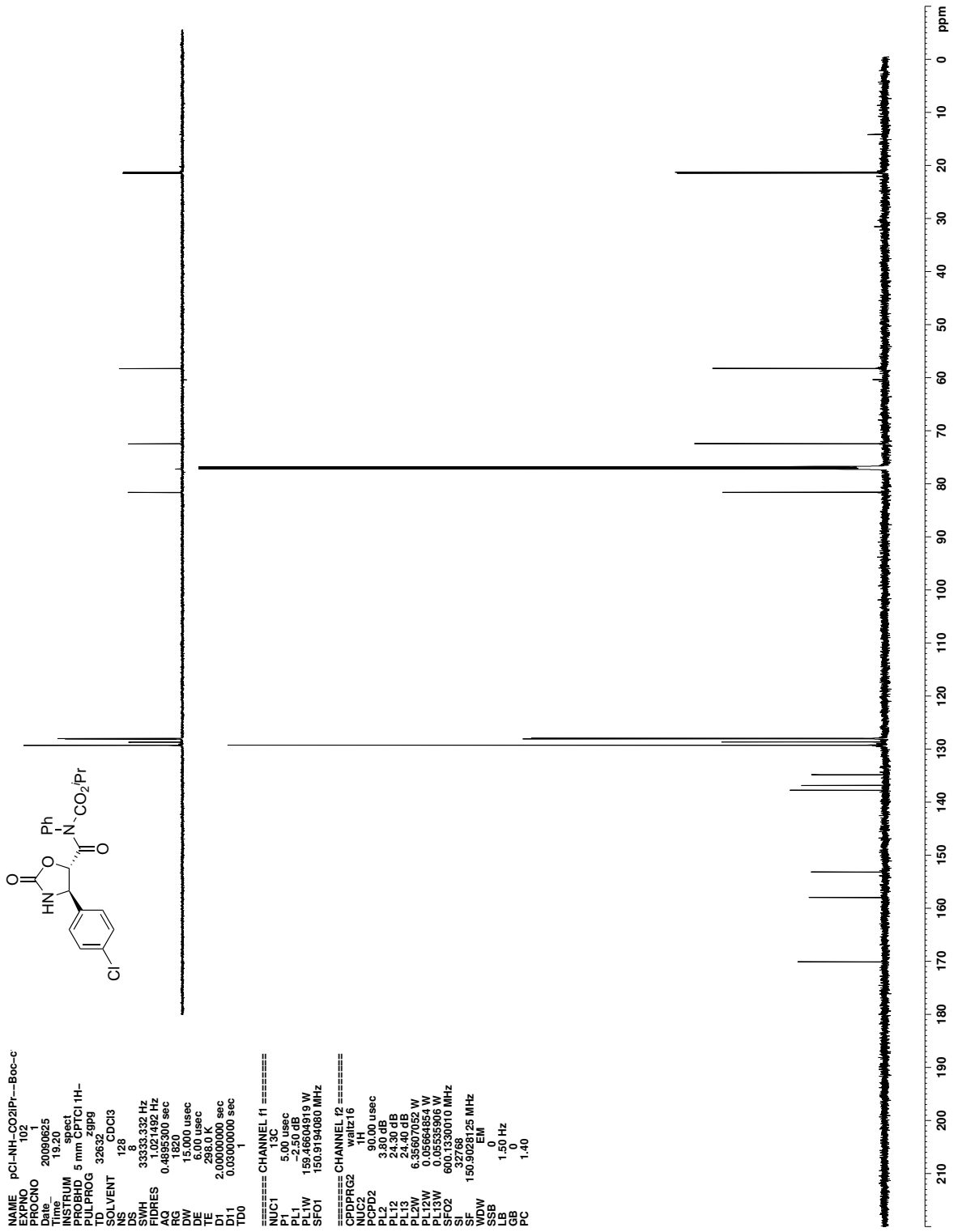


Figure C.68. ¹³C NMR (CDCl₃) of 219

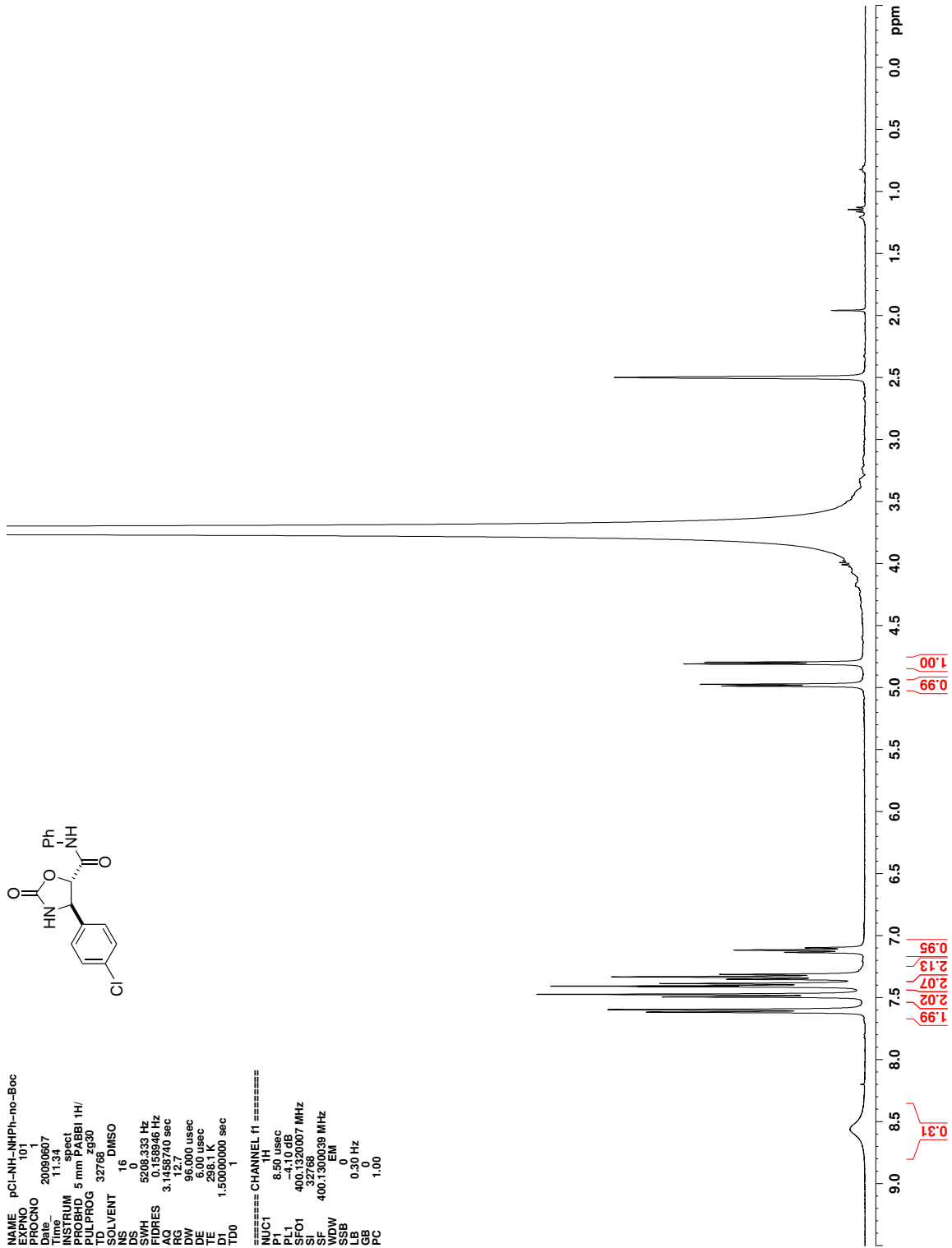


Figure C.69. ^1H NMR (DMSO- d_6) of 223

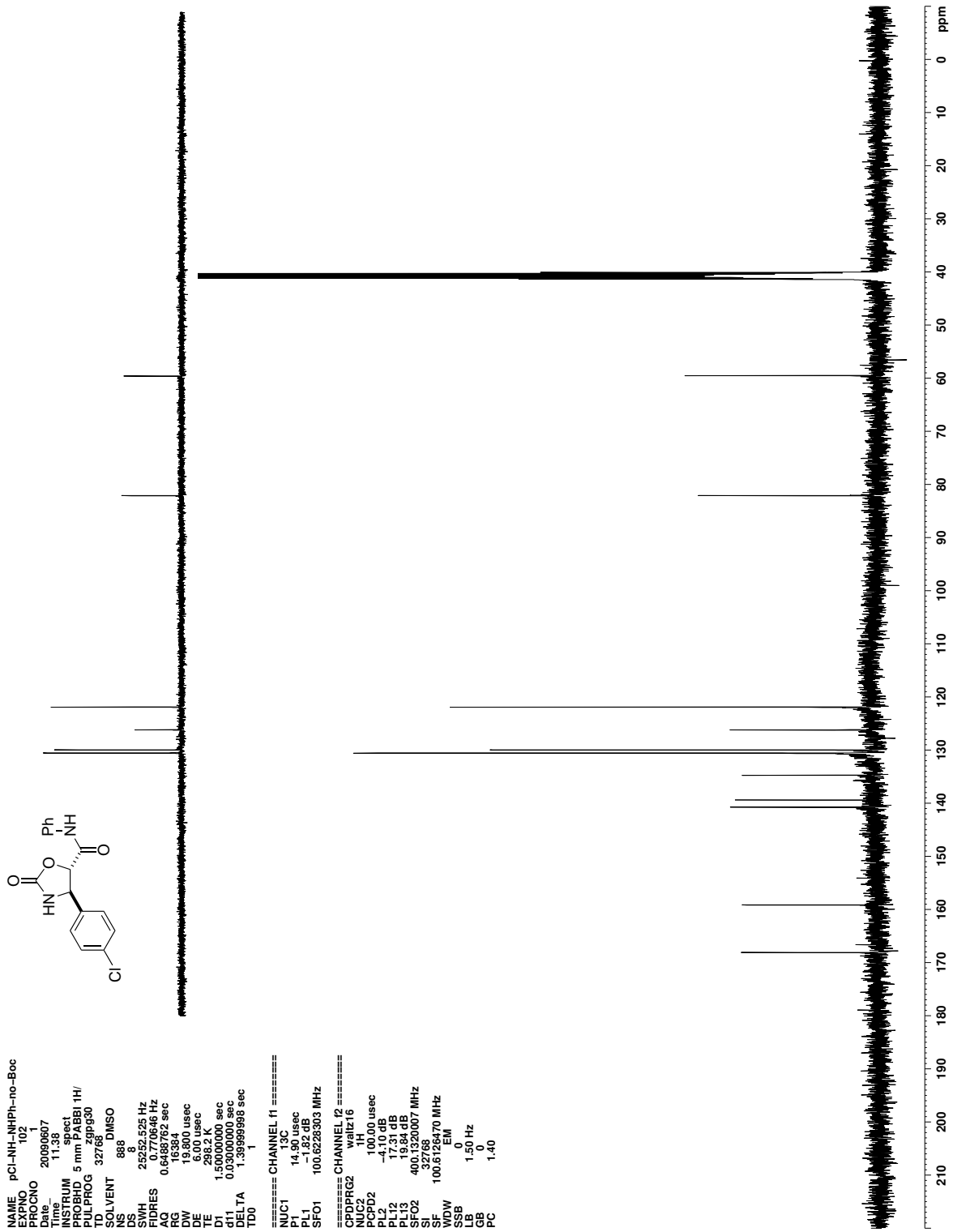


Figure C.70. ¹³C NMR (DMSO-*d*₆) of 223

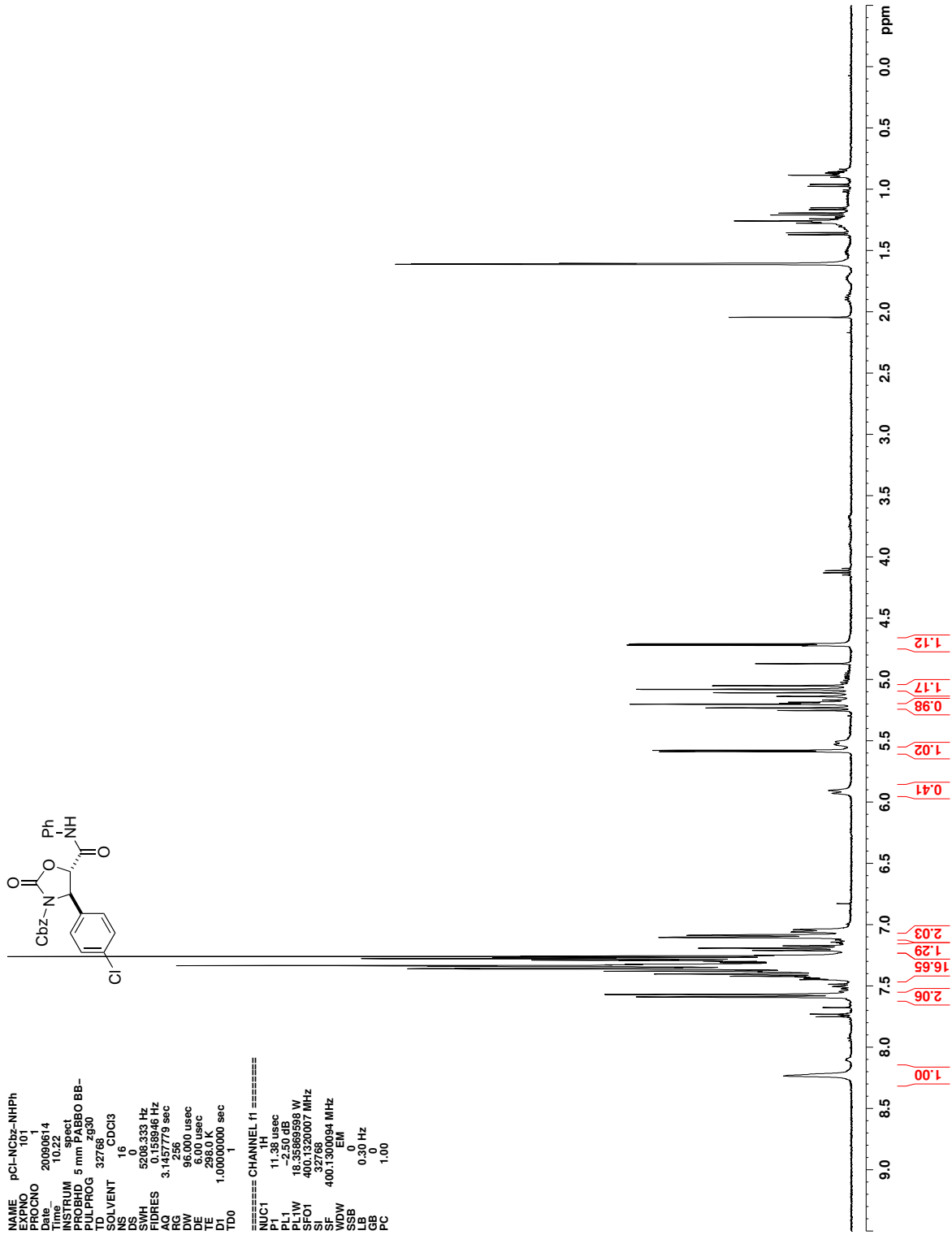


Figure C.71. ^1H NMR (CDCl_3) of 236

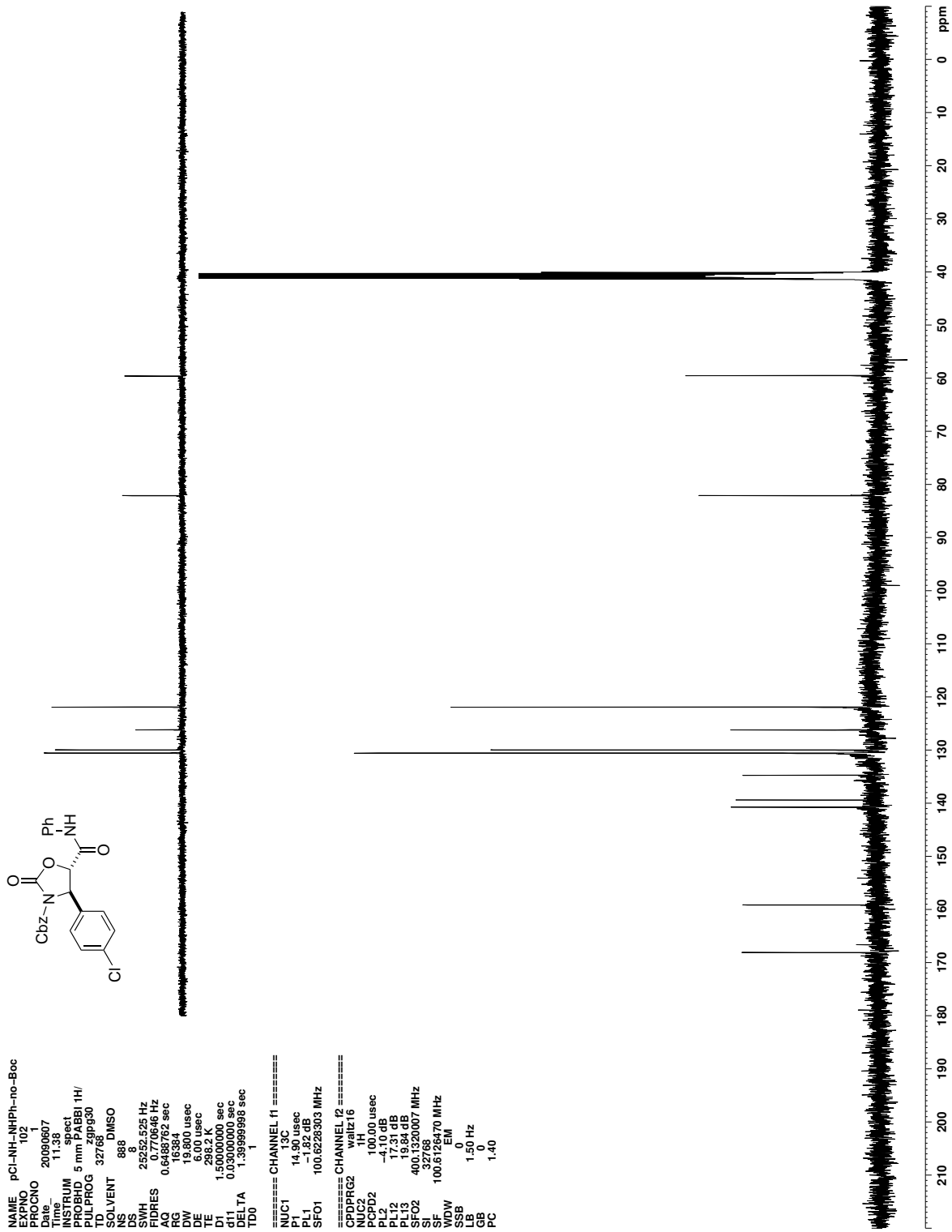


Figure C.72. ^{13}C NMR (CDCl_3) of 236

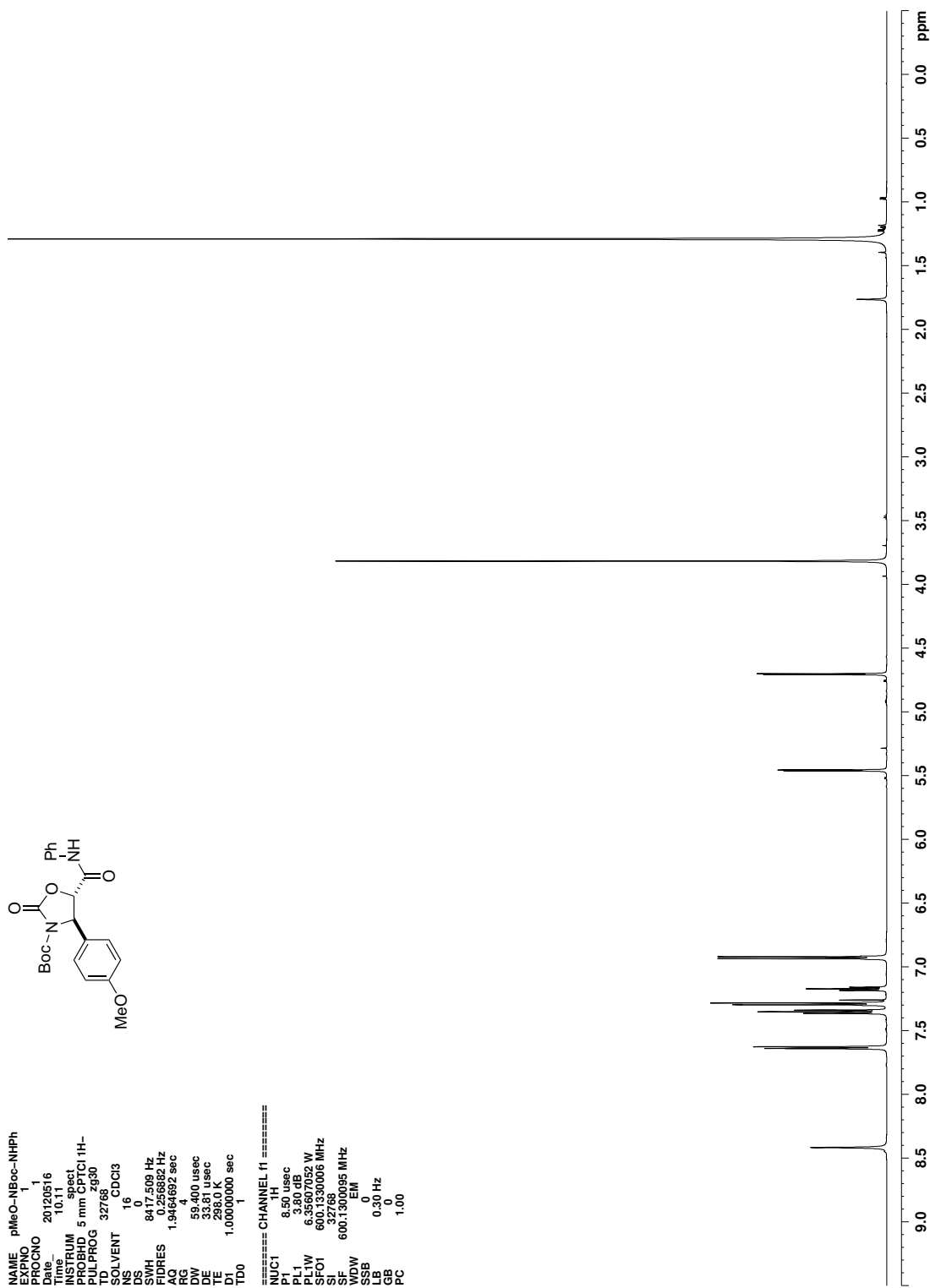


Figure C.73. ^1H NMR (CDCl_3) of 420

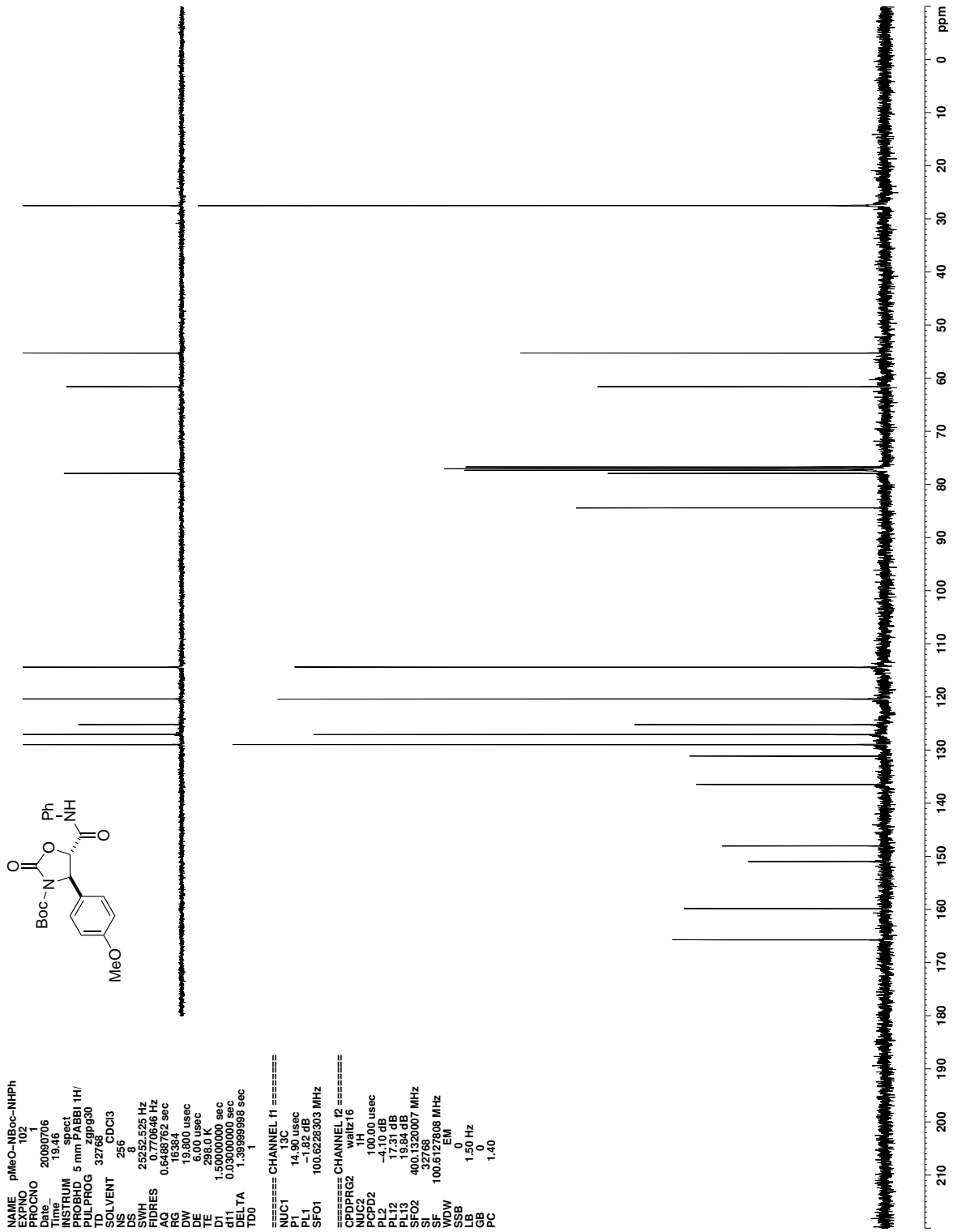


Figure C.74. ¹³C NMR (CDCl₃) of 420

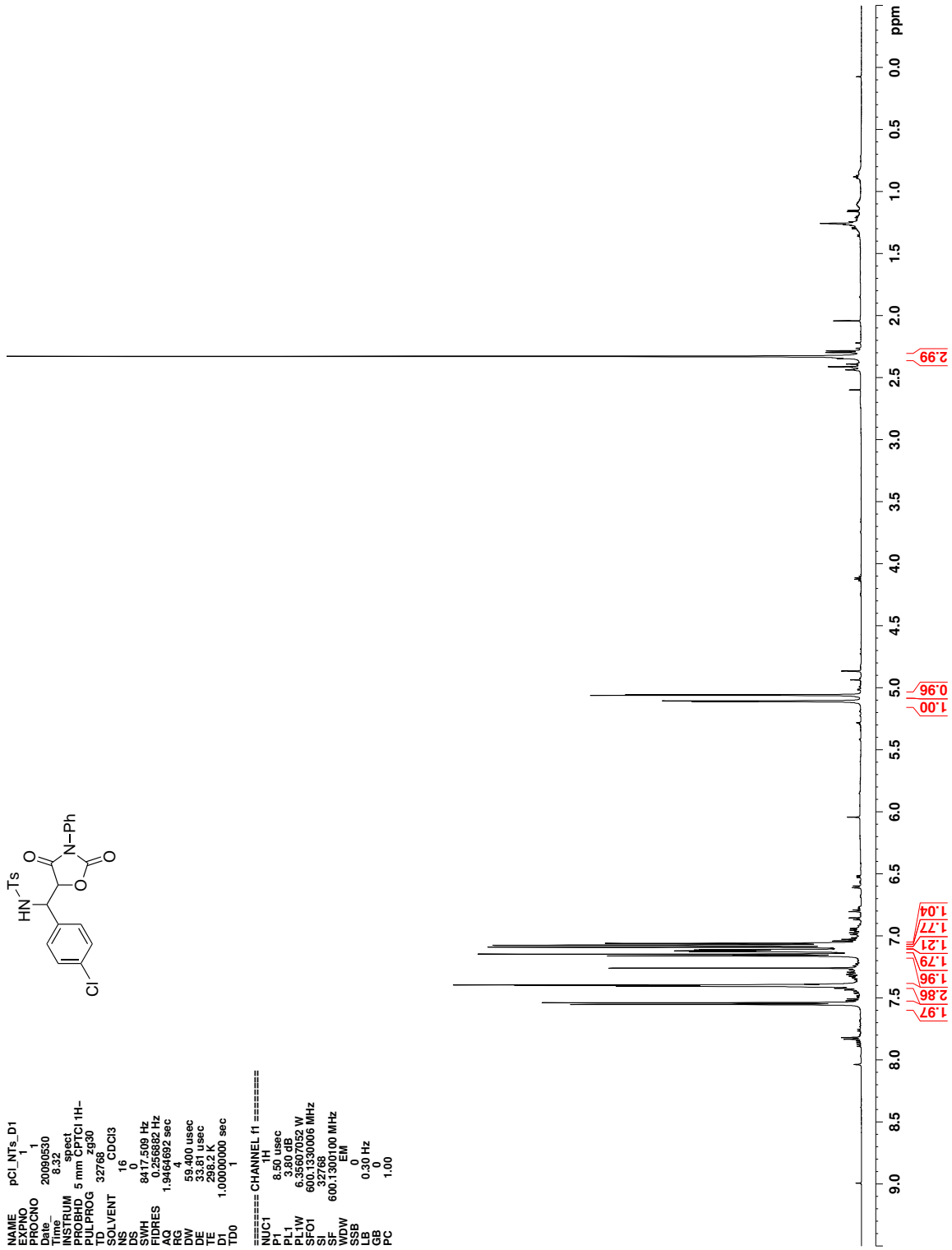


Figure C.75. ^1H NMR (CDCl_3) of 230a

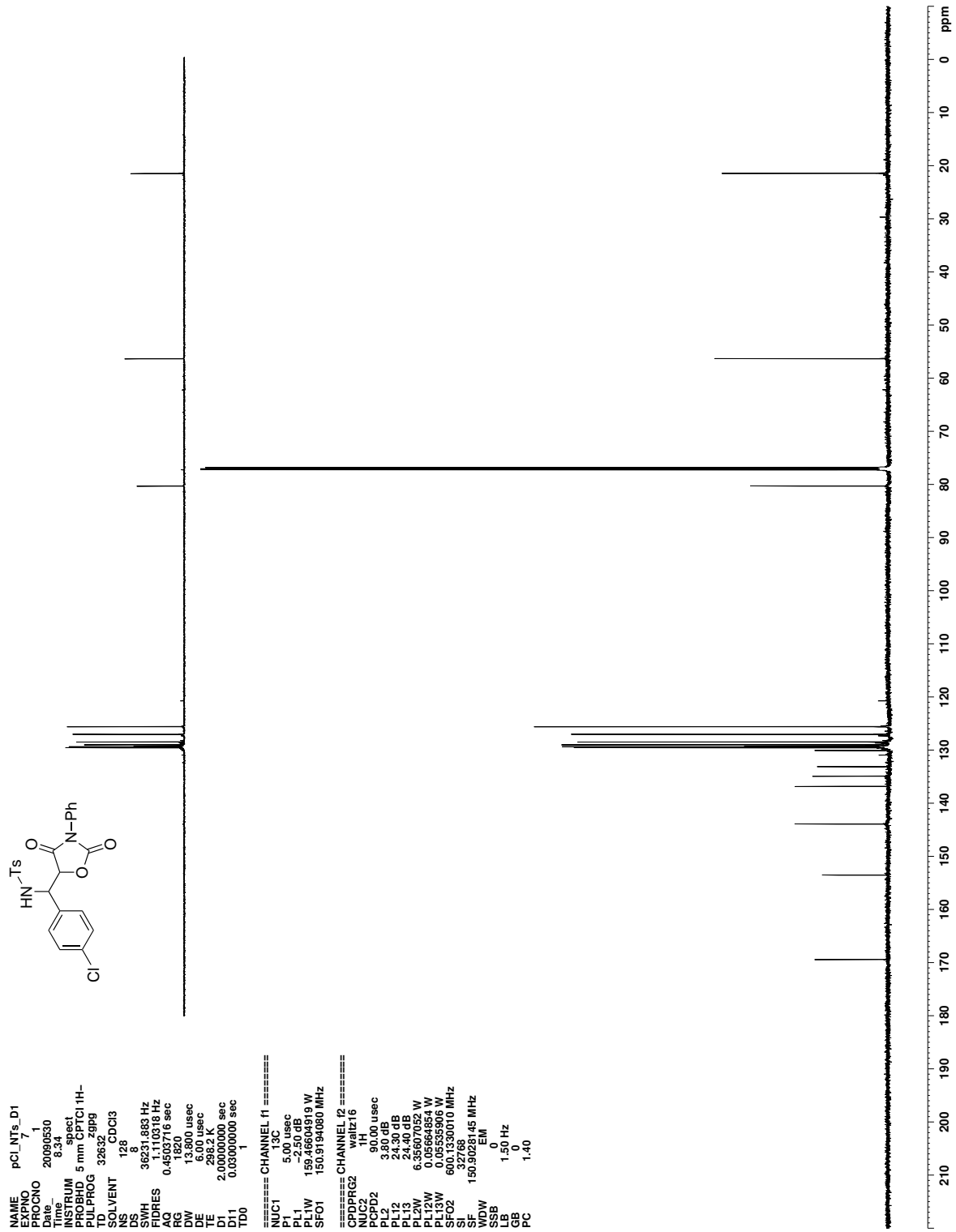


Figure C.76. ^{13}C NMR (CDCl_3) of 230a

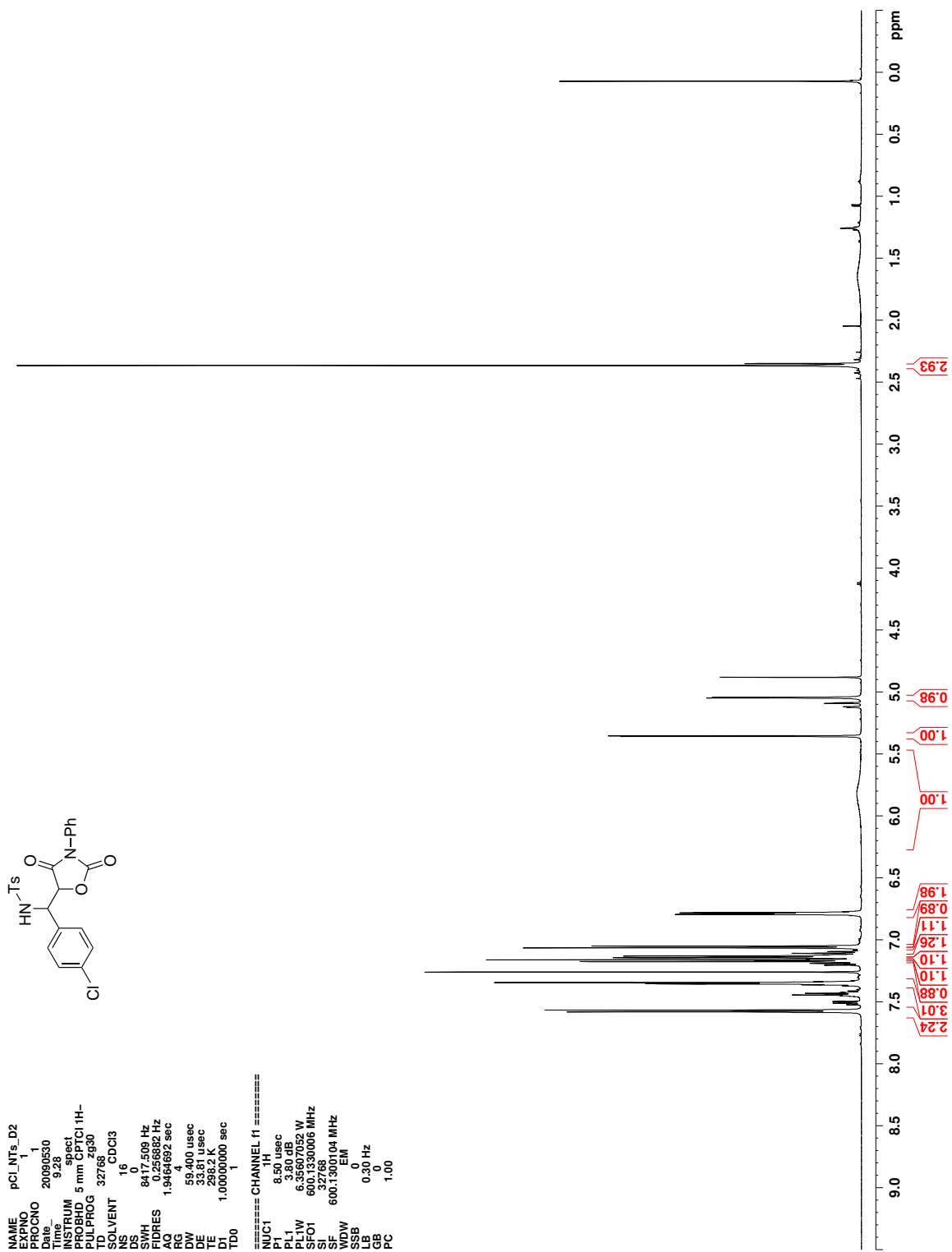


Figure C.77. ^1H NMR (CDCl_3) of 230b

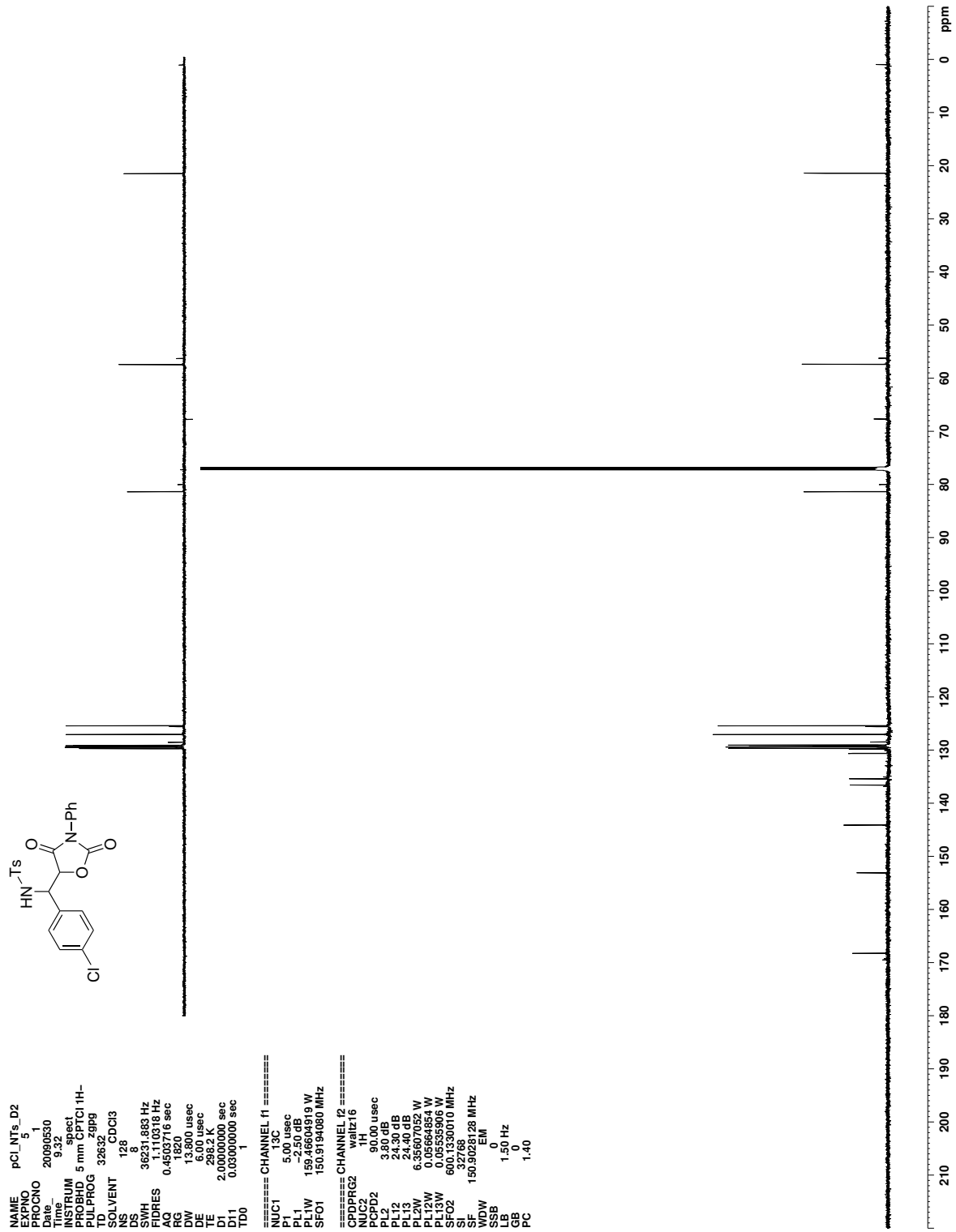


Figure C.78. ^{13}C NMR (CDCl_3) of 230b

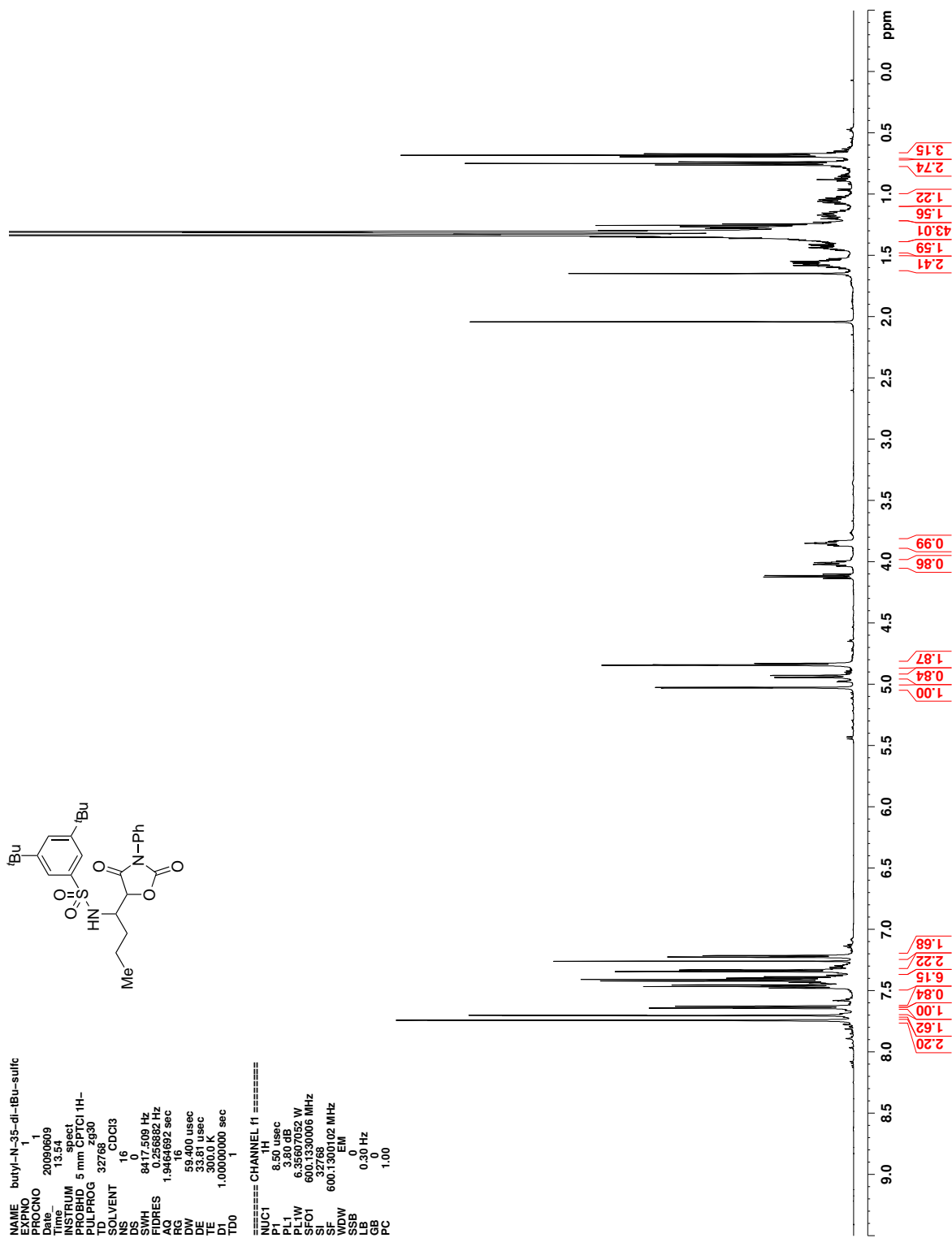


Figure C.79. ^1H NMR (CDCl_3) of **232**

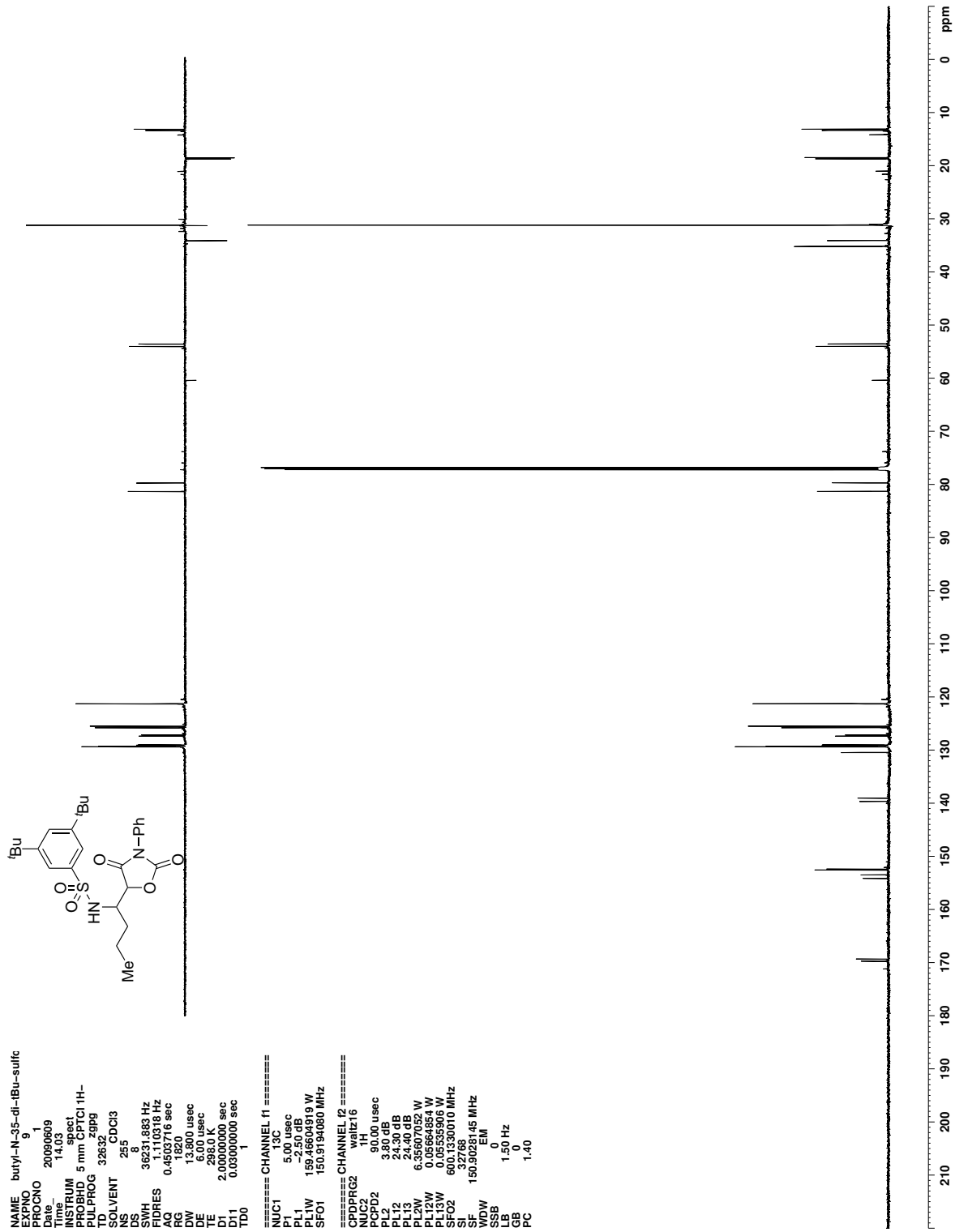


Figure C.80. ^{13}C NMR (CDCl_3) of 232

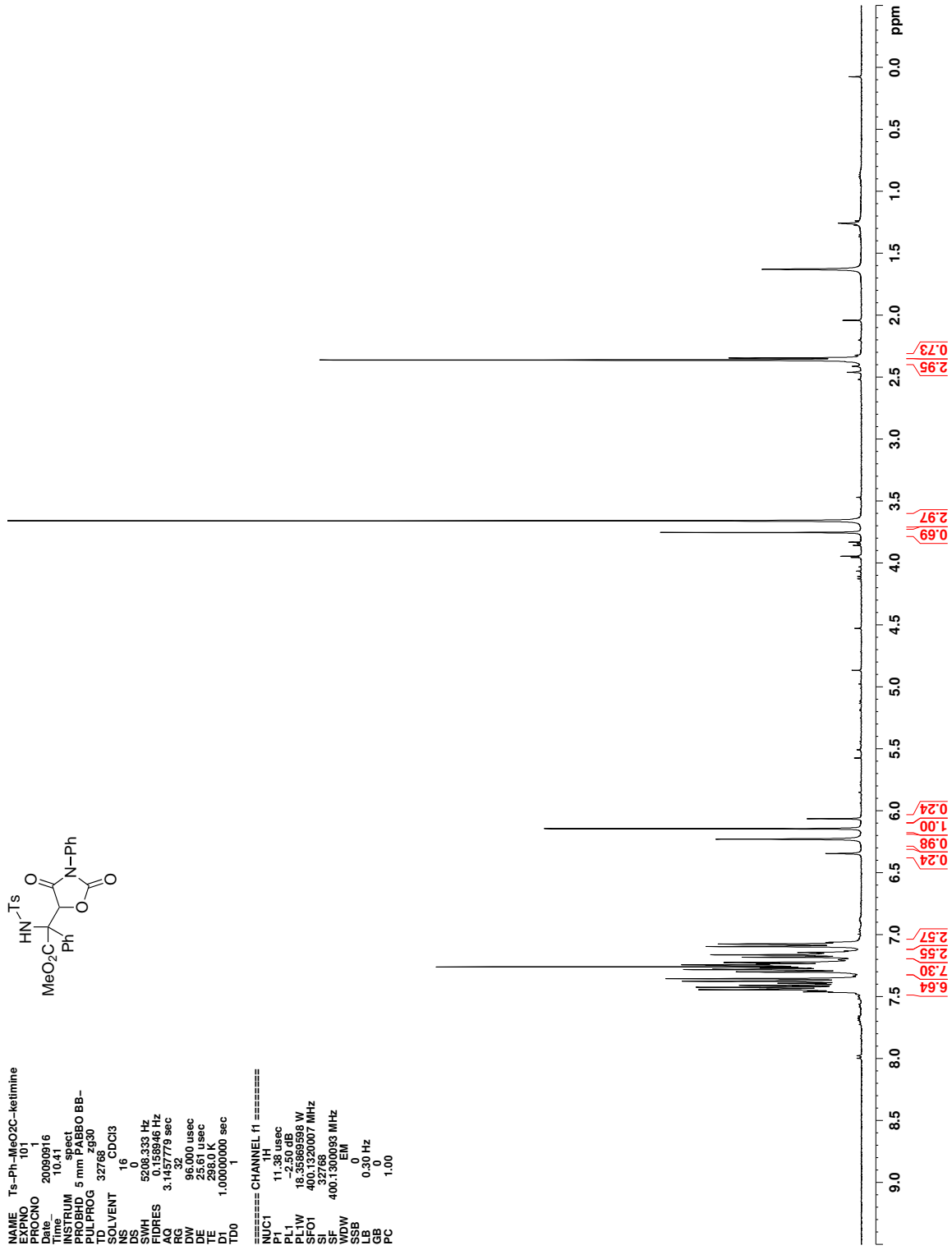


Figure C.81. ¹H NMR (CDCl₃) of 421

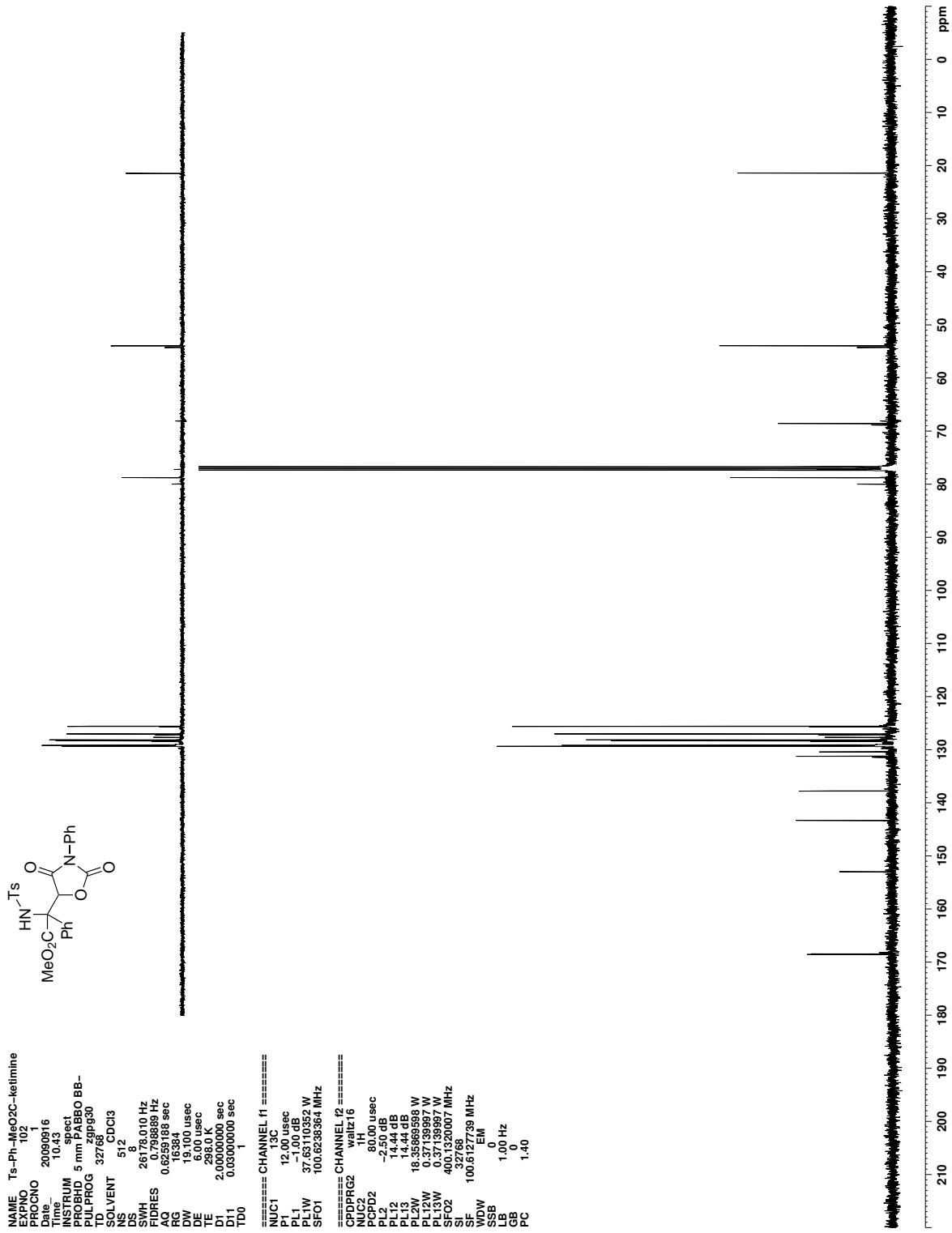


Figure C.82. ¹³C NMR (CDCl₃) of 421

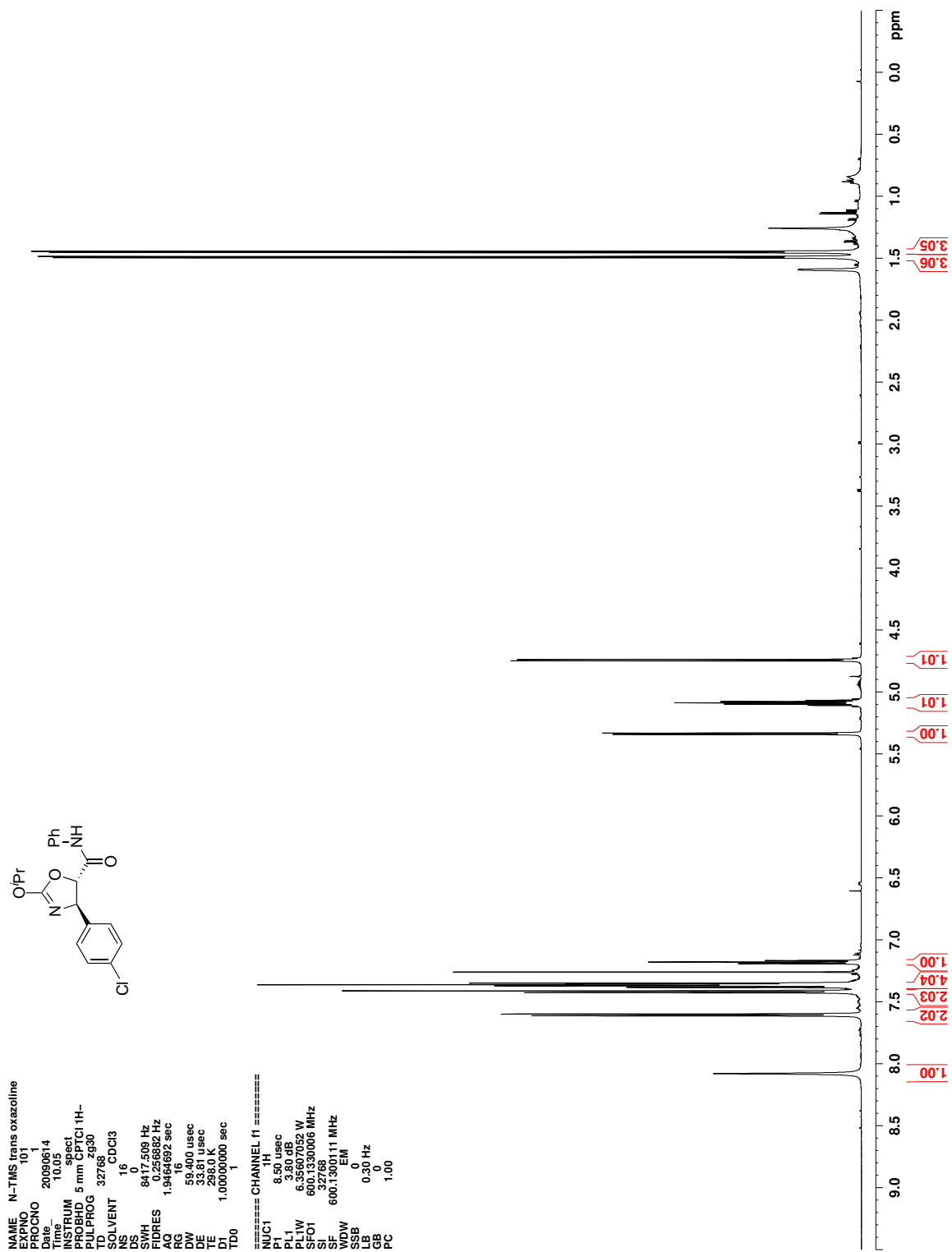


Figure C.83. ^1H NMR (CDCl_3) of 236

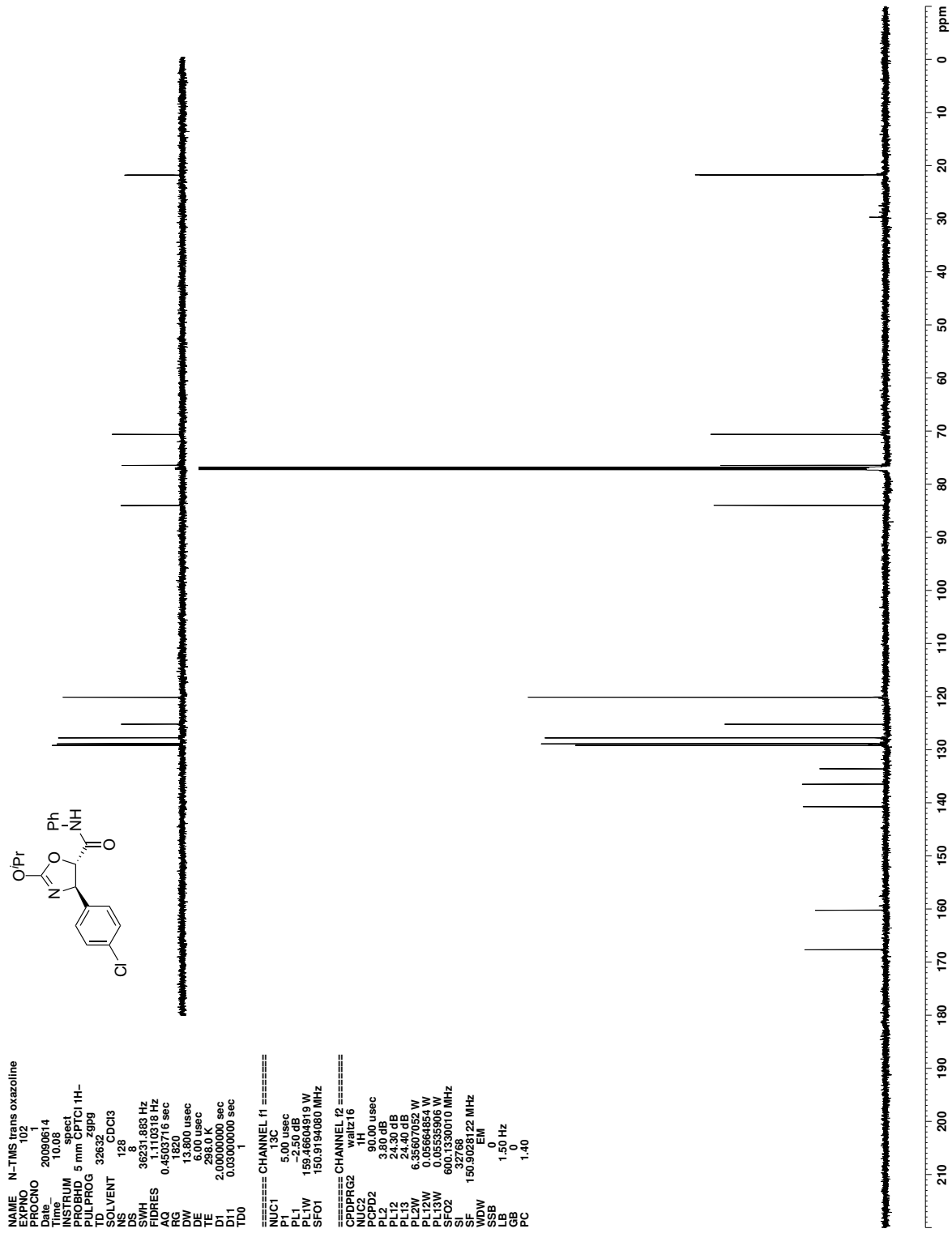


Figure C.84. ¹³C NMR (CDCl₃) of 236

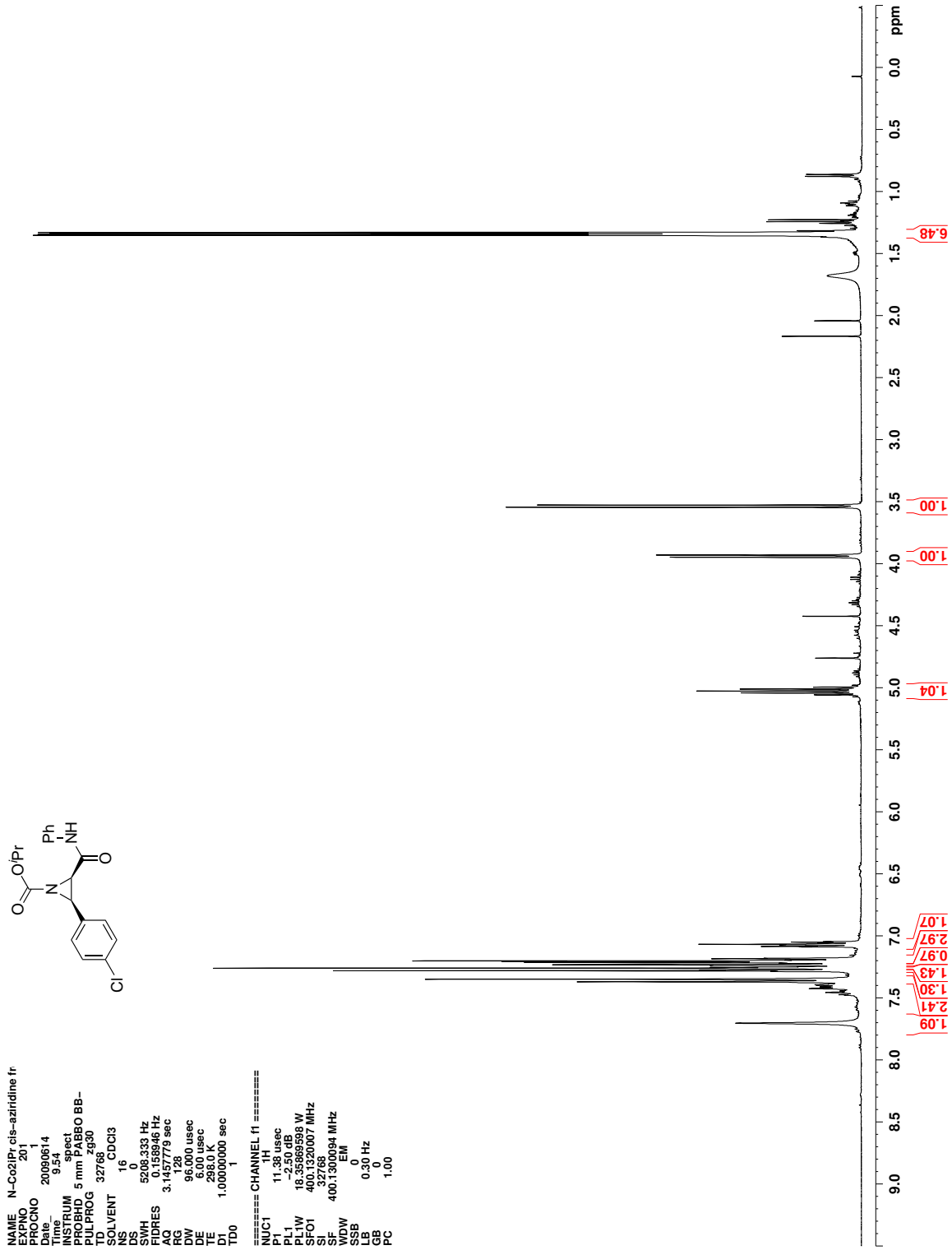


Figure C.85. ^1H NMR (CDCl_3) of 237

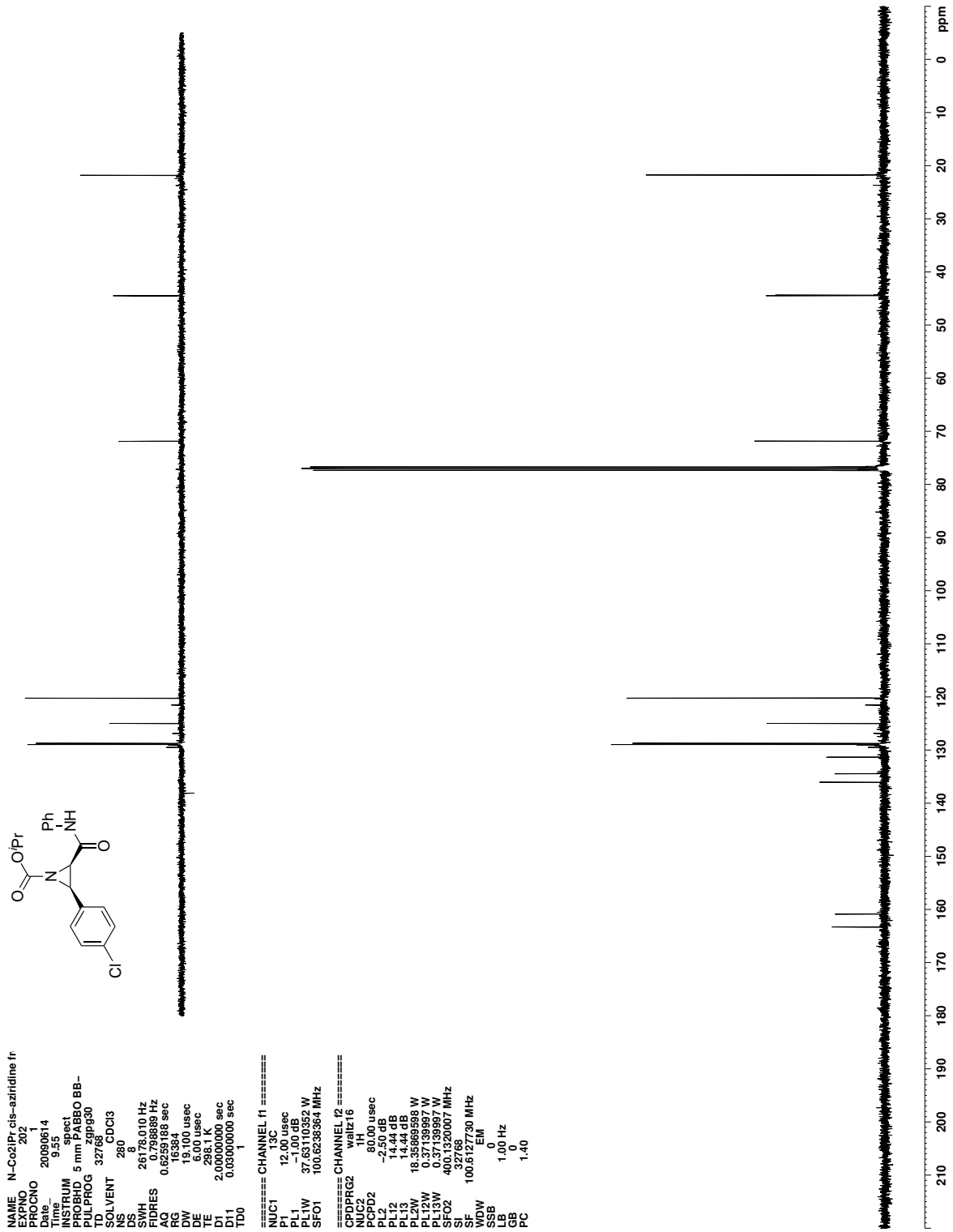


Figure C.86. ^{13}C NMR (CDCl_3) of 237

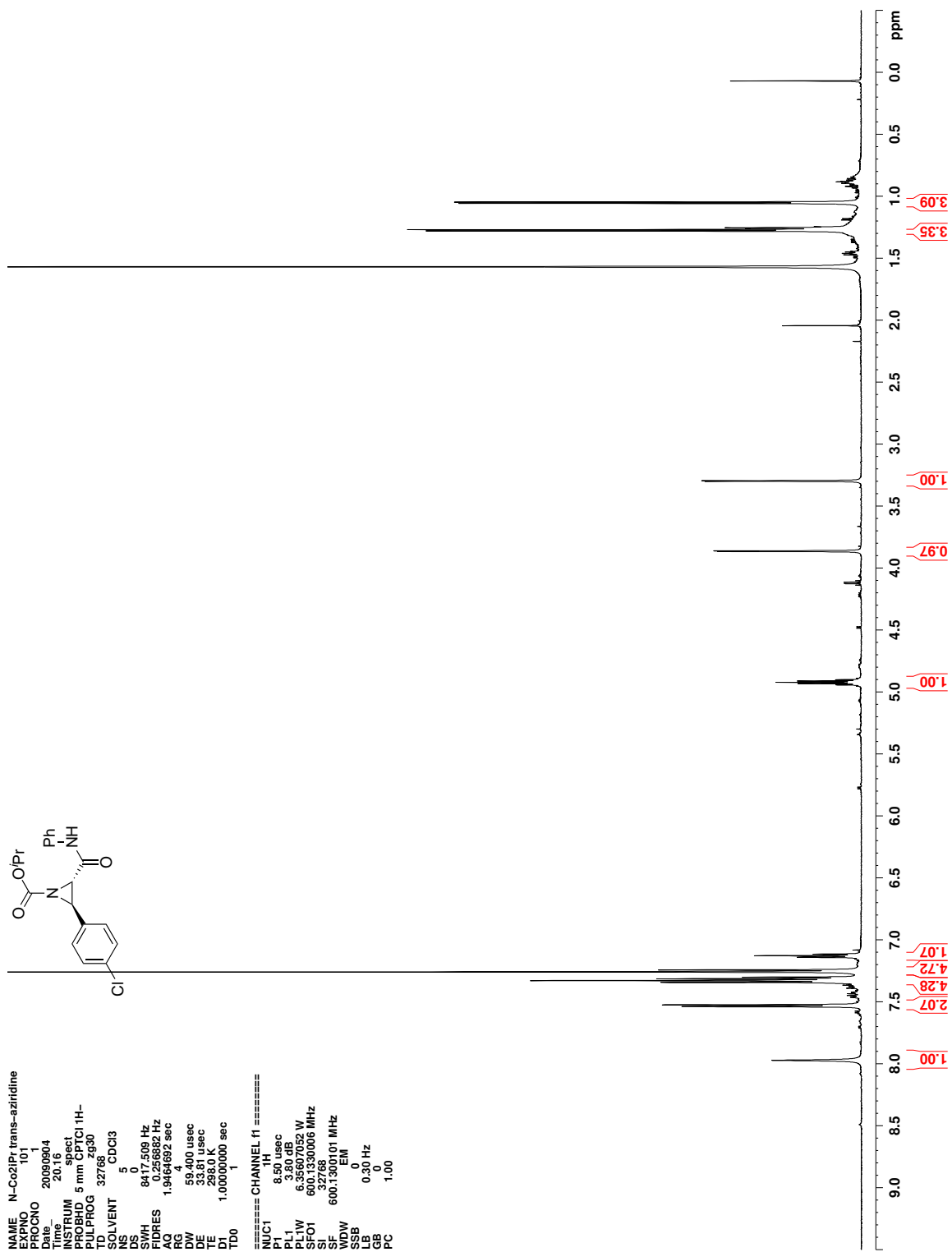


Figure C.87. ^1H NMR (CDCl_3) of 238

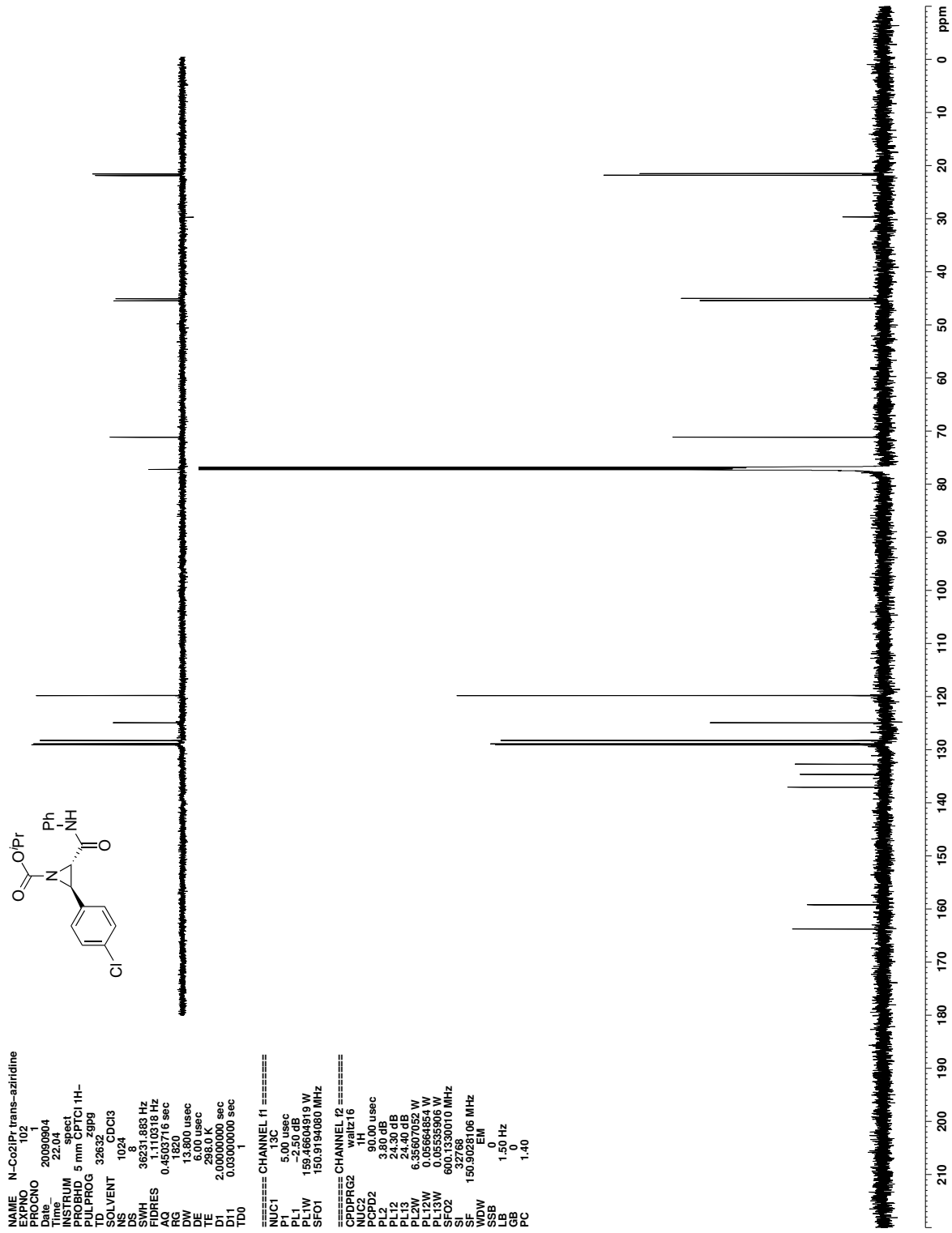


Figure C.88. ¹³C NMR (CDCl₃) of 238

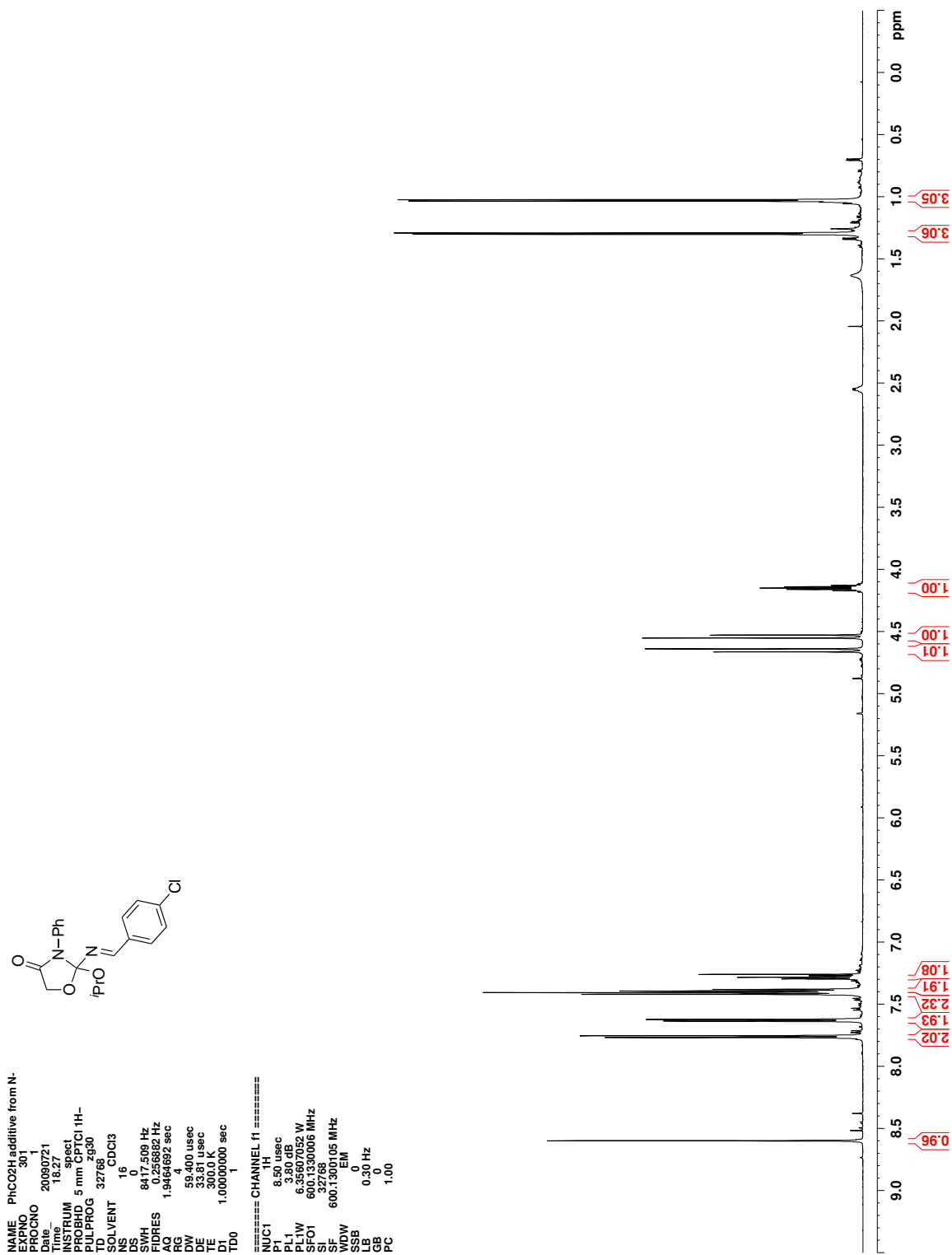


Figure C.89. ^1H NMR (CDCl_3) of 240

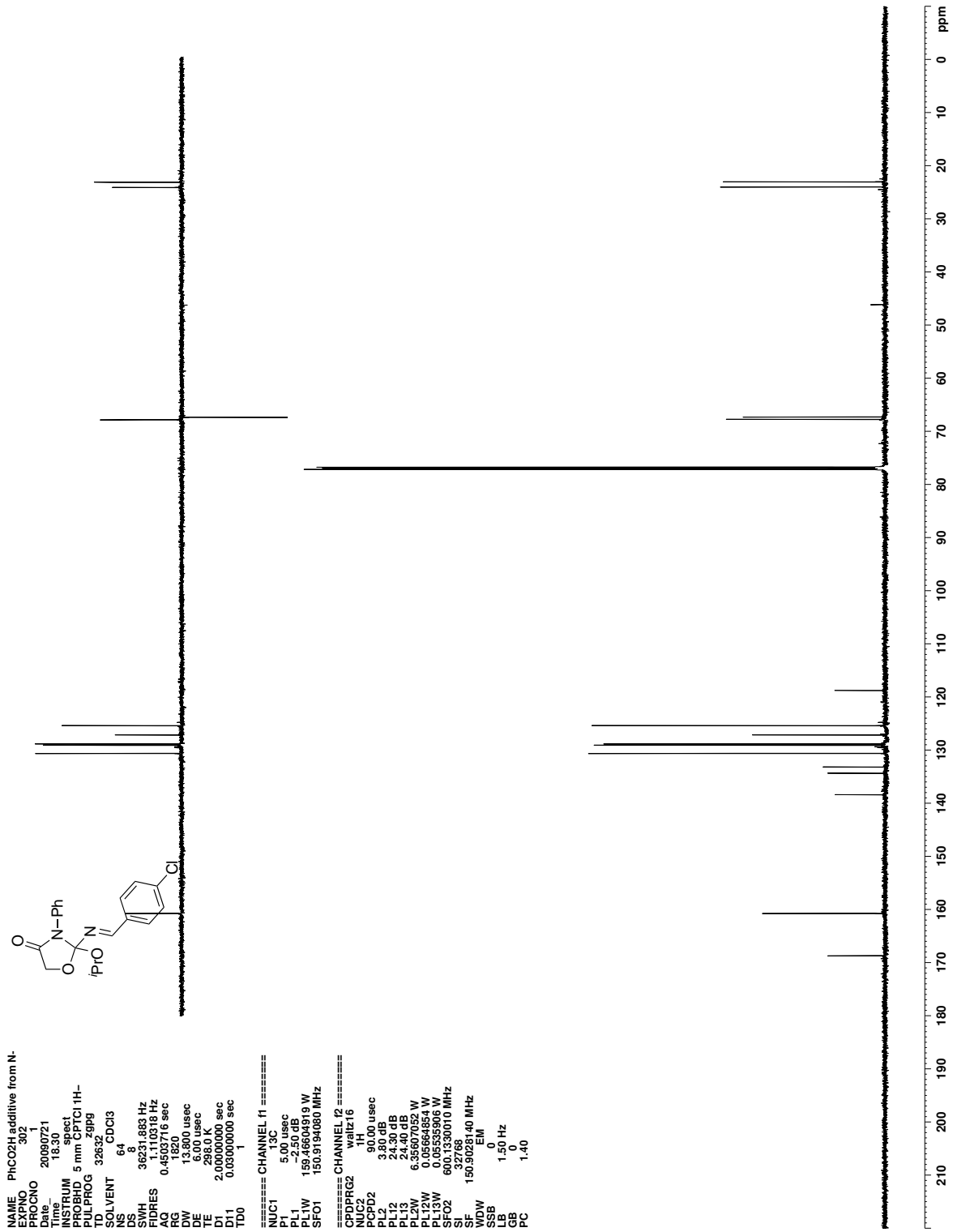


Figure C.90. ^{13}C NMR (CDCl_3) of 240

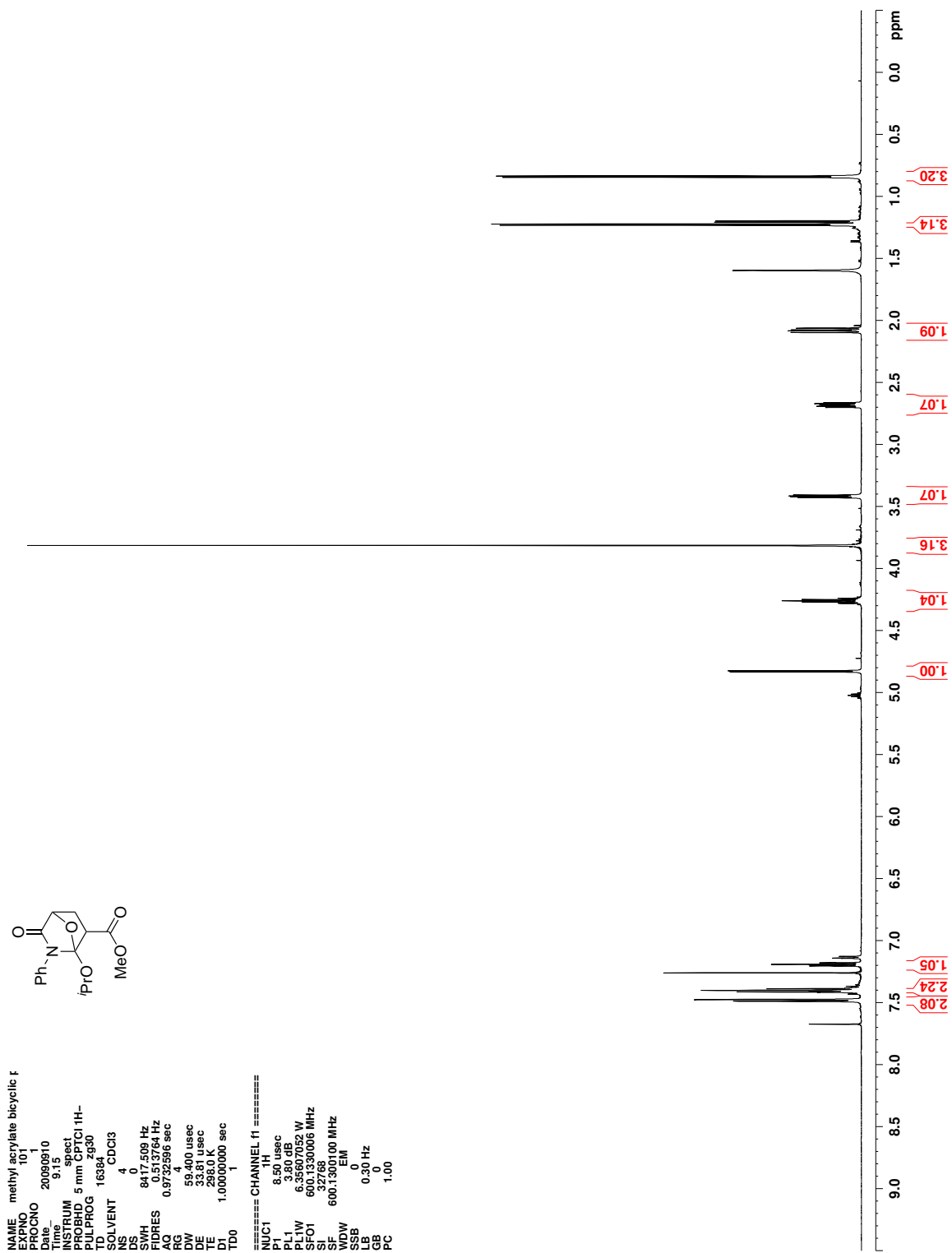


Figure C.91. ^1H NMR (CDCl_3) of 242

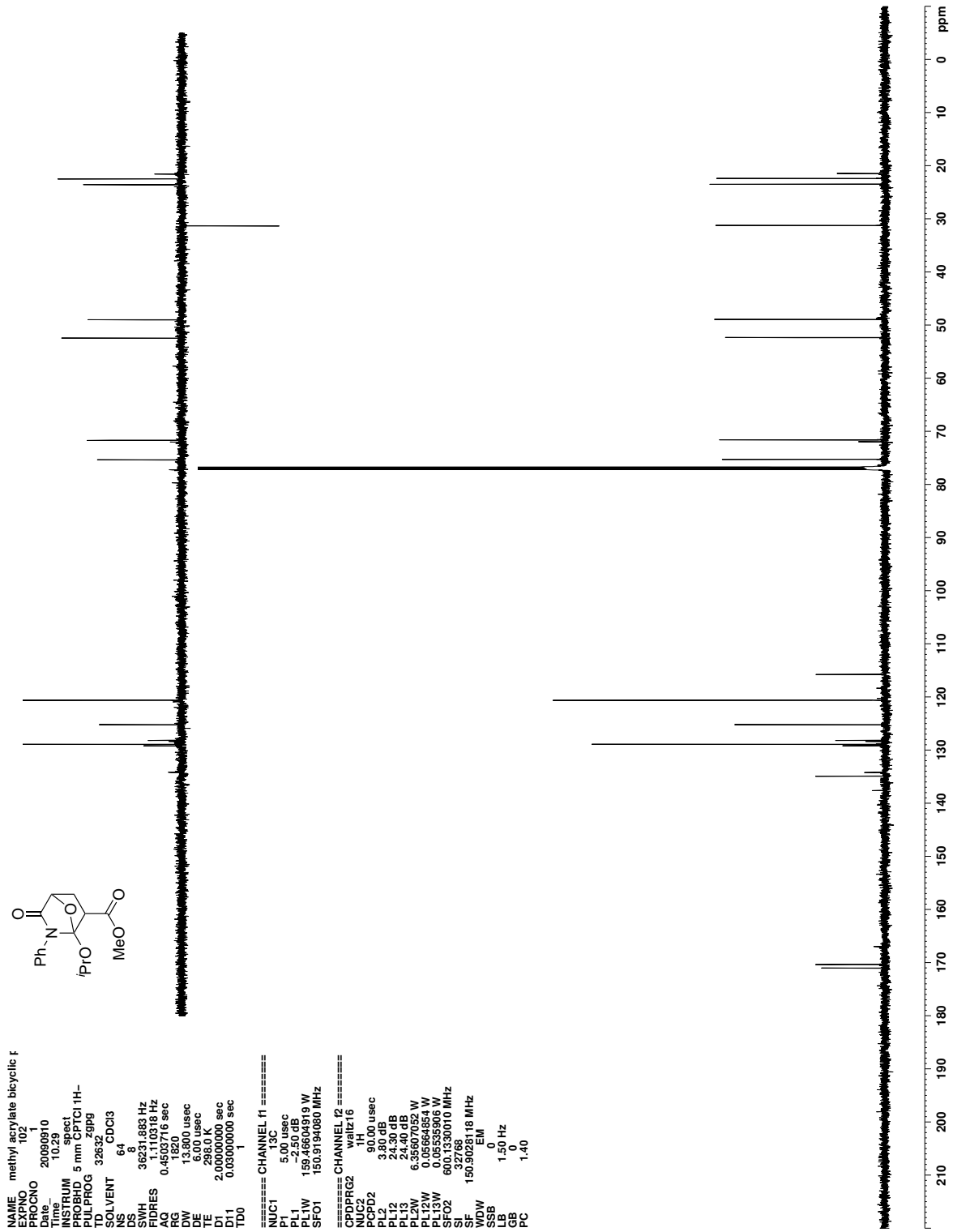
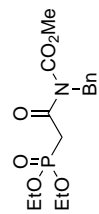


Figure C.92. ^{13}C NMR (CDCl_3) of 242



```

NAME imidiphos-omebn
EXPNO 20
PROCNO 1
Date_ 20100227
Time 9.50
INSTRUM spect
PROBHD 5 mm CPTCI 1H-
TD 65536
AQ 0.04
RG 655
SOLVENT CDCl3
NS 16
DS 0
SWH 8417.508 Hz
FIDRES 0.258652 Hz
AQRES 1.946492 sec
RG 655
DW 59.400 usec
DE 33.81 usec
TE 300.0 K
D1 1.00000000 sec
TD0 1
===== CHANNEL f1 =====
NUC1 1H
P1 8.50 usec
PL1 3.80 dB
PL2 0.00 dB
PL3 0.00 dB
PL4 0.00 dB
PL5 0.00 dB
PL6 0.00 dB
PL7 0.00 dB
PL8 0.00 dB
PL9 0.00 dB
SFO1 600.1330006 MHz
SI 32768
SF 600.1300102 MHz
WDW EM
SSB 0
GB 0
PC 1.00

```

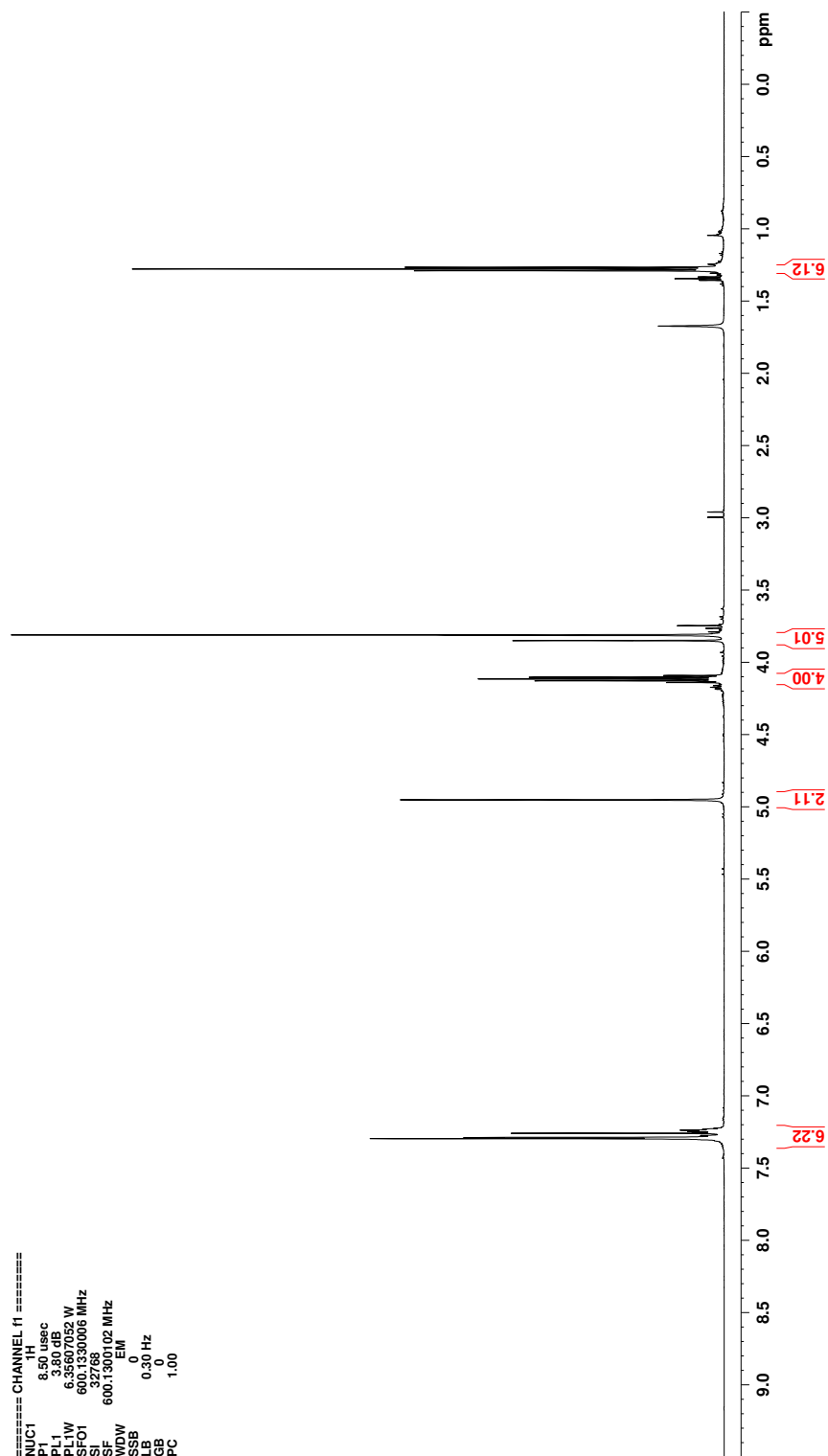


Figure C.93. ¹H NMR (CDCl₃) of 319

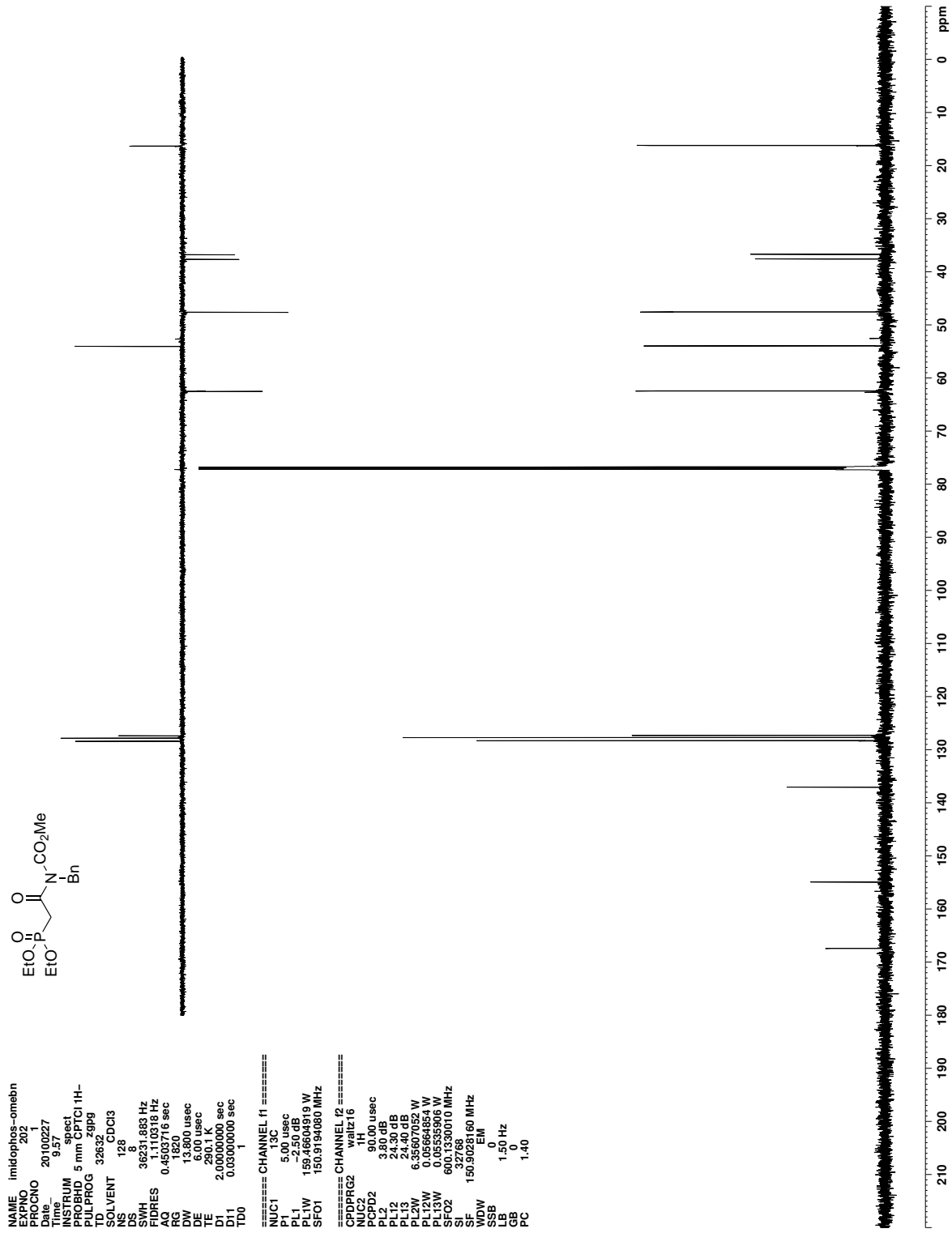


Figure C.94. ^{13}C NMR (CDCl_3) of 319

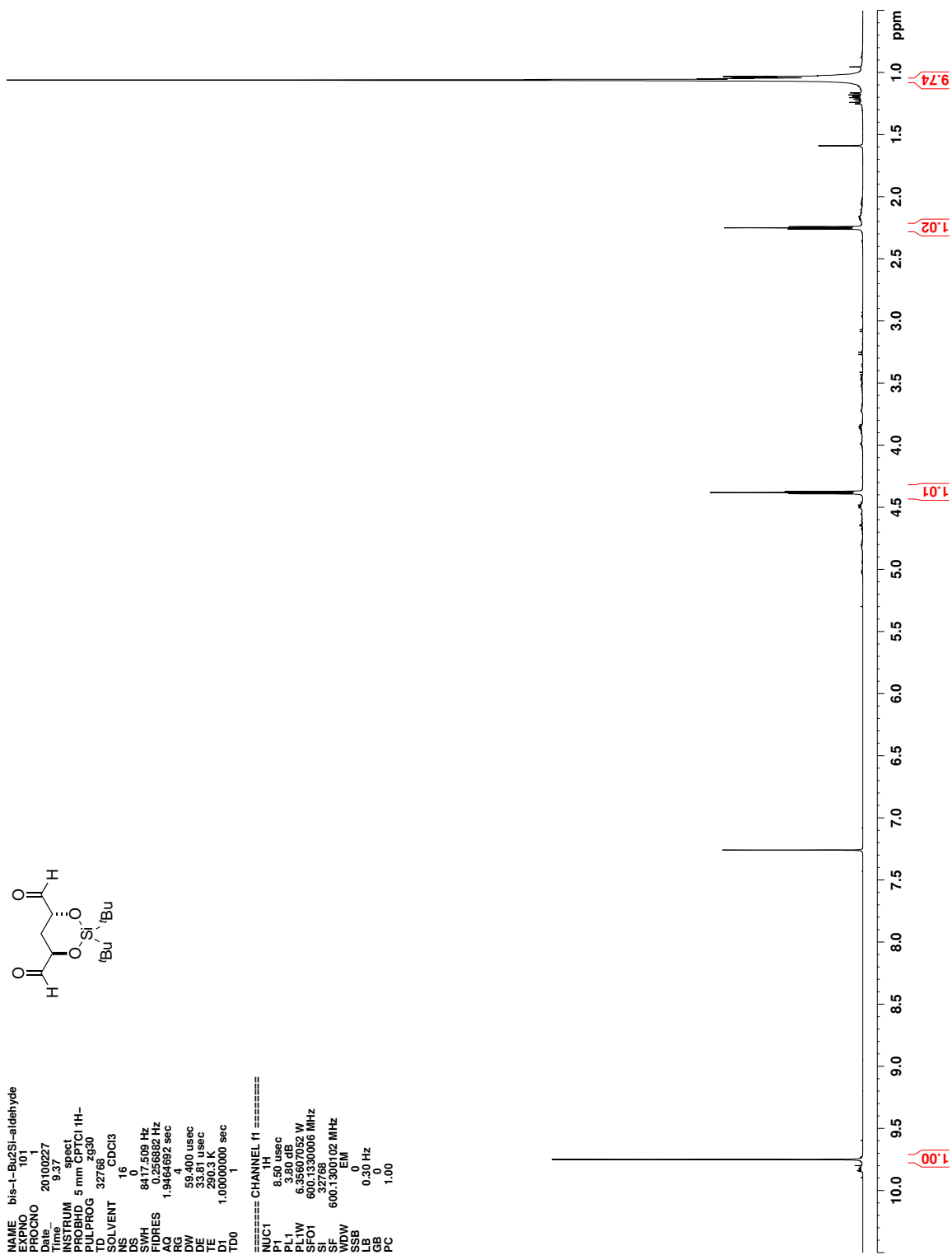


Figure C.95. ^1H NMR (CDCl_3) of **322**

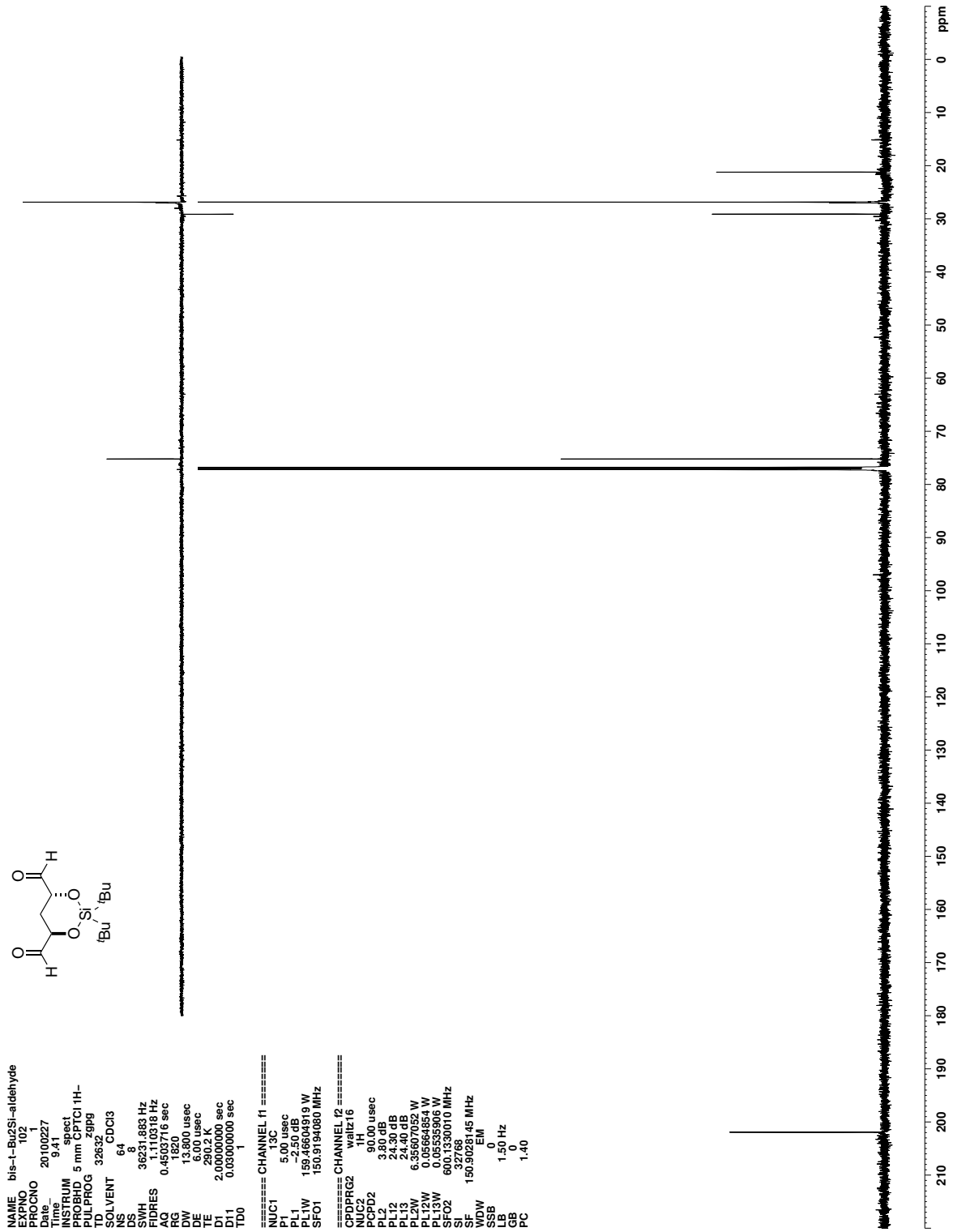


Figure C.96. ^{13}C NMR (CDCl_3) of **322**

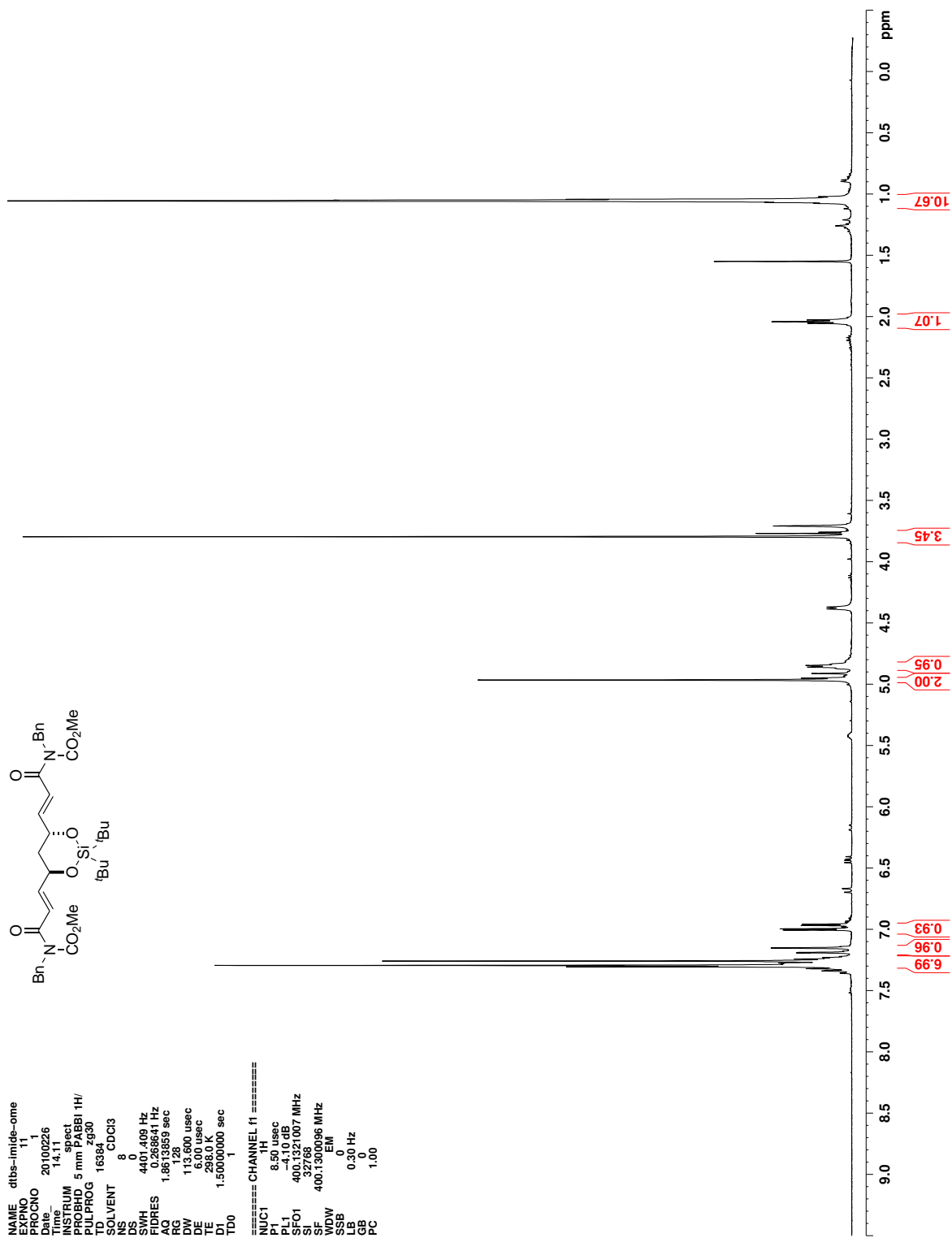


Figure C.97. ^1H NMR (CDCl_3) of 312

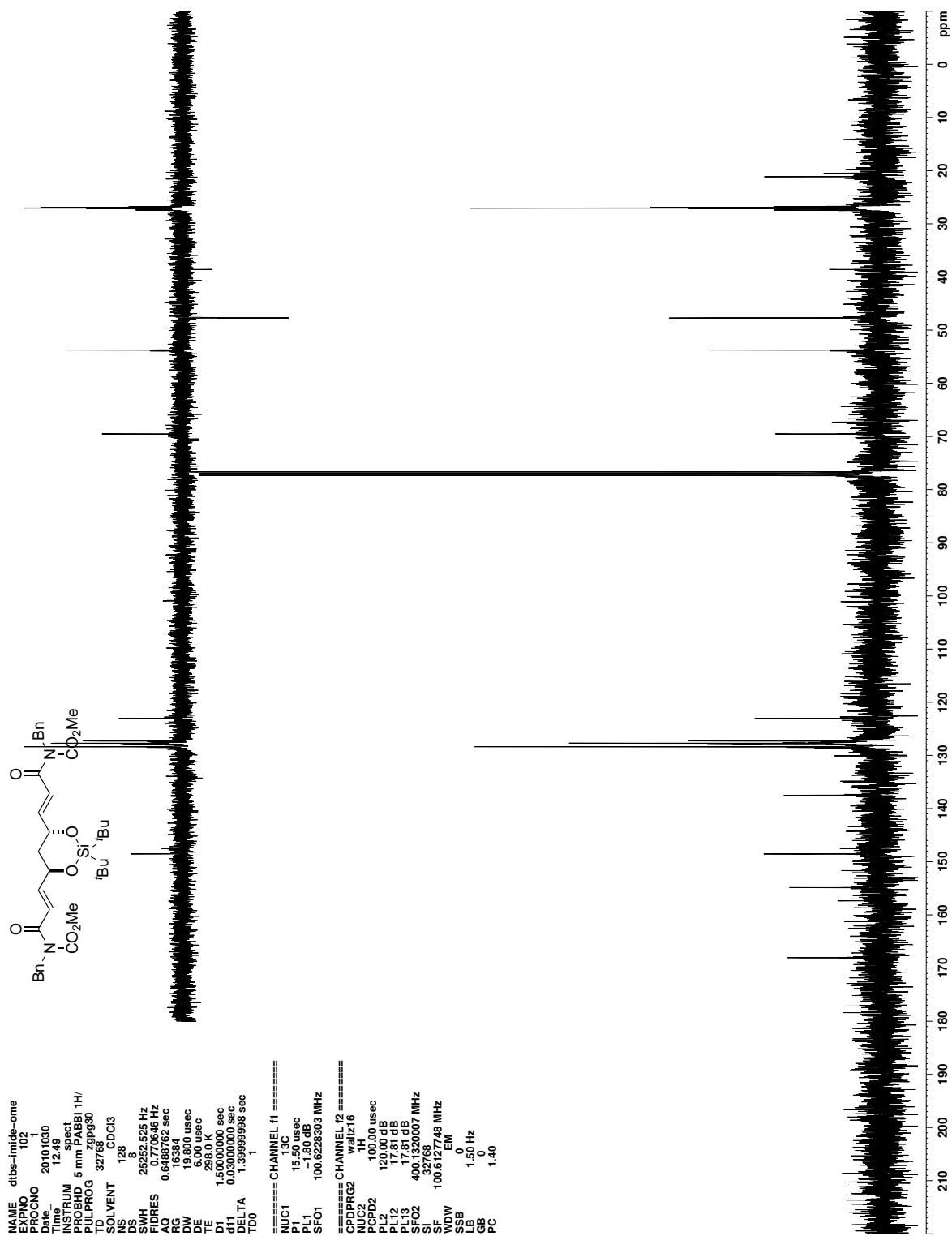


Figure C.98. ¹³C NMR (CDCl₃) of 312

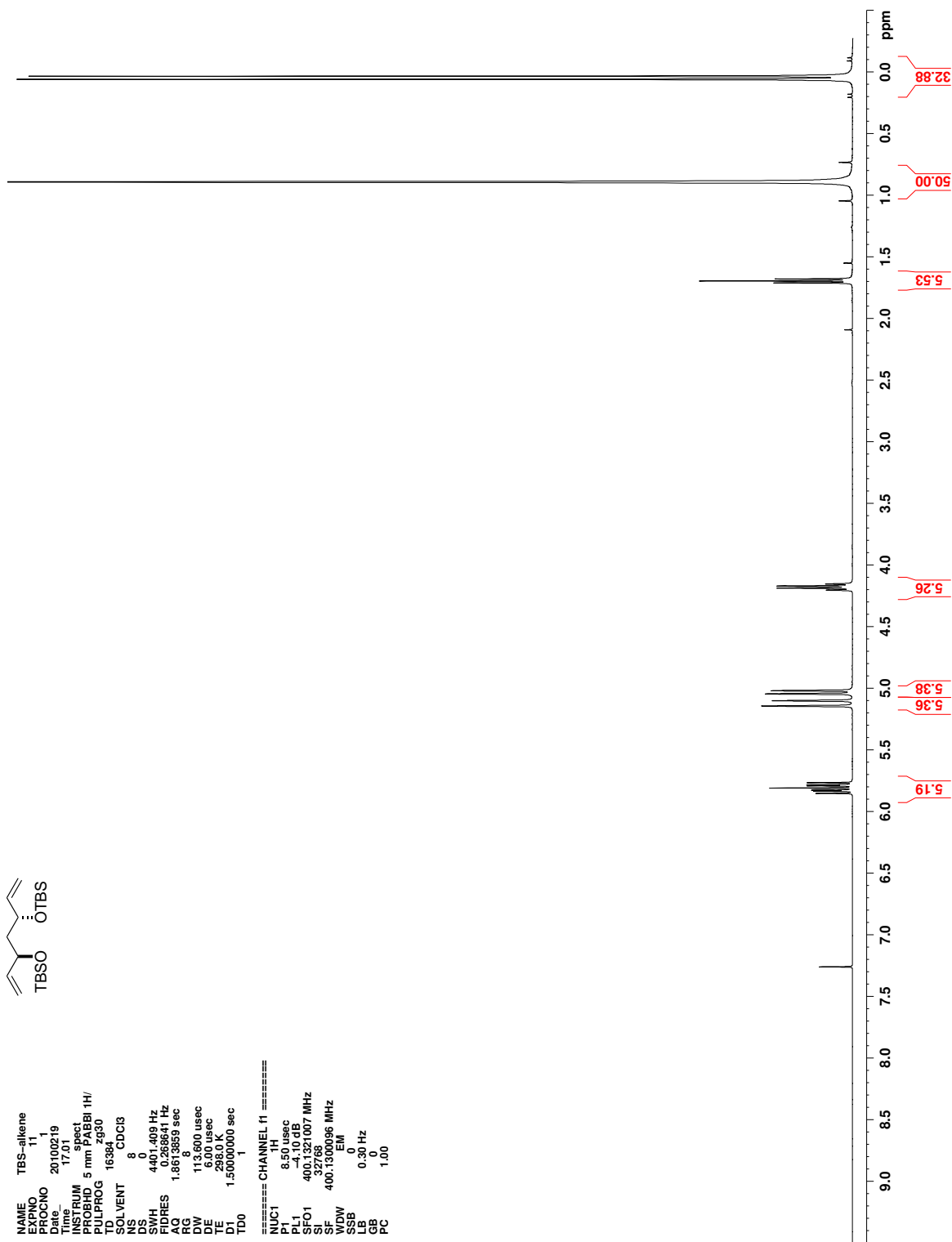


Figure C.99. ^1H NMR (CDCl_3) of 422

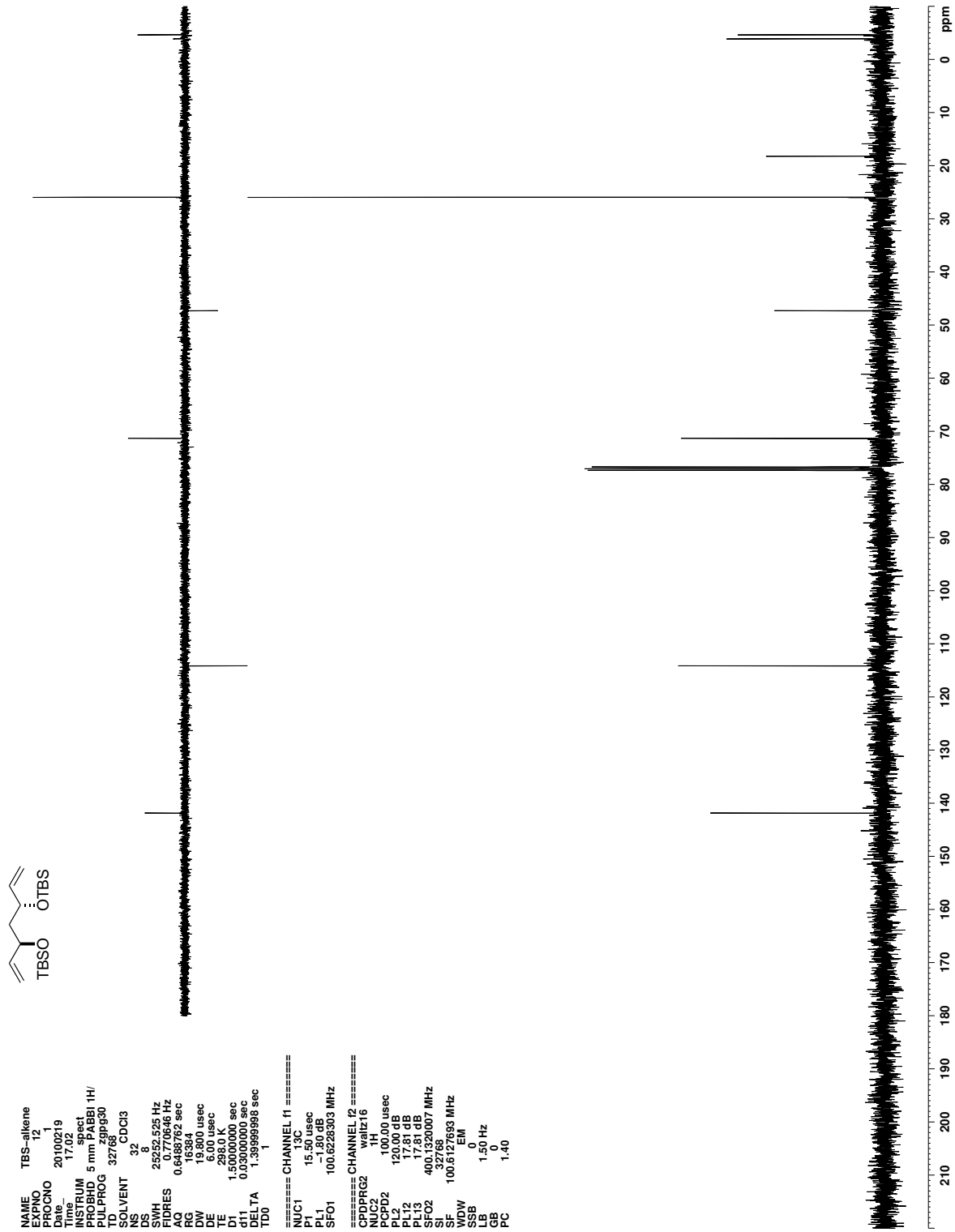


Figure C.100. ^{13}C NMR (CDCl_3) of 422

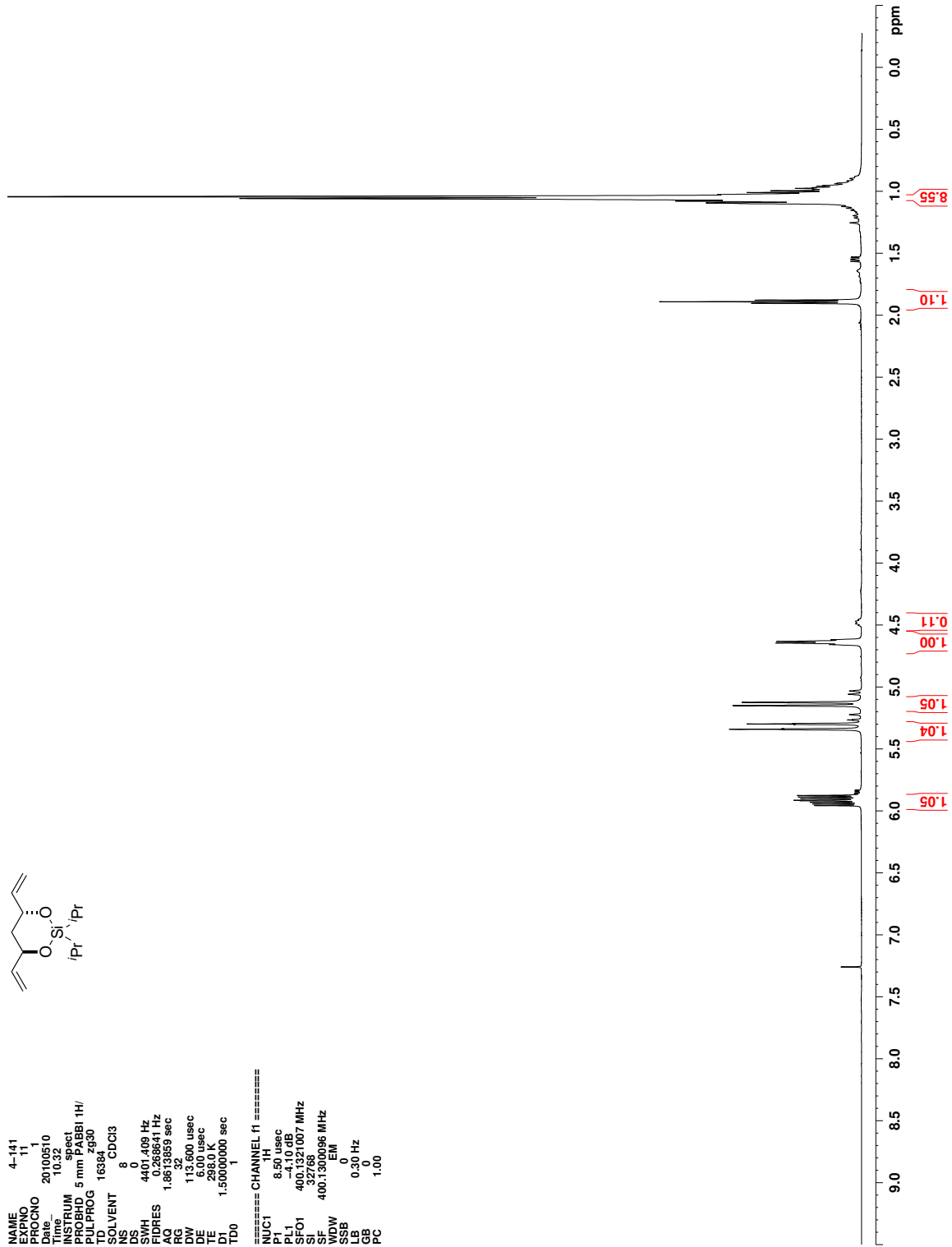


Figure C.101. ^1H NMR (CDCl_3) of 423

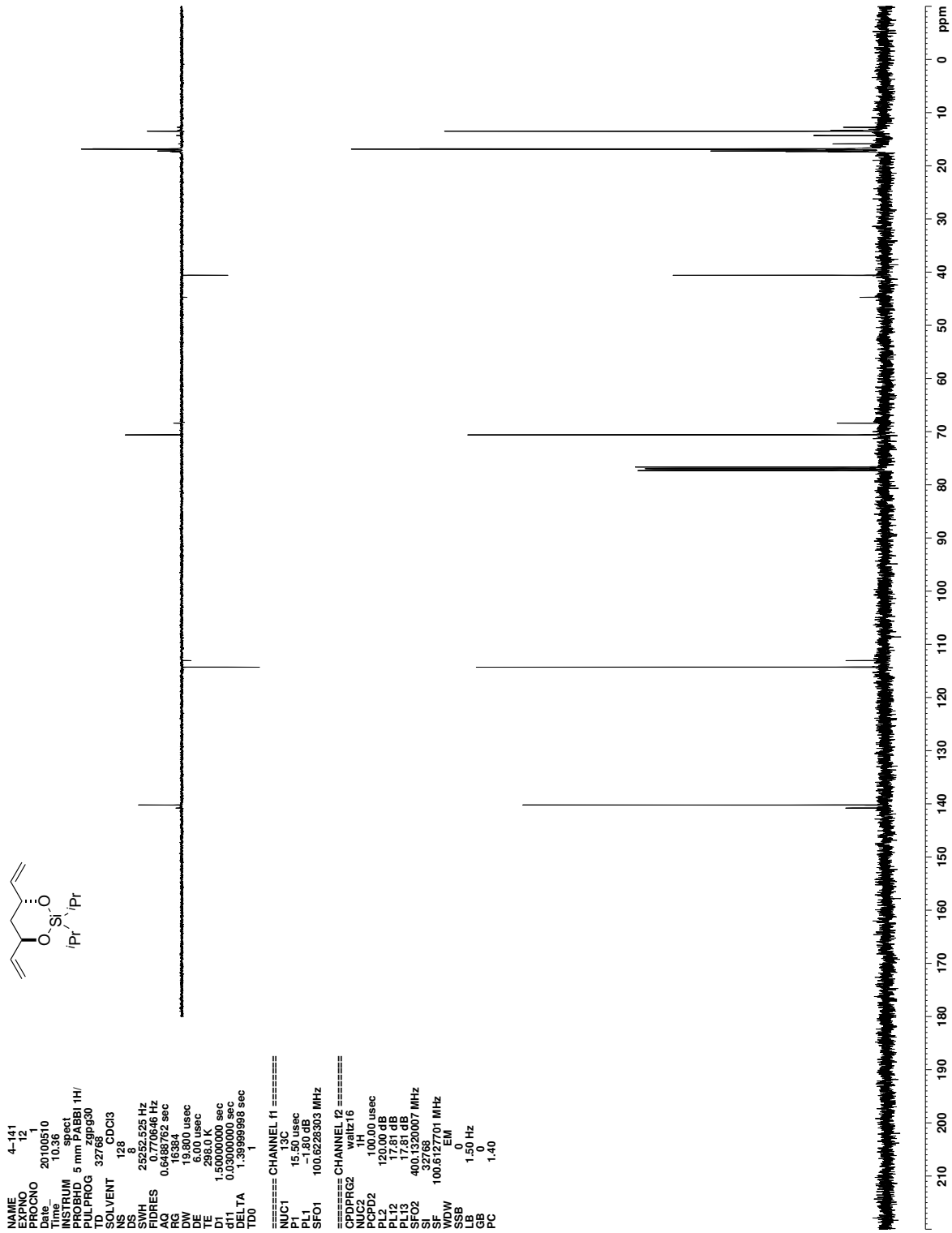


Figure C.102. ¹³C NMR (CDCl₃) of 423

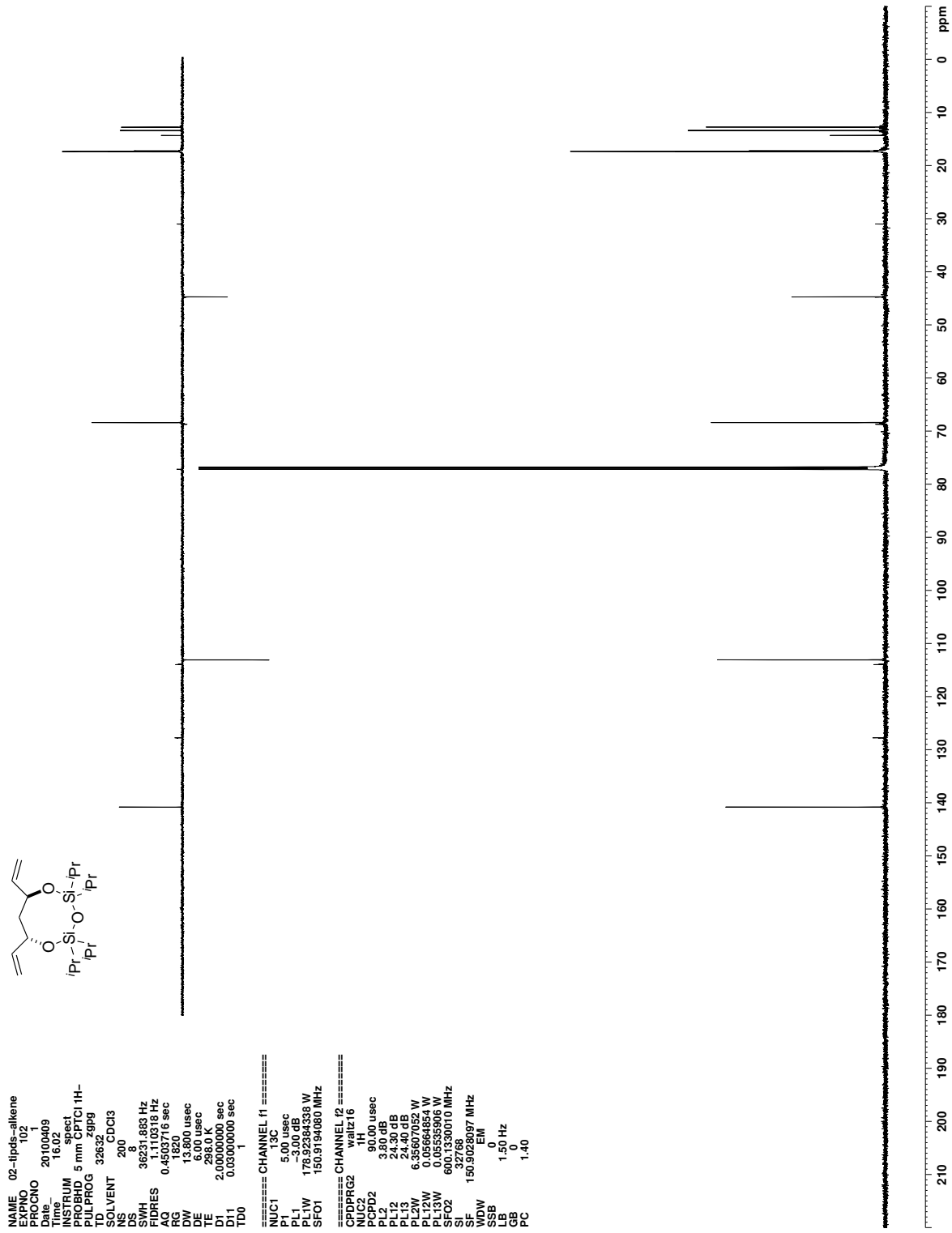


Figure C.104. ¹³C NMR (CDCl₃) of 328

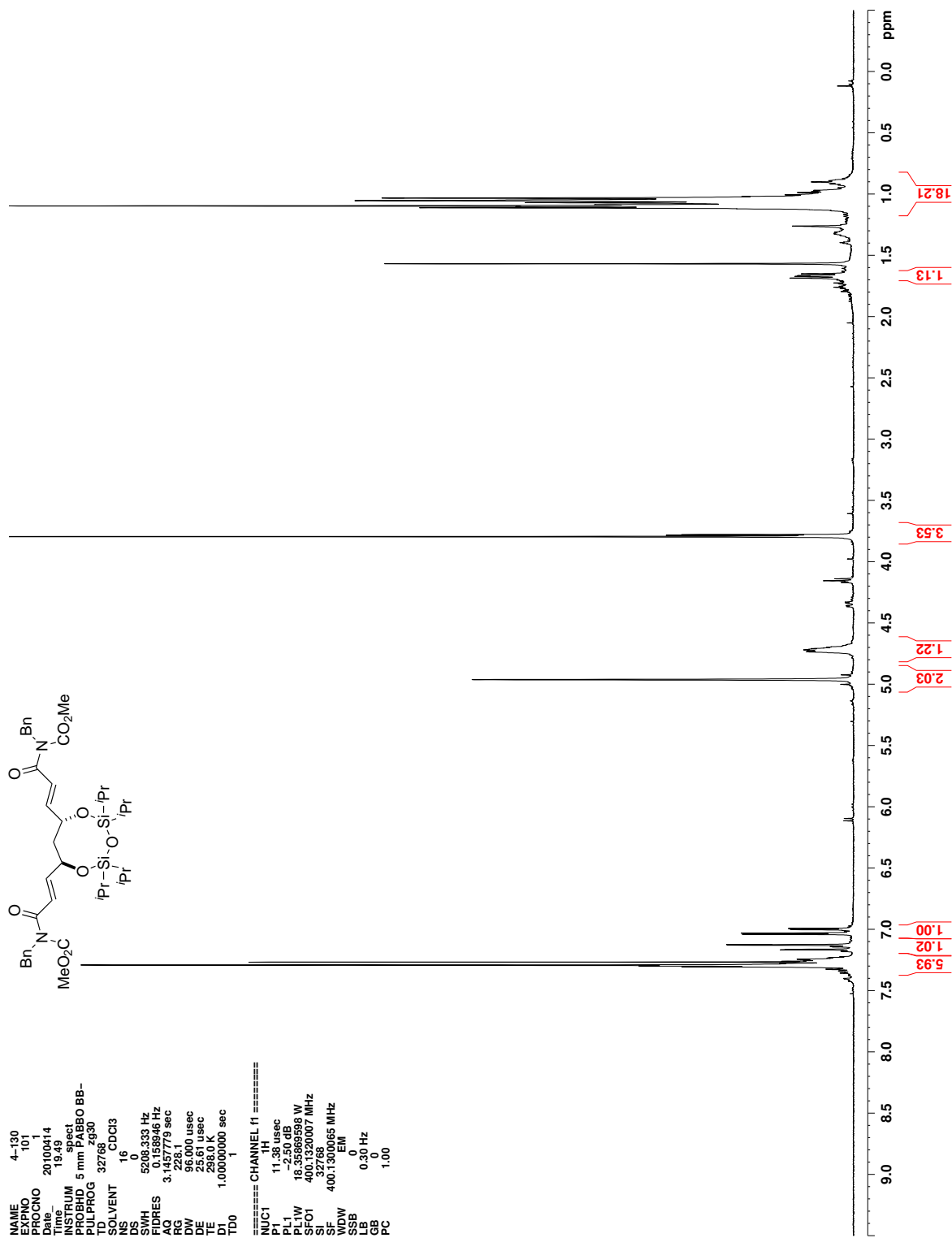


Figure C.105. ^1H NMR (CDCl_3) of 331

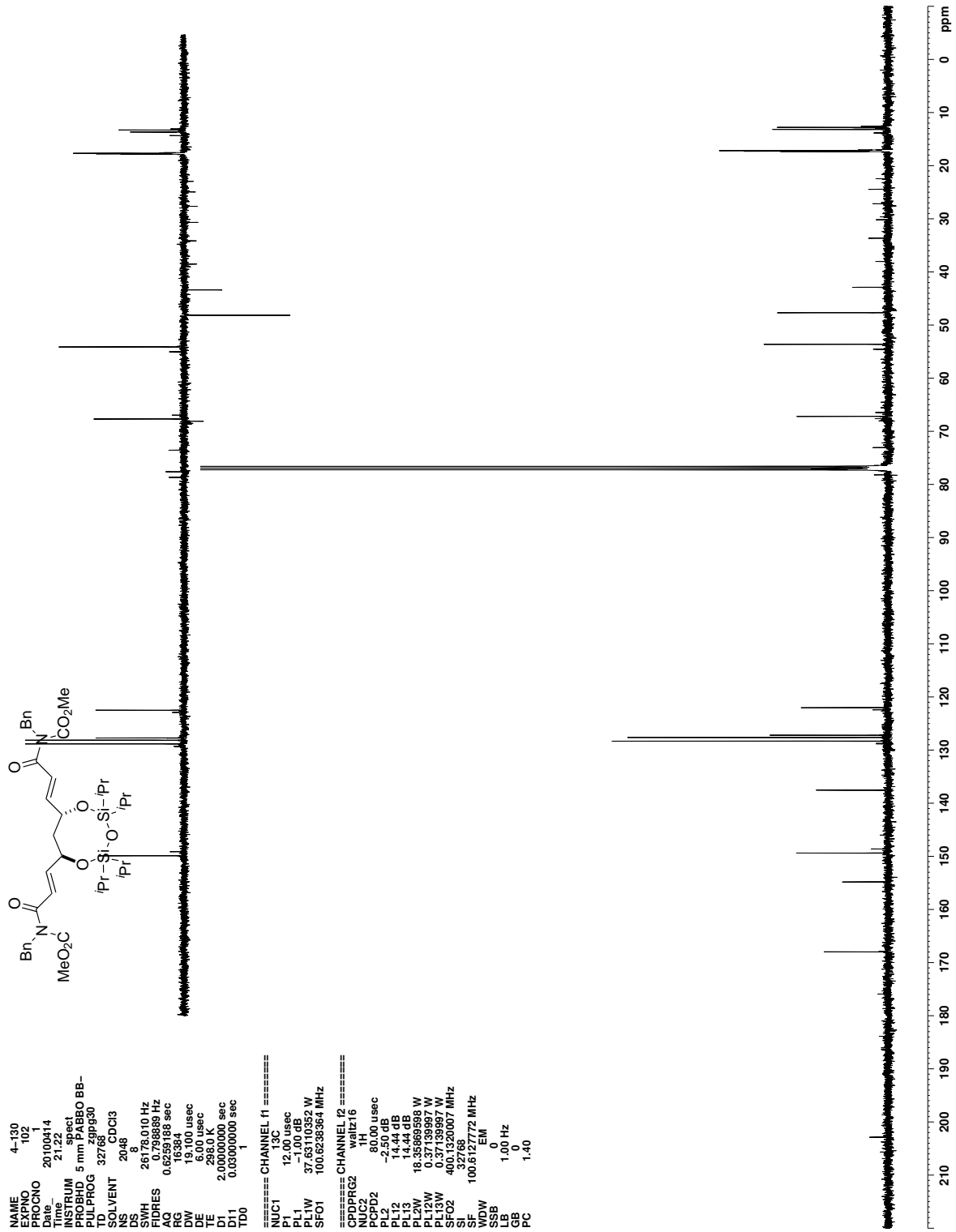


Figure C.106. ^{13}C NMR (CDCl_3) of 331

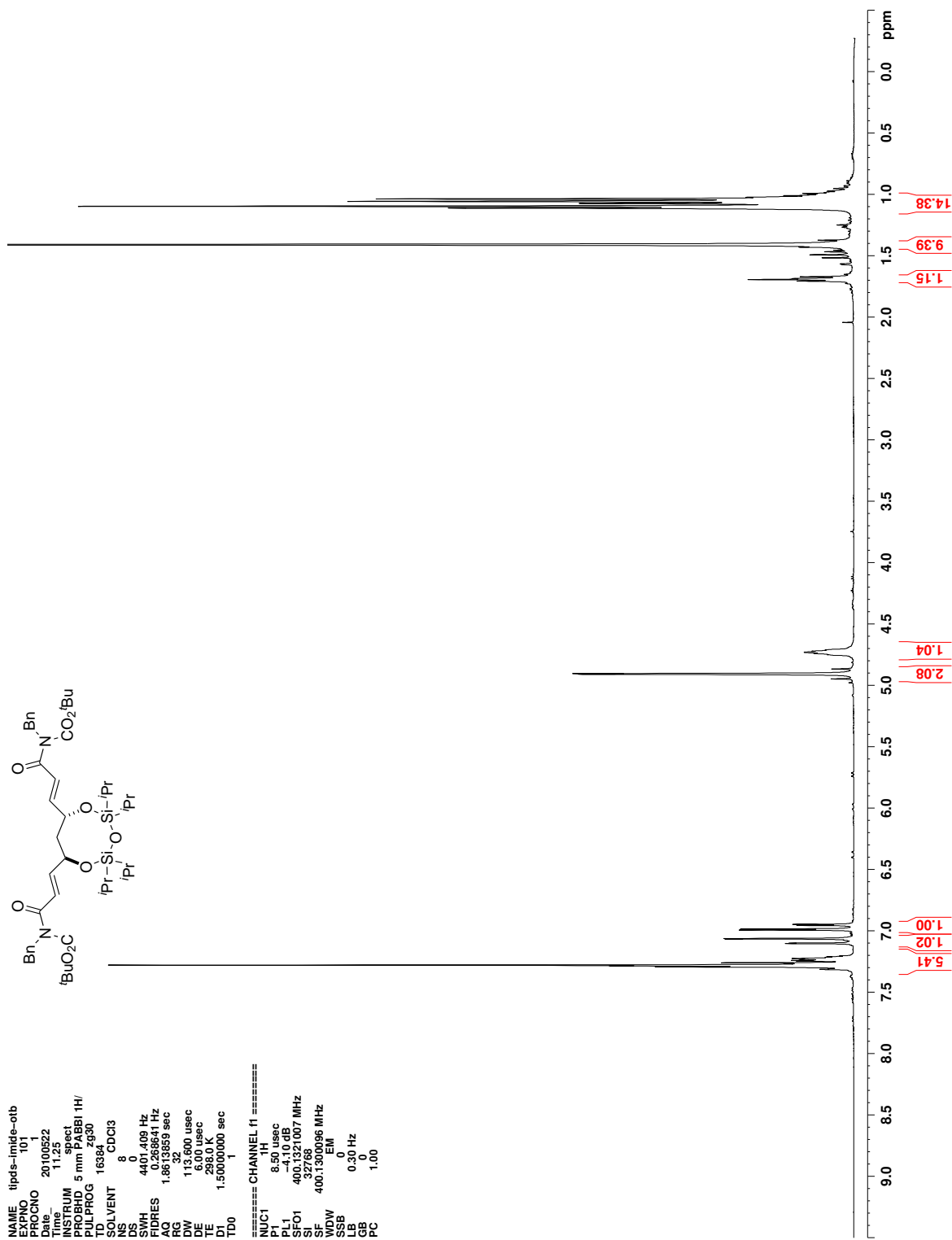


Figure C.107. ^1H NMR (CDCl_3) of 335

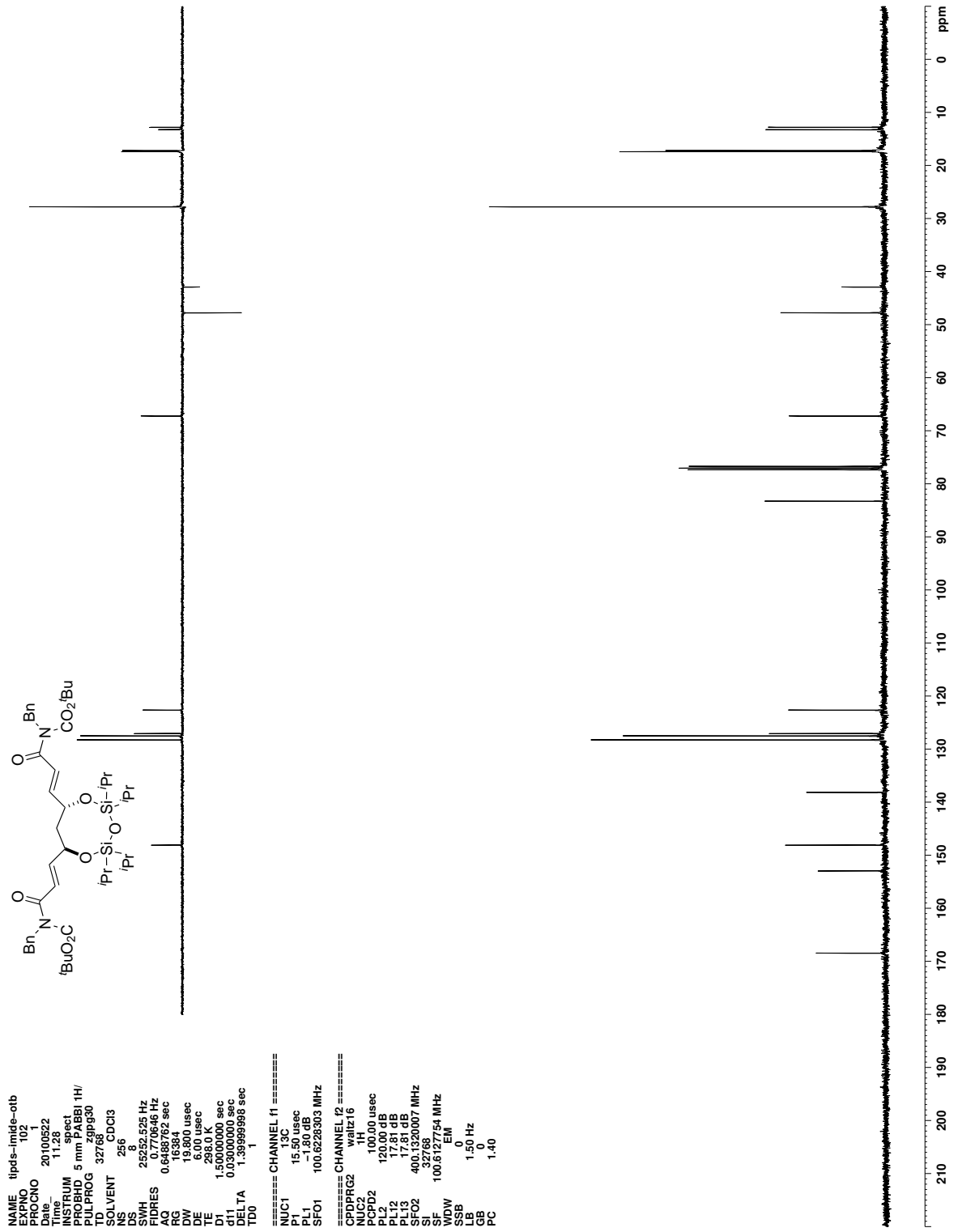


Figure C.108. ¹³C NMR (CDCl₃) of 335

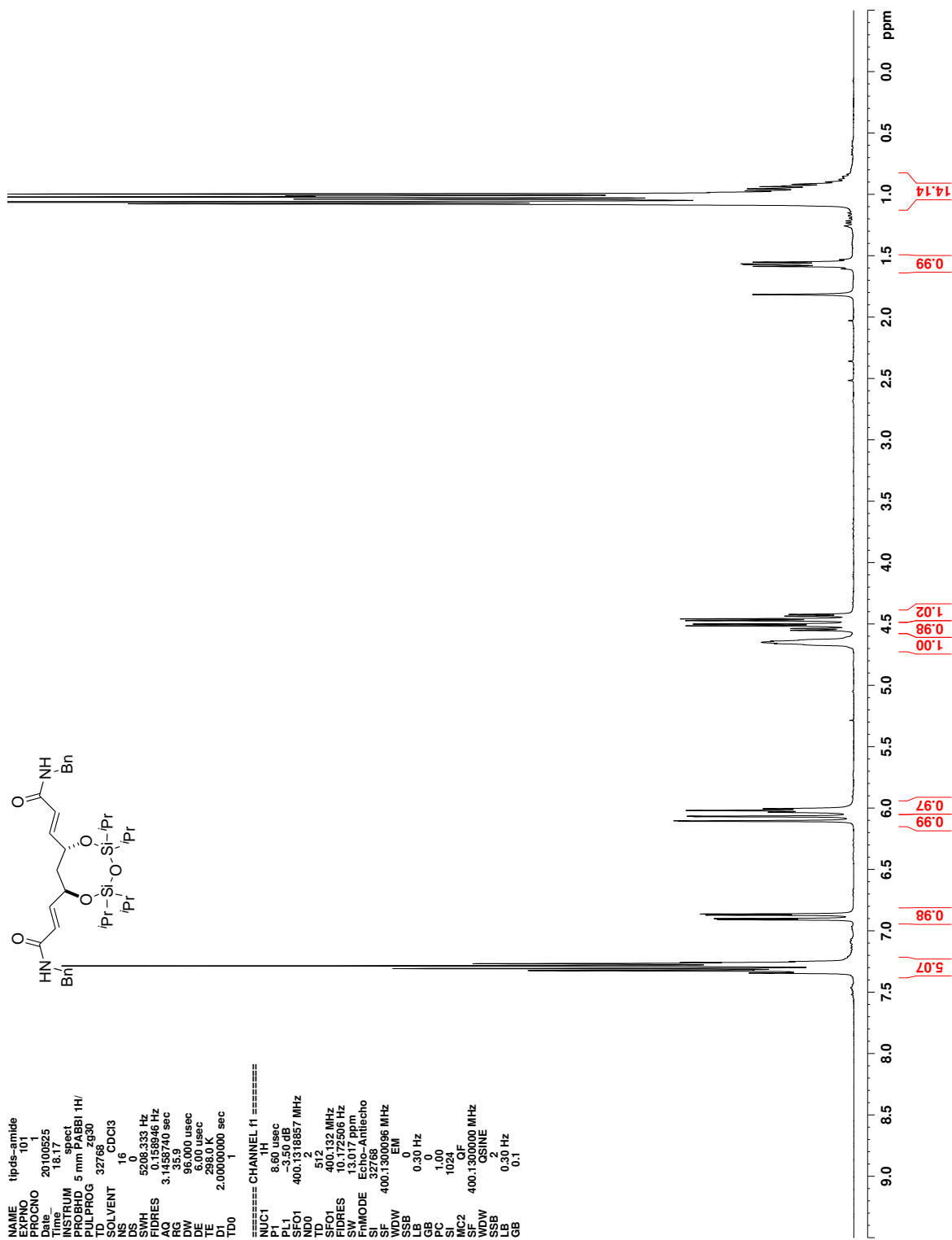


Figure C.109. ^1H NMR (CDCl_3) of 336

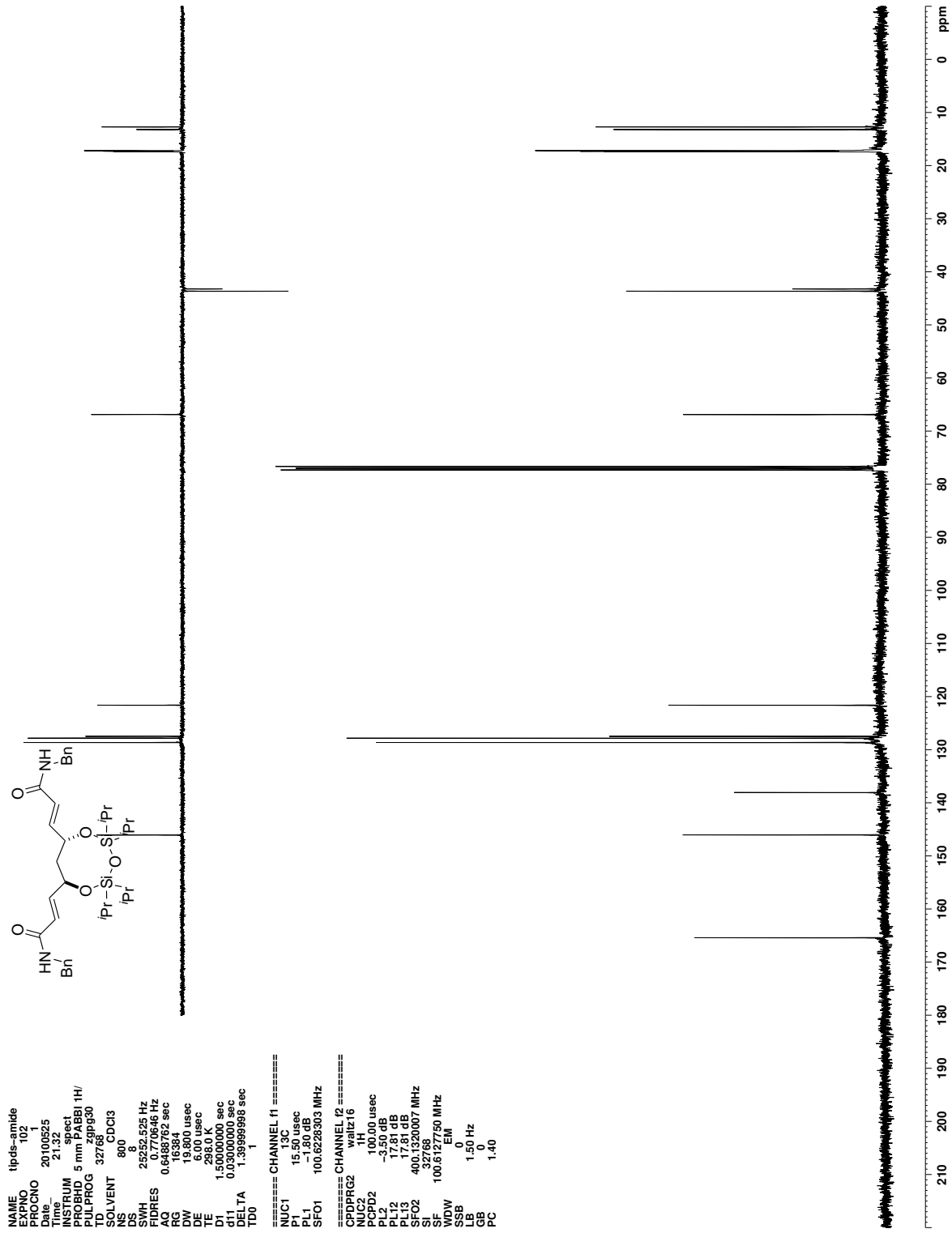


Figure C.110. ¹³C NMR (CDCl₃) of 336

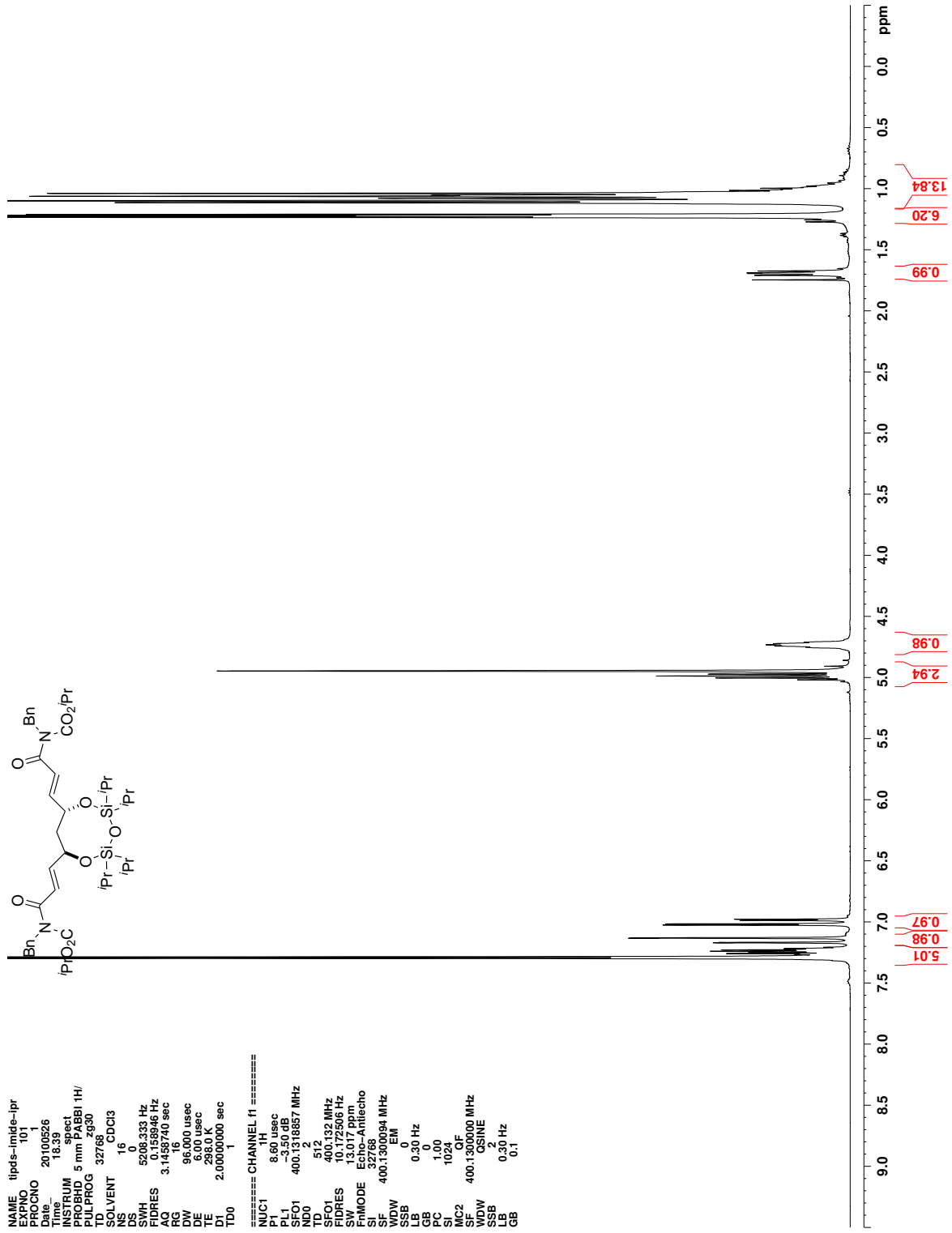


Figure C.111. ¹H NMR (CDCl₃) of 337

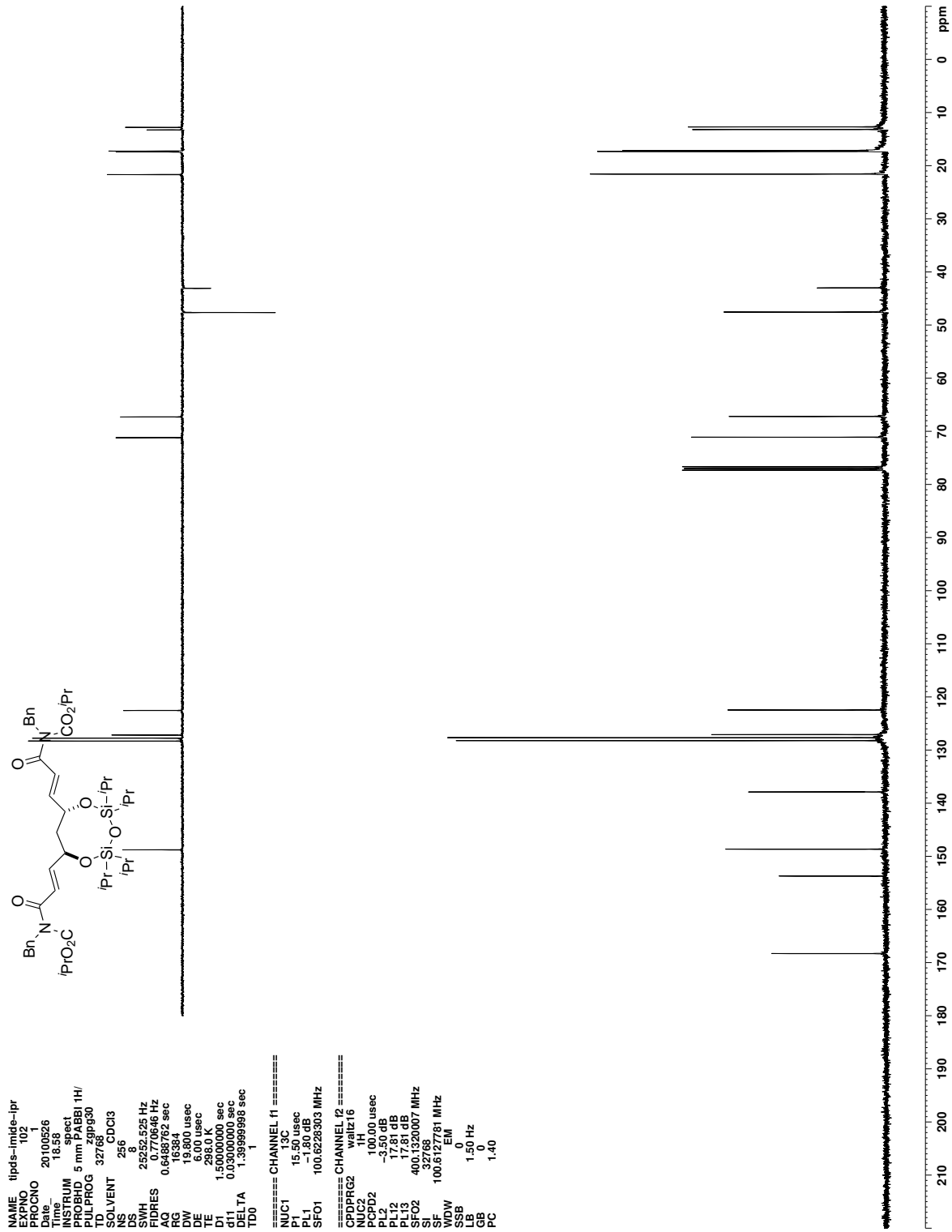


Figure C.112. ¹³C NMR (CDCl₃) of 337

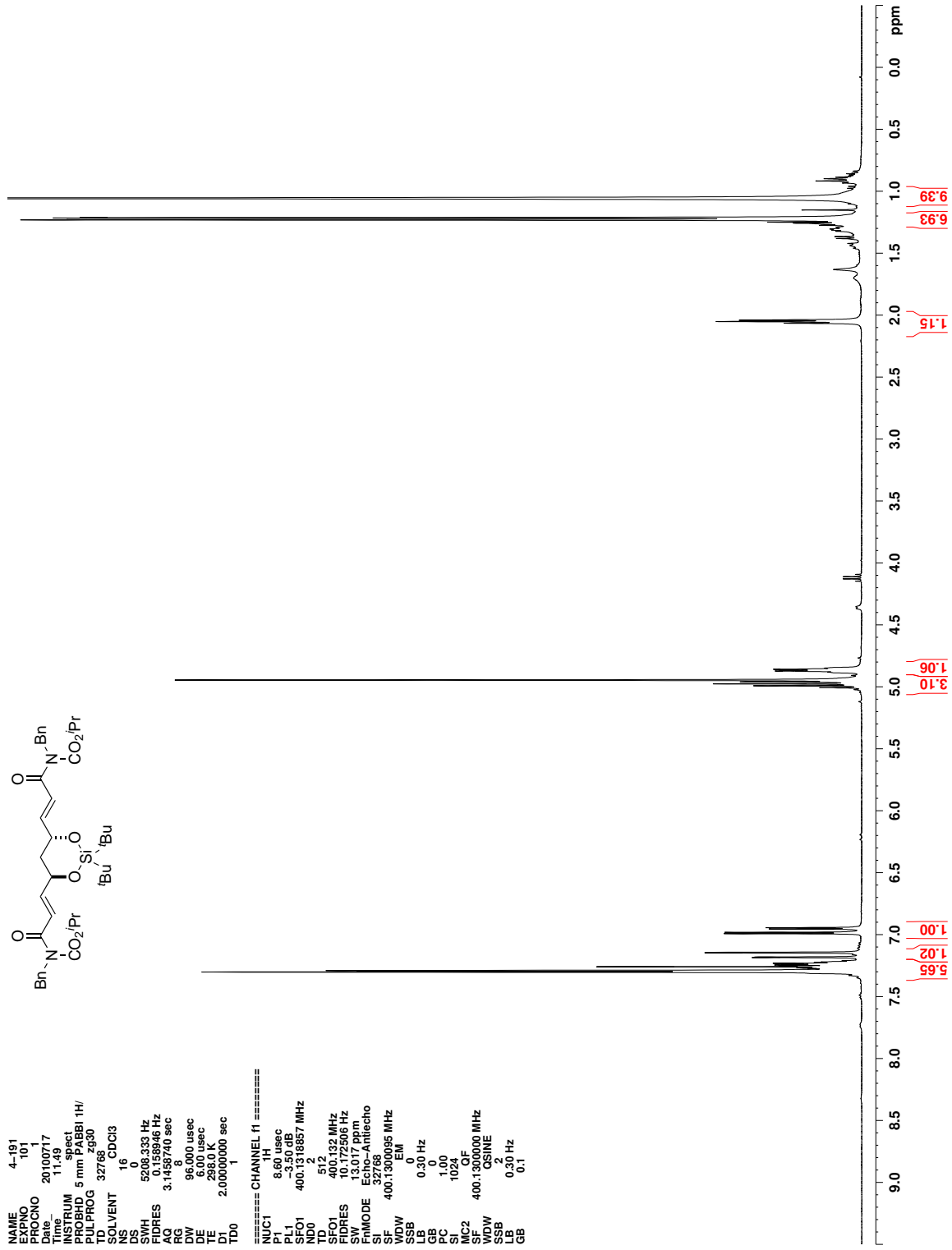


Figure C.113. ^1H NMR (CDCl_3) of 338

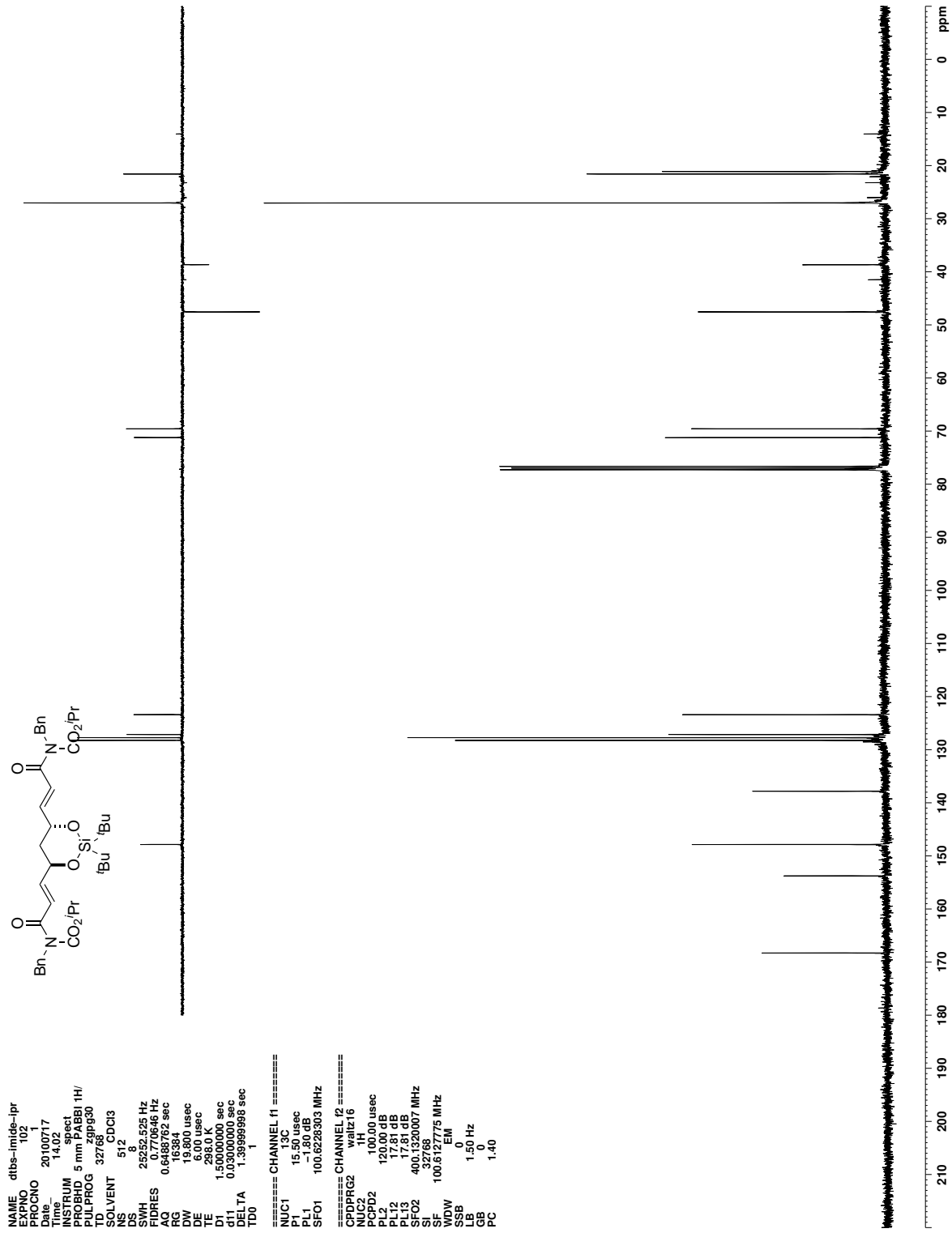


Figure C.114. ¹³C NMR (CDCl₃) of 338

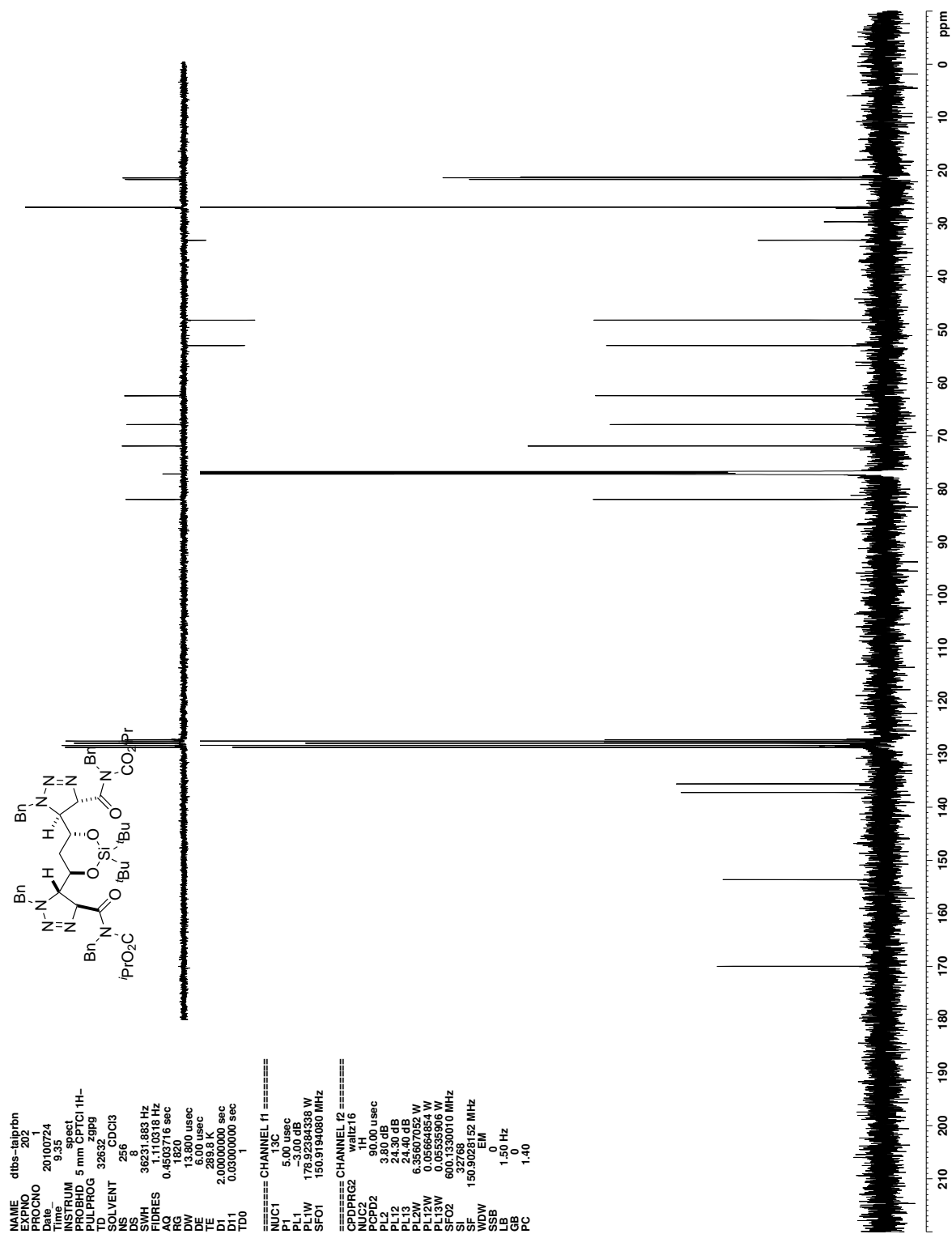


Figure C.116. ^{13}C NMR (CDCl_3) of **339**

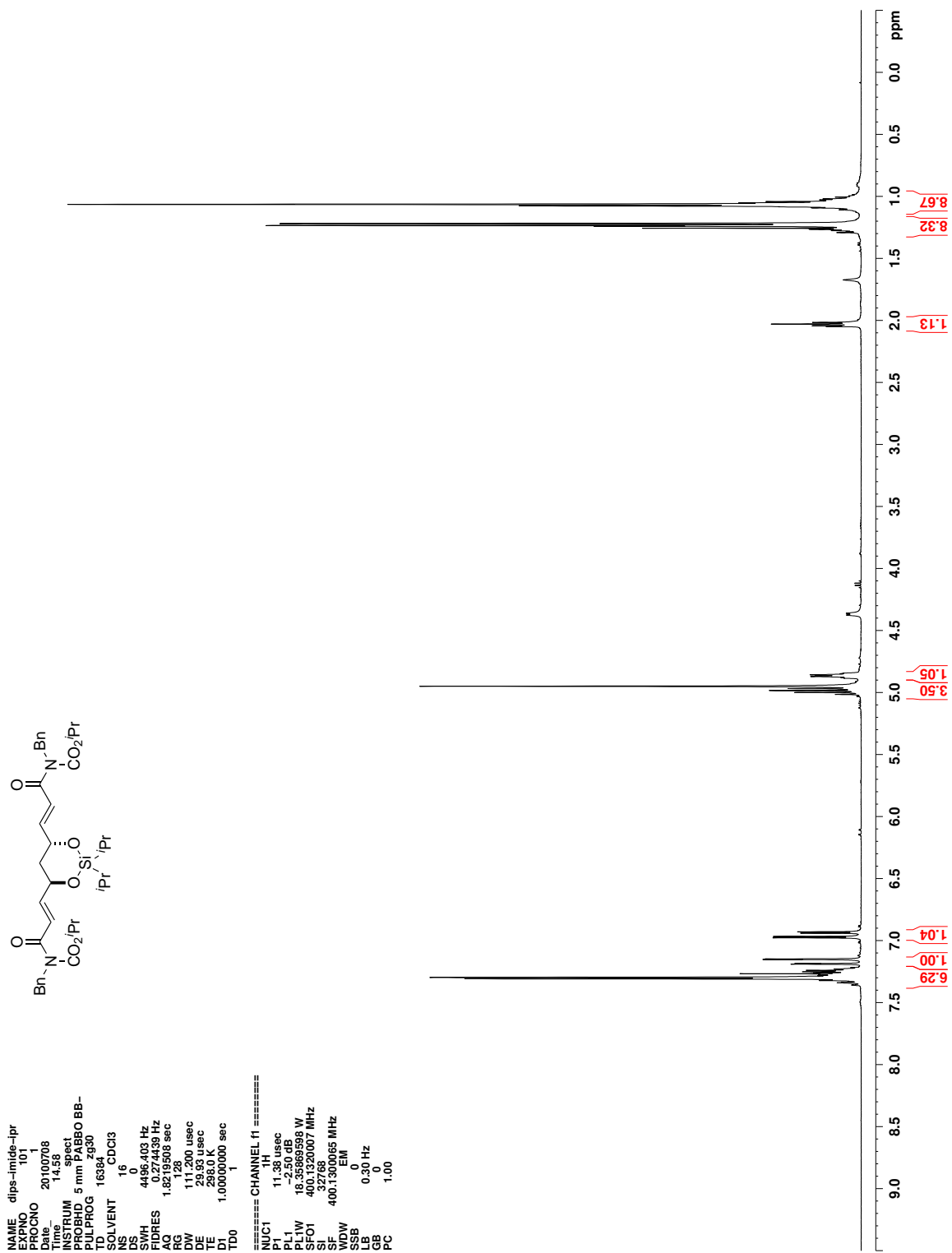


Figure C.117. ^1H NMR (CDCl_3) of 340

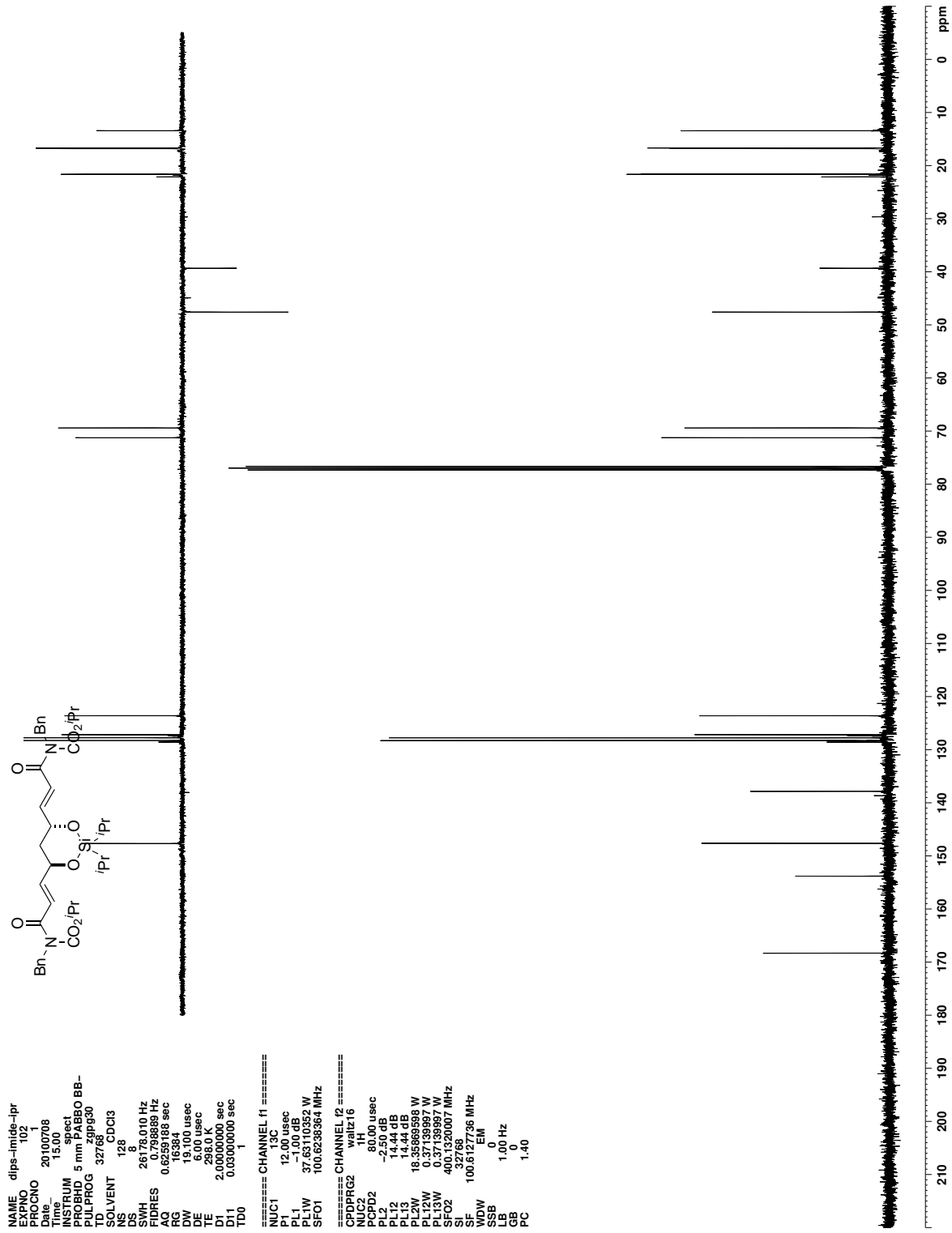


Figure C.118. ¹³C NMR (CDCl₃) of 340

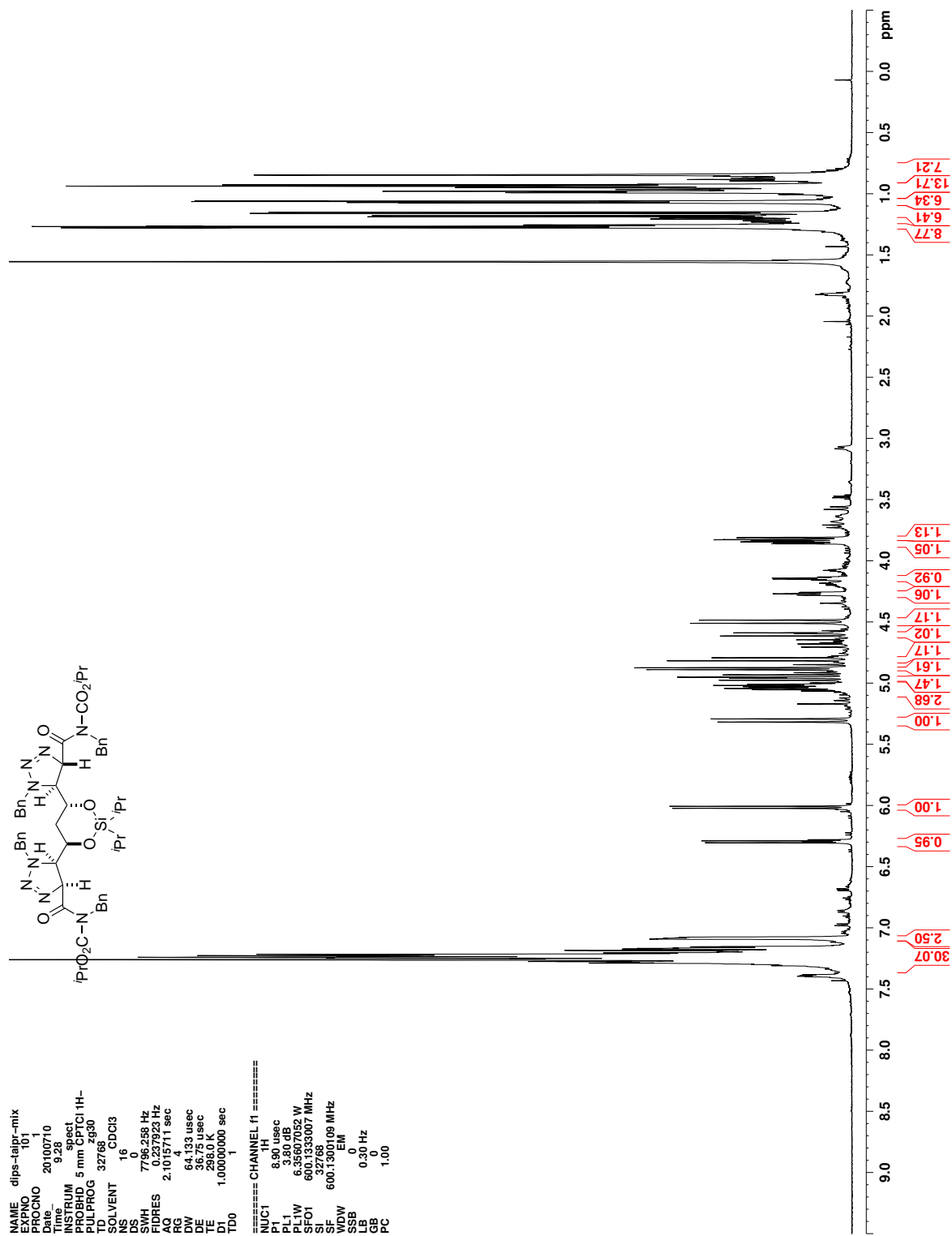


Figure C.119. ¹H NMR (CDCl₃) of 341

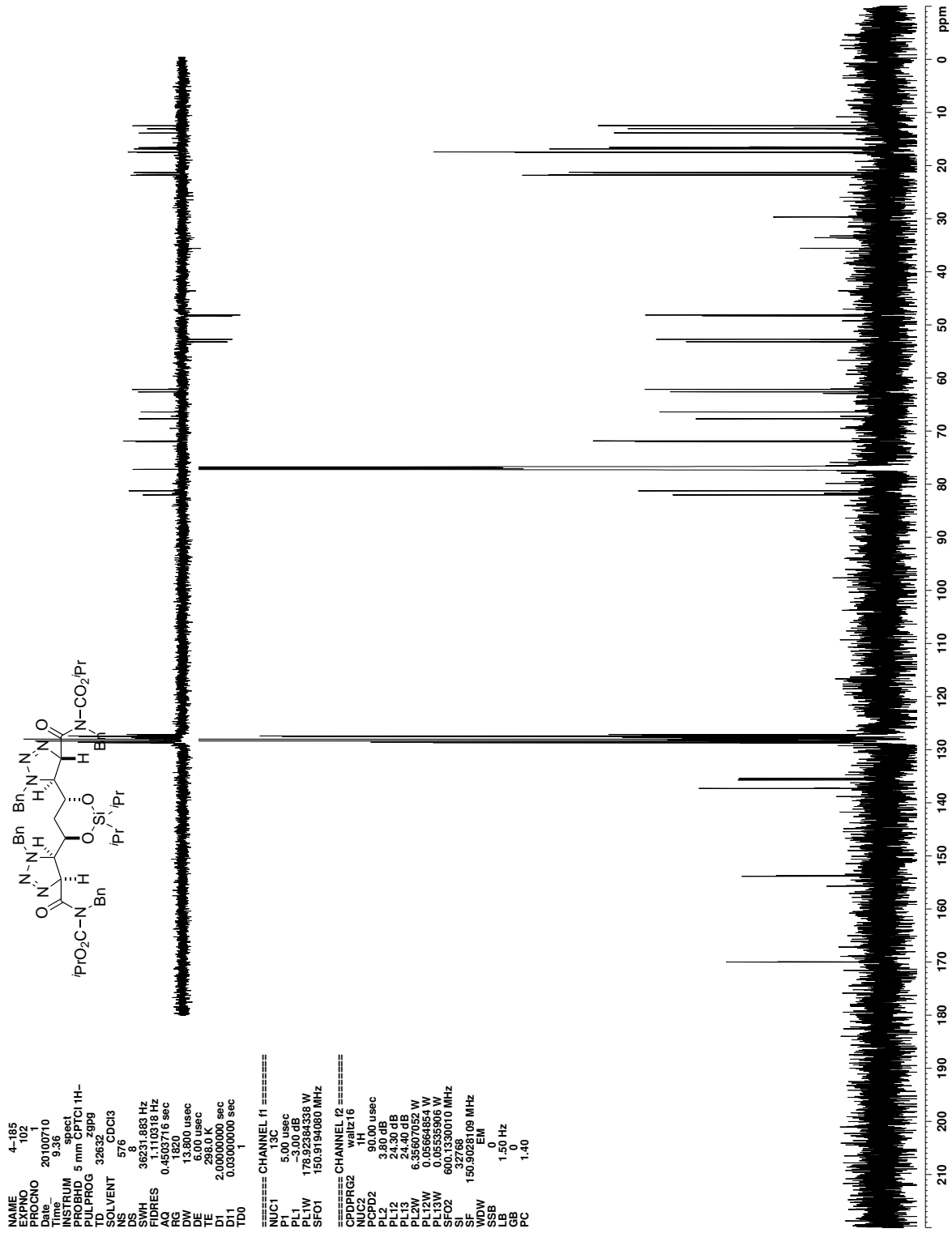


Figure C.120. ¹³C NMR (CDCl₃) of 341

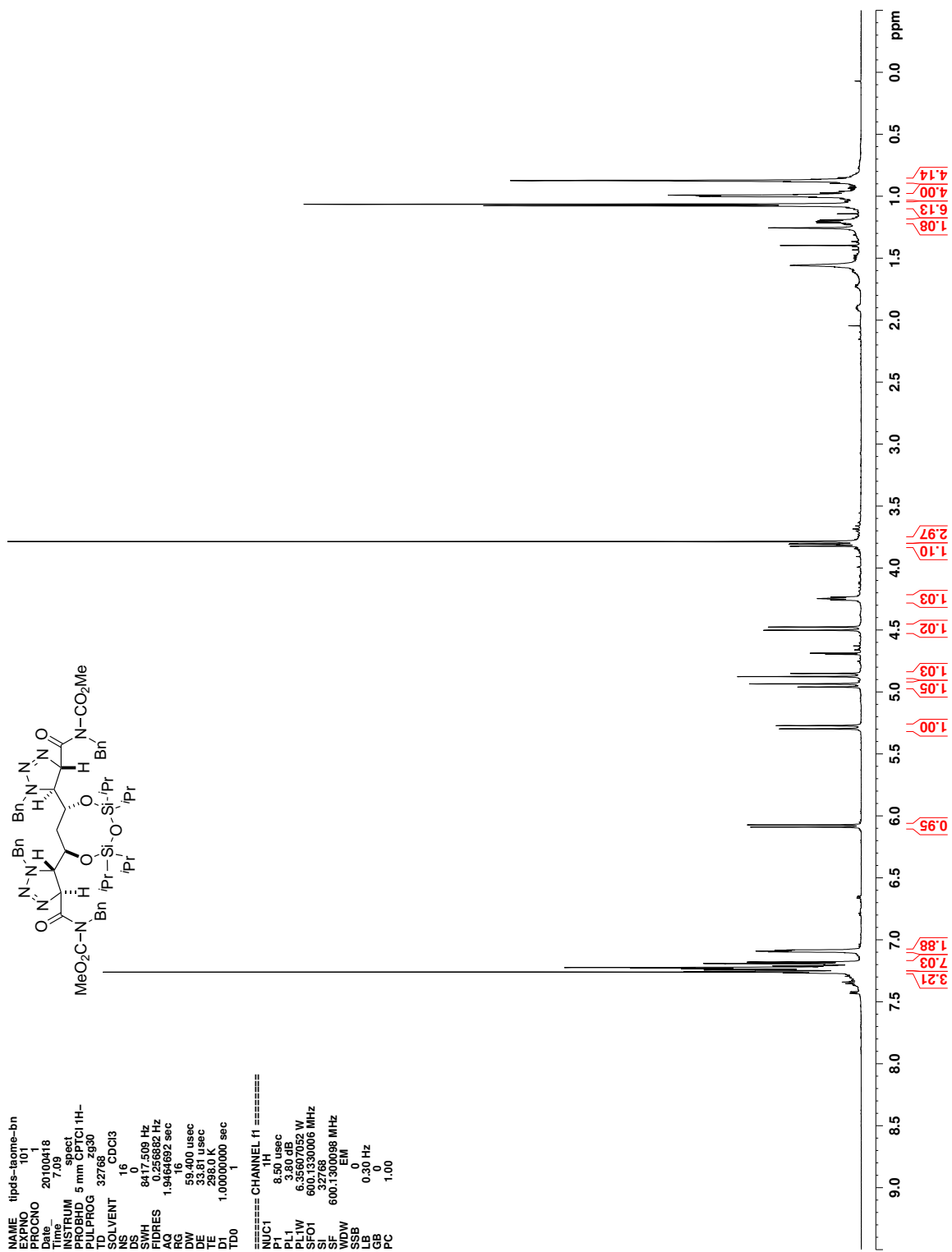


Figure C.121. ^1H NMR (CDCl_3) of 342

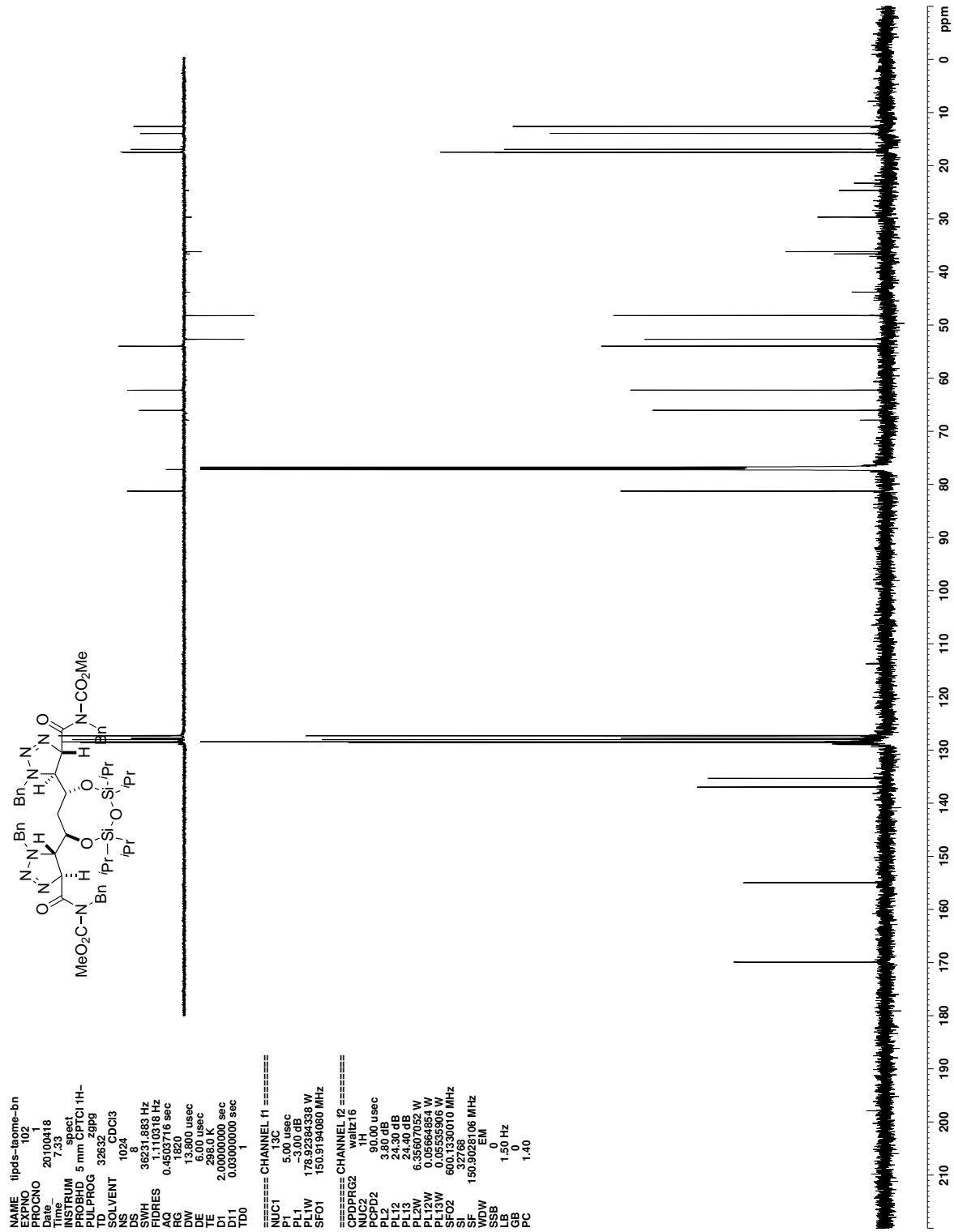


Figure C.122. ^{13}C NMR (CDCl_3) of 342

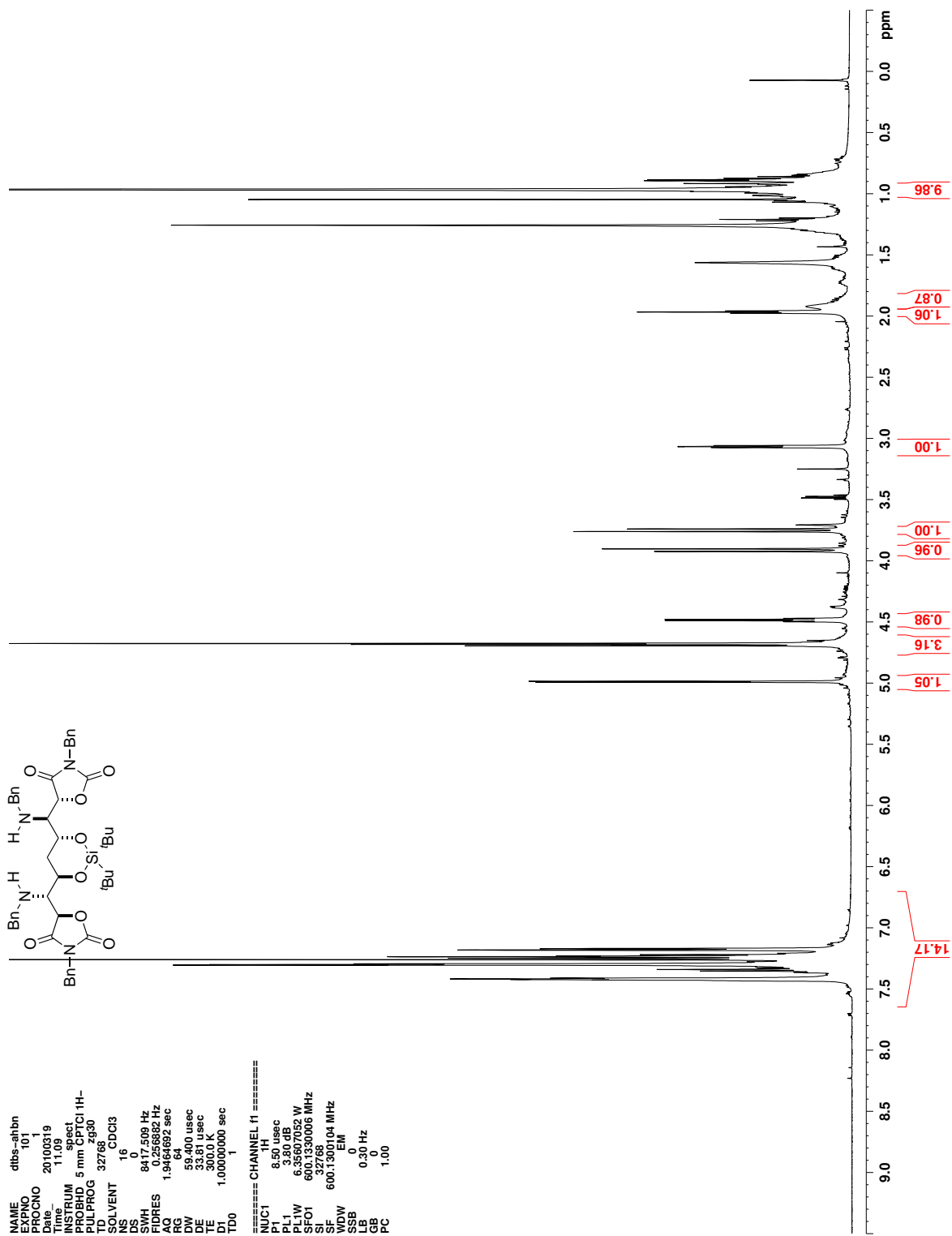


Figure C.125. ^1H NMR (CDCl_3) of 316

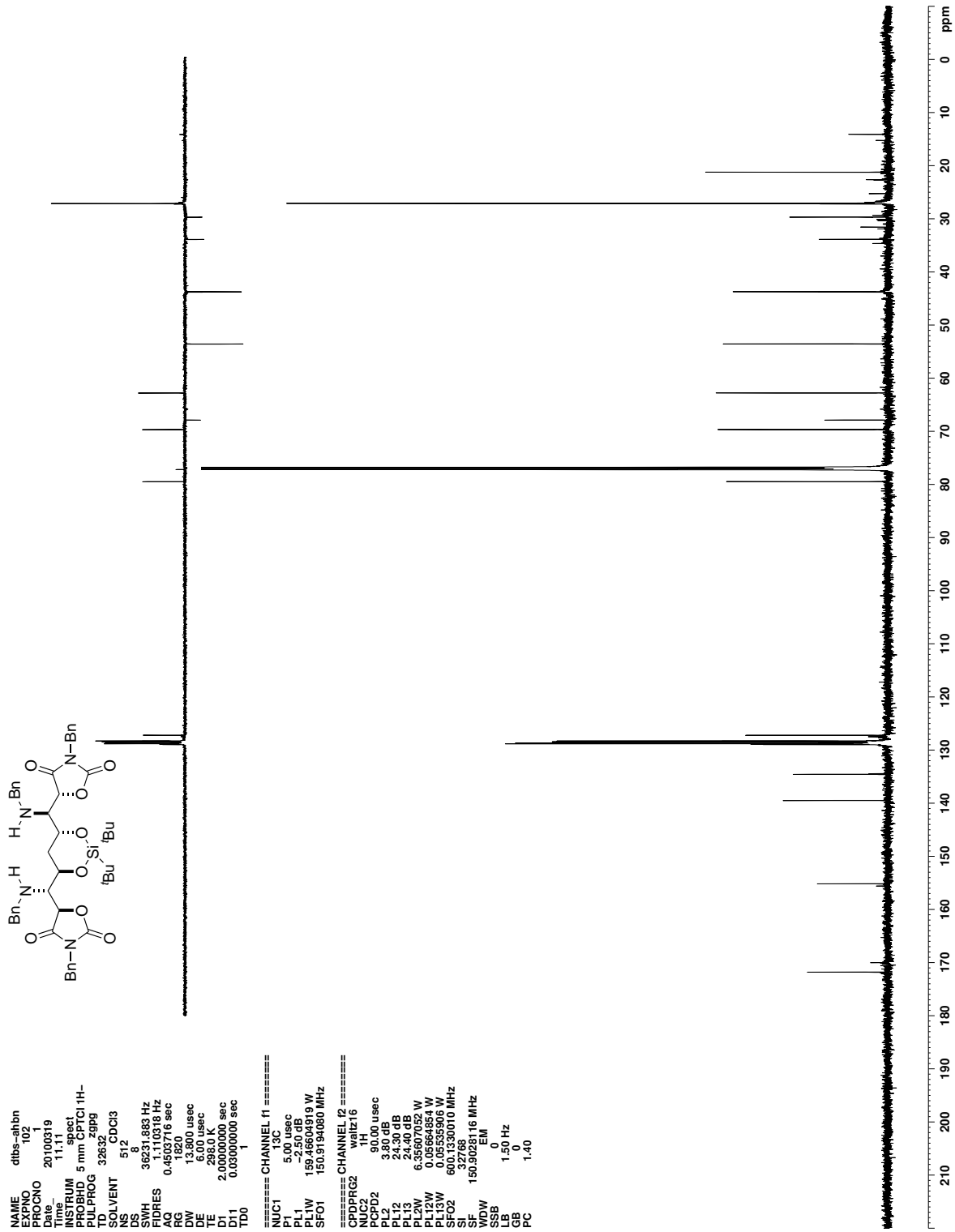


Figure C.126. ^{13}C NMR (CDCl_3) of 316

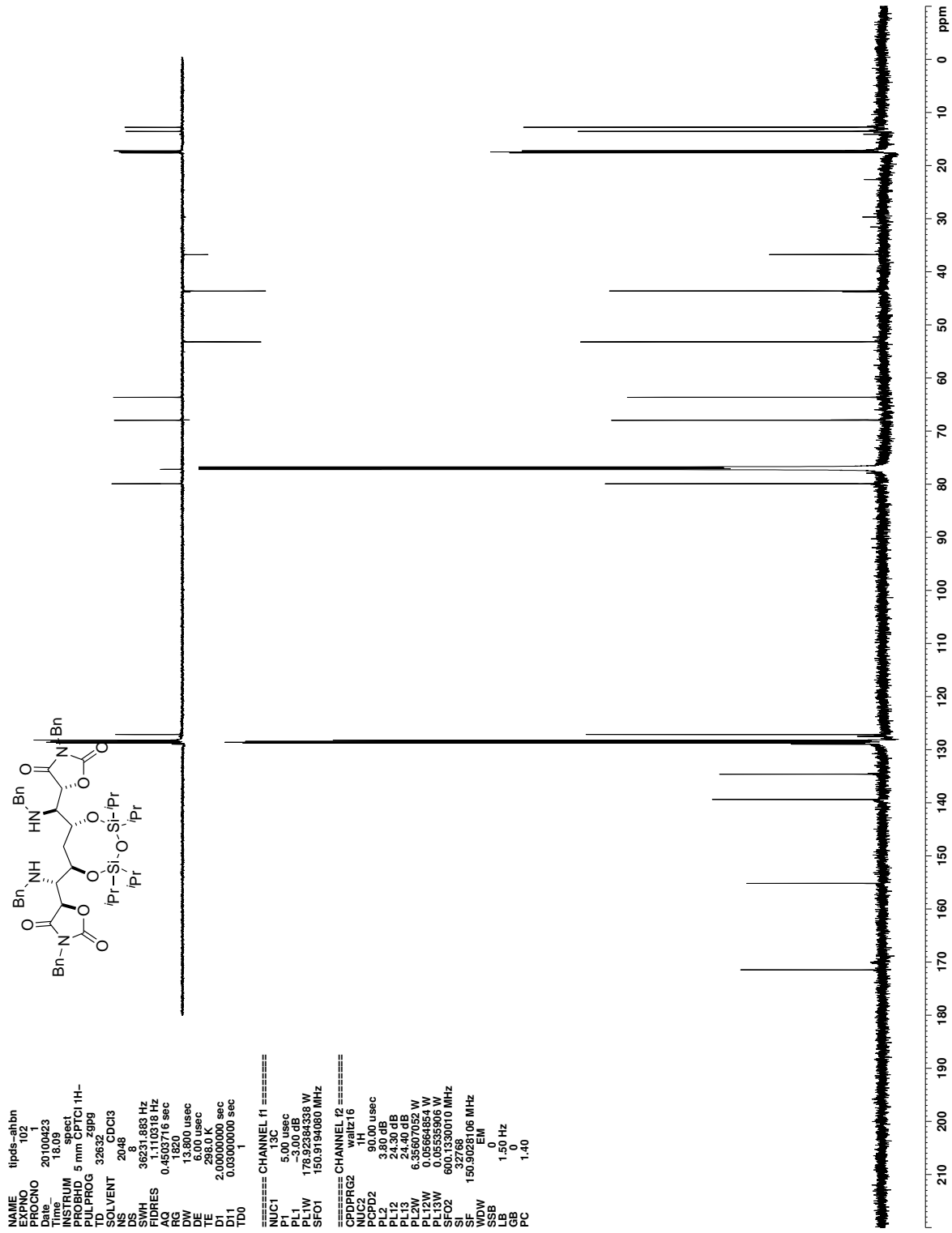


Figure C.128. ¹³C NMR (CDCl₃) of 344

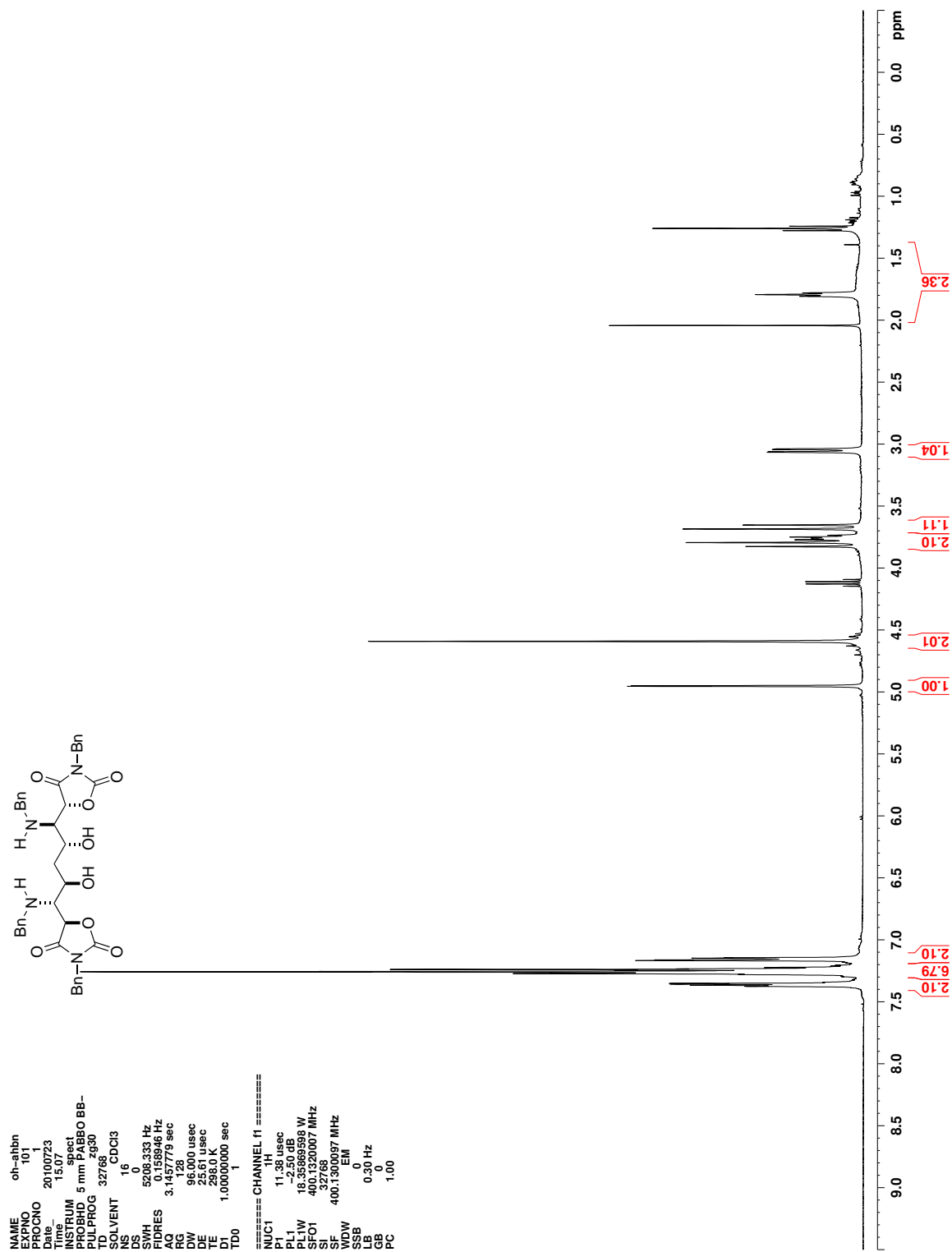


Figure C.129. ^1H NMR (CDCl_3) of 345

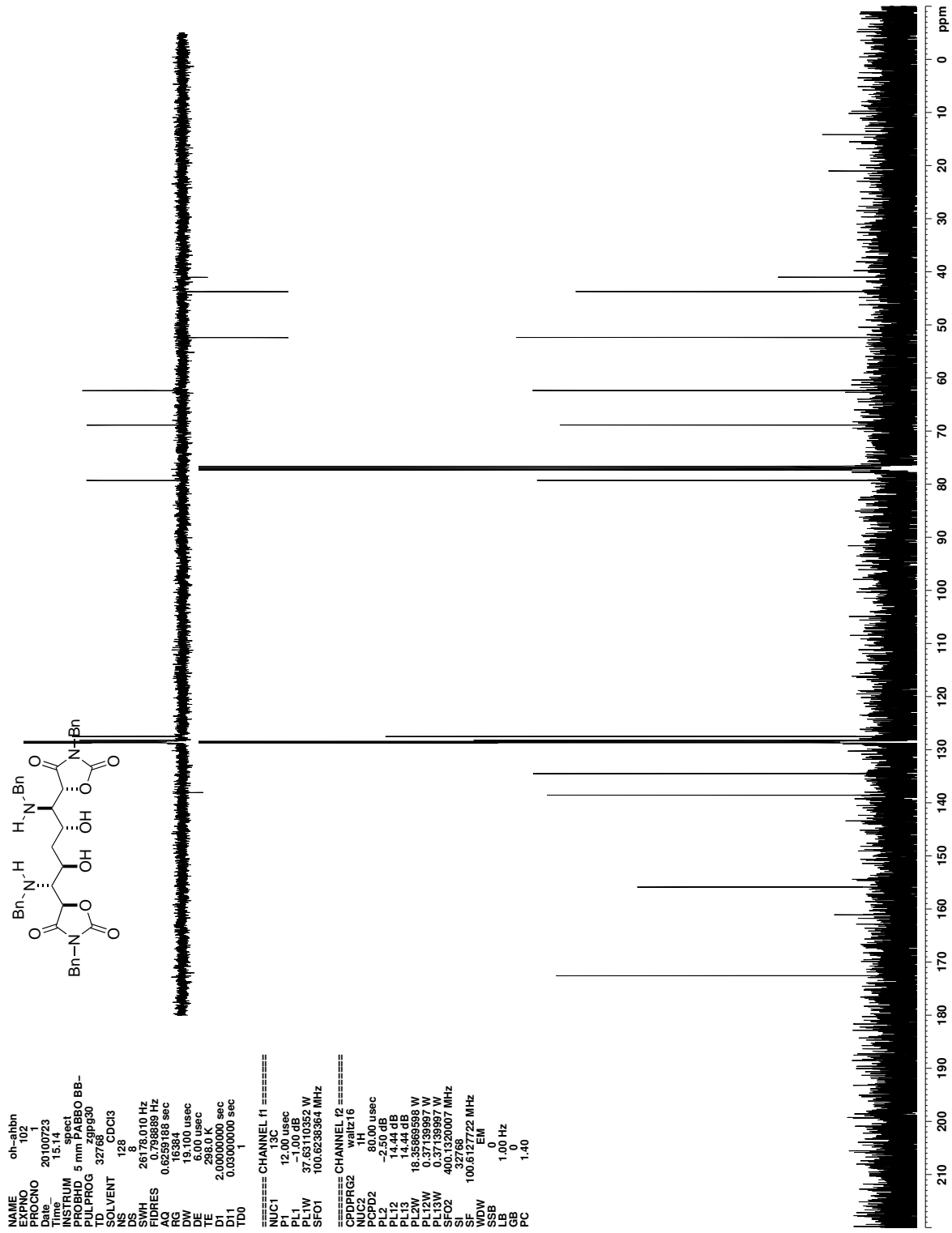


Figure C.130. ^{13}C NMR (CDCl_3) of 345

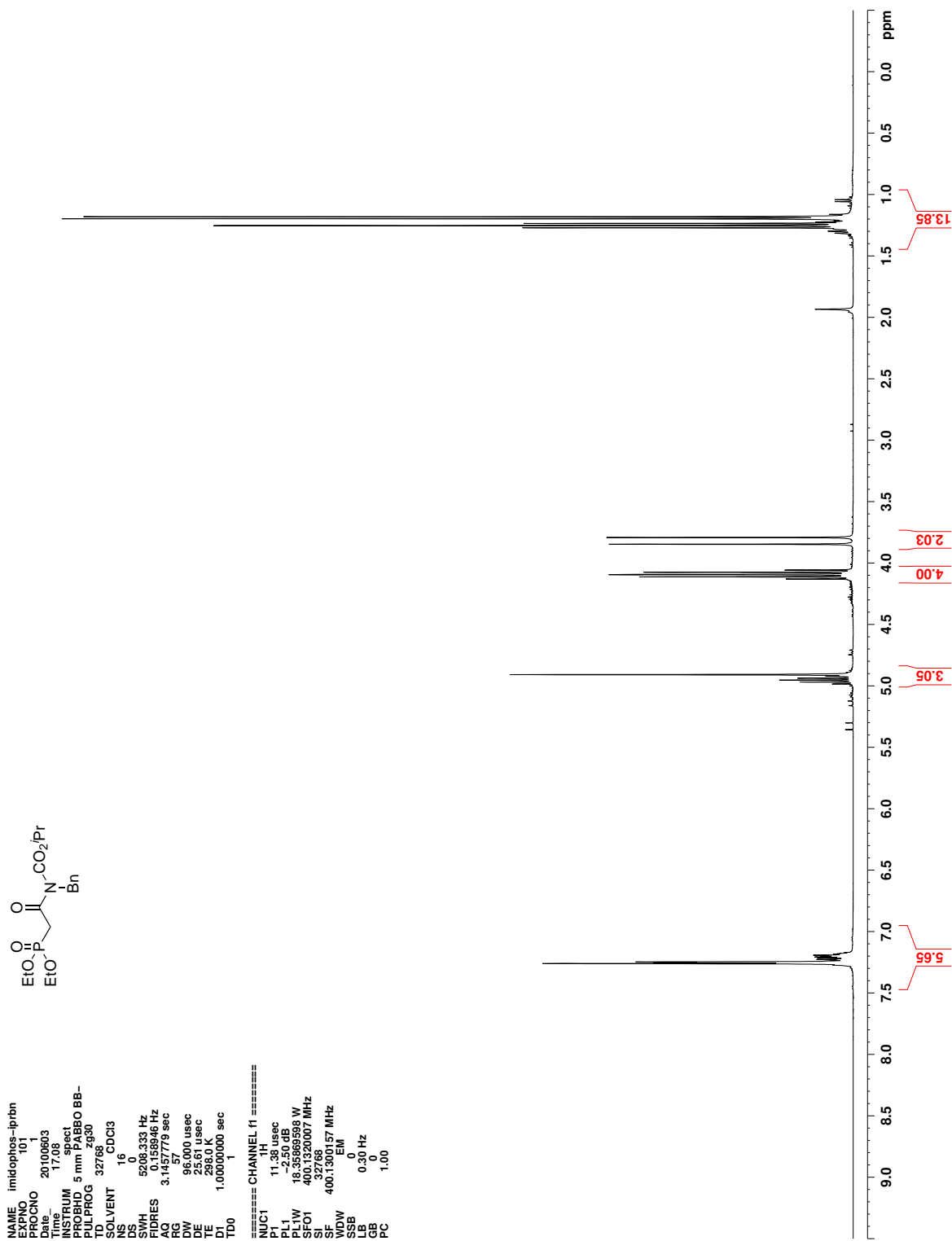


Figure C.131. ^1H NMR (CDCl_3) of 424

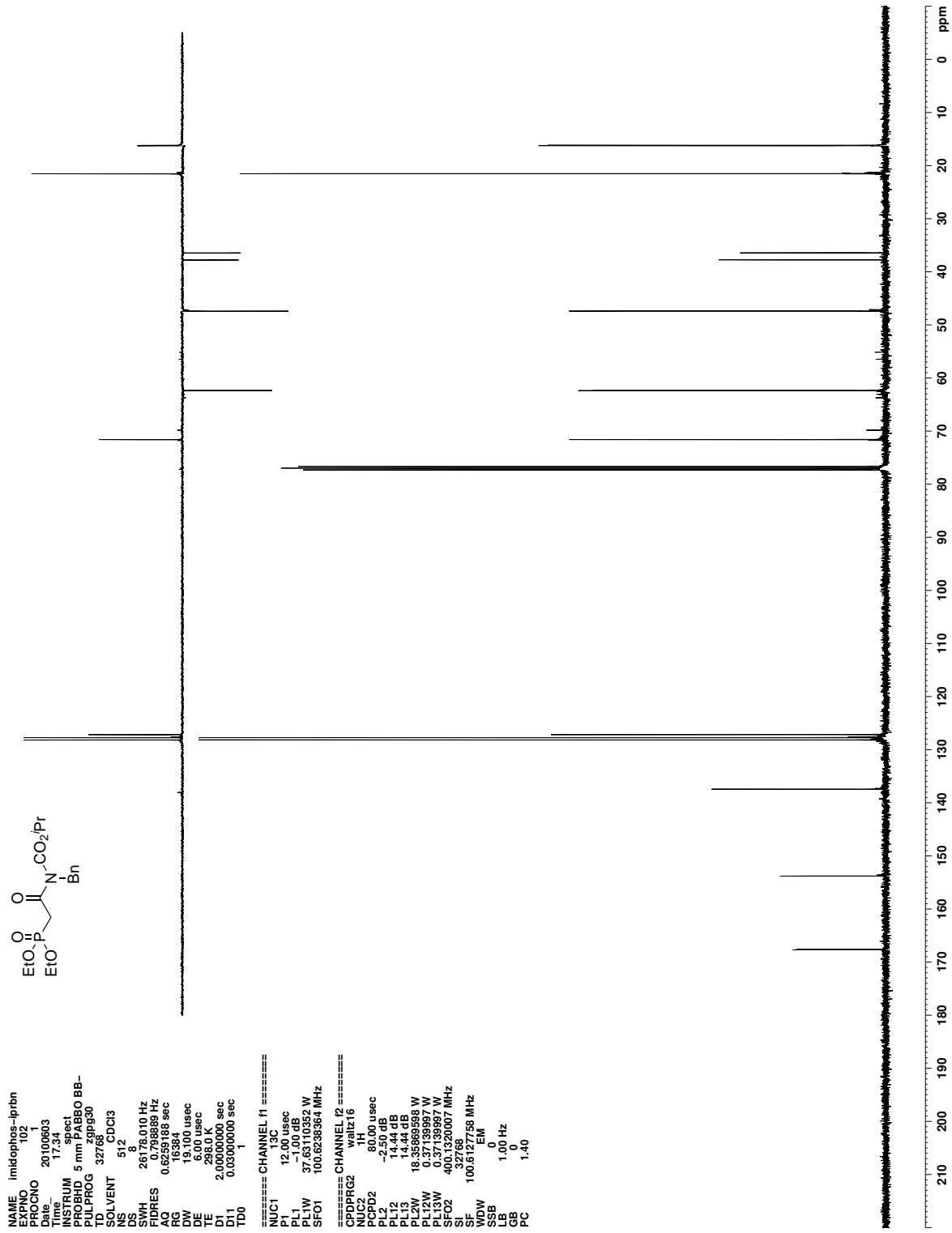


Figure C.132. ¹³C NMR (CDCl₃) of 424

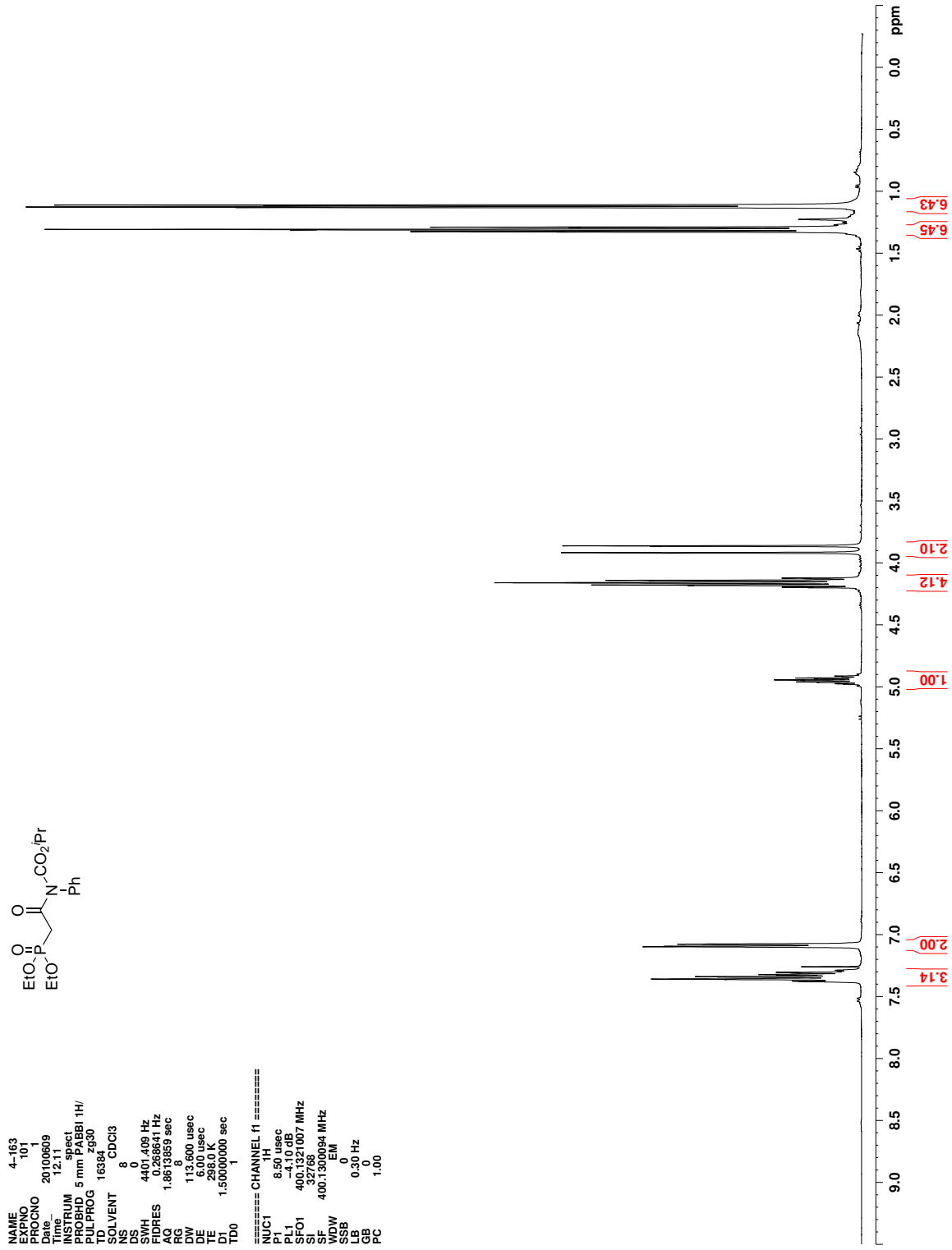


Figure C.133. ¹H NMR (CDCl₃) of 347

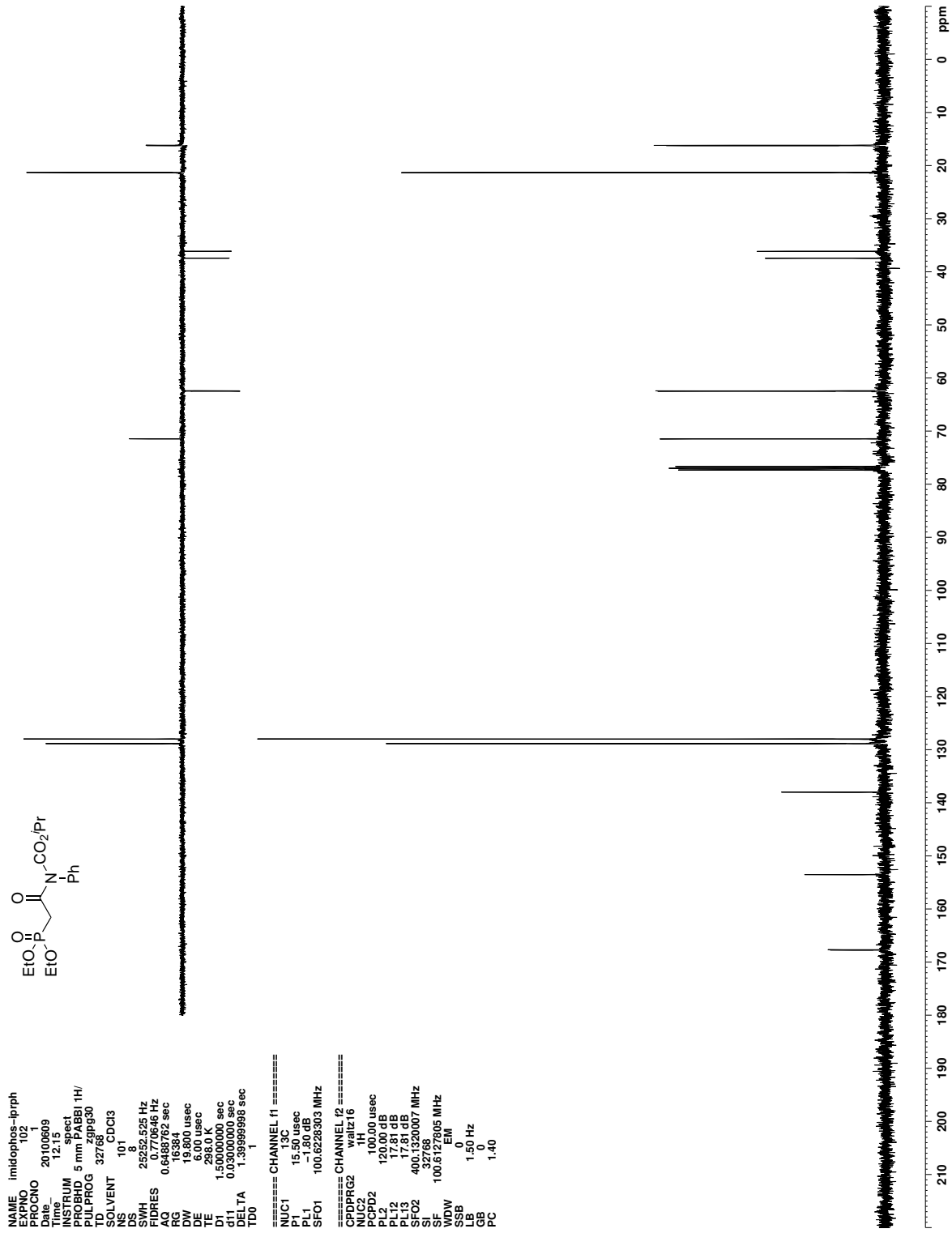


Figure C.134. ¹³C NMR (CDCl₃) of 347

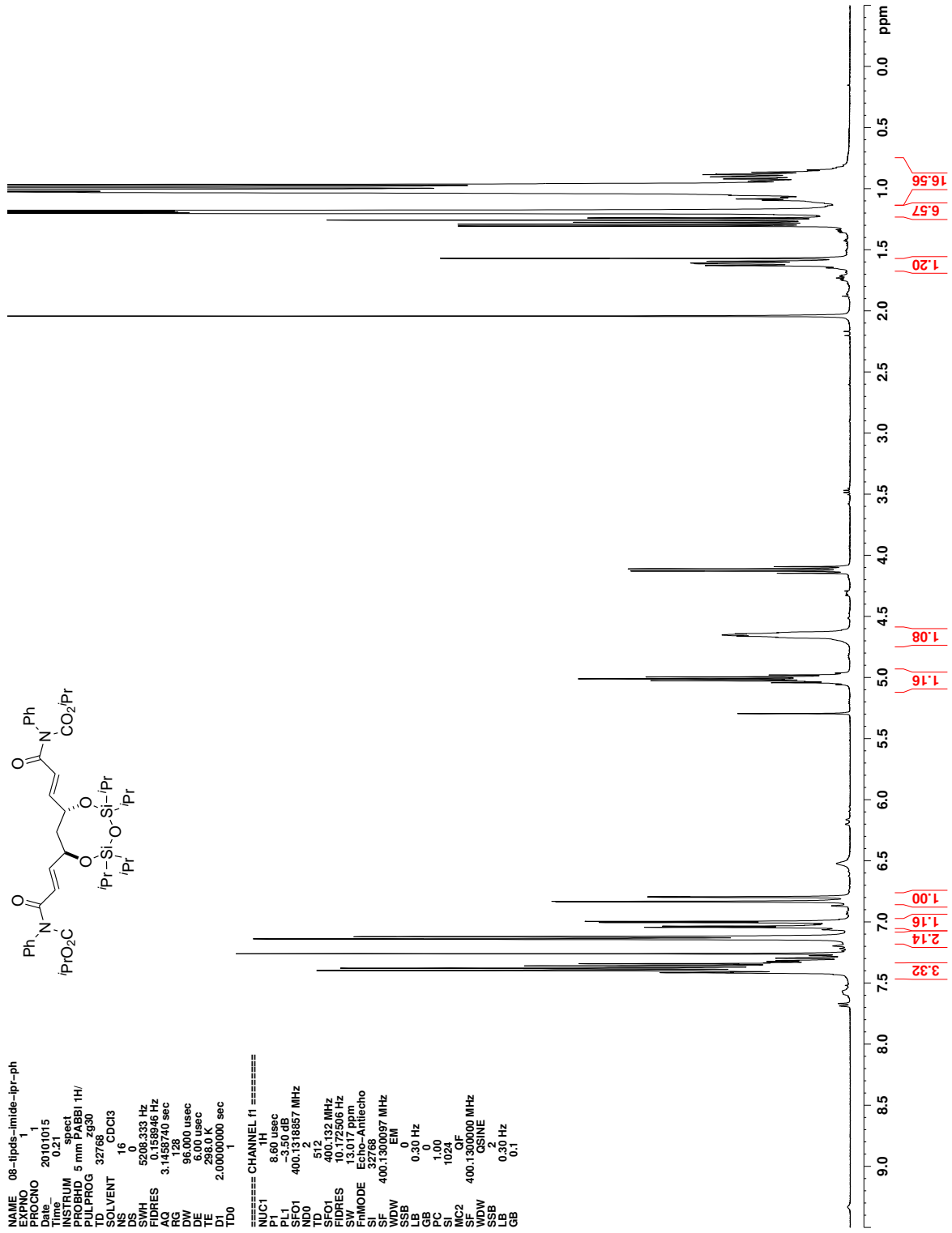


Figure C.135. ^1H NMR (CDCl_3) of 350

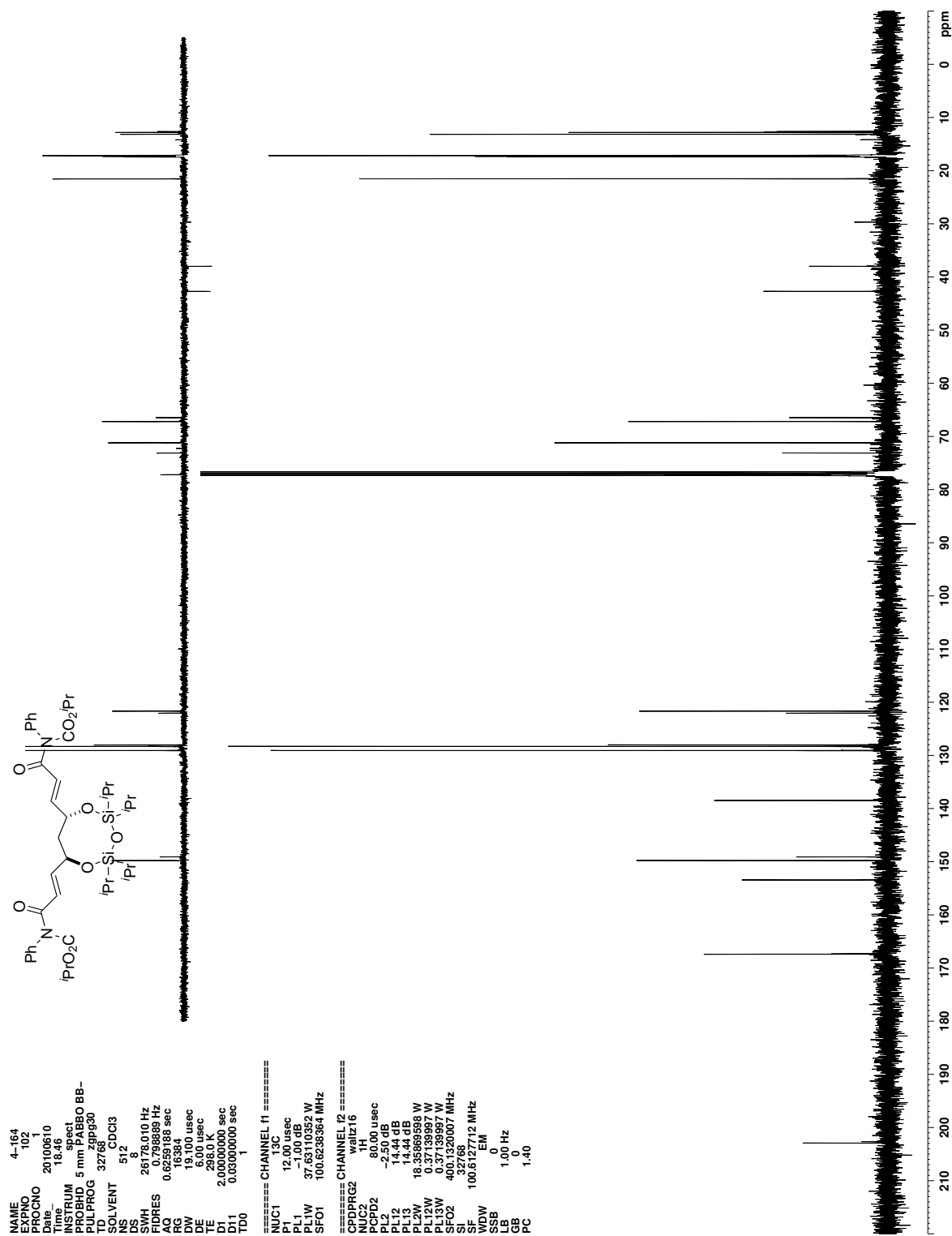


Figure C.136. ¹³C NMR (CDCl₃) of 350

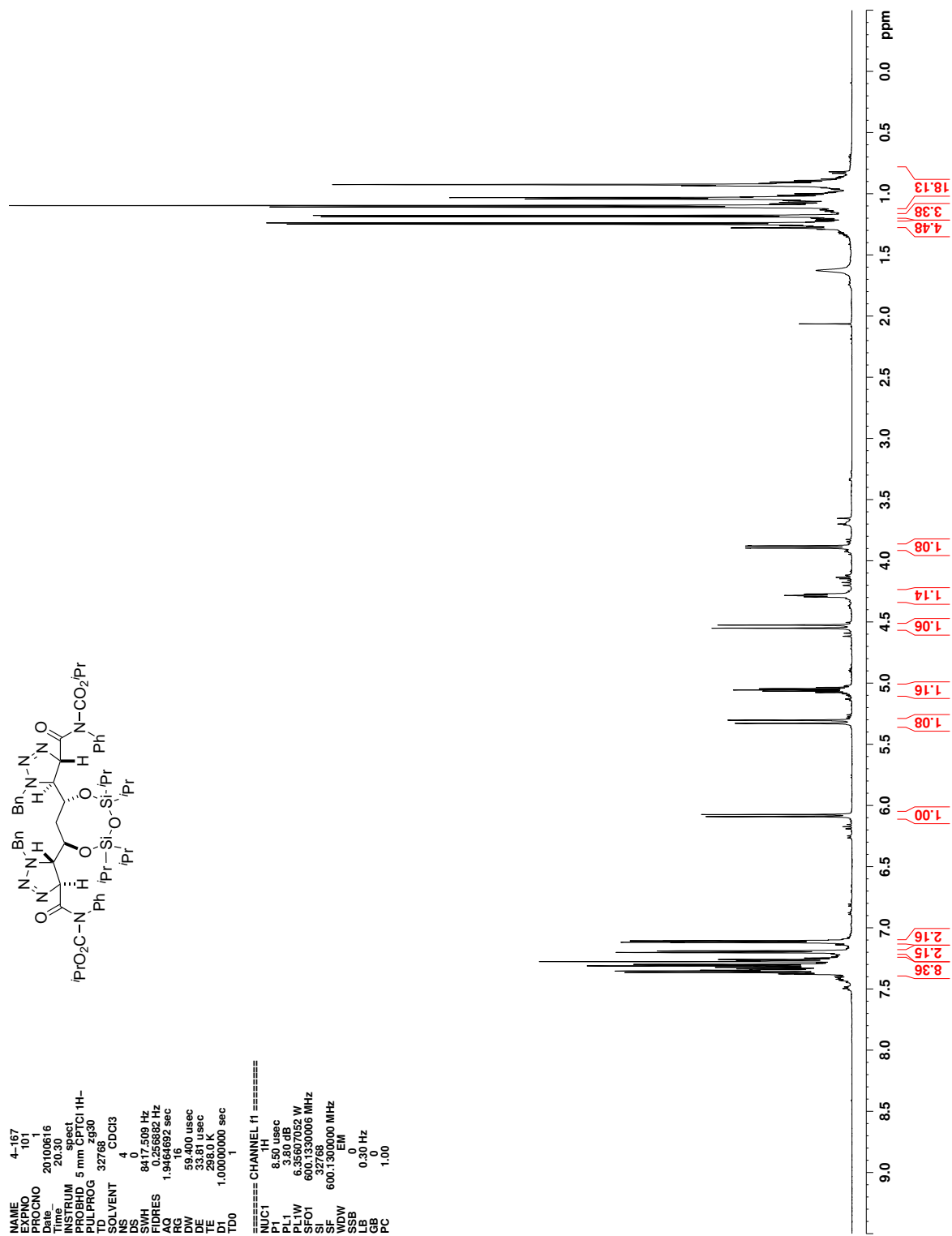


Figure C.137. ^1H NMR (CDCl_3) of 351

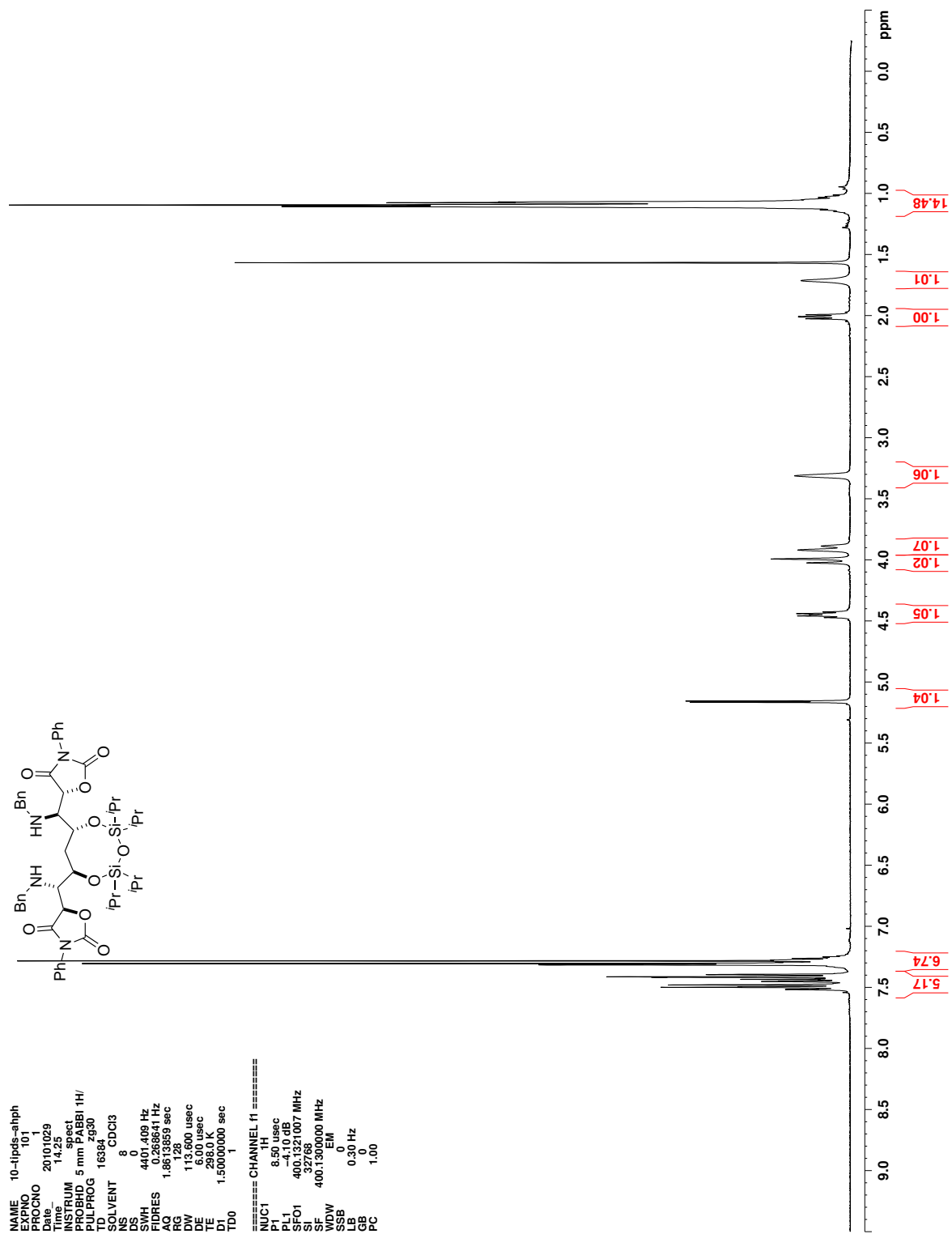


Figure C.139. ^1H NMR (CDCl_3) of 346

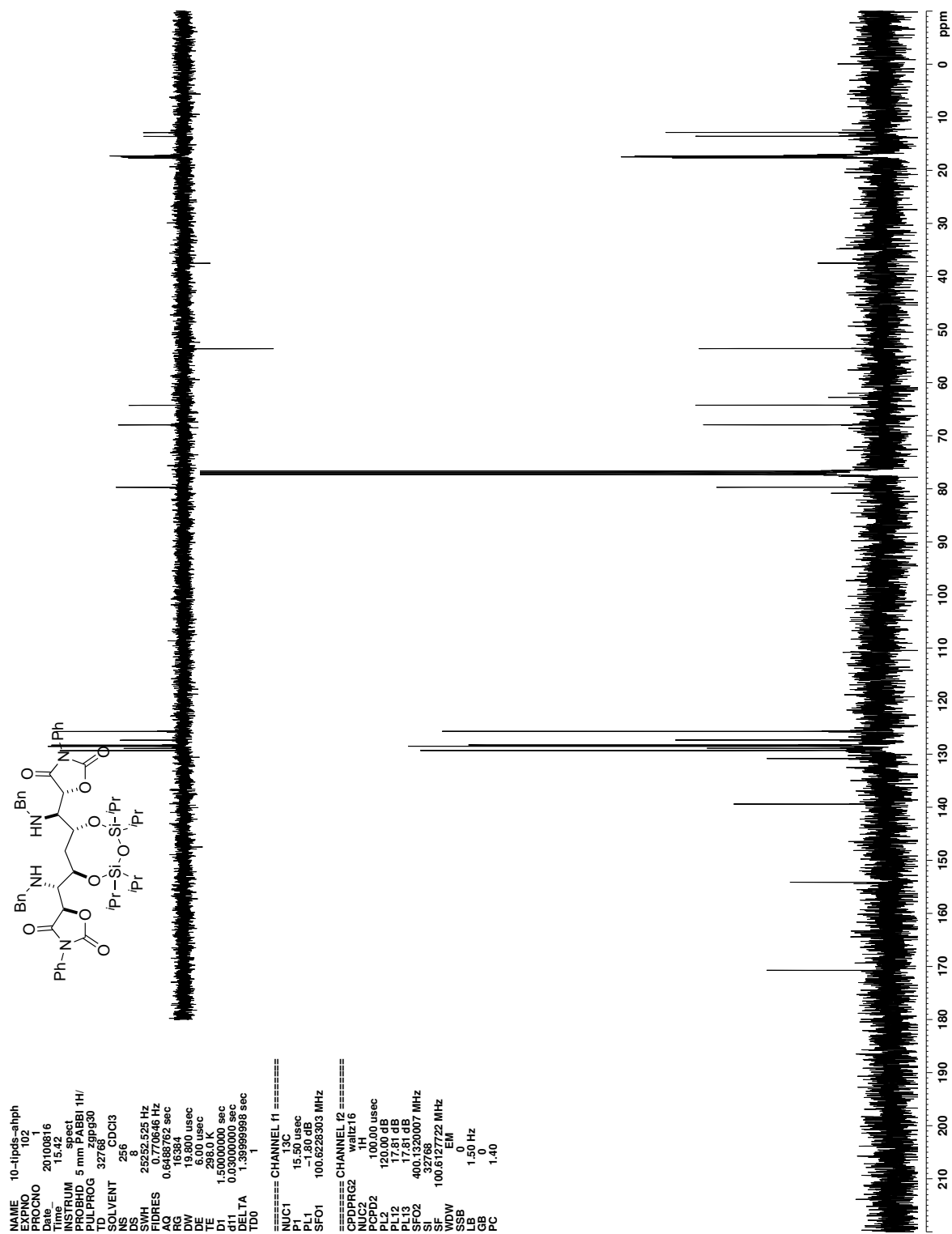


Figure C.140. ¹³C NMR (CDCl₃) of 346

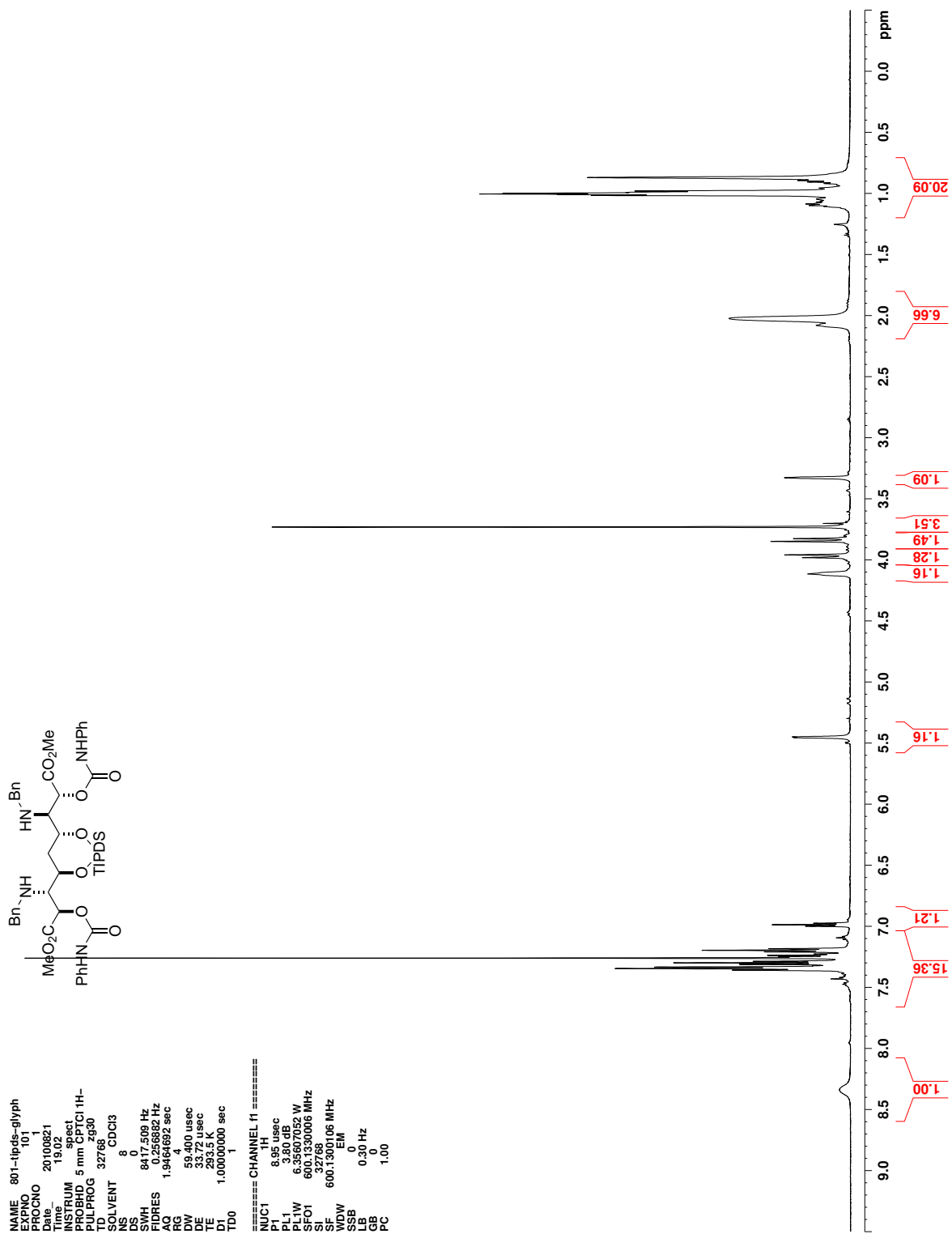


Figure C.141. ^1H NMR (CDCl_3) of **352**

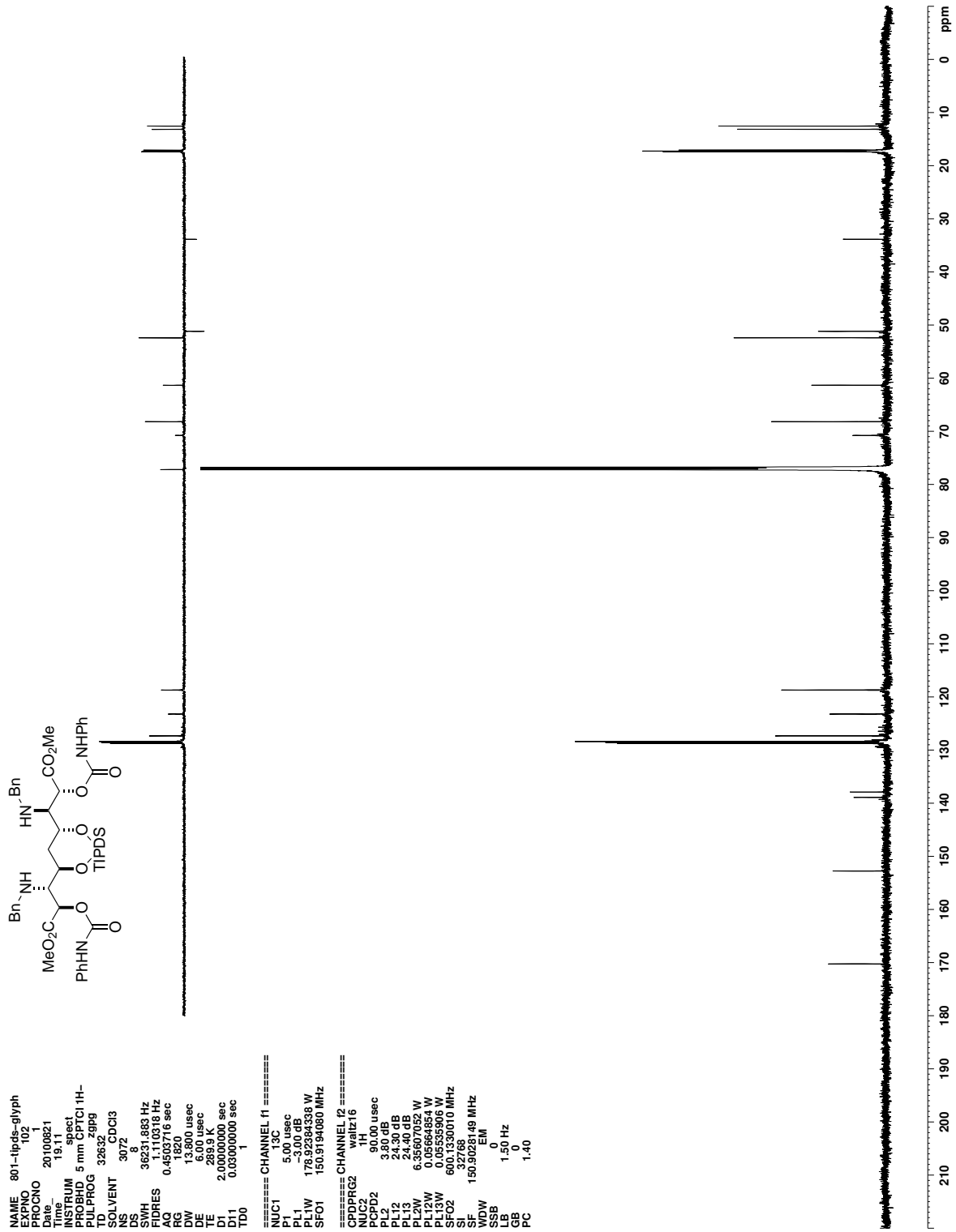


Figure C.142. ^{13}C NMR (CDCl_3) of **352**

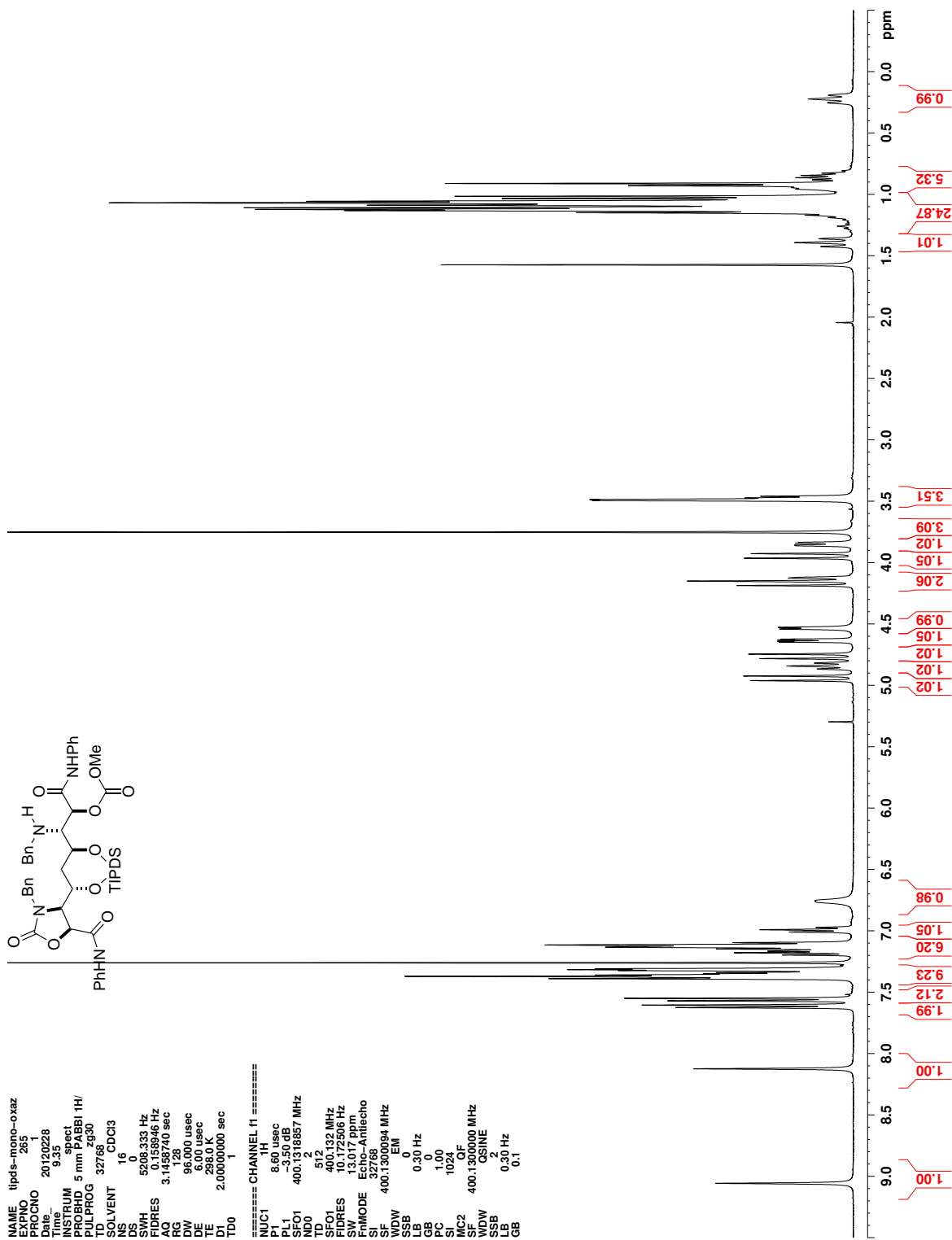


Figure C.143. ^1H NMR (CDCl_3) of 355

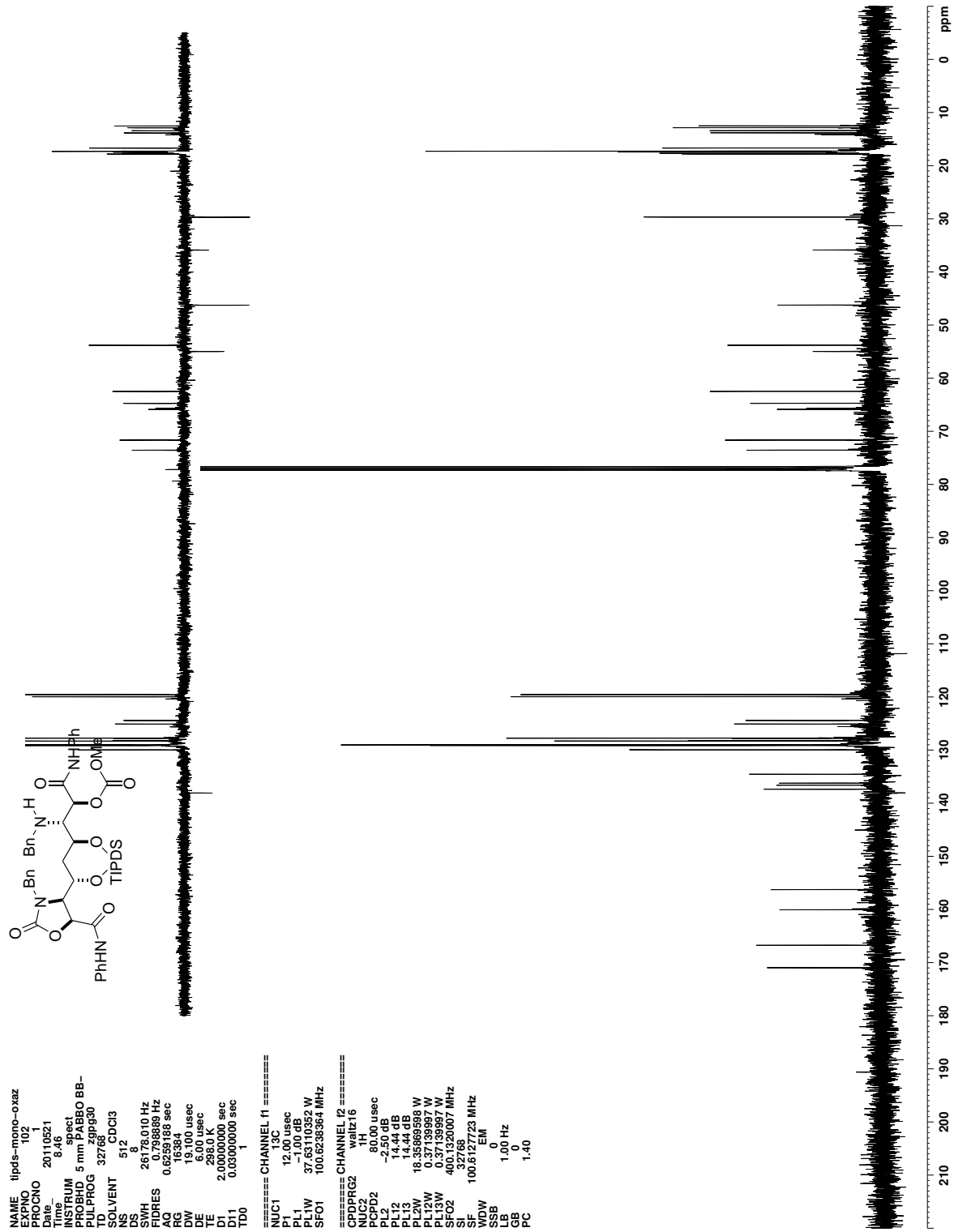


Figure C.144. ^{13}C NMR (CDCl_3) of 355

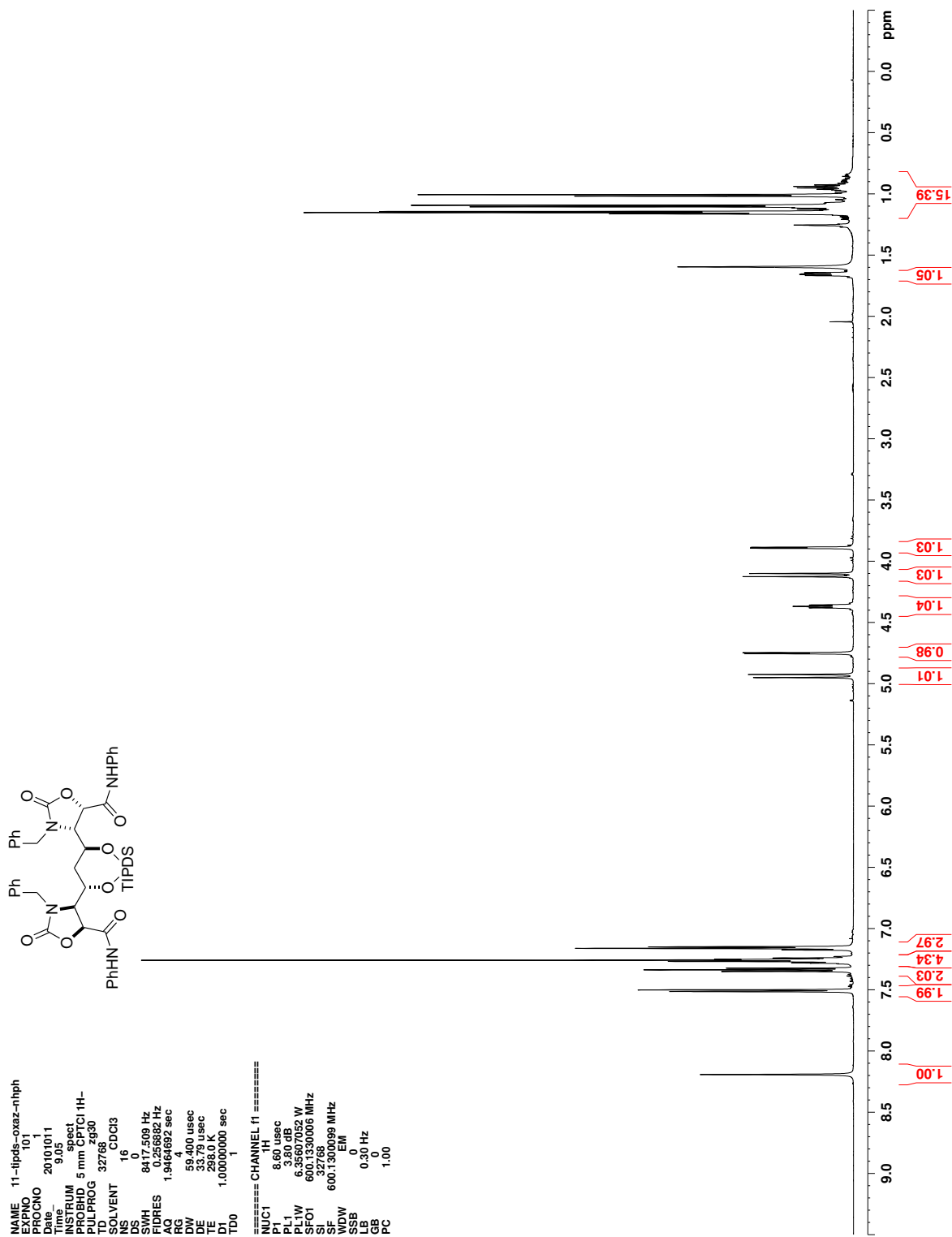


Figure C.145. ^1H NMR (CDCl_3) of 353

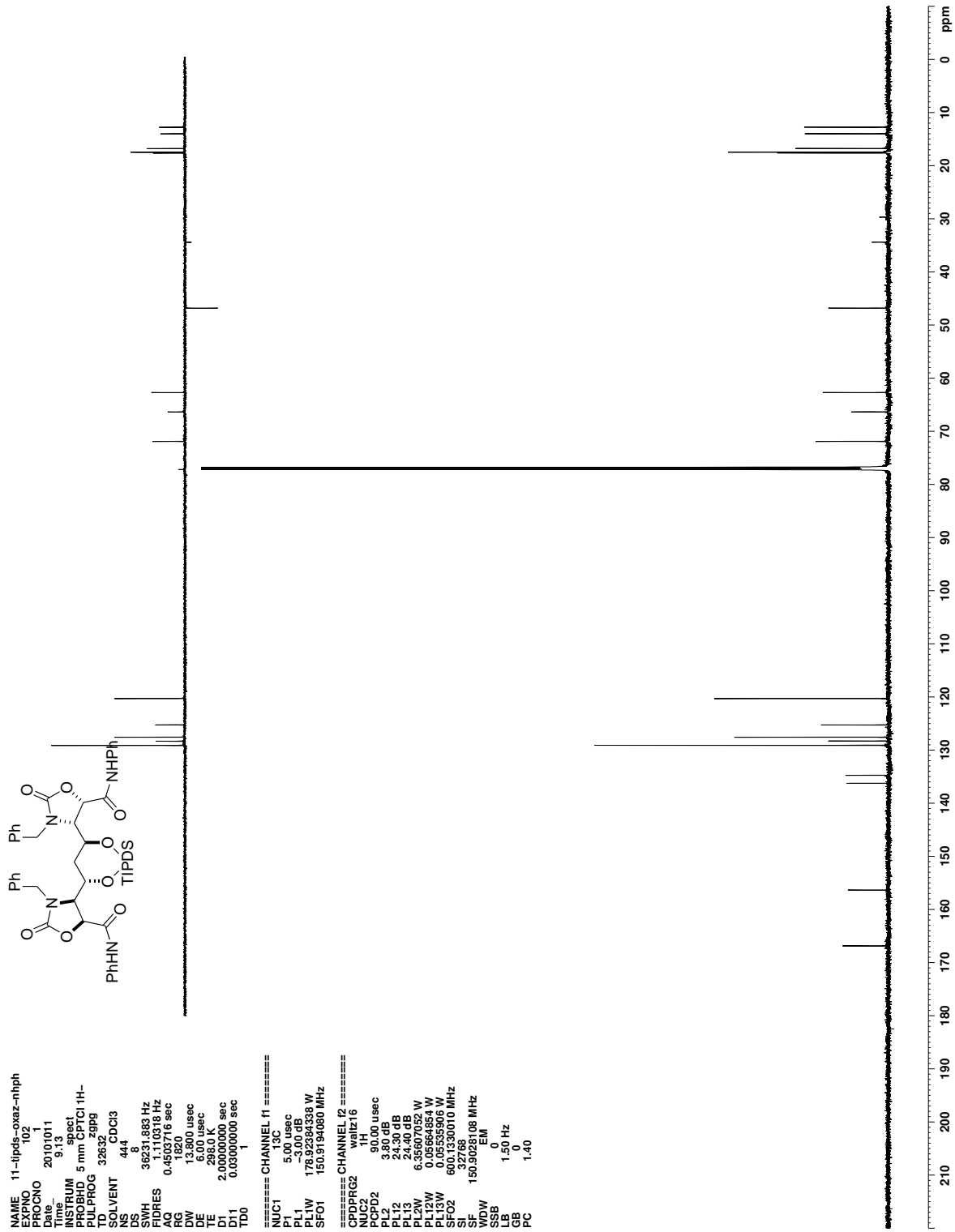


Figure C.146. ^{13}C NMR (CDCl_3) of 353

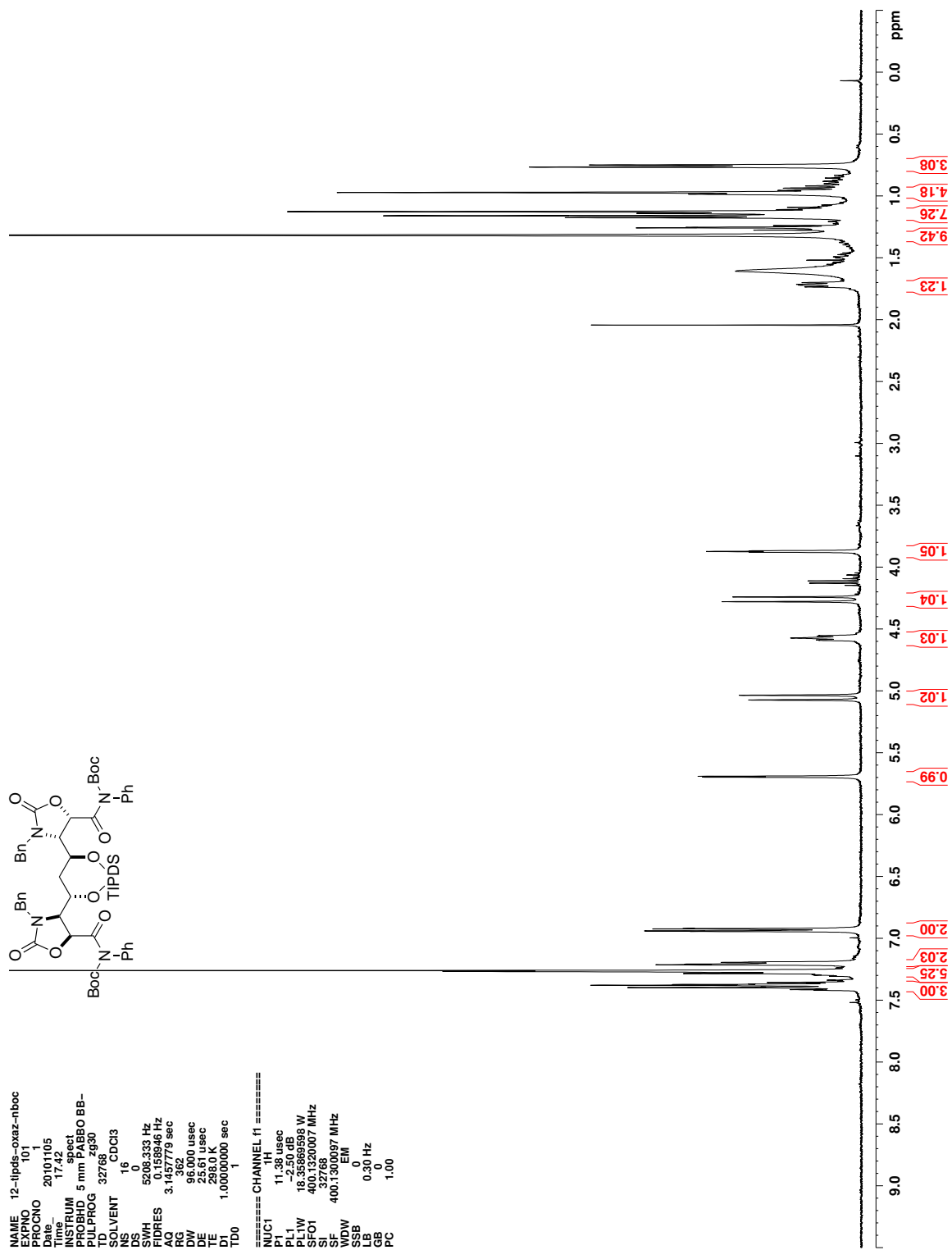


Figure C.147. ^1H NMR (CDCl_3) of 359

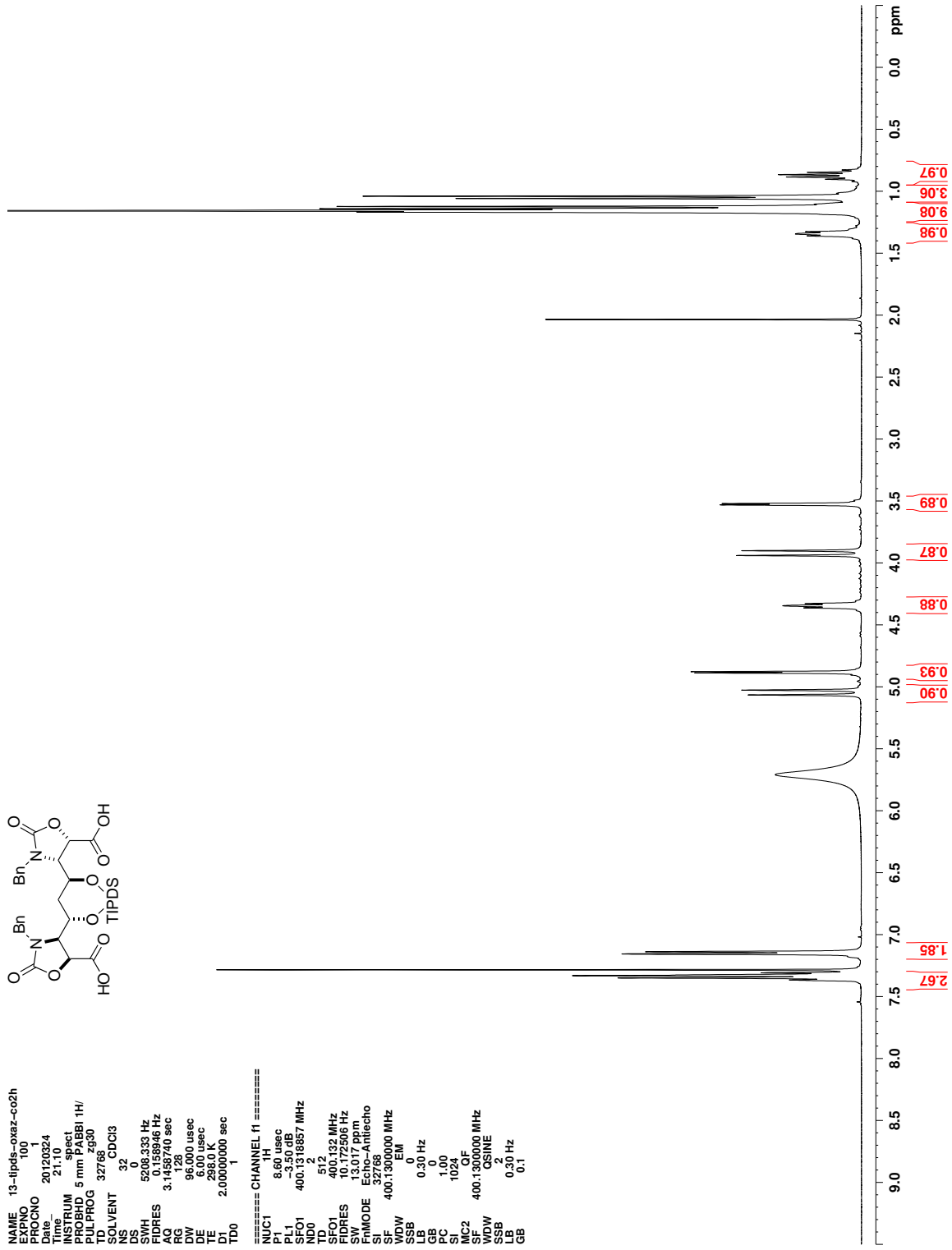


Figure C.149. ^1H NMR (CDCl_3) of 360

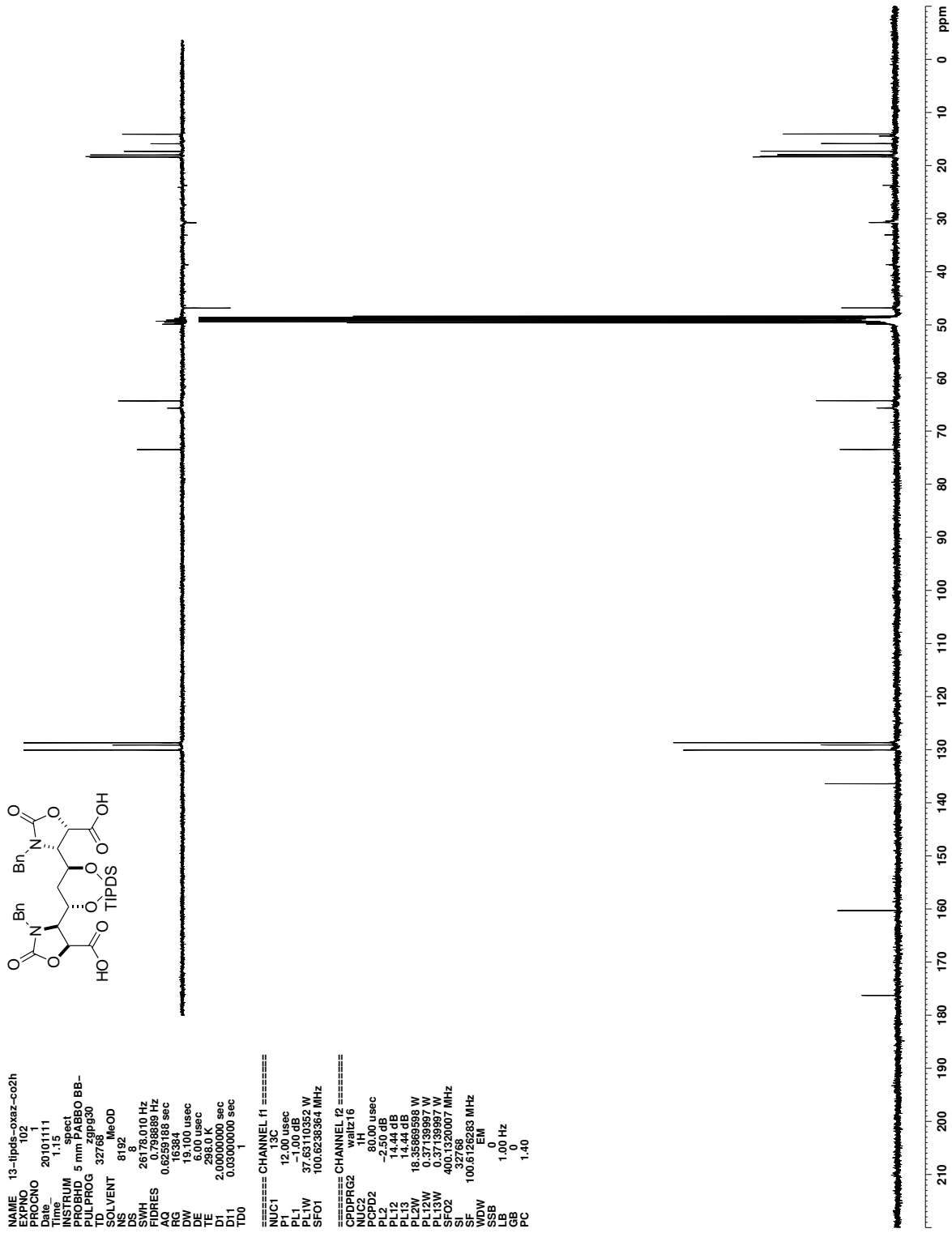


Figure C.150. ¹³C NMR (MeOD) of 360

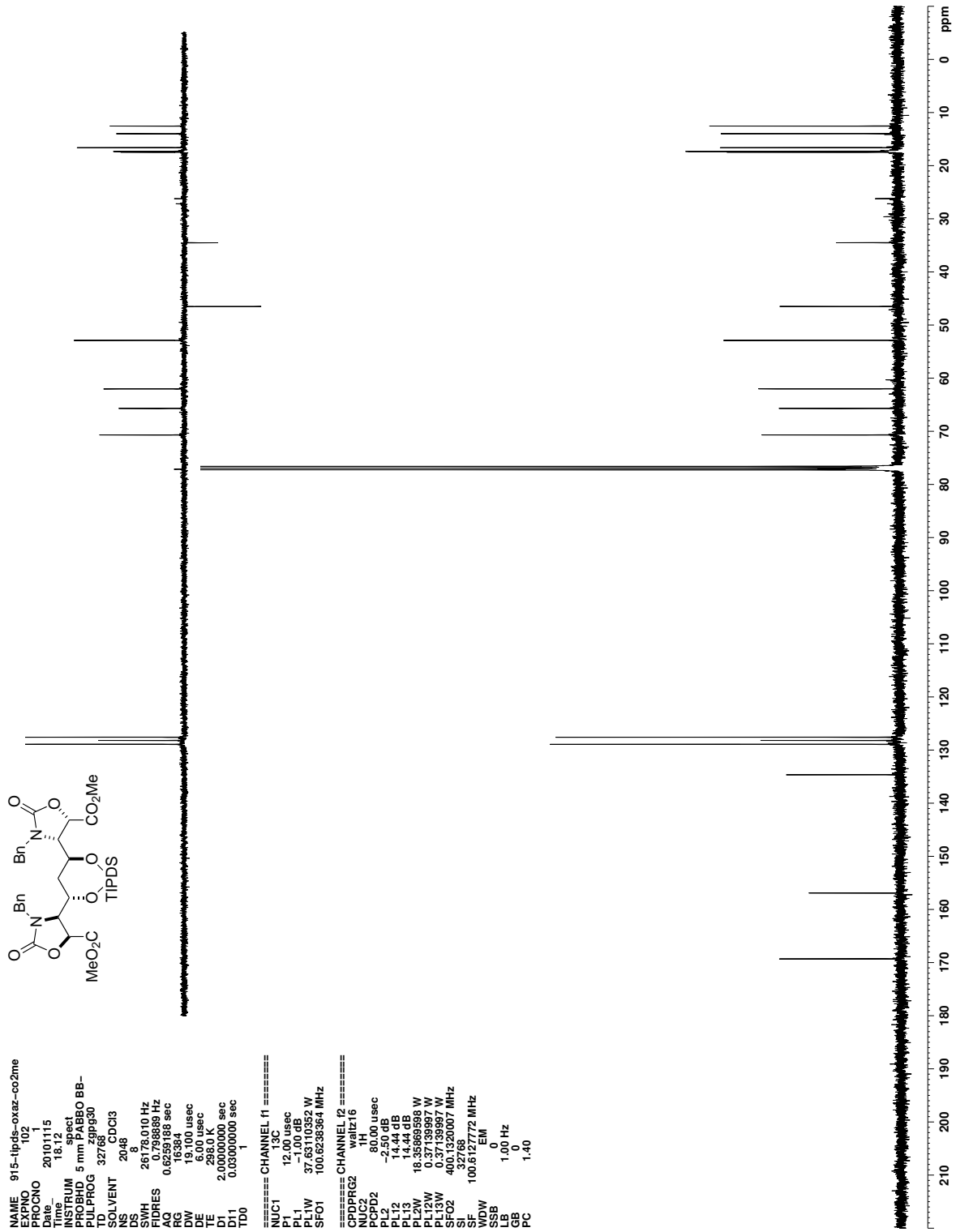


Figure C.152. ¹³C NMR (CDCl₃) of 361

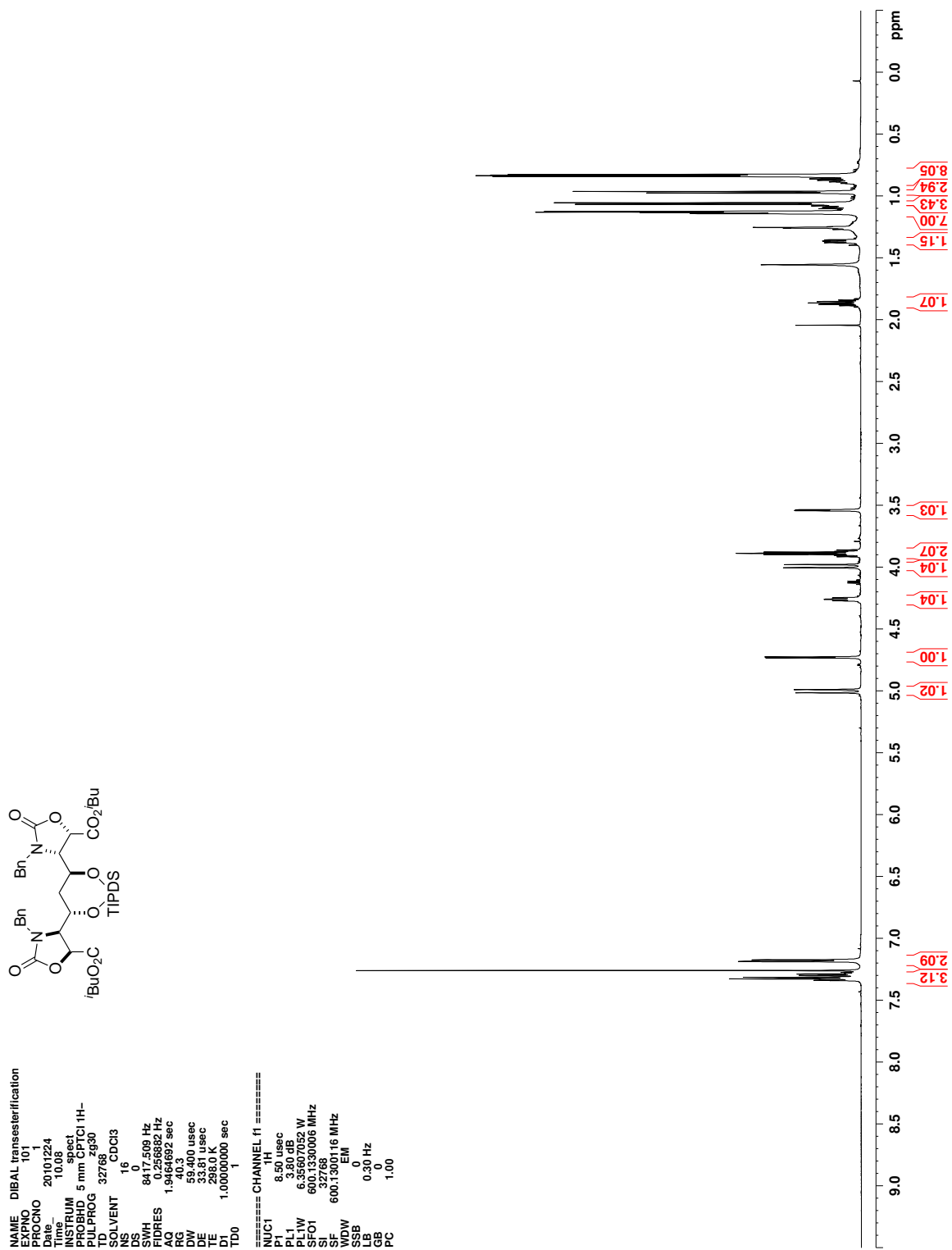


Figure C.153. ^1H NMR (CDCl_3) of 361

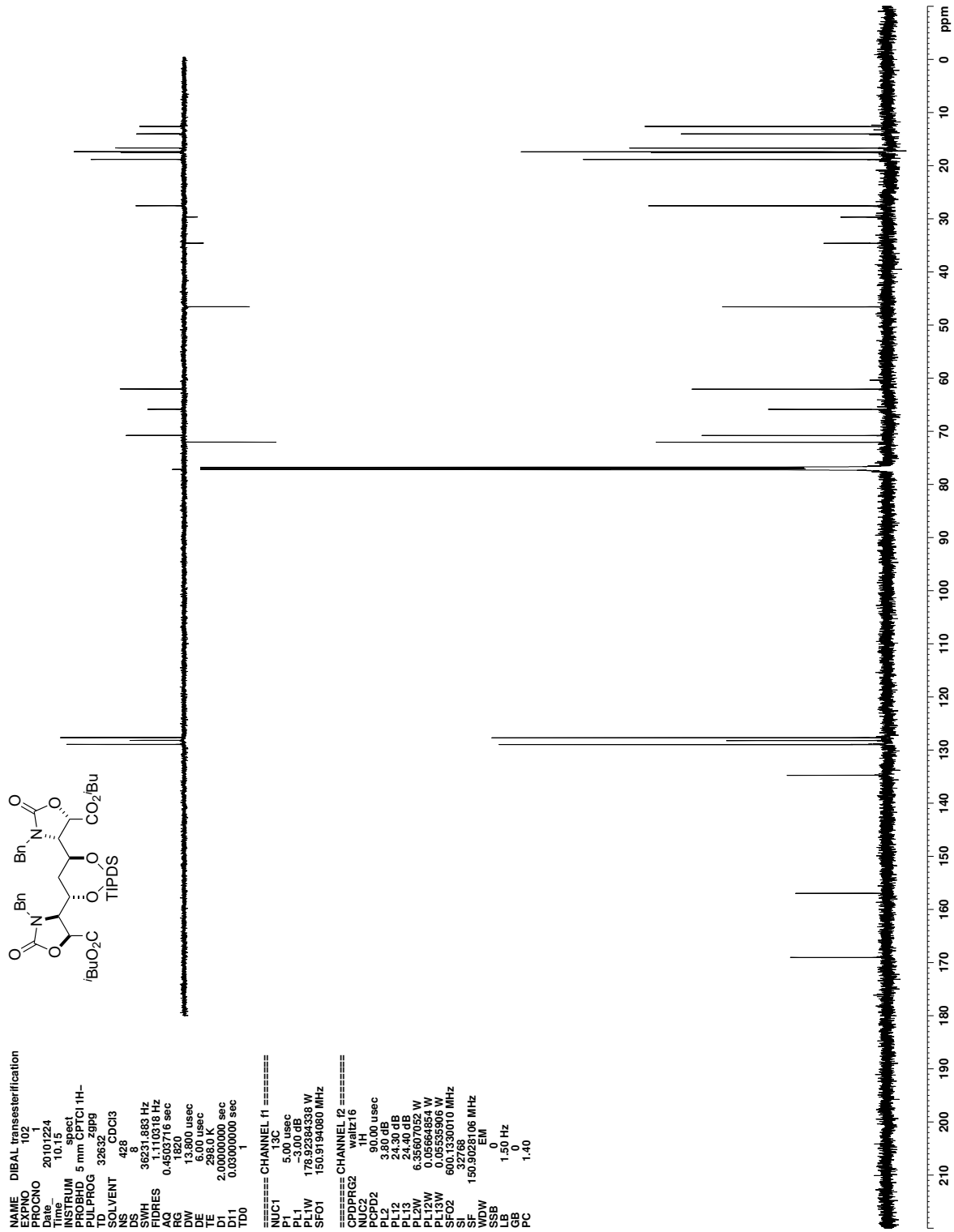


Figure C.154. ¹³C NMR (CDCl₃) of 361

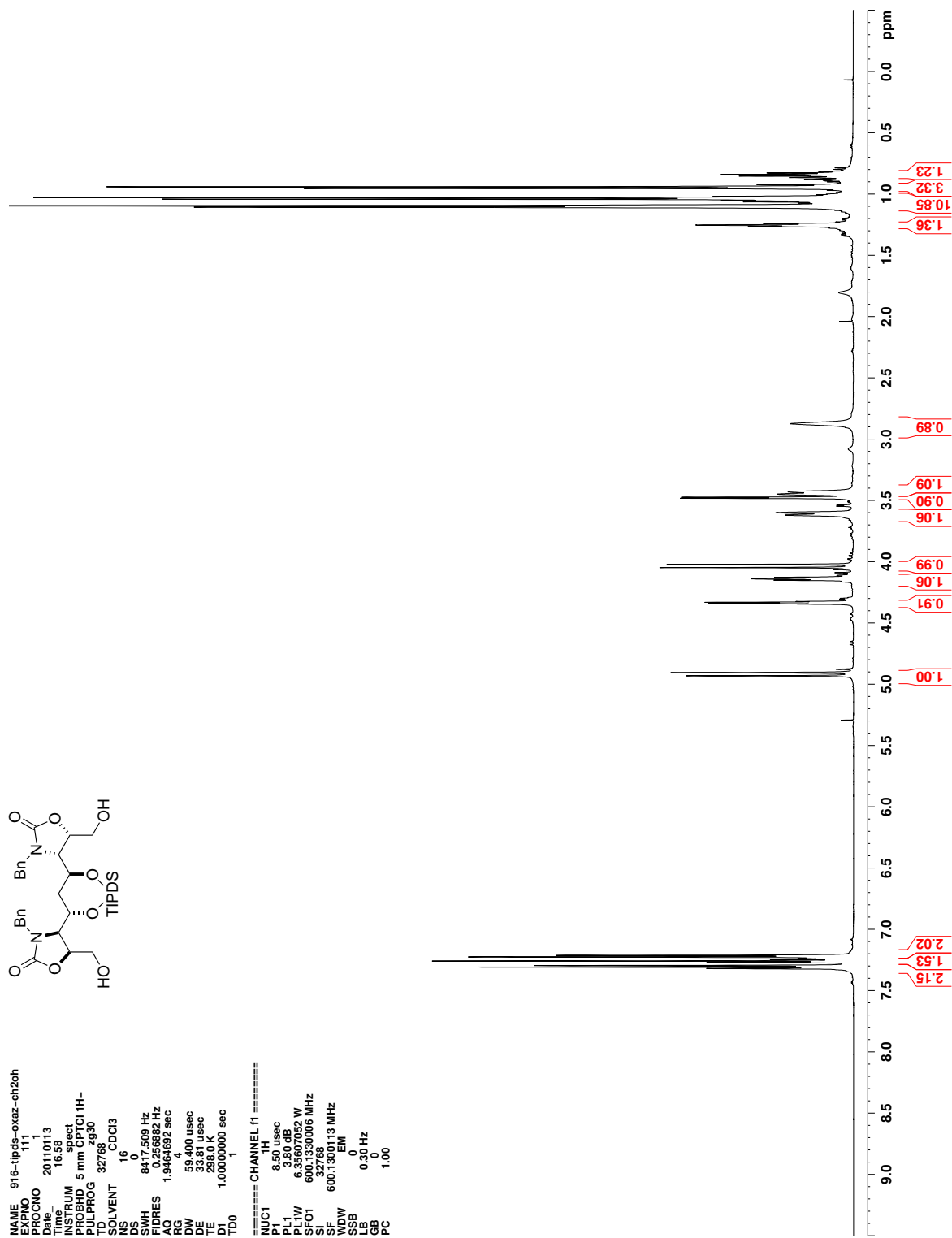


Figure C.155. ^1H NMR (CDCl_3) of 356

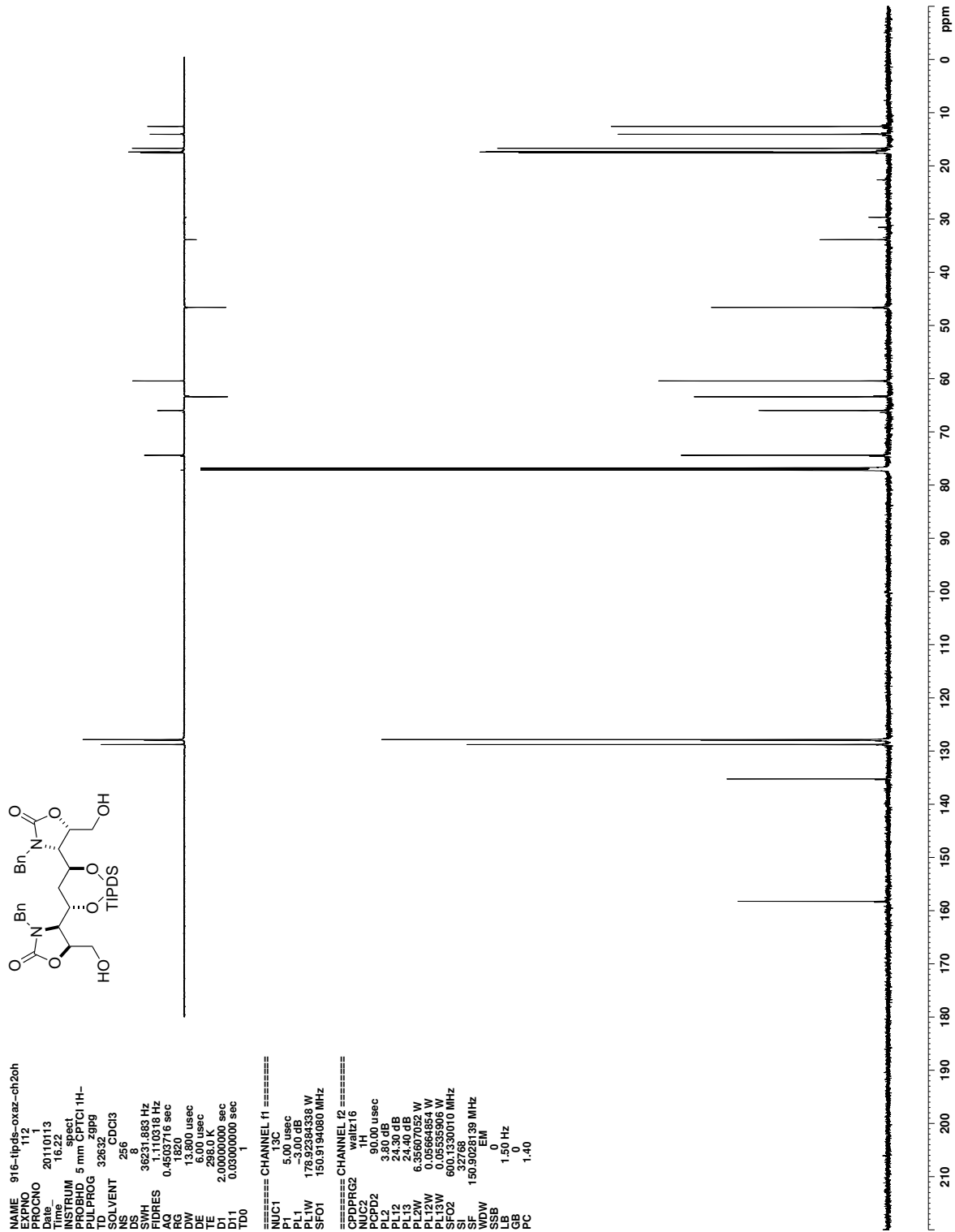


Figure C.156. ^{13}C NMR (CDCl_3) of 356

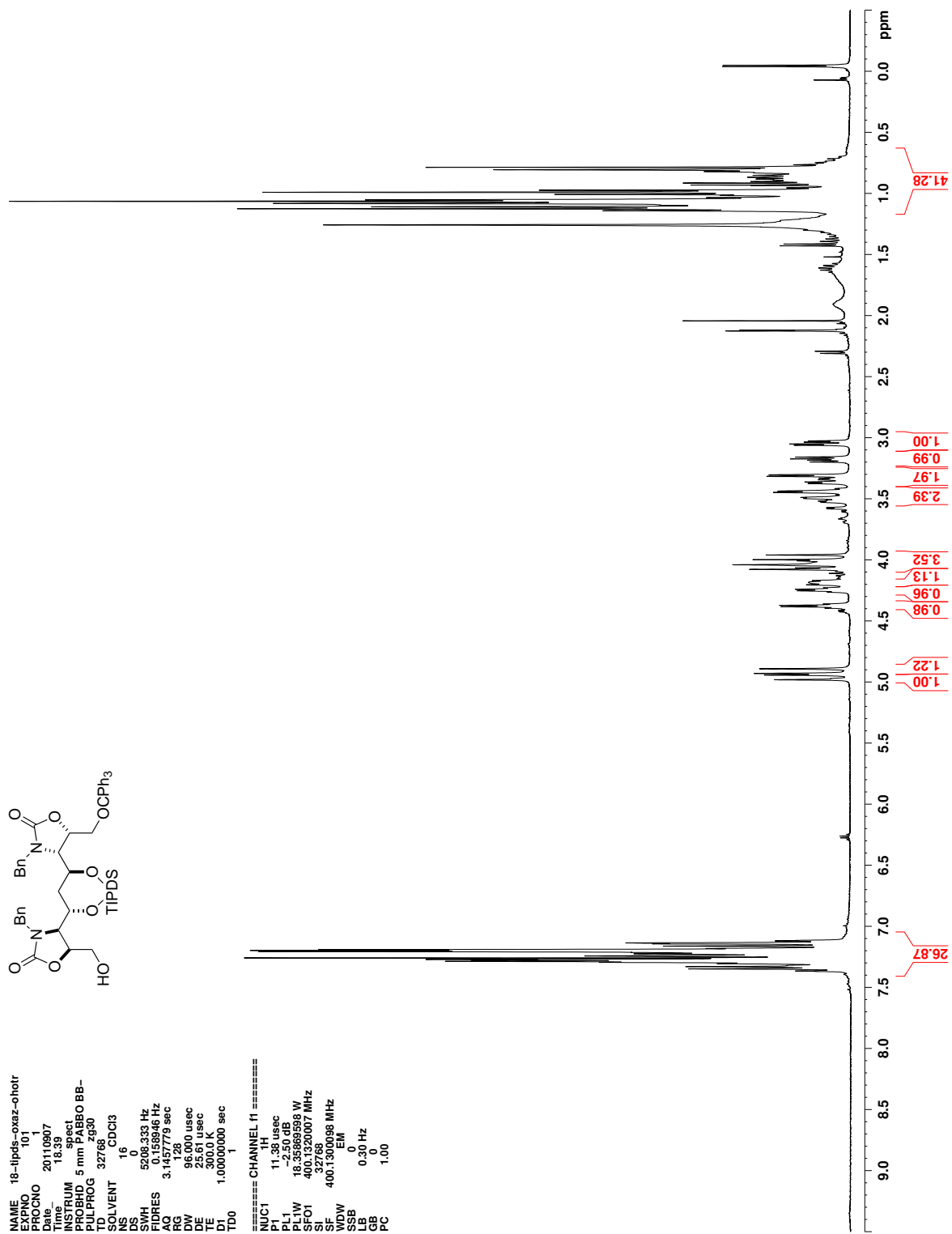


Figure C.159. ^1H NMR (CDCl_3) of 357

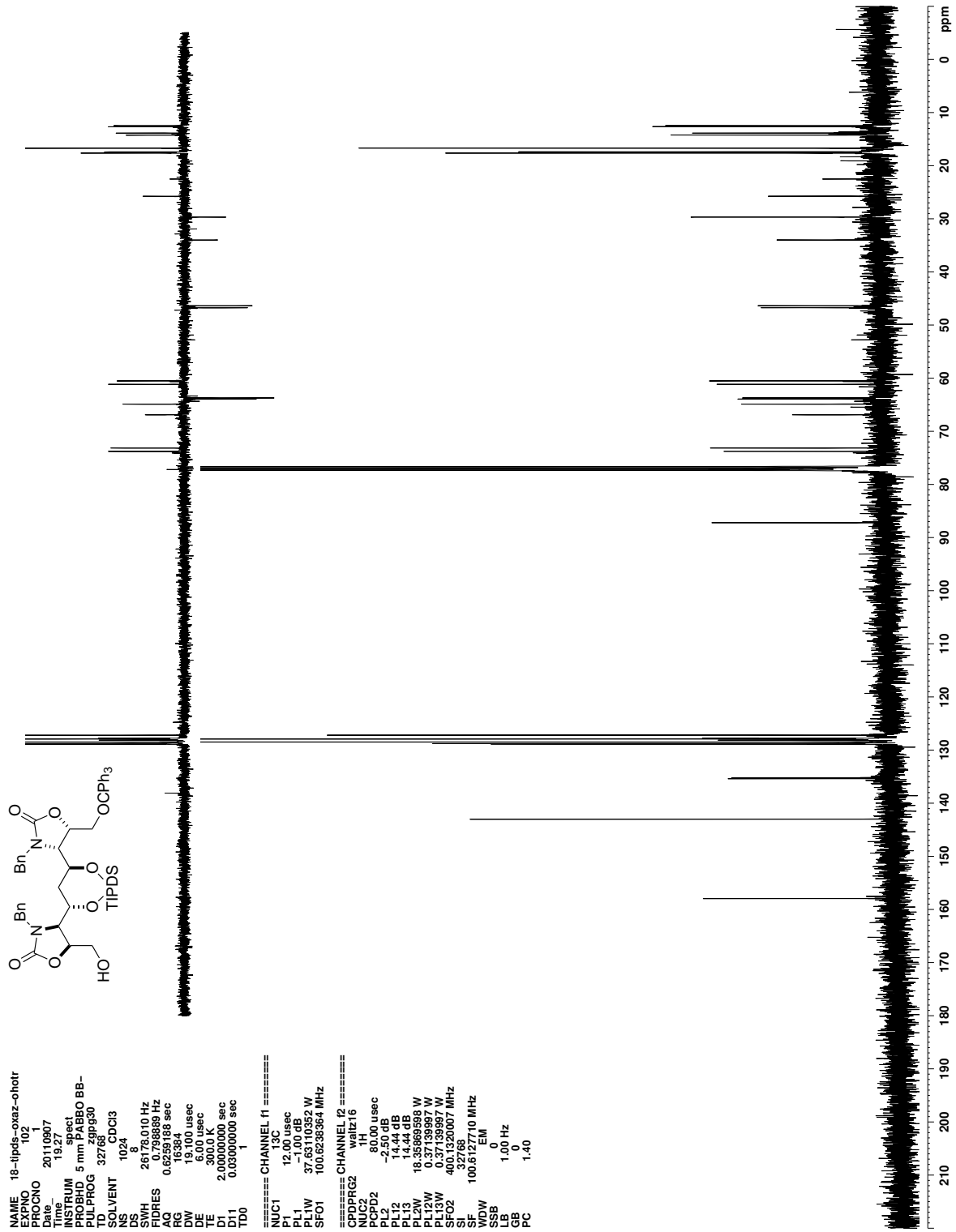


Figure C.160. ^{13}C NMR (CDCl_3) of 357

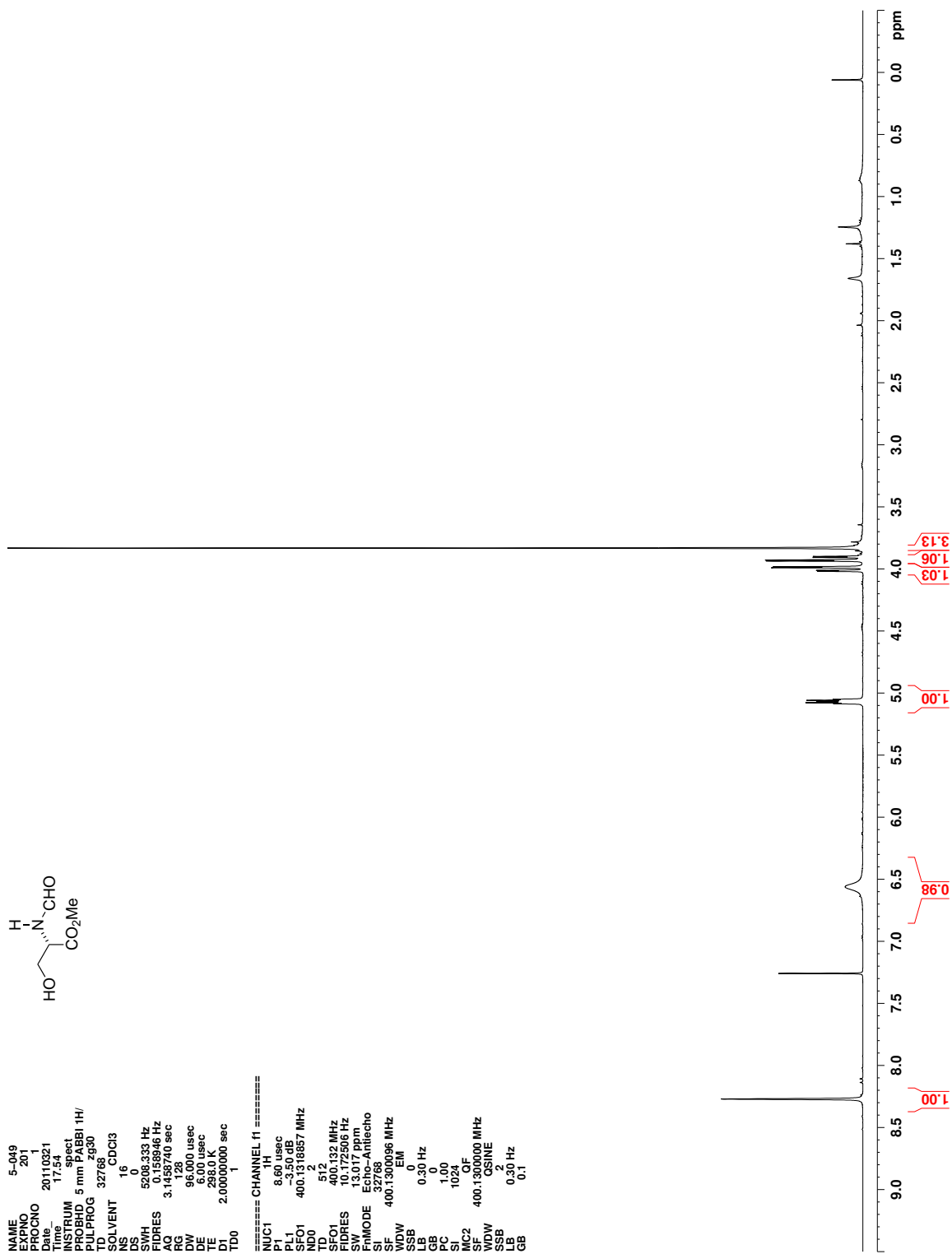
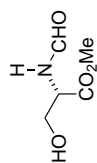


Figure C.161. ^1H NMR (CDCl_3) of 376



```

NAME serome-mcho-oh
EXPNO 202
PROCNO 20110321
Date_ 20110321
Time 21.01
INSTRUM spect
PROBHD 5 mm PABBI 1H/
TD 32768
AQ 0.657787 sec
RG 16384
DS 8
SWH 25252.625 Hz
FIDRES 0.770646 Hz
AQ 0.657787 sec
RG 16384
DW 19.800 usec
DE 6.00 usec
TE 298.0 K
D1 1.50000000 sec
d11 0.10000000 sec
DELTA 1.3598998 sec
TD0 1

===== CHANNEL f1 =====
NUC1 13C
P1 15.00 usec
PL1 -3.00 dB
SFO1 100.6228303 MHz

===== CHANNEL f2 =====
CPDPRG2 waltz16
NUC2 13C
PCPD2 100.00 usec
PL2 -3.50 dB
PL12 17.81 dB
PL13 17.81 dB
SFO2 400.1320007 MHz
SF 32769
SI 100.617720 MHz
WDW EM
SSB 0
LB 1.50 Hz
GB 0
PC 1.40

```

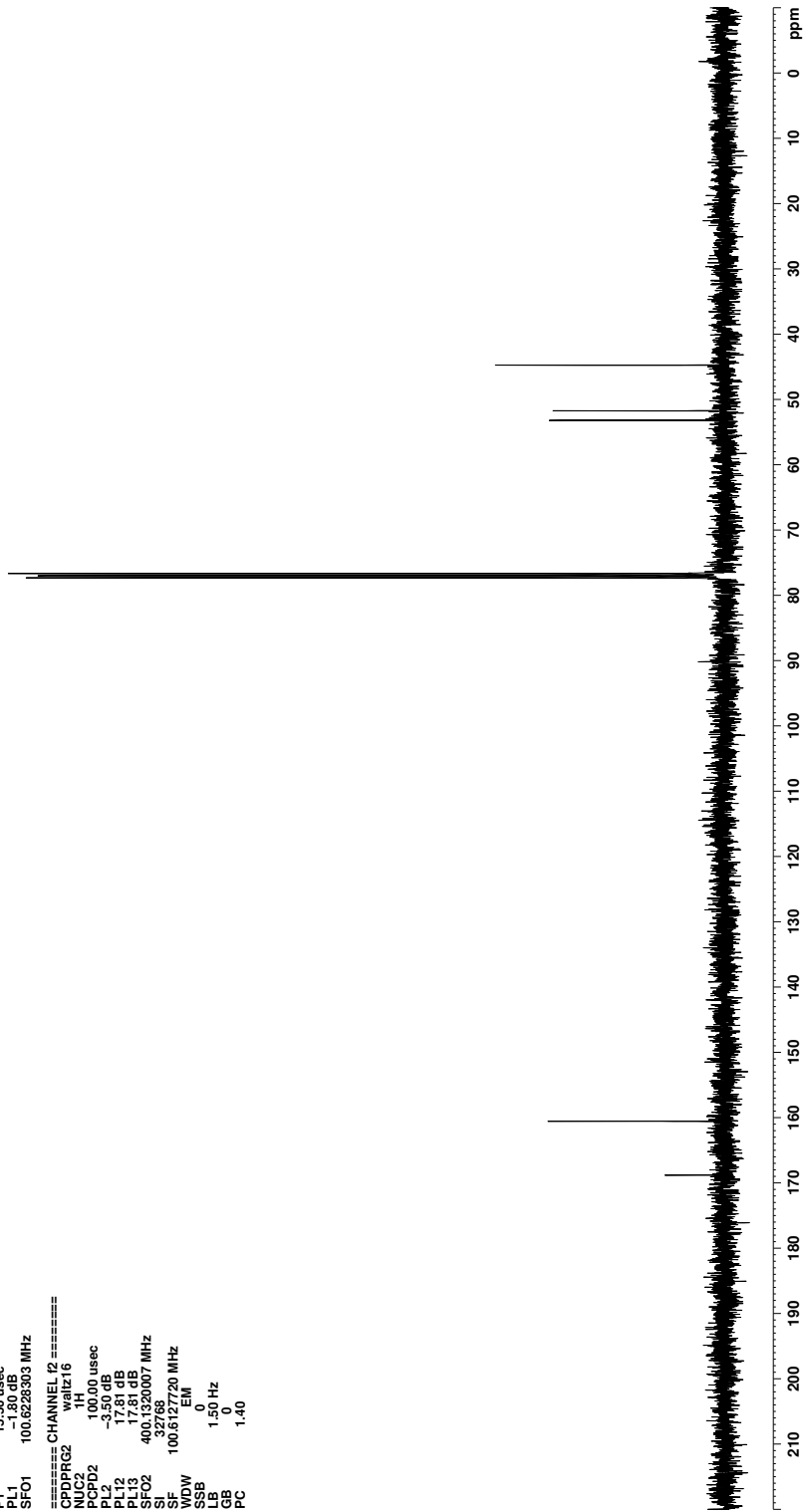


Figure C.162. ¹³C NMR (CDCl₃) of 376

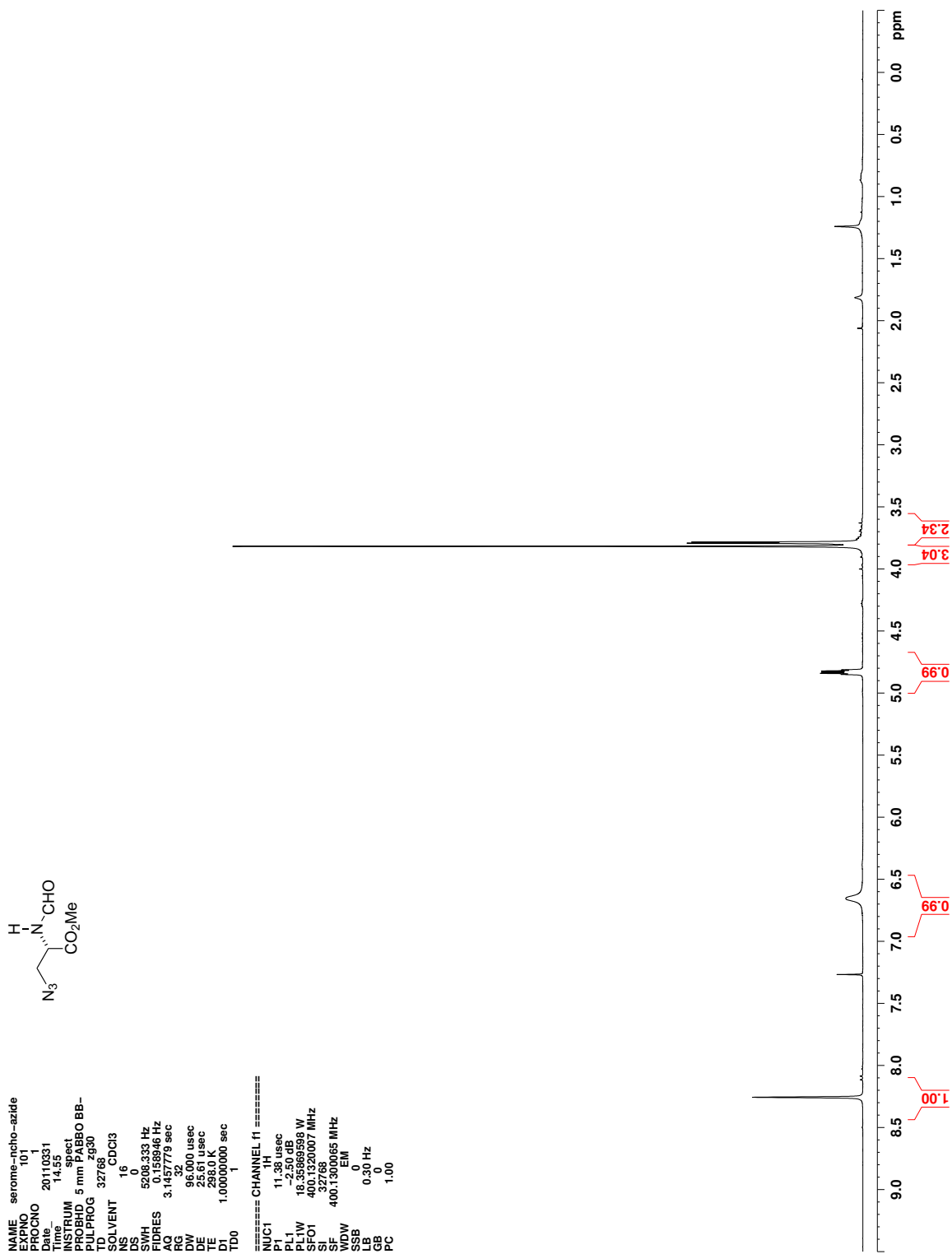


Figure C.163. ^1H NMR (CDCl_3) of 374

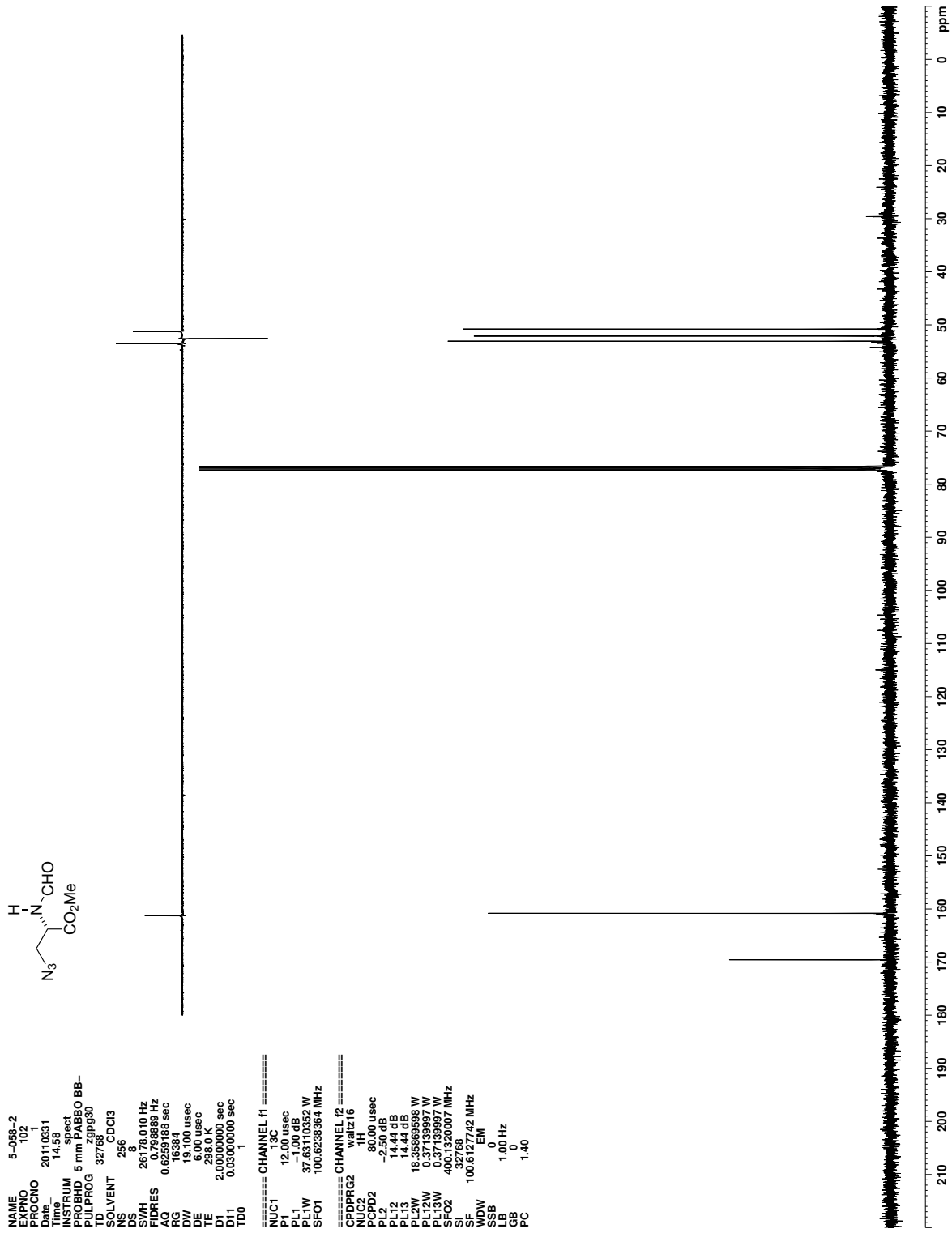


Figure C.164. ¹³C NMR (CDCl₃) of 374

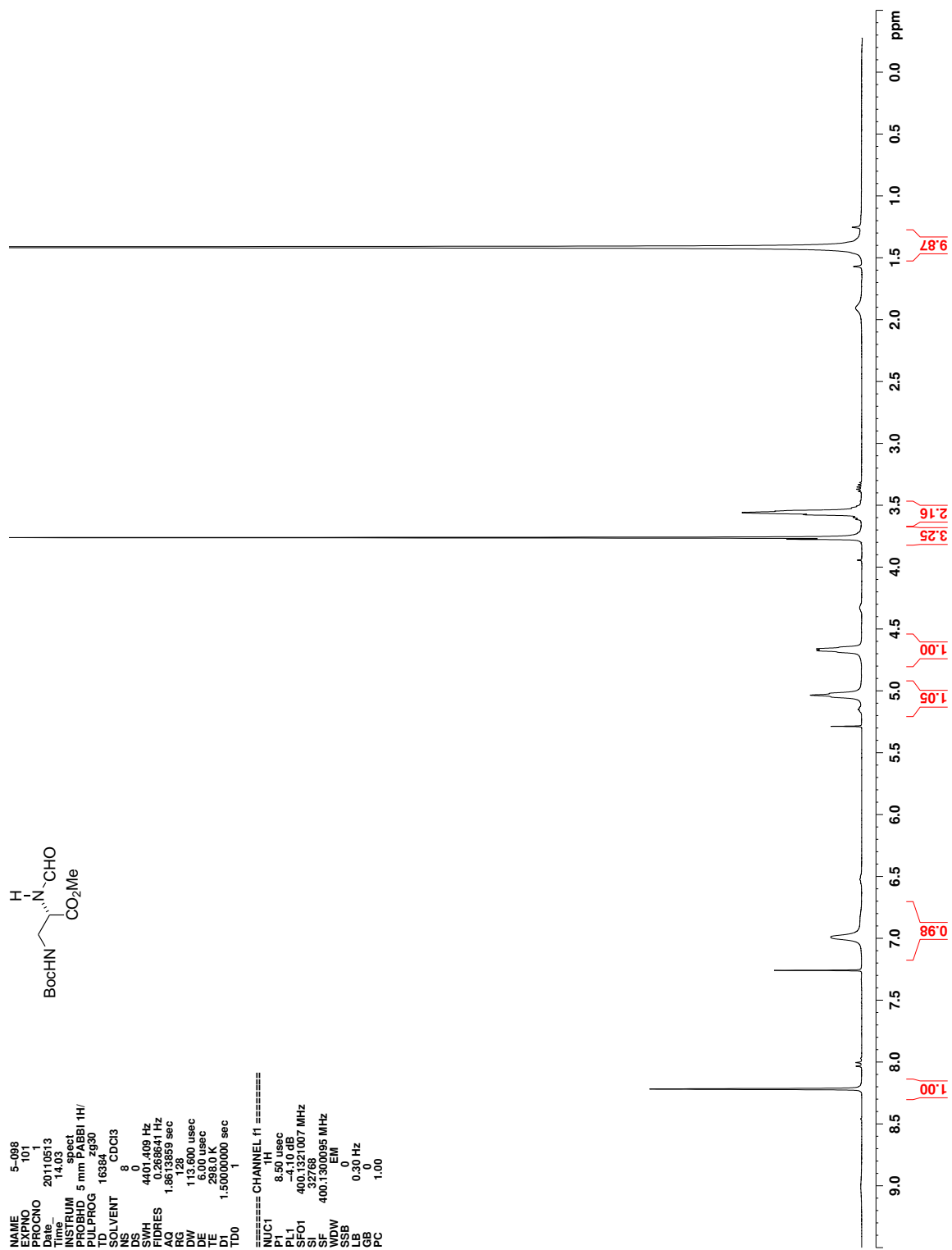


Figure C.165. ^1H NMR (CDCl_3) of 380

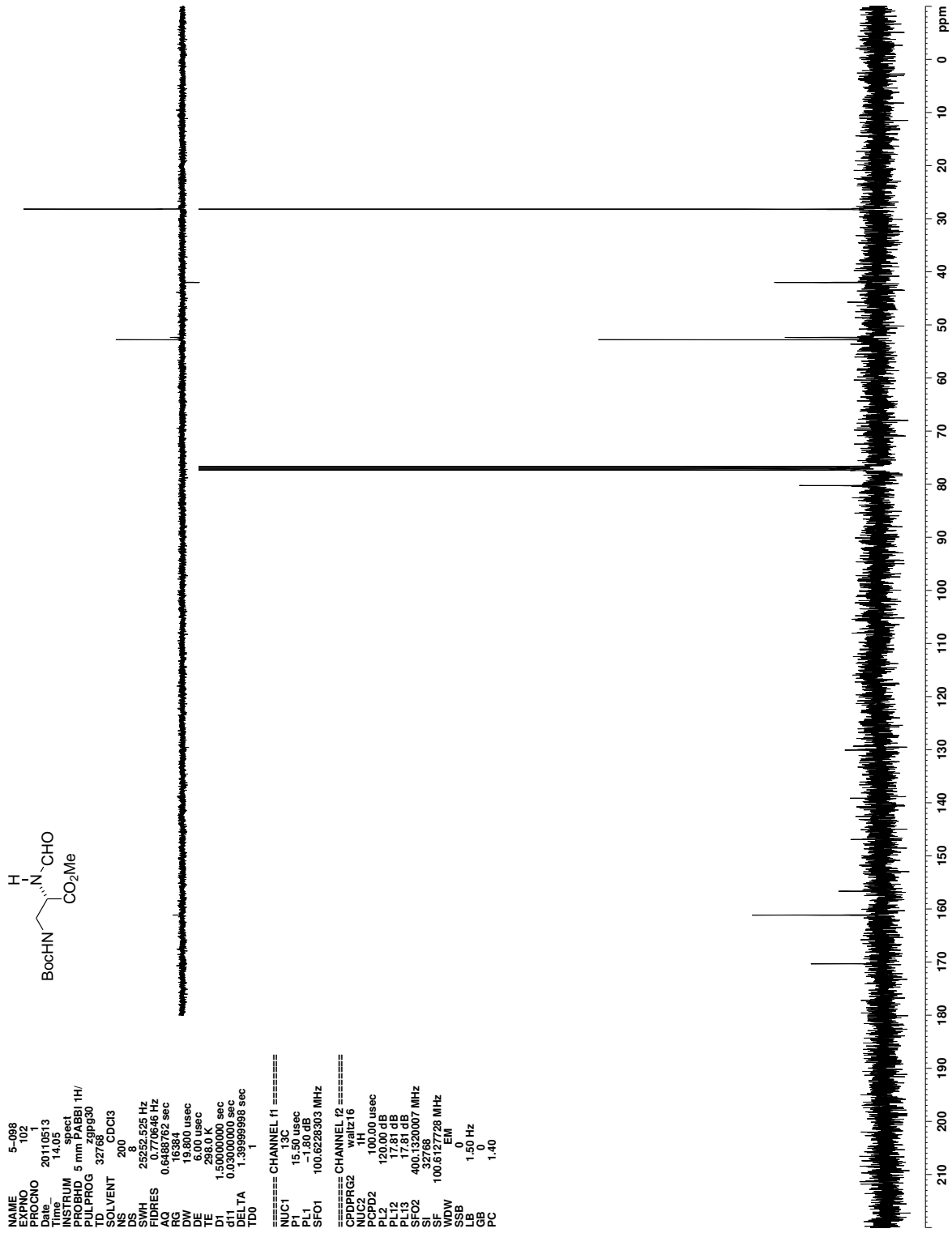


Figure C.166. ¹³C NMR (CDCl₃) of 380

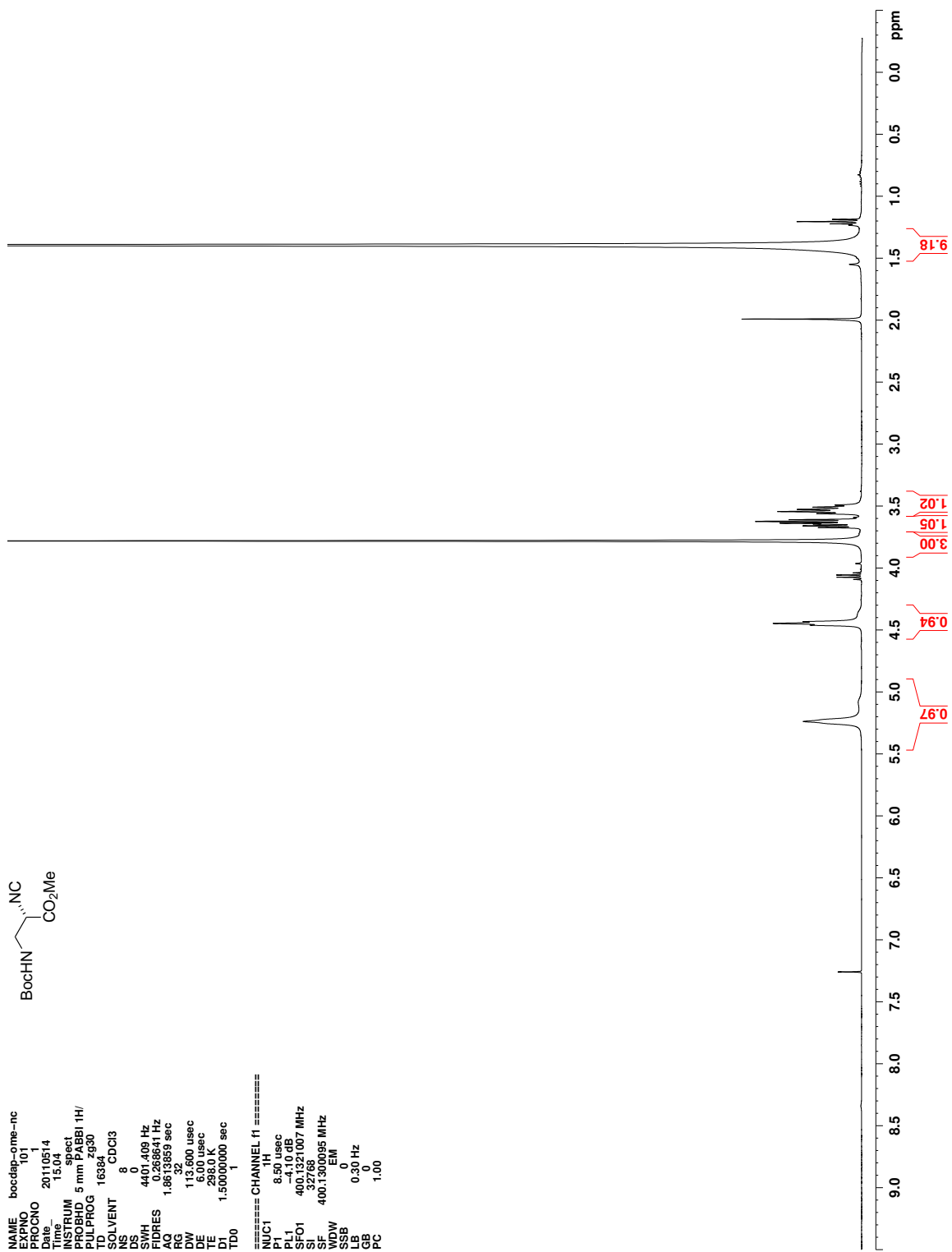


Figure C.167. ^1H NMR (CDCl_3) of 381

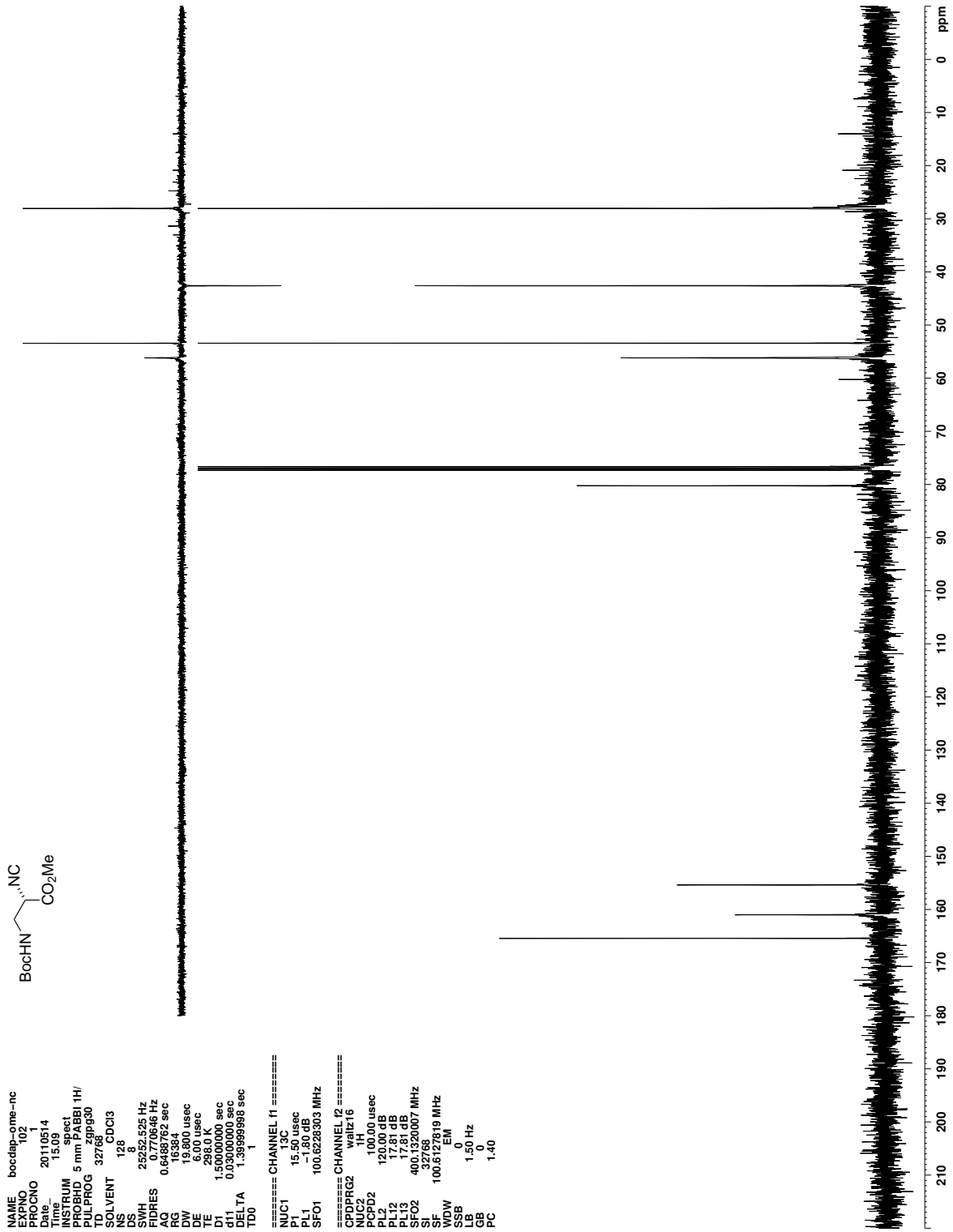


Figure C.168. ¹³C NMR (CDCl₃) of 381

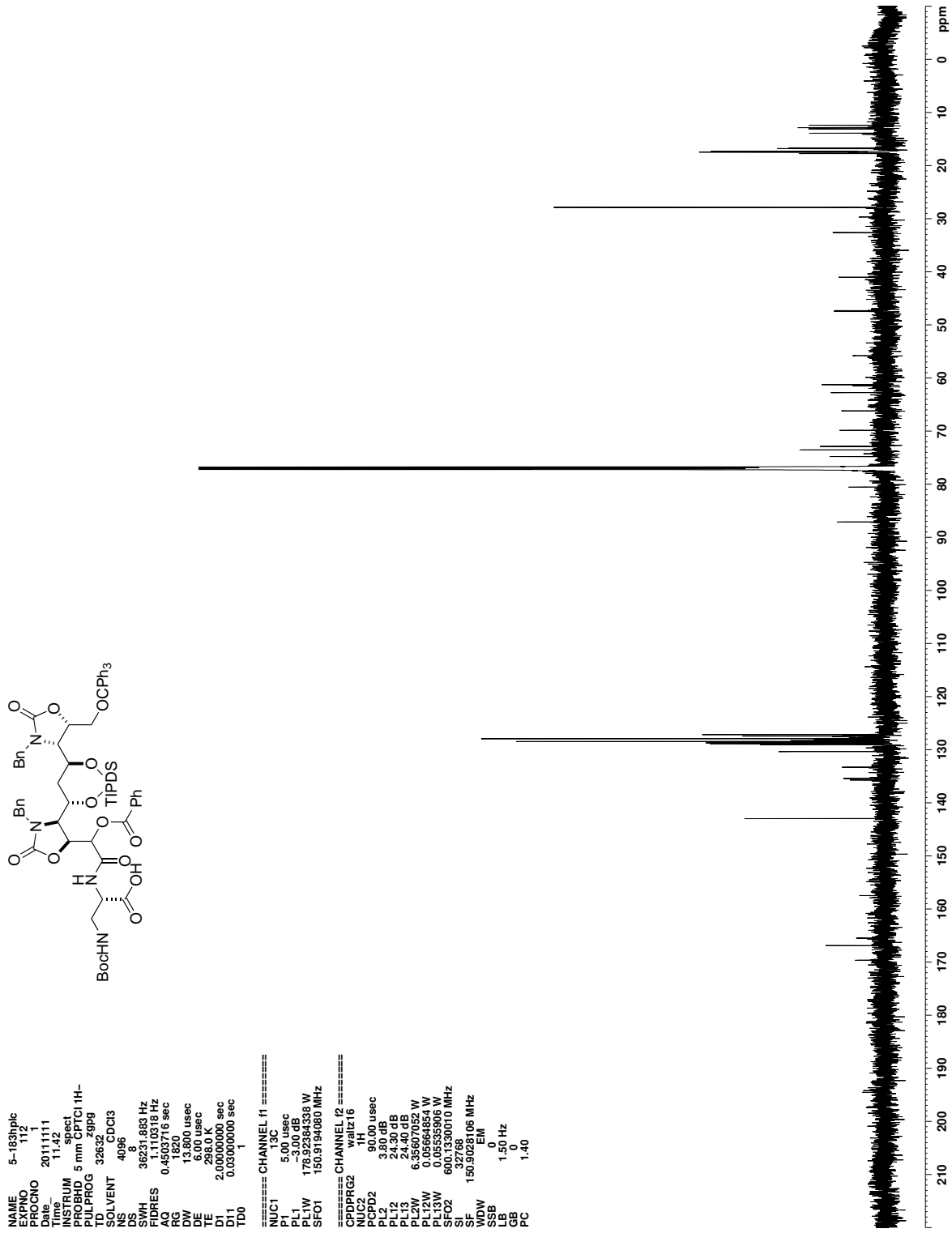


Figure C.170. ¹³C NMR (CDCl₃) of 385

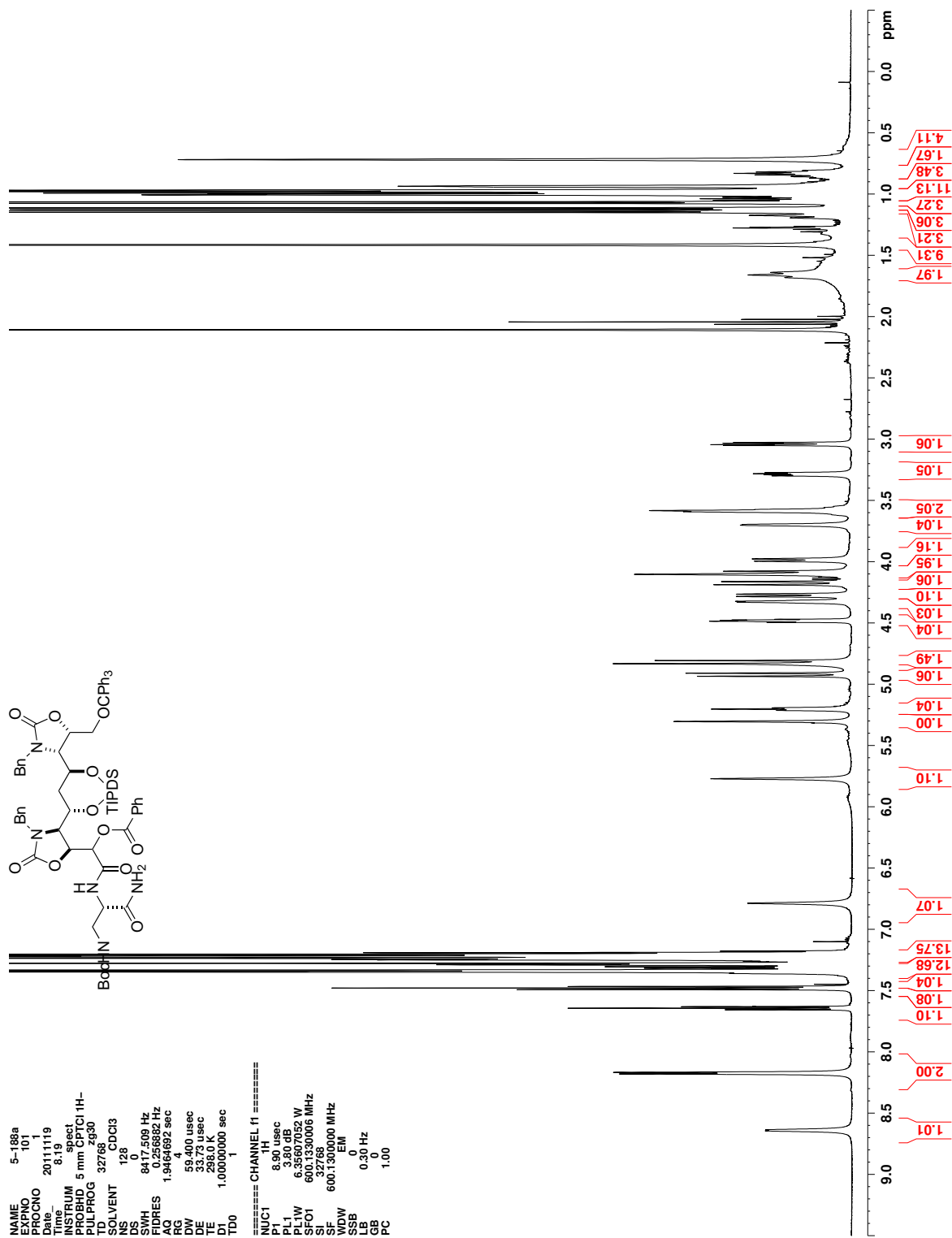


Figure C.171. ^1H NMR (CDCl_3) of 386a

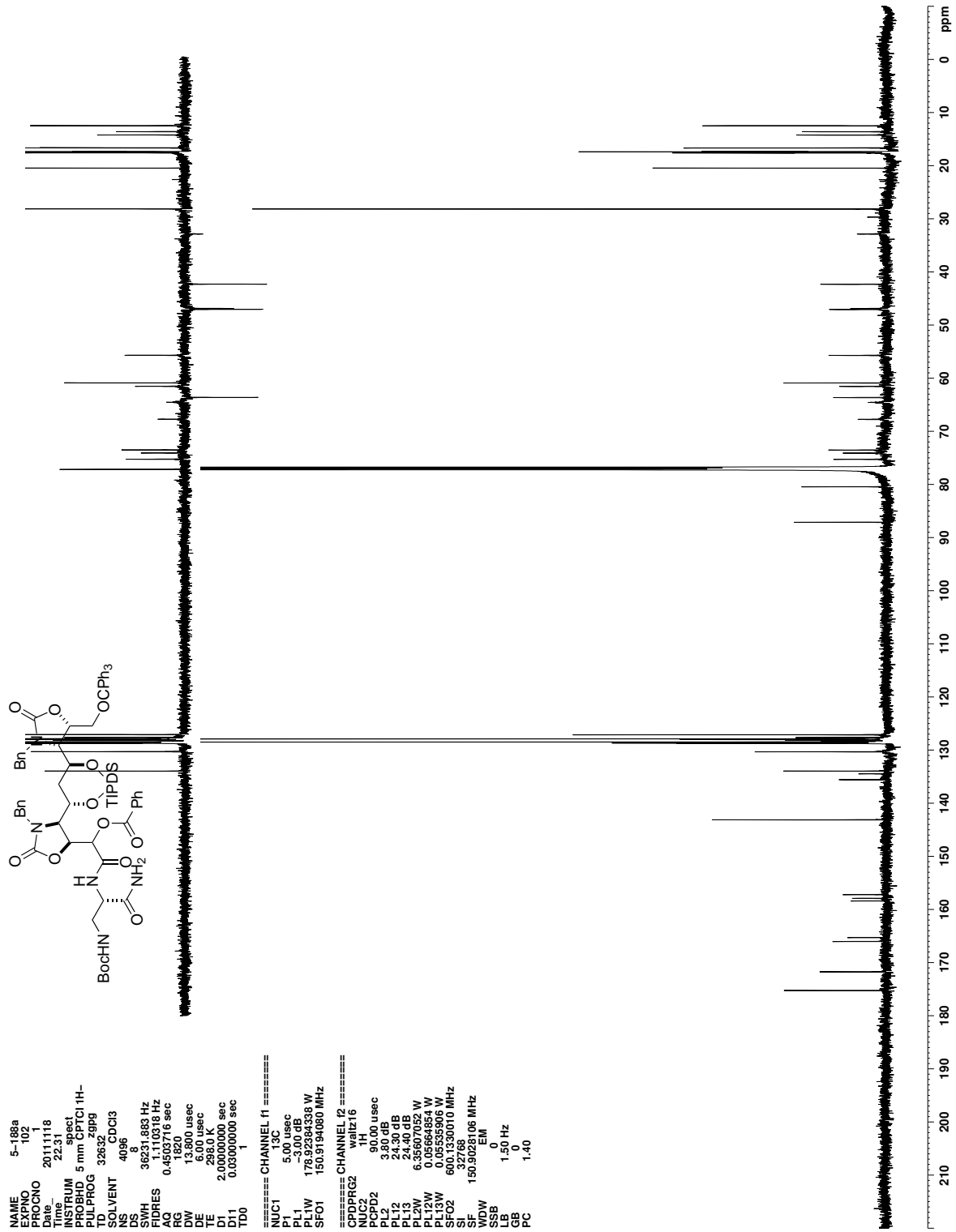


Figure C.172. ^{13}C NMR (CDCl_3) of 386a

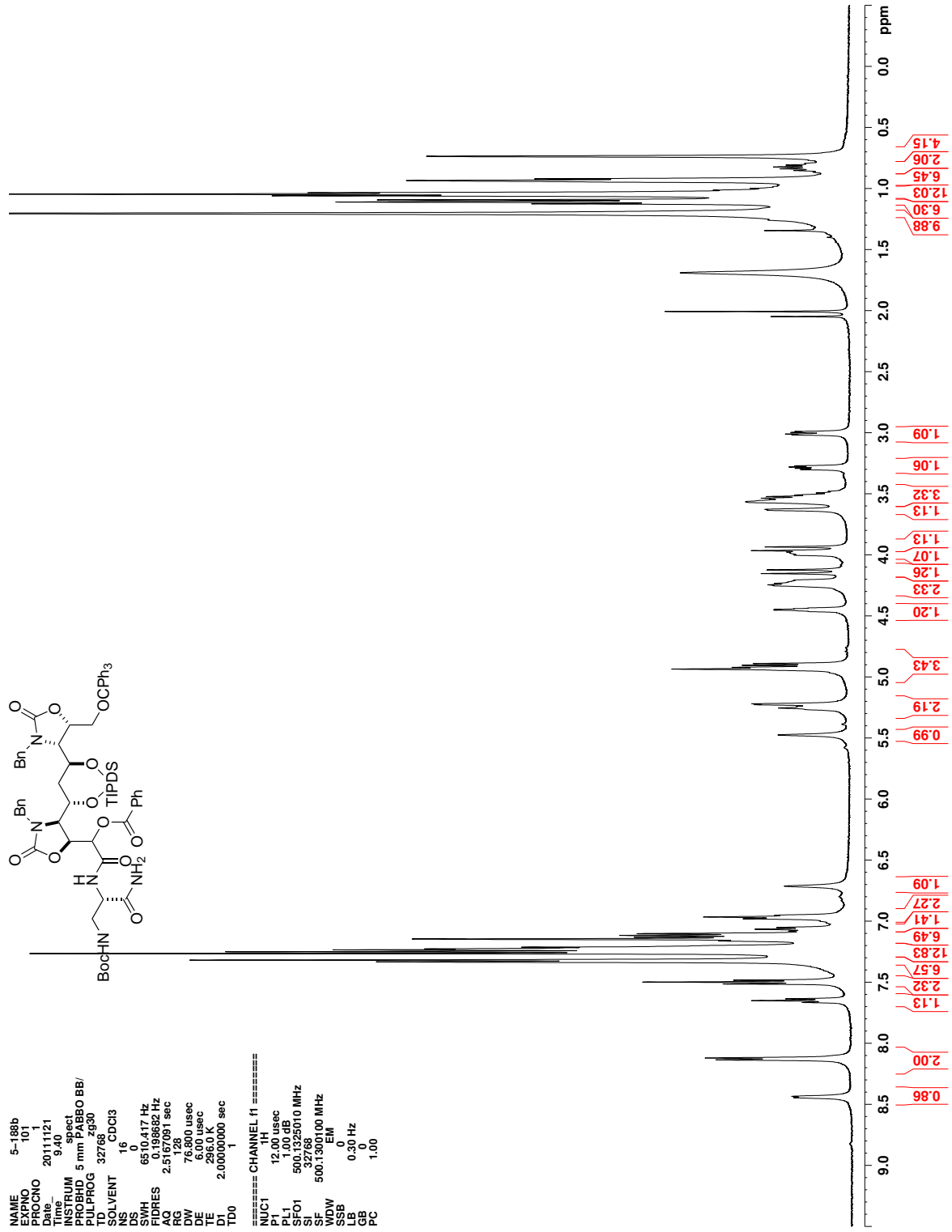


Figure C.173. ^1H NMR (CDCl_3) of 386b

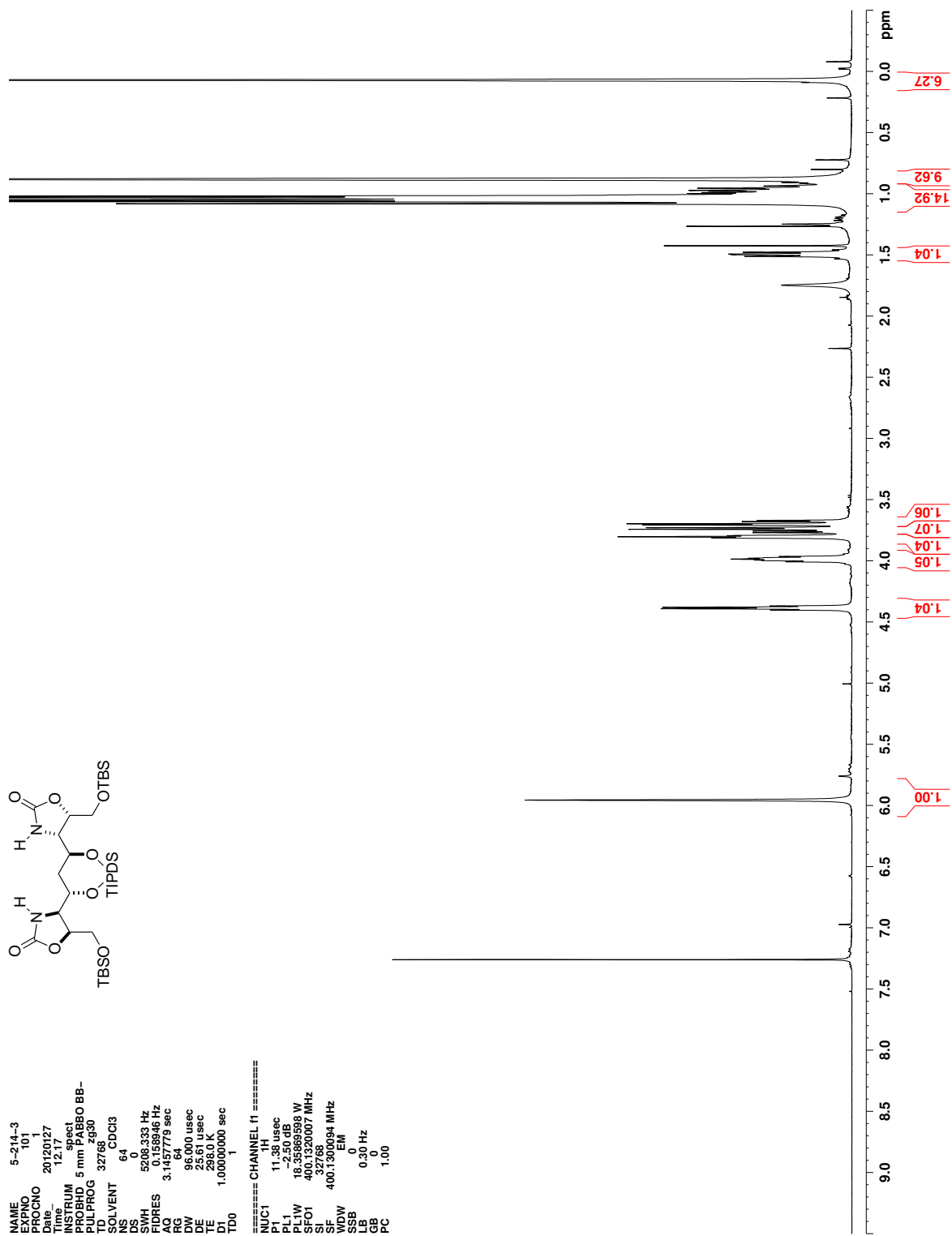


Figure C.175. ^1H NMR (CDCl_3) of 391

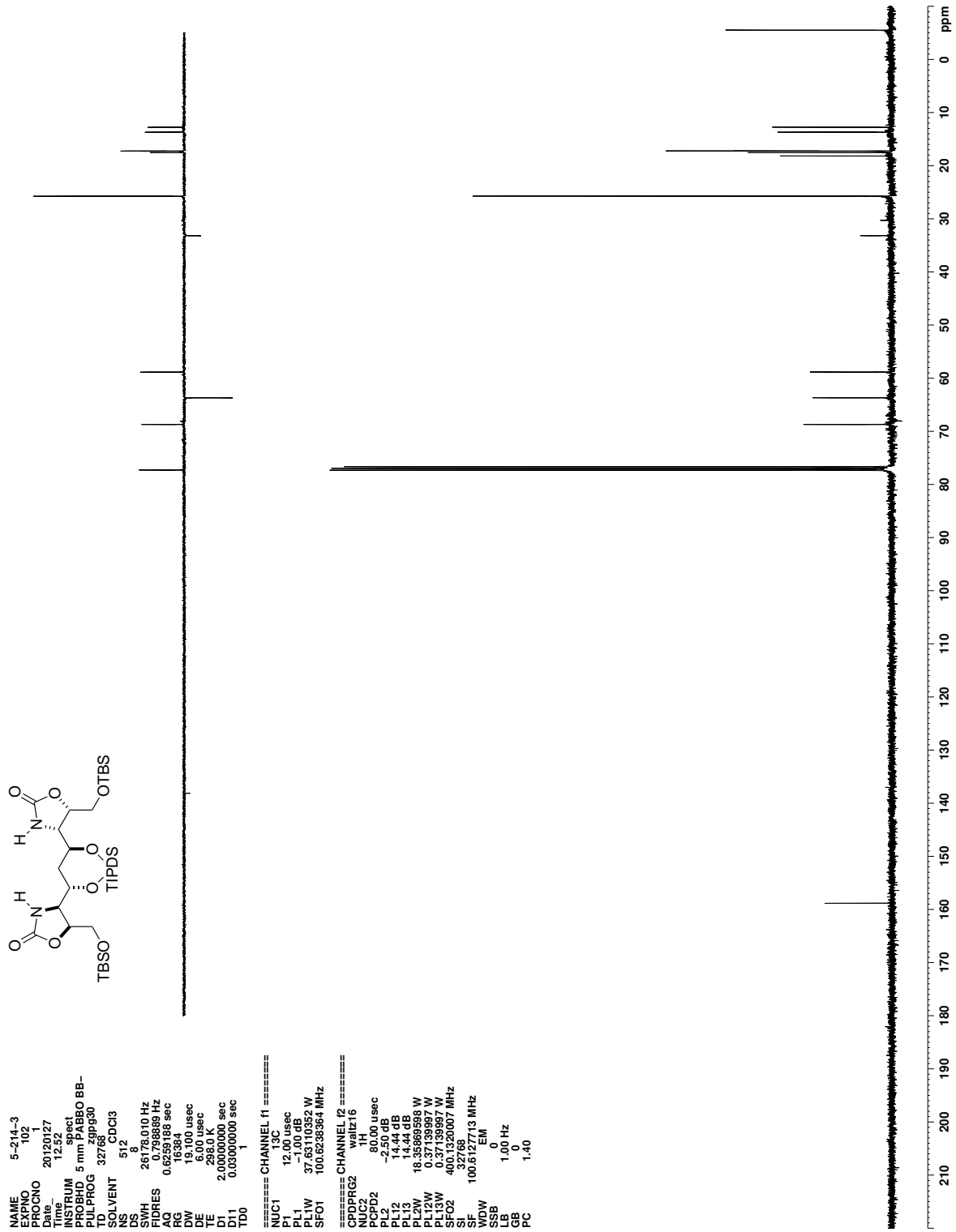


Figure C.176. ^{13}C NMR (CDCl_3) of 391

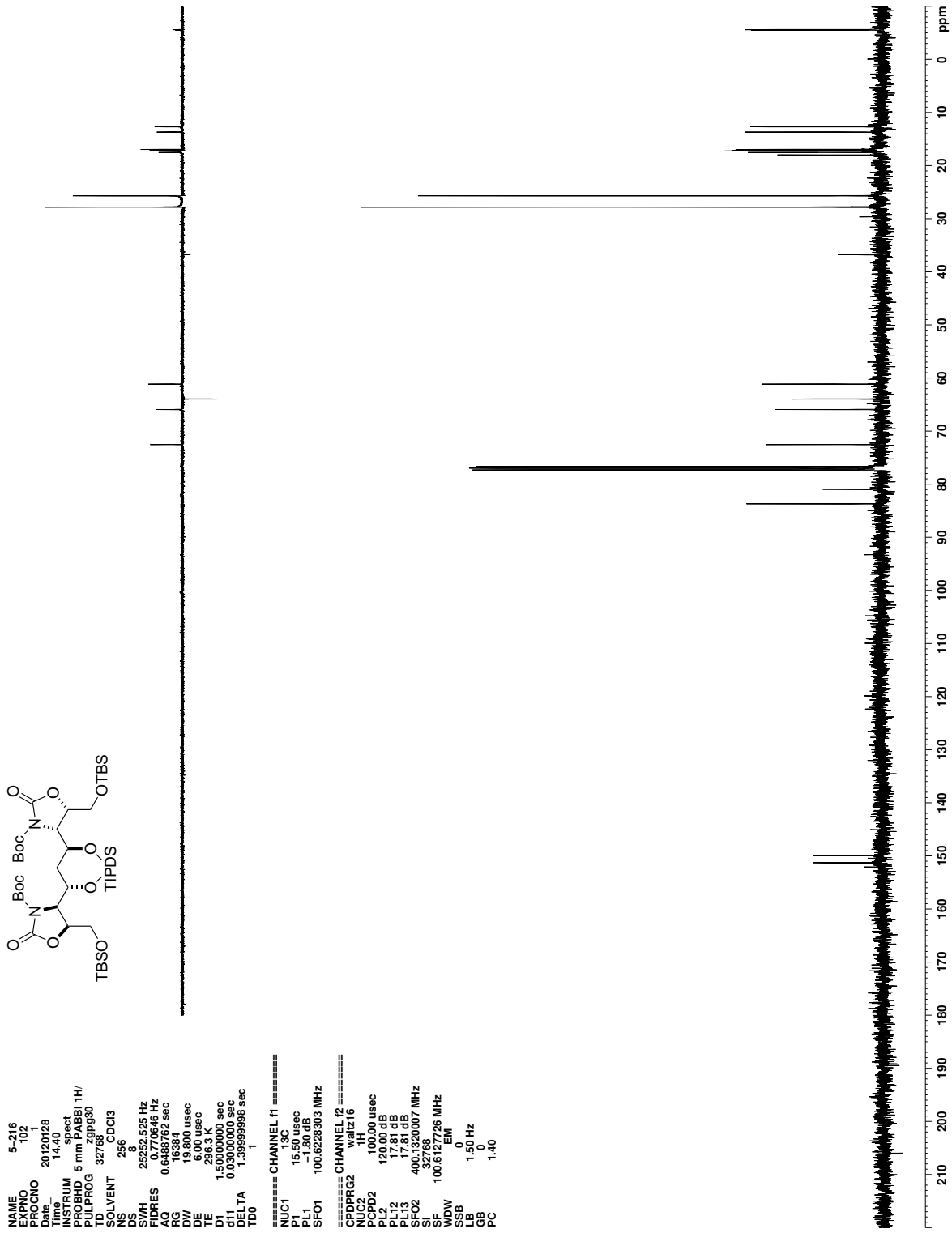


Figure C.178. ^{13}C NMR (CDCl_3) of 392

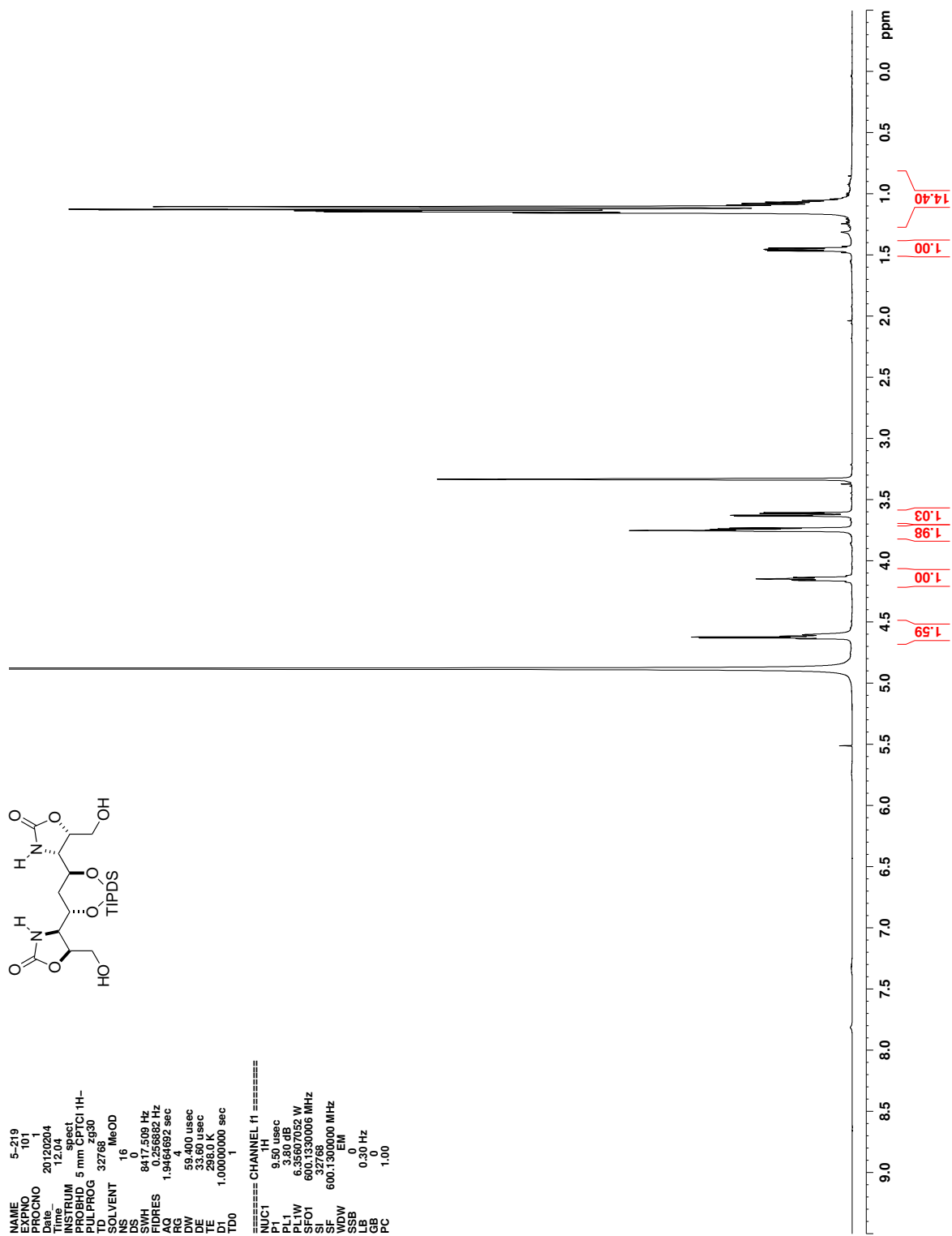


Figure C.179. ^1H NMR (CDCl_3) of 431

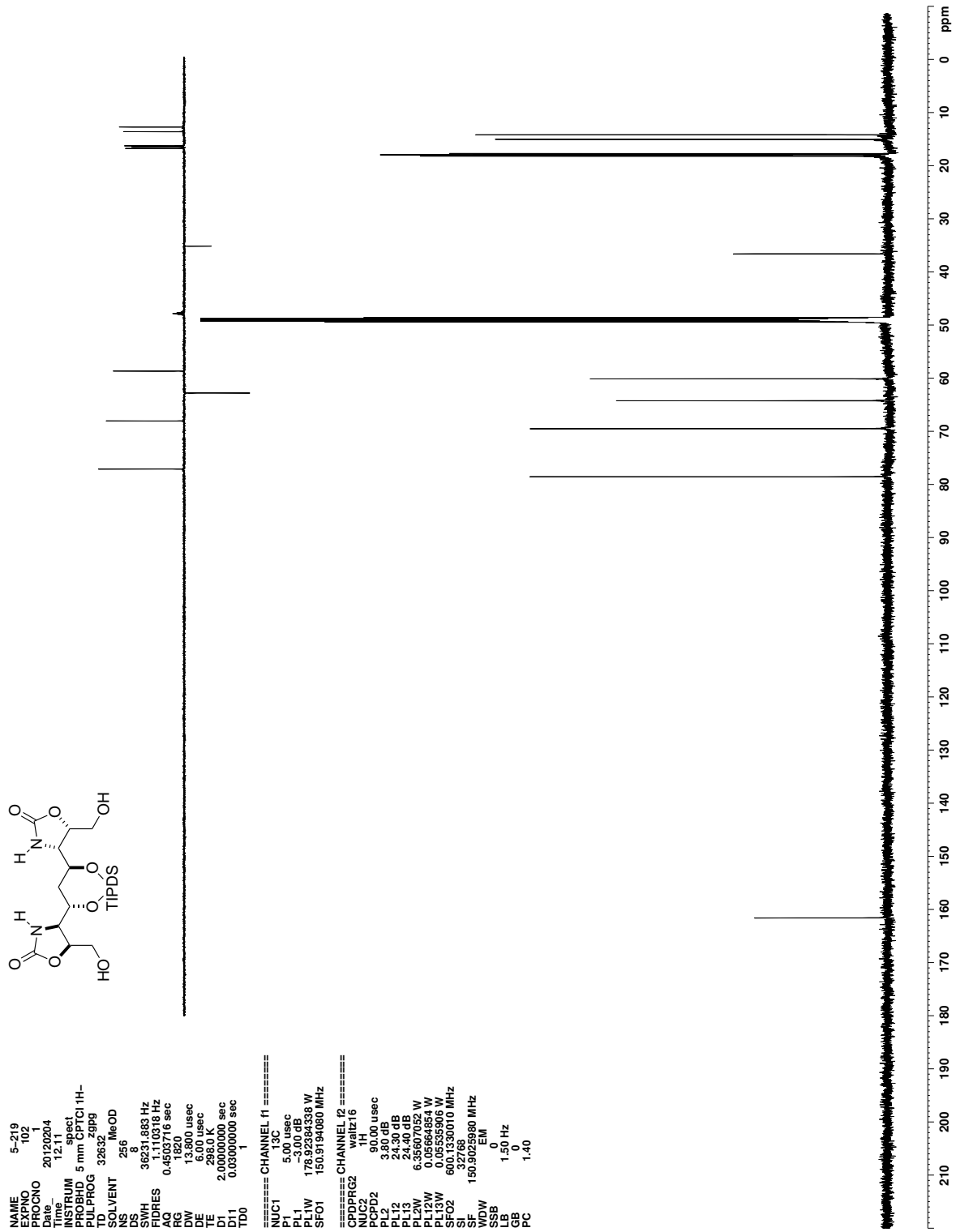


Figure C.180. ^{13}C NMR (CDCl_3) of 431

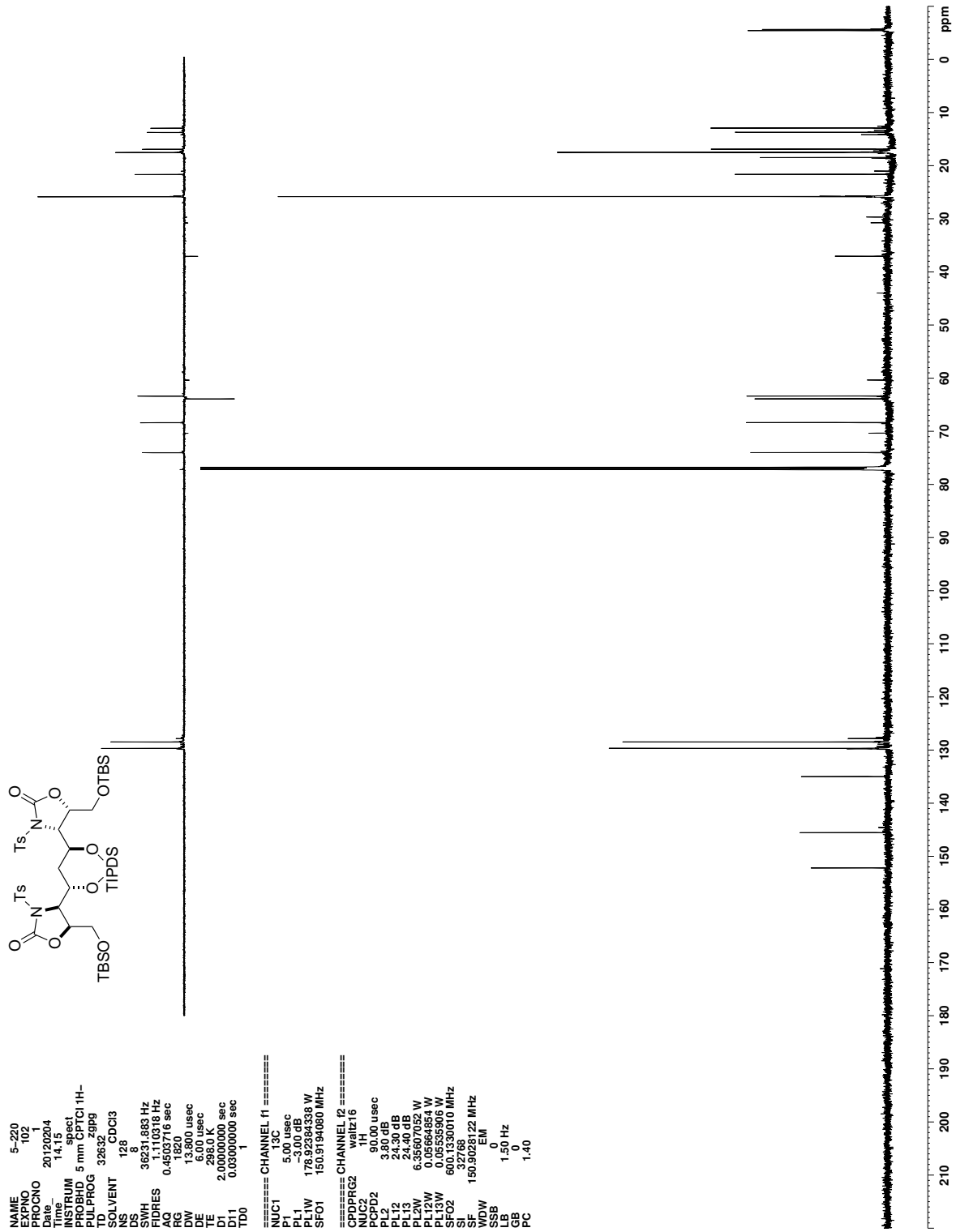


Figure C.182. ^{13}C NMR (CDCl_3) of 394

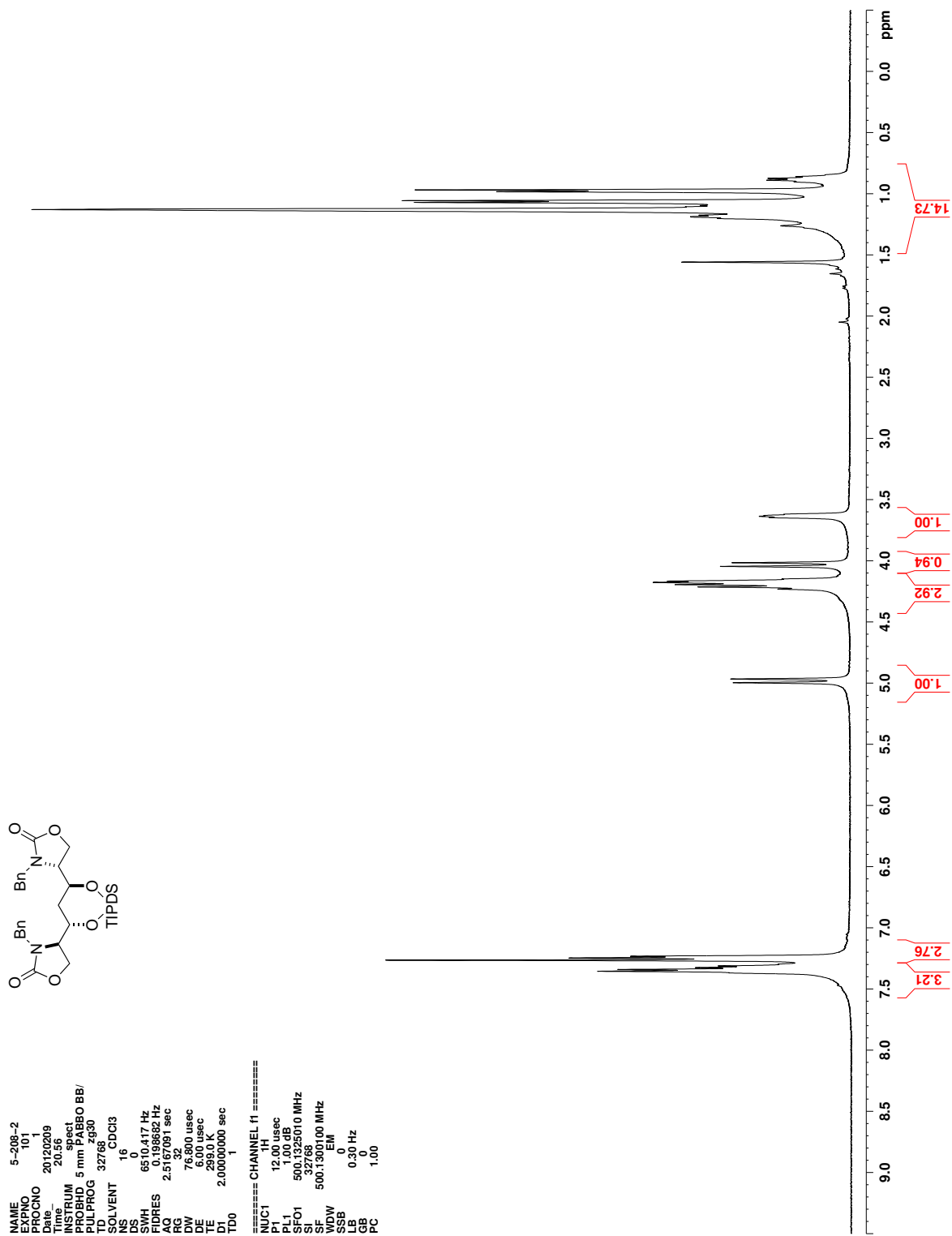


Figure C.185. ^1H NMR (CDCl_3) of 394

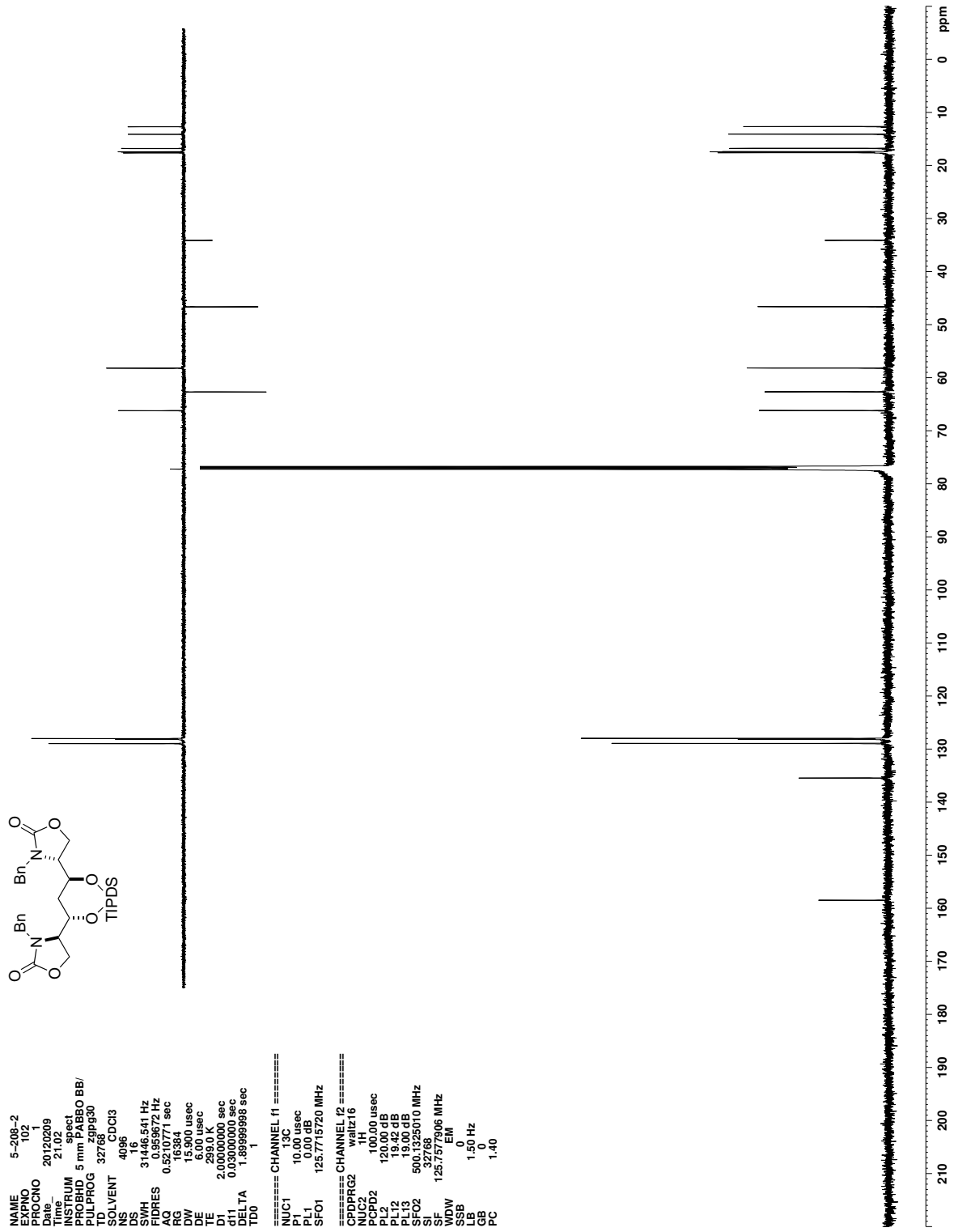


Figure C.186. ¹³C NMR (CDCl₃) of 394

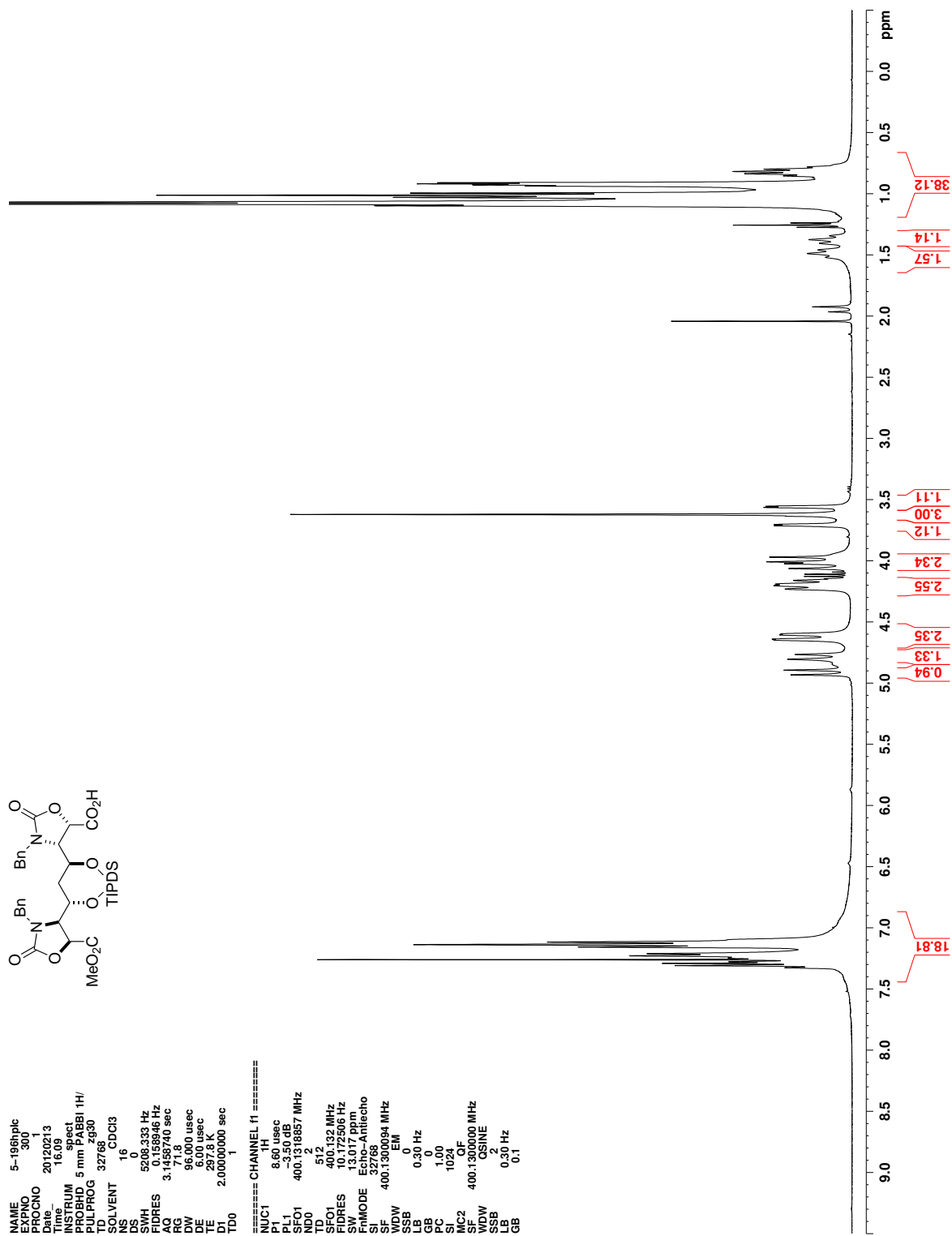


Figure C.187. ¹H NMR (CDCl₃) of 398

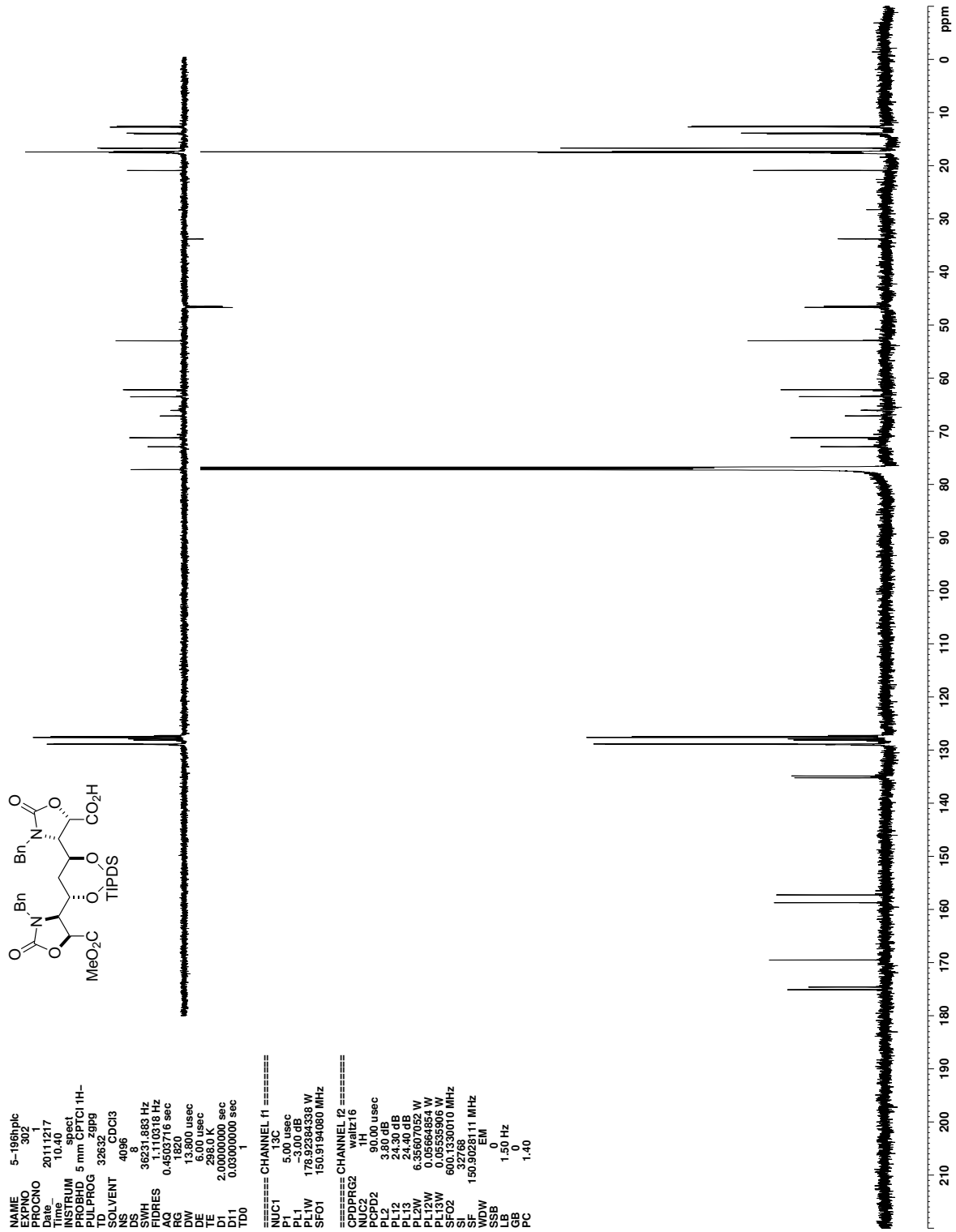


Figure C.188. ^{13}C NMR (CDCl_3) of 398

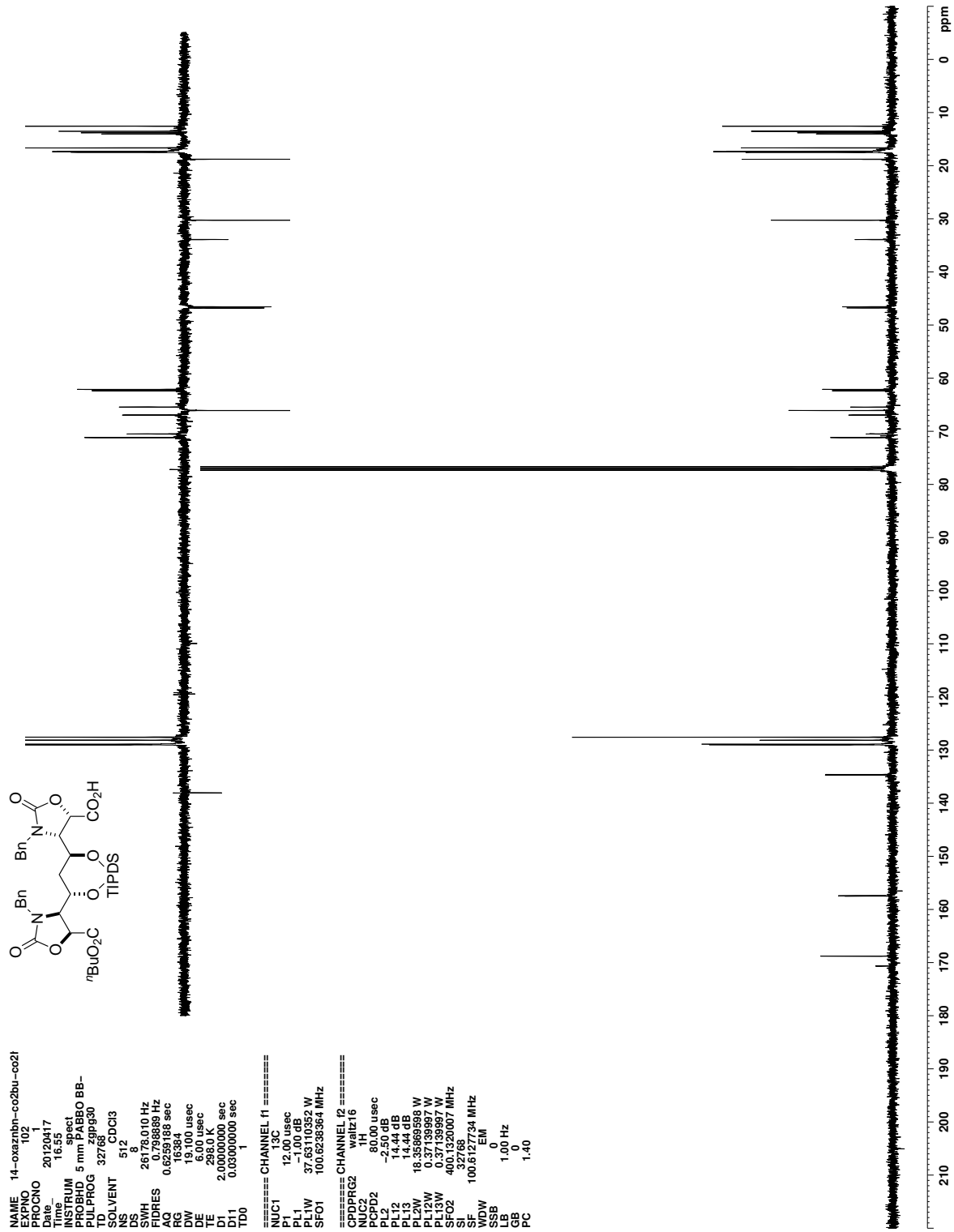


Figure C.190. ¹³C NMR (CDCl₃) of 399

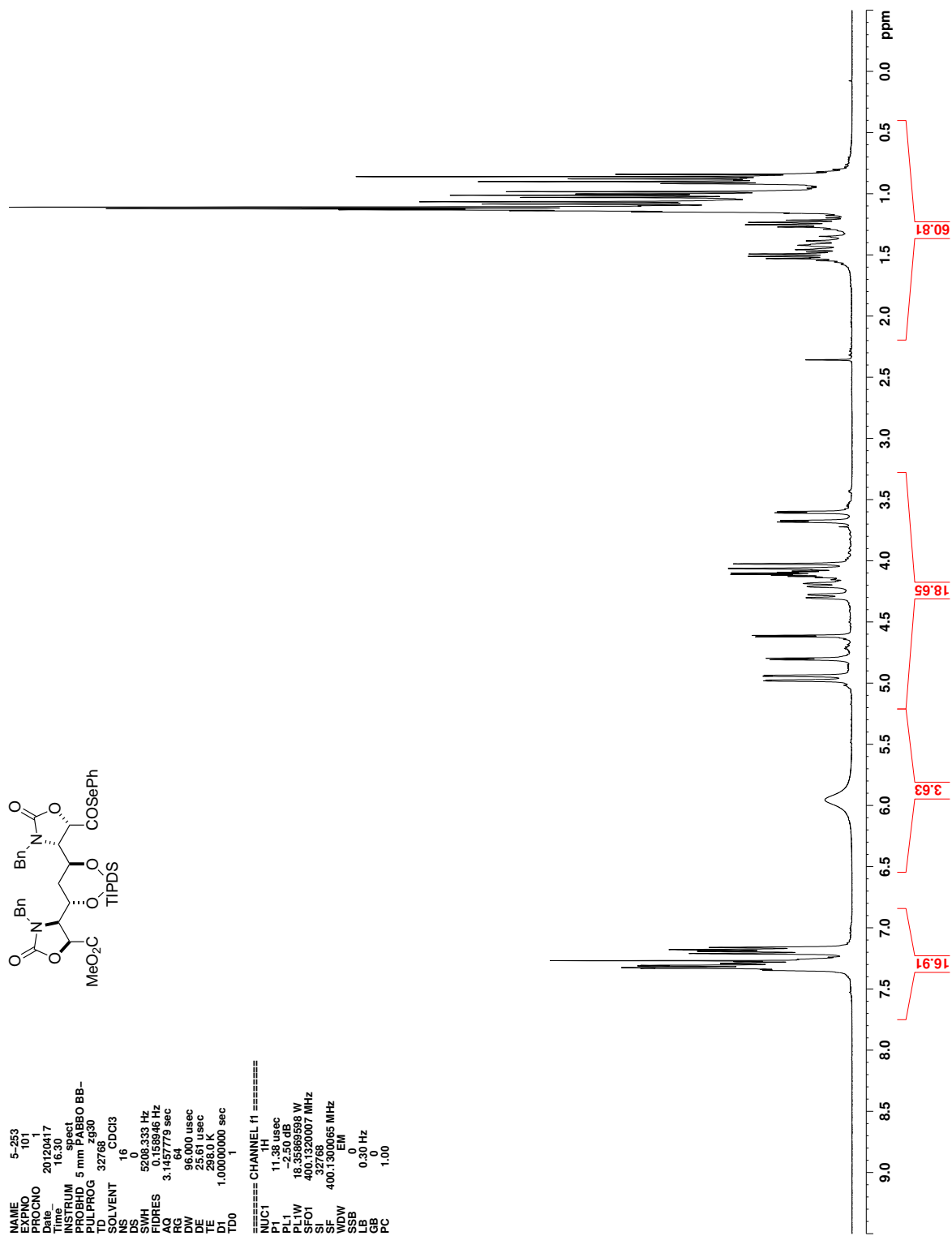


Figure C.191. ¹H NMR (CDCl₃) of 432

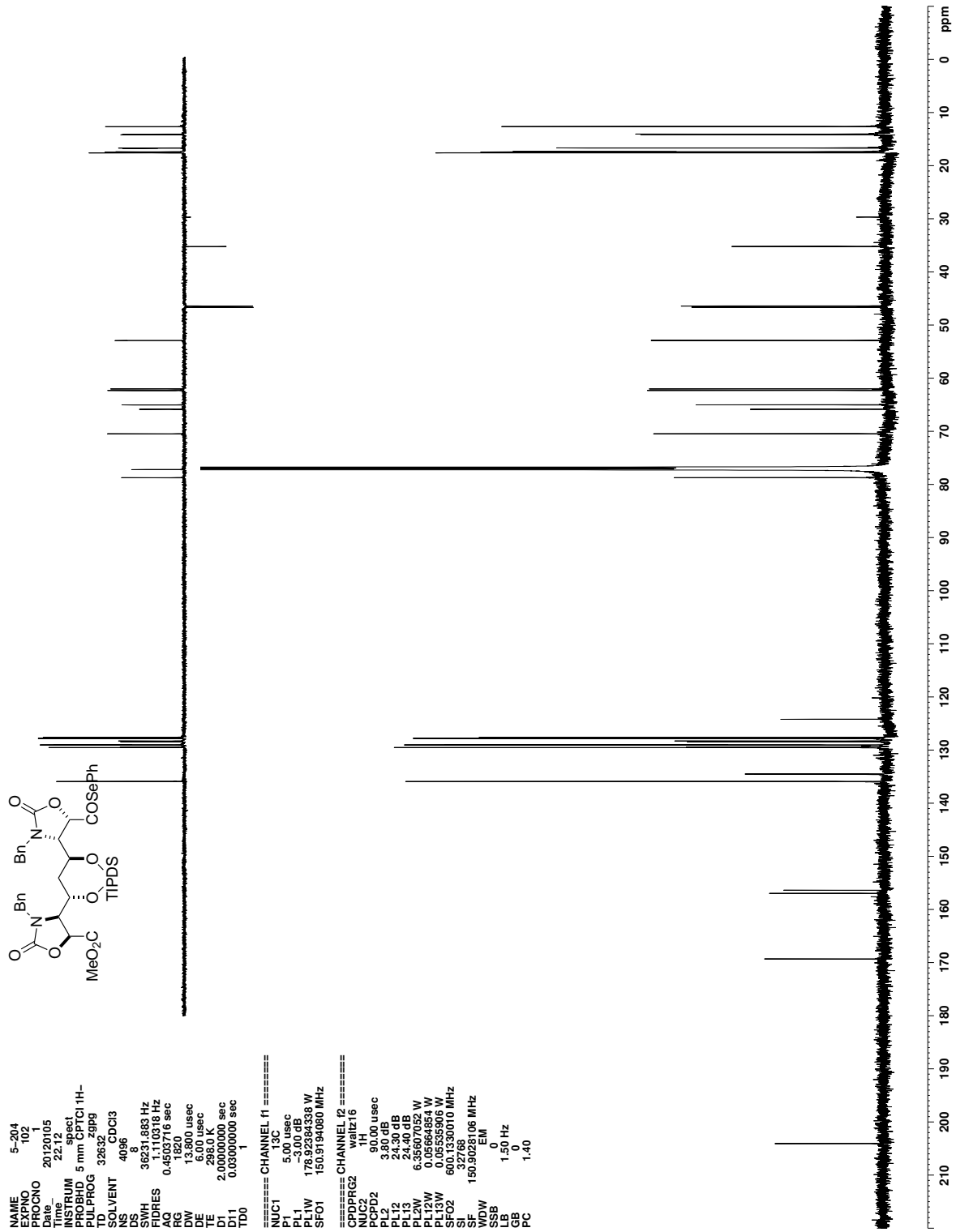


Figure C.192. ¹³C NMR (CDCl₃) of 432

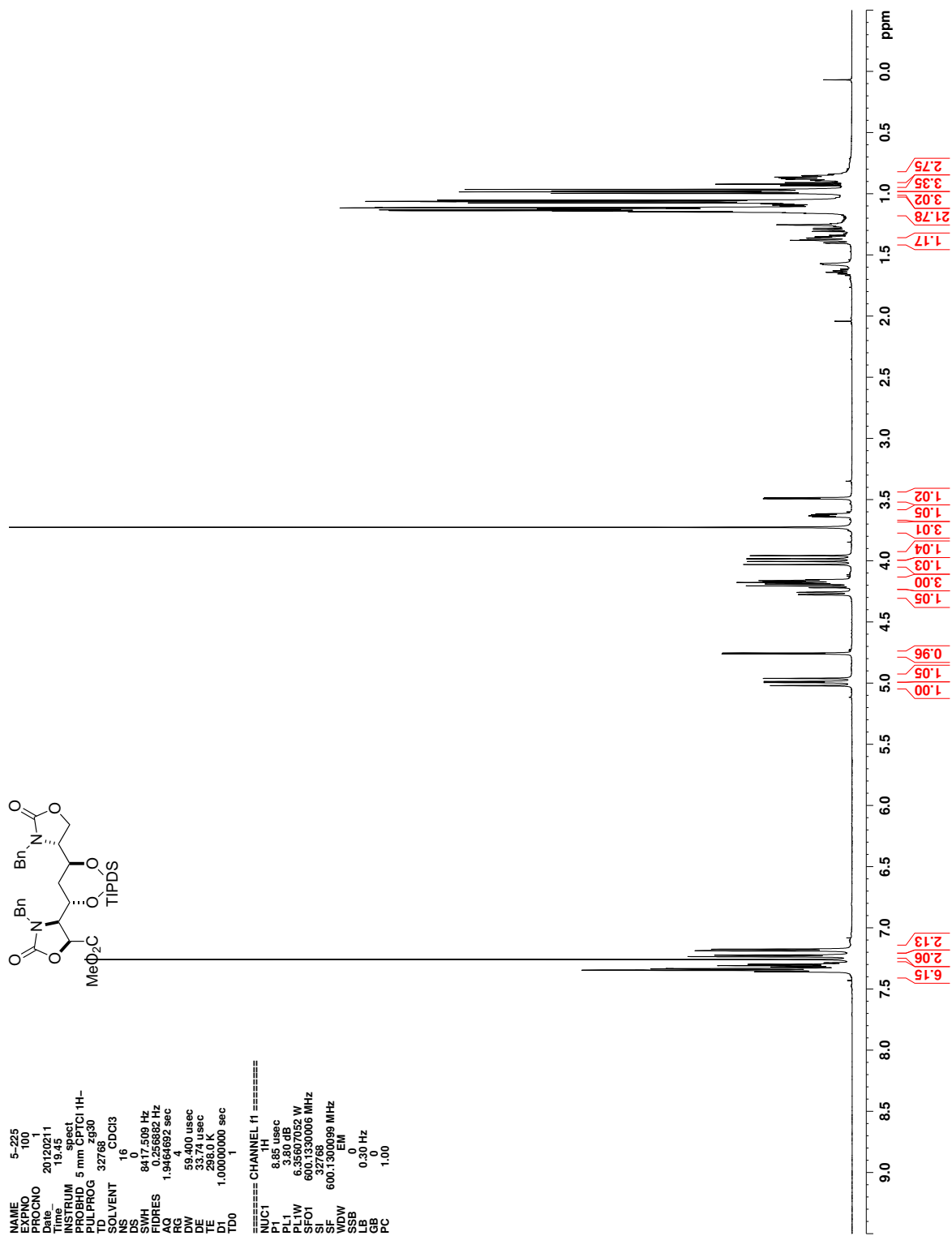


Figure C.193. ^1H NMR (CDCl_3) of 433

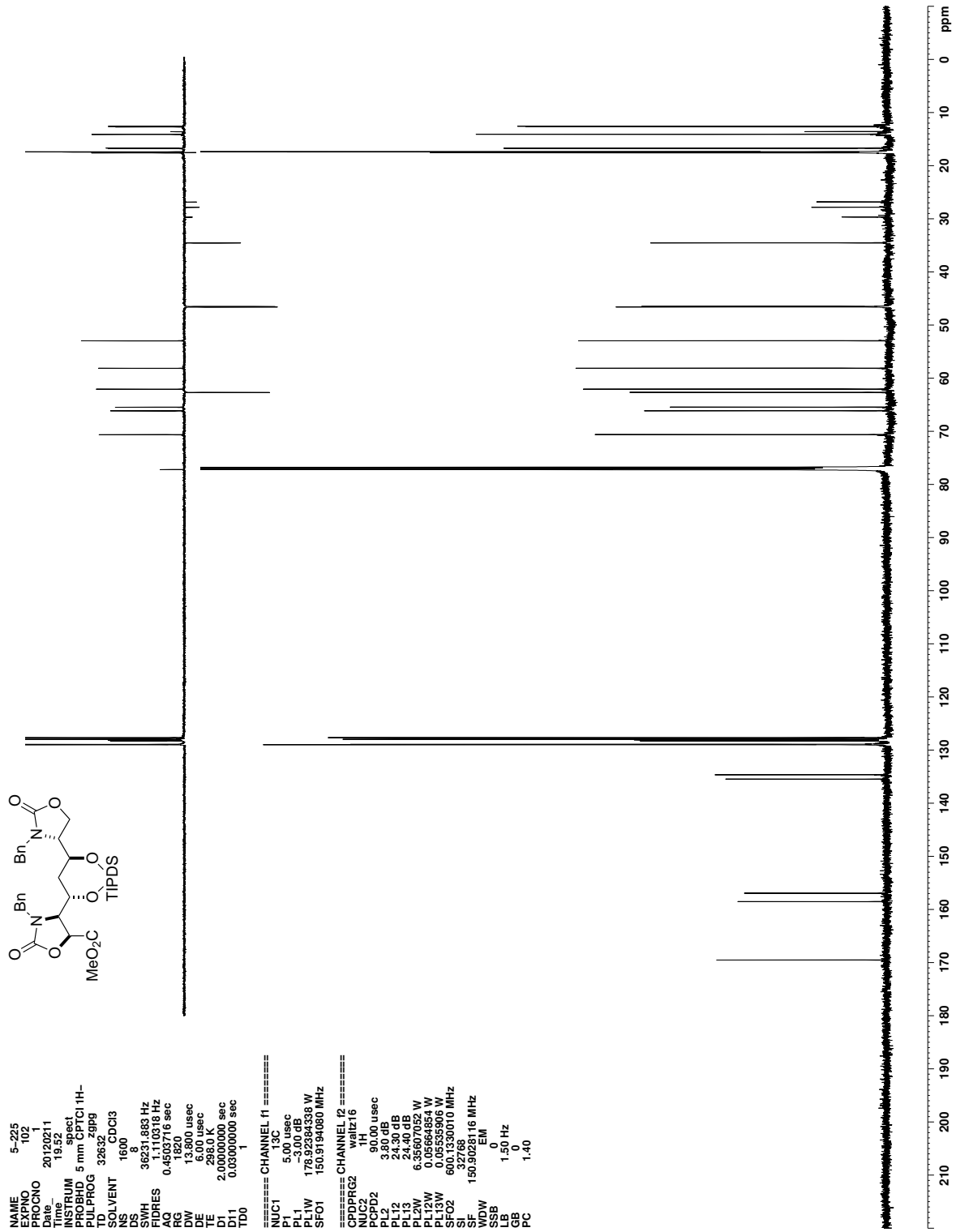


Figure C.194. ^{13}C NMR (CDCl_3) of 433

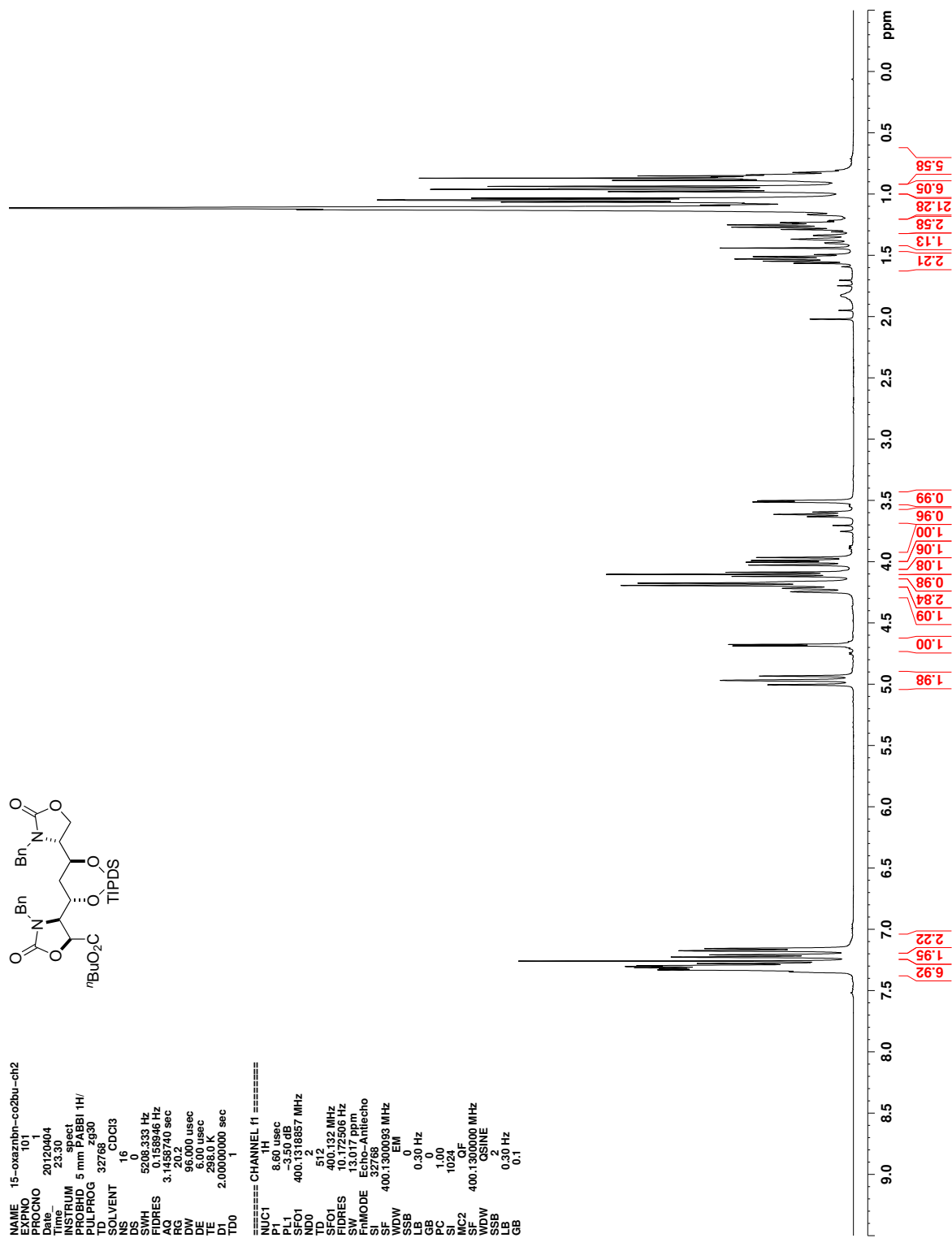


Figure C.195. ¹H NMR (CDCl₃) of 402

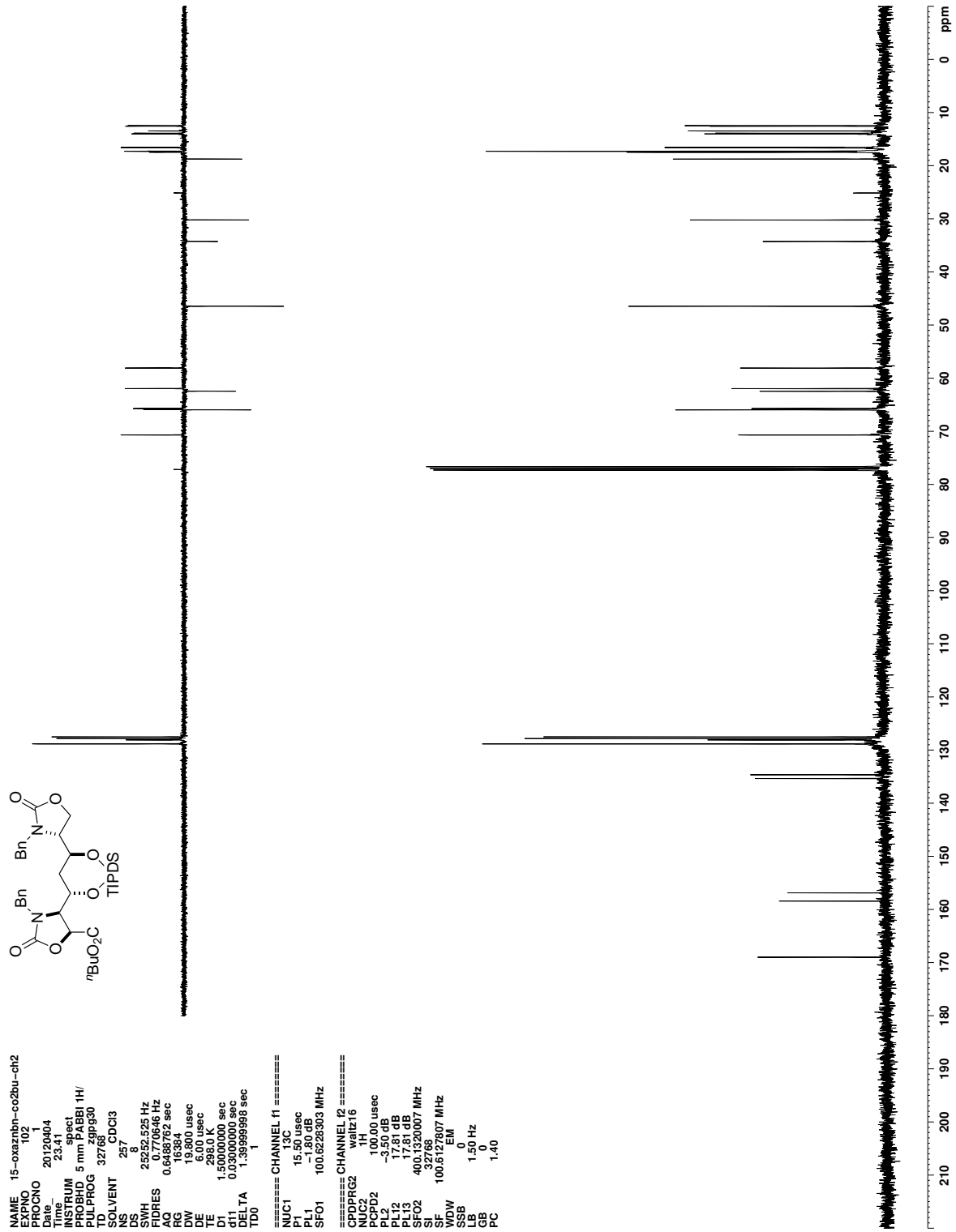


Figure C.196. ¹³C NMR (CDCl₃) of 402

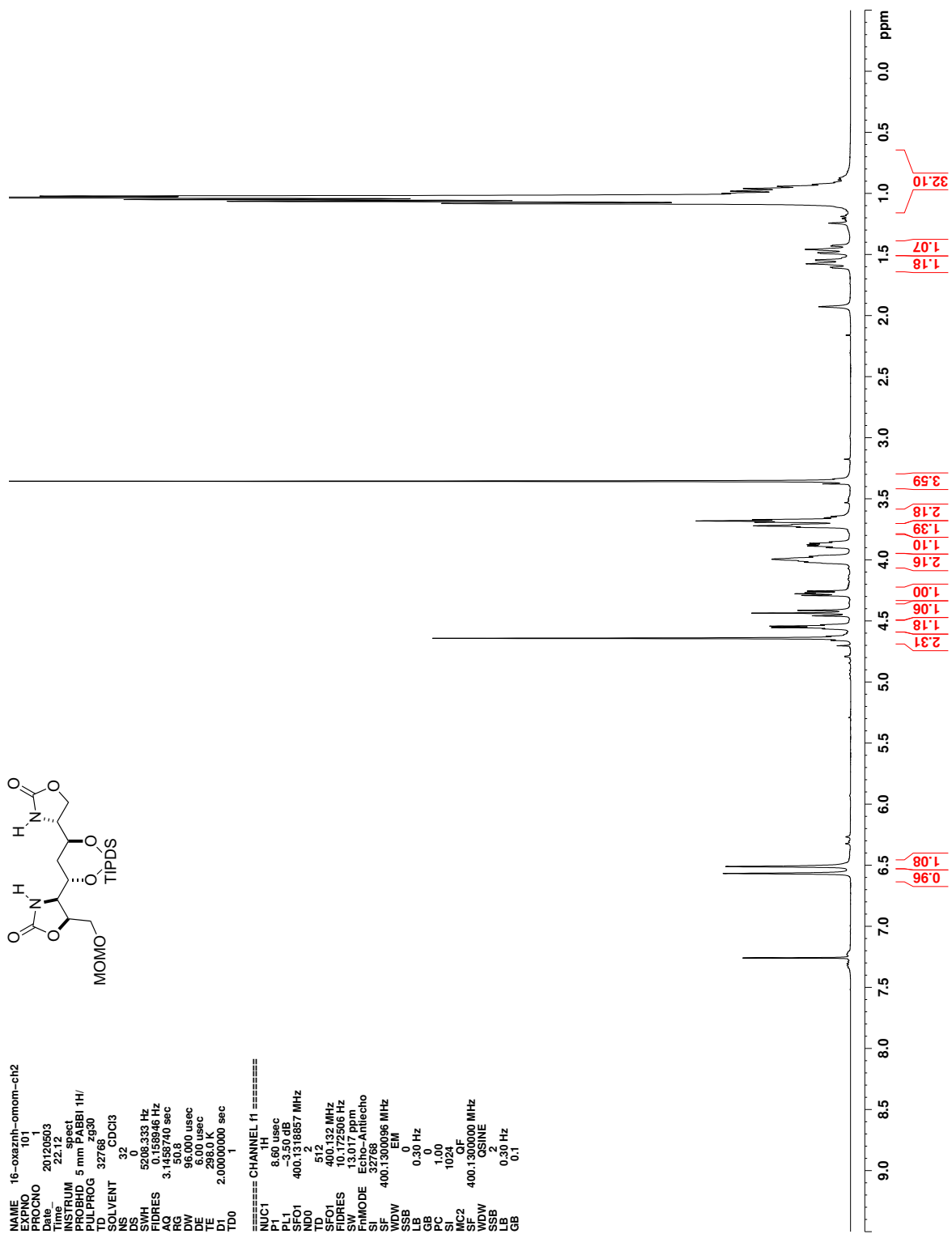


Figure C.197. ^1H NMR (CDCl_3) of 404

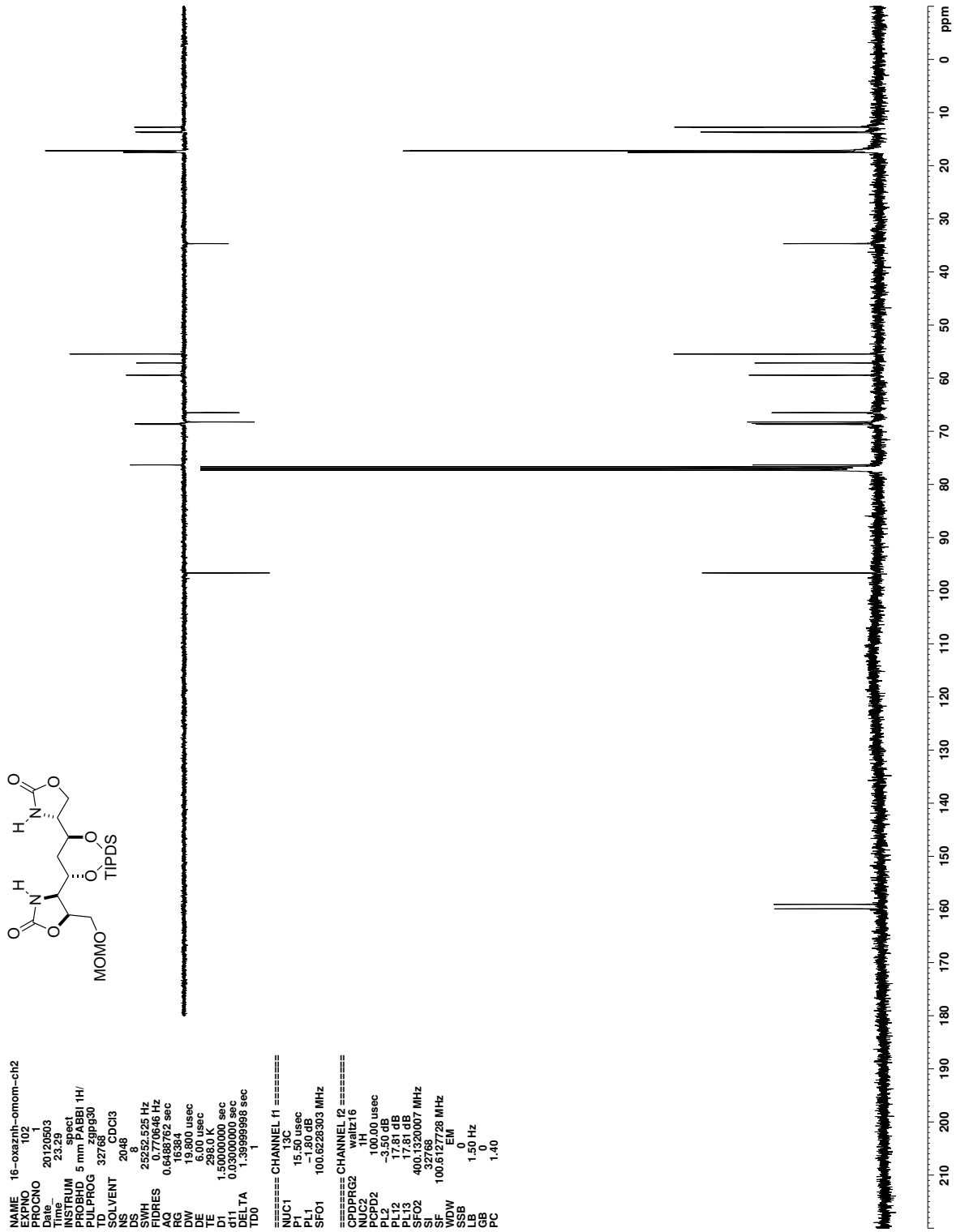


Figure C.198. ^{13}C NMR (CDCl_3) of 404

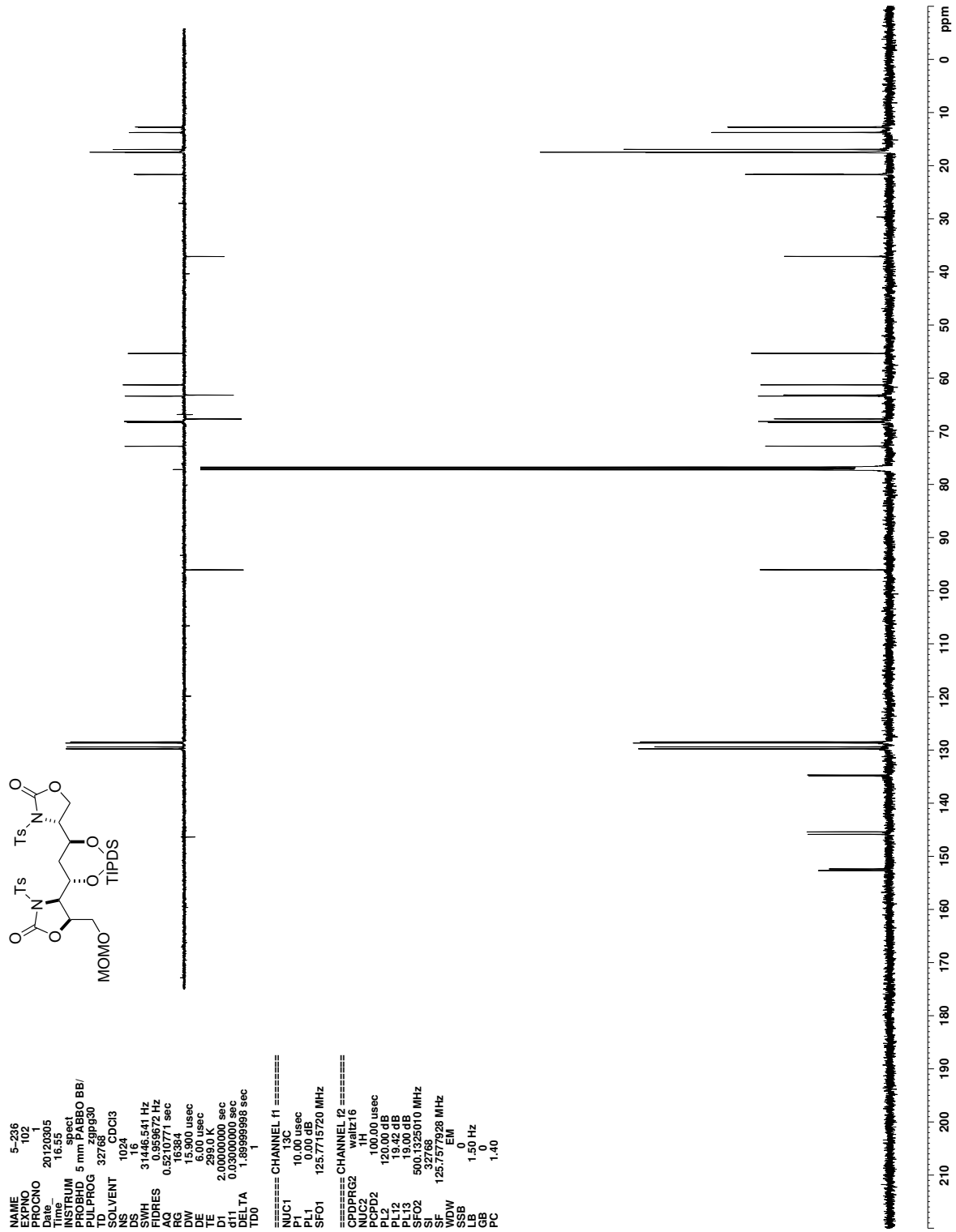


Figure C.200. ^{13}C NMR (CDCl_3) of 405

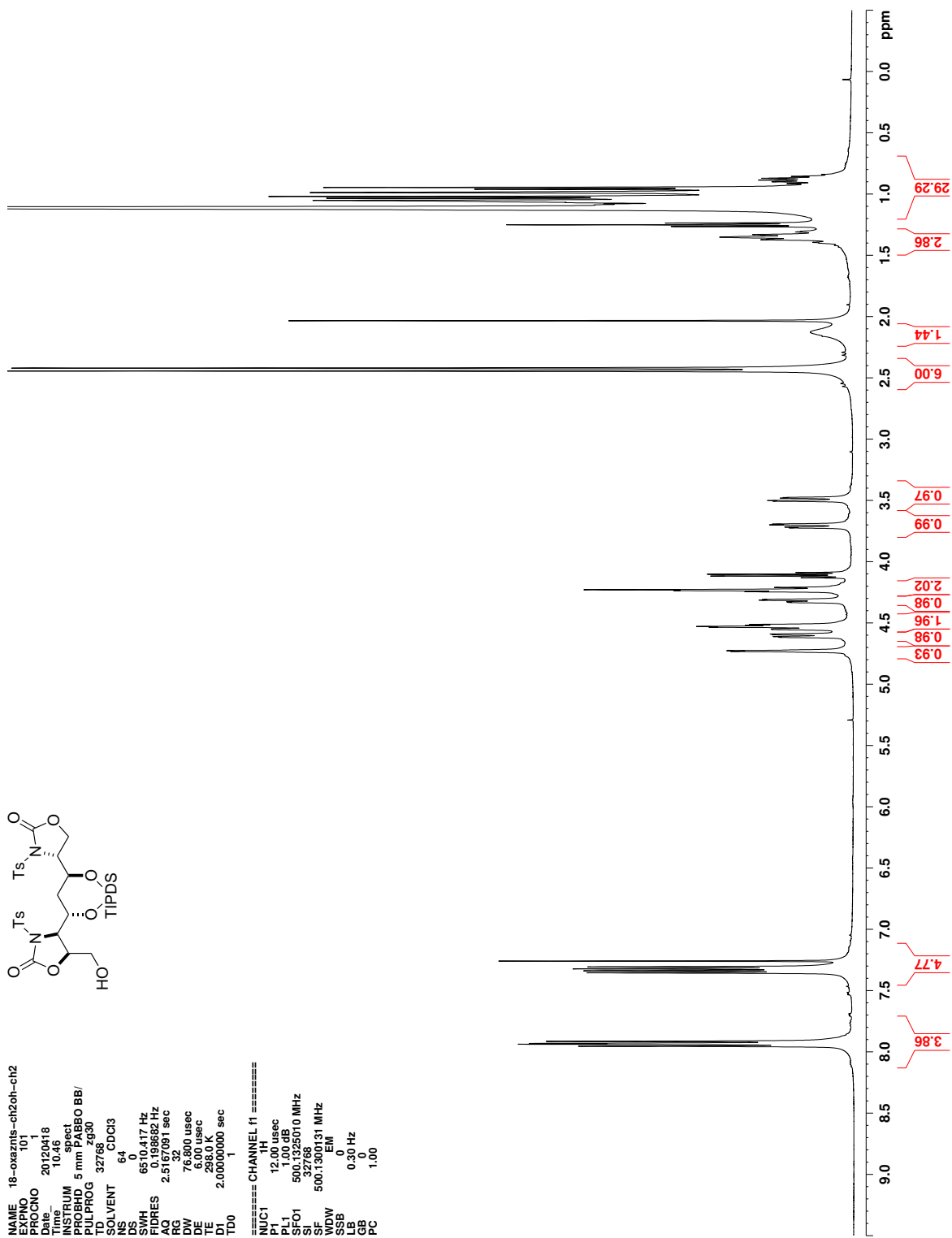


Figure C.201. ^1H NMR (CDCl_3) of 406

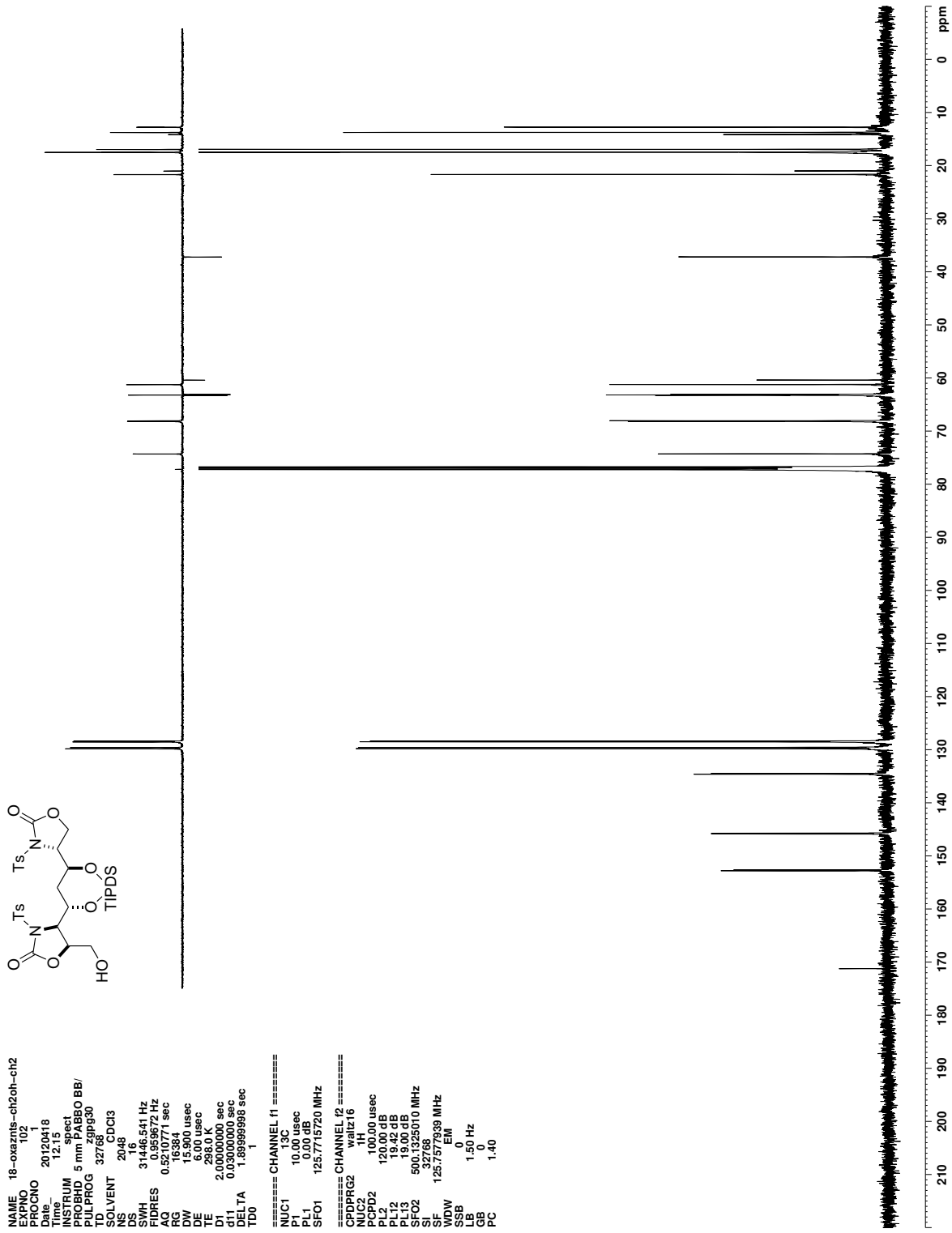


Figure C.202. ¹³C NMR (CDCl₃) of 406

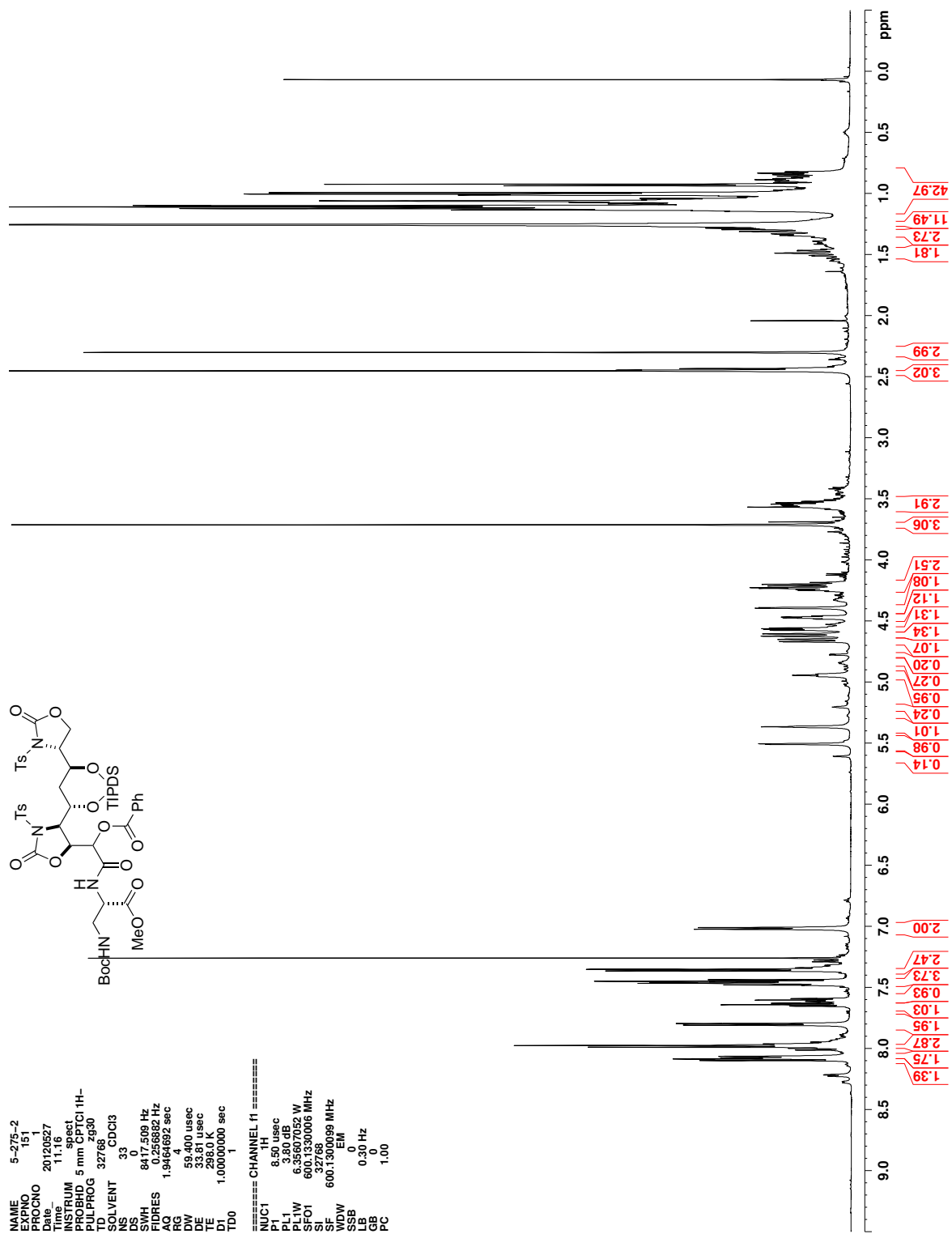


Figure C.203. ^1H NMR (CDCl_3) of 408

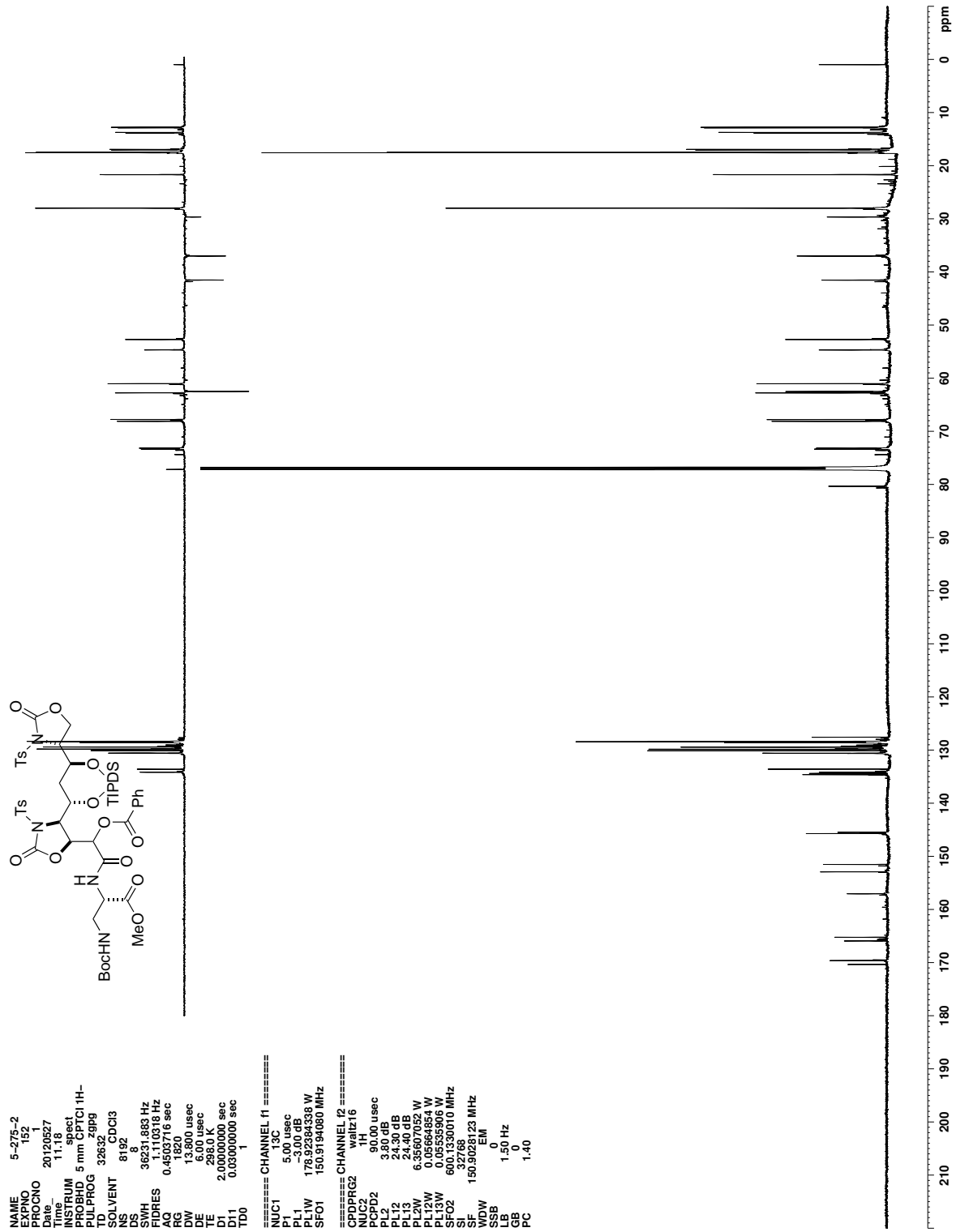


Figure C.204. ^{13}C NMR (CDCl_3) of 408

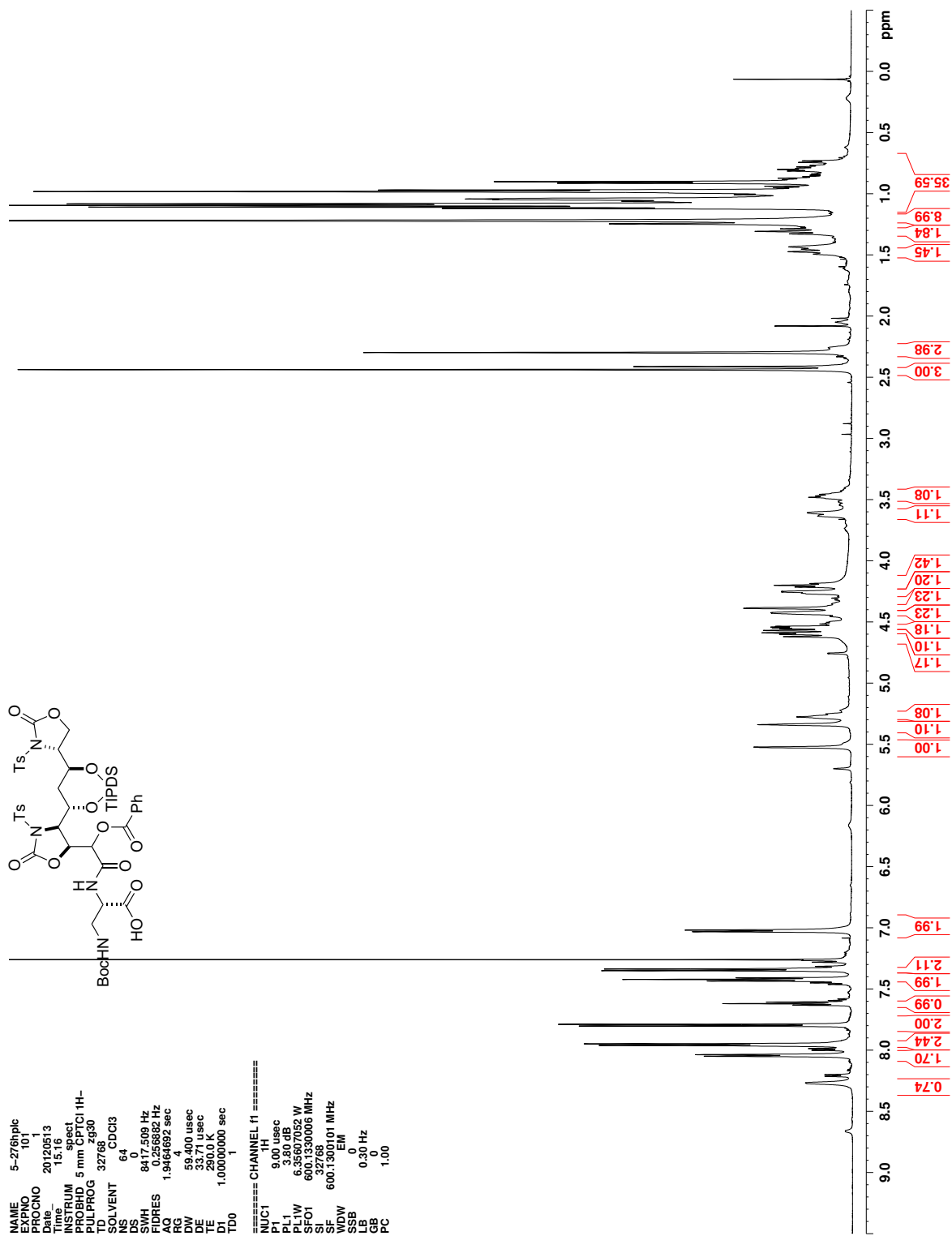


Figure C.205. ^1H NMR (CDCl_3) of 409

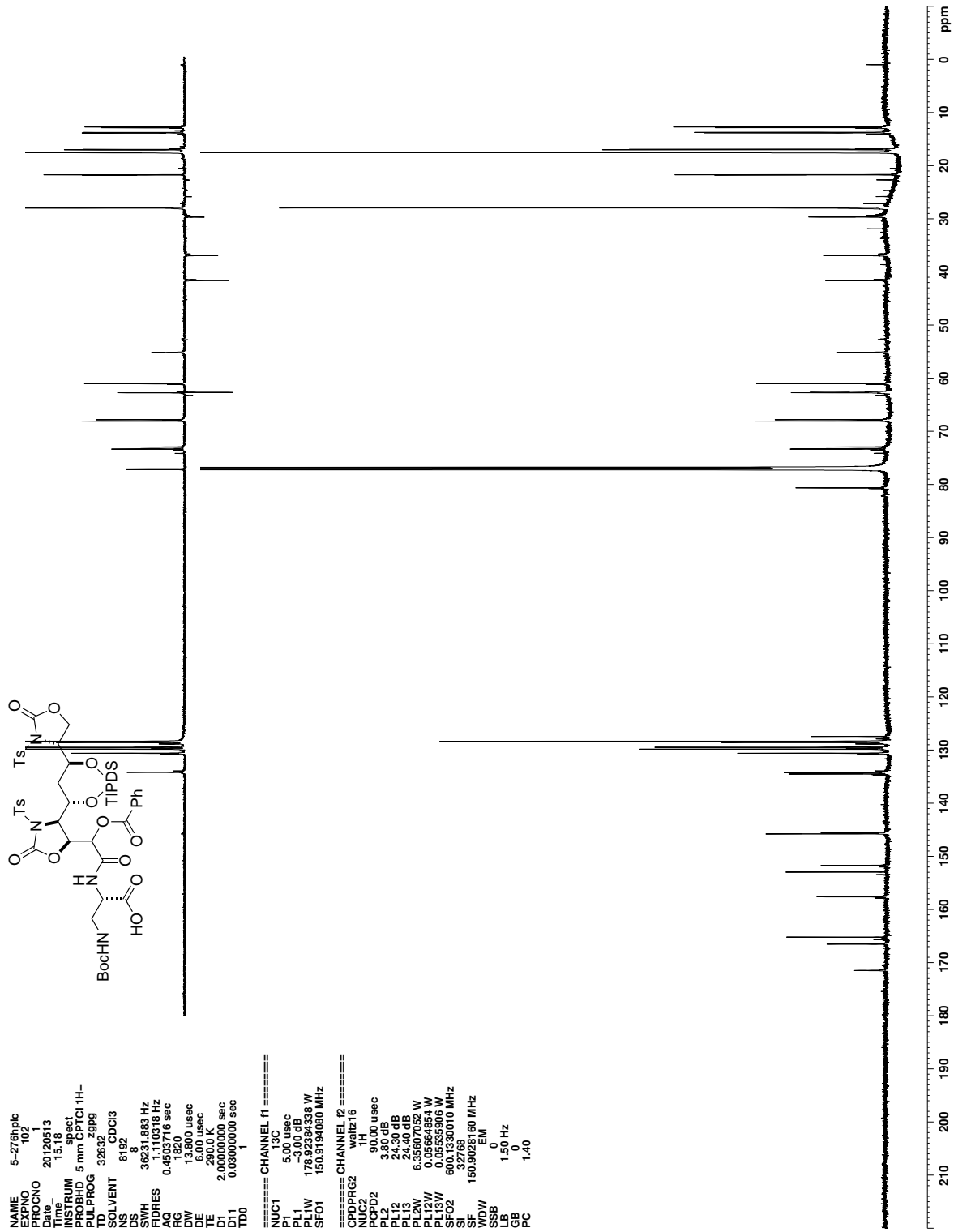


Figure C.206. ^{13}C NMR (CDCl_3) of 409

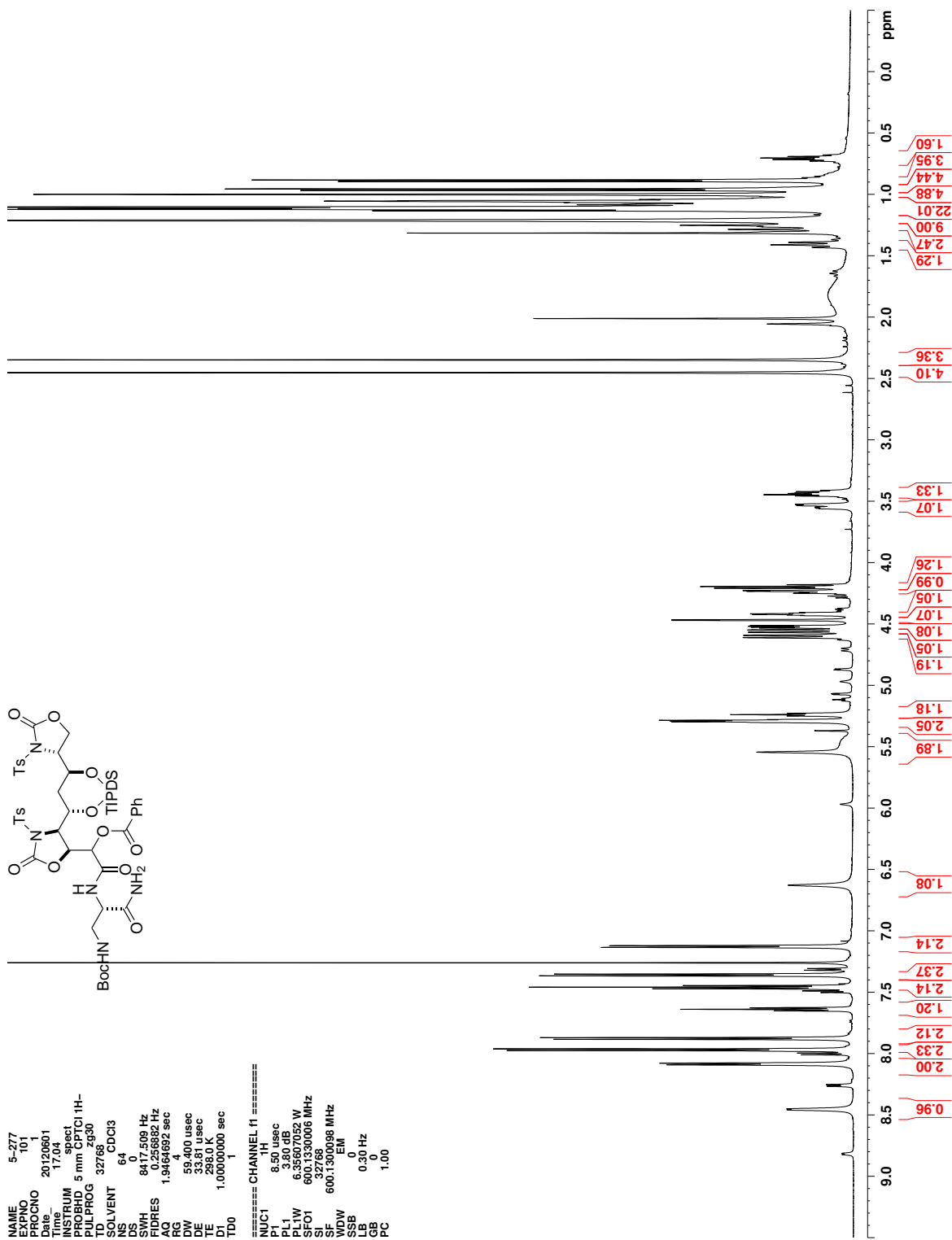


Figure C.207. ^1H NMR (CDCl_3) of 410

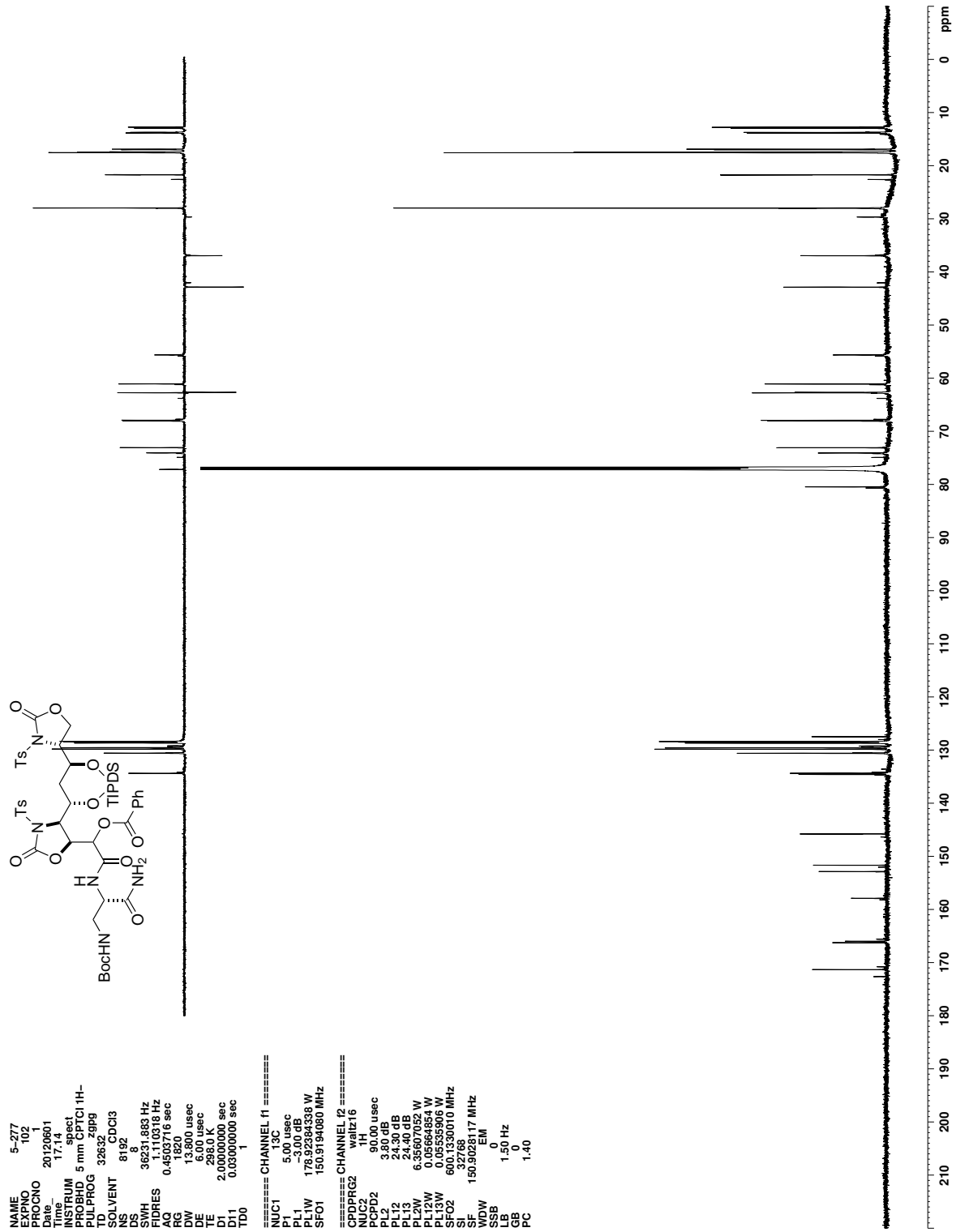


Figure C.208. ^{13}C NMR (CDCl_3) of 410

References

- [1] Curtius, T. *Ber. Dtsch. Chem. Ges.* **1883**, *16*, 2230–2231.
- [2] Kano, T.; Hashimoto, T.; Maruoka, K. *J. Am. Chem. Soc.* **2006**, *128*, 2174–2175.
- [3] Li, W.; Wang, J.; Hu, X.; Shen, K.; Wang, W.; Chu, Y.; Lin, L.; Liu, X.; Feng, X. *J. Am. Chem. Soc.* **2010**, *132*, 8532–8533.
- [4] Davies, H. M. L.; Bois, J. D.; Yu, J.-Q. *Chem. Soc. Rev.* **2011**, *40*, 1855–1856.
- [5] Davies, H. M. L.; Manning, J. R. *Nature* **2008**, *451*, 417–424.
- [6] Davies, H. M. L.; Morton, D. *Chem. Soc. Rev.* **2011**, *40*, 1857–1869, and references therein.
- [7] Davies, H. M.; Yang, J.; Nikolai, J. *J. Organomet. Chem.* **2005**, *690*, 6111–6124.
- [8] Huang, H.; Wang, Y.; Chen, Z.; Hu, W. *Adv. Synth. Catal.* **2005**, *347*, 531–534.
- [9] Roy, M.-N.; Lindsay, V. N. G.; Charette, A. B. In *Stereoselective Synthesis 1: Stereoselective Reactions of Carbon–Carbon Double Bonds*; Vries, J. G. D., Ed.; Georg Thieme Verlag KG: Stuttgart, 2011; Chapter 1.14 Cyclopropanation, pp 731–819.
- [10] Mazet, C.; Koehler, V.; Pfaltz, A. *Angew. Chem. Int. Ed.* **2005**, *44*, 4888–4891.
- [11] Austin, W. F.; Zhang, Y.; Danheiser, R. L. *Org. Lett.* **2005**, *7*, 3905–3908.
- [12] Regitz, M.; Maas, G. *Diazo compounds: properties and synthesis*; Academic Press, Inc.: Orlando, FL, 1986.
- [13] Patai, S. *The Chemistry of diazonium and diazo groups*; J. Wiley, 1978.
- [14] Doyle, M. P.; McKervey, M. A.; Ye, T. *Modern catalytic methods for organic synthesis with diazo compounds : from cyclopropanes to ylides*; Wiley: New York; Chichester, 1998.
- [15] Maas, G. *Angew. Chem. Int. Ed.* **2009**, *48*, 8186–8195.
- [16] Regitz, M. *Angew. Chem. Int. Ed. Eng.* **1967**, *6*, 733–749.
- [17] Regitz, M.; Bartz, W. *Chem. Ber.* **1970**, *103*, 1477–1485.
- [18] Koskinen, A. M. P.; Munoz, L. *J. Chem. Soc. Chem. Commun.* **1990**, 652–653.
- [19] Davies, H. M. L.; Cantrell, J.; William, R.; Romines, R., Karen; Baum, J. S. *Org. Synth.* **1992**, *70*, 93.
- [20] Hazen, G. G.; Weinstock, L. M.; Connell, R.; Bollinger, F. W. *Synth. Commun.* **1981**, *11*, 947–956.
- [21] Baum, J. S.; Shook, D. A.; Davies, H. M. L.; Smith, H. D. *Synth. Commun.* **1987**, *17*, 1709–1716.

- [22] Kitamura, M.; Tashiro, N.; Miyagawa, S.; Okauchi, T. *Synthesis* **2011**, *2011*, 1037–1044.
- [23] Doyle, M. P.; Dorow, R. L.; Terpstra, J. W.; Rodenhouse, R. A. *J. Org. Chem.* **1985**, *50*, 1663–1666.
- [24] Danheiser, R. L.; Miller, R. F.; Brisbois, R. G.; Park, S. Z. *J. Org. Chem.* **1990**, *55*, 1959–1964.
- [25] Arnold, B.; Regitz, M. *Angew. Chem. Int. Ed. Eng.* **1979**, *18*, 320–320.
- [26] Forster, M. O. *J. Chem. Soc., Trans.* **1915**, *107*, 260–267.
- [27] Corey, E.; Myers, A. G. *Tetrahedron Lett.* **1984**, *25*, 3559–3562.
- [28] House, H. O.; Blankley, C. J. *J. Org. Chem.* **1968**, *33*, 53–60.
- [29] Toma, T.; Shimokawa, J.; Fukuyama, T. *Org. Lett.* **2007**, *9*, 3195–3197.
- [30] Creary, X.; Butchko, M. A. *J. Org. Chem.* **2001**, *67*, 112–118.
- [31] Aggarwal, V. K.; de Vicente, J.; Bonnert, R. V. *Org. Lett.* **2001**, *3*, 2785–2788.
- [32] Aggarwal, V. K.; Alonso, E.; Hynd, G.; Lydon, K. M.; Palmer, M. J.; Porcelloni, M.; Studley, J. R. *Angew. Chem. Int. Ed.* **2001**, *40*, 1430–1433.
- [33] Aggarwal, V. K.; de Vicente, J.; Bonnert, R. V. *J. Org. Chem.* **2003**, *68*, 5381–5383.
- [34] Aggarwal, V. K.; Alonso, E.; Bae, I.; Hynd, G.; Lydon, K. M.; Palmer, M. J.; Patel, M.; Porcelloni, M.; Richardson, J.; Stenson, R. A.; Studley, J. R.; Vasse, J.-L.; Winn, C. L. *J. Am. Chem. Soc.* **2003**, *125*, 10926–10940.
- [35] Fulton, J. R.; Aggarwal, V. K.; Vicente, J. d. *Eur. J. Org. Chem.* **2005**, *2005*, 1479–1492.
- [36] Arndt, F. *Org. Synth.* **1935**, *15*, 3.
- [37] Proctor, L. D.; Warr, A. J. *Org. Process Res. Dev.* **2002**, *6*, 884–892.
- [38] Sweeney, J. *Eur. J. Org. Chem.* **2009**, 4911–4919.
- [39] Sweeney, J. B. *Chem. Soc. Rev.* **2002**, *31*, 247–258.
- [40] Gabriel, S. *Dtsch. Chem. Ges.* **1888**, *21*, 1049.
- [41] Muchalski, H.; Johnston, J. N. In *Stereoselective Synthesis 1: Stereoselective Reactions of Carbon–Carbon Double Bonds*; Vries, J. G. D., Ed.; Georg Thieme Verlag KG: Stuttgart, 2011; Chapter 1.4 Aziridination, pp 155–185.
- [42] Muller, P.; Fruit, C. *Chem. Rev.* **2003**, *103*, 2905–2920.
- [43] Hubert, A. J.; Feron, A.; Warin, R.; Teyssie, P. *Tetrahedron Lett.* **1976**, *17*, 1317–1318.
- [44] Bartnik, R.; Mloston, G. *Synthesis* **1983**, 924–925.
- [45] Bartnik, R.; Mloston, G. *Tetrahedron* **1984**, *40*, 2569–2576.

- [46] Rasmussen, K. G.; Jorgensen, K. A. *J. Chem. Soc. Chem. Commun.* **1995**, 1401–1402.
- [47] Hansen, K. B.; Finney, N. S.; Jacobsen, E. N. *Angew. Chem. Int. Ed. Eng.* **1995**, *34*, 676–678.
- [48] Casarrubios, L.; Perez, J. A.; Brookhart, M.; Templeton, J. L. *J. Org. Chem.* **1996**, *61*, 8358–8359.
- [49] Rasmussen, K. G.; Jorgensen, K. A. *J. Chem. Soc., Perkin Trans. 1* **1997**, 1287–1292.
- [50] Rasmussen, K. G.; Hazell, R. G.; Jorgensen, K. A. *Chem. Commun.* **1997**, 1103–1104.
- [51] Rasmussen, K. G.; Juhl, K.; Hazell, R. G.; Jorgensen, K. A. *J. Chem. Soc., Perkin Trans. 2* **1998**, 1347–1350.
- [52] Juhl, K.; Hazell, R. G.; Jorgensen, K. A. *J. Chem. Soc., Perkin Trans. 1* **1999**, 2293–2297.
- [53] Antilla, J. C.; Wulff, W. D. *J. Am. Chem. Soc.* **1999**, *121*, 5099–5100.
- [54] Antilla, J. C.; Wulff, W. D. *Angew. Chem. Int. Ed.* **2000**, *39*, 4518–4521.
- [55] Patwardhan, A. P.; Pulgam, V. R.; Zhang, Y.; Wulff, W. D. *Angew. Chem. Int. Ed.* **2005**, *44*, 6169–6172.
- [56] Zhang, Y.; Desai, A.; Lu, Z.; Hu, G.; Ding, Z.; Wulff, W. D. *Chem.–Eur. J.* **2008**, *14*, 3785–3803.
- [57] Zhang, Y.; Lu, Z.; Wulff, W. D. *Synlett* **2009**, 2715–2739.
- [58] Hu, G.; Huang, L.; Huang, R. H.; Wulff, W. D. *J. Am. Chem. Soc.* **2009**, *131*, 15615–15617.
- [59] Williams, A. L.; Johnston, J. N. *J. Am. Chem. Soc.* **2004**, *126*, 1612–1613.
- [60] Uraguchi, D.; Sorimachi, K.; Terada, M. *J. Am. Chem. Soc.* **2005**, *127*, 9360–9361.
- [61] Hashimoto, T.; Maruoka, K. *J. Am. Chem. Soc.* **2007**, *129*, 10054–10055.
- [62] Zhang, H.; Wen, X.; Gan, L.; Peng, Y. *Org. Lett.* **2012**, *14*, 2126–2129.
- [63] Akiyama, T.; Suzuki, T.; Mori, K. *Org. Lett.* **2009**, *11*, 2445–2447.
- [64] Hashimoto, T.; Uchiyama, N.; Maruoka, K. *J. Am. Chem. Soc.* **2008**, *130*, 14380–14381.
- [65] Zeng, X.; Zeng, X.; Xu, Z.; Lu, M.; Zhong, G. *Org. Lett.* **2009**, *11*, 3036–3039.
- [66] Desai, A. A.; Wulff, W. D. *J. Am. Chem. Soc.* **2010**, *132*, 13100–13103.
- [67] Hashimoto, T.; Nakatsu, H.; Watanabe, S.; Maruoka, K. *Org. Lett.* **2010**, *12*, 1668–1671, PMID: 20232814.
- [68] Hashimoto, T.; Nakatsu, H.; Yamamoto, K.; Maruoka, K. *J. Am. Chem. Soc.* **2011**, *133*, 9730–9733.
- [69] Huang, L.; Wulff, W. D. *J. Am. Chem. Soc.* **2011**, *133*, 8892–8895.

- [70] Troyer, T. L. Brønsted acid promoted additions of diazoalkanes to imines: the interplay of mechanism and stereochemical outcome as a tool to discover and develop a new *syn*-glycolate Mannich reaction. Ph.D. thesis, Vanderbilt University, 2008.
- [71] Troyer, T. L.; Muchalski, H.; Hong, K. B.; Johnston, J. N. *Org. Lett.* **2011**, *13*, 1790–1792.
- [72] Mahoney, J. M.; Smith, C. R.; Johnston, J. N. *J. Am. Chem. Soc.* **2005**, *127*, 1354–1355.
- [73] Hong, K. B. Brønsted acid-promoted olefin functionalization (*anti*-aminohydro-xylation) and progress toward (+)-zwittermicin A. Ph.D. thesis, Vanderbilt University, 2010.
- [74] Hong, K. B.; Donahue, M. G.; Johnston, J. N. *J. Am. Chem. Soc.* **2008**, *130*, 2323–2328.
- [75] Chandra, A.; Viswanathan, R.; Johnston, J. N. *Org. Lett.* **2007**, *9*, 5027–5029.
- [76] Wilt, J. C.; Pink, M.; Johnston, J. N. *Chem. Commun.* **2008**, 4177–4179.
- [77] Guenard, D.; Gueritte-Voegelein, F.; Potier, P. *Acc. Chem. Res.* **1993**, *26*, 160–167.
- [78] Okino, T.; Matsuda, H.; Murakami, M.; Yamaguchi, K. *Tetrahedron Lett.* **1993**, *34*, 501–504.
- [79] Matsuura, F.; Hamada, Y.; Shioiri, T. *Tetrahedron* **1994**, *50*, 11303–11314.
- [80] Salimbeni, A.; Paleari, F.; Poma, D.; Criscuoli, M.; Scolastico, C. *Eur. J. Med. Chem.* **1996**, *31*, 827–832.
- [81] Umezawa, H.; Aoyagi, T.; Suda, H.; Hamada, M.; Takeuchi, T. *J. Antibiot.* **1976**, *29*, 97.
- [82] Nishizawa, R.; Saino, T.; Takita, T.; Suda, H.; Aoyagi, T.; Umezawa, H. *J. Med. Chem.* **1977**, *20*, 510–515.
- [83] Zhu, J.; Ma, D. *Angew. Chem. Int. Ed.* **2003**, *42*, 5348–5351.
- [84] Kunze, B.; Bohlendorf, B.; Reichenbach, H.; Hofle, G. *J. Antibiot.* **2008**, *61*, 18–26.
- [85] Sharpless, K. B.; Patrick, D. W.; Truesdale, L. K.; Biller, S. A. *J. Am. Chem. Soc.* **1975**, *97*, 2305–2307.
- [86] Li, G.; Chang, H.-T.; Sharpless, K. B. *Angew. Chem. Int. Ed. Eng.* **1996**, *35*, 451–454.
- [87] Christie, S. D. R.; Warrington, A. D. *Synthesis* **2008**, 1325–1341.
- [88] Donohoe, T. J.; Chughtai, M. J.; Klauber, D. J.; Griffin, D.; Campbell, A. D. *J. Am. Chem. Soc.* **2006**, *128*, 2514–2515.
- [89] Alexanian, E. J.; Lee, C.; Sorensen, E. J. *J. Am. Chem. Soc.* **2005**, *127*, 7690–7691.
- [90] Liu, G.; Stahl, S. S. *J. Am. Chem. Soc.* **2006**, *128*, 7179–7181.
- [91] Michaelis, D. J.; Shaffer, C. J.; Yoon, T. P. *J. Am. Chem. Soc.* **2007**, *129*, 1866–1867.
- [92] Michaelis, D. J.; Ischay, M. A.; Yoon, T. P. *J. Am. Chem. Soc.* **2008**, *130*, 6610–6615.
- [93] Williamson, K. S.; Yoon, T. P. *J. Am. Chem. Soc.* **2010**, *132*, 4570–4571, PMID: 20232850.

- [94] Cochran, B. M.; Michael, F. E. *Org. Lett.* **2008**, *10*, 5039–5042.
- [95] Hart, D. J.; Ha, D. C. *Chem. Rev.* **1989**, *89*, 1447–1465.
- [96] Kobayashi, S.; Mori, Y.; Fossey, J. S.; Salter, M. M. *Chem. Rev.* **2011**, *111*, 2626–2704.
- [97] Kobayashi, S.; Ishitani, H.; Ueno, M. *J. Am. Chem. Soc.* **1998**, *120*, 431–432.
- [98] Akiyama, T.; Itoh, J.; Yokota, K.; Fuchibe, K. *Angew. Chem. Int. Ed.* **2004**, *43*, 1566–1568.
- [99] List, B.; Pojarliev, P.; Biller, W. T.; Martin, H. J. *J. Am. Chem. Soc.* **2002**, *124*, 827–833.
- [100] Cordova, A.; Notz, W.; Zhong, G.; Betancort, J. M.; Barbas, C. F. *J. Am. Chem. Soc.* **2002**, *124*, 1842–1843.
- [101] Trost, B. M.; Terrell, L. R. *J. Am. Chem. Soc.* **2003**, *125*, 338–339.
- [102] Trost, B. M.; Jaratjaroonphong, J.; Reutrakul, V. *J. Am. Chem. Soc.* **2006**, *128*, 2778–2779.
- [103] Harada, S.; Handa, S.; Matsunaga, S.; Shibasaki, M. *Angew. Chem. Int. Ed.* **2005**, *44*, 4365–4368.
- [104] Matsunaga, S.; Yoshida, T.; Morimoto, H.; Kumagai, N.; Shibasaki, M. *J. Am. Chem. Soc.* **2004**, *126*, 8777–8785.
- [105] Sugita, M.; Yamaguchi, A.; Yamagiwa, N.; Handa, S.; Matsunaga, S.; Shibasaki, M. *Org. Lett.* **2005**, *7*, 5339–5342.
- [106] Yamaguchi, A.; Matsunaga, S.; Shibasaki, M. *Tetrahedron Lett.* **2006**, *47*, 3985–3989.
- [107] Martin, S. F.; Lopez, O. D. *Tetrahedron Lett.* **1999**, *40*, 8949–8953.
- [108] Carswell, E. L.; Snapper, M. L.; Hoveyda, A. H. *Angew. Chem. Int. Ed.* **2006**, *45*, 7230–7233.
- [109] Wieland, L. C.; Vieira, E. M.; Snapper, M. L.; Hoveyda, A. H. *J. Am. Chem. Soc.* **2009**, *131*, 570–576.
- [110] Mandai, H.; Mandai, K.; Snapper, M. L.; Hoveyda, A. H. *J. Am. Chem. Soc.* **2008**, *130*, 17961–17969.
- [111] Muchalski, H.; Doody, A. B.; Troyer, T. L.; Johnston, J. N. *Organic Syntheses* **2011**, *88*, 212–223.
- [112] Evans, D. A.; Britton, T. C.; Ellman, J. A. *Tetrahedron Lett.* **1987**, *28*, 6141 – 6144.
- [113] Ihmels, H.; Maggini, M.; Prato, M.; Scorrano, G. *Tetrahedron Letters* **1991**, *32*, 6215–6218.
- [114] Jencks, W. P.; Carriuolo, J. *J. Am. Chem. Soc.* **1960**, *82*, 675–681.
- [115] Jencks, W. P.; Carriuolo, J. *J. Am. Chem. Soc.* **1960**, *82*, 1778–1786.
- [116] Nugent, B. M.; Yoder, R. A.; Johnston, J. N. *J Am Chem Soc* **2004**, *126*, 3418–3419.

- [117] Davis, T. A.; Wilt, J. C.; Johnston, J. N. *J. Am. Chem. Soc.* **2010**, *132*, 2880–2882, PMID: 20151644.
- [118] Davis, T. A.; Danneman, M. W.; Johnston, J. N. *Chem. Commun.* **2012**, *48*, 5578–5580.
- [119] Myers, E. L.; Butts, C. P.; Aggarwal, V. K. *Chem. Commun.* **2006**, 4434–4436.
- [120] Sibi, M. P.; Cook, G. R. In *Lewis Acids in Organic Synthesis*; Yamamoto, H., Ed.; Wiley-VCH: Weinheim, 2000; Vol. 2; Chapter 12, pp 543–544.
- [121] Doyle, M. P. *Chem. Rev.* **1986**, *86*, 919–939.
- [122] Desimoni, G.; Faita, G.; Jorgensen, K. A. *Chem. Rev.* **2006**, *106*, 3561–3651.
- [123] Koskinen, A. *Asymmetric Synthesis of Natural Products*; Wiley, 1993.
- [124] Mckee, B. H.; Gilheany, D. G.; Sharpless, K. B. *Org. Synth.* **1992**, *70*, 47.
- [125] Wang, Z. M.; Sharpless, K. B. *J. Org. Chem.* **1994**, *59*, 8302–8303.
- [126] Chang, H.-T.; Sharpless, K. B. *J. Org. Chem.* **1996**, *61*, 6456–6457.
- [127] Denmark, S. E.; Nakajima, N.; Nicaise, O. J. C.; Faucher, A.-M.; Edwards, J. P. *J. Org. Chem.* **1995**, *60*, 4884–4892.
- [128] Evans, D. A.; Peterson, G. S.; Johnson, J. S.; Barnes, D. M.; Campos, K. R.; Woerpel, K. A. *J. Org. Chem.* **1998**, *63*, 4541–4544.
- [129] Desimoni, G.; Faita, G.; Mella, M. *Tetrahedron* **1996**, *52*, 13649–13654.
- [130] Handelsman, J.; Raffel, S.; Mester, E. H.; Wunderlich, L.; Grau, C. R. *Appl. Environ. Microbiol.* **1990**, *56*, 713–718.
- [131] Handelsman, J.; Nesmith, W. C.; Raffel, S. J. *Curr. Microbiol.* **1991**, *22*, 317–319.
- [132] Smith, K. P. *Plant Disease* **1993**, *77*, 139.
- [133] Phipps, P. *Biological and Cultural Tests for Plant Disease* **1992**, *7*, 60.
- [134] He, H.; Silo-Suh, L. A.; Handelsman, J.; Clardy, J. *Tetrahedron Lett.* **1994**, *35*, 2499–2502.
- [135] Silo-Suh, L. A.; Lethbridge, B. J.; Raffel, S. J.; He, H.; Clardy, J.; Handelsman, J. *Appl. Environ. Microbiol.* **1994**, *60*, 2023–2030.
- [136] Silo-Suh, L. A.; Stabb, E. V.; Raffel, S. J.; Handelsman, J. *Curr. Microbiol.* **1998**, *37*, 6–11.
- [137] Broderick, N. A.; Goodman, R. M.; Raffa, K. F.; Handelsman, J. *Environ. Etnomol.* **2000**, *29*, 101–107.
- [138] Thomson, J. A. *J. Nutr.* **2002**, *132*, 3441S–3442S.
- [139] Rogers, E. W.; Molinski, T. F. *Org. Lett.* **2007**, *9*, 437–440.
- [140] Rogers, E. W.; Dalisay, D.; Molinski, T. *Angew. Chem. Int. Ed.* **2008**, *47*, 8086–8089.

- [141] Rogers, E. W.; Molinski, T. F. *J. Org. Chem.* **2009**, *74*, 7660–7664.
- [142] Hoffmann, R. W.; Kahrs, B. C.; Schiffer, J.; Fleischhauer, J. *J. Chem. Soc., Perkin Trans. 1* **1996**, 2407–2414.
- [143] Sasaki, M.; Tanino, K.; Hirai, A.; Miyashita, M. *Org. Lett.* **2003**, *5*, 1789–1791.
- [144] Emmert, E. A. B.; Klimowicz, A. K.; Thomas, M. G.; Handelsman, J. *Appl. Environ. Microbiol.* **2004**, *70*, 104–113.
- [145] Kevany, B. M.; Rasko, D. A.; Thomas, M. G. *Appl. Environ. Microbiol.* **2009**, *75*, 1144–1155.
- [146] Müller, I.; Weinig, S.; Steinmetz, H.; Kunze, B.; Veluthoor, S.; Mahmud, T.; Müller, R. *ChemBioChem* **2006**, *7*, 1197–1205.
- [147] Poss, C. S.; Schreiber, S. L. *Acc. Chem. Res.* **1994**, *27*, 9–17.
- [148] Magnuson, S. R. *Tetrahedron* **1995**, *51*, 2167–2213.
- [149] Holland, J. M.; Lewis, M.; Nelson, A. *The Journal of Organic Chemistry* **2003**, *68*, 747–753.
- [150] Inoue, M.; Sato, T.; Hirama, M. *Journal of the American Chemical Society* **2003**, *125*, 10772–10773.
- [151] Roe, S. J.; Stockman, R. A. *Chem. Commun.* **2008**, 3432–3434.
- [152] Hudlicky, T.; Reed, J. W. *Chem. Soc. Rev.* **2009**, *38*, 3117–3132.
- [153] Cortijos, A. M.; Snape, T. J. *Tetrahedron: Asymmetry* **2008**, *19*, 1761–1763.
- [154] Candy, M.; Audran, G.; Bienayme, H.; Bressy, C.; Pons, J.-M. *J. Org. Chem.* **2010**, *75*, 1354–1359, PMID: 20128625.
- [155] Lubineau, A.; Bouchain, G. *Tetrahedron Lett.* **1997**, *38*, 8031–8032.
- [156] Zhang, Y.; Arpin, C. C.; Cullen, A. J.; Mitton-Fry, M. J.; Sammakia, T. *J. Org. Chem.* **2011**, *76*, 7641–7653.
- [157] Kireev, A. S.; Manpadi, M.; Kornienko, A. *J. Org. Chem.* **2006**, *71*, 2630–2640.
- [158] Cailleau, T.; Cooke, J. W. B.; Davies, S. G.; Ling, K. B.; Naylor, A.; Nicholson, R. L.; Price, P. D.; Roberts, P. M.; Russell, A. J.; Smith, A. D.; Thomson, J. E. *Org. Biomol. Chem.* **2007**, *5*, 3922–3931.
- [159] Rychnovsky, S.; Griesgraber, G.; Powers, J. *Org. Synth.* **2004**, *Coll. Vol. 10*, 276–280.
- [160] Whitehead, A.; McReynolds, M. D.; Moore, J. D.; Hanson, P. R. *Org. Lett.* **2005**, *7*, 3375–3378.
- [161] Guan, Y.; Wu, J.; Sun, L.; Dai, W.-M. *J. Org. Chem.* **2007**, *72*, 4953–4960.
- [162] Nicolaou, K. C.; Adsool, V. A.; Hale, C. R. H. *Org. Lett.* **2010**, *12*, 1552–1555.
- [163] Pappo, R.; Allen, D. S., Jr.; Lemieux, R. U.; Johnson, W. S. *J. Org. Chem.* **1956**, *21*, 478–479.

- [164] Zhong, Y.-L.; Shing, T. K. M. *J. Org. Chem.* **1997**, *62*, 2622–2624.
- [165] Markiewicz, W. T. *J. Chem. Res. (S)* **1979**, 24.
- [166] Ziegler, T.; Dettmann, R.; Bien, F.; Jurisch, C. *Trends in Organic Chemistry* **1997**, *6*, 91–100.
- [167] Kocienski, P. *Protecting groups*, 3rd ed.; Thieme: Stuttgart; New York, 2004.
- [168] Wuts, P. *Greene's protective groups in organic synthesis.*, 4th ed.; Wiley-Interscience: Hoboken N.J., 2007.
- [169] Evans, D. A.; Carter, P. H.; Dinsmore, C. J.; Barrow, J. C.; Katz, J. L.; Kung, D. W. *Tetrahedron Lett.* **1997**, *38*, 4535–4538.
- [170] Carter, P. H. Total Synthesis of the Bryostatins. Ph.D. thesis, Harvard University, 1998.
- [171] Tojo, G. *Oxidation of alcohols to aldehydes and ketones : a guide to current common practice*; Springer: New York, 2006.
- [172] Meyer, S. D.; Schreiber, S. L. *J. Org. Chem.* **1994**, *59*, 7549–7552.
- [173] Rao, S. L. N. *Biochemistry* **1975**, *14*, 5218–5221.
- [174] Kurtz, A. C. *J. Biol. Chem.* **1938**, *122*, 477–484.
- [175] Kurtz, A. C. *J. Biol. Chem.* **1949**, *180*, 1253–1267.
- [176] Kjaer, A.; Larsen, P. O. *Acta Chem. Scand.* **1959**, *13*, 1565–1574.
- [177] Anders, K. r.; Vesterager, E. *Acta Chem. Scand.* **1960**, *14*, 961–964.
- [178] Rogers, E. W. Zwittermicin A: Determination of its Complete Configuration and Total Synthesis of its Enantiomer. Ph.D. thesis, University of California, San Diego, 2008.
- [179] De Luca, L.; Giacomelli, G.; Porcheddu, A.; Salaris, M. *Synlett* **2004**, 2570–2572.
- [180] Kim, J.; Jang, D. *Synlett* **2010**, 2093–2096.
- [181] Kotha, S.; Behera, M.; Khedkar, P. *Tetrahedron Lett.* **2004**, *45*, 7589–7590.
- [182] Lei, M.; Ma, L.; Hu, L. *Tetrahedron Lett.* **2010**, *51*, 4186–4188.
- [183] Zhu, J.; Wu, X.; Danishefsky, S. J. *Tetrahedron Lett.* **2009**, *50*, 577–579.
- [184] Muramatsu, I.; Murakami, M.; Yoneda, T.; Hagitani, A. *Bull. Chem. Soc. Jpn.* **1965**, *38*, 244–246.
- [185] Kisfaludy, L.; Ötvös, L., Jr. *Synthesis* **1987**, *1987*, 510–510.
- [186] Egbertson, M. S.; Homnick, C. F.; Hartman, G. D. *Synth. Commun.* **1993**, *23*, 703–709.
- [187] Nicolaou, K. C.; Estrada, A. A.; Zak, M.; Lee, S. H.; Safina, B. S. *Angew. Chem. Int. Ed.* **2005**, *44*, 1378–1382.

- [188] Ogawa, H.; Chihara, T.; Taya, K. *J. Am. Chem. Soc.* **1985**, *107*, 1365–1369.
- [189] Ogawa, H.; Hiraga, N.; Chihara, T.; Teratani, S.; Taya, K. *Bull. Chem. Soc. Jpn.* **1988**, *61*, 2383–2386.
- [190] Ogawa, H.; Ichimura, Y.; Teratani, T. C. S.; Taya, K. *Bull. Chem. Soc. Jpn.* **1986**, *59*, 2481–2483.
- [191] de la Zerda, J.; Barak, G.; Sasson, Y. *Tetrahedron* **1989**, *45*, 1533–1536.
- [192] Klivanov, A. M. *Acc. Chem. Res.* **1990**, *23*, 114–120.
- [193] Saitoh, M.; Fujisaki, S.; Ishii, Y.; Nishiguchi, T. *Tetrahedron Letters* **1996**, *37*, 6733–6736.
- [194] Nishiguchi, T.; Ishii, Y.; Fujisaki, S. *J. Chem. Soc., Perkin Trans. 1* **1999**, 3023–3027.
- [195] Inokuchi, T.; Matsumoto, S.; Nishiyama, T.; Torii, S. *The Journal of Organic Chemistry* **1990**, *55*, 462–466.
- [196] Andreana, P. R.; Liu, C. C.; Schreiber, S. L. *Org. Lett.* **2004**, *6*, 4231–4233.
- [197] Denney, D. B.; Goldstein, B. *J. Org. Chem.* **1956**, *21*, 479–479.
- [198] Arndt, F. *Org. Synth.* **1943**, *Coll. Vol. 2*, 165.